Vehicle noise and vibration refinement

Related titles:

Advanced direct injection combustion engine technologies and development Volume 1: Gasoline and gas engines
(ISBN 978-1-84569-389-3)
Direct injection (DI) enables precise control of the fuel/air mixture so that engines can be tuned for improved power and fuel economy, but ongoing research challenges remain in improving the technology for commercial applications. As fuel prices escalate, DI engines are expected to gain in popularity for automotive applications. This important book, in two volumes, reviews the science and technology of different types of DI combustion engines and their fuels. Volume 1 deals with direct injection gasoline and CNG engines, including history and essential principles, approaches to improved fuel economy, design, optimisation, optical techniques and their application.

Advanced direct injection combustion engine technologies and development Volume 2: Diesel engines
(ISBN 978-1-84569-744-0)
Direct injection (DI) enables precise control of the fuel/air mixture so that engines can be tuned for improved power and fuel economy, but ongoing research challenges remain in improving the technology for commercial applications. As fuel prices escalate DI engines are expected to gain in popularity for automotive applications. This important book, in two volumes, reviews the science and technology of different types of DI combustion engines and their fuels. Volume 2 investigates diesel DI combustion engines, which despite their commercial success are facing ever more stringent emissions legislation worldwide. Three main sections address light-duty diesel engines; heavy-duty diesel engines; and the all-important exhaust emission control strategies, including combustion diagnostics and modelling.

Tribology and dynamics of engine and powertrain: Fundamentals, applications and future trends
(ISBN 978-1-84569-361-9)
Tribology is one element of many interacting within a vehicle engine and powertrain. In adopting a detailed, theoretical, component approach to solving tribological problems, the minutiae can be overwhelmingly complex and practical solutions become elusive and uneconomic. The system perspective generally adopted in industry, however, can lead to shortcuts and oversimplifications, industrial projects are subject to *ad hoc* trial and error, and subsequent 'fire-fighting' activity is required. This book seeks to bridge this divide, using a multi-physics approach to provide sufficient fundamental grounding and understanding of both detailed and approximate analyses – thereby making 'first time right' design solutions possible. Tribological issues and solutions in piston systems, valve train systems, engine bearings and drivetrain systems are addressed. New developments in materials, micro-engineering, nano-technology and MEMS are also included.

Details of these and other Woodhead Publishing books can be obtained by:

• visiting our web site at www.woodheadpublishing.com
• contacting Customer Services (e-mail: sales@woodheadpublishing.com; fax: +44 (0) 1223 893694; tel.: +44 (0) 1223 891358 ext. 130; address: Woodhead Publishing Limited, Abington Hall, Granta Park, Great Abington, Cambridge CB21 6AH, UK)

If you would like to receive information on forthcoming titles, please send your address details to: Francis Dodds (address, tel. and fax as above; e-mail: francis.dodds@woodheadpublishing.com). Please confirm which subject areas you are interested in.

Vehicle noise and vibration refinement

Edited by
Xu Wang

CRC Press
Boca Raton Boston New York Washington, DC

WOODHEAD PUBLISHING LIMITED
Oxford   Cambridge   New Delhi

Contents

v

6 Theory and application of modal analysis in vehicle noise and vibration refinement 117
M. K R O N A S T, Ford-Werke GmbH, Germany

7 Mid- and high-frequency problems in vehicle noise and vibration refinement – statistical energy analysis and wave approaches 142
X. W A N G, RMIT University, Australia

8 Advanced simulation techniques in vehicle noise and vibration refinement 174
N. H A M P L, Ford-Werke GmbH, Germany

Contributor contact details

(* = main contact)

Chapters 1, 2, 3, 4, 5, 7 and 16

Dr Xu Wang
RMIT University
School of Aerospace, Mechanical
    and Manufacturing Engineering
PO Box 71, Bundoora
Victoria 3083
Australia
E-mail: xu.wang@rmit.edu.au

Chapter 6

Dr Michael Kronast
Vehicle NVH Europe
Ford-Werke GmbH
D-50725 Köln
Germany
E-mail: mkronast@ford.com
delkro@netic.de

Chapter 8

Dr Norbert Hampl
Vehicle NVH Europe
Ford-Werke GmbH
D-50725 Köln
Germany
E-mail: nhampl@ford.com

Chapter 9

Mr Thomas Ahlersmeyer
Vehicle NVH Europe
Ford-Werke GmbH
D-50725 Köln
Germany
E-mail: tahlersm@ford.com

Chapter 10

Professor Simon Watkins
RMIT University
School of Aerospace, Mechanical
    and Manufacturing Engineering
PO Box 71, Bundoora
Victoria 3083
Australia
E-mail: simon.watkins@rmit.edu.au

Chapter 11

Professor Steve J. Elliott
Institute of Sound and Vibration
    Research
University of Southampton
Southampton SO17 1BJ
UK
E-mail: sje@isvr.soton.ac.uk

Chapter 12

Dr David C. Baillie
Engineering Department
General Motors Holden Ltd
GPO Box 1714
Melbourne
Victoria 3001
Australia

Chapter 13

Davide Vigé
Vehicle Architectures, NVH and
  Aerodynamics Department
Centro Ricerche Fiat
Strada Torino, 50
10043 Orbassano
Italy
E-mail: davide.vige@crf.it; davide.
  vige@fiat.com

Chapter 14

Björn Reff
Vehicle NVH Europe
Ford-Werke GmbH
D-50725 Köln
Germany
E-mail: breff@ford.com

Chapter 15

Greg M. Goetchius
Material Sciences Corporation
6855 Commerce Blvd
Canton, MI 48363
USA
E-mail: greg.goetchius@matsci.com

Preface

Noise and vibration of motor vehicles are increasingly important for the automotive industry and are concerns for both vehicle manufacturers and component suppliers. While noise pollution legislation is driving down vehicle exterior noise, customers are becoming more discerning in relation to noise and vibration inside the vehicle. Noise and vibration are now considered to be two of the most important quality factors in vehicle design.

This book provides a review of noise and vibration refinement principles, control methods and advanced experimental and modelling techniques. There is also a review of palliative treatments necessary in vehicle design, development and system integration processes in order to meet noise and vibration targets and standards. A comprehensive reference list is provided in order to direct further studies and to assist readers to develop in-depth knowledge of the sources and transmission mechanisms of noise and vibration in motor vehicles. The book aims to support product design and development engineers and managers in automotive engineering companies as well as researchers and students. Chapters 1–4 and 6–8 are focused on the introduction of fundamental principles and methods. Chapters 9–13 present engineering case studies. Chapters 14–16 present advanced techniques.

The authors include specialists working in noise and vibration departments of major automotive manufacturers, component suppliers and universities. An additional aim of the book is to improve automotive education and to bridge the gap between the automotive industry and universities. The authors believe that the key to an efficient automotive industry is close liaison between universities and industry, while maintaining a good balance between academic and commercial needs.

1

Rationale and history of vehicle noise and vibration refinement

X. WANG, RMIT University, Australia

Abstract: Vehicle noise and vibration performance are important aspects of vehicle design validation criteria, and have significant influence on the overall image of a vehicle. This chapter summarizes the objectives and significance of vehicle noise and vibration refinement, defines its scope and illustrates its relationship to the vehicle development process. Some vehicle noise and vibration terms are defined and a brief history of motoring and vehicle refinement is presented.

Key words: noise, vibration, refinement, vehicle development process, target setting, benchmarking, design, development, testing, validation, audit.

1.1 Introduction

Vehicle noise and vibration performance is an important vehicle design validation criterion, since it significantly affects the overall image of a vehicle. Noise and vibration degrade the driver's and passengers' comfort and induce stress, fatigue and feelings of insecurity. Modern vehicle development requires noise and vibration refinement to deliver the proper level of customer satisfaction and acceptance. It is common for a customer's perception of vehicle quality to relate closely to the noise and vibration characteristics of the vehicle.

Globalization combined with increased competition in the marketplace requires a vehicle's noise and vibration characteristics to be well optimized. The sound present in the interior of a vehicle consists mainly of powertrain noise, road noise and wind noise. Given the increased market demand for lighter and more powerful vehicles, it becomes evident that powertrain-induced noise is a key component of the vehicle's interior noise. Automotive manufacturers are increasing the number of powertrains available on vehicle programs because of the potential for improved fuel economy. For example, diesel-powered vehicles are one of the popular alternatives in the global automotive market. This presents and further complicates a unique set of noise and vibration challenges that need to be solved during the vehicle development process. This means not only eliminating squeaks and

3

rattles and suppressing overall noise levels, but also tuning the sound of the automobile to reflect the high quality and distinction of the brand.

1.2   Objectives and significance of vehicle noise and vibration refinement

Noise, vibration and harshness (NVH) have become increasingly important as a result of the demand for increasing refinement. Vibration has always been an important issue closely related to reliability and quality. Noise is of increasing importance to vehicle users and environments. Harshness is related to the quality and transient nature of vibration and noise. Noise and vibration problems may originate from systems such as the engine, pumps, drivetrain, wheels and tyres, or may be related to system integration issues, for example matching between powertrain and body and between chassis and body. Controlling vibration and noise in vehicles poses a severe challenge to designers because motor vehicles have several sources of vibration and noise which, being interrelated and speed dependent, are different from many machine systems. Vehicle noise and vibration refinement has been considered essential for vehicle design and development because of legislation, marketing needs and customer expectations. In order to minimize the impact of the automobile on the environment, legislation has become increasingly demanding on vehicle noise emission and vibration controls. Noise and vibration refinement distinguishes a vehicle from its competitors, thereby attracting new customers.

1.3   Scope of vehicle noise and vibration refinement

Vehicle refinement encompasses noise and vibration refinement, ride and driveability. Vehicle refinement affects the customer's buying decision and the business of selling passenger cars, as it directly affects the driving experience. A refined vehicle should have the following characteristics:

- High ride quality
- Good driveability
- Low wind noise
- Low road noise
- Low engine noise
- Idle refinement (low noise and vibration)
- Cruising refinement (low noise and vibration, good ride quality)
- Low transmission noise
- Low levels of shake and vibration
- Low levels of rattles, squeaks and sizzles

- Low level of exterior noise of good quality
- Low level of interior noise of good quality
- Noise that is welcome as a 'feature'.

Customers have come to expect continuous improvement in new vehicles. They expect their new purchase to be better equipped and more comfortable, and to perform better than the vehicle they have just traded in. If the new vehicle is better in all respects than the old one, but lacks refinement, the customer will not be fully satisfied. Vehicle refinement aims to enhance vehicle performance, styling and acoustics. The motivations for vehicle refinement are therefore:

- Brand image
- Drive comfort
- Quality enhancement
- Cost and weight reduction
- Customer satisfaction.

Noise and vibration refinement is an important aspect of vehicle refinement. It deals with noise and vibration suppression, noise and vibration design, rattle and squeak suppression. The vehicle noise and vibration refinement process covers the following tasks:

- Benchmarking
- Target setting
- Noise and vibration design and development
- Prototype NVH testing and design validation
- Noise and vibration diagnostics and problem solving
- NVH design solutions for production
- NVH audits on production vehicles.

1.4 The vehicle development process and vehicle noise and vibration refinement

Figure 1.1 shows the four-phase vehicle development process. This consists of program definition (phase one), design and development (phase two), product verification (phase three) and production (phase four). Theme (phase one), content definition and design (phase two), test (phase three) and manufacturing and assembly (phase four) are implemented in the four-phase process. Connection of the phases has a timing overlap. Fuzziness in design is large at the beginning of the process and small at the end of the process. The process cycle lasts 3–6 years. The production volume for the process is approximately 100,000—1,000,000 vehicles per year.
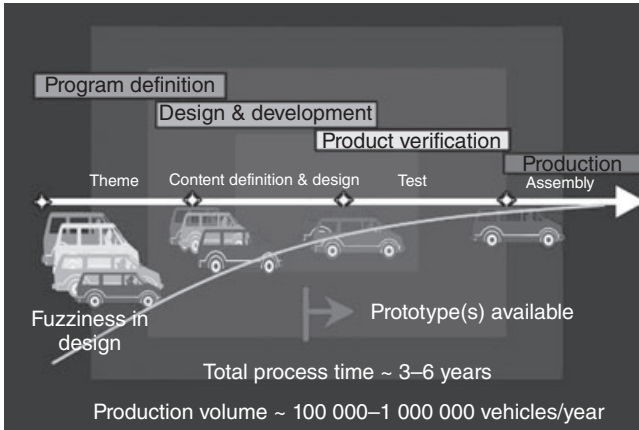
1.1 A four-phase vehicle development process (reproduced by permission, Wang, X., *Introduction to Motor Vehicle Design*, RMIT Publisher, 2005).

Phase one starts from product planning, which identifies:

- Demographic trends
- Buyer profiles
- Economic trends
- Anticipated sales volumes
- Balancing economic opportunity with compliance to the strategic plan and acceptable risks.

In phase one, market research information is analysed, the performance of competing companies and their sales are studied, and the established product cycles are investigated to determine whether current tooling life has expired. Strategies for the replacement of existing models or the introduction of totally new ones must be formulated. Design characteristics, features, options and systems are determined by quality function deployment, benchmark study and existing warranty data.

Quality function deployment identifies:

- The voice of the customers
- Specific performance targets
- Measurable processes towards the targets
- Matrices to inject the customer's needs into the product design and manufacturing processes.

Benchmark study provides insights into design, features, quality and price. It identifies:

- Customer requirements
- Trends in the marketplace
- Important features.

Warranty data identifies:

- Existing design problems
- Desirable and undesirable features
- Product functions that may result in unexpected performance (such as operator misuse, unexpected environmental conditions, or interaction with other vehicle components).

Corresponding to the four-phase vehicle development process, some automotive manufacturers set up a four-phase prototype vehicle development program (Alpha, Beta, Gamma, Pilot). From the past vehicle development program, the unsolved NVH issues are passed on to the current vehicle development program, and NVH engineers address those issues in the program definition phase. Computer Aided Engineering (CAE) tools are used for NVH design and to resolve NVH issues. Mule vehicles are built by modifying the previous vehicle development models in the prototype Alpha where components or system designs are installed. These component or system designs are early prototype or concept designs. The prototype Alpha vehicle is tested according to the experimental plan of the program. The test data are used to validate the component or system designs of the vehicle. NVH development, validation and audit tests are conducted on the prototype. In prototype Alpha, the vehicle body is usually developed from the previous model and the prototyped powertrain may be installed.

The prototype Alpha is usually available at the beginning of the program definition (phase one). More component and/or system designs are added onto the prototype Beta, the early version concept designs evolving to the next level in the prototype based on the development, validation test and audit data. More NVH development, validation and audit tests are conducted in the prototype Beta where the early version of body structure design is installed, the powertrain system design is upgraded, and parts of the chassis and suspension system and component designs are installed. The installed designs in the prototype Beta evolve into the next level based on the prototype development test results. The prototype Beta is usually built at the beginning of the design and development phase.

In the prototype Gamma, all component and system designs are installed. Most of them are upgraded and finalized for the stage of design freeze. The prototype vehicle must pass national design rules and standards/requirements such as impact and crashworthiness, durability, emission and engine calibration, pass-by noise, etc. The prototype Gamma is usually built at the beginning of the product verification–test phase.

In the prototype Pilot, engineers focus on NVH diagnostics and trouble-shooting, auditing vehicle NVH performance and investigating NVH issues related to variations of the manufacturing process such as noise seals/leaks, rattle, squeak, etc. Engineers are requested to organize vehicle NVH assessment rides with a vehicle development team and engineering management, to conduct NVH subjective evaluation and analysis, diagnose NVH problems and troubleshoot them. NVH engineers must propose low-cost, production-friendly design solutions. They are also encouraged to drive and audit the vehicles near the assembly plants, work and communicate with plant engineers to sort out process-variation-related NVH issues and reinforce the process quality control.

In parallel with the four-phase prototype vehicle tests, the component and system designs in the four phases are concurrently tested and validated in laboratories. There are usually two or three vehicle development program overlaps in the typical workload of NVH engineers. These are previously released vehicle-model service fixes, the current-vehicle development program and the future-vehicle development program. NVH engineers are therefore involved not only in problem solving and service fixes, but also in research and development, as well as noise and vibration design to avoid NVH problems at the early design stages. Figure 1.2 shows that the central area of vehicle integration is vehicle noise and vibration refinement in which NVH engineers investigate system matching-related NVH issues, such as NVH issues from matching body with powertrain, matching chassis with body and matching chassis with powertrain. Noise and vibration design for vehicle integration is one of the key tasks in this model; CAE tools are used in vehicle integration and noise and vibration refinement. Good communication is essential between NVH engineers, CAD/CAE engineers, vehicle integration engineers and vehicle plant engineers as shown in the model of Fig. 1.2. Figure 1.3 shows that noise and vibration refinement is the central area of system design and development in which the systems include powertrain, chassis and suspension, body and trim, electrical and HVAC; NVH engineers must compel system suppliers to resolve their system/component NVH problems that appear in vehicle assembly and to meet their NVH targets by the existing quality control processes.

Vehicle noise and vibration refinement is a process requiring team effort. Good communication, a cooperative relationship and trust must be established between NVH engineers, design and development engineers, suppliers, experimental planning, CAE engineers, test technicians, program and engineering managers for the vehicle development process in order for the whole vehicle engineering team to feel integrated and harmonized. Teamwork motivates the parties to generate enthusiasm and commitment, and is conducive to a high standard of work. Communication can be conducted in many ways, for example through group meetings, project and
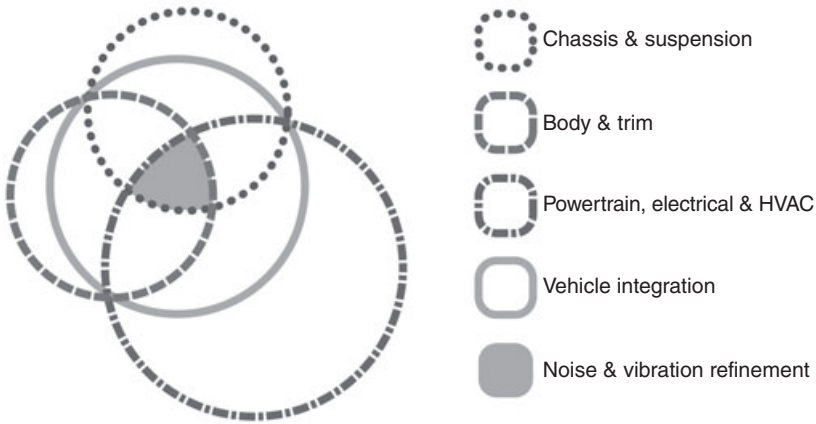
1.2 Interaction model of noise and vibration refinement in vehicle integration (copyright RMIT University, 2008, Wang, X.).
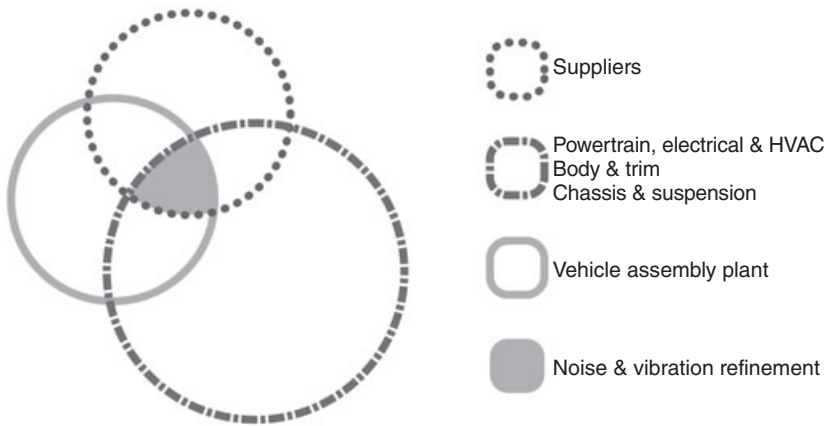
1.3 Interaction model of noise and vibration refinement in system design and development (copyright RMIT University, 2008, Wang, X.).

program meetings, supplier design and development meetings, on-site problem-solving task force meetings, test requests, work instructions, test reports, test procedures, test result presentations, Avoid Verbal Orders (AVOs), emails, telephone conversations, etc.

Standard steps for NVH problem solving are:

- Identify the problems in vehicle operating conditions with the relevant engineering party on site.
- Instrument and test the vehicle, reproducing the problems under the same vehicle operating conditions.
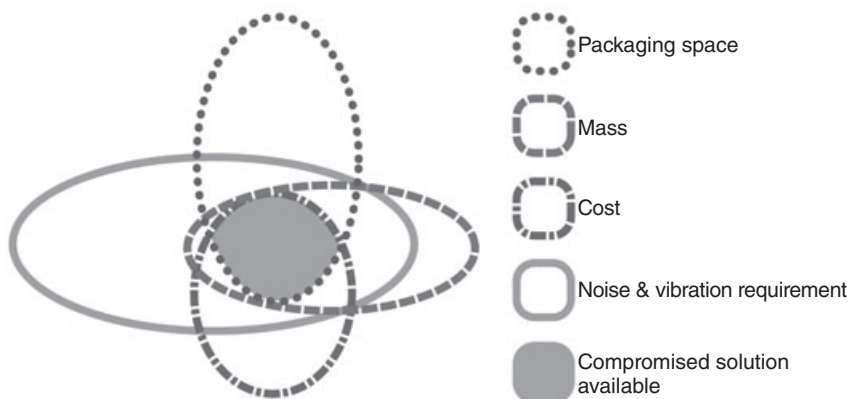
1.4 Compromised solutions in the vehicle development process (copyright RMIT University, 2008, Wang, X.).

- Analyse the test results and suggest solutions for the problems to the relevant engineering party.
- Install the design solutions supplied by the relevant engineering party into the vehicle and validate them under the same vehicle operating conditions.

NVH engineers must recognize that there are many trade-offs between NVH performance, engine power, fuel economy, development time, cost, weight, etc. A compromise must be reached in the development process as shown in Fig. 1.4.

Figure 1.5 shows the steeply increasing committed cost as the commitment to tooling is made during the program. Therefore maximum utilization of virtual testing to identify potential issues prior to the tooling stage will significantly reduce development time and cost, although physical testing of the subsystems and the complete vehicle is still required to ensure that the 'as manufactured' vehicle consistently meets the performance targets set.

In order to reduce vehicle development cost and time, an improved vehicle development process is proposed as shown in Fig. 1.6 where a target setting, cascading, synthesis and confirmation approach is applied to design instead of the traditional design–build–test–redesign approach. This approach facilitates the use of analytical prediction tools early in the process, reducing the use of expensive physical prototype testing. It also allows for design efforts to be shared across the automotive manufacturer and supplier chain. The process can be implemented with a variety of tools and specific applications. The overall requirement is to maintain communication between the independent tasks as the results from each sub-process become available. The activities in the arrowed process flow are
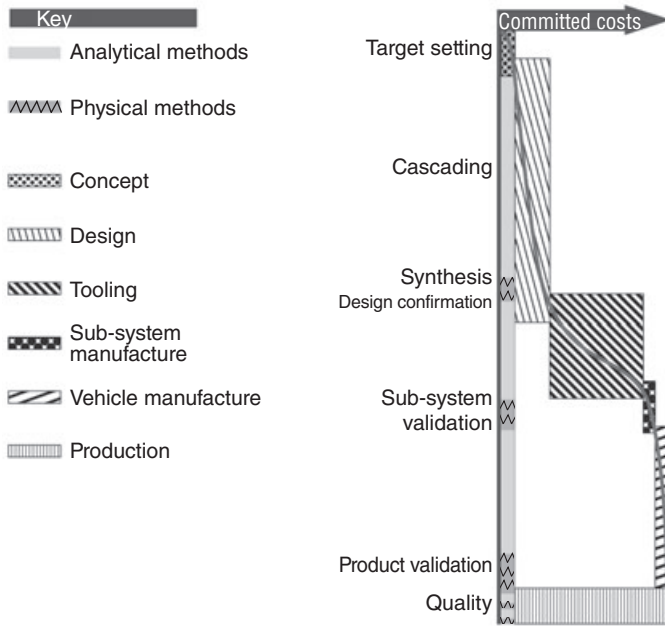
1.5 Integration of physical and analytical methods (copyright Grote, P. and Sharp, M., 'Defining the vehicle development process', Keynote Paper, Symposium on International Automotive Technology, 2001, SAE).

positioned relative to time, with the initial target setting activity occurring first. The intention is for the virtual validation to lead the physical validation and thus accelerate the overall design process. The parallel 'V' image indicates that both validation paths are required. The virtual path is the optimization path that leads to the release of design elements requiring long lead times such as component tooling. The physical path is the confirmation path that must capture effects that cannot be modelled with certainty, such as abrasion and wear, joint fatigue and progressive NVH degradation. The image also shows that the product development process must be advanced through continuous virtual and physical correlation.

The overall design engineering process begins with the initial vehicle target setting as the first stage. The end customers and their demands for specific vehicle characteristics drive the basic requirements. This 'voice of the customer' is combined with the existing internal knowledge and benchmarks of competitive vehicles already in the marketplace, along with cost, weight and performance targets to define the primary vehicle assumptions. The initial assumptions create the top-level design goals for the complete vehicle.
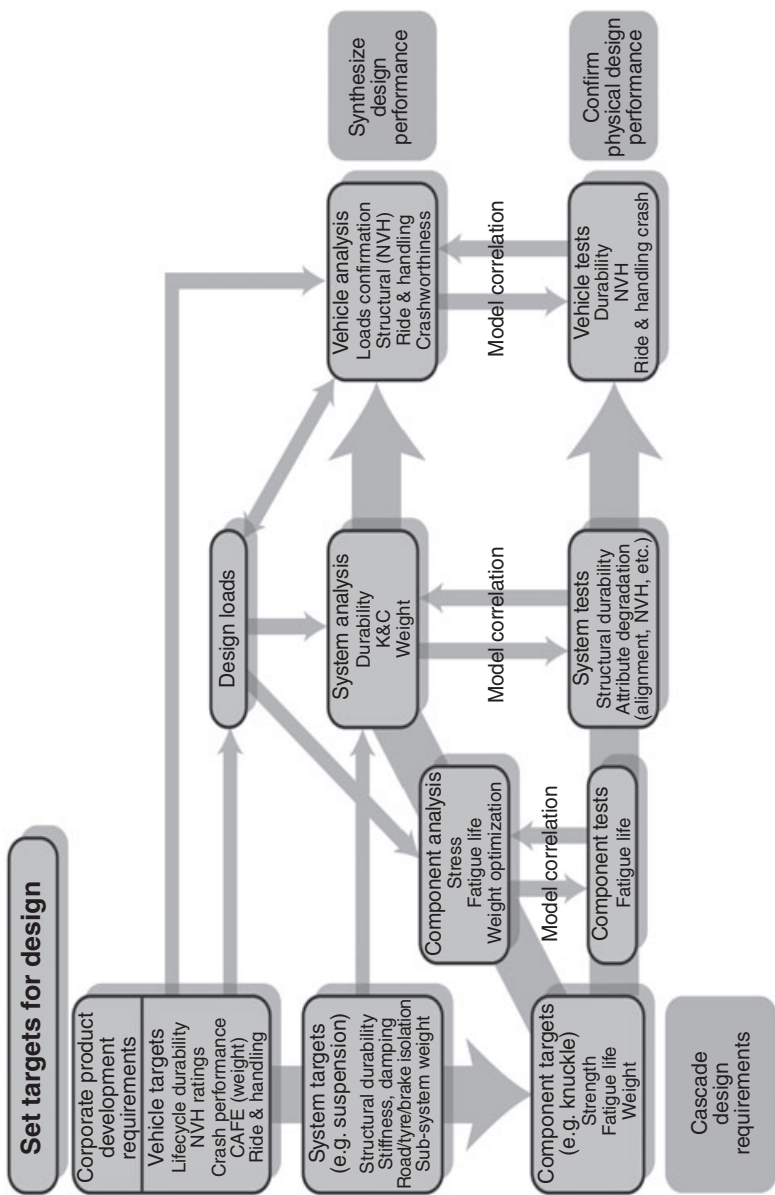
1.6 The emerging vehicle development model (copyright Grote, P. and Sharp, M., 'Defining the vehicle development process', Keynote Paper, Symposium on International Automotive Technology, 2001, SAE).

The second stage is target cascading which subdivides the top-level design goals into system, subsystem and individual component goal levels. This stage relies heavily on CAE tools to define all of the vehicle components with individual target loads and constraints in a digital model. There may be several iterations as the targets are interpreted for each layer of design. There are many trade-offs to be determined with different criteria for safety, performance, NVH, durability and other disciplines.

The third stage is synthesis where the designs for individual components and sub-assemblies are completed using a variety of computer aided design (CAD) tools. This stage utilizes CAE tools to generate virtual test results which may require modification to the initial target values and thus additional trade-offs. These tools typically allow for analysis and prediction of expected results that can be compared to the target data values previously established. One goal of this stage is to identify these necessary trade-offs before committing to specific product design, thus accelerating the overall design process. This stage is therefore referred to as 'virtual testing' as various design levels can be tested with computer simulation methods prior to the manufacture of any prototype physical parts. The sequence of the virtual testing process is component, sub-assembly, sub-system and the full vehicle. The design goals at each level are thus validated with corresponding virtual tests at each level.

The fourth stage is confirmation by physical testing where prototype parts, sub-systems and systems are subsequently evaluated and validated in a similar sequence to the virtual testing process until the complete vehicle is ready for final evaluation. Each activity within the physical testing stage results in additional data that can be used to validate computer models. The continuous feedback may require additional changes to the target levels and vehicle design parameters.

The hybrid simulation is also used to set targets for vehicle development in the 'V' approach. The process starts with full-vehicle performance targets that are cascaded down to requirements for sub-systems (drivetrain, chassis, suspension, etc.), and finally to components (bushings, mounts, struts, etc.). Hardware is then designed, built and assembled into a prototype vehicle in the bottom part of the 'V' where physical testing usually leads to several redesign cycles to iron out problems. In this 'V' approach, most car companies use simulation tools such as Finite Element Analysis (FEA) to help speed the process after CAD has defined the geometry of sub-systems, assemblies and parts. By that time, important design decisions have been made and considerable time and expense are required for any reconfiguration. This problem can be eliminated with function-driven design that aims to accurately establish functional performance requirements through target setting, much earlier in the process before the detailed design has started. This eliminates the repetitive build–test–redesign cycles later in

development by performing analysis earlier with more system-level full-vehicle simulation during the conceptual target-setting stage. By performing up-front engineering, the performance targets can be more accurately established, and thus better strategic decisions on vehicle design can be made. In this way, time and expense can be saved later in the bottom part of the 'V', as fewer prototype testing cycles are required.

1.5   Vehicle noise and vibration term definitions

Noise, vibration and harshness, also known as noise and vibration, abbreviated to NVH and N&V respectively, is the name given to the field of measuring and modifying the noise and vibration characteristics of vehicles, particularly cars and trucks. Harshness is somewhat of an historical misnomer. Noise and vibration can be measured, but harshness is a more subjective assessment. There is a psychoacoustic measurement called harshness but it does not correlate very well with many harshness issues. Interior NVH is the noise and vibration experienced by the occupants of the vehicle cabin, while exterior NVH is largely concerned with the noise radiated by the vehicle, and includes drive-by noise. The noise being generated by fluid pressure fluctuation and passage through the air is called airborne noise. The noise radiated from a structure's surface that is vibrating is called structure-borne noise. Noise is used here to describe audible sound, with particular attention paid to the frequency range from 30 to 4000 Hz. Vibration is used to describe tactile vibration, with particular attention paid to the frequency range from 30 to 200 Hz.

1.6   History of motoring and vehicle refinement

It is frequently difficult to trace the earliest examples of automobiles. In 1885, Karl Benz invented a motorized tricycle in which the wheels were made of timber and steel. Those who rode such a vehicle experienced bad harshness. In 1888, John Dunlop invented air-filled or pneumatic tyres. In 1904 Continental presented the world's first automobile tyre with a patterned tread. The wheel/road-induced noise and vibration were reduced by the air-filled or pneumatic tyres. Other vibration isolators such as rubber bushes and engine mounts were also invented and introduced in vehicles for the reduction of noise vibration harshness. Figure 1.7 shows a 1905 four-cylinder Tarrant with chain-driven rear wheels. In 1909, Henry Ford launched his mass production method for the Model T which made cars available to a large section of the public. The hard, tedious, repetitive work created resentment, resulted in poor workmanship and quality and produced badly finished, unreliable vehicles. Vehicle refinement became necessary. The Volkswagen 'Beetle' had little refinement but many innovative

1.7 The 14–16 horsepower four-cylinder Tarrant – the Melbourne-built car that set an Australian 1000-mile (1600-km) speed record in 1905 (copyright Tuckey, B., *Australians and Their Cars*, Bondi Junction, NSW: Focus, 2003).

features. This vehicle was designed by Ferdinand Porsche in the late 1930s at the behest of Adolf Hitler. By the 1970s, its styling was antiquated, its air-cooled engine was noisy, yet it sold well throughout the world, in particular in the USA. In fact, the metallic sound of the air-cooled engine is not recognized as noise but accepted as one of the brand characteristics of today's Porsche cars. Today's VW 'Beetles' have been well refined in all aspects, including noise vibration harshness. Vauxhall and HSV are refined vehicle brands for GM passenger cars, while Tick Ford and FPV are refined vehicle brands for Ford in which the driveability and ride are upgraded. Lexus are refined Toyota passenger cars in which noise and vibration are greatly reduced. High series passenger cars are refined from low series ones by improving noise vibration harshness, driveability and ride. The term 'vehicle refinement' is placed in the mind of the customer as being a relevant factor in the decision making process of buying a car.

The early vehicle noise and vibration refinement materials were grease, motor oil, rubber bushes, washers, gaskets, springs, mass dampers, bolts and nuts, cushions, earplugs and gloves; the early noise and vibration refinement tools were stereoscopes, screwdrivers, earphones, tape recorders, dial gauges, balancers, water bulb levelling meters, hands, eyes and ears, which are still practical for use and popular today. Engineers subjectively evaluated vehicle noise and vibration performance and solved the NVH problems by traditional mechanical tools and methods.

1.8 Peirce 55-B dictation wire recorder from 1945 (copyright
http://en.wikipedia.org/wiki/Wire_recorder).

1.9 Solidyne GMS200 tape recorder with computer self-adjustment,
Argentina, 1980–1990 (copyright http://en.wikipedia.org/wiki/
Tape_recorder).

In 1876, Emile Berliner, Elisha Gray and Alexander Graham Bell
invented the first microphone used as a telephone voice transmitter. The
microphone associated with the first articulate telephone transmitter was
the liquid transmitter of 1876. In 1938, Hans J. Meier at MIT was the first
person to construct a commercial strain gauge accelerometer. Magnetic
recording was conceived as early as 1877 by Oberlin Smith. The first wire
recorder was the Valdemar Poulsen Telegraphone of the late 1890s. Since
their first introduction, analogue tape recorders have experienced a long
series of progressive developments resulting in increased sound quality,
convenience and versatility, and Fig. 1.8 shows such a recorder from 1945.
Computer-controlled analogue tape recorders were introduced by Oscar
Bonello in Argentina as shown in Fig. 1.9 where the mechanical transport
used three DC motors and introduced two new advances: automated micro-
processor transport control and automatic adjustment of bias and frequency
response. In 30 seconds the recorder adjusted its bias and provided best

1.10 A mechanical calculator from 1914. Note the lever used to rotate the gears (copyright http://en.wikipedia.org/wiki/History_of_computing_hardware).

frequency response to match the brand and batch of magnetic tape used. The microprocessor control of transport allowed fast location of any point on the tape. Around 1820, Charles Xavier Thomas created the first successful, mass-produced mechanical calculator, the Thomas Arithmometer, that could add, subtract, multiply and divide. It was based mainly on Leibniz's work. Mechanical calculators, like the base-10 addiator, the comptometer, the Monroe, the Curta and the Addo-X, were used throughout the twentieth century (e.g. see Fig. 1.10) right up until the 1970s. The IBM PC AT 286, 386 and 486 appeared in the early 1980s, then came PC Pentium technology. PC data acquisition and sound card technology have replaced digital and analogue tape recording technology for recording and analysing noise and vibration test data.

1.7   References and bibliography

Grote, P. and Sharp, M. (2001), 'Defining the vehicle development process', Keynote Paper, Symposium on International. Automotive Technology, SAE.

Happian-Smith, J. (2002), *An Introduction to Modern Vehicle Design*, SAE International, Butterworth-Heinemann.

Harrison, M. (2004), *Vehicle Refinement – Controlling Noise and Vibration in Road Vehicles*, SAE International, Elsevier Butterworth-Heinemann.

Tuckey, B. (2003), *Australians and Their Cars*, Bondi Junction, NSW: Focus.

Wang, X. (2005), *Introduction to Motor Vehicle Design*, RMIT Publisher.

2

Target setting and benchmarking for vehicle noise and vibration refinement

X. WANG, RMIT University, Australia

Abstract: In order to develop new vehicle products with well-refined noise and vibration performance, noise and vibration targets must be set up. Market research helps to select the best-in-class competitors' vehicles and determine benchmark vehicles to be studied. Benchmark analysis together with CAE modelling facilitates vehicle noise and vibration target setting and target cascading. This chapter summarizes objectives, significance and scope of vehicle noise and vibration target setting and benchmarking. Examples are given to illustrate how to conduct vehicle noise and vibration benchmarking, target setting and target cascading.

Key words: target setting, target cascading, benchmarking, interior noise target, exterior noise target, subjective evaluation, objective testing, whole-vehicle noise and vibration, components/subsystems noise and vibration, sound pressure level, sound quality, sound power, articulate index, statistical energy analysis, transfer path analysis.

2.1   Introduction

As mentioned in Chapter 1, in the first phase of a vehicle development program, market analysis, benchmark study and target setting are important tasks. The object of benchmark study is to determine the best-in-class competitors. Requirement, design and performance constitute the three stages of the vehicle development process as shown in Fig. 2.1. The purpose of target setting is to establish design requirements. Vehicle targets are set based on the benchmark study, the voice of the customer and business/industry/government regulation, as shown in Fig. 2.2.

Market analysis determines which group of customers the vehicle is targeting; customer wants from this group and competitors' vehicles for benchmark study are then determined. The competitors' vehicles are analysed to determine the competitor best-in-class systems and subsystems; overall vehicle specifications and targets are then determined as shown in Fig. 2.3.

18
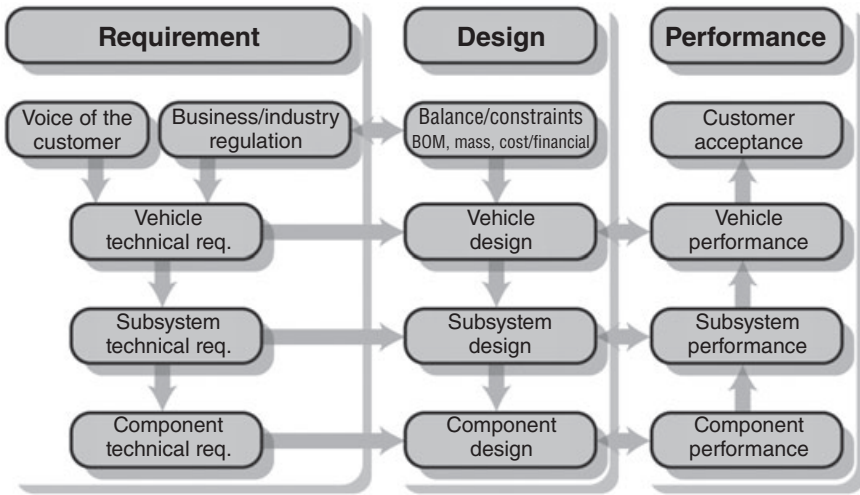
2.1 Vehicle development process.
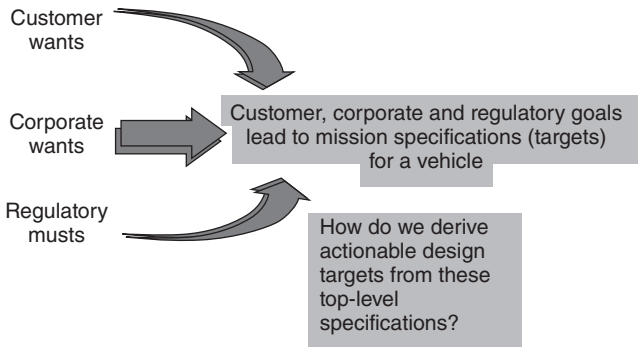
2.2 Basic inputs for vehicle development target setting [2].

2.1.1 Objectives and significance of vehicle noise and vibration target setting and benchmarking

Benchmarking allows for greater understanding of vehicle systems, subsystems and components and their design targets. Apple-to-apple, back-to-back comparisons give information about what are good designs, and what are poor designs, and what are realistic design targets. The development focuses are then better calibrated. The purpose of the benchmark study is to identify the competitor best-in-class and facilitate noise and vibration target setting for the vehicle system, subsystems and components.

Benchmarking & market analysis

Determine what group of customers the vehicle is targeting

Determine the customer wants for this group

Determine the competition vehicles

Analyse the competition vehicles using the matrix provided

Determine competitor best-in-class systems and subsystems

Complete the overall vehicle specifications (OVS)

Complete the vehicle system/ subsystem targets

2.3 Vehicle target setting process [2].

Setting vehicle noise and vibration targets is important for the successful operation of a vehicle development program, as it ensures that planned resources and efforts are directed towards better vehicle noise and vibration performance than that of competitors in order to satisfy customers at the beginning of the development process. Without it, individual system suppliers would determine their own interpretation of an appropriate level of noise and vibration. The final vehicle would most likely be truly refined only in some aspects and not in others. Excessive noise and vibration caused by one component or subsystem in the intended production vehicle would cause its design validation test to fail, lead to a large cost increase and time delay for the program, and jeopardize the program targets. The purpose of vehicle noise and vibration target setting is to ensure that the newly developed vehicle has no noise and vibration complaint issues and that it has superior noise and vibration performance when released to market.

2.1.2   Scope of vehicle noise and vibration target setting and benchmarking

Vehicle noise and vibration targets consist of interior and exterior targets, subjective and objective targets, noise level and sound quality targets. Exterior noise targets include whole-vehicle exterior targets and single-component exterior noise targets. The exterior pass-by noise targets must conform to the national design rules and standards. Interior targets include the whole-vehicle and single-component noise targets inside the vehicle cabin and ride quality (vibration) targets at idle, constant speeds and slow

accelerations, wide open throttle run-up and overrun/coast-down driving conditions.

The noise and vibration targets for the whole vehicle system, individual components and subsystems are documented in the overall vehicle specification and system specifications by the brand holder, and adherence to them has become a condition of contract for any suppliers who implement an advanced product quality planning process.

Corresponding to vehicle noise and vibration targets, a benchmark study needs to be conducted on competitors' vehicles for noise and vibration performance of the interior and exterior, both subjectively and objectively, of the whole vehicle and of components/subsystems, and of the level and quality in all vehicle operating conditions.

2.2   Benchmarking of vehicle noise and vibration

Benchmark vehicles are selected according to similar style/platform capacity, cost, weight and targeted market segment agreed by the program team. They are tested for exterior noise including pass-by and idle; for interior disturbing noise including rattle/squeak, resonance noise, road noise, powertrain noise, auxiliaries, load reversal and gear noise; for communication and audio acoustics including hi/fi qualification and articulation index; for interior actuation noise including servo actuators and door closing; and for interior driving noise in conditions of acceleration and constant speed. The interior and exterior disturbing noise will need to be minimized, while interior driving noise, actuation noise and communication/audio acoustics can be designed as shown in Fig. 2.4. The vibration and ride quality are also tested in all vehicle operating conditions.

Subjective evaluation is an important part of vehicle development because its results are directly related to customers' feelings. Subjective evaluations are conducted in a group of people (more than three) and the results are produced from the statistical average of the group. Table 2.1 shows a vehicle subjective evaluation rating scale and rules. Table 2.2 shows a typical vehicle NVH subjective evaluation form.

2.3   Target setting for vehicle noise and vibration

Both subjective and objective vehicle evaluation tests must be conducted on the selected benchmark vehicles. The test results plus previous vehicle model test data and service warranty data of released vehicles are analysed to set vehicle noise and vibration targets. According to the vehicle noise and vibration subjective rating scale shown in Table 2.1, the noise and vibration subjective evaluation target rating should be typically set as R8 for a future vehicle development model. The engine combustion order

Vehicle acoustics: minimization

| Exterior noise | Pass-by |
| | Idle |

Interior noise	Squeak/rattle	Disturbing noise
	Resonance effect	
	Road noise	
	Auxiliaries	
	Load reversal	
	Gearbox noise	
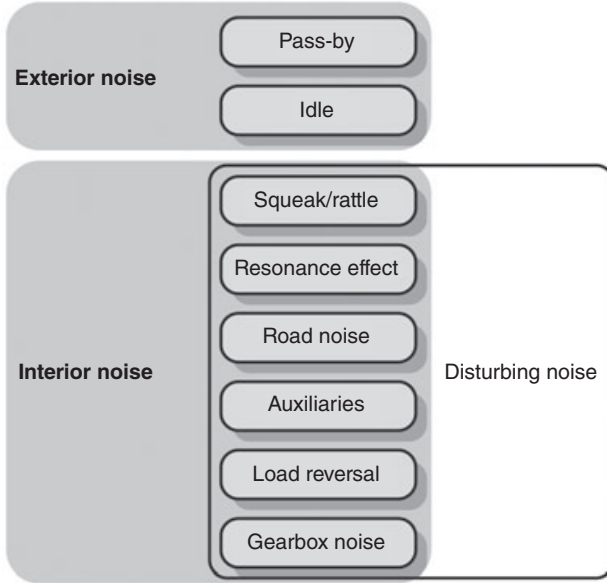
Vehicle acoustics: design

	HiFi qualification	Communication audio/acoustics
	Articulation index	
Interior noise	Servo actuators	Actuation noise
	Door closing	
	Acceleration	Driving noise
	Constant speed	
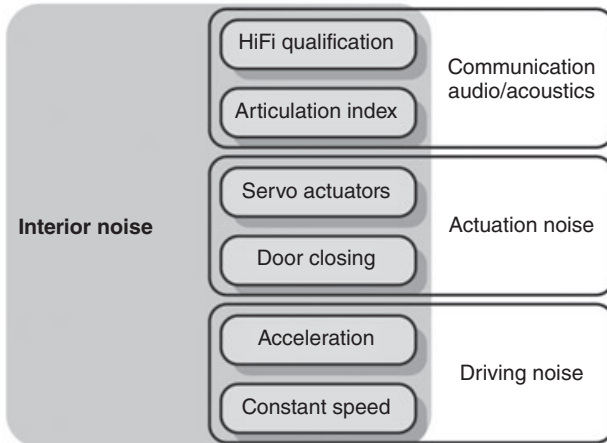
2.4 Benchmarked vehicle noise [4].

tracking boundary lines of the second gear slow acceleration test data, the first gear wide open throttle acceleration test data and overrun coast-down test data will be powertrain noise and vibration target lines, and the constant speed spectrum boundary lines will be target lines of the whole vehicle tyre/road noise, wind noise, driveline and wheel-induced noise and vibration as well as idle noise and vibration.

Table 2.1 Vehicle subjective rating scale (courtesy of General Motors Holden Ltd, 1999)

No. in scale	Criterion
Commercial	
10	Not noticed even by trained evaluators
9	Noticeable only by trained evaluators
8	Noticeable only by critical customers
7	Noticeable by all customers
6	Rated disturbing by some customers
5	Rated disturbing by all customers (border line)
Non-commercial	
4	Rated as failure by all customers
3	Complained as bad failure by all customers
2	Limited operation
1	Non-operation

Acoustic target setting and hybrid simulation assist in engineering the sound characteristics of vehicles. State-of-the-art CAE technology and processes are used to combine test data on existing components with virtual models of new parts to accurately represent entire vehicles and set acoustic targets up-front during development. In this way, the whole-vehicle noise and vibration targets can be cascaded into vehicle subsystem and component targets, and vehicle development can be achieved by predicting and tuning passenger compartment sound early in the conceptual stage, even before the detailed design of the vehicle is started.

Transfer Path Analysis (TPA) cascades system-level noise and vibration targets down to subsystem level targets (Fig. 2.5). In the early stages of a vehicle design program, targeted vehicles for the new vehicle are selected based on their subjective noise, vibration and harshness (NVH) performance. A reference vehicle for the new product will be selected which will be used as a baseline vehicle for the whole vehicle program. Noise and vibration measurements will be taken on both the reference and targeted vehicles under multiple load conditions. The simulation target for the new product will be derived from the measurements of the reference vehicle, measurements of the targeted vehicle, and the simulation of the reference vehicle model. Reverse Transfer Path Analysis tools will be used to quantify the subsystem targets for the new vehicle based on the simulation targets and design intent simulation models of new products.

The stiffness design of hard points between chassis and body structure plays an important role in vibration isolation and noise reduction. The hard points are engine mounting brackets, engine sub-frame/cross-member, transmission cross-member, shaker towers, etc. Structural

Table 2.2 Vehicle NVH subjective evaluation form (courtesy of General Motors Holden Ltd, 1999)

1. ENGINE CRANKING		
Engine cranking noise		
Engine cranking vibration		
2. IDLE		
Idle sound and vibration		
Fan noise		
A/C noise		
Alternator whine inside vehicle		
Power steering noise – when turning the steering wheel from left to right full lock		
Fuel pump noise inside the cabin		
Exterior engine noise level & quality		
Radiator or condenser fan noise		
Exhaust tail pipe sound		
3. ACCELERATION		
Off idle boom		
Quiver 25 km/h		
Shudder 60 to 100 km/h		
2nd gear slow acceleration noise		
1st gear wide open throttle noise		
Gear shift noise and vibration (auto transmission) in normal acceleration		
Gear shift noise and vibration (auto transmission) in wide open throttle		
4. CRUISING		
Noise and Vibration Rating at 40 km/h		
Noise and Vibration Rating at 60 km/h		
Noise and Vibration Rating at 80 km/h		
Noise and Vibration Rating at 100 km/h		
Noise and Vibration Rating at 120 km/h		
Doors, windows, pillars sealing		
Mirror vibration		
Road impact		
Shake, throttle tip-in tip-out		
Torque converter lock-up boom		
5. OVERRUN		
Noise when decelerating with the 2nd gear engaged		
Noise when decelerating with the neutral gear engaged and engine off		
6. BRAKING		
Noise when braking		
Vibration felt when braking		
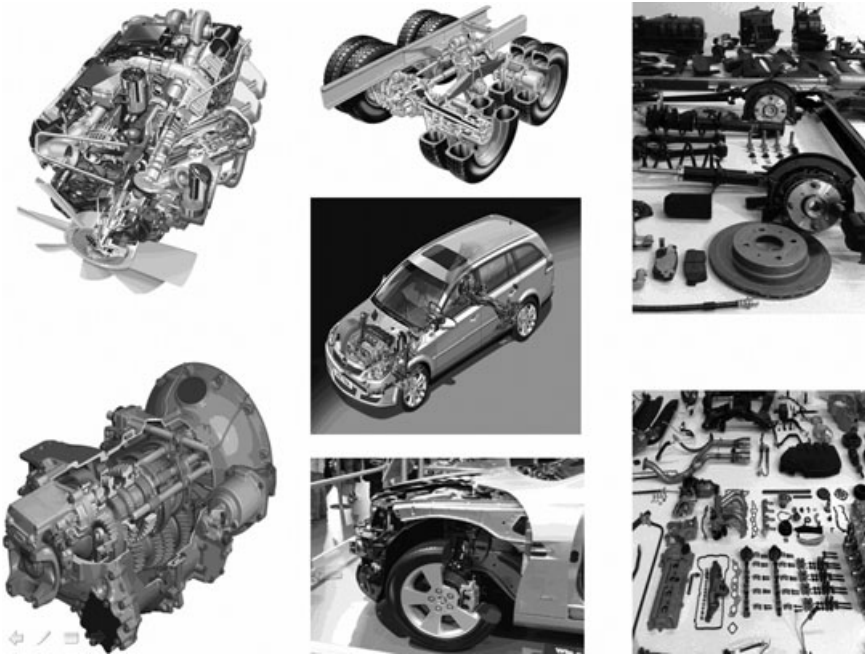
2.5 Vehicle noise and vibration target cascading (source: FEV website).

mobility functions are used to evaluate their stiffness. A structural mobility function is defined as a transfer function or frequency response function between a force and the response velocity. An acoustic mobility function is defined as a frequency response function or a transfer function between a force and the acoustic pressure response at the driver's ear. The design target for the acoustic mobility functions at the hard points is set as 55–60 dBL/N. The design target for the structural mobility function is set as 0.312 mm/s/N. Finite element analysis and frequency response testing are used to verify the design targets. Structural and acoustic mobility functions at the hard points are measured and analysed, and the mobility function values at the hard points are reasonably distributed and designed to achieve a performance compromise of NVH and ride handling. This will be further illustrated in the following chapters.

Statistical Energy Analysis (SEA) is an established technique for predicting high frequency vehicle noise and vibration performance. SEA is more sensitive to certain parameters such as material properties, damping, absorption and treatment thickness and coverage than to fine details of geometry. Using SEA is especially practical and it can be particularly advantageous in the early design phase of a vehicle development program to set subassembly noise and vibration targets.
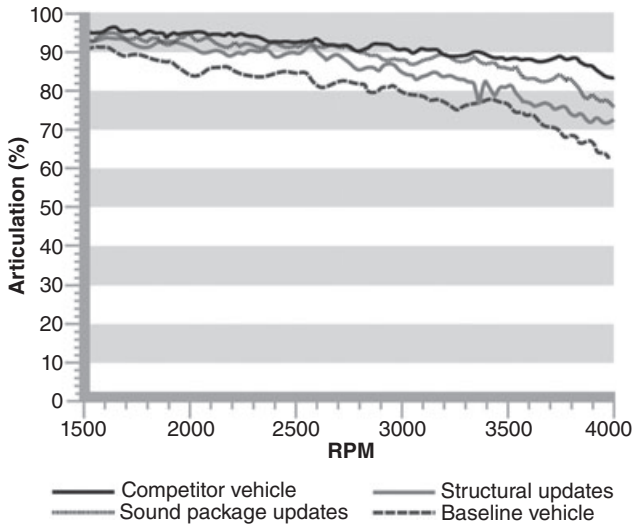
2.6 Articulation index of sound pressure at the driver's ear in the centre for vehicles in first gear slow acceleration sweeps [5].

Power plant sound pressure level (SPL) target setting is the first critical step to develop an efficient NVH strategy that guides computer aided engineering analysis and hardware research to achieve a desired goal in the early stage of a program. Traditionally, specifications have been set by comparing a baseline power plant SPL average from several measurement locations with its target; an effective method can be used to break down the power plant SPL target into individual component levels at desired frequencies quantitatively. The method is based on the inverse square law that the reduction of sound power level equals the reduction of sound pressure level at a fixed point in a free field. The SPL target could be test data or theoretical calculations.

Figure 2.6 shows the articulation index of competitive vehicle, baseline vehicle and development vehicles over an engine speed range from 1500 to 4000 rpm where the target of the articulation index can be set close to that of the competitive vehicle. Figure 2.7 shows the noise reduction or engine firewall noise attenuation of baseline, prototype vehicles and the target line. The engine noise attenuation of the baseline vehicle is less than that of the target line. The engine noise attenuation of the development prototype has reached the target line.

Figures 2.8 and 2.9 show a sound power contribution analysis of a vehicle sound package using a window method where the vehicle was tested under second gear slow acceleration on a chassis dynamometer in an anechoic
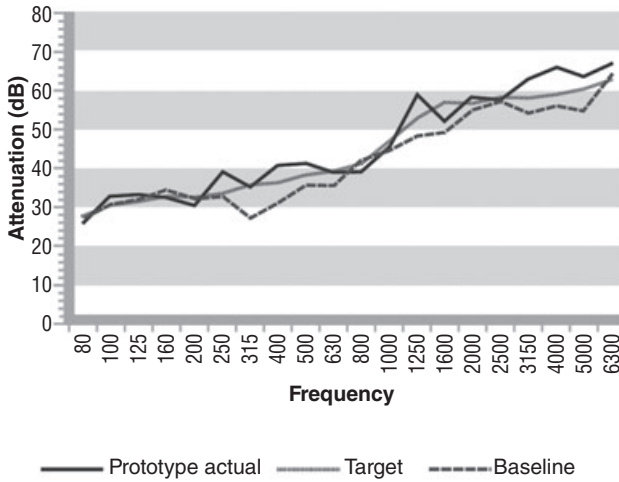
2.7 Engine firewall attenuation (noise reduction).
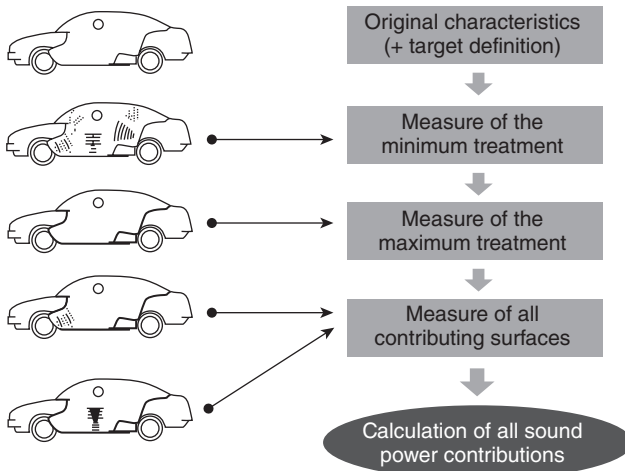
2.8 Window method for sound power contribution analysis.

room for the original condition as delivered, the minimum treatment, the maximum treatment, and all individual contributing trim components on/off. If the vehicle is the competitor best-in-class vehicle, then Fig. 2.9 presents the sound power targets for individual trim components in the vehicle sound package.

Figure 2.10 shows typical SPL targets for different types of vehicle noise sources. Figure 2.11 compares sound quality targets of a test vehicle.
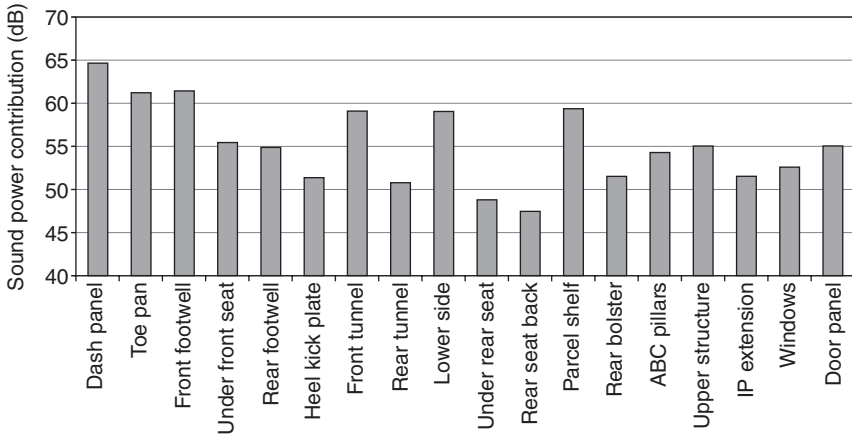
2.9 Sound power contributions (second gear slow acceleration sweep from 500 rpm to 5000 rpm) from a vehicle sound package components using window methods.
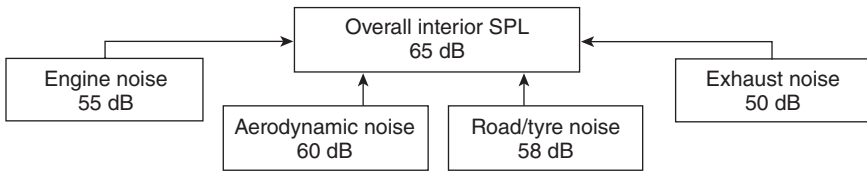
2.10 Targeted SPL for different types of vehicle noise [5].
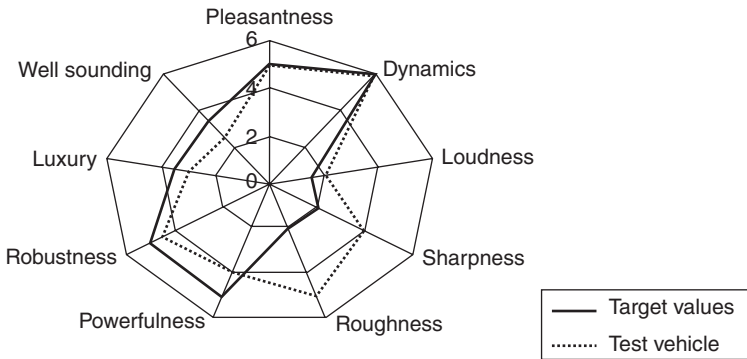
2.11 Sound quality target comparison for a test vehicle [5].

2.4   References and bibliography

1. Harrison, M. (2004), *Vehicle Refinement – Controlling Noise and Vibration in Road Vehicles*, SAE International, Elsevier Butterworth-Heinemann.

2. Wang, X. (2005), *Introduction to Motor Vehicle Design*, RMIT Publisher.
3. Happian-Smith, J. (2002), *An Introduction to Modern Vehicle Design*, SAE International, Butterworth-Heinemann.
4. LMS Engineering Innovation (2007), 'More than a quiet car: Acoustic target setting supports BMW's premium brand image'.
5. Gossler, J.V. (2007), 'NVH benchmarking during vehicle development using sound quality metrics', Masters degree thesis, Department of Mechanical and Mechatronic Engineering, Stellenbosch University, South Africa.
6. Zeng, P.W. (2003), 'Target setting procedures for vehicle power plant noise reduction', *Sound and Vibration*, July 2003.

3

Vehicle vibration measurement and analysis

X. WANG, RMIT University, Australia

Abstract: This chapter introduces the basic concept of vibration measurement, illustrates the pre-requirements for vibration testing and environment testing, and provides tips for the installation of vibration objects. The quotation method for vibration levels and the measurement method for complex modulus and damping loss factor are also discussed. The principles of vibration isolation and vibration absorber are briefed. Two case studies are given to illustrate how the principles and methods are applied to solve engineering problems.

Key words: vibration transducers, accelerometers, subjective evaluation, hand sensing, proximity sensors, velocity sensors, charge amplifier, power supplier, Young's modulus, damping loss factor, human vibration limit, vibration isolation, vibration absorber.

3.1   Introduction

After completing benchmark study and setting vehicle development targets, vehicle noise and vibration refinement starts with a vehicle development process. Vibration is one of the most common customer complaint issues. Vibration may be caused by faulty engine combustion, wheel–tyre imbalance, prop shaft imbalance, driveline angle induced torsional vibration, brake shudder, etc. In order to identify the root cause of vibration, a series of diagnostic tests has to be conducted. Vibration measurement plays a key role in the vehicle development process. In order to avoid vibration problems in the early design stages, vibration isolation and absorber design have to be conducted; in particular, powertrain vibration isolation design has to be carefully carried out to minimize the structure-borne vibration transmitted from power plant to chassis and body structure. This chapter introduces the vibration measurement fundamentals and quotation indexes, and illustrates design principles and methods of vibration isolation and vibration absorption for solving engineering problems. This includes the subjective vibration evaluation method as illustrated below.

3.2   Hand sensing

Humans are sensitive to vibrations. Before any instruments became available all vibration analysis was done by listening and feeling. This method

33

is still used by those who do not have access to instruments. We have some built-in sensors in our skin and our ears. These biological transducers served a survival function and still do. The human ear is amazingly sensitive to the smallest pressure change. The pressure sensors in our skin can detect constant pressure, and also oscillating pressure or vibration.

Humans can directly detect vehicle noise, loudness and vibration smoothness by listening and feeling before any electronic instruments are connected. This is a valid sensing method for vibration analysis if certain precautions are taken, namely calibration and frequency analysis. It is difficult to compare one vehicle with vibration 'readings' separated by several days, especially if many similar vehicles are seen during the interval. The 'measurements' are also highly subjective. One person's judgement of 'rough' could be another person's 'acceptable'. This system of human perception gives an overall vibration reading. The best that can be obtained with hand sensing of vibration is a crude, overall, subjective vibration measurement that sounds an alarm when mechanical failure is imminent. The method of hand sensing works satisfactorily in vehicle noise, vibration and harshness (NVH) departments where some human calibration techniques are employed by NVH engineers and technicians. First, one NVH engineer/technician is given responsibility for a specific vehicle line program, which is his or hers and no-one else's. So the human variable is removed. Second, this one person checks the vehicle on a daily basis, so there is not a long interval between 'measurements'; and third, there are usually identical vehicles nearby to compare against. Using these methods of calibration the NVH engineer/technician can be successful in identifying noise and vibration problems within the vehicle by human hand feeling measurements.

In order to identify the sources of the noise and vibration problems, frequency analysis is necessary. Humans are equipped with a frequency analyser. The combination of the human ear and brain is actually a pretty good spectrum analyser and is extremely sensitive. Human hearing has a sensitive bandwidth of about 40 Hz or less for people with a good musical ear. The human ear is sensitive to air vibrations from about 20 Hz to 20,000 Hz. This is also the frequency range of most annoying vibrations of mechanical equipment. 30 Hz is barely audible for most people but it can certainly be felt with the pressure sensors in the fingertips. A metal object, such as a coin, can be held between the fingertips while probing for vibrations. Evidently there is some amplification from the metal object pressed against a vibrating surface. Hand sensing works for low-frequency vibrations (less than 100 Hz). For higher frequencies, you should listen to the tones, as the majority of mechanical vibrations are within the frequency range of the human ear to detect.

Using the human ear for frequency analysis of vehicle noise is more effective when the ear can be coupled directly to the vehicle. This means

using a stethoscope, a wooden stick or a screwdriver. Any vibration analysis should always be done first by listening and feeling to give the analyst a subjective frame of reference.

If no objectionable vibration or noise can be felt or heard, you can be confident that there is probably no vibration problem in terms of mechanical design and wear. Humans are well calibrated in this respect to mechanical damage criteria, but this judgement depends on no interfering background noise.

Human judgement of vibration severity can be quantified by the level of acceleration:

- 0.001–0.01 g is the threshold of perception.
- 0.1 g is considered unpleasant.
- 0.5 g is considered intolerable by most subjects.

Vibration problems and human sensitivity to them are well correlated in the absence of background vibration. If vibration is uncomfortable to people, then it is probably causing serious damage to the vehicle or machine. As vibration analysts we are looking for vibration. We want to amplify and take a closer look at it. This is the whole purpose of vibration instruments – to amplify vibration and display it in a way that we can better understand.

Instruments increase the signal-to-noise ratio. Suppose you wanted to examine the vibration from one of three running pumps. You could approach the pump of interest and place your hand on it, or couple your ear to its housing with a wooden stick. This will increase the signal of interest above the background noise. Alternatively, you could turn everything else off and run only the pump of interest – this will reduce the background noise and again increase the signal-to-noise ratio. By placing a transducer directly on a vehicle structure of interest, we couple directly to that source of vibration and separate out the background vibrations. The signal-to-noise ratio is increased.

To perform any significant vibration analysis the important parameters to measure are frequency and amplitude. Hands and ears can make both of these measurements subjectively. The rotational speed is the most fundamental number required to do any vibration analysis. A stroboscope with accurate speed readout, or a tachometer, should be the first instrument to be purchased. The stroboscope is, however, not reliable for 'stopping' motion below 300 rpm.

The methods described above using the hands, ears and a stroboscope/ tachometer (and perhaps a stethoscope, wooden stick or screwdriver) are not yet outdated. Keep these tools available in your toolbox and use them frequently to correlate with your instruments as a check.

3.3   Basic vibration measurements

Ears, hand and watch/timer can be subjectively used to sense vibrations. Most of us, however, want a hard number that we can compare to. Transducers, along with a readout instrument, can provide this number.

3.3.1 Types of vibration transducer

A transducer is a device for converting the mechanical motion of vibration into an electrical signal. It is commonly called a 'pickup'. There are generally three types of vibration transducers: displacement, velocity and acceleration. The most common type of displacement transducer is the proximity probe as shown in Fig. 3.1. It operates on the eddy current principle. It sets up a high-frequency electric field in the gap between the end of the probe and the metal surface that is moving. The proximity probe includes an oscillator–demodulator and a cable.

The proximity probe senses the change in the gap and therefore measures the relative distance, or displacement, between the probe and the tip of the surface. The probe measures the gap between 10 and 90 mils. The practical maximum frequency that proximity probes can sense is about 1500 Hz. The minimum frequency is 0 Hz – it can measure static displacement.

The velocity transducer is an adaptation of a voice coil in a speaker. It consists of an internal mass (in the form of a permanent magnet) suspended
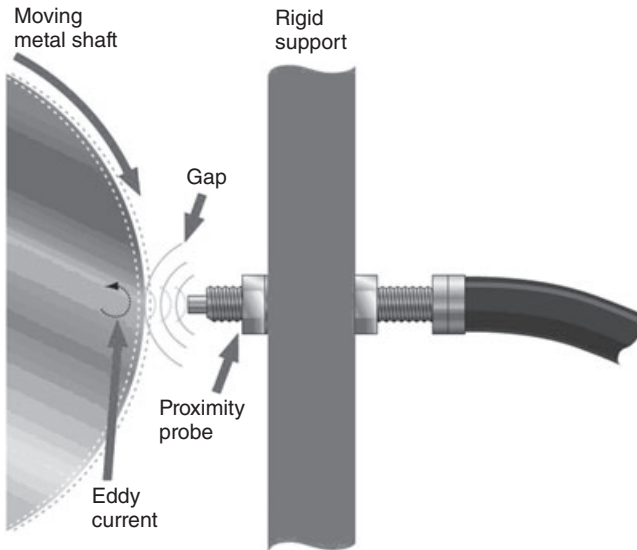
3.1 Proximity probe.
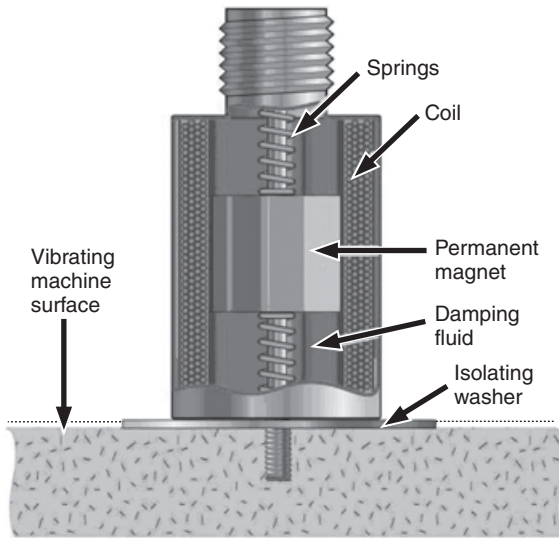
3.2 Velocity transducer.

on springs. Surrounding this mass is a damping fluid, usually oil. A coil of wire is attached to the outer case as shown in Fig. 3.2.

In operation, the case is held against and moves with the vibrating object, while the internal mass remains stationary suspended on the springs. The relative motion between the permanent magnet and the coil generates a voltage that is proportional to the velocity of the motion, hence it is a voltage pickup.

Velocity transducers provide a direct measure of vibration velocity (SI unit – m s^{-1}, although mm s^{-1} is commonly used). The main points regarding velocity transducers are:

- They are often moving coil devices – an electric coil is suspended around a permanent magnet that is kept static.
- They are designed to have a low natural frequency (typically a few Hz), chosen to be much lower than the anticipated excitation frequency range (typically 10–1000 Hz).
- They are usually large and fairly heavy, but robust.
- They cannot be used on lightweight structures due to the mass loading effect – they change the vibration characteristics of the component whose vibration they are trying to measure.
- Multi-axis transducers are available. These usually stand on their own base – often an adjustable tripod is provided to cater for use on sloping or uneven surfaces.
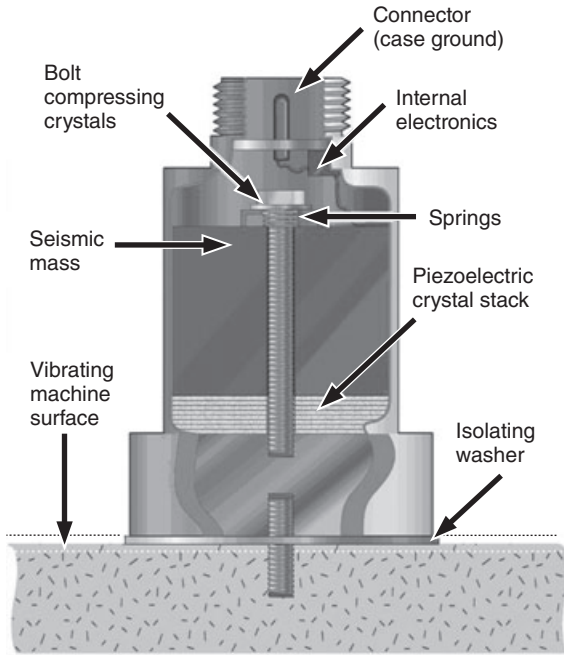
3.3 Piezoelectric accelerometer.

• They are simple – low-cost voltage amplification is commonly used. Battery usage is relatively efficient and the transducer and its signal conditioning are often housed in a single rugged package.

The most common acceleration transducer is the piezoelectric accelerometer (Fig. 3.3). It consists of a quartz crystal (or barium titanate – a manufactured quartz) with a mass bolted on top. In operation, the accelerometer case is held against the vibrating object and the mass wants to stay stationary in space. With the mass stationary and the case moving with the vibration, the crystal stack gets compressed and relaxed. The piezoelectric crystals generate a charge output that is going positive and negative as the crystals are alternately compressed tighter and relaxed about the preload. The charge output is proportional to force, therefore acceleration according to Newton's Second Law; hence the name accelerometer.

The accelerometer is self-generating, but the signal output has such high impedance that it is not usable by most analysis equipment. The output impedance of the accelerometer must be matched to the impedance of the readout instrument for accepting the signal from the accelerometer. The output signal from the accelerometer must be converted to a low-impedance signal by special electronics. This electronic circuitry can be outside or inside the accelerometer. There are two types of accelerometer that you can explore with the following links:

- Voltage type
- Charge type.

The charge-mode accelerometer must have a charge amplifier nearby. This provides the proper impedance matching. The short piece of cable between the accelerometer and the charge amplifier is critical. It must be a low-noise cable and its length cannot be changed. The accelerometer, cable and charge amplifier must be calibrated as a unit and not changed.

The voltage-mode accelerometer has the impedance-matching electronics built inside. It needs no charge amplifier, and the cable length is not critical. All it needs is a low-cost power supply to power the internal electronics. Some readout instrument manufacturers provide built-in power supplies to power their electronics.

It is important to use charge amplifiers with charge accelerometers and power supplies with voltage accelerometers. When the electronics are built into the accelerometer, this simplifies their use. The voltage accelerometers are labelled ICP (integrating circuit piezoelectric) by some manufacturers. Accelerometers provide a direct measure of vibration acceleration (SI unit – m s^{-2}, or g, where 1 g = 9.81 m s^{-2}).

The main points regarding accelerometers are:

- They are designed to have a natural frequency well above the anticipated excitation frequency range.
- They offer a wide frequency range from 0.2 Hz to 10 kHz for better than 5% linearity.
- They are usually small in size and light in weight (can be less than 1 gram).
- For high-temperature applications the charge mode system should be used.
- The accelerometer is sensitive to vibration frequencies much higher than the proximity probe or the velocity pickup.
- A wide dynamic range (160 dB) and good linearity means they can detect very small vibrations and not be damaged by very large vibrations in a wide frequency range.
- The accelerometer is the only transducer that can accurately detect pressure wave vibrations in high frequencies.

Other transducers that are used today for vibration measurement are the strain gauge, piezo-resistive accelerometer, piezo-film/piezo-patch, etc.

3.3.2   Selection of appropriate accelerometers

The first decision to make is whether to use a high-impedance or a low-impedance accelerometer. The advantages of the high-impedance accelerometer are:

- Wide dynamic range
- Ability to use long connector cables between the accelerometer and the charge amplifier.

The main disadvantage of high-impedance accelerometers is their cost.
   The advantages of low-impedance accelerometers are:

- Low cost
- Simpler signal conditioning.

   The main disadvantages of low-impedance accelerometers are:

- Size and mass (once the electronics are built in)
- Intolerance to being overloaded
- A rather high limit on the lowest frequency at which they may be used.

   Subsequent choice of accelerometer will depend on the following factors.

- *Sensitivity*: The larger transducers have greater sensitivity. Higher-amplitude motions require a low-sensitivity accelerometer. A low-level motion should be measured by a high-sensitivity accelerometer.
- *Frequency range*: The upper limit is determined by the natural frequency of the piezoelectric elements. Generally, smaller transducers may be used to measure higher frequency vibrations. The lower-frequency limit is determined by the time constant of the signal conditioning. Only the charge-amplified accelerometer is capable of measuring down to (almost) 0 Hz.
- *Physical size*: As a general rule the mass of the accelerometer should be less than 10% of the mass of the vibrating structure to which it will be attached. Otherwise the additional mass of the attached accelerometer will alter the vibration characteristics of the structure. This is often termed the mass loading effect.
  - Larger accelerometers have lower natural frequencies and are more sensitive but cannot be used for measuring high-frequency vibration or on lightweight panels due to the mass loading imposed by them.
  - Smaller accelerometers have higher natural frequencies and will not mass load lighter panels.
- *Mounting accessories*: The preferred method of mounting the accelerometer for high-frequency measurements is with a screw-threaded stud. However, various hard epoxy or cyanoacrylate adhesives are also available as alternatives. Other mounting methods include magnetic mounts, beeswax, plasticine and double-sided adhesive tape for lower frequencies (below 2 kHz). All of these, although convenient, will restrict the upper frequency limit of the measurement. Some accelerometers are made with their cable terminations on top of the casing to facilitate stud mounting. The mass of the mounting adds to the mass loading effect.

- *Cables*: Low-impedance accelerometers with built-in amplification can be used directly even with long lengths of coaxial cable before the frequency response is affected. High-impedance transducers require special low-noise/high-insulation-resistance cables known as microdot cables, which are of limited length and also fragile. The cables impose limitations on:
  - Temperature exposure
  - Linearity
  - Transverse sensitivity
  - Damping
  - Strain sensitivity.

3.3.3   Charge amplifiers

A good-quality charge amplifier (such as the Brüel & Kjær Type 2626 shown in Fig. 3.4) will have the following features:

3.4 A typical charge-type amplifier.

- A charge input, with a microdot cable termination on the front or rear panel
- A facility for the user to enter the transducer sensitivity to three significant figures (commonly as pC per m/s^2)
- A variable amplifier to allow input signals of amplitude between 0.1 mV per m/s^2 and 1 V per m/s^2
- An indicator that warns the user when the amplifier is being overloaded
- A low-frequency limit to suppress low-frequency noise (particularly if signal integration is to be used)
- Integration circuits to allow the direct measurement of velocity or displacement
- A low-pass filter to remove unwanted signal components prior to amplification
- Battery and external supply via a mains transformer.

Modern intelligent data acquisition and analysis systems (such as Brüel & Kjær Pulse) integrate charge amplifier or voltage power supply units into the data recording instrumentation in which a transducer database can be established and maintained by a Brüel & Kjær default transducer database or other key-in transducer data selection and a factory calibration chart and details of transducer sensitivity can be downloaded.

3.3.4　Calibration of accelerometers

For a good-quality charge amplifier the factory calibration chart and sensitivity data can be used along with charge amplifier gain to calculate a calibration factor (V/m s^{-2}).

In order to get confidence on the measured data, calibration must be conducted before measurements are made. A calibrator exciter can be used to calibrate the entire signal chain from the accelerometer to the display. By comparing a known exciter vibration (B&K 4294) level of 10 m s^{-2} rms (±3%) at 159 Hz with the voltage measured by the transducer which is mounted on the top part of the exciter, the calibration factor is determined (V/m s^{-2}).

With high-impedance accelerometers and good-quality charge amplification, the calibration factor is independent of the (reasonable) length of the microdot lead. Therefore, subsequent to initial calibration, a replacement microdot lead (perhaps of longer length) does not need recalibration of the transducer chain.

For the intelligent data acquisition and analysis systems (such as B&K Pulse), a transducer can be directly connected to the front end without any charge amplifier or power supply in between.

3.3.5 Excitation

To produce a defined vibration, an electromagnetic vibration exciter (also called a shaker) is used. This converts an electrical signal into a mechanical movement, being controlled to maintain a specific vibration level or force.

In principle, the electromagnetic vibration exciter operates like a loudspeaker, where the movement is produced by a current passing through a coil in a magnetic field. The force used to accelerate the moving element is proportional to the drive current and the magnetic flux. Therefore, by controlling the current the vibration level of the exciter can be controlled. A basic setup for excitation consists of an exciter, a power amplifier, an exciter control, an accelerometer (or force transducer), and a conditioning amplifier, as shown in Fig. 3.5. The exciter is selected primarily according to the force or acceleration required, but other parameters may be important such as its ability to take up side loads, the transverse vibration and the distortion of the excitation waveform.

The exciter is isolated from its base by springs, in most cases, giving sufficient protection from environmental vibration when bolted directly on the floor. However, to reduce the vibration transmitted to the building by exciters used for high-load applications, the exciter must be mounted on resilient material or a seismic block. Instead of using an exciter, a broadband excitation can be produced by an impact hammer integrally mounted with a force transducer. The impact method is fast: the impulse contains energy at all frequencies and will therefore excite all modes simultaneously as shown in Fig. 3.6. The setup time is minimal and equipment requirements are small. However, the signal-to-noise ratio is poor for large, fragile structures. With a high degree of damping it would be impossible to get sufficiently large
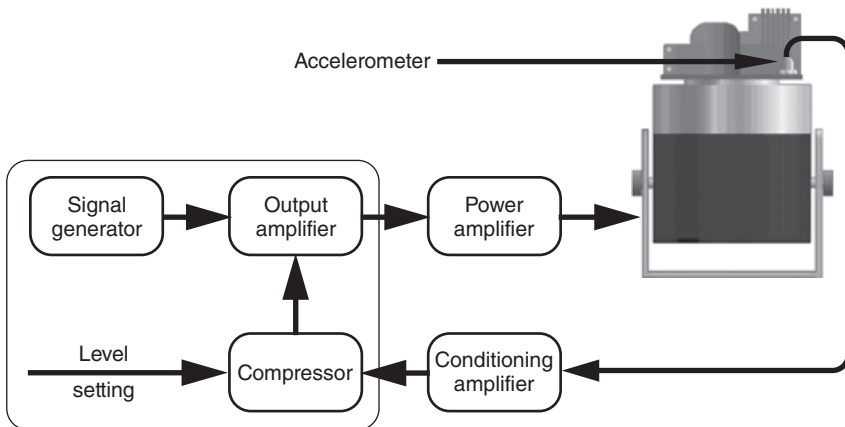
3.5 Basic exciter instrumentation.
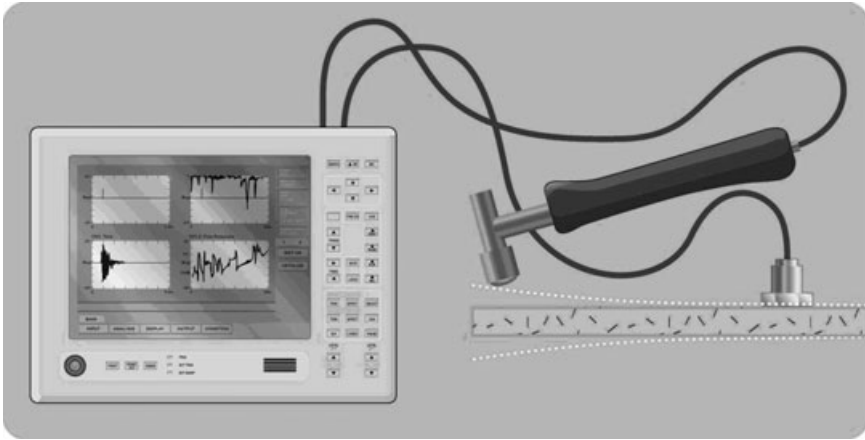
3.6 Impact hammer exciter.
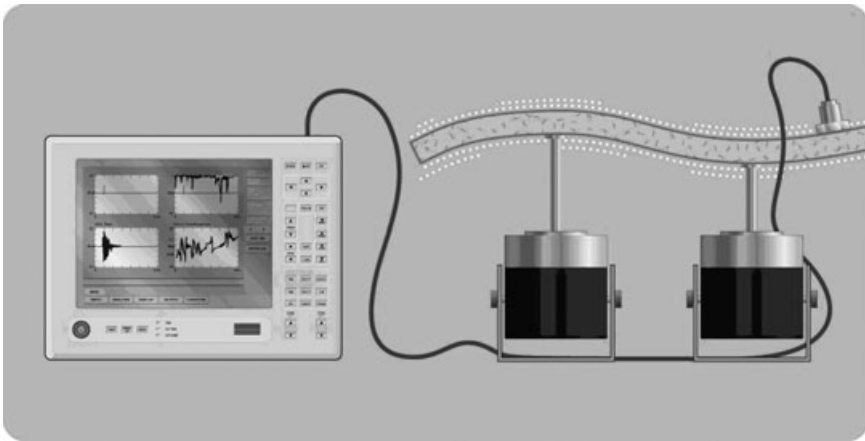
3.7 Electromagnetic exciter.

response without damaging the test object. The vibration exciter has a high
signal-to-noise ratio, easy control with the choice of excitation waveforms,
and the possibility of exciting several points at the same time as shown in
Fig. 3.7.

The vibration excitation signals that can be applied include:

- Sinusoidal signals
- Swept frequency sinusoidal signals
- Random excitation signals
- Swept narrowband random excitation
- Impact hammer excitation.

Sine signals, which are swept or at a single frequency, are by far the most
commonly used excitation inputs. The control is relatively simple. A large

amount of reference materials exist for this type of excitation signals. The response signals are easy to measure. Sine signals are described by their frequency and amplitude. In vibration testing the amplitude is normally expressed in terms of peak values (displacement as peak-to-peak) with frequency ranges from 2 Hz to 10 kHz (10,000 Hz).

In the swept sine test the signal to the exciter is continuously swept back and forth over the appropriate frequency range. The main control parameter is the acceleration level, but below a specified frequency (the cross-over point) a constant displacement is chosen.

A random signal used in vibration testing has a continuous spectrum, with amplitudes varying according to a Gaussian distribution at a frequency. Within the specified frequency range, limited amplitudes should be present. In vibration testing it is generally demanded that a random signal should contain peak values that are three times the rms value.

The force produced by an exciter is limited mainly by the heating effect of the current, i.e. the rms value, whereas the power amplifier rating is influenced by the peak values. To give the same force the amplifier must therefore be larger when used with random excitation than when used with sine excitation. The random capacity of an exciter is specified as the maximum acceleration spectral density at different loads of a spectrum, shaped according to the International Standard ISO 5344. Another advantage of random testing is that the time of endurance is shorter because it acts on all resonances at the same time. The random test is described by its power spectral density or acceleration spectral density, ASD ($(m/s^2)^2/Hz$).

One approach combining a simple feedback control with many of the advantages of the random spectrum is the swept narrowband technique. In a standard sine control the single-frequency signal is substituted by a random band. With a fairly narrow bandwidth the control is satisfactory even for low damped resonances. A vibration exciter is an excellent means of providing the force input to the structure to be analysed by applying either a sine or a broadband signal. In the latter case the input as well as the output are measured and analysed using fast Fourier technique (FFT). The frequency response is calculated from the input spectrum, measured with a force transducer, and the output spectrum, normally measured with an accelerometer.

3.4   Vibration response investigation and vibration testing

In order to check the test object's function and examine the influence of resonances throughout the frequency range, a vibration response will have to be investigated. For all types of tests the resonances are found by sine sweep or random broadband noise (white noise). The resonance
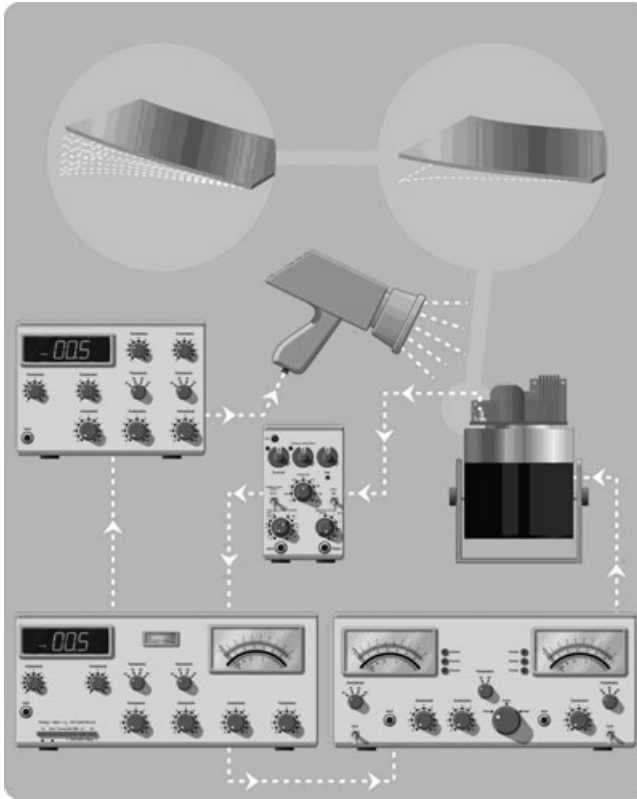
3.8 Vibration response investigation using triggered stroboscopic lamp.

frequencies are measured and the behaviour of the structure is studied in detail by manually controlling the frequency.

The behaviour of the structure is most easily studied by stroboscopic lamp, triggered by the exciter control to follow the excitation frequency as shown in Fig. 3.8. Better, however, is to use a trigger signal which differs slightly from the excitation frequency, giving a slow-motion-like image. This slow-motion frequency (normally 3–5 Hz) can be set on the stroboscope to follow the excitation. A further study of the behaviour can be made by manually delaying the trigger signal to move the image through one or more cycles, or by using dual flashes to give a picture of the extreme positions of the resonating part.

If the expected environment is dominated by one or a few discrete frequencies, the endurance conditioning is most realistically performed only at these frequencies, often as fatigue testing to breakdown of the material. Specimens showing some clearly evident resonances can successfully be tested at these resonances. Due to changes in the structure during the test,
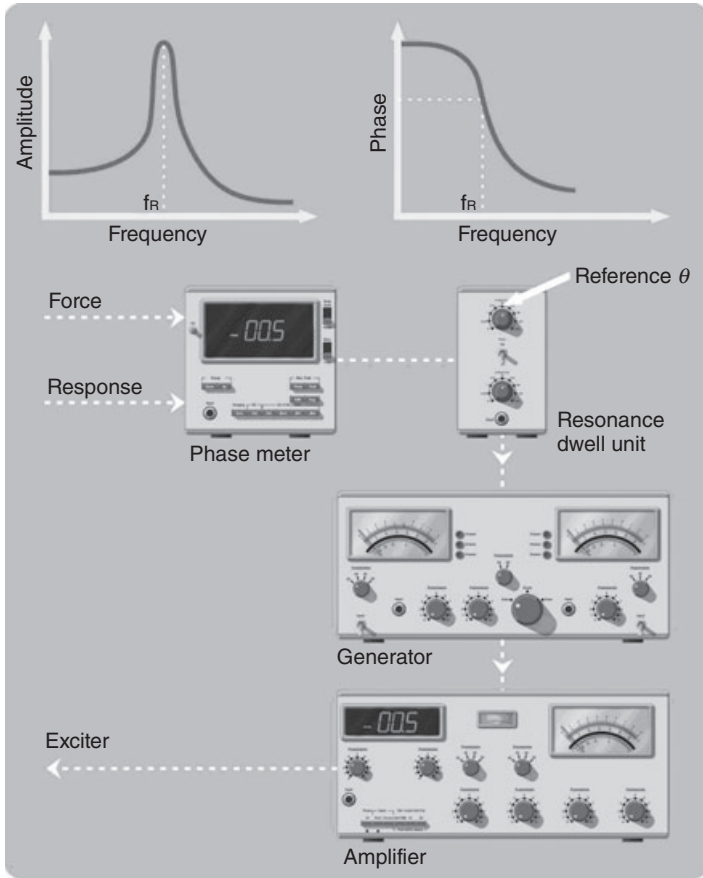
3.9 Vibration response investigation.

the resonance frequency is likely to move around. In order to change the excitation frequency automatically, a resonance dwell unit is used. The resonance dwell unit works on the fact that at resonance the phase angle between excitation and the response signals will change drastically as shown in Fig. 3.9. It is therefore possible to consider the phase angle as characteristic of the resonance, and it is measured and used as a reference in a servo loop controlling the excitation frequency.

Due to the demand of high-speed vehicle operation and the use of light structures in modern vehicles, static measurements of stress/strain properties are not sufficient to validate vehicle design. Dynamic measurements are necessary and vibration testing has therefore found widespread use.

In the environmental laboratory, vibration testing is performed as part of a company's quality assurance. The test object is exposed to a specified vibration level according to a procedure specified in national and interna-

tional standards. To find the dynamic properties of a structure the response to a vibration force is of interest rather than the actual vibration level. This concept is found, for instance, in the determination of the ability to transmit or damp vibrations, or in the description of vibration modes of a structure at resonances. In the calibration of transducers a comparison is made between the transducer to be calibrated and a reference transducer at a prescribed vibration level.

3.5   Environmental testing

An environmental test is performed to determine the ability of vehicle parts to withstand specified severities of vibration, shock, temperature, humidity, etc. The requirements may be set by the user or the supplier with reference to some national, international or OEM standards. These standards describe the test procedures but do not state the individual test levels. During the endurance conditioning the specimen is subjected to vibration, which in severity (frequency range, level and time) should ensure that it can survive in the real environment. Depending on these, the conditioning is performed by sine sweeping, by sine testing at resonance frequencies or other prede-termined frequencies, or by random vibration.

3.6   Mounting the test object

As the test is performed to simulate the environmental influence, the object must be mounted on the exciter table by its normal means of attachment. In most cases this requires a special fixture that allows the specimen to be vibrated along specified axes.

The mounting method must be described in the test, and so must the point on the specimen to which the control accelerometer is attached. Also, it must be specified whether the object should be operating during the test. In cases where the test object cannot be mounted directly on the exciter table, a fixture sometimes of a rather complex nature is required for fasten-ing the object. The fixture must be stiff enough to transmit the generated force or motion uniformly to the test object, thus not introducing any reso-nances. It is important to check the design by measuring the vibration levels on the surface of the fixtures by means of accelerometers. All resonances must lie outside the test frequency range. The natural frequency of a con-struction will be almost the same whether the material is steel or alumin-ium; as the total weight of the test object and fixture is a restricting factor in the application of an exciter, aluminium will normally be the best choice. To obtain a high resonance it will always be necessary to over-dimension the structure, so no considerations normally have to be taken concerning the mechanical strength. If resonances cannot be avoided, the damping can
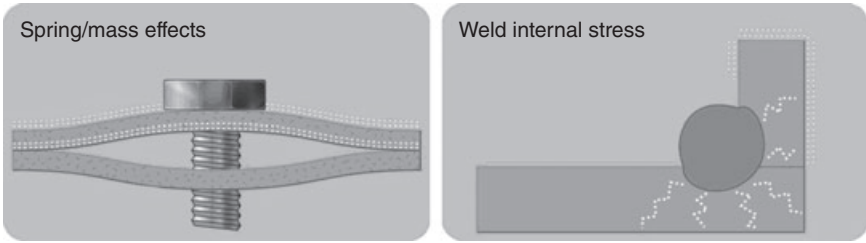
3.10 Introduction of vibration test fixtures.
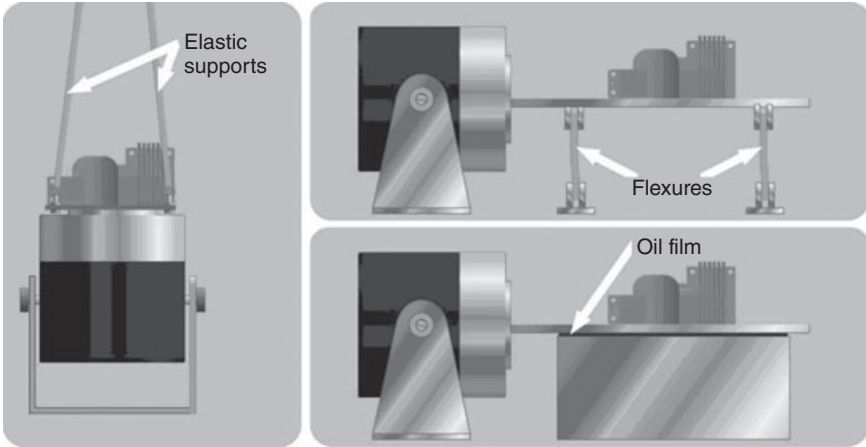
3.11 Static compensation of the exciter table.

be increased by laminating with a damping material such as rubber or by filling cavities with foamed plastic.

For minimizing the weight of the fixture it can be constructed of relatively thin plates, supported by braces. The plates are of simple geometric shapes with responses that are easy to calculate. Much care should be taken in assembling: bolts can introduce spring/mass effects; welding can introduce internal stresses as shown in Fig. 3.10.

Heavy test objects will cause a static deflection of the exciter table, depending on the stiffness of the fixtures. This decreases the available displacement for the dynamic performance and it may be necessary to compensate for this static loading when operating with large dynamic displacements, i.e. especially in the low-frequency range. A simple means of compensating is to apply a DC current to the moving coil, but as this current contributes to the heating of the exciter and power amplifier, the dynamic performance will be reduced. The compensation is therefore more often made by external mechanical supports, e.g. springs suspended from the ceiling or a horizontal slip table supported by fixtures, or sliding on an oil film, as shown in Fig. 3.11.

3.7   Measuring the complex elastic modulus

The modulus of elasticity, E, of a structure is defined as the ratio of the stress, σ, to strain, ε. A static determination of the modulus does not take into account the internal damping, which results in the stress and strain not being in phase under vibration conditions. Where the internal damping is to be considered, e.g. in plastics, asphalt, concrete and other viscoelastic materials, the complex modulus of elasticity must be measured. The modulus is the vector sum of the elastic and the damping modulus. It is related to the loss factor, η, of the material, η being the tangent of the phase angle, φ, between the elastic and complex modulus.

A dynamic test will therefore consist of an excitation with a constant force and measurement of corresponding values of displacement and phase. Figure 3.12 shows one method with a simplified formula for a cantileval beam excited by a sinusoidal force at its free endpoint. The formula includes correction factors for compensating the effects of mounting probe, transducers, etc. The standard method for the measurement of complex modulus is the resonance technique illustrated in Fig. 3.13. The measured system is modelled as a weighted spring with dashpot:

$$f(t) = m\ddot{x}(t) + c\dot{x}(t) + kx(t) \tag{3.1}$$

The frequency response function, FRF, is given by:
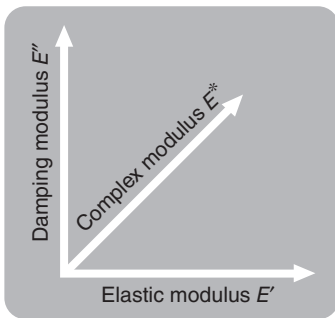
$$E^* = E' + iE''$$

$$\begin{cases} E^* = E'(1 + i\eta) \\ \eta = \tan\phi \end{cases}$$
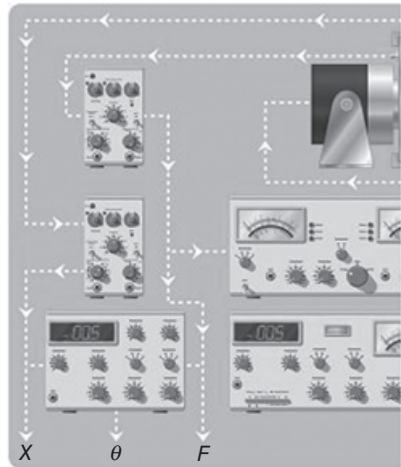
At low frequencies:

$$E^* = k\frac{F}{x}\cos\phi, \quad \eta = \tan\phi$$

3.12 The complex modulus of elasticity.
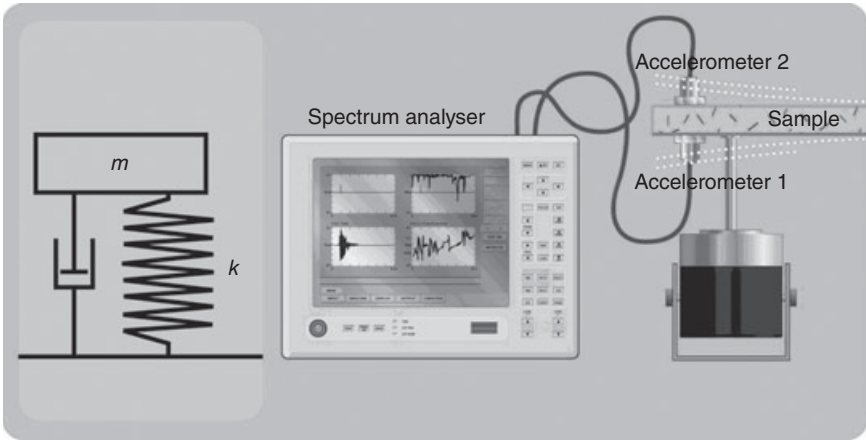
3.13 Diagram of complex modulus measurement principle.

$$H(\omega) = \frac{X(\omega)}{F(\omega)} = \frac{1}{k - m\omega^2 + ic\omega} \qquad (3.2)$$

At the resonance frequency ω_0 the real part of Equation 3.2 becomes zero and the amplitude is determined by the damping mechanism c. The resonance formula is given by:

$$\omega_0 = 2\pi f_0 = \sqrt{\frac{k}{m}} \qquad (3.3)$$

and so, from a measurement of the resonance frequency and knowledge of the mass, the bending stiffness k is obtained:

$$k = 4\pi^2 f_0^2 m \qquad (3.4)$$

The modulus E' is obtained from the sample stiffness, k, as:

$$E' = \frac{k \times d}{A} \qquad (3.5)$$

where d is the sample thickness and A is the sample surface area.

The damping is characterized by the loss factor, η, which is given by the 3 dB bandwidth divided by the resonance frequency:

$$\eta = \frac{\Delta f}{f_0} \qquad (3.6)$$

This method works well for stiff and moderately stiff materials. The complex modulus is given by:

$$E^* = E'(1 + i\eta) \qquad (3.7)$$

3.8   Quoting vibration levels

3.8.1 Single-value index methods

The following single-value index measures of vibration can be displayed as time histories or runs:

- Vibration acceleration (m/s^2 or g, where 1 g = 9.81 m/s^2)
- Vibration velocity (m/s, or commonly mm/s)
- Vibration displacement (m, or commonly mm).

In each case any frequency weighting applied to the data must be declared. Acceleration, velocity and displacement levels (dB) are often used. Care must be taken when quoting vibration levels to:

- distinguish between vibration acceleration, velocity and displacement levels (dB);
- distinguish between peak amplitude, peak-to-peak amplitude (twice peak amplitude – not commonly used), and rms value; and
- quote all units carefully (use SI units where possible, although the use of mm/s for velocity is common).

3.8.2 Acceleration levels (dB)

The usual practice is to measure in rms. Levels are measured in m/s^2 and the level reference is usually taken as one micrometre per second squared rms ($a_{ref} = 10^{-6}$ m s^{-2}):

$$L_a = 20 \log_{10}\left(\frac{a}{a_{ref}}\right) dB \qquad (3.8)$$

3.8.3 Velocity levels (dB)

The usual practice is to measure in rms. Levels are measured in mm/s and the level reference is usually taken as one nanometre per second rms (= 10^{-9} m s^{-1} or 10^{-6} mm s^{-1}):

$$L_v = 20 \log_{10}\left(\frac{v}{v_{ref}}\right) \quad dB \qquad (3.9)$$

Note that the time integral:

- of acceleration yields the velocity–time history;
- of velocity yields the displacement–time history.

Numerical methods may be used to post-process time histories and yield the time integral. Alternatively, electrical circuits are available to perform

the integration at the point of recording the signal. These often become unreliable for double integration of acceleration, limiting signal-to-noise ratio and suffering from DC drift.

For simple harmonic motion analysed in the frequency domain, the integral may be obtained by dividing the amplitude of a spectral component by iω where i is the square root of -1 and $\omega = 2\pi f$ (f is the frequency in Hz).

3.8.4 Assessing vibration levels – human response to vibration

Two ISO standards deal with the human response to vibration. They are:

- ISO 2631 Part 1 (1985) – Mechanical Vibration and Shock: Evaluation of Human Exposure to Whole Body Vibration – Part 1: General Requirements.
- ISO 5349 (1986) – Mechanical Vibration Guidelines for the Measurement of Human Exposure to Hand-transmitted Vibration.

The ISO 2631 Part 1 (General Requirements) offered user-friendly guidance on the effects of vibration acceleration amplitude (1–80 Hz). Three boundaries are given for various exposure periods between 1 minute and 24 hours. These are:

- Reduced comfort boundary
- Fatigue-decreased proficiency boundary
- Exposure limits (for health and safety).

The boundaries often still form part of contemporary performance specifications for vehicles. Part 1 of ISO 2631 was revised in 1997. The guidance on safety, performance and comfort boundaries was removed. In its place, there are the following:

- The main body of the text describes a means of measuring a weighted rms acceleration according to:

$$a_\mathrm{w} = \left[\frac{1}{T} \int_0^T a_\mathrm{w}^2(t)\,\mathrm{d}t \right]^{1/2} \tag{3.10}$$

    where $a_\mathrm{w}(t)$ is the weighted acceleration time history in m/s^2, and T is the duration in seconds.
- Different weightings are given for health, comfort perception, the different axes and the position of the human subject (standing, seated and recumbent).

A weighting W_k is used for assessing the effects of vibration on the comfort and perception of a standing person with vertical acceleration in

the head-to-toe axis. Weighting W_k suggests that a standing person is most susceptible to vertical vibration in the frequency range 4–8 Hz. Annexes to the main text give limited guidance on the health, comfort and perception and motion sickness effects of vibration. This guidance is in terms of weighted rms acceleration. The vibration dose value (VDV) is introduced but it is not used in any guidance on the likely effects of vibration. VDV is defined as:

$$\text{VDV} = \left[\int_0^T [a_w(t)]^4 \, dt \right]^{1/4} \tag{3.11}$$

where the units of VDV are m s$^{-1.75}$.

If the VDV is repeated n times during a period, the total VDV period is then:

$$\text{VDV}_{\text{total}} = \sum_{i=1}^n \left(\frac{t_{\text{total}}}{t_i} \right)^{1/4} \times \text{VDV}_i \tag{3.12}$$

Approximate indications of the likely reaction to various magnitudes of frequency-weighted rms acceleration are listed according to ISO 2631 Part 1 as:

- <0.315 m s^{-2} not comfortable
- 0.315–0.63 m s^{-2} a little uncomfortable
- 0.5–1.0 m s^{-2} fairly uncomfortable
- 0.8–1.6 m s^{-2} uncomfortable
- 1.25–2.5 m s^{-2} very uncomfortable
- >2.0 m s^{-2} extremely uncomfortable

Responses of human behaviour to vibration in different frequency ranges are shown in Fig. 3.14 which shows that motion sickness occurs between 0.1 and 0.63 Hz. Major body resonances occur between 1 and 80 Hz. Vibration disturbs speech at 2–20 Hz, and vibration causes potential annoyance between 0.1 and about 400 Hz. Vibration may cause spinal damage at about 5 to 20 Hz. Figure 3.15 shows that the acceleration of the human body can be written as a weighted acceleration sum:

$$\text{WAS} = \sqrt{(1.4a_x)^2 + (1.4a_y)^2 + a_z^2} \tag{3.13}$$

If a human is exposed to three different vibration environments, the dose is defined as:

$$\text{Dose} = \sum_{i=1}^n \frac{t_i}{\tau_i} \times 100\% \tag{3.14}$$

where t_i is elapsed time and τ_i is allowed time.

EFFECTS ON HUMANS	FREQUENCY - Hz						
	0.1	1	10	100	10^3	10^4	10^5

AIRBORNE NOISE
- Tonal auditory sensation
- Pulsatile auditory sensation
- Non-auditory sensation
- Potential annoyance
- Subjective after-failure
- Speech Interference
- Loss of work efficiency
- Hearing loss
- Middle ear damage*

STRUCTURE-BORNE VIBRATION
- Vibratory sensation
- Disequilibrium
- Motion sickness
- Major body resonances
- Disturbance of speech
- Blurring of vision
- Interference of tasks
- Potential annoyance
- Subjective after-failure
- Spinal damage+
- Gastrointestinal disorders+
- Reynaud's phenomenon etc.^

INFRASONICS	AUDIBLE RANGE	ULTRASONICS

KEY

──────	Frequency range
··········	Uncertain range of occurrence
*	Pressure Injury (barotrauma) at extreme intensities
+	Chronic disorders associated clinically with repeated occupational exposure to whole body vibration
^	Chronic diseases affecting the blood vessels, bones and joints of the hand and forearm associated with cumulative occupational exposure to vibration from hand-held power tools.

3.14 Response of human hearing behaviour to vibration.
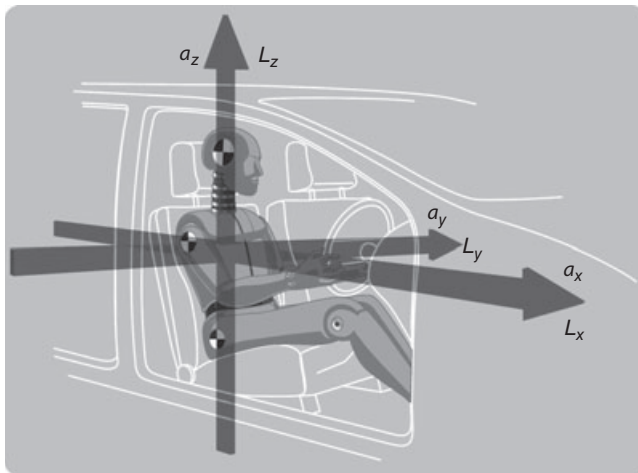
3.15 Acceleration of the human body.

$$\tau_i = \left(\frac{a_0}{a_{eq_i}}\right)^2 \times t_0 \tag{3.15}$$

where $a_0 = 2.8 \times \sqrt{3} = 4.85 \text{ m/s}^2$ ($a_{0x} = a_{0y} = 2 \text{ m/s}^2$, $a_{0z} = 2.8 \text{ m/s}^2$) and energy equivalent acceleration is defined as:

$$a_{eq}(T) = \sqrt{\frac{1}{T} \int_0^T a_{rms}^2 \, dt} \tag{3.16}$$

where T is sampling time and a_{rms} is root mean square acceleration.

If $t_0 = 10$ minutes, the four-hour energy equivalent acceleration is:

$$a_{eq}(4) = a_{eq}(t_0)\sqrt{\frac{T}{4}} \tag{3.17}$$

where $T = \sum_{i=1}^{n} t_i$ is total exposed time in one event.

The exposure from several events can be calculated from:

$$a_{eq}(T) = \sqrt{\frac{\sum_{i=1}^{n} a_i^2 T_i}{\sum_{i=1}^{n} T_i}} \tag{3.18}$$

where T_i is the total elapsed time in the ith event and a_i is the equivalent acceleration in the ith event.

Vibration exposure is defined by:

- Vibration + time = vibration exposure
- Vibration exposure + time = tissue damage.

Vibration exposure is measured according to national and international standards. In order to avoid breaking occupational health legislation, at lowest cost, you will need to conduct the following monitoring and risk assessment:

- Is there a problem?
- How big is the problem?
- What causes the problem?
- How do we reduce the problem?
- How do we prevent the problem?
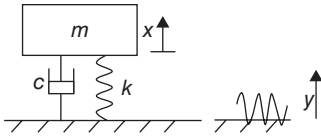
3.16 A single-degree-of-freedom system being excited at the base support.

3.9   Vibration isolation

Consider the situation when the support to a single-degree-of-freedom system has a motion applied to it as shown in Fig. 3.16. In Fig. 3.16 both the support and the mass are moving rather than just the mass, and so it is the relative displacement between the mass and the support that is important. The equation of motion for free vibration becomes:

$$m\ddot{x} = -k(x - y) - c(\dot{x} - \dot{y}) \tag{3.19}$$

Declaring that:

$$z = x - y, \quad \dot{z} = \dot{x} - \dot{y}, \quad \ddot{z} = \ddot{x} - \ddot{y} \tag{3.20}$$

then:

$$m(\ddot{z} + \ddot{y}) = -kz - c\dot{z} \tag{3.21}$$

$$m\ddot{z} + kz + c\dot{z} = -m\ddot{y} \tag{3.22}$$

and, if it is a harmonic excitation:

$$y = Ye^{i\omega t} \tag{3.23}$$

Then:

$$\dot{y} = i\omega Ye^{i\omega t} \tag{3.24}$$

$$\ddot{y} = -\omega^2 Ye^{i\omega t} \tag{3.25}$$

and so:

$$m\omega^2 Ye^{i\omega t} = m\ddot{z} + kz + c\dot{z} \tag{3.26}$$

Now we can assume that:

$$z = Ze^{(i\omega t - i\phi)} \tag{3.27}$$

Then:

$$\dot{z} = i\omega Ze^{(i\omega t - i\phi)} \tag{3.28}$$

$$\ddot{z} = -\omega^2 Ze^{(i\omega t - i\phi)} \tag{3.29}$$

$$m\omega^2 Ye^{i\omega t} = -m\omega^2 Ze^{(i\omega t - i\phi)} + kZe^{(i\omega t - i\phi)} + ci\omega Ze^{(i\omega t - i\phi)}$$

$$Ze^{(i\omega t - i\phi)} = \frac{m\omega^2 Y e^{i\omega t}}{k - m\omega^2 + ci\omega}$$

$$Ze^{-i\phi} = \frac{m\omega^2 Y}{k - m\omega^2 + ci\omega} \tag{3.30}$$

Now:

$$
\begin{aligned}
x = y + z &= \left(Y + Ze^{-i\phi}\right)e^{i\omega t} \\
&= \left(Y + \frac{m\omega^2 Y}{k - m\omega^2 + ci\omega}\right)e^{i\omega t} \\
&= \frac{k + i\omega c}{k - m\omega^2 + ci\omega} Y e^{i\omega t}
\end{aligned}
\tag{3.31}
$$

Now:

$$x = Xe^{i\omega t - \phi i} \tag{3.32}$$

$$Xe^{i\omega t - \phi i} = \frac{k + i\omega c}{k - m\omega^2 + ci\omega} Y e^{i\omega t} \tag{3.33}$$

$$\frac{Xe^{-\phi i}}{Y} = \frac{k + i\omega c}{k - m\omega^2 + ci\omega} = \frac{k(k - m\omega^2) + \omega^2 c^2 - imc\omega^3}{(k - m\omega^2)^2 + c^2\omega^2} \tag{3.34}$$

$$\left|\frac{X}{Y}\right| = \sqrt{\frac{k^2 + (c\omega)^2}{\left[(k - m\omega^2)^2 + (c\omega)^2\right]}} \tag{3.35}$$

Dividing the numerator and denominator by k^2:

$$\left|\frac{X}{Y}\right| = \sqrt{\frac{1 + \left(\dfrac{c\omega}{k}\right)^2}{\left[\left(1 - \dfrac{m\omega^2}{k}\right)^2 + \left(\dfrac{c\omega}{k}\right)^2\right]}} \tag{3.36}$$

where

$$\frac{m}{k} = \left(\frac{1}{\omega_n}\right)^2 \tag{3.37}$$

and

$$\frac{c}{k} = 2\xi \frac{1}{\omega_n} \tag{3.38}$$

Then Equation 3.36 becomes:

$$\left|\frac{X}{Y}\right| = \sqrt{\frac{1+\left(\dfrac{2\xi\omega}{\omega_n}\right)^2}{\left[\left(1-\dfrac{\omega^2}{\omega_n^2}\right)^2+\left(\dfrac{2\xi\omega}{\omega_n}\right)^2\right]}} \tag{3.39}$$

From Equation 3.34:

$$\tan(-\phi) = \frac{-mc\omega^3}{k(k-m\omega^2)+c^2\omega^2} \tag{3.40}$$

$$\phi = \tan^{-1}\frac{\left(+\dfrac{2\xi\omega^3}{\omega_n^3}\right)}{\left(1-\dfrac{\omega^2}{\omega_n^2}\right)+\left(\dfrac{2\xi\omega}{\omega_n}\right)^2} \tag{3.41}$$

Equations 3.40 and 3.41 have been used to generate Fig. 3.17.
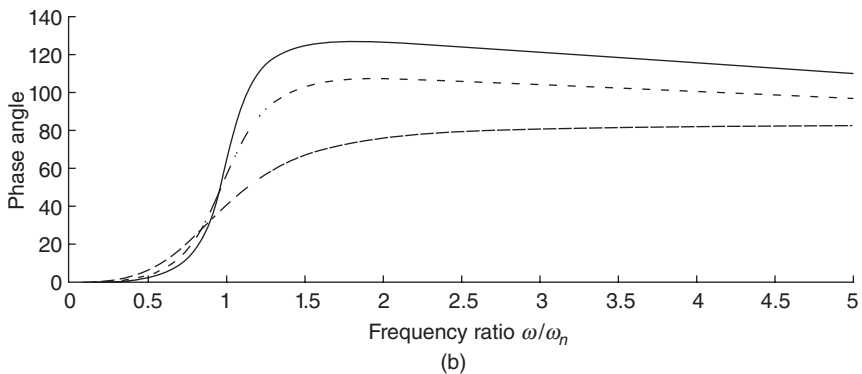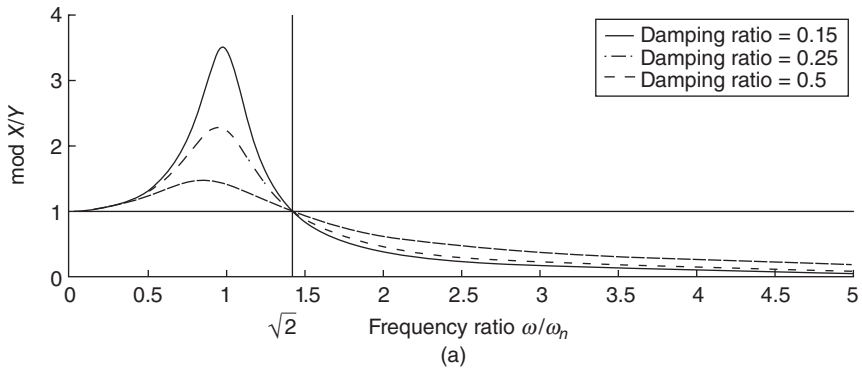
3.17 The response of a single-degree-of-freedom system when forced at its support.

In many systems of the type shown in Fig. 3.17 we are interested in transmitting as little vibration as possible to the base. This problem can become critical when the excitation is harmonic. Clearly the force transmitted to the base is through springs and dampers. The transmitted force can be written as:

$$F_{tr} = m\ddot{x} = -m\omega^2 X e^{-i\phi} e^{i\omega t} \tag{3.42}$$

$$F_{tr} = kY e^{i\omega t} \frac{k + ic\omega}{k - m\omega^2 + ic\omega} \left[-\left(\frac{\omega}{\omega_n}\right)^2 \right] \tag{3.43}$$

Assume $F_0 = kY e^{i\omega t}$ is the amplitude of the actual excitation force.

$$F_{tr} = -F_0 \left(\frac{\omega}{\omega_n}\right)^2 \frac{1 + 2\xi i\left(\frac{\omega}{\omega_n}\right)}{1 - \left(\frac{\omega}{\omega_n}\right)^2 + 2\xi i\left(\frac{\omega}{\omega_n}\right)} \tag{3.44}$$

$$TR = \left|\frac{F_{tr}}{F_0}\right| = \left| \frac{-1 - 2\xi i\left(\frac{\omega}{\omega_n}\right)}{1 - \left(\frac{\omega}{\omega_n}\right)^2 + 2\xi i\left(\frac{\omega}{\omega_n}\right)} \right| \left(\frac{\omega}{\omega_n}\right)^2 \tag{3.45}$$

$$TR = \sqrt{\frac{1 + \left(2\xi \frac{\omega}{\omega_n}\right)^2}{\left(1 - \left(\frac{\omega}{\omega_n}\right)^2\right)^2 + \left(2\xi \frac{\omega}{\omega_n}\right)^2}} \left(\frac{\omega}{\omega_n}\right)^2 \tag{3.46}$$

When damping is negligible:

$$TR = \frac{1}{\left|1 - \left(\frac{\omega}{\omega_n}\right)^2\right|} \left(\frac{\omega}{\omega_n}\right)^2 = \frac{\omega^2 \left(\frac{\Delta X_0}{g}\right)}{1 - \omega^2 \left(\frac{\Delta X_0}{g}\right)} \tag{3.47}$$

From Equation 3.36:

$$\left|\frac{X}{Y}\right| = \frac{1}{\left|1 - \left(\frac{\omega}{\omega_n}\right)^2\right|} = \frac{1}{1 - \omega^2 \dfrac{\Delta X_0}{g}} \tag{3.48}$$

ΔX_0 is the static deflection of the mass on the spring stiffness k. To reduce transmissibility at a given frequency the stiffness may be increased. This

will reduce the static deflection of the mass, and therefore reduce the transmissibility.

3.10   The vibration absorber

By tuning the two-degrees-of-freedom system in Fig. 3.18 to the frequency of the exciting force, the system acts as a vibration absorber, and in the ideal case reduces the motion of the main mass m_1 to zero.

The equation of motion for the system shown in Fig. 3.18 can be written in matrix form as:

$$m_2\ddot{x}_2 + k_2(x_2 - x_1) = 0 \tag{3.49}$$

$$m_1\ddot{x}_1 + k_1x_1 + k_2(x_1 - x_2) = F_0\sin\omega t \tag{3.50}$$

$$\begin{bmatrix} m_1 & 0 \\ 0 & m_2 \end{bmatrix}\begin{Bmatrix} \ddot{x}_1 \\ \ddot{x}_2 \end{Bmatrix} + \begin{bmatrix} k_1 + k_2 & -k_2 \\ -k_2 & k_2 \end{bmatrix}\begin{Bmatrix} x_1 \\ x_2 \end{Bmatrix} = \begin{Bmatrix} F_0\sin\omega t \\ 0 \end{Bmatrix} \tag{3.51}$$

Consider excitation force in the complex domain:

$$F = F_0e^{i\omega t} \tag{3.52}$$

$$x_1 = X_1e^{i\omega t}, \quad x_2 = X_2e^{i\omega t}$$

$$\begin{bmatrix} k_1 + k_2 - m_1\omega^2 & -k_2 \\ -k_2 & k_2 - m_2\omega^2 \end{bmatrix}\begin{Bmatrix} X_1 \\ X_2 \end{Bmatrix} = \begin{Bmatrix} F_0 \\ 0 \end{Bmatrix} \tag{3.53}$$

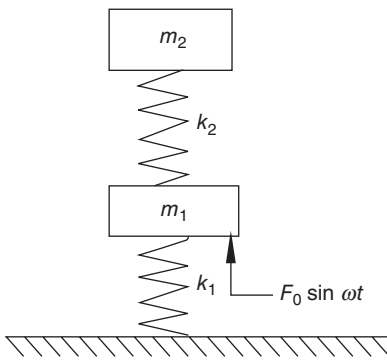$$\begin{Bmatrix} X_1 \\ X_2 \end{Bmatrix} = \begin{bmatrix} k_1 + k_2 - m_1\omega^2 & -k_2 \\ -k_2 & k_2 - m_2\omega^2 \end{bmatrix}^{-1}\begin{Bmatrix} F_0 \\ 0 \end{Bmatrix} \tag{3.54}$$

3.18 The vibration absorber.

The determinant of the left-hand matrix of Equation 3.53 can be written as:

$$\text{Det}[K] = (k_1 + k_2 - m\omega^2)(k_2 - m_2\omega^2) - k_2^2 \tag{3.55}$$

Two natural frequencies of the system can be calculated from:

$$\text{Det}[K] = (k_1 + k_2 - m\omega^2)(k_2 - m_2\omega^2) - k_2^2 = 0 \tag{3.56}$$

$$\omega_{12}^2 = \frac{\omega_{11}^2\left(1 + \dfrac{k_2}{k_1}\right) + \omega_{22}^2 \pm \sqrt{\left[\omega_{11}^2\left(1 + \dfrac{k_2}{k_1}\right) + \omega_{22}^2\right] - 4\omega_{11}^2\omega_{22}^2}}{2} \tag{3.57}$$

$$\omega_1^2 < \omega_{22}^2 < \omega_2^2 \tag{3.58}$$

where $\omega_{11}^2 = k_1/m_1$ and $\omega_{22}^2 = k_2/m_2$.

$$X_1 = \frac{(k_2 - m_2\omega^2)F_0}{(k_1 + k_2 - m_1\omega^2)(k_2 - m_2\omega^2) - k_2^2} \tag{3.59}$$

$$X_2 = \frac{k_2 F_0}{(k_1 + k_2 - m_1\omega^2)(k_2 - m_2\omega^2) - k_2^2} \tag{3.60}$$

Dividing the numerator and the denominator of Equation 3.59 by $k_1 k_2$ gives:

$$X_1 = \frac{\left(\dfrac{1}{k_1} - \dfrac{m_2\omega^2}{k_1 k_2}\right)F_0}{\left(\dfrac{1}{k_2} + \dfrac{1}{k_1} - \dfrac{m_1\omega^2}{k_1 k_2}\right)\left(\dfrac{1}{k_2} - \dfrac{m_2\omega^2}{k_1 k_2}\right) - \dfrac{k_2}{k_1}} \tag{3.61}$$

$$X_1 = \frac{\dfrac{1}{k_1}\left(1 - \dfrac{\omega^2}{\omega_{22}^2}\right)F_0}{\left(1 + \dfrac{k_2}{k_1} - \dfrac{\omega^2}{\omega_{11}^2}\right)\left(1 - \dfrac{\omega^2}{\omega_{22}^2}\right) - \dfrac{k_2}{k_1}} \tag{3.62}$$

$$X_2 = \frac{\dfrac{F_0}{k_1}}{\left(1 + \dfrac{k_2}{k_1} - \dfrac{\omega^2}{\omega_{11}^2}\right)\left(1 - \dfrac{\omega^2}{\omega_{22}^2}\right) - \dfrac{k_2}{k_1}} \tag{3.63}$$

In Equation 3.55, if $\omega = \omega_{22} = \sqrt{k_2/m_2}$, the amplitude $X_1 = 0$ but the absorber mass has a displacement equal to

$$X_2 = \frac{-F_0}{k_2} \tag{3.64}$$

k_2 and m_2 depend on the maximum allowable X_2. Note that although the vibration absorber is effective at $\omega = \omega_{22}$ there are two natural frequencies

of the system on either side of ω_{22} and these have the effect of increasing X_1 at those frequencies. These increases can be controlled to some extent with the addition of damping, but this will decrease the effectiveness of the absorber at ω_{22}.

3.11 Case studies

Two case studies are given to illustrate how the principles and methods are applied to solve engineering problems.

3.11.1 Case study 1

A V8 engine was tested on an engine dynamometer. Torsion vibration of the crankshaft system at the main pulley was measured over the speed range for three load cases. Figure 3.19 shows the engine dynamometer setup. The fourth-order peak-to-peak amplitudes (degrees) are plotted in Fig. 3.20 for the three load cases. Three situations were investigated:

- No harmonic balancer (dotted line)
- Current production balancer (grey solid line)
- New development harmonic balancer. (black solid line)

The fourth-order in the eight-cylinder 4-stroke engine is the main combustion order and contributes most to the torsional vibration.

There are two resonance peaks at 4100 rpm and 4700 rpm in the fourth-order curve (dotted line). The two resonant frequencies are given by:

3.19 Engine dynamometer setup.
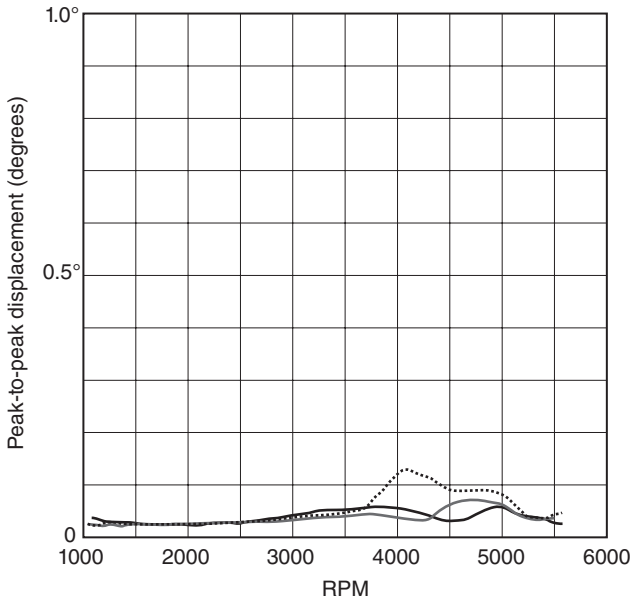
3.20 Torsional angle amplitude (degrees) plot for case study 1.

$$f_1 = 4100 \times \frac{1}{60} \times 4 = 273 \text{ Hz} \tag{3.65}$$

$$f_2 = 4700 \times \frac{1}{60} \times 4 = 313 \text{ Hz} \tag{3.66}$$

In order to select the best harmonic balancer, candidate parts were supplied to measure natural frequencies. The natural frequencies of torsional and lateral modes were measured using the impact frequency response technique. The torsional dampers (harmonic balancers) were clamped onto the back plate at the crankshaft end through butts and a bracket. An accelerometer was attached to the external ring of the damper. A hose clamp was mounted on the outside cylindrical surface of the damper's ring in order to provide a place for impact, as shown in Fig. 3.21. The masses of both the accelerometer and the clamp are negligible. Both torsional and lateral modes of vibration were identified by the tests in Figs 3.21 and 3.22. The measured natural frequencies are shown in Table 3.1. Which part ID is the best choice for the engine torsional damper?

3.11.2 Case study 2: rotational unbalanced masses

In order to illustrate a system subjected to harmonic excitation we consider Fig. 3.23. Two eccentric masses ($m/2$) rotate in opposite directions with
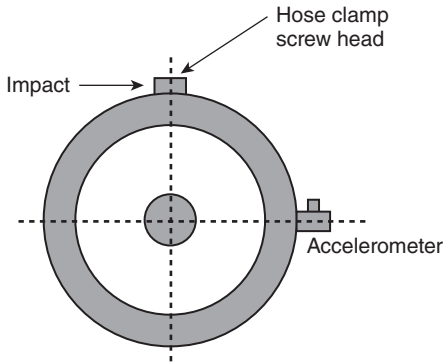
3.21 Torsional mode test setup.
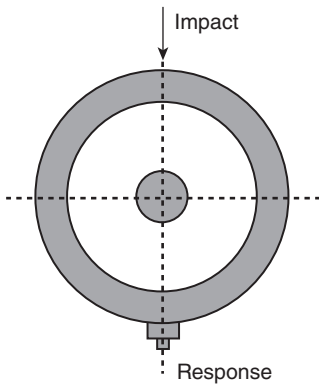
3.22 Lateral mode test setup.

Table 3.1 Natural frequencies of torsional and lateral modes of engine harmonic balancer

Part ID	Frequency of torsional mode (Hz)	Frequency of lateral mode (Hz)
1	328	392
2	320	376
3	344	400
4	324	376
5	356	360
6	352	400
7	208	320
8	276	320
9	336	352
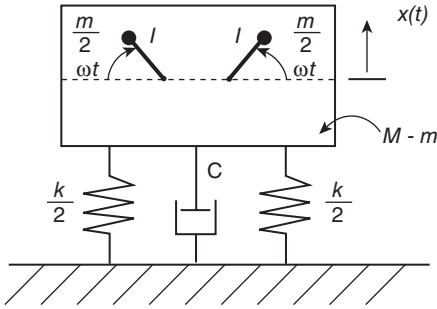
3.23 System subjected to harmonic excitation.

constant angular velocity ω. The reason for having two equal masses rotating in opposite directions is that the horizontal components of excitation of the two masses cancel each other out. On the other hand, the vertical components of excitation add. The vertical displacement of the two eccentric masses is $x + l\sin\omega t$, where x is measured from the equilibrium position. In view of this, it is not difficult to show that the differential equation of the system is:

$$(M - m)\frac{d^2x}{dt^2} + m\frac{d^2}{dt^2}(x + l\sin\omega t) + c\frac{dx}{dt} + kx = 0 \tag{3.67}$$

which can be rewritten in the form:

$$M\ddot{x}(t) + c\dot{x}(t) + kx(t) = ml\omega^2\sin\omega t = \text{Im}(ml\omega^2 e^{i\omega t}) \tag{3.68}$$

where Im denotes the imaginary part of the expression within the parentheses.

In a complex domain where $x(t) = Xe^{i\omega t - i\phi}$,

$$-M\omega^2 Xe^{i\omega t - i\phi} + ci\omega Xe^{i\omega t - i\phi} + kXe^{i\omega t - i\phi} = ml\omega^2 e^{i\omega t}$$

$$[k - M\omega^2 + ci\omega]Xe^{-i\phi} = ml\omega^2$$

$$Xe^{-i\phi} = \frac{ml\omega^2}{k - M\omega^2 + ci\omega} \tag{3.69}$$

If

$$|H(\omega)| = \frac{1}{\left\{\left[1 - \left(\frac{\omega}{\omega_n}\right)^2\right]^2 + \left[2\xi\frac{\omega}{\omega_n}\right]^2\right\}^{1/2}} \tag{3.70}$$

$$\frac{M|X|}{ml} = \left(\frac{\omega}{\omega_n}\right)^2 |H(\omega)| \tag{3.71}$$
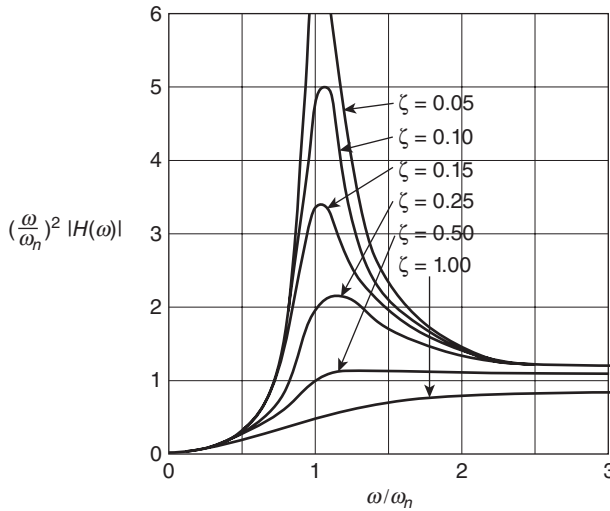
3.24 Transmissibility plot for case study 2. ζ is damping ratio as defined in Equation 3.38 where $\xi = \dfrac{c}{2\sqrt{km}}$.

When $\omega \to 0$ $(\omega/\omega_n)^2|H(\omega)| \to 0$, whereas for $\omega \to \infty$ $(\omega/\omega_n)^2|H(\omega)| \to 1$ (see Fig. 3.24).

It is seen that a small eccentric radius and a large mass ratio of machine versus unbalanced mass reduce vibration amplitude. The vibration amplitude tends to be a constant at high frequencies. The constant is determined by the mass ratio and the eccentric radius of the unbalanced mass.

3.12   Bibliography

Happian-Smith, J. (2002), *An Introduction to Modern Vehicle Design*, SAE International, Butterworth-Heinemann.

Harrison, M. (2004), *Vehicle Refinement – Controlling Noise and Vibration in Road Vehicles*, SAE International, Elsevier Butterworth-Heinemann.

Wang, X. (2005), *Introduction to Motor Vehicle Design*, RMIT Publisher.

4

Vehicle noise measurement and analysis

X. WANG, RMIT University, Australia

Abstract: In order to develop new vehicle products with well-refined noise performance, vehicle noise measurements and analysis have to be conducted to validate designs and acoustic refinement. This chapter introduces the physics of sound, sound evaluation methods, vehicle noise fundamentals, human response characteristics to vehicle noise, psychoacoustics and conventional vehicle noise measurement instrumentation, test and analysis methods.

Key words: wavelength, frequency, amplitude, sound speed, free-field, diffuse field, condenser microphone, sound pressure level, airborne sound, structure-borne sound, time and frequency weightings, decibel scale, environment noise, calibration, octave band frequency analysis, order tracking analysis, waterfall contour spectrum, artificial head technology, psychoacoustics.

4.1 Introduction

Noise results directly from inferior vehicle design giving rise to large structural vibrations or poor cabin insulation. In order to eliminate noise, the source, transfer path and receiver have to be investigated by noise measurement and analysis, customer feelings about noise have to be studied, and the root causes of the noise need to be identified. Troubleshooting solutions should be production friendly. The best solutions involve reduction at source and good design in the early stages of the vehicle development process so as to avoid program timing delays and extra tooling costs.

In order to identify the root causes of vehicle noise, develop new refinements in design and validate the solutions, vehicle noise measurements and analysis have to be conducted. For this purpose, the physics of sound, sound evaluation methods and vehicle noise fundamentals need to be understood, human response characteristics to vehicle noise and psychoacoustics need to be studied, and conventional vehicle noise measurement instrumentation, test and analysis methods have to be illustrated.

4.2 Sound fundamentals

Sound is from air in vibration. Excessive amplitude (or volume) is damaging to the ears. The vehicle cabin spaces need to be especially quiet. This is the

Wavelength in metres
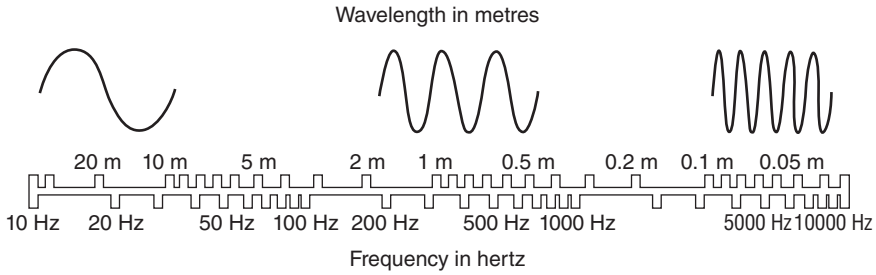
4.1 Wavelength of sound (courtesy of Brüel & Kjær Sound & Vibration A/S, from *Measuring Sound*, 1988, p. 5).

field of vehicle interior acoustics. The significant factors in acoustics for vehicle interiors are reduction of reverberation time and background noise.

The Occupational Safety and Health Administration (OSHA, see http://www.osha.gov/) has placed limits on the maximum noise exposure a worker can receive in an eight-hour workday to avoid permanent hearing loss. The scientific field concerned with hearing damage is called audiology.

Unwanted sound is defined as noise, and noise is perceived as a form of environmental pollution. People are becoming more sensitive to noise pollution. Acoustic emissions and ultrasonics are two other related fields. Acoustic emissions are the sounds generated by materials when they are strained. For example, in vehicles the sounds are usually very minute and are actually the shock waves generated when vehicle body panel boundaries deform along their slip planes. Ultrasonics is the generation of vibration above the human range of hearing (i.e. greater than 20 kHz). These vibrations are used for testing materials, welding plastics, imaging of interior soft body tissues and detecting vehicle cabin noise leakage.

Sound is a periodic process (at least at the practical level within the medium). The conversion relationship between sound wavelength and frequency is shown in Fig. 4.1. Sound involves energy transport. The propagation of sound may involve the transfer of energy but it does not cause the transport of matter. Particles of the medium are excited into oscillation about their usual position of rest but they do not get swept along with the passing sound. By way of illustration, the molecules of air within a speaker's mouth do not need to find their way to the listener's ear for the listener to hear the speaker's voice.

In order that the particles may oscillate about their usual position of rest, the medium through which sound propagates must have both elasticity and inertia so that a restoring force is imposed on a displaced particle and a returning particle overshoots its original position of rest and oscillates to and fro.

Table 4.1 Altitude and the speed of sound

Altitude (m)	Temperature (K)	Pressure		Air density	Speed (m/s)
		(standard atmospheres)		(kg/m³)	
0	288	1		1.225	340.3
1000	281	0.887		1.1117	336.4
10000	223	0.262		0.4135	299.5

Table 4.2 Media type and the speed of sound

Medium	Speed (m/s)
Water (fresh)	1481
Water (salt)	1500
Concrete	3100
Steel	6100

The speed of sound in air, c, increases with temperature. For example:

- At 600 K, $c = 487$ m/s (in air).
- At 900 K, $c = 590$ m/s (in air).

The speed of sound in air also decreases with altitude. Table 4.1 shows how the speed of sound varies with altitude, temperature and pressure.

Sound travels faster in a high density medium than in a low density medium. Most of the sound we hear is a pressure variation in air. It is a longitudinal compressive wave. A moving, vibrating, oscillating or pulsing object sets the air into motion. Sound is a form of mechanical energy radiating out from the source. In air, sound travels at 344 m/s at standard temperature and pressure. The intensity drops off with distance in accordance with the inverse square law; i.e. the sound intensity in air decreases by a factor of 4 when the distance doubles. This assumes free-field conditions with no barriers or other interfering objects.

In steel, sound travels at 5060 m/s, and the inverse square law does not apply. Sound travels about 15 times faster in steel than in air. In metal objects, the sound energy does not radiate equally in all directions but is confined within the metal boundaries to some extent. The sound energy is directed along the metal path. In air, sound attenuation is quite rapid. In solids or liquids, attenuation is much lower. Table 4.2 shows the media type and the speed of sound.

Sound has a source, a path and a receiver. All three of these must be positively identified to solve noise problems. The source and receiver are usually straightforward. Identifying the path presents the most difficulties, and this is also where most noise control measures are applied. Sound has a very low level of energy intensity. Sound energy is typically measured in picowatts (pW, i.e. 10^{-12} watts). This extremely small amount of energy is offset by the extreme sensitivity of the human ear. This extraordinary sensitivity is comparable to that of modern electronic sensors.

Sound propagation in air can be compared to ripples on a pond. If an obstacle is placed in the direct or free field in the sound path, part of the sound will be reflected, part absorbed and the remainder transmitted through the object or obstacle.

4.2.1 Sound evaluation

Sound evaluation can be made with electronic instruments or human biological instruments. In some respects the biological instruments are superior, especially when identifying the character of the sound.

Objectionable sound can be a pure tone or a multiplicity of tones. The human ear and brain constitute a good spectrum analyser that can identify pure tones subjectively. When the sound is composed of a multiplicity of tones, possibly harmonics, the human instruments outclass the electronic spectrum analyser. The spectrum analyser can measure the amplitude and frequency of each component part but has difficulty assigning a fingerprint to it – this is what human instruments do best.

The entire symphony of sound has a characteristic that the human ear and mind can readily identify and remember. For example, middle C from a piano, violin and trumpet all have the primary component of 256 Hz but differ in harmonic content. This is what makes them different to the human ear, and people are readily capable of distinguishing the difference. This can be used to advantage for vehicle noise evaluation. First, a change in harmonic content will be obvious to a person who regularly hears the vehicle. This is embodied in phrases like 'it sounds different' and 'something's not right'. Second, supposedly identical vehicles differ in their sound signatures and the human can immediately discern this without expensive instruments and spectrum analysis. And third, the sound of a specific component or system can be tracked in the presence of other, louder sounds to the point of origin by focusing on the character of the sound. Spectrum analysers can also do this, but not so quickly or inexpensively.

There are other indicators of noise outside the normal range of hearing. At low frequencies and high amplitudes, a pressure fluctuation can be felt, possibly even in the chest cavity. At high frequencies and high
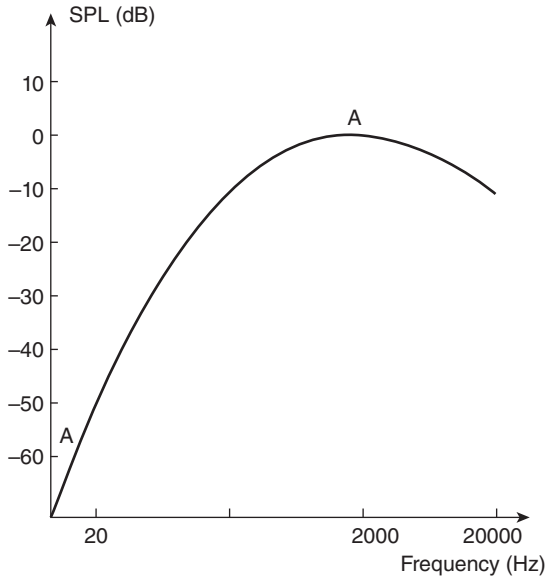
4.2 Human hearing response (copyright RMIT University (Geoff Marchiori), adapted from Brüel & Kjær Sound & Vibration A/S, *Measuring Sound*, 1984, p. 11).

amplitudes pain can be felt. Electronic measurement of sound is done with a microphone as a transducer and a readout instrument.

4.2.2 Human hearing: frequency versus sound pressure level

The human ear does not respond uniformly to sounds at all frequencies. We are deaf to low-frequency sounds (below about 20 Hz) and high-frequency sounds (above about 20,000 Hz), and are most sensitive to sounds around 2000 Hz. The responsiveness of human hearing changes with age. The typical human hearing response is illustrated in Fig. 4.2.

To compensate for this, an A weighting response of a sound-level meter adjusts the meter's response to approximate the human ear's response. The linear (LIN) weighting on the sound-level meter is no weighting at all. The raw signal from the microphone passes through the meter with the LIN characteristic unmodified. Therefore, to make amplitude measurements approximate human hearing sensitivity the A weighting characteristic is used. However, when doing investigative work using frequency analysis, it is undesirable to modify any part of the spectrum, so the LIN weighting is appropriate.
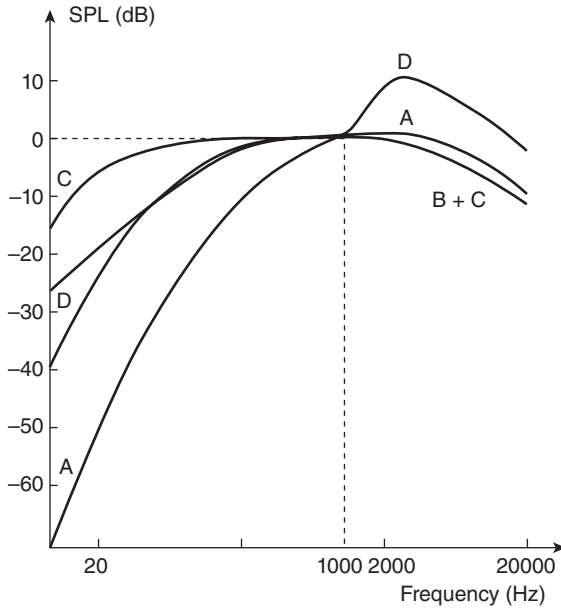
4.3 Weighting curves for sound-level meters (courtesy of Brüel & Kjær Sound & Vibration A/S, *Measuring Sound*, 1984, p. 11).

Figure 4.3 shows the A, B, C and D weighting sound pressure level (SPL) curves. As mentioned already, the A weighting network weighs the signal in a manner which approximates to the human hearing response (as shown in Fig. 4.2), i.e. the A weighting corresponds to an inverted equal loudness contour at low SPLs. The B weighting corresponds to a contour at medium SPLs, and the C weighting to an equal loudness contour at high SPLs. The D weighting has been the standard for aircraft noise measurement. The A weighting is well correlated with subjective evaluation and most widely used; B and C weightings do not correlate well with subjective tests.

Figure 4.4 shows a family of equal loudness contours, i.e the sound pressure level required at any frequency to give the same apparent loudness as a 1 kHz tone. The amplitude scale for sound work is a logarithmic scale (to base 10). It ranges from 0 dB (the threshold of hearing) to 140 dB (typical of the sound level near a jet aircraft engine). An office area typically measures around 60 dB. Three decibels is the minimum change in level that humans can perceive; a change in sound pressure level less than 3 dB will go unnoticed. Ten decibels of change is required before the sound subjectively appears to become twice as loud or quiet.

To obtain frequency information using a sound level meter, octave analysis is done with filters. An octave is a doubling of frequency. It gets its name
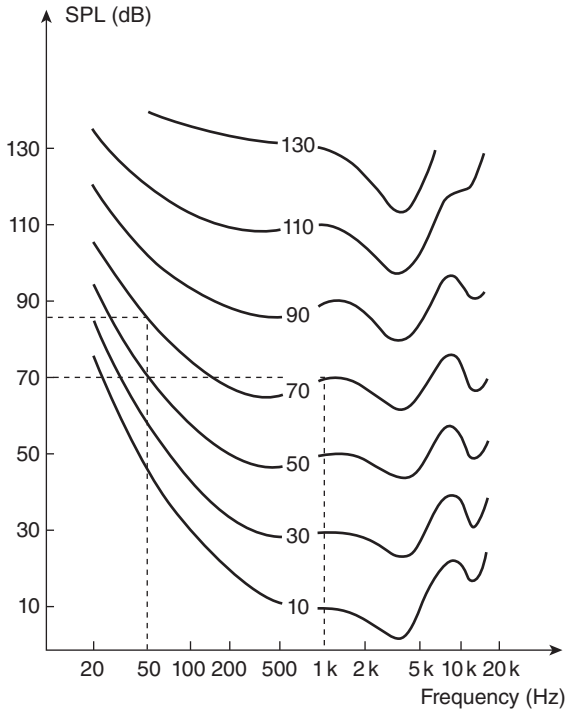
4.4 Equal loudness contours (courtesy of Brüel & Kjær Sound & Vibration A/S, *Measuring Sound*, 1984, p. 8).

from the musical scale where one octave covers eight notes of the diatonic musical scale. For example, the 1 kHz octave band filter passes the frequencies from 707 to 1414 Hz (centred on 1 kHz). Remember that filters are not perfect and the frequency limits are not sharp cut-offs – there is some slope to the sides, and some signals outside this band will sneak in. To get finer resolution of frequency analysis, 1/3-octave bands are available on some filter sets. In 1/3-octave bands the highest frequency of the pass-band is 1.26 times the lowest frequency. The same 1 kHz pass-band in a 1/3-octave filter will have frequency limits of 891 Hz to 1120 Hz. A significant amount of acoustic data is still measured and reported in octave and 1/3-octave filtered measurements, but these measurements are crude compared to those from a spectrum analyser that can perform narrowband analysis. A 400-line analyser set to a frequency span of 2000 Hz will have band-pass filters set at 5 Hz, i.e. 2000/400. The 1000-bin filter in this analyser will have lower and upper cut-off frequencies of 997.5 and 1002.5 Hz. With zooming this can get much narrower. The superiority of spectrum analysers to obtain precise frequency information should be evident.

Table 4.3 Typical sound power levels for different sources

Source	Sound power output (W)
Saturn rocket	25–40 million
Military jet engine with afterburner	100 000
Turbojet engine	1000–10 000
Propeller airliner with four engines	100–1000
75-piece orchestra	10–1000
Small aircraft engine	1–10
Piano	0.1–1
Car alarm	0.1
Hi-fi	0.01
Moving car	0.001–0.01
Fan	0.001
Person shouting	0.0001–0.001
Conversational voice	0.000 01
Whispering voice	0.000 000 001

Table 4.4 Typical sound pressure levels in different environments

Environment	Sound pressure amplitude (Pa)	Description
100 m from Saturn rocket	200	Ear pain threshold
At front of rock concert	20	Potentially damaging
Noisiest factory	2	Harmful
Next to road or railway	0.2	Noisy
Busy restaurant	0.02	
Quiet suburban street	0.002	Quiet
Recording studio	0.0002	Very quiet
	0.000 02	Threshold of hearing

4.2.3 Decibel scales

Sound levels are commonly described in terms of the sound power (W) output of noise sources and the sound pressure (Pa) amplitude at a given location. However, decibel scales (dB) are useful due to the wide range of powers and sound pressure amplitudes that can be encountered.

Table 4.3 shows that sound power outputs of everyday machines lie in the 0.001 to 1000 W range (a factor of one million times) and the human voice has a power output in the range of 0.000 000 001 to 0.001 W (also a factor of one million times).

Table 4.4 shows that everyday noise environments relate to pressure amplitudes in the range of 0.000 02 to 20 Pa (a factor of one million times). The human ear can detect sound pressure amplitudes over this whole range (beyond, in fact: from 20×10^{-6} to 60 Pa).

To simplify the situation, sound levels are usually described by using the decibel scale:

$$L = 10 \log_{10} \left[\frac{X}{X_{ref}} \right] dB \qquad (4.1)$$

where:

$$X = X_{ref} \frac{10^{L/10}}{10} \qquad (4.2)$$

The sound pressure level (L_p) is expressed as the ratio of the squared sound pressure amplitude to the threshold of hearing:

$$L_p = 10 \log_{10} \left[\frac{p^2}{p_{ref}^2} \right] = 20 \log_{10} \left[\frac{p}{p_{ref}} \right] dB \qquad (4.3)$$

where $p_{ref} = 20 \times 10^{-6}$ Pa.

According to this scale, everyday noise environments fall in the sound pressure level range of 0–120 dB. By way of comparison, the typical operating pressures associated with internal combustion engines are:

- Peak cylinder pressure $\approx$ 60 bar $\approx$ 230 dB.
- Exhaust pressure wave $\approx$ 0.8 bar $\approx$ 192 dB.
- Intake pressure wave $\approx$ 0.2 bar $\approx$ 180 dB.

The sound power level (L_w) is expressed as the ratio of the sound power to a reference power of 10^{-12} W:

$$L_w = 10 \log_{10} \left[\frac{W}{W_{ref}} \right] dB \qquad (4.4)$$

where:

$$W_{ref} = 10^{-12} \text{ W} \qquad (4.5)$$

As a result, everyday machine power outputs fall in a sound power range of 70–160 dB and the human voice produces sound power levels in the 30–70 dB range.

4.2.4 Decibel arithmetic

If the sound levels from two or more machines have been measured separately and you want to know the total sound pressure level (SPL) made by the machines when operating together, the sound levels must be added. However, decibels cannot just be added together directly (because of the logarithmic scale). Addition of decibels can be done simply using the chart in Fig. 4.5 where the sound pressures of different machines are uncorrelated to each other.
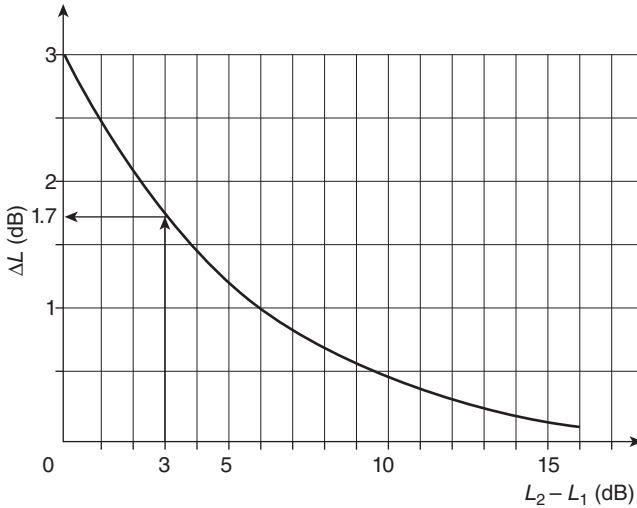
4.5 Adding sound levels (courtesy of Brüel & Kjær Sound & Vibration A/S, *Measuring Sound*, 1988, p. 30).

1. Measure the SPL of each machine separately (L_1, L_2).
2. Find the difference between these levels ($L_2 - L_1$).
3. Enter the bottom of Fig. 4.5 with this difference. Go up until you intersect the curve, then go to the vertical axis on the left.
4. Add the value indicated (ΔL) on the vertical axis to the level of the noisier machine (L_2); this gives the sum of the SPLs of the two machines (L_{1+2}).
5. If three machines are present, repeat steps 1 to 4 using the sum obtained for the first two machines and the SPL of the third machine.

Example:

1. Machine 1 has $L_1 = 82$ dB; machine 2 has $L_2 = 85$ dB.
2. Difference $L_1 - L_2 = 3$ dB.
3. Correction (from chart) $\Delta L = 1.7$ dB.
4. Total noise = 85 + 1.7 = 86.7 dB.

Mathematically, decibel addition has this structure:

$$L_{L_1+L_2} = [L_1 + L_2] = 10\log_{10}[10^{L_1/10} + 10^{L_2/10}] - 10\log_{10} X_{\text{ref}} \qquad (4.6)$$

and decibel subtraction has this structure:

$$L_{L_1-L_2} = [L_1 - L_2] = 10\log_{10}[10^{L_1/10} - 10^{L_2/10}] - 10\log_{10} X_{\text{ref}} \qquad (4.7)$$

where the sound pressures of different sources L_1 and L_2 are uncorrelated to each other.

The combination of two identical sound levels produces a sum which is 3 dB greater than the individual levels. Combining a sound level with another which is 10 dB less in magnitude, it produces a sum that is negligibly greater than the highest sound level.

4.3   Vehicle noise

Whenever vehicle power is generated, transmitted or used, a fraction of this energy is converted into sound power and radiated into the air. Generally the fraction of available vehicle power that is converted into acoustical power is very small. However, very little acoustical power is needed to make a sound source audible.

A vehicle generates two types of noise: noise that travels in air is called airborne noise, while noise that travels in vehicle structures is called structure-borne noise. There are two types of noise – broadband and narrowband, or pure tones. The broadband noise can be desirable or objectionable depending on the frequency content, amplitude and structure-borne versus airborne content. The pure tones are almost always objectionable.

Resonances, which also cause pure tones, may be of two kinds: structural or acoustical. Structural resonance is the easier of the two to identify and correct. Simply find the 'singing' part and stiffen it. An acoustical resonance is found by matching a length of ductwork with the wavelength of the objectionable tone.

4.3.1   Direct sound-generation mechanics: airborne sound

An arbitrary noise is generated by a physical mechanism and then radiated. The physical mechanism could be:

- Hot displacement of fluid mass or volume (loudspeaker, exhaust tailpipe)
- Unsteady combustion (engine, furnace, boiler)
- Unsteady fluid transport (flow noise)
- Fluctuating force on a fluid (fans, wires in a flow)
- Fluctuating shear force (shear layer noise in a jet).

When controlling the sound power output from a direct sound generation mechanism at source, the following strategies can be employed:

- Reduce the source strength by alternating the parameters within the physical process itself, such as the rate of combustion, flow rate, the force imparted to the fluid, etc.
- Reduce the physical size of the source as a means of reducing the source strength.

4.3.2 Indirect sound-generating mechanism: structure-borne sound

An arbitrary noise is generated from a fluctuating force which excites structural responses and sound radiation from the structure. The common indirect sound sources on vehicles are:

- Casing vibration
- Bearing noise
- Electric motor or generator noise
- Belt, chain or gear drives
- Internal combustion engine structural noise.

Controlling noise at the indirect sound sources is done by one or more of the following means:

- Reducing the amplitude of the force or, where a number of independent cyclic forces are present, arranging their phasing so as to obtain cancellation.
- Reducing the vibration response of the structure to a given force input.
- Improving the acoustic radiation efficiency of the structure at a given frequency by altering the critical frequency of the radiating component.

The wavelength of sound is calculated by using:

$$\lambda = \frac{344 \, \text{m/s}}{f} \, \text{m} \tag{4.8}$$

where:

λ = wavelength (m)
f = frequency (Hz)
344 m/s is the speed of sound in air (at 1 atm pressure and 300 K).

It is useful at this point to look at some numbers:

- The lowest frequency audible to the typical human subject is 20 Hz, wavelength in air 17.15 m.
- The highest frequency audible to the typical human subject is 20 kHz, wavelength in air 17.15 mm.
- The lowest amplitude audible to the typical human subject is 20×10^{-6} Pa, particle velocity in air 0.00005 mm/s.
- The highest amplitude audible to the typical human subject without experiencing ear pain is 200 Pa, particle velocity in air 481 mm/s.

4.4   Measuring microphones

Measurements provide definite quantities which describe and rate sounds. Sound measurements also permit precise, scientific analysis of annoying sounds. The measurements give us an objective means of comparing annoying sounds under different conditions.

Sound levels are measured using a microphone attached to some form of electrical signal conditioning and analysis equipment. There are many types of microphone with different operational means of converting fluctuating pressure (or pressure difference) into an electrical signal. Two basic types of microphone are condenser and electro-dynamic. The condenser microphone is favoured for vehicle noise investigations because of its frequency response. Electro-dynamic microphones start to lose sensitivity around 80 Hz and are down considerably at 50 Hz. Condenser microphones, on the other hand, remain linear below 50 Hz and some are linear even down to 20 Hz. Condenser microphones are also more sensitive than electro-dynamic types because of their use of pre-amplifiers.

The pre-amplifier converts the microphone's high output impedance to low impedance suitable for feeding into the input of accessory equipment. This impedance conversion next to the microphone serves to minimize the pickup of noise in the signal cable to the accessory equipment.

4.4.1   Condenser microphones

The operating principle of a condenser microphone is to use a diaphragm as the moving electrode of a parallel plate air capacitor. It features a tensioned metal (nickel) diaphragm supported close to a rigid metal back-plate. The microphone's output voltage signal appears on a gold-plated terminal mounted on the back-plate which is isolated from the microphone casing (or cartridge) by an insulator. The cartridge's internal cavity is exposed to atmospheric pressure by a small vent and the construction of the microphone is completed with the addition of the distinctive diaphragm protective grid.

The diaphragm and back-plate form the parallel plates of a simple air capacitor which is polarized by a charge on the back-plate. When the diaphragm vibrates in a sound field the capacitance varies and an output voltage is generated. The voltage signal replicates the sound-field pressure variations as long as the charge on the microphone back-plate is kept fixed. The sensitivity of the condenser microphone is discussed below.

Sensitivity

As might be expected, the larger the electrodes within the microphone, the greater is the voltage produced by a given deflection of the diaphragm, and the greater is the sensitivity of the microphone.

Precision condenser microphones usually come in four sizes, denoted by their external diameters:

- One inch (25.4 mm)
- Half inch (12.7 mm)
- Quarter inch (6.35 mm)
- Eighth inch (3.175 mm).

Most of them are omnidirectional, i.e. sensitive to sound arriving from all directions. The two smallest microphones have the best omni-directional characteristics at audio frequencies. They respond equally to all frequencies arriving from all directions because their physical presence in the sound field does not have a big influence on incoming sound waves. The larger (one-inch) microphones, as a direct result of their size, are not sensitive to frequencies above 5 kHz which approach from the sides and rear of the microphone. The omnidirectionality of the one-inch microphone can be improved by fitting a nose cone or the special windscreen.

The open-circuit sensitivity is usually quoted for direct comparison between microphones. This is the voltage (mV) produced per pascal of pressure at 250 Hz with 200 V polarization (except for a few microphones requiring 28 V or 0 V polarization). The open-circuit sensitivity is the sensitivity of the capsule on its own before it is electrically loaded by being attached to a pre-amplifier. The sensitivity of the microphone varies with temperature and atmospheric pressure.

Frequency response

There are three basic types of microphone:

- Free-field-response
- Pressure-response
- Random-response.

Free-field-response microphones are used for measuring sound coming mainly from one direction. Their frequency response curve is designed to compensate for the pressure build-up at the diaphragm caused by interference and diffraction effects. Measured sound-pressure levels are assumed equal to those that would exist in the sound field if the microphone were not present. This means that the physical size of the microphone is small compared with the wavelength of the impinging sound, its presence does not affect the local sound field and it measures the true fluctuating pressure. The response of the microphone in these conditions is known as the free-field response. At higher frequencies – near the resonant frequency of the microphone – the impinging sound is reflected and diffracted by the presence of the microphone and, as a result, the pressure at the diaphragm is

increased from its free-field value. The response of the microphone to this artificially higher pressure is the pressure response.

It is also possible to construct microphones that respond linearly with frequency (up to a limiting frequency) to the actual pressure at the diaphragm. These are known as pressure-response microphones. Pressure-response microphones do not compensate for the pressure build-up at the microphone diaphragm – they measure the actual sound-pressure level at the diaphragm. Uses include measuring sound pressure levels at a surface or in a closed cavity. Pressure-response microphones can be used as free-field microphones if they are oriented at right angles to the direction of sound propagation, but their effective frequency range is then reduced. When making measurements within small cavities or couplers or when the microphone diaphragm is mounted flush with a hard surface, it is the pressure response that is of interest. When making measurements in a diffuse field it is the random incidence response that is of interest and a random incidence microphone should be used.

The frequency response of any device that operates over a range of frequencies is that range of outputs that are within 3 dB of a 0 dB reference line as shown in Fig. 4.6. This −3 dB point usually occurs at between 1 and 3 Hz at low frequencies, above which the open-circuit sensitivity of a precision condenser microphone remains constant with changing frequency. However, the sensitivity does become frequency-dependent at higher frequencies. The change in sensitivity with frequency is known as the frequency response of the microphone. At higher frequencies the microphone's
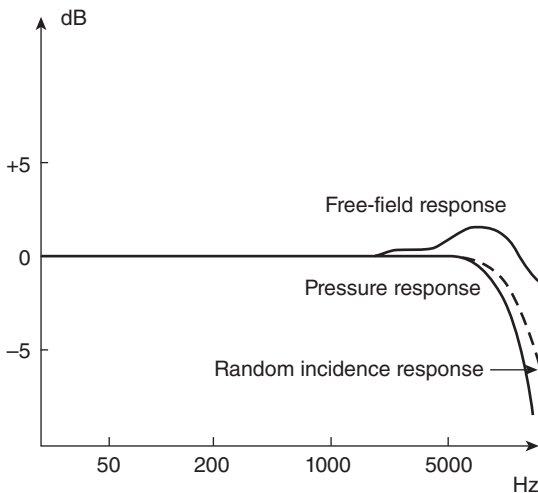
4.6 Frequency responses of free-field, pressure- and random-response microphones (courtesy of Brüel & Kjær Sound & Vibration A/S, *Measuring Sound*, 1988, p. 22).

frequency response curve tails off after the diaphragm resonance. The high frequency cut-off is the frequency at which the frequency response curve falls 2 dB below the 0 dB reference line.

Dynamic range

The lower limit of the dynamic range of the condenser microphone and pre-amplifier combination is determined by the levels of internal (electrical) noise. The upper limit is determined by distortion, i.e. the unacceptable change to the wave shape of the sound waves being sensed by the microphone. Typical dynamic ranges are:

- One-inch microphone: 12–150 dB(A)
- Half-inch microphone: 25–155 dB(A)
- Quarter-inch microphone: 40–170 dB(A)
- Eighth-inch microphone: 55–175 dB(A).

Significant levels of distortion can be expected with any size of microphone at very high sound levels (140 dB and above, i.e. 200 Pa and above).

Pre-amplifiers

Pre-amplifiers are designed to have input impedance of around 10–50 GΩ. The input capacitance is usually around 0.2 pF, which is rather small compared with the capacitance of the polarized microphone capsule (around 3–65 pF at 250 Hz, with the smallest value for eighth-inch microphones and the largest for one-inch microphones). The high input impedance produces a reasonable voltage level from the charge output of the microphone capsule. The noise floor of the pre-amplifier is dependent on the capacitance load imposed by the microphone capsule. In general, larger capsules with the highest capacitance yield the lowest noise.

Pre-amplifiers are designed to have low output impedance (around 25–100 Ω) in order to preserve high frequency response (usually flat in the range of 1–200 kHz). The capacitive output load given by the microphone cable and the input impedance of the next device in the signal chain also determine the frequency response. For this reason, microphone cables are restricted in length to a few metres. Typical pre-amplifiers have a gain of 0 dB, reflecting their role in impedance conversion rather than voltage amplification in the usual sense.

Power supplies

The stabilized polarization voltage (200 V or 28 V) is provided by the microphone power supply: a large battery-operated box (or mains via an

adaptor) used within a few metres from the pre-amplifier. Low output impedance permits the use of longer cables (usually of a BNC-connected coaxial type) between the power supply and the next device in the signal chain.

Time and frequency weightings

Sound pressure data are commonly fitted with three time weightings:

- Fast – having an exponential time constant of 125 ms corresponding approximately to the integration time of the ear
- Slow – having an exponential time constant of 1 s to allow for the average level to be estimated by the ear with greater precision
- Peak – having an exponential time constant of below 100 µs to respond as quickly as possible to the true peak level of transient sounds.

They may also be fitted with one further time weighting:

- Impulse – having a 35 ms exponential rise but a much longer decay time, which is thought to mirror the ear's response to impulsive sound.

Sound pressure data are also fitted with the following three frequency weightings:

- A-weighting approximately follows the inverted shape of the equal loudness contour passing through 40 dB at 1 kHz.
- B-weighting approximately follows the inverted shape of the equal loudness contour passing through 70 dB at 1 kHz.
- C-weighting approximately follows the inverted shape of the equal loudness contour passing through 100 dB at 1 kHz.

4.5   Measuring amplifiers

Measuring amplifiers are available that both provide the power supply and also convert the fluctuating electrical output of the pre-amplifier into either:

- an amplified voltage for tape recording or digital storage, or
- rms level (with optional time and frequency weightings) for quantifying noise levels.

4.6   Calibration

Each microphone cartridge is supplied with an individual calibration chart that includes a complete frequency response curve along with sensitivity data. In the field, the entire signal chain from microphone capsule to analyser display can be calibrated using either of the following devices:

- An acoustic calibrator – a small cylindrical device that fits over the microphone capsule and produces a reference sound pressure level at a given frequency (usually 94 dB at 1000 Hz; the level of accuracy is usually ±0.2 dB for a Type 1 calibrator)
- A piston-phone – a larger device operating at 124 dB and 250 Hz. Full piston-phone kits are supplied with a barometer to allow compensation for atmospheric pressure. The level of accuracy is ±0.09 dB under reference conditions.

It is routine to calibrate the signal chain at the start of every measurement session.

If the microphone picks up the 94 dB sound at 1000 Hz from the Type 1 calibrator and displays it as 94 dB in the end of the signal chain, it means the microphone channel passes the calibration. Otherwise the sensitivity setting will be adjusted and updated automatically to make up the difference. Many people also confirm the calibration at the end of the measurement session.

4.7   Background noise

One factor that may influence the accuracy of measurements is the level of the background noise compared to the level of sound being measured. Obviously the background noise must not 'drown out' the sound of interest. In practice this means that the level of the sound must be at least 3 dB higher than the background noise.

4.8   Recording sound

There are four conventional sound recording types:

- Sound card in PC (two channels is common, but 24-channel sound cards are available)
- Computer data acquisition system (straight onto the hard disk of a PC)
- Digital audio tape (DAT)
- Analogue audio tape.

There are some important points worthy of note here:

- The first three types are digital techniques with high signal-to-noise ratio (around 90 dB) and wide frequency response range (10 Hz to 20 kHz is common).
- The performance of analogue audio tape is poor by comparison (50–80 dB, 25 Hz to 20 kHz for a professional-grade unit).

- The sampling frequency limit for each digital channel will be the upper limit of the frequency response range divided by the number of channels.
- Record levels are set carefully to avoid overloads (a recording level of a recording medium should be selected to suit the dynamic range of the sound).
- High-pass and low-pass filters are set for the correct frequency range to improve the signal-to-noise ratio.

4.9   Analysis and presentation of noise data

There are many ways of analysing sound data. The methods broadly fall into two categories:

- Single-value indices
- Frequency-dependent indices.

4.9.1   Single-value indices: pressure–time history

This is a two-dimensional plot of calibrated pressure (Pa) on the vertical axis against time (s) on the horizontal axis. Such plots are useful as a preliminary check on the quality of the data. The root mean square pressure is given by

$$\overline{p}_{rms} \approx \frac{p_{max}}{\sqrt{2}} \tag{4.9}$$

The sound pressure level is given by

$$L_p = 20 \log_{10} \left[\frac{p_{rms}}{p_{ref}} \right] dB \tag{4.10}$$

where $p_{ref} = 20 \ \mu Pa$ (20×10^{-6} Pa).

The time-varying sound pressure level offers a compact means of displaying a fluctuating sound field on a two-dimensional plot. It is commonly used for both interior and exterior vehicle noise levels as well as for internal combustion (IC) engines and other machines with a wide operating speed range including cooling fans, alternators, pumps and injectors. Frequency weightings may be applied to the data (A, B and C weightings). It is usual to use the fast time weighting (rather than impulse or slow). In any case, it is important to state the use of any weightings in the vertical axis level – the usual form being, for instance, L_{pf} dBA at 1 m from the source. This means fast time weighting and A frequency weighting applied to the raw data. The main application of pressure–time history is the total level of constant-speed tests including idle tests and pass-by noise.

4.9.2 Frequency-dependent index methods: frequency spectrum

The frequency spectrum is commonly used in vehicle tests for octave band analysis and order tracking. In order to understand the octave band analysis, narrowband filters are illustrated as below.

Noise bandwidth of narrowband filters

Before discussing frequency-dependent indices, the noise bandwidth B_n of a narrowband filter must be defined. The noise bandwidth B_n is defined as the bandwidth of the ideal filter that would pass the same signal power as the real filter when each is driven by stationary random noise:

$$B_n = f_2 - f_1 = \int_0^\infty |H(f)|^2 df \tag{4.11}$$

In the ideal filter the modulus of the amplitude transfer function $H(f)$ is zero outside the pass band and unity within the pass band:

$$H(f) = \frac{\overline{x}_{out}}{\overline{x}_{in}} \tag{4.12}$$

where the over-score denotes a complex quantity.

A real filter will have an amplitude transfer function that is not unity right across the pass band and does not go immediately to zero outside the pass band.

Two common classes of narrowband filter are used for analysis of sound data:

- The constant bandwidth type where B_n is the same for all filter centre frequencies f_c
- The constant percentage bandwidth type where B_n is a constant percentage of f_c throughout the frequency range.

Constant percentage bandwidth filters

The constant percentage bandwidth class will be considered first. Commonly available filters of this type have widths of one octave, 1/3 octave, 1/12 octave and 1/24 octave as shown in Table 4.5.

The levels of narrowbands that fit within the bandwidth of coarser filters (for instance, the three 1/3-octave bands that fit within the bandwidth of the one-octave filter) may be combined to give the band levels of the coarser filter. The combination of band levels must be done by logarithmic addition:

Table 4.5 Characteristics of constant percentage bandwidth filters
(n = band number)

Filter	Centre frequency f_c (Hz)	Lower frequency f_1 (Hz)	Upper frequency f_2 (Hz)	Integer values of n for the audio range	Bandwidth around centre frequency (%)
Octave	$10^{n/10}$	$10^{(n-1.5)/10}$	$10^{(n+1.5)/10}$	12–43	69
1/3 octave	$10^{n/10}$	$10^{(n-0.5)/10}$	$10^{(n+0.5)/10}$	12–43	23
1/12 octave	$10^{(n+0.5)/40}$	$10^{n/40}$	$10^{(n+1)/40}$	48–172	6
1/24 octave	$10^{(n+0.5)/80}$	$10^{n/80}$	$10^{(n+1)/80}$	96–344	3

$$L_{\text{total}} = 10 \log_{10}\left[\sum_{i=1}^{n} 10^{L_i/10} \right] \text{dB} \tag{4.13}$$

Following this logic, 1/24-octave bands may be combined to give a 1/12-octave spectrum, the 1/12 bands may be combined to give a 1/3-octave spectrum and so on, until the overall level is obtained (single index). The main application of constant percentage bandwidth filters is octave frequency spectrum analysis of constant-speed tests and order tracking analysis of run-up and run-down tests. Plate I (between pages 114 and 115) shows a constant-speed 1/12 octave noise spectrum of a vehicle.

Constant bandwidth frequency analysis methods

One of the most commonly used outputs from a constant bandwidth spectrum analyser is the power spectral density (psd). In this case, the word 'power' is perhaps a misnomer as in general the psd has units of volts squared per hertz (V^2/Hz) rather than watts per hertz (W/Hz). It may have true units of power if calibrated accordingly. For instance, in the far free-acoustic field:

$$W = \frac{P_{\text{rms}}^2 S}{\rho_0 c} \tag{4.14}$$

where S is the surface area of the wave-front (m^2), ρ_0 the undisturbed air density (kg/m^3) and c the speed of sound (m/s).

The power in each spectral band i is given by:

$$W_i = \frac{S}{\rho_0 c} P_{\text{rms}(i)}^2 = \frac{1}{T}\left[\int_0^{\infty} P_i^2(t)\,\mathrm{d}t \right] \times \left[\frac{S}{\rho_0 c} \right] \tag{4.15}$$

$$W = \sum_{i=1}^{n} W_i \tag{4.16}$$

$$\mathrm{psd}_i = \lim_{B_i \to 0} B_i \to 0 \frac{W_2}{B_2} \tag{4.17}$$

where B_i is the bandwidth of band i.

The psd of the signal from a stationary random process is a smooth continuous function of frequency. For a cyclic process the psd is not smooth as it consists of a series of harmonically related peaks.

Spectral analysis may be performed using either:

- contiguous filters (analogue or digital) or
- Fourier analysis.

The main application of constant bandwidth frequency analysis is frequency spectrum analysis of constant-speed tests and order tracking analysis of run-up and run-down tests.

Order tracking

When analysing the sound from rotating machinery such as internal combustion engines, it is common to use the order-tracking technique. The now obsolete but instructive analogue method was as follows:

1. Obtain an electrical signal that is proportional in some way to the speed of rotation of the machine, for instance a tachometer signal. Calculate the rotational frequency of the machine, f (Hz).
2. Set a constant percentage bandwidth filter (6% is common for 1/12 octave) to have f_c equal to the rotational frequency of the machine, and organize by electrical means for it to follow or track changes in the rotational frequency f_0.
3. Set other constant percentage bandwidth filters (6% is common for 1/12 octave) to follow, or track, changes in the rotational frequency, each one with f_c set to a different order, or harmonic, of the rotational frequency of the machine f_0:

   $f_c = nf_0$ for $n > 0$, not necessarily an integer value

4. Plot the output from each filter against the rotational speed of the machine.

Order track analysis separates noise characteristics of the order of interest from overall noise. Figure 4.7 shows the engine combustion order spectrum of a vehicle.

Waterfall contour plot

Some spectrum analysers allow the use of a tachometer signal to produce a three-dimensional contour plot of frequency spectra against time or

Autospectrum (DE) – Input – slice
Working : Input : Multi-buffer 1 : FFT Analyser
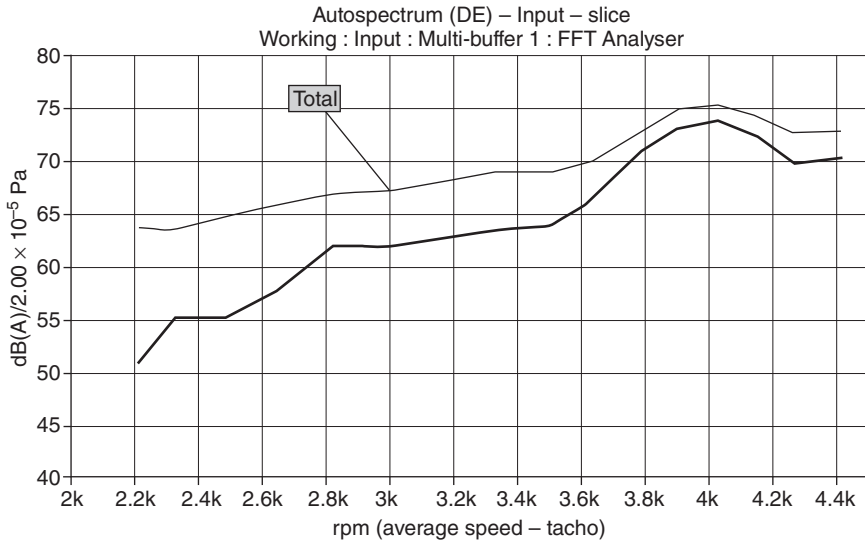
4.7 Engine combustion order spectrum of a vehicle.

machine speed. These are known as waterfall contour plots as shown in Plate II (between pages 114 and 115).

Each horizontal 'slice' is an individual spectrum, gathered over a user-defined averaging period. Beware, with rapid changes in machine speed, that the averaging time for each spectrum will have to be short and therefore individual band levels will only be estimates of the true band levels. Vertical lines of peaks signify resonances – high amplitudes at particular frequencies that are independent of machine speed. Diverging lines of peaks signify different orders. The first order is usually caused by imbalances or misalignments. For a four-stroke internal-combustion engine, half of the number of cylinders is the number of the combustion order, since for every two rotations all of the cylinders fire once, which gives the number of cylinders for combustion pulses. For every rotation half of the cylinders have combustion pulses; therefore half of the number of cylinders is the combustion order of the engine.

The waterfall contour diagram is often used for evaluation of powertrain noise and vibration in the intake and exhaust development, engine and transmission mounting development, and prop shaft and differential mounting development.

4.10 Artificial head technology and psychoacoustics

A human is able to locate a sound source in three dimensions. The locating takes place automatically by means of delay and level differences of the

acoustic signal at both ears because the outer ear causes a direction-dependent filtering of the sound signal. The filter impact results from modification of the sound wave diffusion through attenuation, deflection, reflection and resonance of the sound waves. The geometry and anatomy of the head and shoulder unit as well as the influence of the pinna play a decisive role. Based on this locating capability of the human auditory apparatus, it is possible for humans to select single sound sources from background noise.

Binaural hearing cannot be simulated by simply using two measurement microphones as 'ear replacements'. Only after having taken the acoustic filter characteristics of the head and ears into account do aurally accurate, unaltered recordings become possible. In many respects the human auditory system is different from the properties of conventional sound sensors. On the one hand, very complex signal processing takes place in the auditory apparatus, which captures the amplitude distribution and the spectral and temporal structure of the acoustic signal. The listener perceives a comprehensive, holistic impression of an acoustic event. On the other hand, people possess only a very short acoustic memory. It is possible for artificial head technology to conduct aurally accurate recordings of acoustic signals and to save them. The playback of an artificial head recording generates the same aural impression as if the listener had heard the sound event directly.

Thanks to the true-to-original recording and playback of arbitrary sound incidents and their digital archives, artificial head technology makes comparative and aurally accurate evaluations of different sound situations possible. And because artificial head technology is compatible with conventional measurement technology, subjective and objective sound field analyses can be combined in one investigation.

Psychoacoustics describes the connection between the physical characteristics of a sound signal and the feeling resulting from it. Transfer functions of the connection serve the concept of the hearing procedure and display the transmission characteristics of human hearing. Psychoacoustics offers:

- Parameters related to human hearing
- Signal processing adapted to human hearing
- Objective description of subjective perceived sound quality
- Defined values instead of expressions like 'rattling', 'rumbling', 'booming', etc.
- Manipulation of sound events regarding sources and transfer paths to design a comfortable sound quality.

The main psychoacoustic parameters are articulation index, loudness, sharpness, roughness, fluctuation strength and tonality. The definitions of articulation index, loudness and sharpness will be given in Chapter 13.

One asper of roughness is defined by 60 dB, 1 kHz tone 100% modulated in amplitude at a modulation frequency of 70 Hz. Roughness describes temporal characteristics of a noise. Modulation of a signal with modulation frequencies between 20 Hz and 250 Hz results in roughness.

One vacil of fluctuation strength is defined by 60 dB, 1 kHz tone 100% amplitude modulated at 4 Hz. Modulation of a signal with modulation frequencies smaller than 20 Hz results in large fluctuation strength.

Tonality is a measure of the proportion of individual tones or of several tone components in a noise. Frequently a high tonality causes an unpleasant noise impression. A 1 kHz, 60 dB sinusoidal tone has a tonality of 1 tu.

4.11   Bibliography

Happian-Smith, J. (2002), *An Introduction to Modern Vehicle Design*, SAE International, Butterworth-Heinemann.

Harrison, M. (2004), *Vehicle Refinement – Controlling Noise and Vibration in Road Vehicles*, SAE International, Elsevier Butterwroth-Heinemann.

Wang, X. (2005), *Introduction to Motor Vehicle Design*, RMIT Publisher.

5

Random signal processing and spectrum analysis in vehicle noise and vibration refinement

X. WANG, RMIT University, Australia

Abstract: Starting from definitions of a linear system, random data and process, the statistical properties of random data, correlation analysis, spectral analysis, the Fourier transform, the impulse response function and the frequency response function are introduced. The digital FFT analysis process is illustrated. The relationships between the correlation function and the power density spectrum function, between the impulse response function and the frequency response function, and between the Fourier spectrum function and the power spectrum function are established. The definition and physical meaning of the coherence function are illustrated. Frequently encountered random signals and their conversions are demonstrated.

Key words: random data, time-history record, ensemble, stationary, non-stationary, ergodic, non-ergodic, time-averaging, expected value, mean square value, variance, standard deviation, probability distribution, Gaussian distribution, Rayleigh distribution, correlation analysis, autocorrelation, cross-correlation, Fourier series, Fourier transform, digital FFT analysis, sampling frequency, spectrum size, windowing, anti-alias filtering, sampling points, Fourier spectrum, FFT versus time spectrum, spectral density function, power spectrum density function, auto-power spectrum density function, cross-power spectrum density function, impulse response function, frequency response function, coherence function, linear system, additive property, homogeneous property, superposition principle, convolution integral.

5.1 Random data and process

Random data are any type of data occurring especially in vehicle tyre–road induced noise and vibration that do not have an explicit mathematical formula to describe their properties. It is impossible to predict the precise level of the disturbance at any given time and hence it is impossible to express such disturbances as continuous functions in the time domain – only statistical representations are possible. Any time-history record represents only one record out of a collection of different time-history records that might have occurred. From the vibration point of view, the frequency content of a random signal is very important. For example, the frequency spectrum of a road input to a vehicle is a function of the spatial random
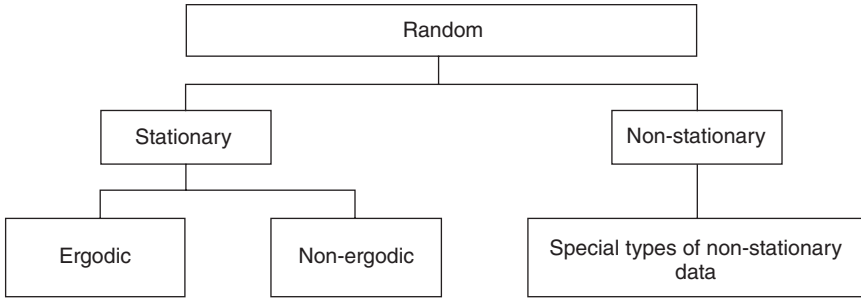
93
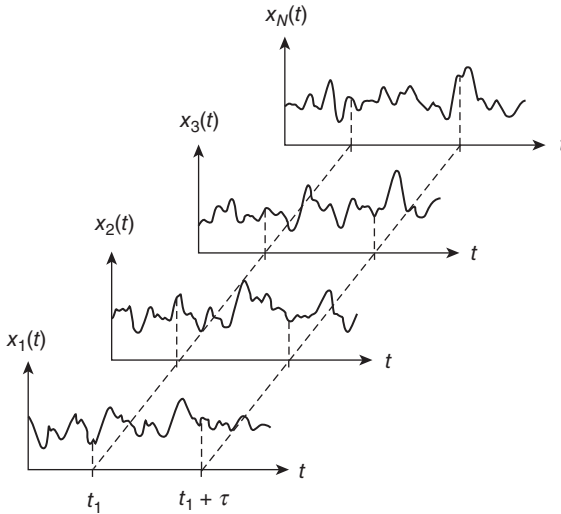
5.1 Ensemble of time-history records defining a random process.

profile of the road surface and the speed of the vehicle. For a given set of conditions, it results in a large number of frequency components distributed over a wide band of frequencies.

5.1.1 Definition of terms

As shown in Fig. 5.1, an ensemble is defined as a collection of records. A random process is defined as a process which is represented by the ensemble and defined by analysing various statistical properties over the ensemble.

Stationary random data is defined as data whose ensemble-averaged statistical properties are invariant with time. For such data, ensemble-averaged mean values are the same at every time. For vehicle applications, stationary processes include idle conditions, constant-speed driving or cruise control driving conditions. Ergodic data is stationary random data where one long-duration average on any arbitrary time-history record gives results that are statistically equivalent to associated ensemble averages over a large collection of records. In practice, stationary random data will automatically be ergodic if there are no sine waves or other deterministic phenomena in the records. Classification of random systems is shown in Fig. 5.2. For example, a white noise, wideband random signal is stationary and ergodic. For such data, one long-duration experiment is sufficient to obtain useful information, as a stationary random record should never have a beginning or an end.

```
          ┌─────────────────────┐
          │       Random        │
          └─────────────────────┘
        ┌────────────┴──────────────────┐
  ┌──────────────┐              ┌──────────────────┐
  │  Stationary  │              │  Non-stationary  │
  └──────────────┘              └──────────────────┘
   ┌──────┴────────┐                     │
┌─────────┐ ┌──────────────┐  ┌─────────────────────────────┐
│ Ergodic │ │  Non-ergodic │  │ Special types of non-stationary │
│         │ │              │  │           data              │
└─────────┘ └──────────────┘  └─────────────────────────────┘
```

5.2 Classification of random systems.

Non-stationary random data is defined as data whose ensemble-averaged statistical properties change with time. Transient random data is a special class of non-stationary random data with a clearly defined beginning and end to the data, for example vehicle second/third gear slow acceleration, first gear wide open throttle (WOT) acceleration, overrun/coastdown deceleration processes, braking, cornering, etc.

When stationary random data pass through constant-parameter linear systems, the output data will also be stationary. When transient random data pass through constant-parameter linear systems, the output will be transient random data. However, when stationary or transient random data pass through time-varying linear systems, the output will be non-stationary. In general, techniques for analysing stationary random data are not appropriate for analysing non-stationary random data.

5.1.2 Time-averaging and expected value

In random data, we often encounter the concept of time-averaging over a long period of time:

$$\bar{x}(t) =< x(t) >= \lim_{T \to \infty} \frac{1}{T} \int_0^T x(t)\, dt \qquad (5.1)$$

or the expected value of $x(t)$, which is:

$$E[x(t)] = \lim_{T \to \infty} \frac{1}{T} \int_0^T x(t)\, dt \qquad (5.2)$$

In the case of discrete variables x_i, the expected value is given by:

$$E[x] = \lim_{n \to \infty} \frac{1}{n} \sum_{i=1}^{n} x_i \qquad (5.3)$$

5.1.3 Mean square value

The mean square value, designated by $\overline{(x^2)}$ or $E[x^2(t)]$, is found by integrating $x^2(t)$ over time interval T and taking its average value according to:

$$E[x^2(t)] = \overline{(x^2)} = \lim_{T \to \infty} \frac{1}{T} \int_0^T x^2(t)\,dt \tag{5.4}$$

5.1.4 Variance and standard deviation

An important property describing the fluctuation in ensemble is the variance σ^2, which is the mean square value about the mean, given by:

$$\sigma^2 = \lim_{T \to \infty} \frac{1}{T} \int_0^T (x - \overline{x})^2\,dt \tag{5.5}$$

By expanding, you can determine that:

$$\sigma^2 = \overline{(x^2)} - (\overline{x})^2 \tag{5.6}$$

so that the variance is equal to the mean square value minus the square of the mean. The positive square root of the variance is the standard deviation σ.

5.1.5 Probability distribution

Refer to the random data in Fig. 5.3. A horizontal line at the specified value x_1 is drawn and the time interval Δt_i ($i = 1, 2, 3 \ldots$) during which $x(t)$ is less than x_1 is summed and divided by the total time, which represents the fraction of the total time that $x(t) < x_1$. The probability density that $x(t)$ will be found less than x_1 is:

$$p(x) = \lim_{\Delta x \to 0} \frac{P(x + \Delta x) - P(x)}{\Delta x} = \frac{dP(x)}{dx} \tag{5.7}$$
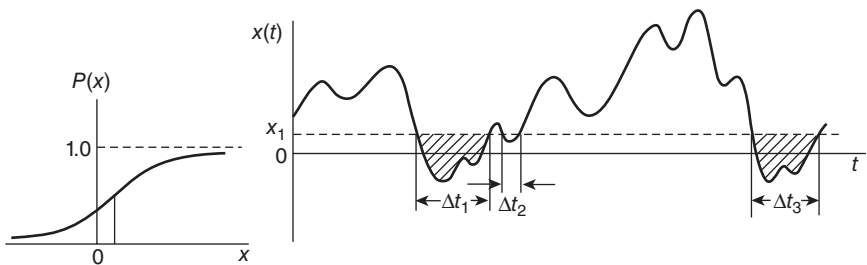
5.3 Calculation of cumulative probability.
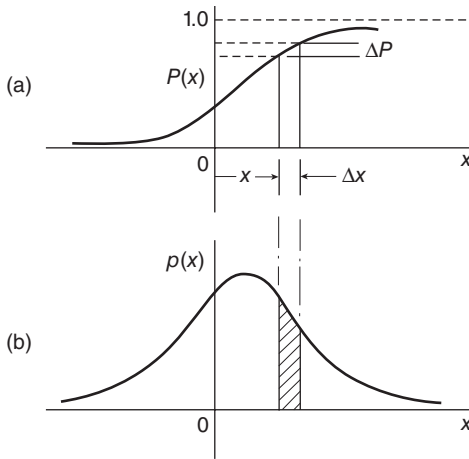
5.4 (a) Cumulative probability; (b) probability density.

From Fig. 5.4 you can see that $p(x)$ is the slope of the cumulative probability distribution $P(x)$:

$$P(x_1) = \int_0^{x_1} p(x)\,dx \tag{5.8}$$

The area under the probability density curve of Fig. 5.4(b) between two values of x represents the probability of the variable being in this interval. Because the probability of $x(t)$ being between $x = \pm\infty$ is certain:

$$P(+\infty) = \int_{-\infty}^{\infty} p(x)\,dx = 1 \tag{5.9}$$

and the total area under $p(x)$ must be unity.

The mean and mean square value defined in terms of the time average are related to this probability density function in the following manner. The mean value $\bar{x}$ coincides with the centroid of the area under the probability density curve $p(x)$, as shown in Fig. 5.4(b), and can be determined by the first moment:

$$\bar{x} = \int_{-\infty}^{\infty} x p(x)\,dx \tag{5.10}$$

The mean square value is determined from the second moment:

$$\overline{(x^2)} = \int_{-\infty}^{\infty} x^2 p(x)\,dx \tag{5.11}$$

which is analogous to the moment of inertia of the area under the probability curve about $x = 0$.

The variance σ^2 is defined as the mean square value about the mean:

$$\sigma^2 = \int_{-\infty}^{\infty} (x - \bar{x})^2\, p(x)\,dx = \int_{-\infty}^{\infty} x^2 p(x)\,dx$$

$$- 2\bar{x} \int_{-\infty}^{\infty} x\, p(x)\,dx + (\bar{x})^2 \int_{-\infty}^{\infty} p(x)\,dx \tag{5.12}$$

$$\sigma^2 = \overline{(x^2)} - 2(\bar{x})^2 + (\bar{x})^2 = \overline{(x^2)} - (\bar{x})^2 \tag{5.13}$$

5.1.6 Gaussian and Rayleigh distributions

The Gaussian and Rayleigh distributions frequently occur in vehicle noise and vibration data. The Gaussian distribution is a bell-shaped curve symmetric about the mean value:

$$p(x) = \frac{1}{\sigma\sqrt{2\pi}} e^{-(x^2/2\sigma^2)} \tag{5.14}$$

The expected value of the product of four Gaussian random process variables, $E[x_1, x_2, x_3, x_4]$, the fourth moment of the Gaussian random inputs, can be reduced to the products of the expected values of two process variables:

$$E[x_1, x_2, x_3, x_4] = E[x_1 x_2]E[x_3 x_4] + E[x_1 x_3]E[x_2 x_4] +$$
$$E[x_1 x_4]E[x_2 x_3] - 2\mu_1 \mu_2 \mu_3 \mu_4 \tag{5.15}$$

where μ_i is the mean value of the x_i process ($i = 1, 2, 3, 4$). In most Gaussian random processes, $\mu_i = 0$ ($i = 1, 2, 3, 4$).

Random variables restricted to positive values, such as the absolute value A of the amplitude, often tend to follow the Rayleigh distribution, defined as:

$$\begin{cases} p(A) = \dfrac{A}{\sigma^2} e^{-(A^2/2\sigma^2)} & A > 0 \\ p(A) = 0 & A < 0 \end{cases} \tag{5.16}$$

The shape is shown in Fig. 5.5. The mean and mean square values for the Rayleigh distribution can be found from the first and second moments:
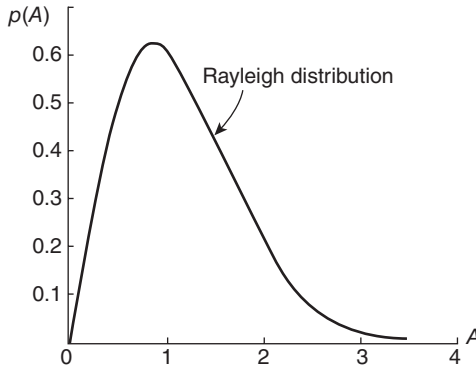
5.5 Rayleigh distribution.

$$\bar{A} = \int_0^\infty A p(A) \, dA = \int_0^\infty \frac{A^2}{\sigma^2} e^{-(A^2/2\sigma^2)} \, dA = \sqrt{\frac{\pi}{2}} \, \sigma \tag{5.17}$$

$$\overline{(A^2)} = \int_0^\infty A^2 p(A) \, dA = \int_0^\infty \frac{A^3}{\sigma^2} e^{-(A^2/2\sigma^2)} \, dA = 2\sigma^2 \tag{5.18}$$

The variance associated with the Rayleigh distribution is:

$$\sigma_A^2 = \overline{(A^2)} - (\bar{A})^2 = \left(\frac{4-\pi}{2}\right)\sigma^2 \tag{5.19}$$

i.e.

$$\sigma_A \approx \frac{2}{3}\sigma \tag{5.20}$$

The probability of A exceeding a specified value $\lambda\sigma$ is:

$$\text{prob } [A > \lambda\sigma] = \int_{\lambda\sigma}^\infty \frac{A}{\sigma^2} e^{-(A^2/2\sigma^2)} \, dA \tag{5.21}$$

The cumulative probability distribution for a sine wave is shown in the first column of the table in Fig. 5.6, and is written as:

$$P(x) = \frac{1}{2} + \frac{1}{\pi}\sin^{-1}\left(\frac{x}{A}\right) \tag{5.22}$$

Its probability density is:

$$\begin{cases} p(x) = \dfrac{1}{\pi\sqrt{A^2 - x^2}} & |x| < A \\ p(x) = 0 & |x| > A \end{cases} \tag{5.23}$$
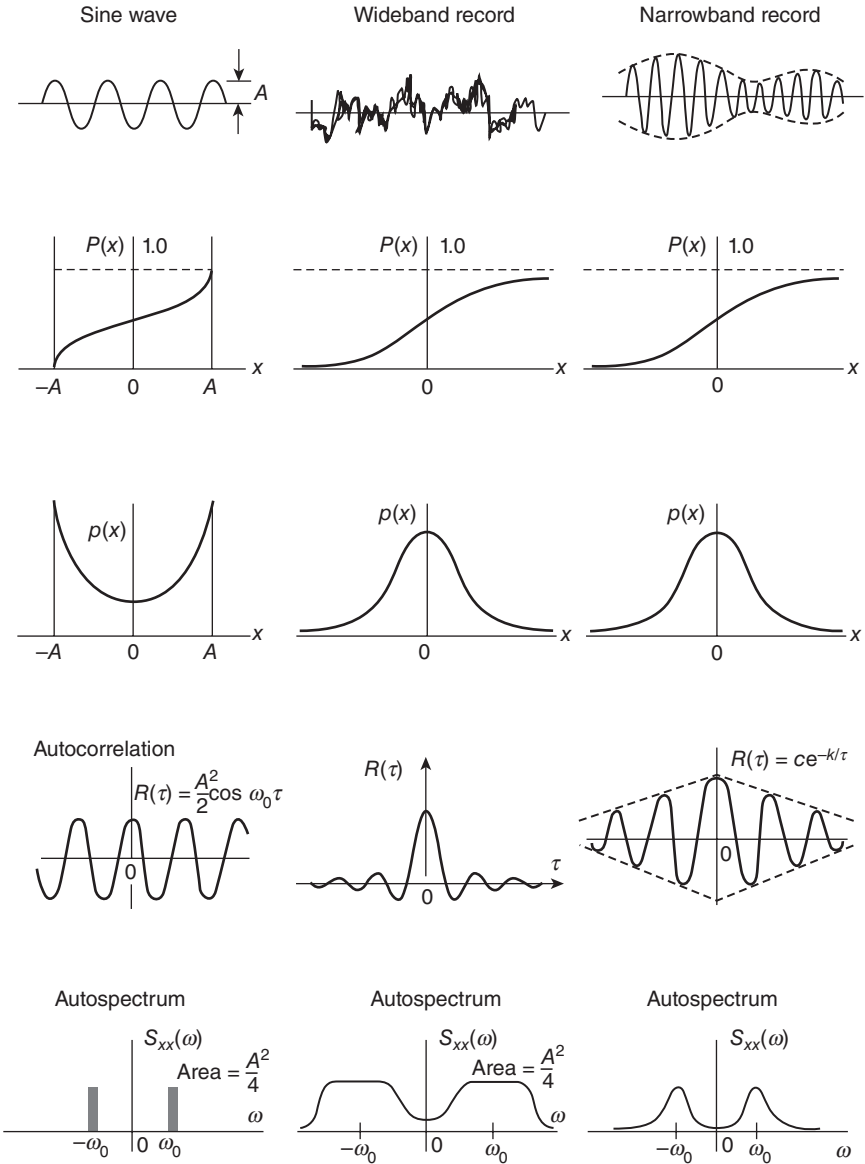
5.6 Three frequently encountered signals and their conversions.

5.2   Correlation analysis

Correlation analysis consists of autocorrelation and cross-correlation analysis. It is a type of analysis in the time domain.
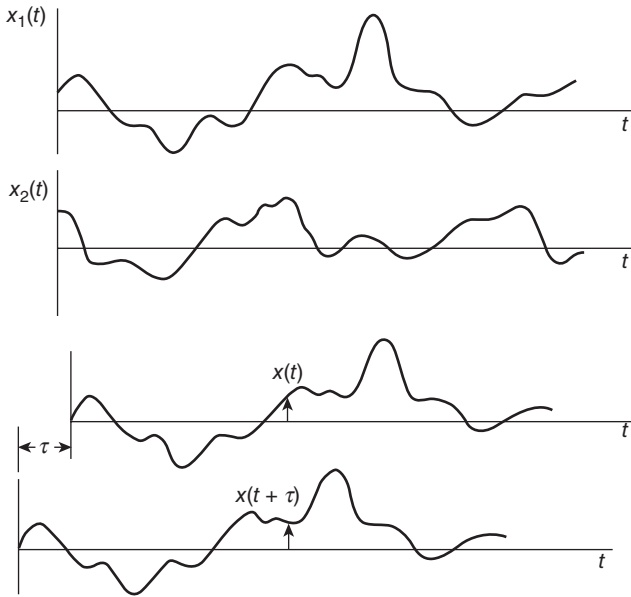
5.7 Correlation between $x(t)$ and $x(t + \tau)$.

5.2.1 Autocorrelation

Correlation is a measure of the similarity between two quantities. Suppose two records $x_1(t)$ and $x_2(t)$ in one ensemble/collection are as shown in Fig. 5.7. The autocorrelation is defined as:

$$R(\tau) = E[x(t)x(t+\tau)] = <x(t)x(t+\tau)> = \lim_{T\to\infty} \frac{1}{T} \int_{-T/2}^{T/2} x(t)x(t+\tau)\,\mathrm{d}t \qquad (5.24)$$

When $\tau = 0$:

$$R(0) = \overline{(x^2)} = \sigma^2 \qquad (5.25)$$

where the random process has a mean of zero. $R(\tau) = R(-\tau)$ is symmetric about the origin τ and the vertical axis which is an even function of τ as shown in Fig. 5.6. Figure 5.8 shows the block diagram of an autocorrelation analyser.

5.2.2 Cross-correlation

Consider two random quantities $x(t)$ and $y(t)$. The cross-correlation between them is defined as:
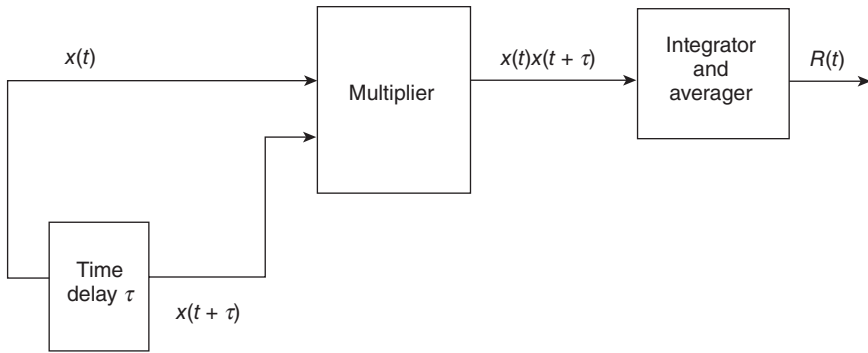
5.8 Autocorrelation analyser block diagram.

$$R_{xy}(\tau) = E[x(t)y(t+\tau)] = < x(t)y(t+\tau) > = \lim_{T \to \infty} \frac{1}{T} \int_{-T/2}^{T/2} x(t)y(t+\tau)\,\mathrm{d}t \quad (5.26)$$

5.3   Fourier series

Generally, random time functions contain oscillations of many frequencies, which approach a continuous spectrum. Although random time functions are generally not periodic, their representations by Fourier series, in which the periods are extended to a large value approaching infinity, offers a logical approach.

The exponential form of the Fourier series is shown to be:

$$x(t) = \sum_{-\infty}^{\infty} c_n \mathrm{e}^{\mathrm{i}n\omega_1 t} = c_0 + \sum_{n=1}^{\infty} (c_n \mathrm{e}^{\mathrm{i}n\omega_1 t} + c_n \mathrm{e}^{-n\omega_1 t}) \quad (5.27)$$

This series, which is a real function, involves a summation over negative and positive frequencies and also contains a constant c_0. c_0 is the average value of $x(t)$ and because it can be dealt with separately we exclude it in future considerations. Moreover, actual measurements are made in terms of positive frequencies, so it would be more desirable to work with:

$$x(t) = 2\,\mathrm{Re}\left[\sum_{n=1}^{\infty} c_n \mathrm{e}^{\mathrm{i}n\omega_1 t}\right] \quad (5.28)$$

where:

$$x(t) = \frac{a_0}{2} + a_1 \cos\omega_1 t + a_2 \cos\omega_2 t + \ldots + b_1 \sin\omega_1 t + b_2 \sin\omega_2 t + \ldots \quad (5.29)$$

and $\omega_1 = 2\pi/T$, $\omega_n = n\omega_1$ and $c_0 = a_0/2$.

If $x(t)$ is a periodic signal of period T, from Equation 5.29, this gives

$$a_n = \frac{2}{T} \int_{-T/2}^{T/2} x(t)\cos\omega_n t\, dt \tag{5.30}$$

$$b_n = \frac{2}{T} \int_{-T/2}^{T/2} x(t)\sin\omega_n t\, dt \tag{5.31}$$

$$c_n = \frac{1}{2}(a_n - ib_n) \tag{5.32}$$

$$c_n = \frac{1}{T} \int_{-T/2}^{T/2} x(t)e^{-n\omega_1 t}\, dt \tag{5.33}$$

Introducing

$$n\omega_1 = \omega_n, \quad \omega_1 = \frac{2\pi}{T} = \Delta\omega_n \tag{5.34}$$

we have

$$x(t) = \sum_{n=-\infty}^{\infty} \frac{1}{T}(Tc_n)e^{i\omega_n t} = \frac{1}{2\pi}\sum_{n=-\infty}^{\infty}(Tc_n)e^{i\omega_n t}\Delta\omega_n \tag{5.35}$$

$$Tc_n = \int_{-T/2}^{T/2} x(t)e^{-i\omega_n t}\, dt \tag{5.36}$$

$$X(\omega) = \lim_{\substack{T\to\infty \\ \Delta\omega_n \to 0}}(Tc_n) = \int_{-\infty}^{\infty} x(t)e^{-i\omega t}dt \tag{5.37}$$

$$x(t) = \lim_{\substack{T\to\infty \\ \Delta\omega_n \to 0}} \frac{1}{2\pi}\sum_{n=-\infty}^{\infty}(Tc_n)e^{i\omega_n t}\Delta\omega_n = \frac{1}{2\pi}\int_{-\infty}^{\infty} X(\omega)e^{i\omega t}d\omega \tag{5.38}$$

5.3.1 Fourier transforms

The Fourier transform of a real-valued function $x(t)$ extending from $-\infty < t < +\infty$ is a complex-valued function $X(f)$ defined by:

$$X(f) = F[x(t)] = \int_{-\infty}^{\infty} x(t)e^{\text{i.e. } -2\pi i f t}dt = \int_{-\infty}^{\infty} x(t)e^{-i\omega t}dt = X(\omega) \tag{5.39}$$

Assuming this complex-valued $X(f)$ exists for all f over $-\infty < f < +\infty$, the inverse Fourier transform brings $X(f)$ back to $x(t)$ as defined by:

$$x(t) = F^{-1}[X(f)] = \int_{-\infty}^{\infty} X(f)e^{2\pi i f t}df = \frac{1}{2\pi}\int_{-\infty}^{\infty} X(\omega)e^{i\omega t}d\omega \qquad (5.40)$$

where

$$X(f) = X_R(f) + i X_I(f) \qquad (5.41)$$

The real part $X_R(f)$ and the imaginary part $X_I(f)$ are:

$$X_R = \int_{-\infty}^{\infty} x(t)\cos 2\pi f t \, dt \qquad (5.42)$$

$$X_I = \int_{-\infty}^{\infty} x(t)\sin 2\pi f t \, dt \qquad (5.43)$$

The magnitude $|X(f)|$ and phase $\phi_x(f)$ are given by:

$$X(f) = |X(f)|e^{+i\phi_x(f)} = |X(f)|(\cos\phi_x(f) + i\sin\phi_x(f)) \qquad (5.44)$$

Therefore:

$$X_R(f) = |X(f)|(\cos\phi_x(f)) \qquad (5.45)$$

$$X_I(f) = |X(f)|(\sin\phi_x(f)) \qquad (5.46)$$

$$|X(f)| = [X_R^2(f) + X_I^2(f)]^{\frac{1}{2}} \qquad (5.47)$$

$$\phi_x(f) = \tan^{-1}\left[\frac{X_I(f)}{X_R(f)}\right] \qquad (5.48)$$

Fourier transforms of several conventional time domain functions are shown in Table 5.1. A number of properties of Fourier transforms are given

Table 5.1 Fourier transforms

$x(t)$	$x(f)$
$\cos 2\pi f_0 t$	$\frac{1}{2}[\delta(f - f_0) + \delta(f + f_0)]$
$\sin 2\pi f_0 t$	$\frac{1}{2i}[\delta(f - f_0) - \delta(f + f_0)]$
$\dfrac{\sin t}{t}$	$\begin{cases} \pi & \left(-\dfrac{1}{2\pi} \leq f \leq \dfrac{1}{2\pi}\right) \\ 0 & \text{otherwise} \end{cases}$
$\dfrac{1}{1+t^2}$	$\begin{cases} \pi e^{-2\pi f} & f > 0 \\ \pi e^{2\pi f} & f < 0 \end{cases}$
$e^{-c|t|}\cos 2\pi f_0 t$	$\dfrac{c}{c^2 + 4\pi^2(f - f_0)^2} + \dfrac{c}{c^2 + 4\pi^2(f + f_0)^2}$

Table 5.2 Fourier transform properties

Operation	Property
Linear	$F[ax(t) + by(t)] = aX(f) + bY(f)$ for any functions $x(t)$, $y(t)$ and constants a and b
Shift	$F[x(t - a)] = e^{-2\pi ifat} X(f)$
Fourier transform of Fourier transform	$F[X(f)] = x(-t)$
Inverse Fourier transform of $X(f)$	$x(t) = F^{-1}[X(f)] = \int\limits_{-\infty}^{\infty} X(f)e^{2\pi ift}\,df$
Odd and even functions	$X(f) = X_R(f) + iX_I(f)$; $x(t)$ is even $\Leftrightarrow X(f) = X_R(f)$ is even; $x(t)$ is odd $\Leftrightarrow X(f) = jX_I(f)$ is odd
Similarity	$F[x(at)] = \dfrac{1}{\vert a\vert}X\left(\dfrac{f}{a}\right)$
Energy	$\int\limits_{-\infty}^{\infty} x^2(t)dt = \int\limits_{-\infty}^{\infty}\vert X(f)\vert^2\,df,\quad \int\limits_{-\infty}^{\infty} x(t)y(t)dt = \int\limits_{-\infty}^{\infty} X * Y(f)\,df$
Autocorrelation	If $R(t) = \int\limits_{-\infty}^{\infty} x(u)x(u + t)\,du$ then $F[R(t)] = \vert X(f)\vert^2$
Product	$F[x(t)y(t)] = X(f) * Y(f)$ where $X(f) * Y(f) = \int\limits_{-\infty}^{\infty} X(u)Y(f - u)\,du$
Convolution	$x(t) * y(t) = \int\limits_{-\infty}^{\infty} x(u)y(t - u)\,du$ where $F[x(t) * y(t)] = X(f)Y(f)$
Parseval's theorem	$\int\limits_{-\infty}^{\infty} x_1(t)x_2(t)\,dt = \int\limits_{-\infty}^{\infty} X_1(f)X_2(f)^*\,df = \int\limits_{-\infty}^{\infty} x_1^*(f)X_2(f)\,df$

in Table 5.2, where $X(f) = F[x(t)]$, $Y(f) = F[y(t)]$ are Fourier transforms of $x(t)$ and $y(t)$.

5.3.2 Digital FFT analysis

In order to implement the above Fourier transform, a quality data acquisition system is required for signal time recording. Ahead of FFT analysis, the time signal is subdivided into *n* time segments of length $\Delta t = n/f_S$ (f_S = sampling frequency) as shown in Fig. 5.9. In order to avoid signal alias, filters and windows will have to be applied to the sampled data. An FFT analysis is conducted from the digital integration of Equations 5.39 and 5.40 using fast computing algorithms for each time signal segment. The number of samples per time segment can then be entered as spectrum size input. If there is more than one time segment (as is normally the case), the individual partial analyses are averaged ahead of representation. The calculated FFT spectrum for side mirror power fold actuator noise of a passenger car is shown in Plate III (between pages 114 and 115).
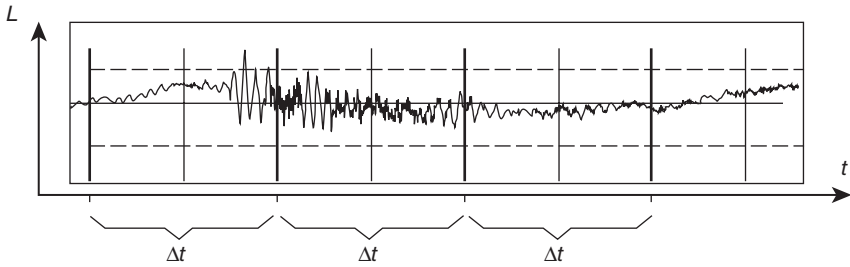
5.9 Time records for digital FFT analysis.

From the averaged FFT spectrum results, the constant percentage bandwidth filters defined in Table 4.5 and Equation 4.13 in Chapter 4 can be used to calculate the constant percentage bandwidth spectrum as shown in Plate IV (between pages 114 and 115).

If a signal process is a non-stationary or transition process, a 3-D spectrum map of FFT versus time will have to be used to present the measured spectrum in both time and frequency domains. In 'standard' FFT analysis, individual partial analyses (spectrum size) are averaged over the entire signal curve. In the analysis versus time, this averaging is not carried out; the analysis result for each time window is graphically displayed. This requires an additional axis. Since the flat monitor screen or paper page allows for only two axes, the third axis (the Z-axis) is represented with the aid of various colours. The three axes are (a) the X-axis (previously the frequency axis), now the time axis; (b) the Y-axis (previously the level axis), now the frequency axis; and (c) the Z-axis, which represents level in the time and frequency domains via different colours as shown in Plate V (between pages 114 and 115).

5.4 Spectral density analysis

For stationary random data, the following expected values of Fourier transform quantities can define the two-sided auto-spectral density functions $S_{xx}(f)$ and $S_{yy}(f)$ and the two-sided cross-spectral density function $S_{xy}(f)$:

$$S_{xx}(f) = \frac{1}{T} E\left[|X(f)|^2\right] \tag{5.49}$$

$$S_{yy}(f) = \frac{1}{T} E\left[|Y(f)|^2\right] \tag{5.50}$$

$$S_{xy}(f) = \frac{1}{T} E[X^*(f)Y(f)] \tag{5.51}$$

where $E[\ ]$ denotes an expected value ensemble average over the quantities inside the brackets. The $X(f)$ and $Y(f)$ are infinite Fourier transforms of

length T for n_d distinct sample records and the frequency f can theoretically be any value in $-\infty < f < \infty$. For digitized data f is restricted to discrete values spaced $1/T$ apart in a bounded frequency range, and Fourier transform formulas become Fourier series formulas.

The spectral density functions $S_{xx}(f)$ and $S_{yy}(f)$ are positive, real-valued even functions of f; the cross-spectral is a complex-valued function of f. If $x(t)$ and $y(t)$ are measured in volts, $S_{xx}(f)$ and $S_{yy}(f)$ will have units of volts^2 per hertz, while t has units of seconds. $S_{xx}(f)$, $S_{yy}(f)$ and $S_{xy}(f)$ always exist for finite-length records.

For stationary random data, the one-sided measurable auto-spectral density functions and cross-spectral density function are zero for $f < 0$ and for $f \geq 0$ defined by:

$$G_{xx}(f) = \frac{2}{T} E\left[|X(f)|^2\right] \tag{5.52}$$

$$G_{yy}(f) = \frac{2}{T} E\left[|Y(f)|^2\right] \tag{5.53}$$

$$G_{xy}(f) = \frac{2}{T} E[X^*(f)Y(f)] \tag{5.54}$$

Note that:

$$\begin{cases} G_{xy}(f) = 2S_{xy}(f) & f \geq 0 \\ G_{xy}(f) = 0 & f < 0 \end{cases} \tag{5.55}$$

which includes $G_{xx}(f)$ and $G_{yy}(f)$ as special cases.

For $f \geq 0$ the following relationships hold:

$$H_{xy}(f) = \frac{S_{xy}(f)}{S_{xx}(f)} = \frac{G_{xy}(f)}{G_{xx}(f)} \tag{5.56}$$

$$|H_{xy}(f)|^2 = \frac{S_{yy}(f)}{S_{xx}(f)} = \frac{G_{yy}(f)}{G_{xx}(f)} \tag{5.57}$$

$$\gamma_{xy}^2 = \frac{|S_{xy}(f)|^2}{S_{xx}(f)S_{yy}(f)} = \frac{|G_{xy}(f)|^2}{G_{xx}(f)G_{yy}(f)} \tag{5.58}$$

where H_{xy} is the frequency response function between variables x and y, and γ_{xy}^2 is the coherence function between two stationary random processes $x(t)$ and $y(t)$. As proved in the works in the bibliography (Section 5.10), this ordinary coherence function for all f is a dimensionless constant that is bounded between zero and one, namely:

$$0 \leq \gamma_{xy}^2(f) \leq 1 \tag{5.59}$$

The coherence function of Equation 5.59 is a causal relationship unless one has other physical grounds for knowing that an input $x(t)$ produces an output $y(t)$. For example, $x(t)$ could be excitation force and $y(t)$ could be vibration response. If a perfect linear relationship exists between $x(t)$ and $y(t)$ at some frequency f_0, then the coherence function $\gamma_{xy}^2(f_0)$ will be unity at the frequency. If $x(t)$ and $y(t)$ are such that $S_{xy}(f_0) = 0$ at frequency f_0, then the coherence function will be zero at that frequency, and $x(t)$ is not correlated to $y(t)$.

There are four main reasons in practice why a computed coherence function between a measured input $x(t)$ and a measured output $y(t)$ will differ from unity. These are:

- Extraneous noise in the input and output measurements
- Bias and random errors in the spectral density function estimates
- Output $y(t)$ being due in part to other inputs as well as the measured input $x(t)$
- Non-linear system operations existing between $x(t)$ and $y(t)$.

If the first three possibilities are ruled out by good data acquisition, proper data processing and physical understanding, it is reasonable to conclude that low coherence at particular frequencies is due to non-linear system effects at these frequencies. Thus the ordinary coherence function can provide a simple practical way to detect non-linearity without identifying its precise nature.

Table 5.3 shows the basic formulas of two- and one-sided spectral density functions for stationary random data. Three frequently encountered signals such as sine wave, wideband random signal and narrowband random signal and their conversions for time traces, the cumulative probability distribution, the probability density distribution, autocorrelation and the auto-spectrum are compared and plotted in Fig. 5.6 where the relationship and trend of the signals changing with bandwidth can be seen.

Table 5.3 Basic spectral density functions, stationary random data

Two-sided spectra

$$S_{xy}(f) = \frac{1}{T} E[X^*(f)Y(f)], \quad -\infty < f < \infty$$

$$S_{xx}(f) = \frac{1}{T} E[X^*(f)X(f)] = \frac{1}{T} E[|X(f)|^2]$$

One-sided spectra

$$G_{xy}(f) = \frac{2}{T} E[X^*(f)Y(f)], \quad f \geq 0 \ \text{only}$$

$$G_{xx}(f) = \frac{2}{T} E[X^*(f)X(f)] = \frac{2}{T} E[|X(f)|^2]$$

5.5 Relationship between correlation functions and spectral density functions

Comparing Equations 5.49 – 5.51 with Equations 5.24 and 5.26 and applying Fourier transform relationships give the conclusion that the relationship between the correlation function and the spectral density function is a Fourier transform pair. That is:

$$R_{xy}(\tau) = \frac{1}{2\pi} \int_{-\infty}^{\infty} S_{xy}(\omega) e^{i\omega\tau} d\omega \tag{5.60}$$

$$S_{xy}(\omega) = \int_{-\infty}^{\infty} R_{xy}(\tau) e^{-\omega\tau} d\tau \tag{5.61}$$

$$F[R_{xy}(\tau)] = S_{xy}(\omega) = S_{xy}(f) \tag{5.62}$$

$$F^{-1}[S_{xy}(f)] = F^{-1}[S_{xy}(\omega)] = R_{xy}(\tau) \tag{5.63}$$

When $\tau = 0$, $x = y$ and

$$R_{xx}(0) = \sigma^2 = \frac{1}{2\pi} \int_{-\infty}^{\infty} S_{xx}(\omega) d\omega = \int_{-\infty}^{\infty} S_{xx}(f) df \tag{5.64}$$

5.6 Linear systems

Ideal physical systems should be linear, physically realizable, have constant parameters and be stable. Properties of ideal physical systems are shown in Table 5.4. A system H is a linear system if, for any inputs $X_1 = X_1(t)$ and $X_2 = X_2(t)$ and for any constants c_1 and c_2:

$$H[c_1 X_1 + c_2 X_2] = c_1 H[X_1] + c_2 H[X_2] \tag{5.65}$$

The additive property is

$$H[X_1 + X_2] = H[X_1] + H[X_2] \tag{5.66}$$

Table 5.4 Properties of ideal physical systems

System property	Requirement	Benefit
Linear	Additive and homogeneous	Output stays Gaussian
Physically realizable	$h(\tau) = 0$ for $\tau < 0$	Output follows input
Constant-parameter	$h(t, \tau) = h(\tau)$	Output stays stationary
Stable	$\int_{-\infty}^{\infty} |h(\tau)| d\tau < \infty$	Output stays bonded

The homogeneous property is

$$H[c_0 X] = c_0 H[X] \tag{5.67}$$

where c_0 is a constant.

For a constant-parameter linear system:

$$y(t + \tau) = H[x(t + \tau)] \tag{5.68}$$

for any τ.

For a second-order dynamic system:

$$H = m\frac{d^2}{dt^2} + c\frac{d}{dt} + k \tag{5.69}$$

$$H[x] = F(t) \tag{5.70}$$

where m is mass, c is damping, k is stiffness and $F(t)$ is excitation force.

If two excitations $F_1(t)$ and $F_2(t)$ are considered, the responses $x_1(t)$ and $x_2(t)$ are given by

$$H[x_1] = F_1(t), \quad H[x_2] = F_2(t) \tag{5.71}$$

If the excitation $F_3(t)$ is a linear combination of $F_1(t)$ and $F_2(t)$, namely

$$F_3 = C_1 F_1(t) + C_2 F_2(t) \tag{5.72}$$

and if the response $x_3(t)$ to the excitation $F_3(t)$ satisfies the relation

$$x_3(t) = C_1 x_1(t) + C_2 x_2(t) \tag{5.73}$$

$$H[x_3(t)] = H[C_1 x_1(t) + C_2 x_2(t)] = F_3(t) = C_1 F_1(t) + C_2 F_2(t)$$
$$= C_1 H[x_1] + C_2 H[x_2] \tag{5.74}$$

and the system satisfies the superposition principle, and is a linear system. Classification of systems is shown in Fig. 5.10.
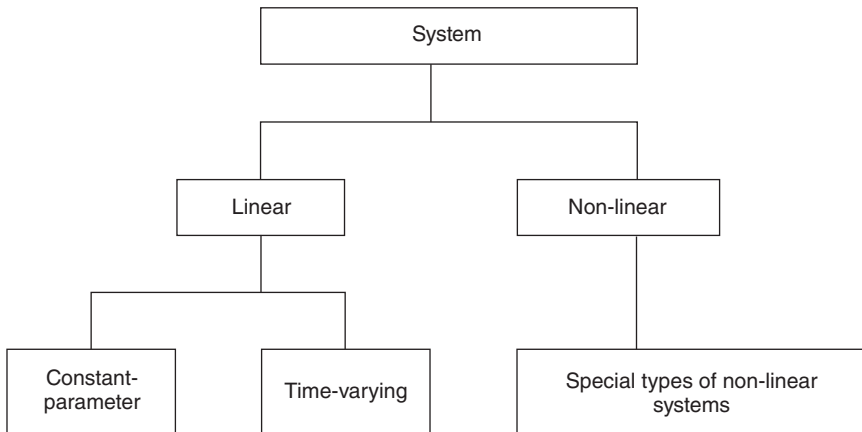
5.10 Classifications of systems.

5.7   Weighting functions

The unit impulse delta function is defined by

$$\begin{cases} \delta(t-a) = 0 & t \neq a \\ \delta(0) = \infty & t = a \end{cases} \tag{5.75}$$

$$\int_{-\infty}^{\infty} \delta(t-a)\mathrm{d}t = 1 \tag{5.76}$$

If $\delta(t-a)$ is multiplied by any time function $f(t)$, as shown in Fig. 5.11, the product will be zero everywhere except at $t = a$, and its time integral will be:

$$\int_{0}^{\infty} f(t)\delta(t-a)\mathrm{d}t = f(a) \quad 0 < a < \infty \tag{5.77}$$

Since $\hat{F} = F\mathrm{d}t = m\mathrm{d}v$, the impulse $\hat{F}$ acting on the mass m will result in a sudden change in its velocity equal to $\hat{F}/m$ without an appreciable change in its displacement.

According to the free non-damped spring–mass system equation with initial conditions $x(0)$ and $\dot{x}(0)$,

$$x = \frac{\dot{x}(0)}{\omega_n}\sin\omega_n t + x(0)\cos\omega_n t \tag{5.78}$$

where ω_n is a natural frequency of the system. The response of a mass–spring system initially at rest and excited by an impulse $\hat{F}$ is:

$$x = \frac{\hat{F}}{m\omega_n}\sin\omega_n t = \hat{F}\,h(t) \tag{5.79}$$
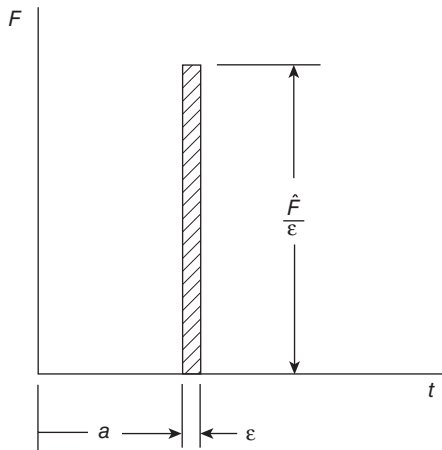
5.11 Unit impulse delta function.

where

$$h(t) = \frac{1}{m\omega_n} \sin \omega_n t \tag{5.80}$$

which is the response to a unit impulse.

When damping is present:

$$x = \frac{\hat{F} e^{-\omega_n \xi t}}{m\omega_n \sqrt{1 - \xi^2}} \sin \sqrt{1 - \xi^2} \, \omega_n t \tag{5.81}$$

where ξ is the relative damping ratio.

$$x = \hat{F} h(t) \tag{5.82}$$

where

$$h(t) = \frac{e^{-\omega_n \xi t}}{m\omega_n \sqrt{1 - \xi^2}} \sin \sqrt{1 - \xi^2} \, \omega_n t \tag{5.83}$$

which is the impulse response function.

For arbitrary force to be considered as a series of impulses as shown in Fig. 5.12, the strength of one of the impulses (shown crosshatched) at time $t = a$ is:

$$\hat{F} = f(a)\Delta a \tag{5.84}$$
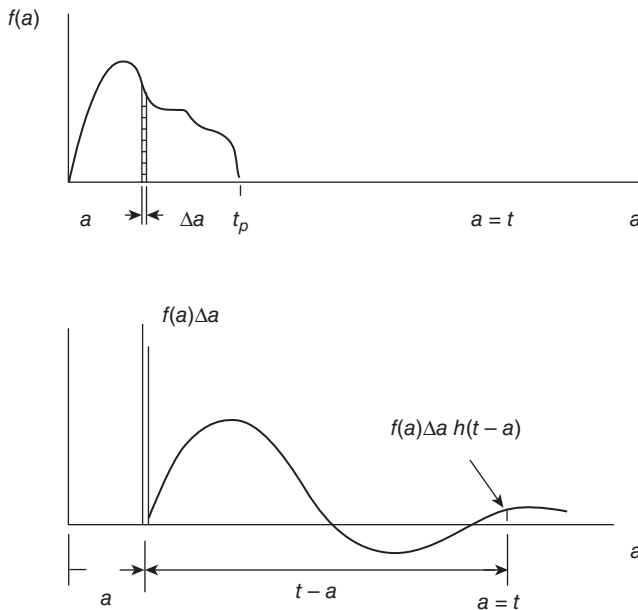
5.12 Excitation force and response.

Its contribution to the response at time t is dependent upon the elapsed time $(t - a)$, or

$$f(a)\Delta a h(t - a) \tag{5.85}$$

where $h(t - a)$ is the response to a unit impulse started at $t = a$. Because the system we are considering is linear the principle of superposition holds.

By combining all such contributions the response to the arbitrary excitation $f(t)$ is represented by the integral:

$$x(t) = \int_0^t f(a)h(t - a)\,\mathrm{d}a \tag{5.86}$$

which is shown in Fig. 5.12. This integral is called the convolution integral. If $\tau = t - a$ then

$$\mathrm{d}\tau = -\mathrm{d}a \tag{5.87}$$

and

$$x(t) = -\int_t^0 f(t - \tau)h(\tau)\,\mathrm{d}\tau = \int_0^t f(t - \tau)h(\tau)\,\mathrm{d}\tau \tag{5.88}$$

For a linear system:

$$x(t) = \int_{-\infty}^{\infty} f(t - \tau)h(\tau)\,\mathrm{d}\tau \tag{5.89}$$

where $h(\tau) = 0$ when $\tau < 0$. $h(\tau)$ is the response of the linear system to the unit impulse delta function input. This relationship is presented in Fig. 5.13.

For a constant-parameter linear system a necessary and sufficient condition for a linear system to be stable is:

$$\int_{-\infty}^{\infty} |h(\tau)|\,\mathrm{d}\tau < \infty \tag{5.90}$$

For a real system to be physically realizable the system cannot respond before the input occurs:

$$h(\tau) = 0 \quad \text{for} \quad \tau < 0 \tag{5.91}$$

$x(t)$ $y(t) = \int_{-\infty}^{\infty} h(\tau)\, x(t - \tau)\,\mathrm{d}\tau$
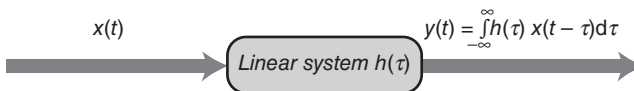
Linear system $h(\tau)$

5.13 Convolution integral relation for ideal constant-parameter linear system.

For constant-parameter systems

$$h(t, \tau) = h(\tau) \tag{5.92}$$

For any linear system, random input data with a theoretical Gaussian probability density function describing its amplitude properties will produce random output data that will also have a theoretical Gaussian probability density function. For a non-linear system, if the random input is a Gaussian process, the random output is a non-Gaussian process.

5.8   Relationship between complex frequency response and impulsive response

If the excitation function $F(\omega)$ in the form of the unit impulse as shown in Fig. 5.14:

$$f(t) = \delta(t), \quad x(t) = h(t) \tag{5.93}$$

is

$$F(\omega) = \int_{-\infty}^{\infty} f(t) e^{-\omega it} dt = \int_{-\infty}^{\infty} \delta(t) e^{-\omega it} dt = 1 \tag{5.94}$$

then the following relationship develops:

$$X(\omega) = F(\omega) H(\omega) = H(\omega) \tag{5.95}$$

From the Fourier transform relationship:

$$x(t) = \frac{1}{2\pi} \int_{-\infty}^{\infty} X(\omega) e^{\omega it} d\omega = \frac{1}{2\pi} \int_{-\infty}^{\infty} H(\omega) e^{\omega it} d\omega = h(t) \tag{5.96}$$
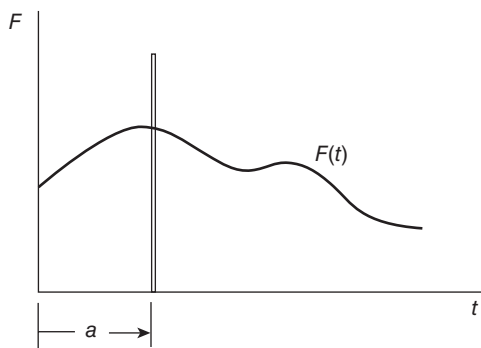
5.14 Excitation force function.

which is

$$h(t) = \frac{1}{2\pi} \int_{-\infty}^{\infty} H(\omega) e^{\omega i t} d\omega \tag{5.97}$$

The inverse Fourier transform relationship of Equation 5.97 gives:

$$H(\omega) = \int_{-\infty}^{\infty} h(t) e^{-\omega i t} dt \tag{5.98}$$

5.9   Frequency response functions

Fourier transforms of both sides of Equation 5.89 give the familiar relation shown in Fig. 5.15 which describes constant-parameter linear systems in the frequency domain, namely:

$$X(f) = H(f)F(f) \tag{5.99}$$

where $X(f)$, $F(f)$ and $H(f)$ are Fourier transforms of $x(t)$, $F(t)$ and $h(\tau)$ respectively, as defined by:

$$X(f) = \int_{-\infty}^{\infty} x(t) e^{-2\pi i f t} dt \tag{5.100}$$

$$F(f) = \int_{-\infty}^{\infty} F(t) e^{-2\pi i f t} dt \tag{5.101}$$

$$H(f) = \int_{-\infty}^{\infty} h(\tau) e^{-2\pi i f \tau} d\tau \tag{5.102}$$

A sufficient condition for $H(f)$ to exist is that this linear system is stable. The lower limit of Equation 5.102 becomes zero for physically realizable systems where $h(\tau) = 0$ for $\tau < 0$.

The complex-valued quantity $H(f)$ is called the frequency response function of the system. It has the following properties:
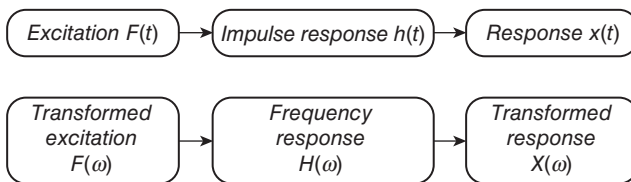
5.15 Block diagram.

$$H(f) = |H(f)|e^{-i\phi(f)} = H_R(f) - iH_I(f) \tag{5.103}$$

$$H_R(f) = |H(f)|\cos\phi(f) \tag{5.104}$$

$$H_I(f) = |H(f)|\sin\phi(f) \tag{5.105}$$

$$|H(f)| = \left[H_R^2(f) + H_I^2(f)\right]^{1/2} \tag{5.106}$$

$$\phi(f) = \tan^{-1}\left[\frac{H_I(f)}{H_R(f)}\right] \tag{5.107}$$

The frequency response function has been widely applied in vehicle noise and vibration measurement and analysis for determination of natural frequency. It is one of the key frequency domain functions applied in modal analysis.

5.10   Bibliography

Bendat, J.S. (1990), *Non-linear System Analysis and Identification from Random Data*, John Wiley & Sons.

Bendat, J.S. and Piersol, A.G. (1985), *Random data – Analysis and Measurement Procedures*, John Wiley & Sons.

Newland, D.E. (1993), *An Introduction to Random Vibrations, Spectral and Wavelet Analysis*, John Wiley & Sons.

Randall, R.B. (1987), *Frequency Analysis*, Brüel & Kjær.

6

Theory and application of modal analysis in vehicle noise and vibration refinement

M. KRONAST, Ford-Werke GmbH, Germany

Abstract: Structural and acoustic resonances can amplify the excitation acting on an operating vehicle to levels that degrade the noise and vibration performance severely. Since one cannot avoid resonances altogether, it is very important during vehicle design to have tools that allow them to be determined and modified. Modal analysis is a mathematical tool that enables engineers to determine characteristic values that describe the resonances and then to build an analytical model from this information. This chapter outlines the theory of vibration, shows how the modal model is derived and discusses the usage of this method in vehicle noise and vibration refinement.

Key words: experimental modal analysis, noise, vibration and harshness (NVH), vehicle sound design, automotive NVH refinement, structural and acoustic resonance.

6.1 Introduction

Every structure or cavity will show a tactile or acoustic response when excited by forces that act on it. Instead of looking at the excitation forces and structural responses in the time domain, it is usual and often more informative to describe these in the frequency domain. If so described, then we will typically see that the amplitudes of both will vary in an uncorrelated way with changing frequency, i.e. a force amplitude decrease going from a lower to a higher frequency may result in either a response amplitude increase, an equal value or even a decrease (see also Fig. 6.1). This behavior is caused by acoustic and structural resonances that will amplify the input excitation at frequencies near the resonance frequency, but that can also attenuate the excitation at frequencies away from the resonance peaks. These resonances can amplify response levels so much that a structure can be destroyed. But even if the structure does not fail, high tactile or acoustic responses are generated that can degrade the noise and vibration performance of a vehicle severely. It is therefore very important to take this into consideration during vehicle noise and vibration development.

Modal analysis is a mathematical tool that is used to determine the characteristic values of the resonances. Based on measurements taken on

117

| Excitation spectrum | | System FRF | | Response spectrum |
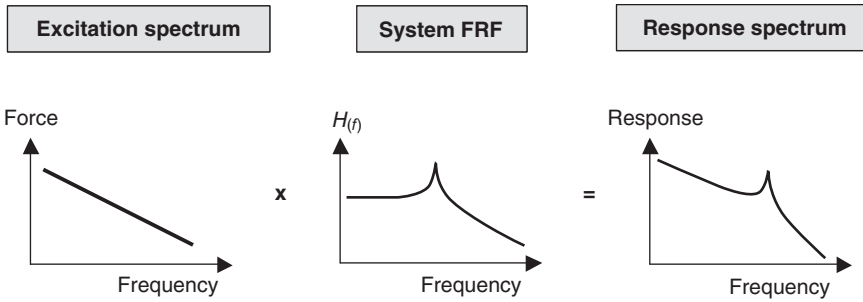
6.1 Distortion of the system response to a linear force input by the transfer characteristics (courtesy of Ford of Europe, Germany).

an existing test object, or using a model of the physical structure or enclosure, the relevant dynamic characteristics can be extracted. With this knowledge the development engineer can plan to avoid having resonances at frequencies with high excitation, or having several resonances very close in frequency to each other, and can therefore reduce the risk of failure or excessively high structural vibration or sound pressure levels. With advances in performance of the test equipment and computer capabilities, modal analysis has become a standard tool in vehicle noise, vibration and harshness (NVH) development throughout the industry.

6.2   Application of modal analysis in vehicle development

For the occupants of a vehicle the operating sound and vibration responses are directly perceivable, contributing to the overall impression of vehicle refinement. It is the development task of the sound and vibration engineer to design the vehicle hardware in such a way that customer expectations, legal requirements and vehicle manufacturing targets with respect to the sound and vibration characteristics are met. This requires a detailed understanding of the complex generation and transfer of sound and vibration to the occupants of the vehicle cabin (Kronast and Hildebrandt, 2000).

A first step in reducing complexity can be attained if the vehicle response is separated into the contributing excitation forces on the one side, and the structural and acoustic properties of the vehicle on the other side. The structural and acoustic properties are then characterized by the sound and vibration transfer functions, which contain all relevant information on the structure's dynamic properties, so these are often also used for comparing vehicles and setting targets. Transfer functions derived by testing a structure can be broken down further through the application of modal analysis. The breakdown into the modal characteristics delivers valuable informa-

```
┌──────────────────┐                    ┌──────────────────────────┐
│  Modal analysis  │                    │ Operating deflection shapes │
└──────────────────┘                    └──────────────────────────┘
          │                                          │
          ▼                                          ▼
Dynamic forces  ┌──────────────────────┐   System responses
   ───────────▶ │ System characteristics│   ──────────────▶
                └──────────────────────┘
                          │
          ┌───────────────┘
          ▼                                          ▼
Imbalance    ┌──────────────────────┐   ┌──────────────────┐
Combustion   │  Natural frequency    │   │     Sound        │
Shock        │  Damping factor       │   │   Vibration      │
Aerodynamic  │  Mode shape vector    │   │    Stress        │
Pressure     └──────────────────────┘   └──────────────────┘
```
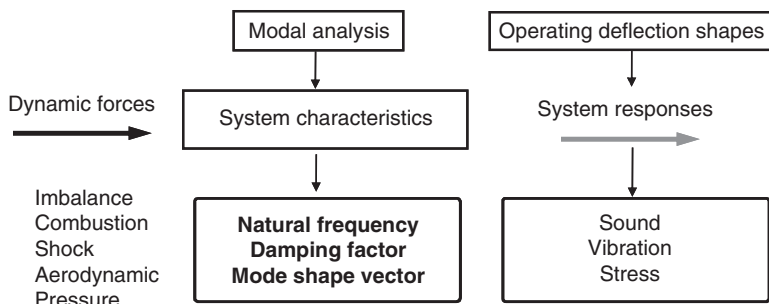
6.2 Contribution of excitation and modal characteristics to a system's forced response (courtesy of Ford of Europe, Germany).

tion for the sound and vibration development engineer, yielding a tool that can be used to assess, change and predict a structure's dynamic properties. In the next sections we will discuss the outlined process.

6.2.1 Spatial, modal and response model

There are several ways to gain an understanding of the root cause of a distinct response. The one with the least amount of analysis work uses sound pressure or vibration data obtained at several locations on the operating vehicle together with a geometrical shape, allowing the generation of 'operating deflection shapes' (ODS) (Johansen and Madsen, 1992). These animated patterns of motion are processed and made visible using a computer. They show areas of high and low response and thus help in identifying the root cause of poor vehicle sound or vibration performance. Near a dominating resonance the ODS can look very similar to an animation of modal analysis eigenvectors, and indeed, as shown in Fig. 6.2, there is a direct relation between a mode shape and an operating deflection shape (de Siqueira and Nogueira, 2001). Often this type of ODS investigation already allows one to draw first conclusions with respect to an NVH concern, but remember that both force excitation and the structural properties are mixed into the result and cannot be separated from each other at this point. When the density of resonances is high but there is no dominating resonance, the ODS will show a complex pattern of motion since several resonances will then be contributing to a deflection pattern at one frequency. At this point it clearly becomes difficult to identify the root cause for an NVH concern.

When the result of an ODS analysis does not yield sufficiently clear information, then modal analysis might be the right tool for the task. Modal analysis employs structural and/or acoustic response data derived through a test with artificial excitation, or a computer model of the object's mass,

Analytical approach (FE)

Physical properties: Modal model:

Mass   Natural frequency   Frequency response
Stiffness   Modal damping   function
Damping   Mode shape vectors

| Acoustic/structural model | Modes | Response properties |

Experimental approach
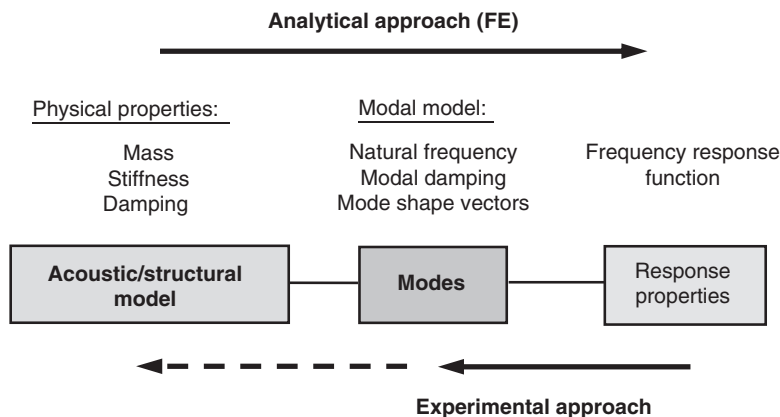
6.3 Analytical and experimental approach to modal analysis (courtesy of Ford of Europe, Germany).

stiffness and damping distribution properties. If the object under investigation fulfills the prerequisites for applying this method, which we will discuss later, then we are able to determine the modes of a structure in a chosen frequency band. Each mode of a structure is characterized by its natural frequency, the modal damping value and the mode shape vectors. Figure 6.3 shows the principle and details for analytical and experimental modal analysis. Avitabile (1998–2008) describes the basics of this method, while Allemang (1992) and He and Fu (2001) present more details.

6.2.2 Application to vehicle NVH development

Having determined the modal parameters as described above, we now have the possibility of formulating a mathematical model of the dynamic properties of the object under investigation (Inman, 2000). This then allows us to calculate the frequency response function, i.e. acceleration/force or pressure/force, between all defined structure points although, in the case of experimental modal analysis, we may not have explicitly measured them. Multiplication of the vibration or noise transfer functions by the respective excitation forces acting on the vehicle and summation of all these contributions then yields the absolute response, or forced response, at the defined response location, as shown in Fig. 6.4. Vice versa, looking at the vehicle development process where absolute vehicle noise and vibration levels are targeted at important response locations, one is now, at least in theory, able to break this down into modal contributions. At the model level the contribution of each mode to the response at a certain frequency can be ranked against the other mode contributions, sensitivity investigations can be performed and the findings can be used to modify the modal model. The
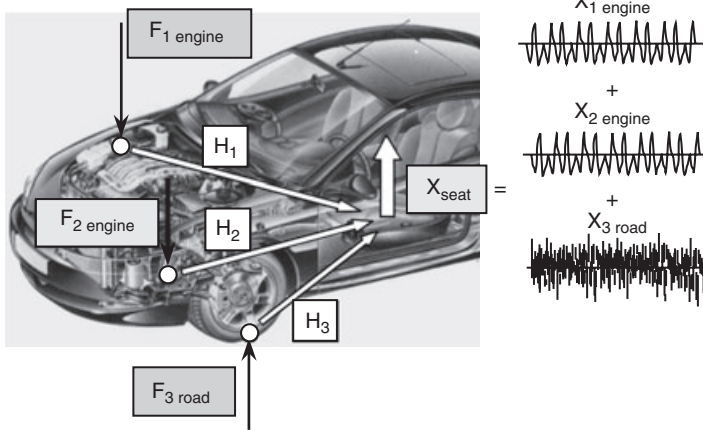
6.4 Multiple excitation and transfer path contributions to the structural response of a vehicle (courtesy of Ford of Europe, Germany).
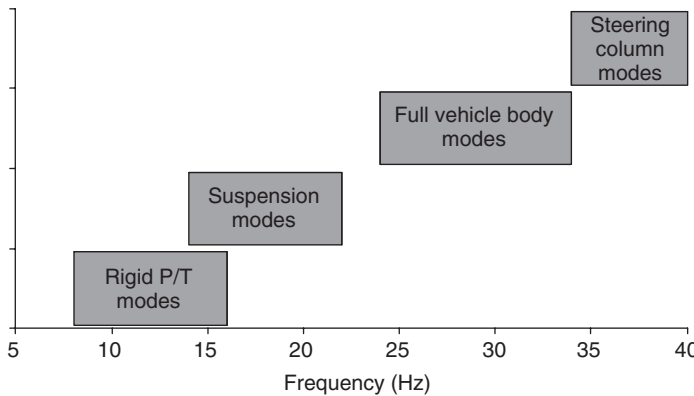
6.5 Typical resonance frequencies of important vehicle systems.

modified model then allows a prediction of how the responses will change if the structural or acoustic dynamic properties of the investigated object are changed. This relation yields a powerful tool for vehicle NVH development.

Often during vehicle development one is not interested in using the modal model to perform calculations. The pure knowledge of a structure's mode frequencies and mode shapes already gives the experienced development engineer sufficient information, enabling him or her to set up a plan for the distribution of these over frequency. This concept is often called modal alignment, although it is really a method to avoid having several modes strongly coupling at one frequency or having a strong excitation and relevant modes near one common frequency. Figure 6.5 shows typical

frequency bands for major passenger vehicle modes. Other usages of the modal properties include the possibility to compare the full vehicle, subsystems or components with competitor dynamic performance, to correlate models to test derived results, or to set targets for system and component development.

6.3   Theory of modal analysis

As shown in Fig. 6.3, determination of the structural dynamic properties can be divided into three steps. The first step is building a physical model, also called a spatial model, which means defining the mass, stiffness and damping distribution for a structure or cavity. The second step is the extraction of the mode frequencies, damping and shapes from this model, which then yields the modal model. Finally, the forced response is derived by applying excitation forces to the modal model (Thomson and Dahleh, 1997). Vice versa, in test-based modal analysis the natural response of a structure to an excitation force is measured. A transfer function is calculated from this data by dividing the acoustic or vibration response by the excitation force. Modal parameters are then derived from these transfer functions (Ewins, 2001; Heylen *et al.*, 1997). In principle it is further possible to derive the spatial model from the test-based modal model, but this is rarely done. In the next sections we will look at the mathematical formulation of the spatial model, see how the modal model is derived from this spatial model and discuss some of its important characteristics.

6.3.1   The physical model

The dynamics of real structures must be represented by a multiple degree of freedom (mdof) model. But a multiple degree of freedom system can be represented by a linear superposition of a number of single degree of freedom (sdof) models. For simplicity we will therefore start our investigations by looking at the characteristics of a single degree of freedom system. Figure 6.6 presents the basic model.
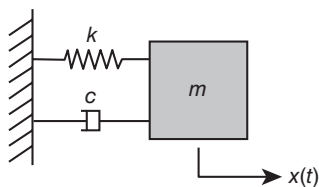
6.6 Free vibration model of a single degree of freedom system.

© Woodhead Publishing Limited, 2010

The governing equation for the free but damped response of this type of system is:

$$m\,\ddot{x}(t) + c\,\dot{x}(t) + k\,x(t) = 0 \tag{6.1}$$

Here the first term containing a lumped mass represents the inertia forces, the second term represents a velocity-proportional viscous damping force, and the third term is the force generated by a linear spring with negligible mass. The solution is assumed to be:

$$x(t) = xe^{st} \tag{6.2}$$

Substituting Equation 6.2 and its derivatives into Equation 6.1 yields Equation 6.3:

$$s^2 + \frac{c}{m}s + \frac{k}{m} = 0 \tag{6.3}$$

This is a quadratic equation whose solutions are:

$$s_{1/2} = -\frac{c}{2m} \pm \sqrt{\frac{c^2}{4m^2} - \frac{k}{m}} = -\omega_n\zeta \pm i\omega_n\sqrt{1-\zeta^2} \tag{6.4}$$

where $\omega_n = \sqrt{k/m}$ represents the undamped natural frequency of the system and $\zeta = c/2m\omega_n$ the damping ratio. Both are important factors that characterize system dynamic properties, oscillation only being possible for a damping ratio below 1. Introducing the above solutions into Equation 6.2 yields the equation of oscillation:

$$x(t) = xe^{-\omega_n\zeta t}e^{i\omega_d t} \tag{6.5}$$

where

$$\omega_d = \omega_n\sqrt{1-\zeta^2} \tag{6.6}$$

is the damped natural frequency of the system.

This result implies that a mode for a damped system consists of two parts, an imaginary part representing the oscillation with a frequency of ω_d and a real part characterizing the decay rate of $\omega_n\zeta$. Figure 6.7 illustrates this behavior.

6.3.2 Forced harmonic vibration

When an excitation force acts on a structure the system is forced to vibrate at those frequencies contained in the excitation spectrum. Although there are many types of excitation it makes sense to consider pure harmonic excitation first. It is often encountered in engineering systems and the analytical handling of the resulting equations is fairly easy. We will therefore
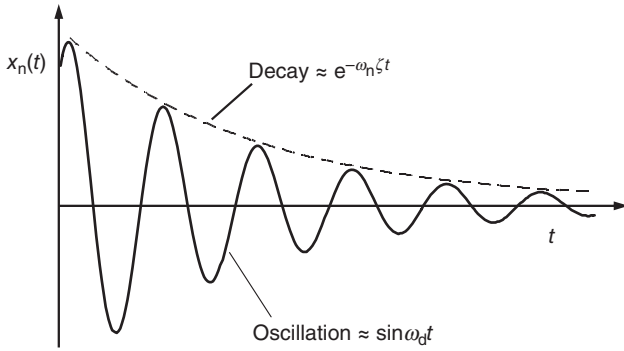
6.7 Real and imaginary solution for the mode of a damped vibration system.

now look at the properties of a viscously damped sdof system undergoing harmonic excitation:

$$m\ddot{x}(t) + c\dot{x}(t) + kx(t) = F(t) \tag{6.7}$$

If we assume that $x(t) = xe^{i\omega t}$ and $f(t) = fe^{i\omega t}$ then we obtain the complex equation:

$$(-m\omega^2 + i\omega c + k)xe^{i\omega t} = fe^{i\omega t} \tag{6.8}$$

Rearranging and substituting ω_n into Equation 6.8 yields the reception form of the system transfer function. This function contains both amplitude and phase information:

$$h_{(\omega)} = \frac{x_{(\omega)}}{f_{(\omega)}} = \frac{1}{m(\omega_n^2 - \omega^2) + i\omega c} \tag{6.9}$$

Figure 6.8 shows a plot of the transfer function on a logarithmic scale. One can distinguish three areas in which one of the influencing factors m, c or k dominates the system response characteristics. For frequencies far below resonance, i.e. $\omega \ll \omega_n$, the transfer function becomes $h_{(\omega \to 0)} = 1/k$. So far below resonance the frequency response function is dominated by the stiffness in the oscillating system. For $\omega \gg \omega_n$ the transfer function reduces to $h_{(\omega \to \infty)} = 1/-m\omega^2$. The response is dominated by the mass of the oscillating system. Finally, for $\omega = \omega_n$ the transfer function can be written as $h_{(\omega = \omega_n)} = 1/i\omega c$. Near resonance the system is dominated by its damping.

These three relations are very important in designing structures. Depending on the relation between the exciting frequency and the system characteristics, one must carefully choose to change either the mass, the stiffness or the damping in a system to best cope with the effects of resonance.
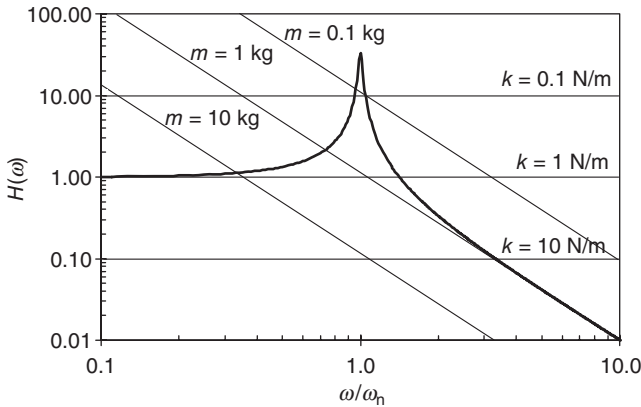
6.8 Single degree of freedom system compliance transfer function
with stiffness (horizontal) and mass (slanted) asymptotes (courtesy of
Ford of Europe, Germany).

6.3.3 Multiple degree of freedom systems and modal properties

In reality the dynamic characteristics of most structures or cavities cannot
be described by a sdof system, but must be modeled as a mdof system. The
equations of a mdof system are similar to that derived in the previous sec-
tions for the sdof system, but now matrices and vectors are used to repre-
sent the numerous contributions to the response. Omitting damping, the
equation for the free vibration of a general mdof system is:

$$[M] \cdot \{\ddot{x}(t)\} + [K] \cdot \{x\} = 0 \qquad (6.10)$$

where $[M]$ is the matrix of mass elements, $[K]$ the matrix of stiffness ele-
ments and $\{x\}$ the vector of displacement versus time. Substituting again an
exponential solution of the form $\{x(t)\} = \{x\}e^{i\omega t}$ and $\{\ddot{x}(t)\} = \omega^2\{x\}e^{i\omega t}$ into
Equation 6.10 yields:

$$([K] - \omega^2[M])\{x\}e^{i\omega t} = 0 \qquad (6.11)$$

The only non-trivial solution for Equation 6.11 is:

$$\det|[K] - \omega^2[M]| = 0$$

This means that we can extract a number of ω_r^2 values, $r = 1, \ldots, N$,
that in this case represent the system's undamped natural frequencies.
Substituting these back into Equation 6.11 yields corresponding displace-
ment vectors $\{x_r\}$ called the mode shape vectors. While natural frequencies
are unique values with a fixed quantity, the mode shape vectors are not.
The mode shape vectors are arbitrarily scaled; the amplitude of the result-
ing mode shape is therefore not unique and fixed. But since the scaling

factor acts on all mode shape vectors in the same way, the mode shape itself is not changed. The following numerical example demonstrates these relationships in more detail.

Although real models may have a very high count of modes, the principles are the same as in very small models. For simplicity we will therefore first study an example of an undamped 2 dof system and derive the modal properties from this system. Finally we will look at some important relations of the modal model.

Numerical example

The system shown in Fig. 6.9 can be seen as a very simple model of a vehicle suspension. The wheel is represented by a lumped mass m with the tire acting as a spring with stiffness $10k$. The attached body is represented by the relevant lumped mass $4m$ and is attached to the wheel by a spring with stiffness k. This is a 2 dof system and we expect it to exhibit two modes. The equations of motion for the free response of this model are:

$$m\ddot{x}_1 + 10kx_1 + k(x_1 - x_2) = 0 \tag{6.12}$$

$$4m\ddot{x}_2 - k(x_1 - x_2) = 0 \tag{6.13}$$

Substituting an exponential solution as in the previous section to Equations 6.12 and 6.13 yields:

$$(10k + k - \omega^2 m)x_1 - kx_2 = 0 \tag{6.14}$$

$$-kx_1 + (k - \omega^2/4m)x_2 = 0 \tag{6.15}$$
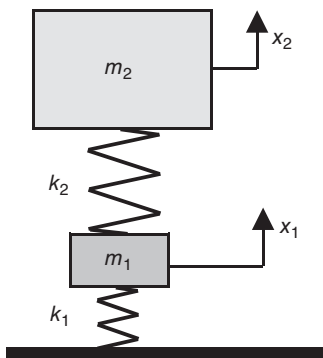
6.9 Free vibration model of an undamped 2 dof system.

Equations 6.14 and 6.15 are satisfied for any x if the following determinant is zero:

$$\begin{vmatrix} (11k - \omega^2 m) & -k \\ -k & (k - \omega^2 4m) \end{vmatrix} = 0 \tag{6.16}$$

This yields the condition that

$$\omega^4 - \frac{45}{4}\left(\frac{k}{m}\right)\omega^2 + \frac{10}{4}\left(\frac{k}{m}\right)^2 = 0 \tag{6.17}$$

If α is substituted for ω^2 then Equation 6.17 is transformed into a quadratic equation for α whose solution is:

$$\alpha_{1/2} = \frac{45}{8}\frac{k}{m} \pm \sqrt{\left(\frac{45}{8}\frac{k}{m}\right)^2 - \frac{10}{4}\left(\frac{k}{m}\right)^2} \tag{6.18}$$

We now have the two modal frequencies of our 2 dof system:

$$\omega_1^2 = \alpha_1 = 11.0232\frac{k}{m}, \quad \omega_2^2 = \alpha_2 = 0.2268\frac{k}{m} \tag{6.19}$$

Assuming $k = 80$ kN/m and $m = 120$ kg, we obtain $f_1 = 13.6$ Hz and $f_2 = 2$ Hz. These are typical modal frequencies for light commercial vehicle suspension systems.

With the knowledge of the modal frequencies we can now determine the ratio of the displacement vectors x. From Equations 6.14 and 6.15 we obtain the two expressions

$$\frac{x_1}{x_2} = \frac{k}{11k - \omega^2 m} = \frac{k - \omega^2 4m}{k} \tag{6.20}$$

Introducing the two modal frequencies from Equation 6.19 into either of these two equations leads to:

$$\frac{x_{1,1}}{x_{2,1}} = \frac{k}{-0.0232k} = -43.1, \quad \frac{x_{1,2}}{x_{2,2}} = \frac{k}{10.7732k} = 0.093 \tag{6.21}$$

This result means that at the higher mode frequency ω_1, the displacement of both masses is opposed in phase, while at the lower mode frequency of ω_2 both masses move in phase. At this stage it is important to realize that the displacement vectors do not possess a fixed value but are arbitrarily scaled and only the ratios of the displacement vectors within one mode are fixed. We therefore choose to set the vectors $x_{1,1}$ and $x_{1,2}$ to 1 and scale the other vector so that the displacement ratio is retained. One thus obtains vectors that are called normal mode shapes and often designated by $\Phi_{i(x)}$. In our example the two normal mode shape vectors are

$$\Phi_{1(x)} = \begin{Bmatrix} 1 \\ -0.0232 \end{Bmatrix}, \; \Phi_{2(x)} = \begin{Bmatrix} 1 \\ 10.8 \end{Bmatrix} \qquad (6.22)$$

6.3.4 Properties of the eigenvalues

The modal model possesses some important properties. These are known as the orthogonal properties of the eigenvectors. It can be shown that the eigenvectors are orthogonal to the mass and stiffness matrices. If $\omega_i^2 \neq \omega_j^2$, i and j being two different modes, then the following relationships exist:

$$\{x\}_i^{\mathrm{T}} \cdot [M] \cdot \{x\}_j = 0 \qquad (6.23)$$

$$\{x\}_i^{\mathrm{T}} \cdot [K] \cdot \{x\}_j = 0 \qquad (6.24)$$

Substituting the normal mode shape vectors and masses from our above example into Equation 6.23 demonstrates that our modal model is orthogonal.

$$(1 \quad -0.0232) \cdot \begin{bmatrix} m & 0 \\ 0 & 4m \end{bmatrix} \cdot \begin{Bmatrix} 1 \\ 10.8 \end{Bmatrix} = (1 \quad -0.0232) \cdot \begin{Bmatrix} m \\ 43.2m \end{Bmatrix} = m - m = 0$$

The same result can be obtained when using Equation 6.24. Finally, if $i = j$ then Equations 6.23 and 6.24 yield:

$$\{x\}_i' \cdot [M] \cdot \{x\}_i = [m_i], \qquad \{x\}_i' \cdot [K] \cdot \{x\}_i = [k_i]$$

The elements on the right-hand side of both equations are called the modal or generalized mass and stiffness. Often the mode shape vectors are scaled with the generalized mass.

6.4   Methods for performing modal analysis

As shown in Fig. 6.3 there are two methods for performing modal analysis. When hardware is available, a test-based modal analysis is possible. In the case of benchmarking of competitor products experimental modal analysis is the only tool available to extract modal information. If a model of the mass, stiffness and damping distribution within a structure is available, then the modal model can be derived by digital calculation. In both cases the modal model can then be used further to perform sensitivity analysis, modification and transfer function prediction. We will now discuss in more detail the application of the two methods in vehicle development.

6.4.1 Test-based modal analysis

The application of test-based modal analysis in road vehicle development became more widespread with the introduction of computers and high-

performance data acquisition equipment in the 1980s. Although equipping a test facility with the necessary software and hardware for multi-channel transfer function measurements and modal analysis is very expensive, in the order of $250,000, test-based modal analysis has become a standard tool throughout the automotive industry. In the vehicle development process it is most often used for benchmarking competitor products, and obtaining a modal status of prototype and production vehicles and their components, e.g. for correlation with FE models or for noise and vibration problem solving. There are some further niche applications, among others determining the center of gravity/inertia characteristics of a structure or determining the equivalent point static stiffness from a single measured transfer function.

An experimental modal analysis can be divided roughly into four stages: first, setup of the test object; second, acquisition of the measurement data; third, test data analysis and determination of the modal model; and fourth, application of the modal model for prediction purposes. With hardware unavailability early in the vehicle development process and the evolution of finite element modal analysis, prediction from test-based modal models has become somewhat less important. In the next section we will therefore focus on the first three stages of experimental modal analysis.

6.4.2   Test object setup

At the beginning of an experimental modal investigation the response locations for the test object need to be defined. The response locations must be chosen so that the mode shapes in the frequency band of interest can clearly be identified during analysis. This means that test objects with high complexity, i.e. structures built up from many components, afford a higher number of response locations than simple structures. An investigation of the global modes of an automobile body structure up to 100 Hz may require only 40 response locations, while the analysis of a complete vehicle up to the same frequency may require 100 and more. The frequency band of interest is another factor when planning the response locations. With increasing frequency the distance between the individual response locations must be reduced, since wavelengths on the structure reduce and higher-order mode shapes are encountered. Once the response locations are defined they are marked on the structure and the geometric positions measured. With this data a grid model is created in the analysis software which afterwards allows one to view the animated mode shapes.

After the definition of the response geometry the test object is set up in the laboratory. There are two possibilities for supporting the test object. The simplest is a suspension which resembles free–free boundary conditions. This means that the test object's possibility of moving freely in space
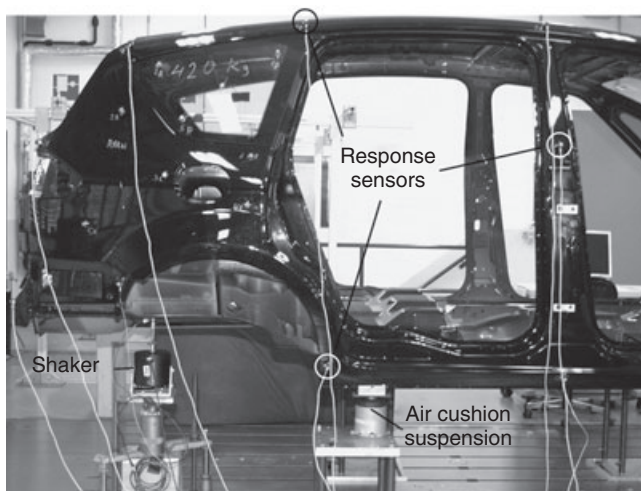
6.10 Unified vehicle sheet metal body setup on air mounts for the measurement of vibration transfer functions. An electrodynamic shaker is attached to the right rear rail for vertical excitation. Small magnets are attached to the thin panels for mass compensation and 3-D sensors measure the vibration response (courtesy of Ford of Europe, Germany).

is restricted as little as possible. In this case the structure is often suspended by soft elastic cords or supported on very soft springs, e.g. air-filled tubes. This separates the six rigid body modes by ideally a factor of 10 in frequency from the lowest frequency flexible test object mode, thus avoiding interaction between rigid and flexible modes. Figure 6.10 shows a vehicle body structure setup to determine the required transfer functions.

When subsystems or components are to be tested, their modal characteristics are often very different from the case when they are attached to the vehicle structure. If a test of these on the vehicle in normal built-in conditions is not possible, the setup becomes more difficult. The subsystem or component must then be attached to a rig for which the attachment points exhibit similar impedance characteristics as the vehicle attachments, or at least the rig modes must be well outside the frequency band of interest. This is important in order to avoid interference from resonances that are characteristic of the rig structure but have nothing to do with the modes of the test object under investigation.

When the test object is set up for data acquisition the excitation locations must be chosen. The most important requirement here is that all modes in the frequency band of interest are excited. For simple structures where one has a good idea of what modes can be expected, it is sufficient to use only one excitation location. For more complex structures or with less knowl-

edge it is often better to apply excitation at two or more locations, in order to reduce the risk of having the excitation near nodal points and therefore not exciting some of the modes. For investigations on the sheet metal body of a car, excitation may be applied at the front and rear load-carrying rails to excite the structure in the vertical and lateral directions. On a complete car additional excitation locations can be used in the middle of the tunnel and on the powertrain.

Two types of excitation mechanisms are commonly used (Brown *et al.*, 1977). The first is a hammer that has a force transducer attached to the tip with which the test object is impacted. This type of excitation is of a transient type and avoids adding an additional system to the test object. When roving excitation measurements are to be made, a hammer reduces the time required to change positions. On the other hand it is more difficult to choose and control a specific excitation force spectrum as closely as with an electrodynamic shaker.

For vehicle structures the electrodynamic shaker is more often used to obtain the necessary frequency response function data. It must be attached carefully to the structure, avoiding force inputs in other directions than the intended, avoiding resonances of the attachment structure, often a rod or wire, and avoiding grounding which can induce unwanted reactions, especially when more than one shaker is used in the setup. On the other hand, since the exciter stays attached to the structure during the entire measurement, it is now possible to measure the driving point with a common element for force and acceleration, called an impedance head. This setup comes very close to the ideal one-point impedance measurement. Also, the amplitude, frequency band and type of excitation can now be controlled very well. A practical disadvantage is of course that the equipment is much more expensive than a hammer, and that changing the excitation location requires more time.

6.4.3   Pre-investigations and data acquisition

The excitation point, also called the driving point, is a very important part of a modal test. It is therefore understandable that some prerequisites that govern modal analysis are checked here before data acquisition. At the driving point where by definition the excitation force and acceleration response act exactly at the same location, the imaginary part of the measured point impedance must exhibit peaks at the resonance frequencies that are all either positive or negative. Since modal analysis is a method based on the linear behavior of a structure, this also needs to be checked. The input force is varied and the resulting measured transfer functions should be checked for changes of resonance amplitudes or frequency shifts. For a multiple excitation setup it is important that the individual excitation
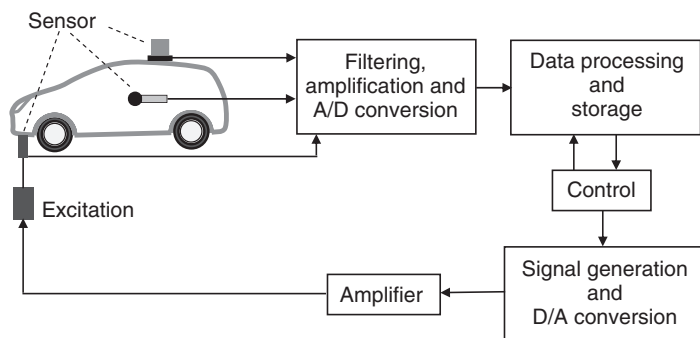
6.11 Excitation and data acquisition equipment layout for the measurement of transfer functions.

spectra are not coherent. If this is the case then the reciprocity of the transfer functions between the driving points can also be checked. A typical measurement equipment setup for the determination of structural and acoustic transfer functions is shown in Figure 6.11.

When the number of measurement locations exceeds the available data acquisition channels on the measurement equipment, the measurements must be taken in several groups over a certain period in time. This is especially true for data acquisition on complex test objects such as a full vehicle where a high number of response locations are required. Here every effort must be made to ensure the integrity of the measurement data, otherwise subsequent analysis of the test data will become difficult or impossible. Complex test objects can change their dynamic characteristics over time, therefore it is essential to track any such changes. This can best be done either by comparing transfer functions of response locations that are not changed during the entire test, or by tracking the driving point frequency response functions for the entire test. Another concern arises from the small but sometimes not negligible mass loading through the accelerometers themselves. This can be avoided by adding dummy masses of equal weight as the sensors to locations where no accelerometers are positioned during a group measurement, and where a not negligible sensitivity to a mass change is presumed.

With a well-prepared test object setup and good results from the pre-investigation, data acquisition is a straightforward task. If the dynamic characteristics of the structure under investigation are susceptible to changing environmental conditions, e.g. effect of temperature on certain materials, then these conditions must be controlled. It is in any case best to try to get all required data in as short a time as possible. Figure 6.12 graphically illustrates the process.
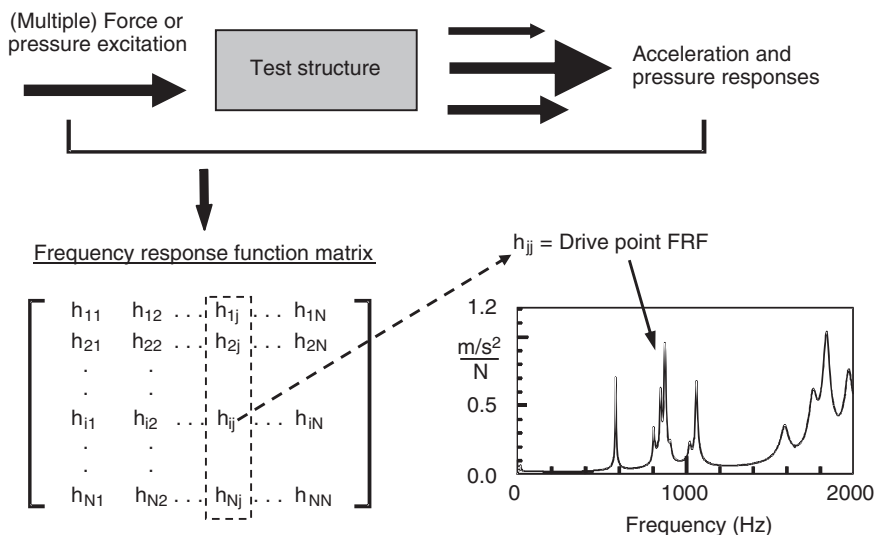
6.12 Example of the data acquisition of transfer functions as required for modal analysis (courtesy of Ford of Europe, Germany).

6.4.4 Data analysis

Before commencing the modal analysis of the measured transfer function data some sanity checks should be done. Transfer functions should show the mass and stiffness line asymptote behaviors already discussed in Section 6.3.2 and shown in Fig 6.8. If these inspections are passed then one can gain an initial overview of the investigated structure's dynamic characteristics by calculating the summation and mode indicator functions: see Fig. 6.13. The summation function is calculated by summing the amplitudes of all measured transfer functions, omitting the phase information, and then normalizing with the number of measured data sets. The resonance peaks are pronounced and one can get a good idea of frequencies that exhibit strong modes and areas of high modal density. For complex test objects the summation functions for subsystems and components can also be calculated. The overview is complemented by the mode indicator function that shows a sharp drop to zero where resonances are detected.

The next step is that of extracting the modal frequencies, modal damping and mode shape vectors from the matrix of transfer function data. This process is often called curve fitting (Lembregts, 1989), which basically means that analytical functions are fitted to the measured individual response functions such that the difference between the measured response function and the analytical expression is minimal. An example of this process will be shown below for a very simple case study, but for more complex systems a computer software package must be used. The modern
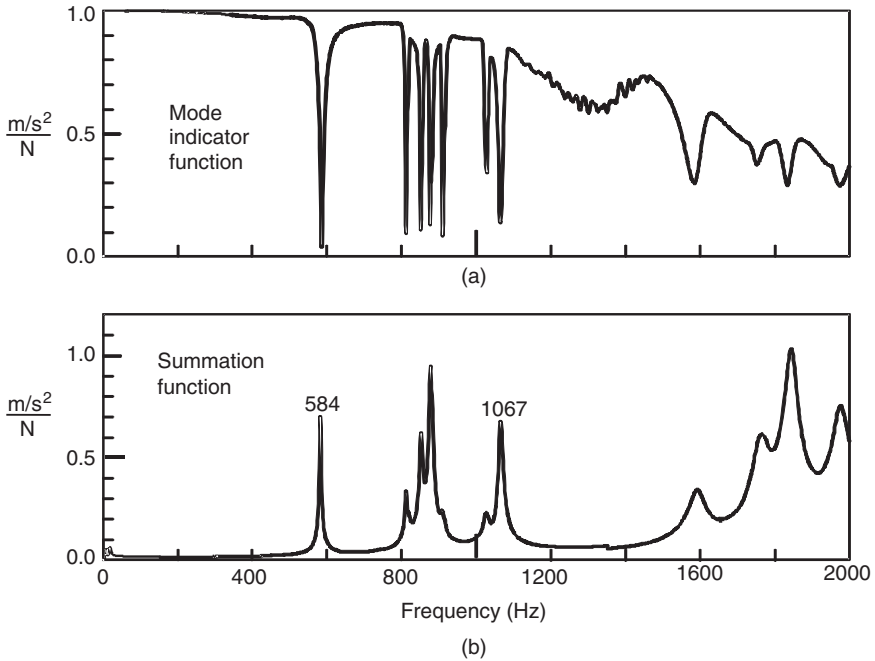
6.13 (a) A mode indicator function dip towards zero indicates the presence of a mode. (b) The summation function enhances resonance peaks. Both give a first impression of mode strength and distribution (courtesy of Ford of Europe, Germany).

poly-reference algorithms implemented in these packages work in the time or frequency domain and are capable of fitting multiple modes across multiple response functions for a number of references.

If we assume damping to be proportional to the stiffness, then the formulation for the problem we are trying to solve is:

$$[K]+i\omega[C]-\omega^2[M]=\left(\frac{\{x\}}{\{f\}}\right)^{-1} \tag{6.25}$$

For a single degree of freedom system the solution of this equation is simple, but for large multiple degree of freedom systems this becomes very inefficient since the inversion of large matrices need to be calculated. Therefore a different formulation of this equation is used. The new formulation can be derived by pre- and post-multiplying Equation 6.25 by the eigenvector matrices $[\Phi]^T$ and $[\Phi]$. For the transfer function of a sdof system this then results in:

$$h_{(\omega)}=\frac{\Phi^2}{(\omega_r^2-\omega^2)+i\omega\dfrac{c}{m}} \tag{6.26}$$
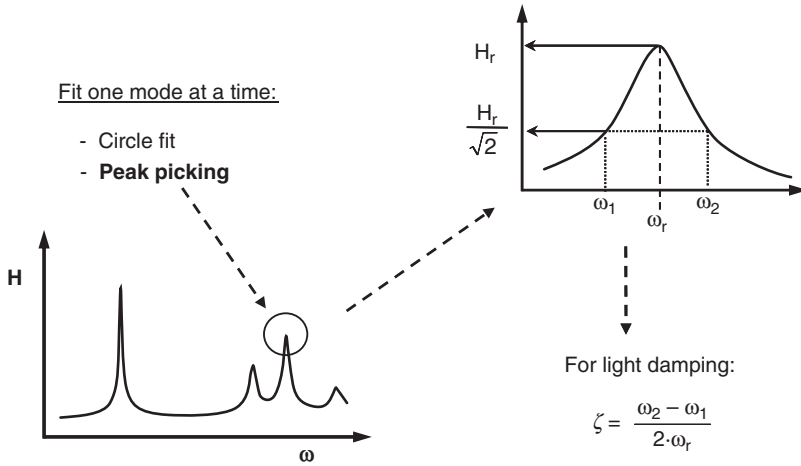
6.14 Example of the determination of the modal frequency and damping by the simple peak picking method.

To illustrate the process of extracting the modal data we will apply a simple method that has been in use for a long time called the peak picking method: see also Fig. 6.14. This method can be applied when the modes are clearly separated from each other and the damping is light, so that contributions from other modes are negligible. Very often this is not the case, but the method is adequate to get a first estimate on the measured transfer function data. We are now looking for a solution to Equation 6.26. The unknowns in this equation are the modal frequency, the modal damping and the mode shape.

First a resonance peak from the plot of the measured transfer function is chosen and the corresponding resonance frequency is read from the frequency axis. Then the half power points to both sides of the chosen reso-nance peak are defined by following the amplitude of the plotted frequency response function downwards until it reaches an amplitude equal to the resonance peak amplitude value divided by $\sqrt{2}$. These points are called the half power points. Again the corresponding frequencies are read from the frequency axis. If the damping is light, i.e. below 3%, then we can calculate the damping factor to be:

$$\zeta = \frac{\omega_2 - \omega_1}{2\omega_r} \tag{6.27}$$

With $2\zeta\omega_r = \dfrac{c}{m}$ we have a solution for the damping. The only unknown left, Φ^2, can now be calculated directly from Equation 6.26. This factor is often represented by an A and is called the modal constant or residue. When the investigated system contains more than one mode, which will be the usual
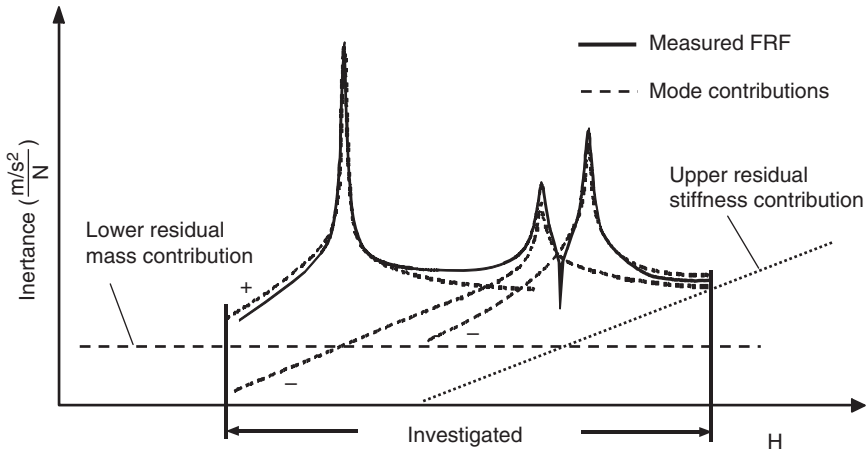
6.15 Mode and residual contribution to a transfer function (courtesy of Ford of Europe, Germany). The signs of neighboring modes govern whether the transfer function exhibits a smooth or a sharp (anti-resonance) transition between peaks.

case for real structures, then the transfer function between two locations will have several single degree of freedom contributions: see Fig. 6.15. The governing equation then becomes

$$h_{i,j}(\omega) = \sum_{r=1}^{n} \frac{\Phi_{i,r}\Phi_{j,r}}{(\omega_r^2 - \omega^2) + i\omega\frac{c_r}{m_r}} \tag{6.28}$$

where r denotes the respective mode number.

6.4.5   Predictive modal analysis

If minor structural changes are made to an existing product then very often these can be cobbled and one has hardware available for an experimental modal investigation. But at the beginning of a vehicle development process for a fully new product, or when major structural changes have been made, there is no hardware available that fully represents the final dynamic characteristics. Since it is not possible to wait for the availability of hardware, which is usually the case, it becomes inevitable that one finds a different means of deriving these. It is therefore usual to use predictive methods based on design intent and using experience from earlier correlation work done on predecessor structures to drive noise and vibration decisions early in a vehicle development program. Here finite element analysis, where mass, stiffness and damping are distributed across a known geometry, and methods that model the structure with lumped masses connected with

springs and damping elements are most commonly used. Since these methods are described in detail in other chapters of this book, we will concentrate in this section on a comparison of experimental and predictive CAE tools, outlining how to best utilize both in developing the required refinement of vehicle noise and vibration.

The increase in performance and confidence for the predictive methods has changed the distribution of modal analysis work between test-based and predictive methods. Today CAE models are used to give design guidance on increasingly complex models, i.e. comparison of dynamic properties such as the frequency response functions for complete vehicle models, and this development is being backed and accelerated by the industry. But the dynamic behavior of a full vehicle is still so complex that both methods are often used in parallel.

When first CAD models of the future product become available, these are taken and, e.g., finite element models created. These models can then be used for forced response or modal analysis calculations. The first step here is to create a grid across the substructures, components and possible cavities, the finite element grid, on which the equations representing the acoustic and structural motion are solved. The substructure and component models are then joined to form the complete vehicle model. At this stage the boundary and coupling conditions must be defined, which is an important and often difficult task.

For full vehicles the meshes have hundreds of thousands of elements, compared to maybe 150 measurement points in experimental investigations. This high element count is necessary if the details of the structure are to be represented properly, which for the test-based analysis is given by the hardware, but they make the work of creating the model, the meshing, more time-consuming and also prolong the time required for computation. This is a serious concern since further refinement of the grids is sometimes considered necessary in order to even better represent important design details of the vehicle. Therefore a balance between the required accuracy of the model and the restrictions in time available for vehicle development is required. The fine distribution of elements leads to the FE model picking up more modes than a test-based model. On the one hand this is an advantage, since the resulting modal model is more 'complete' than the test-based model; on the other hand the evaluation of the FE data is more difficult and again time-consuming since many of the calculated modes are not important for the noise and vibration characteristics of the vehicle as experienced by the passengers.

The predictive models are in general of linear type, the damping often modeled as being proportional to the mass and stiffness matrices. In reality the full vehicle exhibits non-linear behavior and this is a point of concern. But this problem also affects the experimental modal analysis investigation,

since the applied excitation forces during a modal test are seldom equal to the forces acting during operation. A typical example is the suspension modes of the vehicle. The piston that moves in the damper strut during on-road driving requires a minimal force to overcome the stick friction. Modal tests seldom reach an excitation level as encountered in real vehicle operating conditions, therefore modal values are not correct in this case. So both approaches struggle with the non-linear behavior of the object under investigation.

The assumption of damping being proportional is also not strictly applicable but makes solution of the finite element problem easier. When damping is chosen to be proportional to the mass and stiffness matrices, the equations can be solved for the undamped case first and the results corrected for the effects of damping afterwards. Further simplifications often need to be made, i.e. one global damping value defined over the entire structure and frequency band of interest. Since the damping encountered in vehicles is mostly at or below 3% critical damping, this assumption does not affect the mode frequency or mode shapes very much, but it does have a strong effect on amplitudes. But it is the amplitudes that engineers have set targets for and are therefore interested in most. Here one must conclude that the prediction of absolute values today is confined to simple structures, and noise and vibration predictions for full vehicles are best used in an A–B comparison to give a design direction. Defining a correct damping is a critical skill and it is here that an intensive exchange between both experimental and predictive tools is a prerequisite for success.

For practical engineering it is not sufficient to describe only the dynamic properties of a full vehicle or its systems in the form of a modal model, but it is also important that in the case when requirements are not met, some indication of what needs to be done is given. Since FE models possess a fine representation of a structure they can also deliver detailed structural change proposals for the vehicle. The modal model extracted from test-based analysis is restricted to structural optimization of general mass, stiffness or damping changes between the rather coarse positions of the response locations. This is a clear drawback in the development of a vehicle's dynamic properties.

In modal analysis, be it test-based or predictive, much depends on the expertise of the engineer doing the evaluation. In the test-based analysis process the evaluator decides how to analyze the data, determining the modal frequency and damping by his or her own judgment and giving the mode shapes a description. The FE engineer does not have to decide what modal frequencies to include in the modal model, but the much higher number of modes derived from the calculation must be evaluated, and also mode shape descriptions must be formulated. The mode shape description can then be used for correlation or sign-off against set mode shape targets.

But in any case, it is a demanding task to manually order two sets of mode shapes for comparison, and one would wish to have a more automated tool to do this. There are parameters available that allow a comparison of mode shapes, be it from calculation or test. The modal scale factor, MSF, and modal assurance criterion, MAC, allow the comparison of two vectors. The MSF gives an estimate of the ratio between two vectors, the MAC a correlation factor describing whether the vector is orthogonal or not. Some investigations have been conducted towards the usage of these two values to automate mode shape comparisons, but unfortunately with only limited success. For full vehicle mode shapes it is still inevitable to visually inspect and agree on an individual description before commencing with the task of correlating two sets of mode shapes.

Last but not least is the fact that a model describes the design intent. When a prototype or series hardware is finally built from this design, then it is certain that there will be deviations and in the case of a series production additional spread within the individual vehicles. This must be kept in mind when correlating models to experimental data, not expecting to find identical properties but realizing that there will be a certain variation. Of course it would be best to investigate a number of test objects to have an idea of the variation and this has been done in single projects. Within the constraints of usual vehicle development this is impossible since sufficient hardware is often not available for testing, and since experimental modal investigations are very resource and time demanding, so that the final result will come too late for actual program application.

6.5   Limitations and trends

The limitations already discussed for test- and model-based modal analysis define the future trend for the application of this method in vehicle design. The use of model-based predictive methods will continue to increase, the focus being on raising the confidence levels when working with complex structures such as full vehicle models, and reducing the time required for the investigation. This method can be applied early in the design process without the need for expensive prototype hardware and facilities and it can give direct design recommendations. The use of test-based modal analysis has declined and might be decreased further, but one cannot avoid it altogether. Correlation of complex structures and benchmarking of competitor products require an experimental input.

To keep up with the growing expectations, experimental modal analysis has been adapted to specific test applications. Mass loading of a test structure through sensors can change the dynamic properties, especially in the case of very light objects such as a sheet metal oil pan, quite a bit. The application of a scanning laser doppler vibrometer helps to avoid this error

(Stanbridge and Ewins, 1999). The upper frequency limit of a modal test depends on the spacing between the response sensors. Holographic modal tests allow the analysis of high frequency and narrow spaced modes (Klingele *et al.*, 1996).

In vehicle sound and vibration analysis there is often a strong coupling between structural and acoustic modes. Modal analysis methods have therefore been developed that allow simultaneous measurement and analysis of the acoustic and structural transfer functions (Wyckaert *et al.*, 1996). Modal-based damage identification methods are not related to sound and vibration refinement, but are an important application of modal testing in failure analysis and prevention (Farrar and Doebling, 1997).

In recent years experimental modal analysis has been extended to a method called operational modal analysis (OMA). In classical experimental modal analysis the test object is built up in a laboratory and artificially excited. The excitation forces are therefore known and used to calculate the required transfer functions to the driving points. For an OMA the test object is investigated in usual operating conditions and only the responses of the system are measured. Since in general there is no defined information on the location and type of the excitation, apart from the engineer's knowledge of the system, the task is to extract the structural modes from the data without getting 'modes' originating from peaks of the excitations. The advantage of this method is that the investigation can be done in the usual environment and with excitation forces encountered when the test object is normally operated. This method is already being used among others for investigations of civil structures such as buildings, bridges and oil platforms, and in the aerospace and automotive industries (Ventura and Gade, 2005).

6.6   References

Allemang R (1992), *Vibrations: Analytical and Experimental Modal Analysis*, UC-SDRL-CN-20-263-662, University of Cincinnati, OH.

Avitabile P (1998–2008), Modal space – back to basics, *Experimental Techniques*, Volume 22, No. 2 to Volume 32, No. 1 and ongoing, http://sem.org/TDIV-ModalAnalysis.asp

Brown D L, Carbon G D and Ramsey K (1977), Survey of excitation techniques applicable to the testing of automotive structures, SAE 770029.

de Siqueira L P and Nogueira F (2001), Application of modal analysis and operating deflection shapes on the study of trucks and buses dynamic behavior, SAE 2001-01-2780.

Ewins D J (2001), *Modal Testing, Theory, Practice and Application*, Research Studies Press, Letchworth, Herts, UK.

Farrar C R and Doebling S W (1997), 'An overview of modal-based damage identification methods', Proc. DAMAS Conf.

He J and Fu Z F (2001), *Modal Analysis*, Butterworth-Heinemann, Oxford.

Heylen W, Lammens S and Sas P (1997), Modal analysis theory and testing, *International Seminar on Modal Analysis*, KU Leuven, Belgium.

Inman D J (2000), *Engineering Vibrations*, Prentice Hall, Englewood Cliffs, NJ.

Johansen S and Madsen K D (1992), Operating deflection shapes – a fast developing technique, *Proc. 10th Int. Modal Analysis Conf.*

Klingele H, Steinbichler H, Freymann R, Honsberg W and Haberstok C (1996), Holographic modal analysis for the separation of narrow-spaced eigenmodes, *Second Int. Conf. on Vibration Measurements by Laser Techniques, SPIE*, Vol. 2868, pp. 412–417.

Kronast M and Hildebrandt M (2000), A high speed boom investigation of a mid-size car using experimental vibro-acoustic modal analysis, *18th Int. Modal Analysis Conf.*

Lembregts F (1989), Parameter estimation in modal analysis, *Proc. ISMA*, Vol. 14, p. 33.

Stanbridge A B and Ewins D J (1999), Modal testing using a scanning laser doppler vibrometer, *Mechanical Systems and Signal Processing*, Vol. 13, pp. 255–270.

Thomson W T and Dahleh M D (1997), *Theory of Vibration with Applications*, Prentice Hall, Englewood Cliffs, NJ.

Ventura C and Gade S (2005), *Operational Modal Analysis course*, IOMAC, Copenhagen.

Wyckaert K, Augusztinovicz F and Sas P (1996), Vibro-acoustical modal analysis: reciprocity, model symmetry and model validity, *JASA*, Vol. 100, pp. 2877–3465.

7

Mid- and high-frequency problems in vehicle noise and vibration refinement – statistical energy analysis and wave approaches

X. WANG, RMIT University, Australia

Abstract: Starting from the statistical energy analysis (SEA) modal approach, energy sharing between two oscillators and energy exchange in a multi-degree-of-freedom system are discussed, from which the SEA power balance equations are derived. Application procedures of the SEA approach are presented and the main SEA assumptions are highlighted. In order to introduce the SEA wave approach, room acoustics is reviewed; the SEA conceptual parameters such as wave number, wave number space, dispersion and modal density for energy storage are defined. In regard to energy transmission, the concepts of direct and reverberant fields, as well as coupling loss factors for different connections, are illustrated; panel acoustic radiations are introduced and evaluated; transfer matrices and insert loss of a trim lay-up are demonstrated; and leaks and aperture effects are discussed. For energy inputs, direct field impedance and input power are illustrated; distributed random loading and turbulent boundary layer loading are defined; and concepts of diffuse acoustic field loading and propagating acoustic field loading are explained. The hybrid deterministic and SEA approach is briefly introduced. An application example of vibro-acoustic analysis on a passenger car roof–cabin cavity system is given to validate the SEA approach.

Key words: modal oscillators, damping loss factor, phase velocity, group velocity, wave number, dispersion property, direct field, reverberant field, diffuse reverberant field, energy input, energy transmission, energy storage, coupling loss factor, acoustic leakage, noise control treatment, poroelastic materials, trim lay-ups, transfer matrix, insert loss, radiation efficiency, mean energy, clamped systems, blocked subsystems, critical wavelength, critical frequency, hybrid deterministic and SEA approach, SEA modal approach, SEA wave approach, distributed random loading, turbulent boundary layer loading, diffuse acoustic field loading, propagating acoustic field loading, acoustic impedance, transmission coefficient, mass law, non-resonant acoustic energy transmission, resonant acoustic energy transmission, energy density, power flow, modal count, wavelength.

7.1 Introduction

Engineering systems with noise and vibration problems are investigated in a model of source, path and receiver where the source can be quantified or modified by changing its frequency content, levels, etc.; the path can be

142

quantified or modified by changing mass, stiffness and damping or changing geometry, adding isolators, foams, fibres, etc.; and the receiver can be quantified or optimized by design for subjective response, sound quality, reduction in levels, etc.

In order to predict noise and vibration, classic low-frequency approaches are applied to establish system dynamic properties or system dynamic equations in a large number of degrees of freedom by use of finite element dynamic analysis or an experimental modal analysis method, then to calculate the system responses from excitation and the dynamic properties or equations. For a typical saloon car, there are 3×10^6 structural modes and 1×10^6 acoustic modes at frequencies less than 10 kHz. Higher-order modes are extremely sensitive to uncertainties in boundary conditions, material properties and physical properties. It takes a long computational time to solve the dynamic equations in the large number of degrees of freedom in the high frequencies, and the results of the solutions are uncertain due to the uncertainties caused by the material, manufacturing and assembly process variations as shown in Fig. 7.1. This is because subsystem properties and boundary conditions are not known precisely; short-wavelength responses in higher-order modes are very sensitive to small uncertainties. Therefore, traditional deterministic analysis methods are not appropriate for problem solutions at high frequencies due to the expense and amount of detail required. Alternative approaches are needed for high-frequency noise and vibration prediction.

Statistical energy analysis (SEA) was originally developed in the 1960s as a method of predicting the high-frequency response of dynamic structures [1]. Statistical energy analysis is a field of study in which subsystems are statistically described in order to simplify the analysis of complicated structural–acoustic problems; the 'S' indicates systems drawn from a population or ensemble, 'E' represents the fact that energy is the primary response quantity of interest, and 'A' illustrates that SEA is an analysis frame instead of one method. The power injection method and experimental techniques in comparison with analytical calculations such as impedance/modal density calculations were developed in the 1970s. Commercial codes such as VAPEPs, SEAM, AutoSEA, etc., appeared in the 1980s. Leppington *et al.* [2] proposed radiation efficiency formulations and *k*-space approaches; more generic coupling loss factor calculations based on line wave impedances were developed in the 1990s. Langley and co-workers [3–6] generalized the wave approach and developed the hybrid FEA–SEA method; based on the wave approach, variance estimation of energy variables was extended to generic subsystems in the 2000s [7].

In SEA, the whole structure and acoustic cavity system are considered as a network of subsystems coupled through joints. A subsystem is defined as a finite region with a resonant behaviour, involving a number of modes
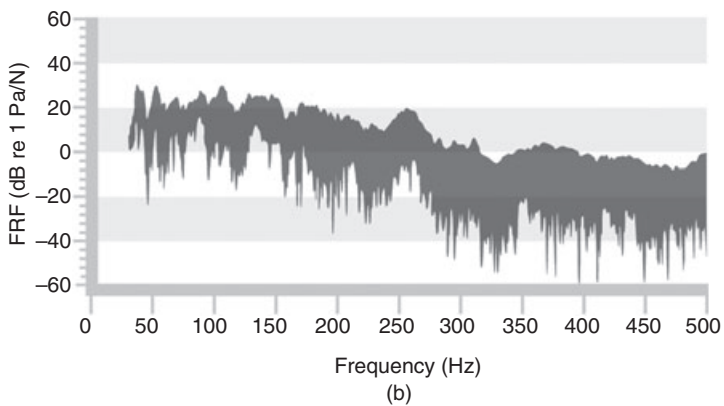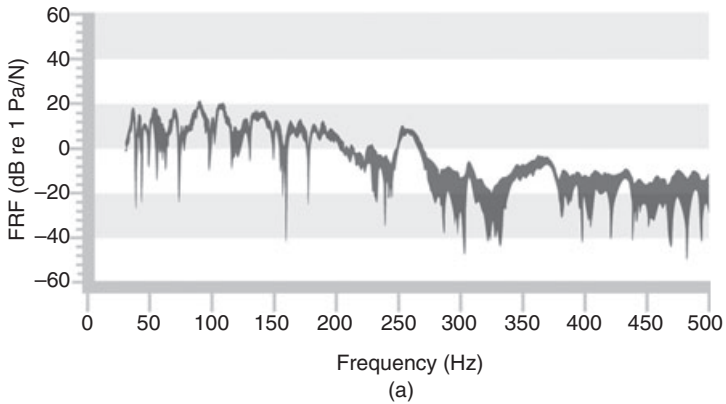
7.1 Uncertainty of measured frequency response functions (FRF); sampled data range: (a) one vehicle, repeated 12 times; (b) 98 nominally identical vehicles. The excitation and response points are identical for the FRF measurement.

of the same type. Each subsystem's response is represented by a space and frequency band averaged energy level. Based on the principle of conservation of energy, a band limited power balance matrix equation for the connected subsystems can be derived and easily resolved. Because of the reduced number of degrees of freedom of the models, the SEA calculations are usually very fast (from few minutes to few hours), allowing a fast analysis process in the design phase. The method predicts the 'mean' energy level in each of the subsystems, in the sense that the system is considered to have random properties. The method would, for example, predict the mean interior noise level for a fleet of cars manufactured on the same production line. A variance prediction method for built-up structures was developed by Langley and Cotoni [7] in which prediction of the statistics of the response of a highly random system without knowledge of the nature of the underlying physical uncertainties became possible. The method

allows for the long-established SEA method to be extended to variance prediction. Both the mean energy level and its variance give estimations of subsystem responses. However, this method is only applicable in mid- to high-frequency ranges.

The objectives of this chapter are to provide an overview of the modern predictive SEA method, to highlight the problems associated with modelling noise and vibration at mid- and high frequencies, to summarize the derivation of the SEA equations and list the main assumptions, and to illustrate the concepts and methods used to derive the parameters of an SEA model.

7.2   Modal approach

In order to predict vibration energy transmission, as mentioned above, a deterministic approach is possible in principle but not practical, and an alternative approach is to adopt a statistical description of response and look at time and spatial averages of vibration energy. The modal approach is based on the assumption that two oscillator results apply to coupled multi-modal systems, that is, the coupling power proportionality of the two oscillators applies to the multi-modal system. In order to illustrate the modal approach, modal resonators and their properties are first illustrated.

7.2.1   Modal resonators and their distribution

If the generalized displacement of the system is denoted by y:

$$\rho \ddot{y} + c_\gamma \dot{y} + \Lambda y = p \tag{7.1}$$

where p is the distributed excitation, ρ is the mass density, c_γ is a viscous resistance coefficient and Λ is a linear operator consisting of differentiations with respect to space.

In the case of a flat plate, for example, ρ is the mass per unit area of the plate and $\Lambda = \beta \nabla^4$, where β is the bending rigidity. The use of simple viscous damping is a valuable simplification and does not affect the utility of our results as long as the damping is fairly small. Where the system is bounded, with well-defined boundary conditions, the solution is frequently sought by expansion in eigenfunctions ψ_n which are solutions to the equation:

$$\frac{1}{\rho} \Lambda \psi_n = \omega_n^2 \psi_n \tag{7.2}$$

where the functions ψ_n satisfy the same boundary conditions that y does, and the quantities ω_n^2 are determined by the boundary conditions and the operator $\rho^{-1}\Lambda$. The response and the excitation are then expanded in the functions

$$y = \sum_n y_n(t)\psi_n(x) \tag{7.3}$$

$$\frac{p}{\rho} = \frac{1}{M}\sum_n f_n(t)\psi_n(x) \tag{7.4}$$

Multiplying Equation 7.2 by ψ_m, and integrating over the region occupied by the structure and subtracting from this the same equation with the indices reversed, we get:

$$\left.\begin{array}{l}\int[\psi_m\Lambda\psi_n - \psi_n\Lambda\psi_m]\,dx = (\omega_n^2 - \omega_m^2)\int\psi_m\rho(x)\psi_n\,dx \\ \int\psi_m\rho(x)\psi_n\,dx = 0 \quad \text{for } n \neq m \\ \int\psi_n^2\rho(x)\,dx = M \quad \text{for } n = m\end{array}\right\} \tag{7.5}$$

Normalization of the amplitude of eigenfunctions gives:

$$\frac{1}{M}\int\psi_m\rho\psi_n\,dx \equiv \langle\psi_m\psi_n\rangle_\rho = \delta_{m,n} \tag{7.6}$$

$$\rho\sum_n\left[\ddot{y}_n + \frac{c_y}{\rho}\dot{y}_n + \omega_n^2 y_n\right]\psi_n = \frac{\rho}{M}\sum_n f_n\psi_n \tag{7.7}$$

if $c_y = \rho\Delta$ where Δ is a constant. Multiplying Equation 7.7 by $\psi_m(x)$ and integrating it over the system domain gives:

$$m_n[\ddot{y}_n + \Delta\dot{y}_n + \omega_n^2 y_n] = f_n(t) \tag{7.8}$$

where modal mass is $m_n = M$, modal stiffness is $\omega_n^2 m_n$ and mechanical resistance is $m_n\Delta = c_n$.

For example, the two-dimensional simply supported isotropic and homogeneous rectangular flat plate of dimensions L_1, L_2 (see Fig. 7.2) has mode shapes for bending motion that are:

$$\psi_{n_1,n_2} = 2\sin\frac{n_1\pi x_1}{L_1}\sin\frac{n_2\pi x_2}{L_2}$$
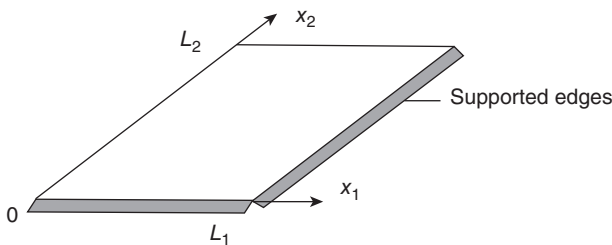
7.2 Mode shapes for bending motion of a 2D simply supported isotropic and homogeneous rectangular flat plate of dimensions L_1, L_2.
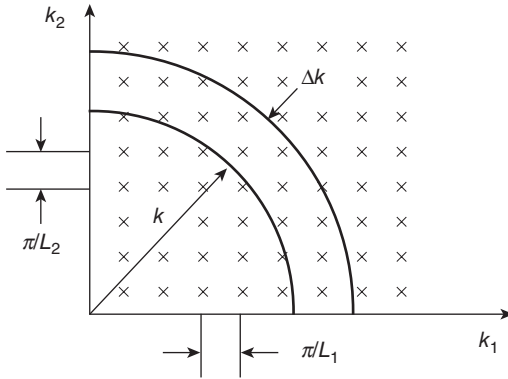
7.3 A convenient ordering of modes.

$$\psi_{n_1,n_2} = 2\sin\frac{n_1\pi x_1}{L_1}\sin\frac{n_2\pi x_2}{L_2} \tag{7.9}$$

The resonance frequencies are given by:

$$\omega^2_{n_1,n_2} = \left[\left(\frac{n_1\pi}{L_1}\right)^2 + \left(\frac{n_2\pi}{L_2}\right)^2\right]^2 R^2 C_l^2 = \left(k_1^2 + k_2^2\right)^2 R^2 C_l^2 = k^4 R^2 C_l^2 \tag{7.10}$$

where n_1 and n_2 are integers, R is the radius of gyration of the plate cross-section, $C_l = \sqrt{E/\rho}$ is the longitudinal wave speed in the plate material, E is Young's modulus and ρ is the material density.

Equation 7.10 suggests a very convenient ordering of the modes, which is shown in Fig. 7.3, where every 'wave number lattice' corresponds to a mode. The distance from the origin to that point will determine the value of the resonance frequency of the mode ω_{n_1,n_2}.

Each lattice corresponds to an area $\Delta A_k = \pi^2/A_p$ where $A_p = L_1 L_2$ is the area of the plate. As the wave number increases from k to $k + \Delta k$ a new area $\frac{1}{2}\pi k\Delta k$ will include $\frac{1}{2}\pi k\Delta k/\Delta A_k$ new modes, therefore the average number of modes per unit increment of wave number,

$$n(k) = \frac{\pi k\Delta k}{2\Delta A_k \Delta k} = \frac{\pi k}{2\Delta A_k} \tag{7.11}$$

which is termed the modal density in the wave number. The modal density in the radian frequency $n(\omega)$ is derived from the relation:

$$n(\omega)\,\Delta\omega = n(k)\,\Delta k \tag{7.12}$$

$$n(\omega) = \frac{\pi k}{2\Delta A_k}\frac{\Delta k}{\Delta\omega} = \frac{\pi k}{2C_g\Delta A_k} \tag{7.13}$$

where $C_g = \Delta\omega/\Delta k$ is the group velocity for waves in a system that has a phase velocity $C_p = \omega/k$.

For a flat plate, the group velocity C_g is twice the phase velocity which is given by

$$C_p = \frac{\omega}{k} = \sqrt{\omega R C_l} \tag{7.14}$$

The modal density in cycles per second (Hz) is:

$$n(f) = n(\omega)\frac{\mathrm{d}\omega}{\mathrm{d}f} = \frac{2\pi^2 \omega A_p}{4C_p^2 \pi^2} = \frac{A_p}{2RC_l} = \frac{\sqrt{3}A_p}{hC_l} \tag{7.15}$$

where $R = h/2\sqrt{3}$, the radius of gyration for a homogeneous plate of thickness h. In this case the modal density is independent of frequency.

The kinetic energy of vibration is:

$$\frac{1}{2}\int \mathrm{d}x\rho\left(\frac{\partial y}{\partial t}\right)^2 = \frac{1}{2}\int \mathrm{d}x\sum_{m,n} y_m'(t)y_n'(t)\rho\psi_m(x)\psi_n(x)$$
$$= \frac{1}{2}M\sum_n [y_n'^2(t)] \tag{7.16}$$

Since the kinetic and potential energies of each resonator are equal at resonance, $\langle y_n'^2 \rangle = \omega_n^2 \langle y_n^2 \rangle$, the total energies of the modes simply add to form the total system energy.

For the response of a system to a point force excitation, a point force of amplitude f_0 is applied at a location x_s on the structures modal amplitude from Equation 7.4:

$$f_m(t) = \int f_0(t)\psi_m(x)\delta(x - x_s)\mathrm{d}x = f_0(t)\psi_m(x_s) \tag{7.17}$$

If the excitation is given by $f_0(t) = F_0 e^{i\omega t}$, Equation 7.8 becomes:

$$M(\omega_n^2 + i\eta\omega\omega_n - \omega^2)y_n = F_0\psi_n(x_s)e^{i\omega t} \tag{7.18}$$

The response is expressed as:

$$y(x, t) = \frac{F_0 e^{i\omega t}}{M}\sum_n \frac{\psi_n(x_s)\psi_n(x)}{\omega_n^2 - \omega^2 + i\eta\omega\omega_n} \tag{7.19}$$

The driving point mobility function is written:

$$Y = \frac{v(x_s, \omega)}{f_0} = \frac{i\omega}{M}\sum_n \frac{\psi_n^2(x_s)}{\omega_n^2 - \omega^2 + i\eta\omega\omega_n} \equiv \mathrm{Re}[Y] + i\,\mathrm{Im}[Y] \tag{7.20}$$

$$\mathrm{Re}[Y] = \sum_n a_n(x_s)g_n(\omega) \tag{7.21}$$

where $a_n = \psi_n^2(x_s)/\eta M\omega_n$ and $g_n = (\xi^2 + 1)^{-1}$ which is defined below.

$$\text{Im}[Y] = \sum_n a_n(x_s) b_n(\omega) \tag{7.22}$$

where $b_n = \xi(\xi^2 + 1)^{-1}$ assuming the damping $\eta < 0.3$ is small enough so that the individual modal mobility $a_n (g_n + ib_n)$ is fairly sharp in frequency where:

$$a_n = \frac{\psi_n^2(x_s)}{\eta M \omega_n}, \quad g_n = \frac{1}{1+\xi^2} \tag{7.23}$$

$$\xi = \frac{\omega_n}{\eta \omega} - \frac{\omega}{\eta \omega_n}, \quad \mathrm{d}\xi \approx \frac{\mathrm{d}\omega_n}{\eta \omega} \tag{7.24}$$

$$Y = \sum_n a_n (g_n + ib_n) \tag{7.25}$$

$$\langle g_n \rangle_{\omega_n} = \frac{1}{2\Delta\omega} \int_{-\infty}^{\infty} \frac{1}{\xi^2+1} \mathrm{d}\omega_n \tag{7.26}$$

Assuming ω is fixed and the ω_n are random variables, ω_n tend to ω. $\Delta\omega$ is the interval of resonance frequency, and if $\Delta\omega \gg \frac{\pi}{2}\eta\omega$,

$$\langle g_n \rangle_{\omega_n} = \frac{\eta\omega}{2\Delta\omega} \int_{-\infty}^{\infty} \frac{1}{\xi^2+1} \mathrm{d}\xi = \frac{\pi\eta\omega}{2\Delta\omega} \tag{7.27}$$

which is simply the ratio of the modal bandwidth to the averaging bandwidth. In the interval $\Delta\omega$ the number of modes that can contribute to the average is $n(\omega)\,\Delta\omega$.

$$\langle \text{Re}[Y] \rangle_{\omega_n, x_s} = \frac{\Delta\omega n(\omega)}{\eta M \omega} \frac{\eta\pi\omega}{2\Delta\omega} \langle \psi_n^2 \rangle = \frac{\pi}{2} \frac{n(\omega)}{M} \tag{7.28}$$

For a flat plate, $n(\omega) = A_p/4\pi R C_l$ and $M = \rho_s A_p$, where ρ_s is the surface density and A_p is the surface area,

$$\langle \text{Re}[Y] \rangle = (8\rho_s R C_l)^{-1} \tag{7.29}$$

If the input force has a flat spectrum of S_f over the band $\Delta\omega$, the power fed into any one mode can be found from the dissipation $\eta\omega_0 M \langle \dot{y}^2 \rangle$:

$$\langle P \rangle = \frac{\pi n(\omega)}{2M} \frac{S_f \Delta\omega}{2\pi} = \langle \text{Re}[Y] \rangle_{\omega_n, x_s} \langle f^2(t) \rangle \tag{7.30}$$

7.3   Energy sharing between two oscillators

As shown in Fig. 7.4, two linear resonators can be coupled by spring, mass and gyroscopic elements. The kinetic and potential energies are given by

$$\text{KE} = \frac{1}{2} m_1 \dot{y}_1^2 + \frac{1}{2} m_2 \dot{y}_2^2 + \frac{1}{8} m_c (\dot{y}_1 + \dot{y}_2)^2 \tag{7.31}$$
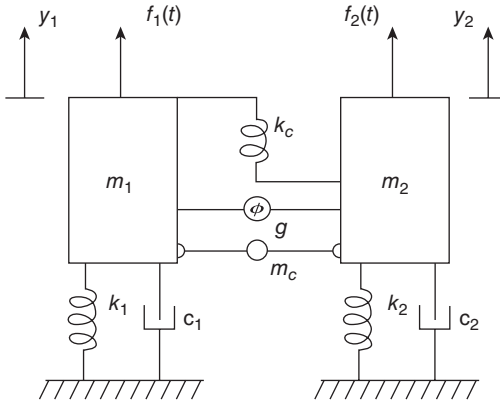
7.4 Coupled linear resonators.

$$PE = \frac{1}{2}k_1 y_1^2 + \frac{1}{2}k_2 y_2^2 + \frac{1}{2}k_c(y_2 - y_1)^2 \qquad (7.32)$$

The equation of motion in the absence of velocity-dependent forces is given by:

$$\frac{d}{dt}\frac{\partial KE}{\partial \dot{y}_i} - \frac{\partial PE}{\partial y_i} = f_i \qquad (7.33)$$

Substituting Equations 7.31 and 7.32 into Equation 7.33 gives:

$$\left(m_1 + \frac{1}{4}m_c\right)\ddot{y}_1 + c_1\dot{y}_1 + (k_1 + k_c)y_1 = f_1 + k_c y_2 + g\dot{y}_2 - \frac{1}{4}m_c\ddot{y}_2 \qquad (7.34)$$

$$\left(m_2 + \frac{1}{4}m_c\right)\ddot{y}_2 + c_2\dot{y}_2 + (k_2 + k_c)y_2 = f_2 + k_c y_1 + g\dot{y}_1 - \frac{1}{4}m_c\ddot{y}_1 \qquad (7.35)$$

where the gyroscopic coupling forece $g\dot{y}$ is included.

If we let $y_2 = \dot{y}_2 = \ddot{y}_2 = 0$ in Equation 7.34 and let $y_1 = \dot{y}_1 = \ddot{y}_1 = 0$ in Equation 7.35, oscillators 1 and 2 become clamped and are called clamped systems 1 and 2. That is, we set the response variables of the other system to be zero in order to obtain the decoupled system.

Equations 7.34 and 7.35 can be rewritten as:

$$\ddot{y}_1 + \Delta_1\dot{y}_1 + \omega_1^2 y_1 + \frac{1}{\lambda}(\mu\ddot{y}_2 + v\dot{y}_2 - Ry_2) = F_1 \qquad (7.36)$$

$$\ddot{y}_2 + \Delta_2\dot{y}_2 + \omega_2^2 y_2 + \lambda(\mu\ddot{y}_1 + v\dot{y}_1 - Ry_1) = F_2 \qquad (7.37)$$

where

$$\Delta_i = \frac{c_i}{\left(m_i + \dfrac{m_c}{4}\right)}, \quad \omega_i^2 = \frac{k_i + k_c}{\left(m_i + \dfrac{m_c}{4}\right)}$$

$$\mu = \left(\frac{m_c}{4}\right)\left(m_1 + \frac{m_c}{4}\right)^{\frac{1}{2}}\left(m_2 + \frac{m_c}{4}\right)^{-\frac{1}{2}}, \quad v = \frac{g}{\left(m_1 + \dfrac{m_c}{4}\right)^{\frac{1}{2}}\left(m_2 + \dfrac{m_c}{4}\right)^{\frac{1}{2}}}$$

$$R = \frac{k_c}{\left(m_1 + \dfrac{m_c}{4}\right)^{\frac{1}{2}}\left(m_2 + \dfrac{m_c}{4}\right)^{\frac{1}{2}}}, \quad \lambda = \left(m_1 + \frac{m_c}{4}\right)^{\frac{1}{2}}\left(m_2 + \frac{m_c}{4}\right)^{-\frac{1}{2}},$$

$$F_i = \frac{f_i}{\left(m_i + \dfrac{m_c}{4}\right)}$$

Considering both f_1 and f_2 as independent white noise sources, the power flows between the resonators are calculated. The power supplied by the source $P_1 = \langle f_1 \dot{y}_1 \rangle$:

$$\langle f_1 \dot{y}_1 \rangle = \left(m_1 + \frac{1}{4}m_c\right)\langle \ddot{y}_1 \dot{y}_1 \rangle + c_1 \langle \dot{y}_1^2 \rangle + (k_1 + k_c)\langle y_1 \dot{y}_1 \rangle - k_c \langle y_2 \dot{y}_1 \rangle$$

$$- g\langle \dot{y}_2 \dot{y}_1 \rangle + \frac{1}{4}m_c \langle \ddot{y}_2 \dot{y}_1 \rangle$$

$$\langle f_1 \dot{y}_1 \rangle = c_1 \langle \dot{y}_1^2 \rangle + \frac{1}{4}m_c \langle \ddot{y}_2 \dot{y}_1 \rangle - k_c \langle y_2 \dot{y}_1 \rangle - g\langle \dot{y}_2 \dot{y}_1 \rangle \tag{7.38}$$

$$\langle f_2 \dot{y}_2 \rangle = c_2 \langle \dot{y}_2^2 \rangle - k_c \langle y_1 \dot{y}_2 \rangle + \frac{1}{4}m_c \langle \ddot{y}_1 \dot{y}_2 \rangle + g\langle \dot{y}_1 \dot{y}_2 \rangle \tag{7.39}$$

Using the fact that:

$$\left\langle \frac{d}{dt}(y_1 y_2)\right\rangle = \langle \dot{y}_1 y_2 \rangle + \langle y_1 \dot{y}_2 \rangle = 0$$

$$\left\langle \frac{d}{dt}(\dot{y}_1 y_2)\right\rangle = \langle \ddot{y}_1 y_2 \rangle + \langle \dot{y}_1 \ddot{y}_2 \rangle = 0$$

summation of Equations 7.38 and 7.39 gives:

$$\langle f_1 \dot{y}_1 \rangle + \langle f_2 \dot{y}_2 \rangle = c_1 \langle \dot{y}_1^2 \rangle + c_2 \langle \dot{y}_2^2 \rangle$$

From Equation 7.38 or 7.39, the power flow from resonator 1 to resonator 2 gives:

$$\langle P_{12} \rangle = -k_c \langle y_2 \dot{y}_1 \rangle - g \langle \dot{y}_2 \dot{y}_1 \rangle + \frac{1}{4} m_c \langle \ddot{y}_2 \dot{y}_1 \rangle$$

If $\Delta_1 = \omega_1 \eta_1$, $\Delta_2 = \omega_2 \eta_2$ and η_i is the loss factor of each uncoupled resonator, therefore when clamping system 2, $y_2 = \dot{y}_2 = \ddot{y}_2 = 0$.

$$\varepsilon_1^{(b)} \equiv \frac{\pi S_{f_1}(\omega)}{2\Delta_1 \left(m_1 + \dfrac{1}{4} m_c \right)} = \frac{\pi S_{f_1}(\omega)}{2\omega_1 \eta_1 \left(m_1 + \dfrac{1}{4} m_c \right)} = \left(m_1 + \frac{1}{4} m_c \right) \langle \dot{y}_1^2 \rangle \quad (7.40)$$

which is the uncoupled or blocked energy of resonator 1 according to Equation 2.1.36 in reference [1]. Similarly,

$$\varepsilon_2^{(b)} \equiv \frac{\pi S_{f_2}(\omega)}{2\Delta_2 \left(m_2 + \dfrac{1}{4} m_c \right)} = \left(m_2 + \frac{1}{4} m_c \right) \langle \dot{y}_2^2 \rangle \quad (7.41)$$

is the energy of resonator 2 when $y_1 = \dot{y}_1 = \ddot{y}_1 = 0$.

The power flow from resonator 1 to resonator 2 is:

$$\langle P_{12} \rangle = A \left(\varepsilon_1^{(b)} - \varepsilon_2^{(b)} \right) \quad (7.42)$$

which states:

1. The power flow is dominated by the resonator interaction between the two resonators. The quantity A is very large when ω_1 and ω_2 are within a resonance bandwidth of each other, but very small otherwise.
2. The power flow is directly proportional to the difference in decoupled energy of the resonators.
3. The quantity A is positive definite; the average power flow is from the resonator of greater energy to the resonator of less energy.
4. A is also symmetric in the system parameters so that an equal difference of resonator energies in either direction ($1 \rightarrow 2$ or $2 \rightarrow 1$) will result in an equal power flow; that is, the power flow is reciprocal.

The power flow is proportional to the difference in the actual kinetic energy, or potential energy, or total energy. The power flow can be calculated either from input power to the system or from measured vibration. The calculation can be based either on uncoupled systems or on the actual vibration energy of the coupled systems.

If the average energy of resonator 1 is ε_1, and the average energy of resonator 2 is ε_2, the power flow between them is:

$$\langle P_{12} \rangle = B(\varepsilon_1 - \varepsilon_2) \quad (7.43)$$

where:

$$B = \frac{\mu^2\left[\Delta_1\omega_2^4 + \Delta_2\omega_1^4 + \Delta_1\Delta_2\left(\Delta_1\omega_2^2 + \Delta_2\omega_1^2\right)\right] + (\gamma^2 + 2\mu R)\left(\Delta_1\omega_2^2 + \Delta_2\omega_1^2\right) + R^2(\Delta_1 + \Delta_2)}{(1-\mu^2)\left[\left(\omega_1^2 - \omega_2^2\right)^2 + (\Delta_1 + \Delta_2)\left(\Delta_1\omega_2^2 + \Delta_2\omega_1^2\right)\right]} \tag{7.44}$$

If resonator 2 has no direct excitation, $S_{f_2} = 0$, then the power dissipated by the resonator must equal the power transferred from 1 to 2.

$$\langle P_{2,\text{dissipated}}\rangle = \langle P_{1,2}\rangle; \qquad \Delta_2\varepsilon_2 = B(\varepsilon_1 - \varepsilon_2)$$

or

$$\frac{\varepsilon_2}{\varepsilon_1} = \frac{B}{\Delta_2 + B} \tag{7.45}$$

The largest value of ε_2 is ε_1, which occurs when the coupling (determined by B) is strong compared to the damping Δ_2.

When the two resonators are identical and have stiffness coupling only, then Equation 7.44 becomes:

$$B = \frac{2\Delta R^2}{4\Delta^2\omega^2} = \frac{R^2}{2\Delta\omega^2} \tag{7.46}$$

$$\frac{\varepsilon_2}{\varepsilon_1} = \frac{R^2/2\Delta^2\omega^2}{1 + R^2/2\Delta^2\omega^2} \tag{7.47}$$

Additional points can now be added in regard to the power flow from resonator 1 to 2:

5. The power flow is proportional to the actual vibration energy difference of the systems, the constant of proportionality being B.
6. The parameter B is positive definite and symmetric in system parameters; the system is reciprocal and power flows from the more energetic resonator to the less energetic one.
7. If only one resonator is directly excited, the greatest possible value of energy for the second resonator is that of the first resonator.

7.4 Energy exchange in multi-degree-of-freedom systems

As shown in Fig. 7.5, the equations for the blocked or decoupled subsystems are:

$$\ddot{y}_i^{(b)} + \left(\frac{c_{r_i}}{\rho_i}\right)\dot{y}_i^{(b)} + \frac{\Lambda_i y_i^{(b)}}{\rho_i} = \frac{P_i}{\rho_i} \quad i = 1, 2, \ldots \tag{7.48}$$

$$\frac{\Lambda_i \psi_{i\alpha}}{\rho_i} = \omega_{i\alpha}^2 \psi_{i\alpha} \quad i = 1, 2, \ldots \tag{7.49}$$
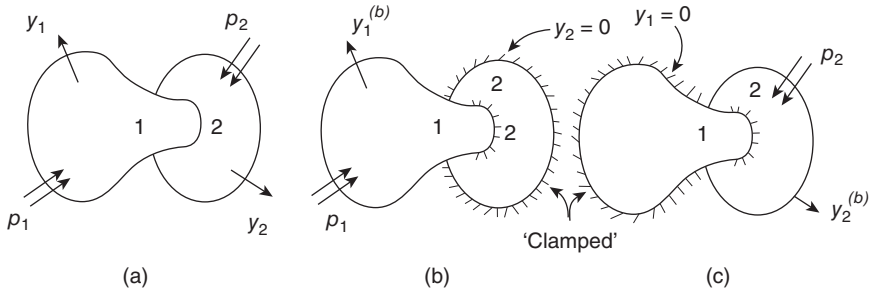
7.5 Blocked or decoupled subsystems.

(a) Blocked   (b) Connected
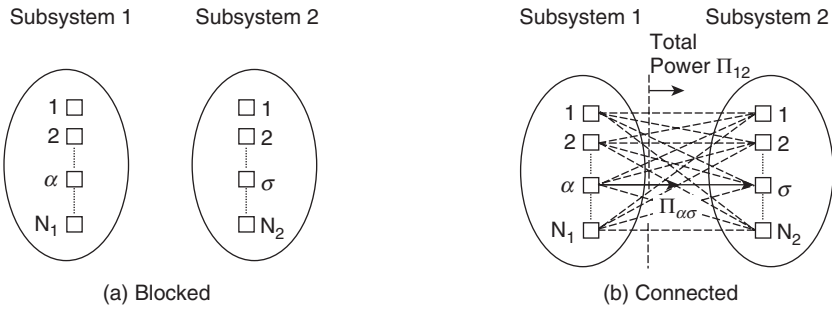
7.6 Modes for subsystems: (a) individual modal groups with subsystems blocked; (b) interactions of mode pairs with subsystems connected at the junction.

with the orthogonal property and normalizations given by

$$\langle \psi_{i\alpha} \psi_{i\beta} \rangle_{\rho_i} = \delta_{\alpha,\beta} \tag{7.50}$$

The boundary conditions satisfied for $\psi_{i\alpha}$ include the clamped condition. Suppose that the spectral densities of the modal excitations $F_{i\alpha}(t) = \int p_i \psi_{i\alpha} dx_i$ are flat over a finite range of frequency $\Delta\omega$ and that within this band there are $N_i = n_i \Delta\omega$ modes of each subsystem. The modes for these subsystems are illustrated in Fig. 7.6(a). Each mode group represents a model of the subsystem.

In the application of SEA, this model has some very particular properties as illustrated below.

1. Each mode α of subsystem i is assumed to have a natural frequency $\omega_{i\alpha}$ that is uniformly probable over a frequency interval $\Delta\omega$. This means that each subsystem is a member of a population of systems that are generally similar physically, but differ enough to have randomly distributed parameters. The assumption is based on the fact that normally identical structures or acoustic spaces will have uncertainties in their modal parameters, particularly at higher frequencies.

2. We assume that every mode in a subsystem is equally energetic and that the modal amplitudes $y_{i\alpha}(t) = \int \dfrac{\rho_i y_i \psi_{i\alpha}}{m} \, dx_i$ are incoherent; that is,

$$\langle y_{i\alpha} y_{i\beta} \rangle = \delta_{\alpha,\beta} \langle y_{i\alpha}^2 \rangle \tag{7.51}$$

3. This assumption requires that we correctly select mode groups, which is an important guide for appropriate SEA modelling. This also implies that the modal excitation functions F_i are drawn from random populations of functions that have certain similarities (such as equal frequency and wave number spectra) but are individually incoherent.

4. The damping of each mode in a subsystem is the same.

'Unlock' the system and consider the new equations of motion, which are:

$$\ddot{y}_i + \frac{c_{r_i}}{\rho_i} \dot{y}_i + \Lambda_i y_i = \frac{p_i + \mu_{ij}(x_i, y_j) \ddot{y}_j + (-1)^j \gamma_{ij}(x_i, y_j) \dot{y}_j + k_{ij} y_j}{\rho_i}$$
$$i \neq j, \quad i, j = 1, 2, \ldots \tag{7.52}$$

One now expands these two equations in the eigenfunctions $\psi_{1\alpha}(x_1)$ and $\psi_{2\sigma}(x_2)$ to obtain:

$$m_1 [\ddot{y}_\alpha + \Delta_1 \dot{y}_\alpha + \omega_\alpha^2 y_\alpha] = F_\alpha + \sum_\sigma [\mu_{\alpha\sigma} \ddot{y}_\sigma + \gamma_{\alpha\sigma} \dot{y}_\sigma + R_{\alpha\sigma} y_\sigma] \tag{7.53}$$

$$m_2 [\ddot{y}_\sigma + \Delta_2 \dot{y}_\sigma + \omega_\sigma^2 y_\sigma] = F_\sigma + \sum_\alpha [\mu_{\sigma\alpha} \ddot{y}_\alpha + \gamma_{\sigma\alpha} \dot{y}_\alpha + R_{\sigma\alpha} y_\alpha] \tag{7.54}$$

where α is for subsystem 1, and σ is for subsystem 2, and $\Delta_i = c_{r_i}/\rho_i$; the mass of the subsystem is m_i. The coupling parameters are [1]:

$$\mu_{\alpha\sigma} = \int\limits_{\text{junction}} \mu_{12}[x_1, x_2(x_1)] \psi_\alpha(x_1) \psi_\sigma[x_2(x_1)] dx_1, \text{ etc.} \tag{7.55}$$

$$\mu_{\sigma\alpha} = \int\limits_{\text{junction}} \mu_{21}[x_1(x_2), x_2] \psi_\sigma[x_1(x_2)] \psi_\alpha(x_2) dx_2, \text{ etc.} \tag{7.56}$$

where the integrations are taken along the junction between the subsystems and, therefore, over the same range of x_1, x_2 in both integrals. Conservative coupling requirements are met by $\mu_{\alpha\sigma} = \mu_{\sigma\alpha} = \mu$, $\gamma_{\alpha\sigma} = \gamma_{\sigma\alpha} = \gamma$, $R_{\alpha\sigma} = R_{\sigma\alpha} = R$, or $\mu_{21} = \mu_{12} = \mu$, $\gamma_{12} = \gamma_{21} = \gamma$, $R_{12} = R_{21} = R$.

The coupled systems may now be represented as shown in Fig. 7.6(b) with the interaction lines showing the energy flows that result from the coupling. Suppose we study the energy flow between mode α of subsystem 1 and mode σ of subsystem 2. Modes α and σ have energies ε_α and ε_σ. The modal energies of the subsystem 1 modes are all equal; that is $\varepsilon_\alpha = \varepsilon_1 =$ constant and $\varepsilon_\sigma = \varepsilon_2 =$ constant.

The inter-modal power flow:

$$\langle P_{\alpha\sigma} \rangle = \langle B_{\alpha\sigma} \rangle_{\omega_\alpha\omega_\sigma} (\varepsilon_1 - \varepsilon_2) \tag{7.57}$$

$$\langle B_{\alpha\sigma} \rangle_{\omega_\alpha\omega_\sigma} = \frac{\pi}{2} \frac{\Delta_1\Delta_2}{\Delta\omega} \langle \lambda \rangle_{\alpha\sigma} \tag{7.58}$$

where

$$\lambda \equiv \frac{[\mu^2\omega^2 + (\gamma^2 + 2\mu R) + R^2/\omega^2]}{\Delta_1\Delta_2} \tag{7.59}$$

when $\mu^2 \ll 1$, $\Delta/\omega \ll 1$ and $\lambda \ll 1$.

The total power flow from all N_1 modes of subsystem 1 to mode σ of subsystem 2 is:

$$\langle P_{1,\sigma} \rangle = \langle B_{\alpha\sigma} \rangle N_1 (\varepsilon_1 - \varepsilon_2) \tag{7.60}$$

Finally the total power flow from subsystem 1 to subsystem 2 is found by summing over the N_2 modes of subsystem 2:

$$\begin{aligned} \langle P_{12} \rangle &= \langle B_{\alpha\sigma} \rangle N_1 N_2 (\varepsilon_1 - \varepsilon_2) \\ &= \frac{\pi}{2} \Delta\omega \frac{\mu^2\omega^2 + (\gamma^2 + 2\mu R) + R^2/\omega^2}{\delta\omega_1 \delta\omega_2} (\varepsilon_1 - \varepsilon_2) \end{aligned} \tag{7.61}$$

when $\delta\omega_i = \Delta\omega/N_i$ is the average frequency separation between modes.

If the total energy of subsystems 1 and 2 is defined as $E_{1(total)}$ and $E_{2(total)}$:

$$\varepsilon_1 = \frac{E_{1(total)}}{N_1}, \quad \varepsilon_2 = \frac{E_{2(total)}}{N_2} \tag{7.62}$$

$$\begin{aligned} \langle P_{12} \rangle &= \langle B_{\alpha\sigma} \rangle N_1 N_2 \left[\frac{E_{1(total)}}{N_1} - \frac{E_{2(total)}}{N_2} \right] \\ &= \omega\eta_{12} \left[E_{1(total)} - \frac{N_1}{N_2} E_{2(total)} \right] \end{aligned} \tag{7.63}$$

where $\eta_{12} = \langle B_{\alpha\sigma} \rangle N_2/\omega$.

If we define $\eta_{21} = N_1\eta_{12}/N_2$ then:

$$\langle P_{12} \rangle = \omega \left(\eta_{12} E_{1(total)} - \eta_{21} E_{2(total)} \right) \tag{7.64}$$

η_{12} and η_{21} are called the coupling loss factors for subsystems 1 and 2. $\omega\eta_{12}E_{1(total)}$ represents the power lost by subsystem 1 due to coupling, just as the quantity $\omega_1\eta_1 E_{1(total)}$ represents the power lost by subsystem 1 due to damping. If subsystem 1 is connected to subsystem 2 with energy $E_{2(total)}$, subsystem 1 will receive an amount of power $\omega\eta_{21}E_{2(total)}$ from subsystem 2.

In the basic relationship $N_1\eta_{12} = N_2\eta_{21}$, replacing the modal count N_i with modal density time, the frequency bandwidth $n_i\Delta\omega$ gives

$$n_1\eta_{12} = n_2\eta_{21} \tag{7.65}$$
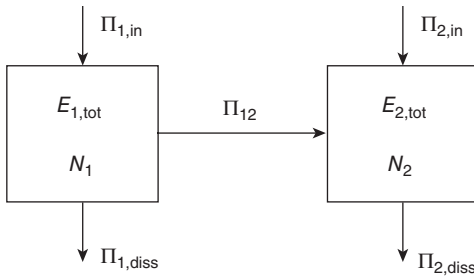
7.7 An energy transfer and storage model.

The system shown in Fig. 7.6(b) is simply represented in Fig. 7.7. The power flow equations for subsystems 1 and 2 are:

$$\langle P_{1,in} \rangle = \langle P_{1,dissipated} \rangle + \langle P_{12} \rangle$$
$$= \omega \left[\eta_1 E_{1(total)} + \eta_{12} E_{1(total)} - \eta_{21} E_{2(total)} \right] \tag{7.66}$$

$$\langle P_{2,in} \rangle = \langle P_{2,dissipated} \rangle + \langle P_{21} \rangle$$
$$= \omega \left[\eta_2 E_{2(total)} + \eta_{21} E_{2(total)} - \eta_{12} E_{1(total)} \right] \tag{7.67}$$

Considering the case where only one of the systems is directly excited by one external source, that is, setting $<P_{2,in}> = 0$:

$$\frac{E_{2(total)}}{E_{1(total)}} = \frac{N_2}{N_1} \frac{\eta_{21}}{\eta_2 + \eta_{21}} \tag{7.68}$$

A solution of Equations 7.66 and 7.67 gives:

$$E_{1(total)} = \frac{\langle P_{1,in} \rangle (\eta_2 + \eta_{21}) + \langle P_{2,in} \rangle \eta_{21}}{\omega D} \tag{7.69}$$

$$E_{2(total)} = \frac{\langle P_{2,in} \rangle (\eta_1 + \eta_{12}) + \langle P_{1,in} \rangle \eta_{12}}{\omega D} \tag{7.70}$$

where

$$D = (\eta_1 + \eta_{12})(\eta_2 + \eta_{21}) - \eta_{12}\eta_{21} \tag{7.71}$$

The dissipated power in subsystem 1 can be evaluated by

$$\langle P_{1,dissipated} \rangle = 2\pi f \eta_1 E_1 \tag{7.72}$$

where E_1 is the total dynamic energy of the subsystem modes at frequency f (Hz) and η_1 is the damping loss factor.

As shown in Fig. 7.7, the net transmitted power can be represented in several different forms, for example

$$\langle P_{12} \rangle = 2\pi \, \Delta f \, \beta_{12}(\varepsilon_1 - \varepsilon_2) \tag{7.73}$$

where ε_1 and ε_2 are the average modal energies (energies per mode) of the two subsystems in a frequency band Δf, and β_{12} is a coupling factor that depends only on the physical properties of the two coupled subsystems:

$$\varepsilon = \frac{E}{N} = E\frac{\overline{\delta f}}{\Delta f} \tag{7.74}$$

where N is the mode number and $\overline{\delta f}$ is the average frequency spacing between the modes of the subsystem in the frequency bandwidth Δf.

$$\langle P_{12}\rangle = 2\pi f(\eta_{12}E_1 - \eta_{21}E_2) \tag{7.75}$$

$$\langle P_{1,\text{in}}\rangle = \langle P_{1,\text{dissipated}}\rangle + \langle P_{12}\rangle = 2\pi f(\eta_1 + \eta_{12})E_1 - 2\pi f\eta_{21}E_2 \tag{7.76}$$

$$\langle P_{2,\text{in}}\rangle = \langle P_{2,\text{dissipated}}\rangle + \langle P_{21}\rangle = 2\pi f(\eta_2 + \eta_{21})E_2 - 2\pi f\eta_{12}E_1 \tag{7.77}$$

$$\frac{\varepsilon_2}{\varepsilon_1} = \frac{\eta_{21}}{\eta_2 + \eta_{21}} \quad (\langle P_{1,\text{in}}\rangle = 0) \tag{7.78}$$

If $N_1 = 1$:

$$\langle P_{12}\rangle = 2\pi\beta_{12}\left(E_1\Delta f - E_2\overline{\delta f_2}\right) \tag{7.79}$$

$$\langle P_{12}\rangle_{\Delta f} = 2\pi\beta_{12}\left(E_1\overline{\delta f_1} - E_2\overline{\delta f_2}\right) = \beta_{12}\left(\frac{E_1}{n_1(\omega)} - \frac{E_2}{n_2(\omega)}\right) \tag{7.80}$$

For a complex system with N subsystems, the SEA equations can be written as

$$\omega\begin{bmatrix} n_1\left(\eta_{11} + \sum_{i\neq 1}\eta_{1i}\right) & -\eta_{21}n_2 & \cdots\cdots & -\eta_{N1}n_N \\ -\eta_{12}n_1 & n_2\left(\eta_{22} + \sum_{i\neq 2}\eta_{2i}\right) & \cdots\cdots & \cdot \\ \cdot & & & \cdot \\ \cdot & \cdots\cdots & \cdots\cdots & \cdot \\ \cdot & & & \cdot \\ -\eta_{1N}n_1 & \cdots\cdots & \cdots\cdots & n_N\left(\eta_{NN} + \sum_{i\neq N}\eta_{Ni}\right) \end{bmatrix}\begin{Bmatrix} \dfrac{E_1}{n_1} \\ \cdot \\ \cdot \\ \cdot \\ \cdot \\ \cdot \\ \dfrac{E_N}{n_N} \end{Bmatrix}$$

$$= \begin{Bmatrix} P_1 \\ \cdot \\ \cdot \\ \cdot \\ \cdot \\ \cdot \\ P_N \end{Bmatrix} \tag{7.81}$$

If each subsystem has n degrees of freedom, the total of $n \times N$ dynamic equations are reduced to the total of N SEA equations, which speeds up the computation.

In summary, modes of a system become localized to various subsystems where local modes of the subsystems of a system are statistically described; local modal properties/wave properties are assumed to be maximally disordered in a state of maximum entropy. Simple expressions for ensemble average energy flow between coupled subsystems exist, since vibration energy flow between coupled subsystems is proportional to difference in modal energies, that is, average energy per mode. The SEA power balance equations which govern response of a system in a given frequency band can be derived from the principle of energy conservation.

The above SEA modal description is good for a qualitative introduction to SEA theory since the SEA equations derived from a modal approach are based on several assumptions, in particular for the extension of the two oscillator results to multimodal systems. The exact SEA equations as per Equations 7.66 and 7.67 can also be derived from a wave approach [8]. This is discussed in the next section.

7.5 Wave approach to statistical energy analysis (SEA)

In order to illustrate the wave approach, room acoustics are first reviewed. A typical room of 100 m^3 has 1×10^7 acoustic modes at frequencies of less than 10 kHz. If the connection between two such rooms is a rigid piston, the component of field associated with the radiation from such a piston into unbounded space/subsystem is called a direct field. The difference between the actual field and the direct field is called the reverberant field. The term 'diffuse' is used to describe a special set of statistics that are obtained when averaging over a large enough ensemble of reverberant fields, where the average can be taken over a set of nominally identical subsystems (or sometimes across a frequency band) and the statistics represent a state of maximum disorder or maximum entropy, in other words to get an equal partition of energy and incoherence of individual modes/ waves.

As shown in Fig. 7.8, the loading on the connecting piston can be represented by the direct field impedance of the fluid in the cavity subsystem and diffuse reverberant loading (incident power or blocked force proportional to the energy of the reverberant field, αE_i). Since the two reverberant fields are incoherent, the responses can be considered separately (Fig. 7.8(b) and (c)) and then superimposed. The power transmission from room cavity 1 to room cavity 2 is given by
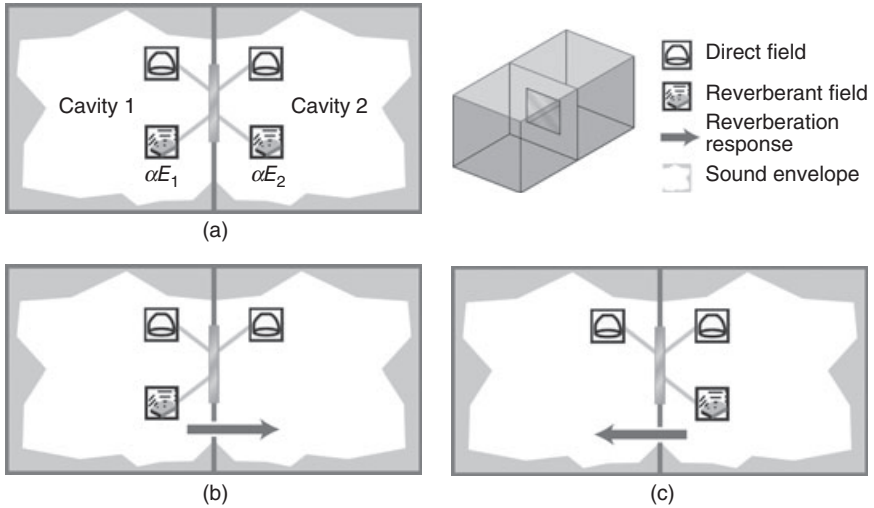
7.8 Subsystem loading on connection.
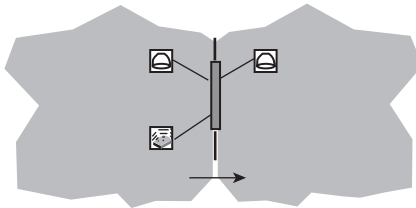
7.9 Power transmission from room cavity 1 to room cavity 2; with reverberant fields incoherent, the responses are calculated separately and then superimposed.

$$P_{12} = \tau P_{\text{inc1}} = \tau \frac{E_1 c_1 A}{4V_1} \qquad (7.82)$$

where the reverberant field αE_2 is not included, as shown in Fig. 7.9; P_{inc} is incident power, E is cavity energy, c is speed of sound, A is area of the connecting piston, V is cavity volume and τ is transmission coefficient.

The power transmission from room cavity 2 to room cavity 1 is given by

$$P_{21} = \tau P_{\text{inc2}} = \tau \frac{E_2 c_2 A}{4V_2} \qquad (7.83)$$

where the reverberant field αE_1 is excluded, as shown in Fig. 7.10. The coupling power between room cavities 1 and 2 is given by
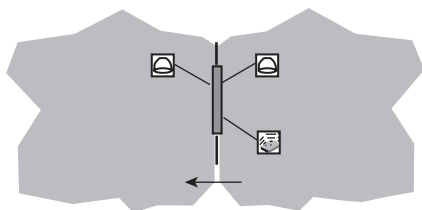
7.10 Power transmission from room cavity 2 to room cavity 1; with reverberant fields incoherent, the responses are calculated separately and then superimposed.

$$P_{12} = \tau P_{\text{inc1}} - \tau P_{\text{inc2}} = \tau A \left(\frac{E_1 c_1}{4V_1} - \frac{E_2 c_2}{4V_2} \right) \tag{7.84}$$

which is proportional to the difference in energy density group velocity.

From the above room acoustics discussion:

- The response of a subsystem can be described in terms of direct and reverberant fields.
- Averaging fields across an ensemble gives a diffuse reverberant field with a state of maximum entropy.
- Two diffuse reverberant fields become incoherent.
- Loading on the connection is related to the direct field impedance and diffuse reverberant field loading.
- The diffuse reverberant field loading is proportional to the energy density and group velocity of the subsystem.
- Net coupling power is proportional to the difference between local incident powers.

In the wave approach to SEA, a system is divided into a series of sub-structures or subsystems that support wave propagation such as beams, plates, shells, acoustic ducts, acoustic cavities, etc. where each substructure or subsystem contains a number of wave types including bending, extensional, shear waves, etc. Each wave type is represented by a separate SEA subsystem which can receive, store, dissipate and transmit energy. From a wave viewpoint, a subsystem is a collection of propagating waves, while from a modal viewpoint it is considered as a collection of resonant modes. A connection is defined as a geometric region which allows energy to flow in or out of a subsystem. A direct field is a component of the response associated with direct field radiation from connections, and is deterministic. A reverberant field is a component of the response associated with reflections from boundaries of the subsystem and blocked connections, and is statistical. Each SEA subsystem is represented in terms of superposition of a direct field and a reverberant field as shown in Fig. 7.11.

(a) Direct field

Component of response
associated with direct
field radiation from
connections –
deterministic

(b) Reverberant field

Component of response
associated with reflections
from boundaries of subsystem
and blocked connections –
statistical
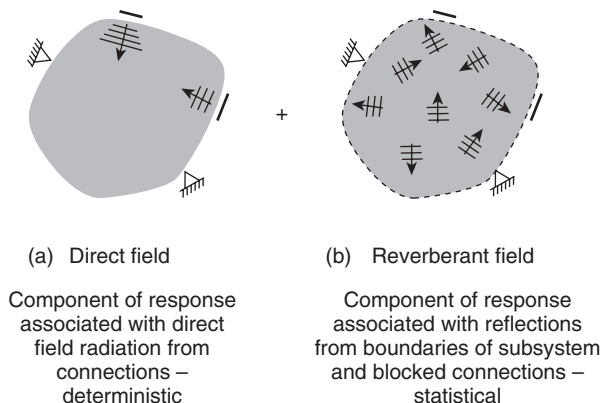
7.11 Each SEA subsystem is represented by superposition of (a) a
direct and (b) a reverberant field.

The SEA wave approach is based on the following assumptions as shown
in Fig. 7.11:

- Neglect coherence between direct fields of different connections to the
  same subsystem as shown in Fig. 7.11(a).
- There is significant uncertainty regarding the properties of each subsystem so that the reverberant fields are diffuse when viewed across the
  ensemble as shown in Fig. 7.11(b).

The first assumption is not valid for problems in which direct field transmission between connections is a domain path, for example heavily damped
subsystems or subsystems that are small compared with a wavelength.
Separate corrections are needed in such cases. The second assumption
implies that the SEA prediction gives the ensemble average response and
leads to incoherence between direct and reverberant fields when averaged
across the ensemble.

In order to apply the SEA approach to engineering problems, the procedures below have to be followed.

7.6   Procedures of the statistical energy analysis approach

In most cases, the following three steps in the application of SEA have to
be followed:

1. Define the system model.
2. Evaluate the model parameters.
3. Evaluate the response variables.

7.6.1 Defining the system model

There are also three steps in defining the system model:

1. Divide the system into physical components of suitable size and combine the natural modes of each component into groups (subsystems) with similar characteristics.
2. Define the physical coupling between subsystems.
3. Define the form of excitation to the system.

7.6.2 Evaluating the subsystem parameters

After defining the system model, there are four steps in evaluating the subsystem parameters:

1. Mode count, modal density and group velocity
2. Damping loss factor
3. Coupling loss factors to connected subsystems
4. Input power from the external sources of excitation

where the definition and evaluation method of the damping loss factor have been given in Chapter 3, and are not duplicated in this chapter.

7.6.3 Evaluating the response variables

After defining the system model and evaluating the subsystem parameters, the response variables can be evaluated by

$$[D]\{\varepsilon\} = \{\langle P_{in} \rangle\} \tag{7.85}$$

where $[D]$ is a symmetric matrix of damping and coupling loss factors. The modal energy vector $\{\varepsilon\}$ can be found from

$$\{\varepsilon\} = [D]^{-1}\{\langle P_{in} \rangle\} \tag{7.86}$$

7.7   Evaluation of the statistical energy analysis subsystem parameters

There are three main SEA parameters for the SEA wave approach:

1. Input power from external excitation – input power as shown in Fig. 7.12(a)
2. Energy storage capacity of the reverberant field – modal density/group velocity as shown in Fig. 7.12(b)
3. Energy transmission from the reverberant field to direct fields of adjacent subsystems – coupling loss factor as shown in Fig. 7.12(c).

External
excitation

(a)   (b)   (c)
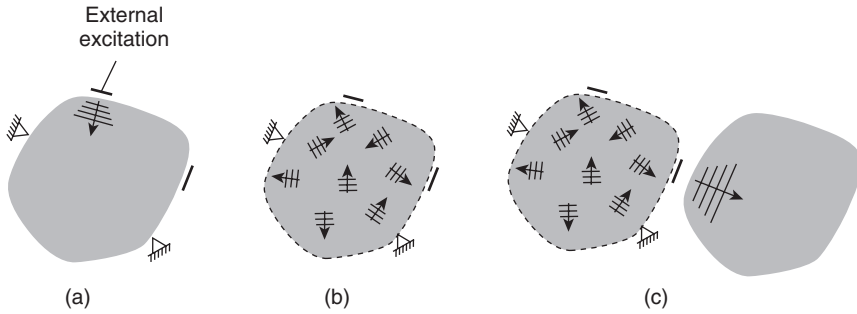
7.12 Three main SEA parameters.

In order to calculate the SEA subsystem parameters using a wave approach, we need to know the following:

- Types of waves that can propagate in a given subsystem, which depends on subsystem dimension, cross-section, etc.
- The dispersion properties of each wave type.

7.7.1 Modal density and group velocity for one-dimensional wave propagation

The exponential displacement field along the one-dimensional waveguide is assumed to be

$$u = U(x, y)e^{ikz}e^{i\omega t} \tag{7.87}$$

From the equation of motion for the assumed displacement field, the roots of the homogeneous equation can be solved for values of U and k that satisfy the homogeneous equation at a given frequency ω. Each root represents a wave type of the waveguide; roots with real k represent propagating waves, while roots with imaginary k represent evanescent waves. U reflects wave type and k represents wave number in rad/m, which is given by

$$k = \frac{2\pi}{\lambda} = \frac{2\pi f}{c_p} = \frac{\omega}{c_p} \tag{7.88}$$

where λ is wavelength in m, c_p is phase velocity in m/s, and the group velocity c_g (m/s) is defined as

$$c_g = \frac{\partial \omega}{\partial k} \tag{7.89}$$

which was mentioned in Equation 7.13. The group velocity is the speed at which energy propagates by a wave. The dispersive relation is given by
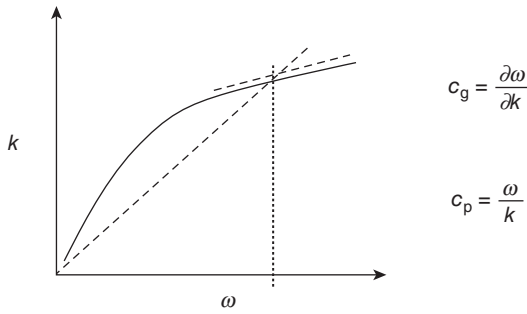
7.13 Dispersion curves.

$$c_g = \frac{\partial \omega}{\partial k}$$

$$c_p = \frac{\omega}{k}$$
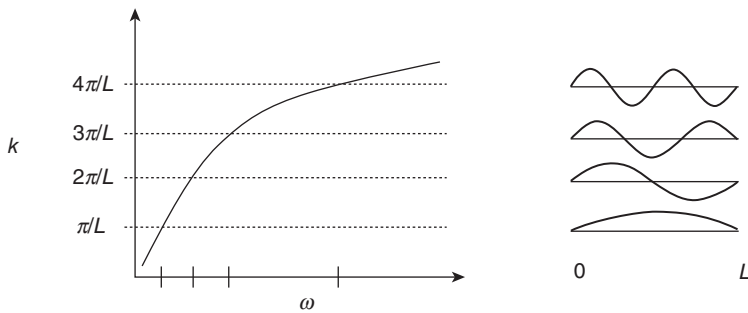
7.14 Wave mode duality.

curves or plots which show how the wave number varies with frequency for each wave type where the group and phase velocity are related to the local and global slopes of the dispersion curve at a given frequency. If group velocity varies with frequency then the wave is said to be dispersive as shown in Fig. 7.13. For a one-dimensional waveguide of length L, one mode is expected on average for every increment in wave number of π/L radians, which is shown in Fig. 7.14 which reflects wave mode duality.

Modal density is defined as the expected number of modes per unit frequency, which is given by:

$$n(\omega) = \frac{\partial N(\omega)}{\partial \omega} = \frac{\partial}{\partial \omega}(kL/\pi) = \frac{L}{\pi c_g} \tag{7.90}$$

where the mode count $N(\omega) = kL/\pi$ is defined as the expected number of modes below frequency ω. Equation 7.90 gives

$$\frac{E}{n} = \pi\left(\frac{E}{L}\right)c_g \tag{7.91}$$

This means that the modal energy E/n is equal to the energy density $\pi(E/L)$ multiplied by the speed c_g at which energy flows, which is the incident

power. From a wave viewpoint, the modal density relates the incident power in a reverberant field to the total energy contained within the reverberant field.

7.7.2 Modal density and group velocity for two-dimensional wave propagation

The exponential displacement field for plates/shells which support wave propagation in two dimensions is assumed to be

$$u = U(z)\,e^{ik_x x}\,e^{ik_y y}\,e^{i\omega t} \tag{7.92}$$

Wave types are calculated in the same way as for a one-dimensional waveguide, but now $U(z)$ describes the displacement field through the thickness; the wave number and wave velocities become vector quantities.

It is helpful to view the response of a panel in wave number space where the wave number space description is obtained by taking the two-dimensional Fourier transform of the physical displacement field. The wave number indicates the number of 'wiggles' per unit distance in a given direction, which is extremely useful for understanding wave propagation and acoustic radiation. For example, infinite isotropic panel resonant wave numbers lie on a circle in wave number space as shown in Fig. 7.3, where the number of modes in a given band is proportional to the area contained between two dispersion curves in the wave number space.

When boundary impedance is random, averaged modal densities for two- and three-dimensional wave propagation are given by [9]

$$n(\omega) = \frac{kA}{2\pi c_g} \tag{7.93}$$

$$n(\omega) = \frac{kV}{2\pi^2 c_g} \tag{7.94}$$

respectively, where A is the surface area of the two-dimensional structure and V is the volume of the three-dimensional acoustic cavity where boundary corrections are sometimes applicable.

For a three-dimensional room with rigid walls, the averaged modal density is given by [9]:

$$n(\omega) = \frac{n(f)}{2\pi} = \frac{L_{1x}L_{2y}H\omega^2}{2\pi^2 c^3} + \frac{\omega(L_{1x}L_{2y} + L_{1x}H + L_{2y}H)}{4\pi c^2} + \frac{L_{1x} + L_{2y} + H}{4\pi c} \tag{7.95}$$

where L_{1x} and L_{2y} are the length and width of the room, H is the depth of the room, c is the speed of sound in air, f is the frequency in Hz and ω is the radial frequency in rad/s.

In summary, energy storage in the SEA wave approach is represented by modal density, which is related to group velocity and dimensions of a subsystem/wave field. The SEA parameters for the wave fields can be found from dispersion curves.

7.7.3 Coupling loss factor

The coupling loss factor describes the rate at which energy flows from the reverberant field of the *i*th subsystem to the direct field of the *j*th subsystem per unit energy in the reverberant field of the *i*th subsystem, which is expressed as

$$\eta_{ij} = \frac{P_{coup,ij}}{\omega E_i} \tag{7.96}$$

According to the SEA wave approach assumption shown in Fig. 7.11(a), that is neglecting direct field transmission between two junctions connected to the same subsystem, or assuming that transmission is incoherent via the reverberant field, the coupling loss factor for each junction can be calculated in isolation. This implies that the SEA ensemble average response does not capture transmission in which coherent phase information is propagated across several subsystems; localization, wave number filtering effects and global modes are not revealed in the SEA ensemble average predictions.

In order to calculate the coupling loss factor, the semi-infinite impedance to a junction has to be added to the direct fields of each subsystem, and the junction has to be loaded by diffuse reverberant loading with a particular type of forcing. The diffuse field wave transmission coefficient from subsystem *i* to subsystem *j* is calculated when a diffuse reverberant field is incident upon the connection. For line and area connections, wave transmission calculation is often simplified by assuming that junctions are planar and/or large compared with a wavelength.

For pointed connected subsystems, direct field impedances of all subsystems connected to a junction are assembled first, that is the 6×6 dynamic stiffness matrix for connection degrees of freedom, and this process is repeated and looped over the excited wave field/subsystem. The force on the junction due to the diffuse incident wave field (with unit energy density) in the excited subsystem is then found. This force is then applied to the junction and the input power to the direct fields of each of the receiving subsystems is calculated. The columns of the coupling loss factor matrix are calculated and the process is repeated.

For line-connected subsystems, the maximum and minimum trace-wave numbers in the excited subsystem are first sought, then a set of incident trace-wave numbers are chosen to describe the diffuse field, and the process loops over all trace-wave numbers. For each trace-number, direct field

impedances of all subsystems connected to the junction are assembled into a 6×6 matrix for connection degrees of freedom. The force on the junction due to an incident trace-wave number (with unit energy density) is then sought in the excited subsystem. This force to the junction is then applied and the input power to the direct fields of each of the receiving subsystems is calculated, the results being averaged over all incident trace-wave numbers.

A formulation is available for predicting diffuse field transmission through pointed and line-connected subsystems such as plates/shells, etc., which can include lumped masses/isolators, in-line beams, etc.; subsystem impedances can be computed from local wave impedances (for example, line wave impedance) which are related to dispersion properties of waves. Coupling loss factors can be related to the matrix of subsystem wave transmission coefficients from which the coupling loss factor matrix is obtained for a given point or line junction. This matrix describes scattering/coupling/transmission between different wave fields.

For area-connected subsystems, resonant energy transmission is governed by the radiation efficiency of resonant modes, while non-resonant energy transmission is governed by the mass law and can be described by additional coupling loss factors. For example, the coupling loss factor between a cavity and a plate is given by [9]

$$\eta_{12} = \frac{\rho_0 c \sigma}{\omega \rho h_t} \tag{7.97}$$

where ρ_0 is the mass density of air, ρ is the mass density of the plate, h_t is the thickness of the plate, and σ is the radiation efficiency of the plate, which is given by [9]

$$\sigma = \frac{\lambda_c^2}{S} * 10^{\frac{1.2(f-f_B)}{f_B}} \qquad (f < f_B) \tag{7.98}$$

$$\sigma = \frac{\lambda_c^2}{S} \qquad (f_B < f,\ f < f_A) \tag{7.99}$$

$$\sigma = \frac{\lambda_c^2}{S} 10^{\frac{0.18(f-f_A)}{f_A}} \qquad (f_A < f,\ f < 0.25 f_c) \tag{7.100}$$

$$\sigma = \left(\frac{\lambda_c^2}{S}\right)^{\frac{4f_c-4f}{3f_c}} 10^{\frac{0.18(f_c-4f_A)}{f_A}\frac{f_c-f}{3f_c}} \left(\frac{P}{2\lambda_c}\right)^{\frac{4f-f_c}{6f_c}} \quad (0.25 f_c < f,\ f < f_c) \tag{7.101}$$

$$\sigma = \left(\frac{P}{2\lambda_c}\right)^{1-\frac{f}{2f_c}} \qquad (f_c < f,\ f < 2f_c) \tag{7.102}$$

where the critical frequency is given by [10]

$$f_c = \frac{c^2}{1.8 c_{Lt} h_t} \tag{7.103}$$

where

$$c_{Lt} = \sqrt{\frac{E}{\rho(1-v^2)}} \tag{7.104}$$

and the critical wavelength is given by

$$\lambda_c = \frac{c}{f_c} \tag{7.105}$$

The perimeter of the plate is given by

$$P = 2(L_{1x} + L_{2y}) \tag{7.106}$$

The radiation area is given by

$$S = L_{1x} L_{2y} \tag{7.107}$$

Frequency limits for the radiation ratio are given by

$$f_B = \frac{c^2}{2 S f_c} \left(\frac{P^2}{8S} - 1 \right) \tag{7.108}$$

$$f_A = 100 \left(\frac{\lambda_c c}{P^2} \right) \tag{7.109}$$

The radiation efficiency can also be calculated from the Leppington–Heron radiation efficiency [2].

7.7.4 Transfer matrices and insert loss of a trim lay-up

It is assumed that there are three characteristic wave types in poroelastic materials: the fluid standing wave, the solid standing wave, and a shear wave of both solid and fluid. Based on inertial/stiffness coupling, Biot equations provide a simple model (semi-empirical) way to describe the three wave types in terms of various measurable properties of a poroelastic material for which the response of a poroelastic material can be solved from known properties, domain and boundary conditions.

Noise control treatment is often encountered by planar lay-ups of poroelastic material where the transfer matrix method provides an efficient numerical method for computing wave propagation through such lay-ups. The method assumes the trim lay-ups are infinite in the lateral direction and homogeneous, and the response across each layer is sought analytically based on transfer properties/matrices for a given layer.

7.7.5 Leaks

Acoustic leakage paths are significant for acoustic energy transmission. Typical leaks arise because of access holes/pass-throughs, grillages, gaps, imperfect coverage, etc. It is important to account for leakage in the SEA model, which can be represented by additional coupling loss factors at area junctions.

7.7.6 Energy inputs

There are five types of energy inputs for the SEA wave approach: direct field impedance and input power, distributed random loading, turbulent boundary layer loading, diffuse acoustic field loading and propagating wave field loading.

Input power from point force excitation applied to point/line/area-type connections can be computed from the direct field impedance, which is identical to calculations performed when calculating coupling loss factors.

Input power from distributed pressure loads is calculated from the auto-spectrum and cross-spectrum. The auto-spectrum function of turbulent boundary layer loading depends on the boundary layer thickness and flow condition, and is typically obtained empirically from wind tunnel tests. The cross-spectrum of turbulent boundary layer loading contains information about spatial correlation structures within a flow in a Corcos model. For convection flows, different characteristic decay lengths in the flow and cross-flow directions are observed. The decay coefficients and convection wavelengths are important parameters.

Loading from diffuse acoustic field excitation can be calculated by the use of the diffuse field reciprocity principle. Spatial correlation in a diffuse field is given by a sine function. Input power from diffuse acoustic field excitation is proportional to radiation efficiency, in principle.

Input power from propagating wave field excitation can be calculated from modal joint acceptance or wave number space integrals in which trace velocities are derived from components of acoustic wave numbers and correlation decays are generally low.

7.8 Hybrid deterministic and the statistical energy analysis approach

A hybrid analysis method was developed in which the various components of a complex vibro-acoustic system can be modelled either deterministically or statistically [3–6]. The coupling between these two types of component is effected by using a diffuse field reciprocity relation, which relates the cross-spectrum of the forces at the boundary of a statistical component to
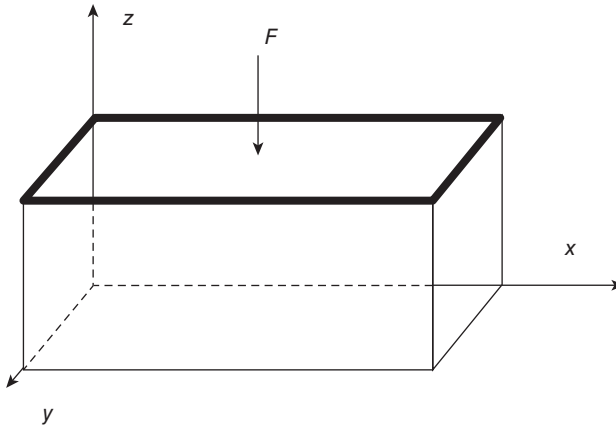
7.15 A plate–room system with a simply supported aluminium plate on the top and an excitation at the centre.

the vibration energy level of the component. This method is most applicable in the mid-frequency ranges.

7.9   Application example

In order to illustrate the above approaches, vibro-acoustic analysis of a plate–room cavity system has been conducted by using deterministic analysis, statistical energy analysis (SEA) and the hybrid approach in which the plate–room cavity system can be considered as a simplified model of a vehicle cabin cavity coupled with a roof panel.

The plate–room cavity system is shown in Fig. 7.15 in which a sine excitation force is acting at the centre of a plate. The aluminium plate is simply supported and has a length of $L_{1x} = 1.2$ m, a width of $L_{2y} = 1.35$ m, a thickness of $h_t = 5$ mm and a damping loss factor of 0.03. The room is a rectangular room with all the walls smooth, rigid and perfectly reflecting except for the top wall of the thin aluminium plate. The room has dimensions of length $L_{1x} = 1.2$ m, width $L_{2y} = 1.35$ m and height $L_{3z} = 1.45$ m, and a damping loss factor of 0.03. The room size is close to a typical passenger car cabin size.

The modal density for the plate is assumed to be $n_1(\omega) = 0.0942/(2\pi)$ s/rad, the modal density for the room cavity is calculated from Equation 7.95, and the coupling loss factor from the plate to the room cavity is calculated from Equation 7.97. The radiation efficiency is calculated from Equations 7.98–7.102. The speed of sound in air, c, is assumed to be 340 m/s; air mass density ρ_0 is 1.3 kg/m³ and mass density ρ of the aluminium plate is 2800 kg/m³. Equations 7.66 and 7.67 are applied to calculate mean plate and room cavity energy for the SEA approach.

In order to validate the SEA mean energy estimations, a deterministic analysis using modal expansion has been conducted in which coupling effects of the solid structure and fluid cavity are considered. Multiple constant bandwidth analysis was conducted on the results of the deterministic analysis, in which mean values of the deterministic energy at frequency sampling points in individual frequency bands were calculated at the central frequencies of the frequency bands and compared with the SEA mean value predictions. A hybrid solution was also sought by applying the deterministic analysis to calculate the mean room cavity energy (master system–room) and by applying the SEA equation to calculate mean plate energy (subsystem–plate). In this way, the coupling effects of the solid structure and the fluid cavity were considered in the SEA coupling loss factors.

The simulation results are shown in Plake VI which shows that the results calculated by the three methods support one another. The SEA and the hybrid methods tend to overestimate the mean response energy levels in comparison with the discrete sample average/median values from the deterministic results in the low to mid-frequencies.

In regard to the computational efficiency for the results in Plate VI (between pages 114 and 115), the SEA computation took 0.5 minutes, the deterministic computation took 10 hours and the hybrid computation took 2 hours. In the frequency range of 0–100 Hz, the deterministic method showed modal information in detail; the SEA method does not provide any modal information and has poor computational accuracy in this frequency range. In the frequency range of 100–600 Hz, the deterministic method showed more modal overlaps and structure variation-induced uncertainty, and its computational speed slowed down; the hybrid method showed the strong fluid–solid coupling mode peak and its computational speed was much faster than that of the deterministic method in this frequency range; and the SEA method does not provide any modal information but its computational accuracy improved in this frequency range.

7.10   References

1. Lyon, R.H. and DeJong, R.G. (1995), *Theory and Application of Statistical Energy Analysis*, Butterworth-Heinemann, Boston, MA.
2. Leppington, F.G., Broadbent, E.G. and Heron, K.H. (1982), The acoustic radiation efficiency of rectangular panels, *Proc. Roy. Soc. Lond.*, A382, 245–271.
3. Langley, R.S. and Cotoni, V. (2007), Response variance prediction for uncertain vibro-acoustic systems using a hybrid deterministic–statistical method, *J. Acoustical Society of America*, 122(6), 3445–3463.
4. Langley, R.S. and Bremner, P. (1999), A hybrid method for the vibration analysis of complex structural–acoustic systems, *J. Acoustical Society of America*, 105(3), 1657–1671.

5. Langley, R.S. and Cordioli, J.A. (2009), Hybrid deterministic–statistical analysis of vibro-acoustic systems with domain couplings on statistical components, *J. Sound and Vibration*, 321(3–5), 893–912.
6. Langley, R.S. (2008), Recent advances and remaining challenges in the statistical energy analysis of dynamic systems, 7th European Conference on Structural Dynamics, Southampton, 7–9 July 2008.
7. Langley, R.S. and Cotoni, V. (2004), Response variance prediction in the statistical energy analysis of built-up systems, *J. Acoustical Society of America*, 115(2), 706–718.
8. Langley, R.S. and Bercin, A.N. (1997), Wave intensity analysis of high frequency vibrations, in *Statistical Energy Analysis – an Overview, with Applications in Structural Dynamics*, edited by Keane, A.J. and Price, W.G., Cambridge University Press, Cambridge and New York.
9. Norton, M.P. (1989), *Fundamentals of Noise and Vibration Analysis for Engineers*, Cambridge University Press, Cambridge and New York.
10. Cremer, L., Heckl, M. and Ungar, E.E. (1990), *Structure Borne Sound: Structural Vibrations and Sound Radiation at Audio Frequencies*, 2nd edn, Springer-Verlag, Berlin.

Advanced simulation techniques in vehicle noise and vibration refinement

N. HAMPL, Ford-Werke GmbH, Germany

Abstract: Application of computer aided engineering (CAE) techniques is a key element of contemporary vehicle development processes. Upfront CAE simulations of vehicle noise and vibration performance are required to select designs that meet vehicle attribute targets. CAE is a key enabler to meet program timing and program cost by design selection right the first time before hardware and prototypes are available.

A wide variety of CAE-tools and analytical methods is available on the market to simulate certain aspects of noise and vibration refinement. Key CAE methods like finite element (FE), boundary element (BE), multi-body dynamics, computational fluid dynamics (CFD), statistical energy analysis (SEA) and transfer path analysis (TPA) are covered in this chapter as well as details on application and deliverables of these tools during the virtual series process. This chapter also includes contemporary applications like x-functional optimization and auralization and a list of links to standard tools used by the author's organization.

Key words: computer aided engineering (CAE), simulation, analytical methods, finite elements (FE), boundary element method (BEM), multi-body dynamics, statistical energy analysis (SEA), computational fluid dynamics (CFD), transfer path analysis (TPA), virtual series, X-functional optimization, design of experiment (DOE), visualization, auralization.

8.1 Introduction

Application of computer aided engineering (CAE) techniques is a mandatory element of contemporary vehicle development processes. It is well known to the public that several simulation loops of virtual crash tests are performed before building and crashing a first hardware prototype. Even if prototypes can still be fully used after noise and vibration testing, upfront CAE simulations of components as well as full vehicle noise and vibration performance are required to 'do it right the first time', i.e. select design concepts capable of meeting required component and full vehicle noise and vibration performance targets to avoid manufacturing, testing and redesign of sub-optimal vehicles or components, for the following reasons:

174

- The prototype build process is time- and resource-consuming and hence cannot be done repeatedly during the vehicle development process; current market constraints require short and efficient development processes to achieve affordable product prices.
- The first 'fully representative' hardware prototypes are available quite late in the development process; late design changes due to late indication of these prototypes for not meeting main attribute requirements would jeopardize program cost and timing.

Hence, early attribute predications are essential well before availability of the first hardware prototypes; in particular, all aspects that cannot be covered by engineering judgement or design guidelines need to be supported by CAE simulations.

Noise and vibration refinement covers many different aspects; therefore a wide variety of CAE tools and methods is available on the market to simulate certain aspects of noise and vibration refinement by analytical methods.

Confidence in CAE predictions for noise and vibration depends highly on the level of modelling details; neither is there one single CAE tool in place that can efficiently simulate all noise and vibration effects with high accuracy nor can a single metric express noise and vibration prediction capabilities.

8.2   Basic simulation techniques

A high-level overview on the most important CAE methods in use for noise and vibration refinement is given in the following.

8.2.1   Finite element-based techniques

Finite element (FE) methods are computational methods to simulate structural performance by use of numerical models. The basic concept of all FE techniques is to represent the geometry of each single component by a set of numerous small-sized elements (finite elements) for which well-known structural performance parameters such as stress, strain, temperature, etc., can be described by analytical (not necessarily linear) formulas [1, 2]. These elements can be simple spring elements, 'Euler–Timoshenko' beams, shell elements of triangular or quadrangular size, volume elements like tetrahedrons or hexahedrons, concentrated mass points (lumped masses), etc. Several so-called 'meshing' tools are available on the market to generate the respective FE models based on CAD geometry. Strictly speaking, the structural performance of each of these finite elements can be described by

the dynamic equation consisting of the element mass matrix, the element stiffness matrix and the 'response' vector.

The overall mass and stiffness matrix as well as the overall response vector are created from the respective individual matrices taking into consideration connections between individual elements as well as boundary conditions. Contemporary computer systems – from high-power computer clusters down to single desktop PCs – are capable of effectively solving these multi-degree-of-freedom equations and of generating requested structural results.

The full vehicle noise and vibration FE model consists of several component FE models, mainly of the following:

- Trimmed body FE model
- (Interior) cavity models
- Fluid–structure boundaries
- Chassis models
- Powertrain model
- Bushing and connections.

The trimmed body itself usually consists of the body in prime (i.e. all body sheet metal with primer and all fixed glazing; this model is created from shell elements and connections representing spot welds, seam welds or bonding), closures, interior trim (e.g. sound package material), instrument panel, seats, and many further parts rigidly mounted to the body structure. The latter can be represented with differing degrees of accuracy from simple concentrated masses to a detailed FE model, depending on the respective CAE task.

Cavity models represent air inside the passenger cabin, in the trunk (boot) and for dedicated under-hood (bonnet) noise analyses, even air in the engine bay. It is obvious that modelling of the boundary conditions for the engine bay cavity is non-trivial and requires correlation exercises ahead of any noise and vibration prediction.

Fluid–structure coupling describes the interrelationship between 'sheet metal vibration' and in-cabin sound pressure. These fluid–structure interactions need to be capable not only of generating sound pressure due to boundary structural vibrations, but also, vice versa, of generating structural vibrations due to sound pressure excitation. State-of-the-art tools are well capable of meeting these requirements with limited modelling and computational efforts.

Chassis noise and vibration models (e.g. suspension cross-members, longitudinal and lateral suspension links, anti-roll bar, twist beam rear axle, knuckle) can be easily derived from the respective CAE models for strength and durability analyses. Even though non-linear FE models are normally used to analyse strain effects and plastic deformation under extreme load-

ings for the latter, linear models can well be used for noise and vibration analyses as even extreme noise loads should never cause any plastic deformation of any load-carrying structure.

Powertrain FE models for application to vehicle noise and vibration refinement represent the engine (this model consists predominantly of solids) and transmission as well as drive shafts. Further FE models represent the exhaust, intake, accessory drive, powertrain mounts, etc. It needs to be noted that real-world operational temperatures need to be taken into account, in particular for exhausts, to correctly represent actual structural performance.

All these individual FE models need to be combined into one single FE model. As almost all currently used FE tools are based on unique 'grid' numbers for each node of uniquely numbered elements, using uniquely assigned material numbers to define material properties, each number must be used just once per category. Sophisticated internal numbering conventions or efficient renumbering mechanisms need to be applied for assembly of a full vehicle FE model to avoid any grid, element or material number duplication which would jeopardize the CAE model. Unlike in the early stages of FE analyses, grid numbers no longer need to be manually allocated to achieve best 'narrowband' system matrices for efficient solution, as up-to-date FE solvers do an internal reordering of system equations anyhow to achieve best computational performance.

The main task for full vehicle analyses is to predict customer perceptions of noise and vibration and to understand overall vehicle behaviour rather than doing detailed subsystem optimizations (e.g. panel thickness, topology optimization, etc.). Hence efficient full vehicle analyses can be achieved using 'superelement' techniques [3] by substructuring the vehicle FE model into individual pieces (e.g. body structure, closures, suspension components, etc.). Each superelement is processed individually at defined boundary conditions; the solutions are then combined to solve the entire model. The final analysis (in which all of the individual superelement solutions are combined) involves much smaller matrices than would be required to solve the entire model in a single solution. This technique has the advantage of reducing computer resource requirements, especially if changes are made to just one component (superelement) of the vehicle; in this case, only the affected superelement needs to be reanalysed and the final analysis repeated.

For standard superelement analysis each piece is represented by a reduced stiffness, mass and damping matrix, including all connection nodes and analysis points, whereas component mode synthesis is a form of superelement dynamic reduction wherein matrices are defined in terms of modal coordinates (corresponding to the superelement modes) and physical coordinates (corresponding to the grid points on the superelement boundaries). The advantage of component modal synthesis is the significantly smaller
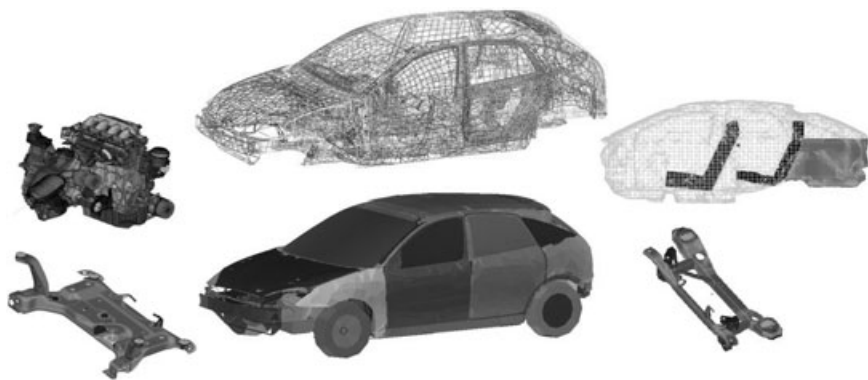
8.1 Finite-element-based full vehicle noise and vibration CAE model of a Ford Focus and its main superelements: trimmed body, interior cavities, rear and front suspension subframes, powertrain.

number of modal coordinates compared to the number of physical coordinates of the detailed model. It should be noted that each superelement could be derived also from physical testing, thereby increasing the accuracy of the overall analysis.

A display model for a full vehicle noise and vibration analysis and its components is shown in Fig. 8.1.

8.2.2   Boundary element-based techniques

The boundary element method (BEM) is an alternative numerical approach to solve linear partial differential equations if these can be formulated as integral equations (i.e. in boundary integral form) [4]. The main application field for BEM in vehicle noise and vibration refinement is sound radiation simulation of engine, exhaust shell, etc.

The boundary element method attempts to use given boundary conditions to fit boundary values rather than values throughout the space defined by a partial differential equation. Once this is done the integral equation can be used in the post-processing stage to numerically calculate the solution at any desired point in the solution domain. The boundary element method is often more efficient than other methods, including finite elements, in terms of computational resources for problems where there is a small surface to volume ratio.

For BE models, unlike FE models, the boundary surface is modelled by surface elements instead of the continuum (e.g. interior cavity of a vehicle, or environment around an engine). FE results as well as test results (e.g. vibration velocity of a powertrain surface) can be used to define boundary conditions.
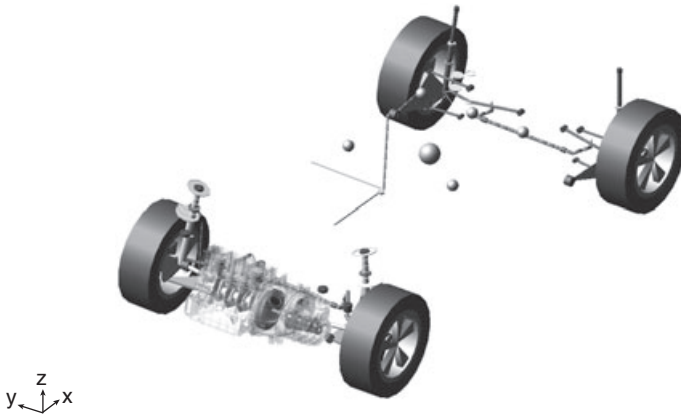
8.2 Multi-body CAE model of Ford Focus to simulate start/stop
vibrations. Suspension is represented by bars and bushes; detailed
model of crank train; trimmed body represented by concentrated
mass.

8.2.3   Multi-body dynamics

Multi-body dynamics tools are well established for simulation of structures
and mechanisms characterized by geometric non-linearity, large deflec-
tions, backlash, etc. [5]. These tools offer a variety of predefined compo-
nents, linear as well as non-linear connections, etc. The equations of motion
for these systems can only be solved in the time domain. Small time steps
are required to correctly cover dynamical effects; selection of proper
numerical solvers and time increments is mandatory to efficiently derive
correct results. To keep computational efforts small, structural elements for
multi-body models are usually represented by significantly simpler ele-
ments than detailed FE component models. Nevertheless, some of these
tools are nowadays capable of including subsystem FE models; both model
assembly and computational effort are significantly increased for such
approaches. Figure 8.2 shows a Ford Focus multi-body CAE model.

In addition to structural systems, some multi-body systems offer inter-
faces to software packages capable of simulating system dynamics and
control strategies.

8.2.4   Tools for system dynamics

Another category of simulation tools use dedicated mathematical and
logical models to define system dynamics of the individual (not necessarily
structural) vehicle components [6]. Hence, even dynamic control algorithms
can be included in this type of CAE model. A typical application for noise
and vibration refinement is upfront simulation of noise attenuation systems

as well as active nibble cancellation tools included in electrical power-assisted steering (EPAS). Libraries of predefined dynamical elements are offered within these toolsets to help users set up new models with minimum effort for developing new system dynamics equations.

8.2.5 Statistical energy analysis methods

Application of the above simulation tools is restricted to frequency ranges where 'exact' dynamic equations can be set up. This is not necessarily the case for mid- to high-frequency noise – for vehicle noise and vibration refinement the lower bound of this frequency range is between 250 and 400 Hz. Statistical approaches such as the so-called Statistical Energy Analysis (SEA) method need to be applied for these types of noise simulation and prediction [7, 8]. The basic principle of SEA is to solve equations for energy balance between individual sub-structures. Consequently, a vehicle needs to be partitioned into sub-structures that can be described by their acoustical or vibration energy within their boundaries, power source or energy loss within their boundaries and energy flow to all neighbouring sub-structures.

Each SEA tool includes libraries of energy equations for different element types; these are derived from FE analyses and correlation tests as well as assumptions for coupling loss factors. Extensive upfront correlation exercises are required until predictions can be made for road noise as well as wind noise. SEA techniques are well established for optimizing sound packages as these predict interior noise changes due to thickness or material changes of sound package material.

8.2.6 Computational fluid dynamics (CFD)

Tools for computational fluid dynamics (CFD) are required to simulate and predict aerodynamic and aeroacoustic vehicle phenomena. All CFD tools use numerical methods and algorithms to solve partial differential equations to analyse problems that involve fluid flows as well as interaction of gases with surfaces defined by boundary conditions.

The traditional approach in CFD in automotive engineering is to start with the Navier–Stokes (N–S) equations which statistically describe a real fluid [9]. The problem is that for most cases of interest, the solutions to these very complex and highly non-linear equations are characterized by many degrees of freedom, thus requiring a high computational effort.

An alternative approach is to use the Lattice Boltzmann method (LBM) which is a special discretization of the continuum Boltzmann equation in space, time and velocity. Conceptually, LBM recovers hydrodynamics by formulating a conservation theorem for any quantity conserved during

collisions of particles. Mass, momentum and energy are each specified in this theorem, generating three equations, recovering compressible mass continuity, a momentum equation and an energy equation [10].

All CFD analyses are normally performed by aerodynamics specialists. They can do all the postprocessing to derive acoustic excitation for noise refinement analyses from regular CFD analyses with just minor enhancements to fulfil aeroacoustic needs. Taking into account the main frequency as well as the structure of wind noise, it is straightforward to use SEA tools to predict wind noise based on CFD excitation data.

8.2.7 Transfer path analyses (TPA)

An entirely different analysis concept is used for transfer path analysis (TPA). For any TPA a vehicle is characterized by its 'noise paths' rather than by actual geometry. The principal concept of TPA is to sum up all individual noise paths (individual noise sources multiplied by respective noise sensitivity) to the full vehicle noise or vibration response. Individual noise sources are typically mount forces, intake and exhaust orifice noise, powertrain noise radiation, high-frequency noise, under-hood sound due to powertrain rigid body motion, etc. For the example of a powertrain mount, the respective noise source would be mount displacement multiplied by mount stiffness; the respective noise sensitivity would be p/F (sound pressure (p) per unit excitation force (F)) and noise transfer function (NTF).

The mathematical effort for TPA methods itself is significantly lower than for FE or BE methods, but valid TPA models require representative data for, e.g., noise sensitivities. If the latter cannot be predicted with high confidence, these need to be based on measured noise sensitivities. Hence these methods will be 'exact' only for installations of 'new' powertrains into given structures. Noise sources can be based on measurements or CAE analyses.

8.3   Frequency or time-domain methods

The majority of FEM and BEM analyses for noise and vibration refinement are performed in the frequency domain rather than in the time domain by applying modal frequency response analyses. This approach significantly reduces CPU time, but should be applied only for quasi-stationary phenomena like idle, cruising road and wind noise, slow speed changes during acceleration or overrun, as well as for calculating transfer functions.

Time-domain analyses are appropriate for non-linear structures as well as for non-periodic load cases. Typical time-domain analyses cover simulation of non-linear systems and materials as well as single impacts, key-on/key-off simulations, brake judder responses, etc. Time increments for any

time-domain analysis need to be small enough to ensure two simulation instances within one complete vibration cycle of the system with highest system eigenfrequency.

8.4   Simulation process

Simulation processes occur in three distinct phases during vehicle development:

1. Early concept selection using simplified (concept) models – these analyses are normally done individually for each attribute, and common concepts need to be agreed before detailed component design starts.
2. Virtual verification and *x*-functional optimization of *x*-attribute agreed 'frozen' design – virtual series.
3. Support of actual attribute issues on 'verification prototypes' and correlation of CAE models.

8.4.1   Virtual series

Once design has achieved a maturity level that allows creation of simulation models for all individual attributes, a so-called 'CAD freeze' will kick-off a 'virtual series' process. The main concept of virtual series is that early assessments for all attributes and teams need to be based on one common design well before the first hardware prototypes are created for the final engineering 'sign-off'. Virtual series are by no means restricted just to typical CAE attributes like safety, durability, noise, cooling, etc., but are also applied to analyses on cost, weight, manufacturing, etc.

Once the design is frozen, all component areas, including their suppliers, will start 'meshing' components they are responsible for. These meshes can still be attribute-independent, i.e. can be used for both safety (high deformation requiring non-linear material laws) as well as noise calculations (small deformations within linearity range).

Each attribute CAE team will then incorporate these FE meshes as well as supplier models into attribute-specific simulation models. Model creation typically consists of 70% chasing for data (e.g. actual dynamic mount stiffness under operational load; mass, centre of gravity and moment of inertia for all parts for which no FE mesh is required or available) and 30% modelling and analysis.

All simulation results need to be jointly reviewed to agree on corrective actions (these may be based on dedicated model modifications) and to incorporate these changes into CAD design for the next 'virtual series freeze'. The timespan between CAD freeze and reporting on the vehicle noise and vibration refinement results is typically in the order of 6–10

weeks; this often causes a significant delay of CAE analyses with respect to design status and the need to kick off the prototype build process before the final virtual series could be completed.

8.4.2   Noise and vibration refinement deliverables for virtual series

Each component CAE model that is required for a full vehicle noise and vibration simulation model will first be checked and analysed by the responsible component area to ensure that the component will meet its targets. Typical noise-relevant component attributes are dynamic stiffness, component eigenfrequencies and mode shapes, noise and vibration transfer functions as well as source levels, e.g. shaking forces and noise radiation of powertrains. If any component significantly fails to meet its noise-related target, full vehicle noise performance will also probably not meet its targets.

Typical virtual series deliverables for full vehicle noise and vibration refinement are:

- Vehicle modal alignment: all component modes should properly be separated to avoid any 'resonance catastrophe' under operating conditions.
- Vehicle sensitivity to 'unit excitation': this can be a vibration transfer function (vehicle response at the customer perception point due to, e.g., unit mount force, calculated by FE tools), a noise transfer function (p/F, also calculated by FE tools) or noise reduction (sound pressure difference between engine bay and passenger cabin, calculated by SEA tools).
- Response to typical vehicle load cases, e.g. structure-borne response to idle excitation (loads of the powertrain applied to a full vehicle FE model), response to wheel imbalance (nibble, solved by FE or system dynamics tools depending on vehicle content for electronic tools to reduce steering wheel rotation – EPAS), response to road excitation or road noise (road surface irregularities applied to tyre patch points using an FE tool); vehicle acceleration noise (including all load paths in the TPA tool); and high-frequency noises like wind noise (derive the shape-related pressure fluctuation on the outer vehicle skin from CFD simulation and apply this as load for SEA analyses).

The 'status assessments' that need to be prepared for the virtual series report will be followed by further activities to identify the root causes for missing attribute targets. Transfer path analyses as well as modal contribution analyses are typical methods applied for these noise and vibration refinement investigations (see Plates VII and VIII between pages 114 and 115).

Based on such findings, high-level corrective actions like increasing local stiffness by adding reinforcements to the CAE model or shifting component modes in the respective CAE model will be investigated. If these changes solve the issues, these concepts will be communicated to the respective component areas to develop feasible solutions that need to be incorporated into the design for the next virtual series or for prototypes, as appropriate.

8.4.3 Simulation of design status versus x-functional optimization

Virtual series as described above would just deliver vehicle noise and vibration refinement status for nominal design. This would not make use of one main advantage of virtual analyses: CAE enables analysis of several different designs within a fraction of the time, efforts and resources that would be needed for creating and testing real hardware variants. Consequently, simulations should

- take into account variability of design parameters such as mount stiffness on attribute performance,
- investigate parameter settings which enable more robust designs,
- include x-functional optimization to find a best compromise between attribute performances. The attributes offering most potential conflicts for noise and vibration refinement are vehicle dynamics, durability, weight and cost.

Each of these tasks requires a series of simulations using different input parameter sets. There is no longer a need to submit each simulation run manually; several optimization packages are available on the market that automatically submit a series of analyses on individual tools as listed above, tailored to variability of input parameters, and that carry out post-processing and optimization.

In real-case applications, every simulation can take hours or even days. In these cases, the time to run a single analysis makes running more than a few simulations prohibitive. The design of experiment (DOE) technique is a smart approach to achieving a maximum amount of knowledge from a reduced number of calculations or tests [11]. Further analyses can be performed on a response surface that is a multi-dimensional hyper-surface created by interpolation of the well-distributed results on the full vehicle CAE model. This response surface represents a meta-model of the original problem and can be used to perform the optimization. Just the outcome of this optimization needs to be verified on the original CAE model.

8.4.4 Confidence in noise and vibration refinement simulations

Quality and confidence in CAE simulation results depend on the quality of each single involved sub-model. Some vehicle noise and vibration refinement phenomena can be predicted with high confidence by CAE (e.g. powertrain rigid body modes in a vehicle, bending frequencies of a powertrain), whereas prediction of some other noise and vibration refinement characteristics (e.g. trimmed body noise transfer functions) cannot be predicted with an accuracy of less than say 3 dB. Consequently, road-induced low-frequency noise – which involves trimmed body noise transfer functions for suspension attachment points – cannot be predicted with sufficient accuracy by CAE.

Consequently, a 'full analytical sign-off' for vehicle noise and vibration refinement is still not achievable. Therefore all attribute assessments should be done jointly between attribute experts and simulation experts. In the case of road noise, any analytical upfront assessment might be based on a surrogate metric by comparing suspension forces of different suspension designs.

In order to enable early CAE analyses for the next vehicle program, CAE teams need to spend reasonable resources on correlating the latest CAE models with current production hardware.

8.5   Application of virtual reality for vehicle noise and vibration refinement

Simulation techniques should be applied to enable evaluations of complete vehicles or subsystems even before hardware is available. Consequently, results of CAE simulations should not be shown just as 'pure numbers' or 'colour curves' but should be presented in a form similar to impressions in real vehicles.

8.5.1 Visualization of simulation results

Modal analysis results have been animated on computer screens for many years; animation speed and quality have improved significantly. For illustration purposes, displacement amplitudes are often magnified by orders of 10 to allow for, e.g., mode interpretation. Recent developments allow 3D display without any magnification in a so-called 'virtual reality cave' to evaluate the real visible impression of driving a vehicle. In addition, simulating seat and steering wheel vibrations in such a cave creates a real in-vehicle 'look and feel' impression [12].

8.5.2 Auralization of simulation results

Auralization techniques are all the techniques required to generate and simulate predicted sounds and noises. The main techniques for auralization approaches are order extraction, sound decomposition and sound synthesis. Order extraction techniques allow identification of order content of any recorded vehicle sound, based on quality 'tacho' signals that enable identification of trigger signals. Sound decomposition is required to separate recorded noise into different orders and 'random noise' contributions. Sound synthesis is the last process step in superposing individual sound components. It is extremely critical for the quality of any synthesized sound that phase relationships between individual orders are representative, otherwise any synthesized sound will sound artificial and cannot be used for jury evaluation. This is relevant for both binaural (two-ear) sounds that are based on artificial head (Aachen Head) measurements as well as monoaural (mono) sounds.

8.6   Conclusions

Computer performance is improving from year to year, thus enabling more noise and vibration refinement CAE simulations as well as analyses on CAE models with more degrees of freedom. Finer meshing itself is not necessarily guaranteeing increased accuracy of simulation results; simulation methods also need to be permanently refined. These method enhancements are usually performed as joint projects between software vendors, universities and OEMs. CAE enhancements and new methods are regularly reported at user software conferences and are included in software releases. A list of URL links to vendors of commercial noise and vibration refinement software packages is given in Section 8.7. A very good overview on the latest state-of-the-art noise simulation methods and projects is given, for example, at the annual SAE Noise and Vibration Conference (Society of Automotive Engineers).

Although many noise and vibration phenomena can be simulated, there is no real need to do this for each and every noise and vibration effect. Strictly following the respective design rules can be more than capable of avoiding recurrence of typical error states such as gear rattle, transmission whine or squeak. Therefore any simulation should be requested and set up only if adding real value to the carline program – never do any CAE simulation just to follow any process. Simulations additionally require dedicated resources for component 'meshing', simulation model creation and finally simulation job execution and analysis; simple component rig tests may be a better alternative than CAE.

A final remark on CAE simulation is that any CAE model that generates error messages definitively delivers wrong results; CAE simulation runs without warnings could be correct – nevertheless it is important to understand both the physics as well as the restrictions of each CAE method and model. Always do sanity checks on results. It is significantly better not to publish doubtful CAE results than to share erroneous CAE results that drive wrong design directions. Nevertheless, developers should make use of simulation techniques for noise and vibration refinement, as they are a viable contributor to quality vehicles.

8.7 Sources of further information and advice

There are hundreds of CAE tools available on the market that can be used for noise and vibration refinement simulation. The following is a small selection of tools used within the Ford Motor Company for noise and vibration refinement:

NASTRAN, Finite Element solver, www.mscsoftware.com

ABAQUS, Finite Element solver, www.simulia.com

RADIOSS, Finite Element solver, www.altairhyperworks.com

AKUSMOD, tool for coupled fluid–structure analysis, www.sfe1.extern.tu-berlin.de

ACTRAN, tool for coupled fluid–structure analysis, www.fft.be

SYSNOISE, boundary element tool for acoustics simulation, now included in **Virtual.Lab**, www.lmsint.com

ADAMS, multibody system software, www.mscsoftware.com

SIMPACK, multibody system software, www.simpack.com

SIMULINK, simulation software for multidynamic systems, www.mathworks.com

VA One, statistical energy analysis tool, www.esi-group.com

SEAM, statistical energy analysis tool, www.seam.com

Star-CD, CFD tool, www.cd-adapco.com

PowerFLOW, CFD tools, www.exa.com

Artemis, sound recording, analysis and playback software, www.head-acoustics.de/eng

modeFRONTIER, optimization and robustness tool, www.esteco.com

I-sigh, optimization and robustness tool, www.simulia.com

HyperStudy, optimization and robustness tool, www.altairhyperworks.com

8.8 References

1. Zienkiewicz, O., *The Finite Element Method*, 3rd edition, McGraw-Hill, New York, 1979
2. Bathe, K., *Finite Element Procedures*, Prentice-Hall, Englewood Cliffs, NJ, 1982

3. MSC/Nastran, *Handbook for Superelement Analysis*, MacNeal-Schwendler Corp., Los Angeles
4. Ciskowski, R.D. *et al.*, *Boundary Element Methods in Acoustics*, Computational Mechanics Publications, Southampton, UK, 1991
5. Schielen, W., *Multibody Systems Handbook*, Springer, Berlin, 1990
6. Harper, B.D., *Solving Dynamic Problems in MATLAB*, Wiley, New York, 2002
7. Lyon, R.H., *Statistical Energy Analysis of Dynamical Systems, Theory and Applications*, MIT Press, Cambridge, MA, 1975
8. Lyon, R.H. and DeJong, R.G., *Theory and Application of Statistical Energy Analysis*, 2nd edition, Butterworth-Heinemann, Boston, MA, 1995
9. Ferziger, J.H. and Peric, M., *Computational Methods in Fluid Dynamics*, Springer, Berlin, 2002
10. Lietz, R., Mallick, S., Kandasamy, S. and Chen, H., Exterior airflow simulations using a Lattice Boltzmann approach, *2002 SAE World Congress*, Detroit, paper 2002-01-0596
11. Grove, D.M. and Davis, T.P., *Engineering Quality and Experimental Design*, Longman, London, 1992
12. Allman-Ward, M. *et al.*, The interactive NVH simulator as a practical engineering tool, *2003 SAE Noise and Vibration Conference*, Traverse City, MI, paper 2003-01-1505

9

Advanced experimental techniques in vehicle noise and vibration refinement

T. AHLERSMEYER, Ford-Werke GmbH, Germany

Abstract: This chapter discusses advanced techniques to correctly measure vehicle noise and to understand its root causes. The chapter covers structure-borne and air-borne contribution analysis for low and high frequencies in general and shows how sound intensity probes and laser vibrometers can help to analyse the test object. In addition, psychoacoustic metrics and material tests typically used in the field of vehicle noise and special aspects of tracked analysis are discussed.

Key words: transfer path analysis, sound intensity, source identification, sound quality, material testing, tracking analysis.

9.1 Transfer path analysis technique

The classical method of noise source identification is to conduct a disconnection test. If a source is disconnected (e.g. by decoupling the engine mount, putting a total muffler on the air intake system, etc.) and the noise amplitude at the receiving point is reduced significantly, the main root cause is found. However, this only works well if there is a single dominant source (or very few). Even then there is an inherent risk that the disconnection test changed the other contributions, which is often the case if engine mounts are decoupled. With multiple sources of similar contributions this method is not able to give clear results.

In such cases, Transfer Path Analysis (TPA) works better. The TPA models each connection between the noise source (e.g. vibrating engine) and the receiver (e.g. interior compartment noise or seat vibration) as an excitation (e.g. force input, N) and a transfer function (e.g. receiver sensitivity, Pa/N or $(m/s^2)/N$). Figure 9.1 shows the source–receiver model. The general thinking is:

$$resp_{ij} = exci_j \times TF_{ij} \tag{9.1}$$

where

$resp_{ij}$ = response at point i caused by excitation at path j
$exci_j$ = excitation at path j
TF_{ij} = transfer function between points i and j.
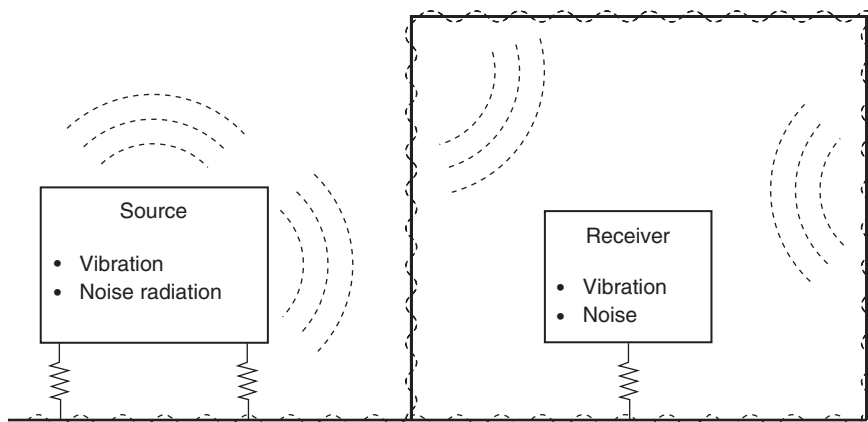
9.1 Source–receiver model.

If all paths are modelled correctly the complex sum of all responses should be equal to the response under operation:

$$\text{resp}_{\text{oper},\,i} = \sum_{i,j} \text{resp}_{ij} \qquad (9.2)$$

where $\text{resp}_{\text{oper},i}$ = response at point i measured under operation.

The difference between the calculated response and the measured response can be used as an indicator of the quality of the TPA model. However, even if the calculated response equals the measured response under operation, this is not a proof that the TPA model is exact in every detail.

The main problem of the TPA is to get the force input.[1–3] There are four principal methods:

1. Force method: measure excitation force by introducing a force sensor.
2. Stiffness method: estimate excitation force through, e.g., rubber mounts by multiplying measured relative displacement by measured dynamic stiffness.
3. Matrix method: estimate excitation force by measuring and inverting the inertance transfer matrix.
4. Operational TPA: estimate excitation force by a least-squares approach of operational data.

The features of each method are:

1. Introducing a force sensor (e.g. 15 mm high) will modify the vehicle (mass and stiffness at the connection point and position of force input) and therefore potentially all path contributions. It can only be applied in special cases. The advantage is that the problems of other methods do not arise (see below).

© Woodhead Publishing Limited, 2010

2. The measurement of relative displacement can be difficult for complex mounts such as engine mounts. The dynamic stiffness of a rubber mount depends on the frequency and the preloads in all directions. Unfortunately the preload changes during operation (wide open throttle = WOT, or overrun = OVR) due to changing engine torque and with temperature, so it is very difficult to test the engine mount under real-world conditions. Commercially available 3D mount testing machines are extremely expensive and work only up to 100 Hz, so they cannot provide the required data.

3. The matrix method only works if all relevant transfer paths are included in the model. A typical vehicle model will include at least 25 structural paths, a model of a rear- or all-wheel drive vehicle may include up to 80 paths (see Table 9.1).

4. The least-squares approach assumes that transfer functions are constant over, e.g., all engine rpms. Since the engine torque changes over rpm this is not valid in detail. As the desired response is used as a target for the least-squares optimisation, the difference between the measured response and the calculated response can no longer be used as a quality indicator of the TPA model.

For the first method the vehicle must be modified significantly; for the second method the vehicle must be modified if the original mounts are to be used. For the first, second and third methods, the transfer functions should be measured with a decoupled excitation side, which again is a modification of the vehicle. These modifications may change the vehicle significantly, therefore making validation of the model impossible.

During the measurement of the transfer functions the vehicle is at room temperature, has no occupants (missing volume and mass load) and is not preloaded with reaction torques from the powertrain. All these conditions differ more or less from operational conditions and may adversely affect the result.

Table 9.1 Typical paths to be included in a TPA

Count	Component	Directions	Paths
3–4	Engine/transmission mounts	*XYZ*	9–12
1	AC hose	*XYZ*	3
1	Clutch cable	*XYZ*	3
3–8	Exhaust hangers	*Z* or *XYZ*	3–8
2	Airborne noise sources	S (scalar)	2
1	Powertrain radiated noise	S (scalar)	Typically 6
2 (4*)	Side shafts*	*XYZ*	6–12

*If the contribution of the side shafts is to be further analysed, they must be split down to link arm (*XYZ*) + top mount (*XYZ*) per side shaft.

The only way to avoid this is to conduct operational TPA, which unfortunately gives the least insight into the vehicle because the excitation forces are not calculated; only the path contribution and the transfer functions (Pa/(m/s^2)) are calculated, which are only valid under the operating conditions used.[4,5]

This situation can be improved by performing noise transfer function (NTF) (Pa/N) and point inertance measurements ((m/s^2)/N). With these values one could better understand the body structure and calculate the exciting forces. However, for physically exact results it is required to disconnect the body and excitation sides in order to ensure that the exciting force is introduced only into the body. Unfortunately this gives the method a disadvantage.

Airborne noise sources such as intake and exhaust orifice noise can be included in the model, e.g. by measuring the noise under operation (Pa) and the transfer function with noise excitation at the orifice (Pa/Pa). Even the radiation from surfaces can be included by measuring the surface averaged acceleration (m/s^2), multiplying it by the surface (m^2) and measuring the volume acceleration transfer function (Pa/(m^3/s^2)).

As the TPA calculates a vector sum of contributions it can only deal with coherent signals with constant phase relationship (e.g. engine excitation). For incoherent excitation (e.g. road noise) the inputs must first be represented by a set of orthogonal vectors (principal components, PRC) by means of a principal component analysis (PRCA).

The number of principal components is identical to the number of reference signals. Nevertheless, a certain principal component cannot be interpreted as being correlated with a certain reference signal. In order to explain the measured response best a high number of PRCs are required. However, for each set of PRCs one has to solve a complete TPA. Therefore it is desired to find the lowest number of reference signals that can explain the measured response well enough in the problem areas. The quality of a road noise TPA depends highly on the selection of the reference signals.

The index of the highest contributing PRC is not constant, so problem range A may be explained mainly by PRC 1 whereas problem range B may be explained mainly by PRC 2. In general a noise phenomenon (e.g., a response peak at a certain frequency) is explained not just by a single PRC but by a combination of PRCs. This requires that the results of multiple TPAs have to be judged in parallel or one has to work with the sum of PRCs.

9.2   Sound intensity technique for source identification

The sound pressure is a scalar value, so by measuring the sound pressure at one point there is no information available concerning where the noise is coming from. For a point source in a free-field environment the sound

pressure at a second point is required in order to estimate the direction of the noise source.

With a more complex source in a more complex environment this no longer works. As well as the sound pressure, the sound velocity is needed to understand how much sound energy is transmitted and in which direction. Sound pressure and sound velocity define the basic properties of the sound field:

$$\vec{Z} = p/\vec{v} \qquad (9.3)$$

$$\vec{I} = p\vec{v} \qquad (9.4)$$

where

Z = sound impedance, $kg/(m^2s)$ = Ns/m^3
I = sound intensity, W/m^2 = $N/(ms)$
p = sound pressure, Pa = N/m^2 = $kg/(ms^2)$
v = sound velocity, m/s.

In the far field of a point source the sound pressure p and the sound velocity v are in phase, so the sound impedance becomes real:

$$Z_0 = p_0/v_0 = \rho c = 400 \text{ Ns/m}^3 \qquad (9.5)$$

where

p_0 = sound pressure reference value = 2×10^{-5} Pa
v_0 = sound velocity reference value = 5×10^{-8} m/s
ρ = density of air = 1.18 kg/m³
c = speed of sound = 339 m/s at 20°C

and the sound intensity may be expressed as:

$$I = pv = p^2/(\rho c) \qquad (9.6)$$

As the reference values p_0 (= 2×10^{-5} Pa) and $I_0 = p_0^2/400$ (= 1×10^{-12} W/m²) are aligned, in the far field of a point source the sound pressure level and sound intensity level are identical. In the near field of a point source the sound pressure p and the sound velocity v are not in phase, so the net sound energy flow is lower than expected from the measured sound pressure and therefore the sound intensity level L_I is lower than the sound pressure level L_p.

In a perfect diffuse sound field there is no net energy transfer, so the intensity level is zero and thus much lower than the sound pressure level. The difference between the sound pressure level L_p and the sound intensity level L_I is called the reactivity index or pressure-intensity index,[6] δ_{pI}

$$\delta_{pI} = L_p - L_I \qquad (9.7)$$
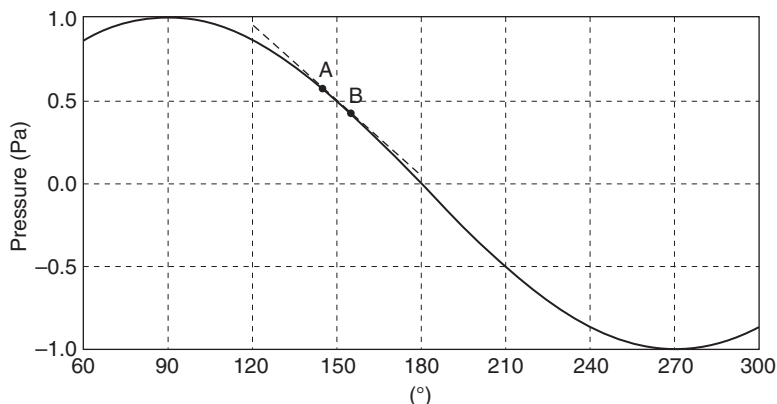
9.2 Approximation of sound velocity.

Table 9.2 Upper frequency limits of intensity probe for −1 dB error

Distance r	Upper frequency
6 mm	10.4 kHz
12 mm	5.2 kHz
25 mm	2.5 kHz
50 mm	1.25 kHz

It can be used as an indicator for the sound field type (0 dB indicates an ideal free field, >20 dB a diffuse sound field).

Unfortunately it is difficult to measure the sound velocity directly but it may be replaced by the pressure gradient $\Delta p/\Delta r$, as shown in Fig. 9.2. The pressure gradient is estimated by measuring the sound pressure at two points A and B at distance r, so the sound velocity v becomes:

$$v = (p_A - p_B)/r \tag{9.8}$$

For the sound pressure p the average value is taken:

$$p = (p_A + p_B)/2 \tag{9.9}$$

This is a good approximation for p and v only if the distance r is much smaller than the wavelength, otherwise the sound intensity is underestimated; Table 9.2 gives the upper frequency limits for an error of −1 dB.

For low frequencies or a diffuse sound field the term $p_A - p_B$ becomes very small, so the level calibration and phase difference of the two pressure sensors becomes very critical. Assuming a pressure-intensity index of 15 dB and a phase error of 0.1°, the lower frequency limits for an error of ±1.0 dB

Table 9.3 Lower frequency limits of intensity probe
for ±1 dB error

Distance r	Lower frequency
6 mm	434 Hz
12 mm	217 Hz
25 mm	104 Hz
50 mm	52 Hz

between the true intensity and the estimated intensity are shown in Table 9.3.

The usual realisation of an intensity probe is to place two small microphones either side by side or face to face with a massive spacer to fill the gap. The latter strategy easily allows one to modify the distance r and thus to adapt the usable frequency range by just changing the spacer. An alternative approach was invented at the University of Twente in 1994 and realised by Microflown: a particle velocity sensor was built based on the two hot wire anemometers concept.[7]

But how can the sound intensity be used to find a noise source? Assuming a point source in a free-field environment, the maximum sound velocity occurs if the two microphones and the point source are located in line. If the microphones are oriented normal to the point source, the pressure at both microphones is identical and thus the sound velocity is zero (Fig. 9.3).

The sound intensity probe has a dipole characteristic which can be used to find a noise source. As there is no sharp maximum (a ±27° misalignment causes only a −1 dB variation in intensity) but a sharp minimum (a 3° misalignment causes a 6 dB variation in intensity), the minimum can be used to manually find the orientation of the intensity vector. Starting at a certain point the intensity probe is oriented such that the measured intensity is minimal. This defines one plane of the intensity vector. In an orthogonal plane the procedure is repeated, thus finding the exact orientation of the intensity vector. Finally the sign is checked by orienting the intensity probe in the direction of the found intensity vector. This procedure must be repeated, e.g., every 20 cm to finally find the noise source. Alternatively a 3D intensity probe can be used to find the exact orientation of the intensity vector at a certain point.

In order to use a sound intensity probe in such a way, a stable sound field is required. For a rotating engine this requires that the engine speed is kept constant during the whole process. In addition, the engine load and the temperature of all the transmission media (metal, air, etc.) involved must be constant. This is impossible for a complete vehicle and can only be realised for a powertrain on a powertrain test rig (e.g., a chassis dynamometer) with external cooling.
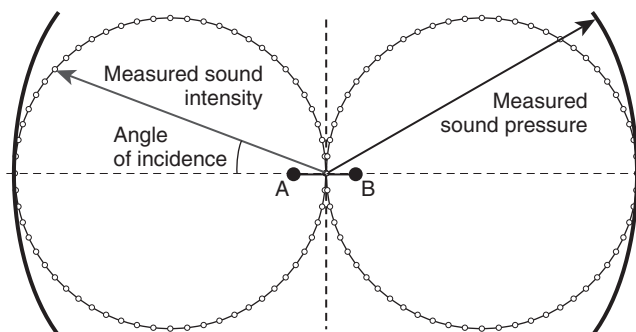
9.3 Directivity of intensity probe.

The main application for sound intensity measurements is the estimation of radiated sound power under non-ideal conditions. If the sound intensity is measured normal to a closed surface, the sound power (W) radiated through this surface can be measured by multiplying the surface averaged intensity (W/m²) by the area of the surface (m²). As the intensity probe can distinguish between energy coming out or going into the surface, this works even in a non-anechoic room and when other sources are present in the neighbourhood. An effective way to perform such measurements is to continuously scan the surface, thus achieving an equally weighted spatial average. The scanning surface may even be close to (i.e. in the nearfield of) the noise source. However, performing a nearfield intensity mapping (e.g. at 10–20 cm from the radiating surface) requires either a high instrumental effort (several 3D intensity probes in parallel) or a long measurement time combined with a very stable device under test. Instead of using an array of 3D intensity probes, under some circumstances it is more efficient to use the same number of microphones in a rectangular array and perform a nearfield acoustic holography analysis (see next section).

9.3   Acoustic camera: beamforming and nearfield acoustic holography techniques for source diagnostics

Sometimes it is difficult or impossible to measure in the near field of a noise source (e.g. a wind generator), or large areas are to be scanned for noise sources (e.g. buildings, body panels of vans, etc.). In such circumstances one needs to measure the sound pressure at certain points in the measurement plane and to estimate the sound pressure distribution at the source plane by beamforming techniques.[8,9]

In other applications the sound pressure can only be measured close to the surface but has to be extrapolated further away from the surface. This

Table 9.4 Frequency range of NAH and beamforming arrays

Type	Spatial resolution	Frequency range
Nearfield acoustic holography	$\min(d, \lambda/2)$	$F_{min} = c/2S$ $F_{max} = c/8D$
Beamforming	$\dfrac{d\lambda}{D}$	F_{min} limited by desired spatial resolution

c = speed of sound in air = 339 m/s at 20°C
λ = wavelength (m) = speed of sound (m/s)/frequency (Hz)
D = diameter of array (m)
d = distance to source (m)
S = averaged distance of array points (m)

can be achieved with nearfield acoustic holography (NAH) techniques. An essential requirement for NAH is that the dimension of the microphone array must be greater than the dimension of the source plane.

In both cases planar microphone arrays are used. With the overall size of the array and the distribution of the microphones within the array, certain properties can be achieved. Typical arrays use 30–90 microphones. Both techniques cover different frequency ranges assuming comparable dimensions of the microphone array used (see Table 9.4)[10].

Both methods follow different strategies. The delay and sum beamforming strategy applies a certain amount of delay on certain microphones. If the signals from all microphones are summed after manipulation an acoustic antenna with a main lobe and suppressed side lobes is created. The side lobes will give error sources, which can be reduced, e.g., by using non-uniformly distributed arrays. By changing the amount of delay, different parts of the surface can be highlighted (i.e. scanned). This works up to an angle of ±30° from the central axis, so relatively small arrays are able to scan relatively large objects. The method requires low background noise in the measurement plane, as all measured noise is assumed to be radiated from the target plane.

The NAH essentially estimates a distribution of correlated volume–velocity point sources in the defined source plane and then uses the Helmholtz equation to calculate the sound pressure distribution in a target plane. The model is tuned in a least-squares sense to achieve the measured sound pressure distribution. This requires that the planar microphone array must enclose the source plane. This is approximately fulfilled if it has the same size as the noise source plus an extension that also covers noise radiated 45° to the outside. The model can then also be used to calculate the far-field radiation and, e.g., the radiated sound power. As the model is based on surface velocity, the impact on virtual source reduction measures

can be predicted as well. When compared to dual microphone intensity measurements both methods correlate well.[11]

Both strategies deliver a map of, e.g., sound pressures on a target surface. The dynamic range of the maps (e.g. the difference between main lobe and side lobes for beamforming) will typically be between 6 and 15 dB depending on the design of the array and the frequency. In general this complicates the interpretation of the results.

For beamforming usually a high sample rate is used for data acquisition to theoretically achieve a high spatial resolution. The delay is realised by just taking later samples (or by interpolation between samples), so the main calculation is done in the time domain and is transferred to the frequency domain only for visualisation. Therefore acoustic cameras based on the beamforming strategy can work nearly in real time and may show transient effects. This is one of the reasons for their popularity.[12]

The most promising application for vehicle NVH is rapid noise source localisation on a powertrain test rig. Whether NAH or beamforming is used is determined by the problem frequency range. Even on a powertrain testrig the conditions are not ideal:

- For beamforming the measurement distance often cannot be made long enough owing to small powertrain test cells. Furthermore, the requirement of free-field radiation and low background noise is often not fulfilled.
- For NAH the source surface is often not plane enough and the microphone array cannot be positioned close enough and must therefore be relatively big to enclose the source. Furthermore, cables and pipes that cross the free sound field may adversely affect the result. Other applications such as squeak and rattle detection often suffer too much from the principal limitations of the method.

Although it is very much desired to localise noise sources or areas of noise radiation or transmission in the vehicle interior, NAH and beamforming are not the right tools here. The source shape is in general too complex and the sound field too diffuse to allow using these techniques. For these applications spherical beamforming was developed.[13] The microphone array is placed on a solid sphere which is placed, for example, at the driver's head position. The algorithm decomposes the measured sound pressures into their spherical harmonic components and then estimates the directional contributions by recombining these spherical harmonics. The angular resolution φ of spherical beamforming is approximated by:

$$\varphi = \frac{180c}{2\pi fa} \qquad (9.10)$$

where

φ = angular resolution (°)
a = diameter of sphere (m)
c = speed of sound (m/s)
f = frequency (Hz).

For low frequencies the method suffers from poor angular resolution; for higher frequencies the dynamic range of the maps is a limiting factor due to side lobes. With a sphere of 20 cm diameter and about 40 pressure sensors, a frequency range of 500 Hz to 4 kHz can be covered with angular resolutions from 98° to 12°. This is in general not enough to locate single sources but it finds areas where further methods (including optical/manual inspection and nearfield microphone measurements) are required to find the root cause of high noise radiation.

9.4   Laser techniques for dynamic analysis and source identification

For light structures (e.g. roof panels) the application of an accelerometer with cabling might already alter the structural properties or might require miniature accelerometers with other limitations such as the signal-to-noise ratio. Here non-contact methods such as laser doppler vibrometers (LDV) can be a better solution. LDVs are also ideal to measure vibrations on very hot surfaces. In production control applications LDVs are preferred because no time is needed to apply a vibrating sensor or a cable.

Especially for extensive structures (e.g. complete body panels of vehicles or aircraft) a method that allows for measuring the complete surface is desired. If stationary conditions can be provided (e.g. shaker excitation or constant engine speed) a scanning LDV is the ideal solution. If non-stationary events are measured, all vibrations must be measured instantaneously. This can be done either with an array of LDVs or by holographic methods.

The laser beam of the LDV is split into a reference beam and a test beam, which is sent towards the desired vibrating surface. The beam is reflected from the vibrating surface which causes a Doppler shift in frequency. The reflected test beam finally interferes with the reference beam. In order to be able to distinguish between positive and negative vibration amplitudes, an additional known frequency shift is introduced to the test beam. A schematic of a typical LDV is shown in Fig. 9.4.

The laser beam with frequency F_L (>10^{14} Hz) is divided into a reference beam and an object beam using a beam splitter. The object beam first passes through a Bragg cell, which adds a known frequency shift F_B (typically 30–40 $\times$ 10^6 Hz). The modified object beam with frequency $F_L + F_B$ then
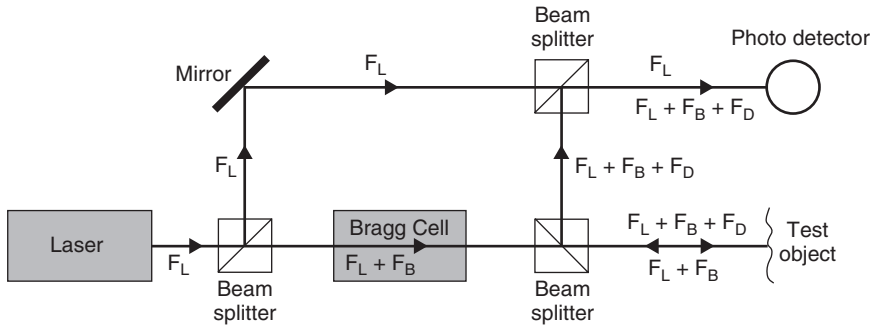
9.4 Schematic of laser Doppler vibrometer (LDV).

hits the target surface. The motion of the target surface adds a Doppler shift F_D to the object beam, given by:

$$F_D = \frac{2v(t)\cos(\alpha)}{\lambda} \tag{9.11}$$

where

$v(t)$ = velocity of target surface (m)
α = angle between object laser beam and velocity vector
λ = wavelength of object laser beam.

Light with frequency $F_L + F_B + F_D$ is reflected by the surface in all directions. A portion of it is collected by the LDV and reflected by a beam splitter to the photodetector. Both beams interfere, but the photodetector senses only the beat frequency $F_B + F_D$ between the two beams, which is a standard frequency-modulated signal with the Doppler shift as the modulation frequency. This signal is then finally demodulated to get the desired velocity versus time signal of the vibrating surface.

Although the LDV can be used as a normal vibration sensor, it is much more complicated than a normal accelerometer, so the cost is much higher. It is used only when its advantages are required.

In a scanning LDV device the object beam is deflected in the *X* and *Y* directions by a specific amount. In order to keep the amplitude error below 0.3 dB (corresponding to an angle error of less than 15°) the LDV is positioned relatively far away from the vibrating surface to allow it to scan a diameter of 0.5/distance or a square of 0.35/distance. The object beam therefore must be deflected in steps of less than 1° with high accuracy, which requires mirrors adjusted with piezoelectric devices. A scanning LDV makes sense only if the actual positions are known to the measurement system and the different points are measured one after the other automatically. So a scanning LDV is always embedded into a software solution which must measure and display the data. This further increases the

costs of such a system. However, 1D scanning LDVs are widely used because they offer a good compromise between problem insight, ease of installation and measurement and analysis time. However, as surface vibrations are measured this provides only indirect information about the radiated noise.

If measurement of in-plane vibrations is required (e.g. for brake squeal on disc brakes) a 3D scanning LDV is required, which is more than three times as expensive as a 1D scanning LDV. Therefore such LDVs are found only where absolutely necessary (e.g. at a brake system manufacturer).

For non-stationary signals holographic methods can be used. Here the object beam is widened to highlight the whole surface of interest. If the test object is stationary on a mechanically isolated bed plate, a reference hologram can be measured without excitation and the interference pattern under operation can be evaluated to find the desired surface vibration. The technique is very similar to the LDV technique, only here the photodetector is an array of photodetectors.

If the test object is operating at a certain rpm it is not possible to use a reference hologram without excitation as the test object may have moved in between. Here a double- or multiple-pulse holographic interferometer technique must be applied, which further complicates the measurement process, thus increasing costs.

9.5   Sound quality and psychoacoustics: measurement and analysis

There are many aspects of product quality: design, durability, functionality, ease and simplicity of use, etc. Besides objective quality aspects, subconscious impressions like feel, smell and noise become more and more important in distinguishing an excellent product from merely good products. So instead of measuring only the objective noise level it is desired to evaluate the subjective noise quality. Unfortunately the human way of listening is pretty much non-linear in several aspects:

*   The frequency and amplitude sensation is not linear but approximately logarithmic (as for most human senses).
*   The frequency response of the ear is not linear.
*   This effect varies with amplitude.
*   Different signals may mask each other in time and frequency.
*   The rating of noise differs individually and depends, e.g., on the ethnic background and the expectation of the listener.

Therefore sound quality ratings are only meaningful in a special context.

Before the advent of digital measurement systems, a fixed spectral weighting was applied in order to simulate the lower sensitivity of the
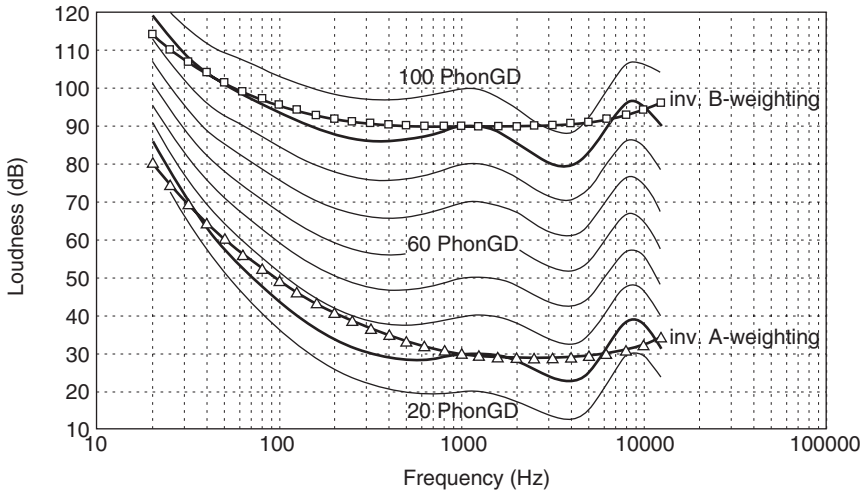
9.5 Equal loudness curves with inverse A- and B-weighting according to ISO 532B (diffuse sound field).

human ear to lower and higher frequencies. For loud noises at low frequencies (e.g. second engine order boom, see Section 9.8) the B-weighting was applied, while for quieter noises or those with less low-frequency energy the A-weighting was applied. Both are rough estimates of the curves of equal loudness according to ISO 532B for medium or low noise levels, respectively (see Fig. 9.5). With the advent of digital measurement systems it was possible to calculate the true loudness (assuming stationary noise), including spectral masking effects, etc.

In order to better distinguish dB(A) and dB(B) and to better correlate loudness values with perceived loudness, loudness is expressed in sone. The relation between sone and phon is

$$\text{sone} \geq 1: \text{loudness (phon)}$$
$$= 40 + 10\log_{10}(\text{loudness (sone)})/\log_{10}2 \qquad (9.12)$$

$$\text{sone} < 1: \text{loudness (phon)}$$
$$= 40 \times (\text{loudness (sone)} + 0.0005)^{0.35} \qquad (9.13)$$

If sound A is perceived to be twice as loud as sound B, which has a loudness of X sone or Y phon, the loudness of sound A is $2X$ sone or $(Y+10)$ phon.

Although the calculation of stationary loudness is standardised in ISO 532B, the underlying data is based on work of Zwicker around 1960.[14] There is not yet a standardised version of time-varying loudness. Several investigations have been performed which indicate that the loudness curves of ISO 532B are no longer valid, because of the rapid changes in unwanted
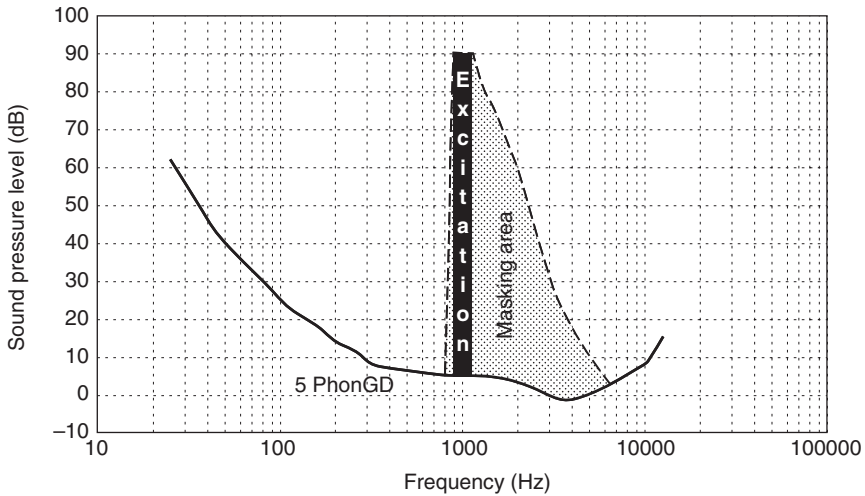
9.6 Spectral masking according to ISO 532B (free sound field).

Table 9.5 Overview of sound quality metrics

Metric	Unit	Description
Loudness	sone, phon	1 sone = 40 phon for 1 kHz tone of 40 dB
Sharpness	acum	1 acum for noise of 60 dB, 1 bark wide, centred around 1 kHz
Roughness	asper	1 asper for 1 kHz tone of 60 dB, 100% amplitude modulated at 70 Hz
Fluctuation strength	vacil	1 vacil for 1 kHz tone of 60 dB, 100% amplitude modulated at 4 Hz

noise pollution and desired high-level music reproduction, e.g. with headphones.

When two signals are received in parallel one of them may be masked by the other, depending on the level and frequency difference. Figure 9.6 shows the situation for a one-third octave band noise at 1 kHz with a level of 90 dB. Each tone that is lower than the spectral masking curve cannot be perceived subjectively.

The concept of loudness and spectral masking helps one to interpret objective data in order to find critical frequency ranges and whether tonal noises are annoying or just inaudible. Other psychoacoustic metrics are sharpness, roughness and fluctuation strength. They are defined only for artificial noises and in general are not standardised (see Table 9.5).

Besides the psychoacoustic metrics there exist several additional metrics such as tonality and impulsiveness that are intended to classify sounds. One

of these additional metrics is Articulation Index (AI), which originates from the telecommunications industry (Fig. 9.7). The AI concentrates on the amplitude (30 dB) and frequency range (200–6300 Hz) of speech. It applies a weighting scheme similar to the above A-weighting but with an additional 9 dB per octave suppression at frequencies of >1 kHz. An additional spectral weighting is applied by adding different percentage values per dB with the highest scores in the 800–5000 Hz frequency range (maximum around 1800 Hz). It is often used to describe acoustic comfort in the interior compartment (or the difference between two conditions) with a single number value.

In each one-third octave band a certain sound pressure level is assigned a percentage value. The AI is the sum of all percentage values for a given one-third octave spectrum. If the background or masking noise is louder than the upper limit, it is assumed that nothing can be understood at all (=0% AI). If the masking noise is below the lower limit, it is assumed that everything can be understood (=100% AI). When applied to vehicle noise it is desired to extend the listening range to higher and lower levels in order to better distinguish an excellent car from good cars, e.g. under extreme operating conditions such as cobblestone excitation. In such circumstances the AI can exceed 100% or be negative. To distinguish both variants the extended AI is often abbreviated to EAI. Note that AI and EAI are among the few metrics for which a high value is desired (higher is better).

With the advent of the diesel powertrain, impulsiveness and modulation become more and more important. Modulations occur, for example, if the combustion noise from each cylinder is not identical. For objective analysis of modulation a quasi-stationary signal is required (e.g. constant engine rpm for several seconds). Depending on the modulation frequency the noise is perceived, e.g., as rough (modulation frequency 15–300 Hz) or fluctuating (modulation frequency <20 Hz).[15]

Often the noise sensation cannot be fully described with a single standard objective measurement. Then the noise of different test objects or different test conditions is recorded and subjectively rated. In order to get a more realistic reproduction an artificial head is used with two microphones placed at the ear locations (binaural head) and the noise is played back via high-quality headphones.

Such a recording can also be used to verify an assumed problem frequency or frequency range. The recorded sound can be filtered (e.g. noise from 1300 to 1400 Hz can be suppressed by 10 dB by a notch filter) and the original and filtered sound can be compared subjectively. This not only gives a hint which frequency band must be improved but also how much the noise must be reduced to achieve a desired improvement.

The subjective rating of a noise is often expressed in complex perception categories such as powerful, aggressive, refined, etc. If all ratings are

9.7 Articulation index according to Leo L. Beranek.
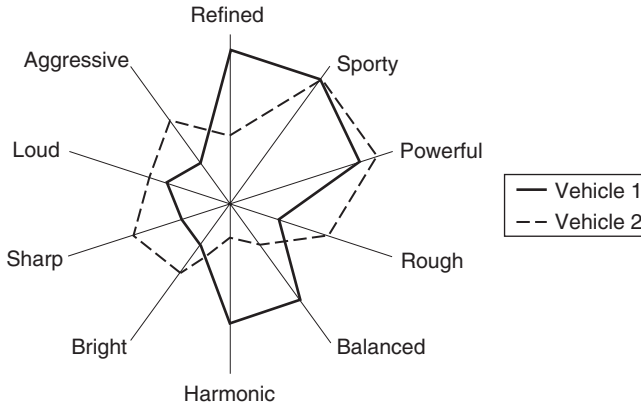
9.8 Description of interior noise by means of sensoric profile.

displayed in a spider diagram, different sensoric profiles can be compared (see Fig. 9.8).

If a group of similar sounds are subjectively rated in given categories by a representative jury and analysed with a variety of objective parameters (e.g. dB(A), AI, spectrum, modulation spectrum, etc.), it is in general possible to correlate the subjective ratings with a combination of objective parameters, e.g.:

$$\text{subjective rating} = \sum_i \text{factor}_i \times (\text{objective parameter}_i)^j \qquad (9.14)$$

If a sufficient correlation is found it is possible to assign a subjective rating to a similar sound or to define the objective parameters of a target sound. As soon as the group of similar sounds is changed significantly the correlation exercise must be repeated.

9.6   Ultrasound diagnostic techniques

In the field of vehicle noise, ultrasound devices are mainly used for leakage detection in sound package or sealing applications. An ultrasonic source (in general battery powered) is placed on one side of a barrier and the ultrasonic receiver (also in general battery powered) on the other side. This is a classical noise reduction setup. Moving from audible noise to ultrasonic noise (typically a warbled tone around 40 kHz) has the advantage that the result is independent of audible background noise, thus allowing ultrasonic leakage tests in workshops or even in a production plant.

The intensity of the received ultrasonic sound is displayed on a scale. Additionally the ultrasonic signal is transferred into the audible range by heterodyning and can be heard, e.g., through headphones. Both items help to localise leaks by looking for locations with high ultrasonic intensity.

However, ultrasonic sound behaves slightly differently from audible sound. Due to its shorter wavelength an ultrasonic wave may pass through a hole which would have been too small for an audible wave in the typical frequency range up to 10 kHz. Small cavities may amplify ultrasonic waves by resonance effects which are not acting on audible waves with higher wavelengths and vice versa. So interpreting the intensity in detail is difficult and the quantitative results with ultrasonic detection may differ from those with audible noise excitation.

A sound source must be small compared to the radiated wavelength in order to radiate omnidirectionally. As ultrasonic waves have very small wavelengths this requirement is in general not fulfilled for an ultrasonic source. Therefore the absolute intensity of the received signal may depend on the exact location and orientation of the ultrasonic source.

Therefore, ultrasonic leakage devices are easy to use even under noisy conditions and give quick and intuitive information on relative ultrasonic intensity changes that in general correlate well with intensity changes of audible noise. However, due to the different wavelength and spectral content the effect of measures in general is not comparable.

9.7   Advanced material testing techniques

In the field of vehicle acoustics it is very important to understand the effect of sound absorbing and sound deadening materials. The sound absorption of small, flat parts for normal sound incidence can be evaluated with a standing wave tube according to ISO 10534 (also called a Kundt tube: see Fig. 9.9). If the diameter of the tube is small compared to the radiated wavelength, plane wave propagation can be ensured. The classical test procedure is to generate a tone with a loudspeaker on one side of the closed tube and to evaluate the standing wave pattern near the surface of the test material backed up with a solid wall (see Fig. 9.10).

From the ratio P_{max}/P_{min} the absorption coefficient α can be derived:

$$\alpha = 1 - r^2 \tag{9.15}$$
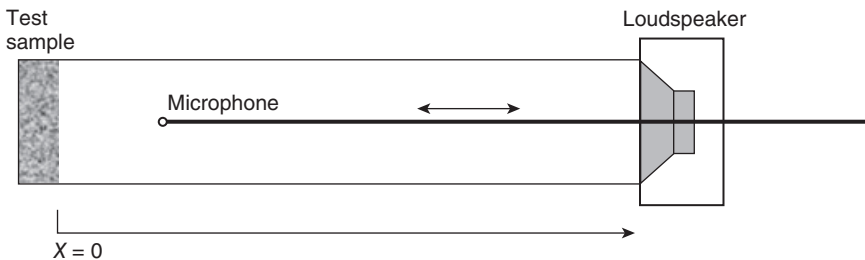
9.9 Scheme of Kundt tube.
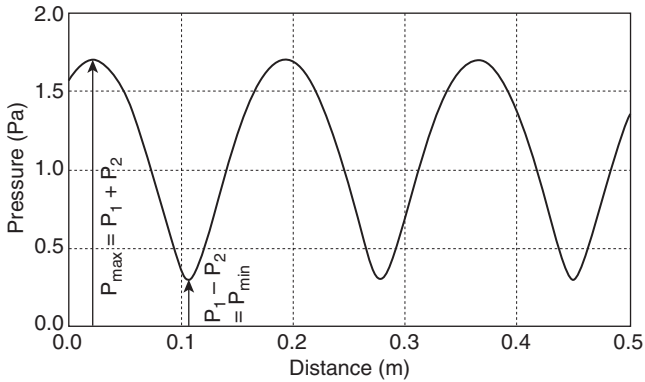
9.10 Standing wave pattern in Kundt tube (1000 Hz, $r = 0.7$).

where

$$r = \frac{(P_{\max}/P_{\min}) - 1}{(P_{\max}/P_{\min}) + 1} \tag{9.16}$$

In order to cover the whole frequency range typically two tubes are required, one with 10 cm diameter for the frequency range from 50 to 1600 Hz and one with 3 cm diameter for 500 to 6300 Hz. In order to avoid the time-consuming manual scanning of the standing wave pattern at successive frequencies, modern Kundt tubes use broadband noise excitation and several microphones at fixed locations together with adapted evaluation software.

For locally acting porous absorbers the tube results are relevant and random incidence results can also be estimated. For plate resonators the results are not representative if the mounting conditions differ from real-world mounting. The advantage of the tube method is that only small test samples are required.

In general the noise comes from all sides. This can be simulated by using a reverberation room with a diffuse sound field according to ISO 354 or ASTM C423. In a first step the reverberation time T_{60_empty} of the empty room is measured. Although no obvious absorbing material is in the room, the reverberation time is not infinitely long, so some parts of the reverberation room are not perfectly reflecting and absorbing the sound energy. A simple model of the room assumes that the effect of the distributed absorption is represented by a lumped element, a perfect (100%) absorber with area A_{equiv}, also called equivalent absorption area.

In a second step the desired material is added to the room and a new reverberation time T_{60_full} is measured, so the total effect can be explained by a new equivalent absorption area. In order to ensure a proper modal

density the volume of the reverberation room must, e.g., be 200 m³ for a cut-off frequency of 100 Hz.

The difference between both conditions is the difference of both equivalent absorption areas:

$$T_{60} = \frac{0.163V}{A_{equiv}} \tag{9.17}$$

$$\Delta A_{full-empty} = 0.163V \left(\frac{1}{T_{60\_full}} - \frac{1}{T_{60\_empty}} \right) \tag{9.18}$$

$$\alpha = \Delta A/S \tag{9.19}$$

where T_{60} = reverberation time = time for 60 dB noise decay (s)
   V = reverberation room volume (m³)
   A = amount of 100% absorbing area equivalent to absorption effect (m²)
   α = absorption coefficient (%)
   S = surface of absorbing material (m²).

In general, 10–12 m² of material (or an equivalent number of complex parts like seats or head liners) is needed to ensure a significant change of the reverberation time. During material development this is a significant disadvantage of the test method. Moreover the measured absorption coefficient depends significantly on the design of the reverberation room, the amount and location of diffusers, the microphone and source location, the estimation of the decay time, etc.[16–18]

Therefore the sound package supplier RIETER (formerly Keller or Interkeller) tried to combine the best of two worlds in a practical package, and created the Alpha Cabin (see Fig. 9.11), which became a *de facto* stan-
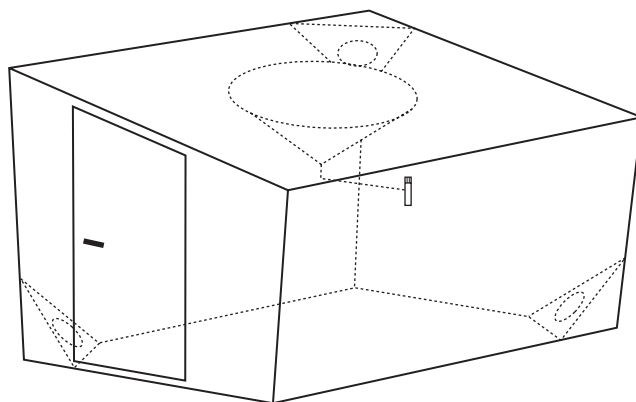
9.11 Alpha Cabin.
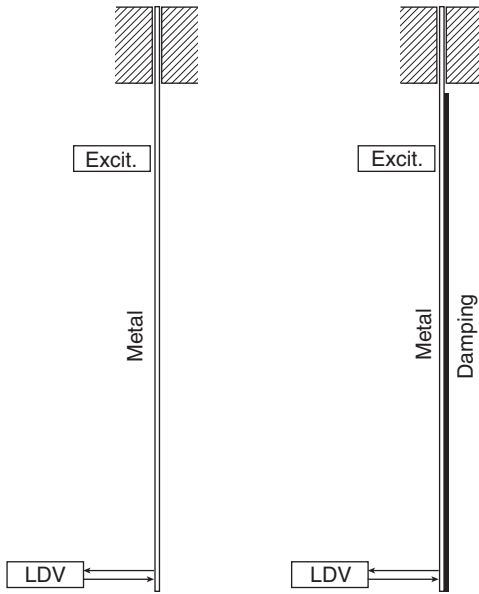
Excit. = excitation with magnetic transducer
LDV = laser doppler vibrometer

9.12 Oberst bar.

dard in the field of absorption measurement, although there is no official standard such as ISO. The Alpha Cabin is a small reverberation chamber on wheels with a volume of 6.44 m^3 (smaller by a factor of π^3 than a standard reverberation room) and a small entrance door, that allows one to evaluate the absorption properties of a sample from 400 Hz (π times higher than for a standard reverberation room) to 10,000 Hz. This provides more realistic diffuse field excitation but allows smaller samples with sizes of approximately 1.2 m^2 (smaller by a factor of π^2 than for a standard reverberation room), so for complex parts often only one sample is required. The Alpha Cabin comes complete with loudspeaker excitation, microphone including positioning system, and data acquisition and post-processing system, thus ensuring consistent results all over the world. Therefore the Alpha Cabin is also used for production quality control.

Another important material property is the viscoelastic damping of sound-deadening material, which is extensively used on body panels, e.g. in the firewall and floor region. The damping factor is estimated indirectly according to the Oberst method (see Fig. 9.12):[19]

1. In the first step a metal strip (e.g. 220 mm long, 12 mm wide and 1 mm thick) is fixed on one side and excited on the free side with a magnetic transducer. At a reference point the vibration response is measured.

The frequency response function (FRF) shows several peaks (high excursion per force input) at the mechanical resonances.

2. In the second step, damping material is applied to the same strip. The thickness of the applied material is measured at several locations (and optionally levelled) and the width is made identical to the strip width by grinding. Finally the FRF is measured again.

3. For both FRFs curve fitting is applied to extract the exact resonance frequencies and damping. The shift of the resonance frequency is the effect of the density, the dimensions and the elastic modulus of the material. The reduction of the peak and Q-factor at the nth resonance frequency is the effect of the damping.

The damping depends on the temperature, so all FRF measurements are performed in a climate chamber with several hours of thermal settling. Typical temperature ranges are −20 to +60°C in steps of 20°C. As the change in frequency and peak amplitude is only small, high accuracy is needed to give reliable results. In general the damping may also vary with frequency, therefore ISO 6721-3 requires one to interpolate the evaluated damping at the resulting resonance frequencies for a target frequency of 200 Hz.[19]

In the floor region often a combination of different materials is used. Damping material is applied to the sheet metal, and on top comes a layer of foam or other porous material covered with a layer of heavy mass and/or carpet. The effect of the sound-deadening material can be measured by using the supporting structure as a wall between two isolated reverberation rooms. Either noise or vibration excitation can be used. The structure is excited in one room and the response is measured in the other room, once with and once without the added material. For a complete floor insulation the test setup is pretty complex and a moulded part must be manufactured, which is very expensive in the prototype phase. For practical reasons a smaller test setup is desired that works with flat material. Again it was RIETER that proposed a device called 'Apamat' for structure-borne excitation with steel balls, and a device called 'Small Cabin' for airborne excitation. The supporting structure in both cases is a plane sheet of metal (84 cm × 84 cm) of desired thickness. On top of that the desired material setup can be positioned. The lower and upper chambers are different for both devices. Measurement with a plane sheet is used for reference. Both devices again became a *de facto* industrial standard.

In many fields of vehicle development CAE tools have to be used. If materials other than metal have to be modelled correctly, their properties must be known or measured in detail. For porous absorbers the properties can be represented by a Biot–Allard model.[20,21] This requires the inputs shown in Table 9.6.

Table 9.6 Parameters for the Biot–Allard model of porous absorbers

Parameter	Type	Symbol	Unit
Composite porosity	acoustic	φ	(–)
Air flow resistivity (AFR)	acoustic	σ	(Pa·s/m²)
Composite tortuosity	acoustic	τ	(–)
Composite pore shape factor	acoustic	c	(–)
Viscous characteristic length	acoustic	Λ	(m)
Thermal characteristic length	acoustic	Λ'	(m)
Young's modulus	structural	E	(Pa)
Damping loss factor (DLF)	structural	η	(–)
Poisson's ratio (for foam materials) (range: 0.15–0.48)	structural	ν	(–)

The full characterisation of porous materials needs to be measured using a variety of special equipment which is very complex. Each supplier of such material must develop its own tools to acquire each of these data, as no standardised devices and processes are available. This further complicates the comparison of different materials from different suppliers by CAE tools. Again, RIETER fills the gap and supplies a complete set of tools under the product name ELWIS.

Besides common FEM–CAE models special software programs are available such as SISAB or WinFlag that are able to estimate the effect of multi-layer systems (absorption and damping).[22,23]

9.8   Advanced tachometer reference tracking techniques

For motor vehicles some noise components are related to the ignition frequency of the engine or other rotational devices such as the fan, alternator, etc. For combustion engines most harmonic responses are a multiple of the rotation frequency. The rotation frequency is called the first engine order; the ignition frequency of a four-stroke, four-cylinder engine is the second order (one ignition after each two revolutions for a four-stroke engine multiplied by the number of cylinders that ignite one after the other). If the rpm of the device is known, these related parts (= engine orders) can be analysed separately.

For quasi-stationary tests on engine test rigs the estimation of the rpm is not a problem, but for fast-varying engine speeds (e.g. second gear wide open throttle (WOT) acceleration) this is more complex. Even more complex is the estimation of rpm fluctuations, e.g. within one ignition cycle. This requires multiple information concerning the current crankshaft angle per revolution, e.g. each 5 degrees. To achieve a resolution of 5° at 6000 rpm

Table 9.7 Parameters used for Fourier transformation and their relationships

Parameter	Symbol	Dimension	Relationship
Sample frequency	F_S	(Hz)	$F_S = BS \times \Delta F$
Block size	BS	(–)	$BS = F_S/\Delta F$
Frequency resolution	ΔF	(Hz)	$\Delta F = F_S/BS$
Block length	ΔT	(s)	$\Delta T = 1/\Delta F$

with <1% error, the rpm signal must be observed more than 720,000 times per second. With only one pulse per revolution and an allowed rpm error of <1% at 6000 rpm, the rpm sample rate must exceed 10,000 Hz.

Instead of installing a dedicated rpm sensor it seems to be very attractive to use on-board sensors, e.g. CAN-bus information. The CAN-bus information is available, e.g., on the onboard diagnostic (OBD2) plug near the steering wheel, so instrumentation is very easy. However, the desired CAN-bus information must be decoded and is not available in real time. The CAN-bus information is typically updated every 10–20 ms, so the CAN-bus rpm always lags slightly behind the real engine rpm. For an rpm change rate of 5000 rpm in 5 s (e.g. second gear full load) the 10–20 ms offset corresponds to a 10–20 rpm error, which can be tolerated for normal applications.

The engine order extraction is basically done by performing a Fourier transformation (FT) on a block of data of length ΔT sampled with a fixed frequency F_S. With information on the average rpm within that block the average energy related to the desired engine order can be extracted. Ideally the rpm should not vary within the timeframe ΔT, so ΔT should be made as small as possible. However, the frequency resolution ΔF of the FT corresponds to $1/\Delta T$, so with conventional FT analysis a compromise must be found between rpm and frequency resolution. Table 9.7 shows the parameters used in the Fourier transformation with their symbols and the relationships between them.

A constant block length ΔT yields a constant frequency resolution ΔF. This corresponds to a varying order resolution ΔO, because the order frequency increases with rpm. For low rpm the order resolution might become critical. This can be improved by adapting the frequency resolution $\Delta F = 1/\Delta T$ to be proportional to the actual rpm. As long as the data are sampled with a fixed frequency, this cannot work perfectly. Even then the rpm (and therefore the order frequency) is still varying within the block, so the order energy is spread across several frequency bands. This can be avoided only if the signal is (re-)sampled synchronously to the actual rpm. Then a block always has, e.g., 64 samples per revolution, yielding a constant order resolution ΔO. Figure 9.13 shows the different strategies.
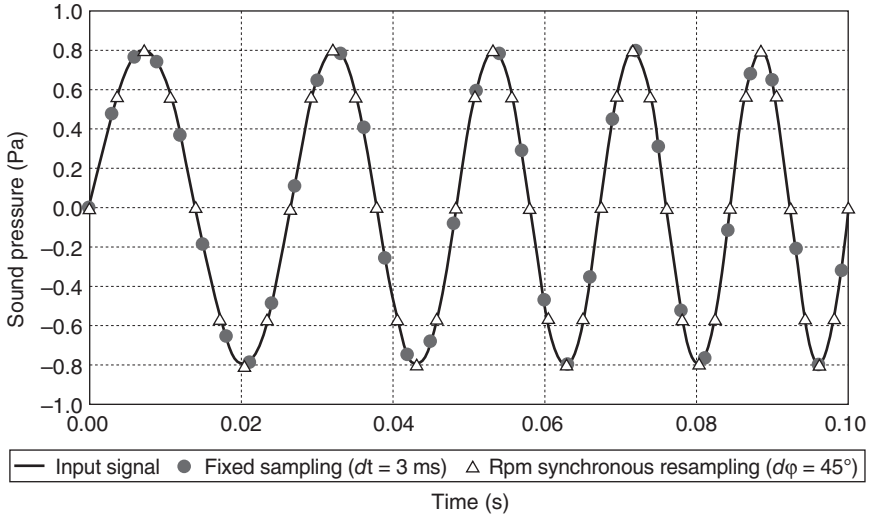
9.13 Fixed versus rpm-synchronous sampling (for engine speed sweep).

Table 9.8 Parameters used for order analysis and their relationships

Parameter	Symbol	Dimension	Relationship
Engine revolution	n	(1/s)	
Block length	ΔT	(s)	$\Delta T = 1/(n \times \Delta O)$
Order resolution	ΔO	(–)	$\Delta O = 1/(n \times \Delta T)$
Maximum order	O_{max}	(–)	
Resample frequency	F_S	(Hz)	$F_S \geq 2nO_{max}$

An order resolution ΔO of 0.5 means that all energy within the orders X – 0.25 to X + 0.25 is summed up and associated with the order X. It also means that a time block of length $1/\Delta O$ revolutions is used to calculate the order spectrum. If the noise consists only of order-related signals of a multiple of ΔO, no window function is required. However, this cannot be guaranteed in general due to uncorrelated noise (e.g. road and wind noise) and rpm-independent resonances. As long as a time window (e.g. Hanning) is applied, it is relevant for the resulting amplitude of lower orders, whether or not an order starts with zero phase offset. The better the order resolution, the longer is the time sample used for analysis. This also has an averaging effect and will reduce the influence of the start position when a time window is used. Table 9.8 shows the parameters used in order analysis with their symbols and the relationships between them.

If an engine order-related signal of frequency X coincides with another signal of the same frequency (either fixed resonance or a signal related to

the order of a different device with uncorrelated rpm) the above methods are unable to split the combined signal into both contributors. Here Kalman–Vold filtering can help, which essentially is a least-squares approach to estimate the amplitude of an order.[24] The estimated value is essentially a weighted average of previous values.

9.9   References

1. Fingberg, U. and Ahlersmeyer, T. (1992), 'Noise path analysis of structure borne engine excitation to interior noise of a vehicle', paper presented at *17th International Seminar on Modal Analysis* (ISMA), Leuven, Belgium

2. De Vis, D., Hendricx, W. and van der Linden, P. J. G. (1992), 'Development and integration of an advanced unified approach to structure borne noise analysis', paper presented at *Second International Conference on Vehicle Comfort*, ATA

3. van der Linden, P. J. G. and Varet, P. (1996), 'Experimental determination of low frequency noise contributions of interior vehicle body panels in normal operation', paper 960194 presented at *SAE Conference*, Detroit

4. Gajdatsy, P., Janssens, K., Gielen, L., Mas, P. and Van Der Auweraer, H. (2008), 'Critical assessment of operational path analysis: effect of coupling between path inputs', *Journal of the Acoustical Society of America (JASA)*, 123(5), 3876

5. Lohrmann, M. (2008), 'Operational transfer path analysis: comparison with conventional methods', *Journal of the Acoustical Society of America (JASA)*, 123(5), 3534

6. Brüel & Kjær, *Sound Intensity*, primer available online at http://www.bksv.com/Library/primers.aspx (accessed 08.01.2010)

7. De Bree, H. E. (2003), 'The Microflown, an acoustic particle velocity sensor', *Australian Acoustics*, 31(3), 91–94

8. LMS, Application note, 'Acoustic holography: noise source identification and quantification', available online at http://www.lmsintl.com/acoustic-holography-noise-source-identification-qualification (accessed 08.01.2010)

9. Brüel & Kjær, 'Technical Review 2004-1 Beamforming', available online at http://www.bksv.com/Library/Technical%20Reviews.aspx (accessed 08.01.2010)

10. Brüel & Kjær, 'Technical Review 2005-1 NAH and beamforming using the same array', available online at http://www.bksv.com/Library/Technical%20Reviews.aspx (accessed 08.01.2010)

11. Bono, R. W., Brown, D. L. and Dumbacher, S. M. (1996), 'Comparison of nearfield acoustic holography and dual microphone intensity measurements', paper presented at *ISMA21*, Leuven, Belgium

12. Heinz, G. (2004), 'Schall orten – verschiedene Lokalisierungstechniken im Vergleich', *GFaI-Report 002*, available online at http://www.gfai.de/~heinz/publications/papers/2004_Vergl.pdf (accessed 08.01.2010)

13. Brüel & Kjær, 'Product data: PULSE array-based noise source identification solutions', available online at http://www.bksv.com/doc/bp2144.pdf (accessed 08.01.2010)

14. Zwicker, E. (1958), 'Über phsychologische und methodische Grundlagen der Lautheit', *Acustica*, 8, 237–258

15. Zwicker, E. and Fastl, H. (1990), *Psychoacoustics: Facts and Models*, Berlin, Heidelberg and New York: Springer

16. Nwankwo, D. D. and Szary, M. L. (1996), 'Calibrating reverberation room for accurate material sound absorption measurements', paper 960191 presented at *SAE Conference*, Detroit

17. Thomasson, S. I. (1982), 'Theory and experiments on the sound absorption as function of the area', report TRITA-TAM-8201, *Department of Technical Acoustics, Royal Institute of Technology*, Stockholm

18. Kath, U. (1983), 'Ein Hallraum-Ringversuch zur Bestimmung des Absorptionsgrades', *Acustica*, 52, 211

19. ISO 6721-3 (1994), 'Determination of dynamic mechanical properties. Part 3: Flexural vibration–resonance curve method'

20. Biot, M. A. (1992), *Acoustics, Elasticity, and Thermodynamics of Porous Media. Twenty-one Papers by M.A. Biot*, New York: Acoustical Society of America

21. Allard, J. F. (1993), *Propagation of Sound in Porous Media: Modeling Sound Absorbing Materials*, London and New York: Elsevier Applied Science

22. Semeniuk, B. (1999), 'The simulation of the acoustic absorption and transmission characteristics of automotive material configurations: the new SISAB software', paper presented at *RIETER Automotive Conference*, Zurich, 1999

23. Zulkifli, R., Mohd Nor, M. J., Mat Tahir, M. F., Ismail, A. R. and Nuawi, M. Z. (2008), 'Acoustic properties of multi-layer coir fibres sound absorption panel', *Journal of Applied Science*, 8(20), 3709–3714

24. Blough, J. R. (2007), 'Understanding the Kalman/Vold–Kalman order tracking filters' formulation and behavior', paper presented at the *SAE Noise and Vibration Conference*, St Charles, IL

10

Aerodynamic noise and its refinement in vehicles

S. WATKINS, RMIT University, Australia

Abstract: Aerodynamically generated noise (commonly known as wind noise) is the major source of noise at high speed in a modern car. The sources of in-cabin noise are reviewed and categorised into the source types (monopole, dipole, quadrupole) and the different hydrodynamic/acoustic mechanisms. Methods of noise reduction are outlined which involve the reduction of the noise source, rather than increases in transmission loss from the external hydrodynamic and acoustic fields to in-cabin. The main tool used in sound measurement (the aeroacoustic wind tunnel) is described.

Key words: aerodynamic, aeroacoustic, wind noise, cavity, vortex shedding.

10.1 The importance of aerodynamic noise

Aerodynamically generated noise is generally the dominant noise inside a modern passenger car travelling at relatively high speed (>~100 km/h). In part this is due to the sensitivity of wind noise to flow velocity, which is related to the vehicle velocity through the air. Generally the sound intensity is proportional to the fourth to sixth power of velocity (see later). At lower speeds, mechanical noise, road/tyre interaction noise, engine noise and transmission noise are so dominant that wind noise is hardly noticed. However, at highway speeds wind noise is significant and is the focus of much attention by car companies. Automobiles are bluff bodies with complex geometries and flows, including many areas of turbulence due to flow separations, both large and small. Large areas of separation include the flow at the rear of the car and over wheel housings, and small areas of separation include flow over small cavities, such as those existing in external rear-view mirrors and door/body gaps. Flow separation can cause strong pressure fluctuations, which generate aerodynamic noises and also impinge upon the side structures, causing them to vibrate and to radiate noise. Noise that is heard inside the cabin is called 'in-cabin' or interior noise. Interior noise is highly non-linear and comprises wind noise and noises generated by flow-induced panel vibration as well as other 'mechanical' noise sources.

In-cabin noise depends on the vehicle's external geometry including the A-pillar, the windshield, seals, cavities and any small openings around the

219

vehicle body, as well as the transmission losses associated with the transition paths through the vehicle structure. Car companies expend considerable effort on sealing the vehicle (costing time and money and increasing vehicle mass) and much of this effort is directed at reducing the levels of aerodynamic noise. Whilst levels are low (well below any potentially damaging effects) the noise can be annoying for long periods. It can also interfere with communications, either between passengers or when listening to in-cabin media or from external sources, such as from emergency vehicles. Thus an increasing measurement focus is put upon aspects such as Articulation Index (a measure of communication ability) and psychoacoustic parameters which attempt to replicate whether humans find the noises desirable or otherwise. In this chapter our focus is on internal noise rather than noise radiated externally. Externally radiated noise is usually dominated by tyre noise and for typical highway speeds externally radiated aerodynamically generated noise is not a significant problem.

10.2   Aerodynamic noise sources: background

Aerodynamically generated noise results from pressure fluctuations in turbulent fluid flow. It is important to draw a distinction between the pressure fluctuations that occur due to hydrodynamics (sometimes known as 'pseudosound') and acoustic waves. Pressure fluctuations are a hallmark of turbulent flow which is a chaotic, semi-random process. Generally there is little or no correlation between hydrodynamically generated pressures at two different points in space. In contrast, acoustic pressure fluctuations are coherent since they are a wave motion in the elastic medium of air (fluctuating about the mean atmospheric pressure). An example of hydrodynamic pressure fluctuations is the noise heard during a mobile phone call when speaking on a very windy day. The sensor used in most acoustic measurement systems, the microphone, can be thought of as an AC-coupled pressure transducer, which responds to pressure fluctuations, irrespective of whether they are hydrodynamic or acoustic. Thus a microphone with a diaphragm flush with a surface over which a turbulent flow is moving will measure the sum of the hydrodynamic and acoustic parts. In general the hydrodynamic fluctuations will be much greater than the acoustic, so care has to be taken with putting microphones in turbulent flows when trying to measure just the acoustic components. This is complicated by the fact that acoustic waves are radiated away from the surface due to the hydrodynamic fluctuations.

The generation and propagation of acoustic pressures is usually amenable to mathematical analysis, whereas pressure fluctuations (and other parameters) involved with turbulence can normally only be analysed from

a statistical point of view. For some types of problem the acoustic and hydrodynamic fields are coupled (such as some cavity problems – see later) which can cause very significant analytical and computational challenges. Many eminent scientists and mathematicians have tried to understand and model the problem and some insights into these are given below.

10.3   Modelling, relevant theory and the possibilities of simulation

The study of noise generated by turbulent flow began with trying to understand propeller noise development in the late 1940s. A major milestone in understanding occurred in 1952 when Sir James Lighthill introduced his acoustic analogy to deal with the problem of jet noise. Lighthill first gave a basic theory of aerodynamic sound generation, and its application to the noise radiated from airflow, in two papers (Part I and Part II) in 1952 and 1954 respectively. Lighthill's 1952 paper theorised how the sound radiates from a fluctuating fluid and its estimation. His 1954 paper detailed the origin of noise from turbulent jets.

Lighthill considered a fluctuating hydrodynamic flow, covering a limited region, surrounded by a large volume of fluid, which is at rest apart from the infinitesimal amplitude sound waves radiated from the flow. It was postulated that all the non-linearities in the motion of matter act as sources of sound. Therefore, sources of sound in a fluid motion were considered to be the difference between the exact equations of fluid motion and the acoustical approximation (this is known as Lighthill's 'Acoustic Analogy'). Lighthill derived his equation reorganising the exact equations of continuity and momentum so that they reduce to the homogeneous acoustic wave equation at large distances from the turbulent flow. However, to this day there remain researchers who question some of the underlying assumptions and simplifications.

Several scientists and mathematicians have developed Lighthill's ideas but due to the somewhat intractable nature of the problem, analytical approaches are not normally used for calculating vehicle wind noise. There have been major efforts in computational aeroacoustics to provide methods that enable wind noise to be predicted in the early design stages of a vehicle (in a similar way that computational fluid mechanics is used to predict the time-average quantities such as drag, lift and sideforce). To date there appears to be little success in accurate and efficient predictive methods adopted by the car companies. However, useful lessons learnt include the classifying of certain noise sources into types such as monopole, dipole and quadrupole. This indicates how the generation mechanism varies with flow speed and an overview of this is given below.

10.3.1 Source types

A *monopole source* can be considered as a small pulsating sphere, contracting and expanding with time. The monopole source can come from unsteady volumetric flow addition, such as one experiences from the exhaust pipe of an unmuffled piston engine. This is considered a primary monopole source and sources that are considered to be in this class are dealt with as high priority during the development process. Thus a well-designed car will have these sources minimised. Such is the case of leaks in the sealings of doors, or unsteady addition of fluid volume to the passenger compartment through some leak path. The sound intensity of a monopole source is proportional to the fourth power of fluctuating velocity:

$$I_{\text{monopole}} \approx \rho \frac{L^2 V^4}{r^2 c} \qquad (10.1)$$

where

L^2 = area of noise
r = distance from noise source
c = speed of sound
ρ = air density
V = fluctuating velocity.

A *dipole source* can be considered as two small adjacent spheres (ie. monopoles) that are pulsating exactly out of phase. Dipole sources are due to the time-varying momentum fluxes. Unsteady pressures due to separated flows and also vortex shedding can be idealised as dipole sources. If two simple sources of equal strength are placed close together and arranged to be always of exactly opposite phase, then as one produces a net outflow, the other produces an exactly opposite inflow. Thus at some distance from the sources there is no net fluid influx. However, being of opposite sign there is a net thrust exerted on the fluid from the more positive to the more negative source, which periodically fluctuates in orientation. It is the time rate of change of this force on the fluid that is important for noise production. Such an arrangement becomes a dipole source in the limit if the separation distance between the sources is made infinitesimally small, i.e. very much less than the radiated wavelength. The noise from turbulent flow over a small obstruction in an airstream provides a good example of fluid mechanical dipole source of aerodynamic noise and many aeroacoustic sources can be approximated in this way. The sound intensity of a dipole source is proportional to the sixth power of the fluctuating velocity:

$$I_{\text{dipole}} \approx \rho \frac{L^2 V^6}{r^2 c^3} \qquad (10.2)$$

A *quadrupole source* can be considered as four monopoles (or two dipoles) caused by collisions of fluid elements and is typical of the turbulent shear layer of a jet. In the extreme, the net shear may reduce to a local stress on the fluid, and the time rate of change of shear or stress plays an important role in producing sound. As fluid can be expected to support such forces poorly, quadrupole sources are relatively poor radiators of noise. However, they do play a dominant part in the mixing region of a fluid jet. For low Mach number flow ($M < 0.3$), which is the case for road vehicle applications, the monopole is the most efficient noise source, followed, in increasing order of effectiveness, by dipoles and quadrupoles. The sound intensity of a quadrupole source tends to increase with the eighth power of flow velocity:

$$I_{quadrupole} \approx \rho \frac{L^2 V^8}{r^2 c^5} \tag{10.3}$$

In turbulent fluid flow the fluctuating velocity V is approximately proportional to the average velocities, which would be of the order of the road speed of the vehicle, if there is negligible atmospheric wind. When considering local noise sources it should be recognised that some over-speed and under-speed regions exist around the vehicle as well as possible atmospheric wind effects (e.g. see Watkins and Oswald, 1999). How the vehicle speed influences the sound intensities of different sources around the vehicle depends upon which type of source is being considered and the local flow velocity.

Whilst the increase of sound intensity with velocity is very large, it should be remembered that in the above equations the units are the standard linear engineering units (e.g. pascals), yet due to the non-linearities of human hearing a decibel scale is required. Thus a doubling of sound pressure (perhaps from a small increase in the flow velocity) will not result in a human perceiving a doubling of sound level.

10.3.2 Possibilities of simulation

Ideally we would like to predict fluctuating hydrodynamic pressures at multiple locations around the vehicle, some of which are very small (e.g. cavities). From these we would then like to predict sounds at frequencies up to the top end of human hearing (~20,000 Hz). This is one of the hardest of mathematical/computational challenges and it is interesting to note that car companies are still building (very costly) aeroacoustic wind tunnels for wind noise determination and reduction. Thus experimental methods dominate development. A rigorous analysis of aeroacoustics is beyond the scope of this book, and the interested reader is referred to dedicated books in the area such as Blake (1986) and Blevins (1990).

10.4   Causes of hydrodynamic pressure fluctuations and their reduction

There are several flow characteristics that cause noise: turbulent boundary layers, separated and reattaching flows, a variety of types of cavity flows, vortex shedding and leak flows. These are dealt with in sequence below.

10.4.1   Turbulent boundary layers

The pressure fluctuation inherent in turbulent boundary layers follows a sixth-power law scaling with flow velocity (idealised as dipole sources). At speeds relevant to road vehicles this type of source does not usually dominate. In some locations, such as at the top front of the roof, there can be some noticeable noise, but the next four sources listed below prove more problematic.

10.4.2   Separated and reattaching flows

Most of the front portion of a well-developed passenger car exhibits only small areas of separated flow. The two exceptions are downstream of the A-pillars and external rear-view mirrors. Both exhibit areas of separation (and associated vorticity). They are areas of known noise problems, particularly since they are in close proximity to the ears of the driver and front passengers. Not only can the fluctuating impinging flow on the side glass cause acoustic waves; the fluctuating pressures cause the vehicle windows and body panels to vibrate and radiate noise into the vehicle interior. A schematic of flow pattern in the A-pillar region is shown in Fig. 10.1.
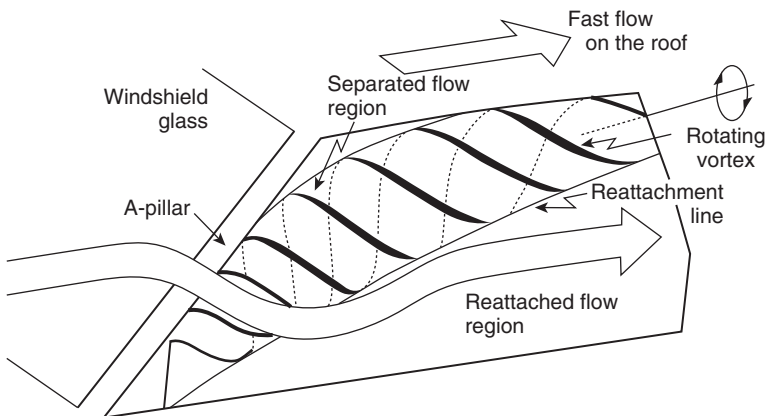
10.1 Schematic of flow field around the A-pillar (Haruna *et al.*, 1990).

For many car shapes, the effective corner radii are sufficiently small such that the local flow breaks away from the surface as it tries to turn around the A-pillars. The intermittency and reattachment of the flow to the side window can generate a broadband wind noise. For a given relative velocity, the strength of these vortices (and hence the noise) depends on the velocity magnitude and the yaw angle, which in itself depends on the strength and orientation of the atmospheric wind. An atmospheric wind with a crosswind component causes this angle to be non-zero. It is likely that angles can vary between zero and 15°, depending upon vehicle and atmospheric wind speeds and direction. Note that most of the aeroacoustic wind noise is between 20 and 10,000 Hz. When yawed, the leeward side of the A-pillar vortex is of greater size and strength than the windward side vortex and therefore the noise on the leeside is generally greater than the windward side. Many studies of the A-pillar flow have been made (e.g. Watanabe *et al.*, 1978) and much commercial work is carried out in the early development stages of new car models.

The effective corner radius is a key parameter in determining separation – the larger the radius the less chance there is of separation. This is illustrated in Fig. 10.2. Here the rms of the maximum surface pressure (measured via a flush-mounted microphone) is plotted against the corner radii for a family of generic rigid shapes. Tests were performed in a low-noise wind tunnel and the C_p rms values are essentially the hydrodynamic pressure fluctuations (i.e. they dominate any acoustic waves radiated away from the models, or background acoustic noise). The magnitude of the hydrodynamic fluctuations gives an indication of the magnitude of any acoustic problems, but unless the exact vehicle structure is used in tests, no direct conclusions can be drawn regarding the acoustic in-cabin pressures.

Three cases are presented in Fig. 10.2: 0, –15 and +15 degrees yaw angle, where a negative yaw angle is defined as being on the leeward (downwind) side. Data were obtained in a wind-tunnel experiment and two of the models, with wool tuft 'telltales', can be seen in Fig. 10.3. The blurring of the tufts for the smallest radii model (Fig. 10.3(a)) indicates unsteady flow. For the largest radius (0.5 m) (Fig. 10.3(b)) the fluctuating pressure coefficient C_p rms has a value of approximately 0.04: see Fig. 10.2. This is typical of the pressure fluctuation in a turbulent boundary layer and the flow (for any of the yaw angles tested) is attached to the surface. The large rises observed as the radius is reduced result from the flow separations, and normally the largest fluctuations occur near the flow reattachment point or line.

To reduce pressure fluctuations (and thus in-cabin wind noise) it would clearly be beneficial to increase the radii, but this is subject to packaging and styling constraints, and complicated by the design requirements for door and window opening. The detailed geometry of the joins at doors and
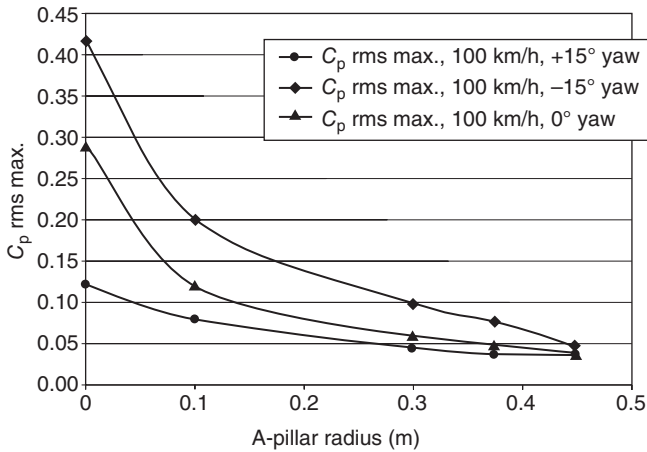
10.2 Maximum rms surface pressure fluctuations as a function of A-pillar radii, 100 km/h on 30% scale model (adapted from Alam, 2000).
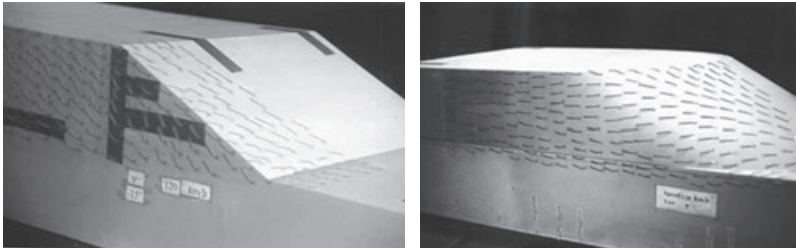
(a)   (b)

10.3 Wool tuft flow surface flow visualisation for (a) the sharp-edged model (A-pillar radii = 0) and (b) the largest radii (A-pillar radii = 0.50 m).

windows is critical to ensure there are no cavity whistles and this is often studied in quiet wind tunnels (see later). This area of the car has many conflicting design requirements including structural integrity (e.g. for rollover strength), ergonomics (for minimising the A-pillar blind spot), water management and, of course, good water and air sealing.

The A-pillar area is also influenced by the external (wing) mirrors. By their very nature a relatively flat mirrored plane is needed at their rear, which necessitates that their shape be a truncated bluff body. For most mirrors the flow is attached over the front half, then separates leading to a wake that can impinge on the sideglass, depending upon yaw angle (for details of the wake flows see Khalighi *et al.*, 2008). Several studies have been performed on mirrors and there exist several aeroacoustic and

Airflow

Depth mode

Airflow

Span mode

(b) Room acoustic resonance

Airflow

(a) Fluid-dynamic (feedback)
resonance

Airflow

(c) Helmholtz
resonance
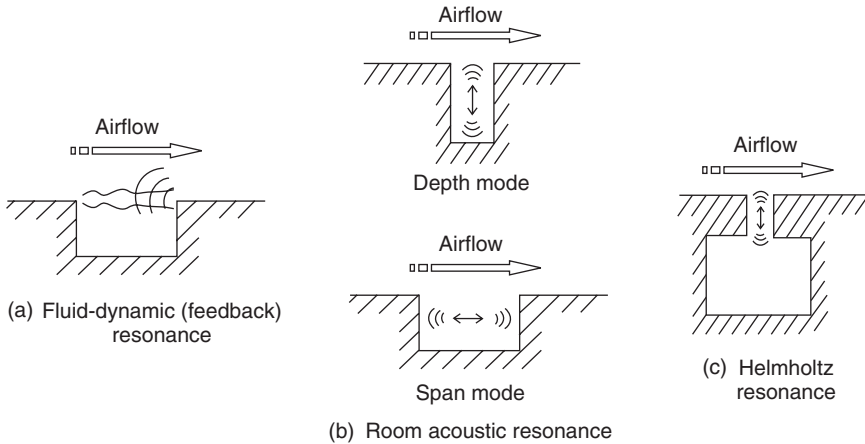
10.4 Commonly encountered cavity mechanisms (from Milbank, 2004).

vibration problems associated with them, including blurring the image due to rotational vibrations of the glass (Watkins, 2004) and cavity whistles (see later). Even relatively small changes in surface texture, such as different surface finishes, can influence the boundary layer, leading to laminar flow whistles (see Lounsberry *et al.*, 2007).

10.4.3 Cavity flows
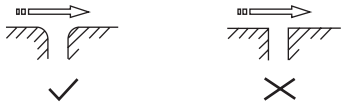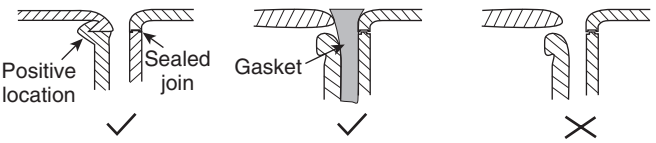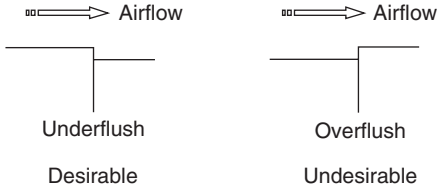
Three different types of cavity flow problems are commonly encountered in cars. These are illustrated in Fig. 10.4. *Fluid-dynamic resonance* is a feedback phenomenon that occurs in compact cavities excited by thin laminar boundary layers. Such conditions are encountered on the cavities found around the periphery of mirror casings (these cavities are often present for styling or water management reasons). There have been many cases of whistling mirrors and the tonal frequencies can easily be predicted with a knowledge of the cavity and local flow conditions. Practical methods of noise reduction are given in Table 10.1. For an extensive coverage of this, including how to predict the frequencies (via Rossiter's equation) and the effects of yaw angle, see Milbank (2004).

Helmholtz resonance can be found anywhere where there is a substantially closed volume with an outlet excited by the flow. This can include the car cabin when a window or sunroof is open. The resonant frequency is given by (Wikipedia, 2008):

$$\omega_H = \sqrt{\gamma \frac{A^2}{m} \frac{P_0}{V_0}} \text{ (rad/s)} \tag{10.4}$$

Table 10.1 Minimising fluid dynamic resonance whistles (from Milbank, 2004)

Measure	Comments
1 Avoid sharp edges	Avoid sharp edges at the cavity opening exposed to the flow. Rounded edges are preferable and the larger the radius the better.
2 Limit the cavity depth	Limit the depth as much as possible, either by making the cavity very shallow, e.g. $L > 13D$, or reducing the depth so that $D < 2\delta$.
3 Block off air access	Block off any air access into interior volumes or spaces within adjacent parts of the mirror. This may require extremely close or interference fits between parts, positive location between parts (as illustrated) or some sort of sealing or gasket.
4 Tight tolerances for mating parts	Overall, the tighter the fit between mating parts the less likelihood that air will be drawn in or out of the mirror assembly and potentially cause a cavity whistle.
5 Underflush conditions between mating parts are preferable	Underflush conditions between mating parts at the assembly surface are preferable to overflush conditions. making a judgement as to whether a joint is underflush or overflush involves knowing the local flow direction over that part of the assembly.

where:

γ = adiabatic index or ratio of specific heats, usually 1.4 for air and diatomic gases

A = cross-sectional area of the neck

m = mass in the cavity

P_0 = static pressure in the cavity

V_0 = static volume of the cavity.

For a typical large car cabin this results in a low frequency noise/vibration of 10–20 Hz, which are frequencies at the lower boundary of human hearing. Solutions are only partially successful (apart from closing the window!) and these can include partially opening other windows (e.g. see Chen and Qian, 2008) or the use of vortex generators at the leading edge of the opening (see Mejia *et al.*, 2007).

10.4.4 Vortex shedding

This occurs from long objects of circular or some other sort of regular constant cross-section and causes noise and in some cases substantial vibration. The resulting noises, sometimes referred to as Aeolian tones, are problematic for circular aerials and for some roofrack bars of relatively bluff cross-section. The frequency of vortex shedding can be found if one knows the Strouhal number S for a particular section; this is generally about 0.20; for circular sections it is 0.21 for the flow regime of interest. The equation for the Strouhal number is given below and can be used to calculate the frequency f of the wind whistle produced:

$$S = \frac{fd}{U} \tag{10.5}$$

where:

U = local flow speed (m/s)
d = cylinder diameter or prism height (m)
f = frequency (Hz).

The solution to reduce this source of noise is to prevent correlated vortex shedding from objects, usually by modifying or changing the shape, some-times by a helical wire, strakes or an inset spiral (see Watkins *et al.*, 1997). Figure 10.5 shows noise spectra obtained in a quiet wind tunnel for two different aerials. Here both axes are scaled in a logarithmic manner; the horizontal scale range is from 50 to 20,000 Hz and the vertical scale is in nominal volts output from a sound pressure meter, thus absolute sound amplitude is not measured. Note the complete absence of the tones gener-ated by each segment for the spirally ground aerial shown in Fig. 10.5(b).

10.4.5 Leak (or aspiration) noise

As mentioned in Chapter 13, leak noise is produced when a flow path can exist between the exterior and interior of the cabin. Often the vehicle external static pressure is lower than the in-cabin static pressure (this depends upon the location around the vehicle and the wind conditions) and this pressure difference causes the air to move through the leak at relatively
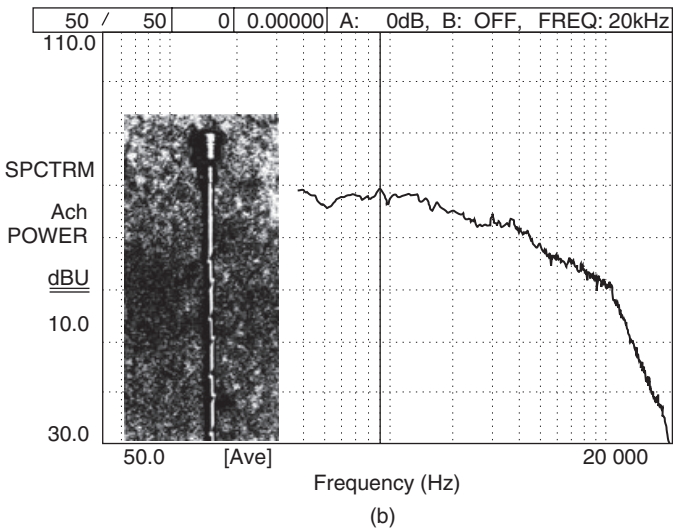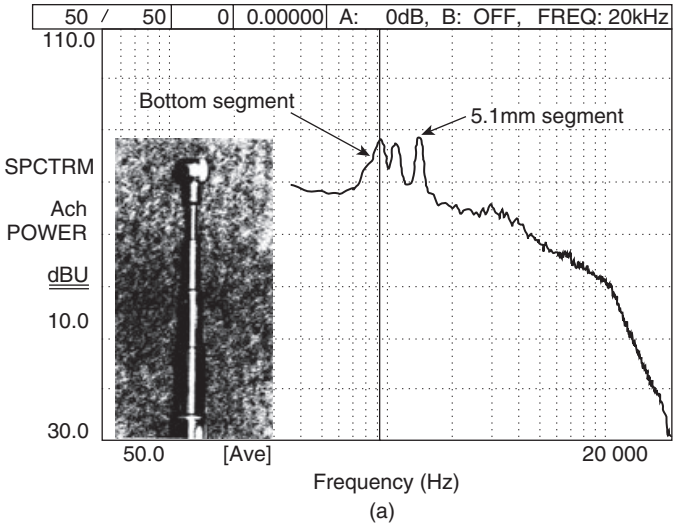
10.5 Noise spectra from (a) standard and (b) optimum spiral grind telescopic aerials (adapted from Watkins *et al.,* 1997).

high speed. Car companies take the sealing of the vehicle very seriously, since noise leaks can increase in-cabin noise substantially and can be loud and short-term in nature. Common locations for leaks are the window seals. Leak noise is of high frequency and short wavelength and is mainly caused by the monopole and dipole type mechanisms (George and Callister, 1991).

Noise can be transmitted through a seal even if there is no flow. If there is a high enough pressure difference the seal will move back and forth and

noise will be transmitted. This movement will be resisted by the seal's stiffness, mass and damping. Multiple seals have better effect compared to the increased mass and stiffness of a single seal. Doubling the stiffness or mass of a seal reduces noise by approximately 3 dB whereas a double seal can reduce noise by up to 6 dB (George and Callister, 1991). Seals need to withstand the pressure differences across the body under all environmental and driving conditions imposed on them.

Leak noise is usually insignificant for a well-sealed car. However, due to the pressure differences that exist around the moving vehicle (which, in strong crosswinds, can vary considerably with time) and dynamic body flex (due to road inputs), movement of door seals can still occur and in some cases can permit a leakage through a seal. When this occurs, significant short-term noise can be generated. Car companies now place considerable emphasis on maintaining effective sealing of the body under the wide spectrum of operating conditions, including high and low temperatures, by good designs, manufacturing processes, quality control and tests (e.g. an ultrasonic leak check).

10.5   Aeroacoustic measurement techniques and psychoacoustic analysis

10.5.1 Aeroacoustic measurement techniques

Experimental work on aerodynamically induced vehicle noise consists of wind-tunnel tests and on-road tests, either full-size or reduced scale. Many car companies now have dedicated wind tunnels and, since a major part of testing for a new car is determining (and reducing) wind noise, tunnels need to be quiet and semi-anechoic. This necessitates an open-jet wind tunnel, usually with a fixed, acoustically reflective floor representing the road. Situated around the jet is a relatively large plenum area which (apart from the floor) has anechoic treatment to provide an acoustic free field. Treatment can either be the traditional anechoic wedges or, more recently, panel-type absorbers. A typical modern aeroacoustic wind tunnel is shown in Fig. 10.6. The photograph is taken from inside the jet nozzle and shows a vehicle located in the open-jet test section; the acoustic wedges can be seen on the plenum walls. Also evident is the collector behind the vehicle which serves to smoothly collect the jet, including any wakes from the vehicle.

Instrumentation is normally standard acoustic instruments, such as sound pressure level meters or one or more binaural head systems. The use of multiple binaural heads enables sound to be measured at all possible passenger ear locations, as well as providing volume 'fill' for the cabin to replicate the driver and passenger(s).

10.6 The open jet test section of an aeroacoustic wind tunnel.

In order to reduce car development time and associated costs, much emphasis is now placed on vehicle simulation and/or scale testing. A significant drawback to the type of test described above is that it requires a full-size vehicle to be available, including trim, sealing, etc., which will clearly be very late in any car development cycle. Model-scale wind-tunnel tests, whilst commonplace for determining aerodynamic drag, etc., cannot generally be used to study aeroacoustics, since (i) the physical mechanisms are not amenable to simple scaling and (ii) the characteristics of the body, including seals, cannot be correctly dynamically replicated in model scale. Whilst analysis and computation can give guidance to some categories of problem (such as described in Section 10.4.2 above) many flows do not have amplitude and frequency characteristics that follow well-known scaling laws, thus the possibilities of using scale models for aeroacoustic testing are severely limited. However, some full-scale tests are conducted prior to the construction of detailed full-size pre-production vehicles. These have included full-size clay models with part-cabin replication (which can be used for some sealing assessments, when a microphone is placed in the part cabin), or studies on isolated parts, such as entire mirror assemblies. Clearly the replicated approach flow must be of a similar nature to that experienced on-road and of low background noise level.

Techniques to assess wind noise in the early design stage include performing measurements on a solid clay model (normally these are produced in the relatively early design stage). Here there is no representation of an internal cabin, thus external acoustic measurements will be required. These can be either in the wind tunnel plenum chamber (where the flow velocity will be very low, thus pseudosound from a microphone will be negligible) or in-flow using a streamlined shield on a microphone. A very carefully designed microphone shield is needed, otherwise the hydrodynamic pressure fluctuations will dominate the acoustic ones. Such techniques provide information on the acoustic waves radiated away from the vehicle. Sometimes microphones are flush-mounted on the external surfaces of the car, such that their diaphragm forms part of the smooth external shape, but

it must be recognised that such techniques measure the sum of hydrodynamic and acoustic pressures and the former will dominate at highway speeds. These techniques do not allow the in-cabin measurements to be gained directly but give data on the exterior surface pressure fluctuations. However, if a knowledge of the cabin body dynamics (including sealing systems) is known, then in-cabin noise levels can be inferred.

10.5.2 Psychoacoustic analysis

The likely subjective effect that in-cabin sounds have on humans is an important and growing area of analysis. This can be as simple as getting subjective feedback from target groups of subjects or simply A-weighting the signals. However, many other sophisticated processing techniques are increasingly being used. These include Articulation Index (AI), roughness and modulation. The reader is directed to the specialist texts in these areas, such as Plack (2005) and Fastl and Zwicker (2007).

10.6   Conclusions

Aerodynamically generated noise is a complex, non-linear phenomenon which can involve feedback mechanisms between the acoustic and hydrodynamic fields. Generally the physics is not amenable to analysis that provides useful engineering answers in a timely manner. The determination and reduction of wind noise continues to be a focus for automotive companies, since other noise sources (e.g. engine, exhaust, tyres) have been reduced substantially over the last few decades. Additionally, new hybrid or all-electric powertrains are likely to have lower levels of noise than their internal combustion equivalents, thus putting a renewed emphasis on wind noise. Wind noise is still a significant source of in-cabin noise at high speeds, due to the strong influence of flow velocity on amplitude and sometimes frequency. Whilst the acoustical energy represents an insignificant proportion of the energy required for propulsion (thus a low-drag car does not mean a low-noise car, or vice versa), in-cabin noise arising from the external flow can still prove troublesome and the sealing required increases vehicle cost and mass. Very small features such as a styling cavity can generate relatively large (and annoying) sounds. Since useful analytical or computational solutions appear far from mature, car companies continue to use experimental methods in aeroacoustic wind tunnels.

10.7   Acknowledgements

10.8 References

Alam F. (2000), 'The effects of car A-pillar and windshield geometry on local flow and noise', PhD Thesis, School of Aerospace, Mechanical and Manufacturing Engineering, RMIT University, Melbourne.

Blake W. K. (1986), *Mechanics of Flow-Induced Sound and Vibration*, Volumes I and II, Academic Press, Orlando, FL.

Blevins R. D. (1990), *Flow-Induced Vibration*, second edition, Van Nostrand Reinhold, New York.

Chen F. and Qian P. (2008), 'Vehicle wind buffeting noise reduction via window openings optimization', SAE paper 2008-01-0678.

Fastl H. and Zwicker E. (2007), *Psychoacoustics: Facts and Models*, Springer, Berlin, Heidelberg and New York.

George A. R. and Callister J. (1991), 'Aerodynamic noise of ground vehicles', SAE paper 911027.

Haruna S., Nouzawa T. and Kamimoto I. (1990), 'An experimental analysis and estimation of aerodynamic noise using a production vehicle', SAE paper 900316.

Khalighi B., Johnson J., Chen K.-H. and Lee R. (2008), 'Experimental characterization of the unsteady flow field behind two outside rear view mirrors', SAE paper 2008-01-0476.

Lighthill M. J. (1952), 'On sound generated aerodynamically. I. General theory', *Proc. R. Soc. Lond. A* **211** (1952) 564–587.

Lighthill M. J. (1954), 'On sound generated aerodynamically. II. Turbulence as a source of sound', *Proc. R. Soc. Lond. A* **222** (1954) 1–32.

Lounsberry, T. H., Gleason M. E. and Puskarz M. M. (2007), 'Laminar flow whistle on a vehicle side mirror', SAE paper 2007-01-1549.

Mejia P., Park J. B. and Mongeau L. (2007), 'Surface pressure fluctuations in separated-reattached flows behind notched spoilers', SAE paper 2007-01-2399.

Milbank J. (2004), '*Investigation of fluid-dynamic cavity oscillations*', PhD Thesis, School of Aerospace Mechanical and Manufacturing Engineering, RMIT University, Melbourne.

Plack C. J. (2005), *The Sense of Hearing*, Routledge, New York.

Watanabe M., Harita M. and Hayashi E. (1978), 'The effect of body shapes on wind noise', SAE paper 780266.

Watkins S. (2004), 'On the causes of image blurring in external rear view mirrors', SAE paper 2004-01-1309.

Watkins S. and Oswald G. (1999), 'The flow field of automobile add-ons – with particular reference to the vibration of external mirrors', *Journal of Wind Engineering and Industrial Aerodynamics*, **83**, 541–554.

Watkins S., Oswald G., Czydel R. and Saunders J.W., "The Noise and Vibration of Automotive Add-ons: Wing Mirrors, Aerials and Roofracks", 9th Int. Pacific Conf. on Automotive Eng. (IPC9), Indonesia, Nov 1997.

Wikipedia (2008), http://en.wikipedia.org/wiki/Helmholtz_resonance

11
Active noise and vibration control in vehicles

S.J. ELLIOTT, University of Southampton, UK

Abstract: Active control works by destructive interference between the original sound or vibration field in the vehicle and that generated by a controllable, secondary, source. Physical limitations generally confine its usefulness to low frequencies so that it complements conventional passive control methods. The development of powerful processors at an affordable cost and the increasing trend towards integration in vehicles has allowed the commercial implementation of active control systems by several manufacturers, mainly for the reduction of low frequency engine noise. As vehicles become lighter to achieve fuel efficiency targets, it is expected that active control will play an important part in maintaining an acceptable NVH environment, in terms of sound quality as well as overall level.

Key words: sound, vibration, active control, sound quality, lightweight vehicles.

11.1 Introduction

Active control involves driving a number of actuators to create a sound or vibration signal out of phase with that generated by the vehicle, thus attenuating it by destructive interference. Its successful application requires that there is both a good spatial and a good temporal matching between the field due to the actuators, or secondary sources, and that due to the vehicle. The requirement for spatial matching gives rise to clear limits on the upper frequency of active noise control, due to the physical requirement that the acoustic wavelength must be small compared with the zone of control. The requirement for temporal matching requires a signal processing system that can adapt to changes in the vehicle speed and load. Both the physical limitations and the signal processing control strategies will be described in this chapter, together with a description of some of the practical systems that have found their way into production at the time of writing. Active noise and vibration control can provide a useful alternative to passive noise and vibration control, particularly at low frequencies and on vehicles with particular problems. Although active control has been experimentally demonstrated in vehicles for over 20 years, it is only recently that the levels of integration within the vehicle's electronic systems have allowed the cost to become affordable. Active control may now allow a reduction in the weight

235

of conventional passive methods of low frequency noise control, helping the push towards lighter, more fuel efficient vehicles.

11.2   Physical principles and limits of active control

Active vibration control in vehicles often involves the isolation of a particular transmission path, particularly of engine orders through engine mounts. Here the spatial matching problem requires that the mechanical actuator drives in the same direction as the dominant transmission path from the source and at more or less the same point. For this reason most systems use combined active/passive mounts, in which the actuator is integrated into a conventional hydromount. Although piezoelectric and magnetostrictive actuators have been considered for this application, the most successful actuator type appears to be electromagnetic. Cost considerations generally limit the number of actuators that can be used, since these are generally the most expensive parts of automotive active vibration control systems, and so the successful use of active control is limited to vehicles with a few dominant transmission paths. The introduction of active mounts can significantly ease the conventional problems in trading off high static stiffness with low dynamic stiffness.

An idealised arrangement to illustrate the function of an active mount is shown in Fig. 11.1. The force transmitted through the mount, assuming it behaves reasonably linearly, can be written at a particular frequency as

$$f_T = f_S + S_M(x_S - x_B) \tag{11.1}$$
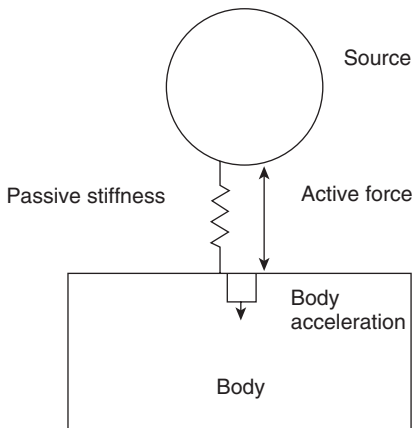
11.1 Idealised active vibration system consisting of a single active mount, which includes passive stiffness S_M and an actuator generating an active force f_S, connecting a vibration source such as an engine to the vehicle's body.

where f_S is the secondary force generated by the actuator, x_S is the displacement of the source above the mount, x_B is the displacement of the body below the mount and S_M is the mount stiffness. The body is assumed to only be driven by this total force, so that if F_B is the flexibility of the body below the mount, then

$$x_B = F_B f_T = F_B f_S + F_B S_M (x_S - x_B) \tag{11.2}$$

so that solving the equation for the displacement of the body gives

$$x_B = \frac{F_B (f_S + S_M x_S)}{(1 + F_B S_M)} \tag{11.3}$$

If x_B is measured using an accelerometer on the body, for example, and, at a particular engine order, an adaptive controller is used to adjust the secondary force, f_S, so that the output of this accelerometer is cancelled, then it can be seen by setting equation 11.3 to zero that f_S under these optimum conditions must be equal to

$$f_{S(optimum)} = -S_M x_S \tag{11.4}$$

Notice that the required force does not depend on the flexibility of the body, since this has been brought to rest. Also, notice that the total force in equation 11.1 has also been set to zero with this control force, and that not only does this total force act down on the body but it also acts up on the source structure. Thus, if the total force becomes zero, the source structure is effectively floating at this control frequency and x_S becomes the free displacement of the source. Equation 11.4 thus provides a useful way of estimating the force requirements of an active mount, depending as it does on only the mount stiffness and the free source displacement at the frequency of interest. There are some advantages to measuring the total transmitted force for use as the control signal, rather than the body acceleration, since it is related to the secondary force in a more straightforward way than the latter. The measurement of the total transmitted force, using a load cell for example, can, however, be more complicated than measuring the acceleration.

The requirement for spatial matching is more complicated for active noise control, since it is the acoustic field inside the vehicle which must be controlled and this is generally excited by the distributed vibration of the whole body, excited by multiple sources. In order to illustrate the frequency limitations of active noise control inside a vehicle, we assume that the sound field is tonal and use the complex pressure at a single frequency, ω, which may be described in modal form as

$$p(\mathbf{x}, \omega) = \sum_{n=0}^{\infty} a_n(\omega) \Psi_n(\mathbf{x}) \tag{11.5}$$

where **x** is the position vector, $a_n(\omega)$ is the amplitude of the *n*th acoustic mode and $\Psi_n(\mathbf{x})$ is its mode shape.

Although in principle an infinite number of modes must be used to describe the sound in the enclosure, the sound field can always be approximated to arbitrary accuracy with a finite modal series. In the low frequency range, where active control is most effective, the modal description is a very efficient representation of the sound field since relatively few modes need be considered. Conventional passive noise control techniques also do not work very well in this low frequency region, unless very massive barriers or bulky absorbers are used, and so active control conveniently complements the effect of passive noise control techniques and can provide significant weight and space savings at low frequencies.

Two active control problems will be briefly considered: global control and local control. The objective of a global control system is to reduce the sound throughout the enclosure by adjusting the amplitudes and phases of a number of secondary sources, which are typically loudspeakers. The fundamental limits of such a strategy can be assessed by calculating the reductions which are possible in the mean square pressure integrated over the whole volume, which is proportional to the acoustic potential energy in the enclosure that may be written as

$$E_p(\omega) = \frac{1}{4\rho_0 c_0^2} \int_V |p(\mathbf{x}, \omega)|^2 dV \qquad (11.6)$$

Assuming that the mode shapes are orthonormal, $E_p(\omega)$ is equal to the sum of the modulus squared mode amplitudes (Nelson and Elliott, 1992). Since the secondary sources linearly couple into each mode amplitude, $E_p(\omega)$ is a quadratic function of the complex secondary source strengths, and this function has a unique global minimum. This minimum value of $E_p(\omega)$ provides a measure of the best performance that can be obtained in a global control system for a given distribution of secondary sources and a given excitation frequency. Figure 11.2(b), for example, shows the result of a number of such calculations for the levels of $E_p(\omega)$ at various excitation frequencies in a computer model of an enclosure of dimensions $1.9 \times 1.1 \times 1.0$ m as shown in Fig. 11.2(a), which are approximately the conditions inside a small car (Elliott, 2001). The solid line in Fig. 11.2(b) shows how the energy due to a primary source in one corner of the enclosure varies with excitation frequency, the dashed line shows the energy after it has been minimised using a single secondary loudspeaker in the opposite corner, and the dot-dashed line shows the energy after minimisation using seven secondary loudspeakers placed at all the corners of the enclosure away from the primary. The first longitudinal resonance, at about 80 Hz, is significantly attenuated by the action of a single secondary loudspeaker, but almost no reduction is achieved in the energy at about 160 Hz, close to which three
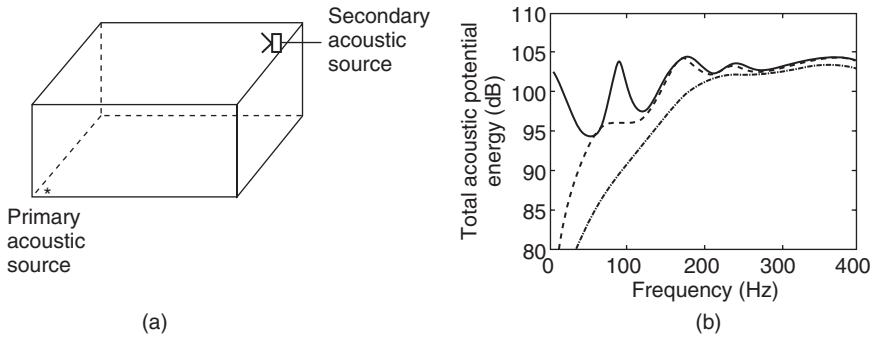
11.2 (a) An active noise control system in which a loudspeaker is used to globally control the sound in an enclosure of about the size of a small car interior. (b) The total acoustic potential energy in the enclosure as a function of excitation frequency, when driven by the primary source alone (solid line), when the energy is minimised using a single secondary source (dashed line) and when the energy is minimised using seven secondary sources (dot-dashed line).

acoustic modes have their natural frequencies. This is to be expected, since in general a single loudspeaker can control only a single mode. Even with seven secondary loudspeakers, however, a reduction in energy of only about 5 dB is achieved at this excitation frequency and this reduction becomes less than 1 dB at about 250 Hz.

The number of secondary sources required to achieve active control is approximately equal to the number of significantly excited acoustic modes, which can be estimated from the modal overlap, i.e., the average number of modes with natural frequencies within the half-power bandwidth of a single mode (Elliott, 2001). The modal overlap in this enclosure is about seven at 250 Hz, which explains the limited performance with seven loud-speakers, but at higher frequencies the acoustic modal overlap in an enclo-sure rises as the cube of the excitation frequency. This sharp rise with frequency in the required number of secondary sources provides a very clear upper frequency limit to global control with a system of reasonable complexity.

An alternative strategy to global control would be to control only the sound at specific locations in an enclosure, such as close to the ears of pas-sengers in a vehicle. Such a local control strategy was originally suggested by Olsen and May (1953) who described an active headrest using a feed-back control system from a microphone to a closely-spaced loudspeaker acting as the secondary source. The acoustic performance of such a system depends on the detailed geometric arrangement of the headset and the position of the passenger's head, but some physical insight can be gained by considering simplified models. Figure 11.3, for example, shows a
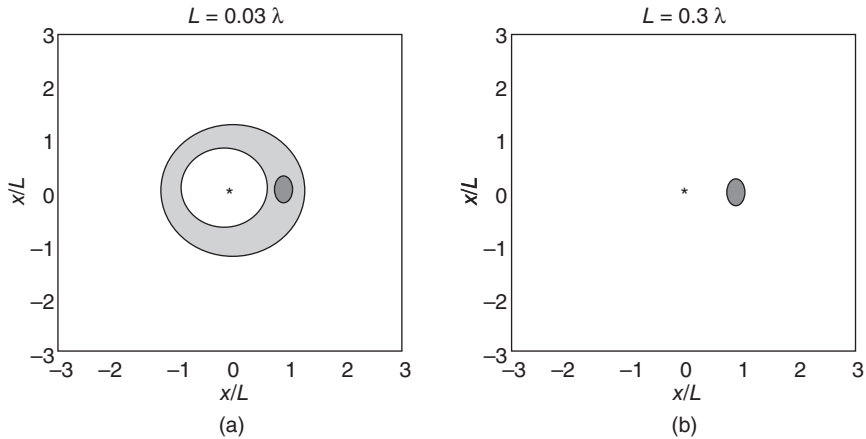
11.3 The zone of quiet, within which a diffuse primary field is attenuated by more than 10 dB for a local control system in which a monopole acoustic source at the origin is arranged to cancel the pressure at $x = L$ for two different excitation frequencies for which (a) L is much larger than the acoustic wavelength, and (b) L is of the order of the acoustic wavelength.

cross-section through the zone of quiet, within which the sound has been attenuated by at least 10 dB, generated when a diffuse primary sound field is cancelled at the point $x = L$ by an acoustic monopole at the origin (Elliott, 2001). The two graphs correspond to an excitation frequency for which L is much smaller than the acoustic wavelength, in which case a 'shell' of quiet is generated around the secondary source, and to an excitation frequency for which L is of the order of the acoustic wavelength, in which case the zone of quiet is spherical with a diameter which is about one-tenth of an acoustic wavelength (Elliott *et al.*, 1988). The rule of thumb that the spatial extent of a local active control system is about one-tenth of a wavelength has proved to be very useful in the initial stages of many practical designs.

11.3   Control strategies

The effective attenuation of a signal using active control requires a high degree of temporal matching between the waveform due to the vehicle alone and that due to the active control system. This is most easily illustrated with a sinusoidal signal, for which a 10 dB attenuation requires that the two signals must be matched within about 2 dB in amplitude and within about 20° in phase. In practice, this temporal matching is achieved by using a control system with a sensor to monitor the residual difference between the two signals. This 'error sensor' may be a microphone, or microphone array, for an active noise control system inside a vehicle, or an accelerom-
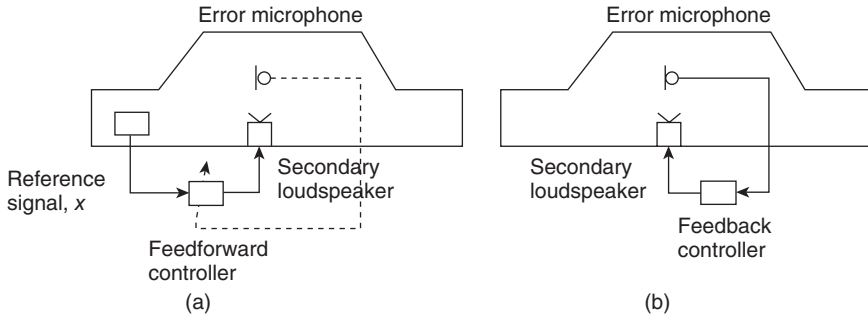
11.4 Illustration of single-channel active noise control systems using (a) a feedforward and (b) a feedback control strategy. Note that the feedforward control signal requires an additional reference signal, *x*, and uses the error signal to adapt the controller.

eter on the chassis next to an active mount for an active vibration control system.

There are two different ways in which the control system can use the signal from this error sensor: using either feedforward control or feedback control. Idealised, single-channel feedforward and feedback controllers are illustrated in Fig. 11.4. In addition to the signal from the error sensor, which is illustrated as a microphone in Fig. 11.4(a), a feedforward control system also requires an independent 'reference' signal, generally denoted x, that is correlated with that being controlled. In an engine noise controller, for example, it is the engine orders that are being attenuated and a reference signal at the frequency of these engine orders is required, which will track these orders as the engine speed changes. Originally, such a reference signal was derived by analogue processing of the ignition signal, but it is now commonly synthesised from knowledge of the engine speed supplied over a CAN bus, for example. The signal driving the secondary loudspeaker is obtained by adjusting the amplitude and phase of this tonal reference signal.

It is not generally effective to operate a feedforward controller with a fixed response, since it is then not responsive to changes in the error signal or the environment, i.e. it is 'open loop'. The error signal is thus used to adapt the response, so that it is able to change with engine speed and load, for example, and the system then becomes 'closed loop'. The need to adapt the controller response means that most practical implementations use digital electronics, operating in sampled versions of the reference and error signals and producing a sampled signal to drive the actuator, which all need to be filtered to remove components above half the sampling frequency. A variety of algorithms have been used to adapt the controller, but most are based on an adaptive filtering method called the 'LMS' (least mean square)

algorithm, which was originally developed in the 1960s for applications such as echo cancellation on telephone lines (Widrow and Stearns, 1985). The modified algorithm required to get the controller to converge reliably in active control applications is called the filtered reference LMS or 'filtered *x* LMS' (Widrow and Stearns, 1985; Elliott, 2001). In practice, multiple loudspeakers are driven to minimise the sum of the mean square responses from a number of microphones, which requires a multichannel generalisation of the filtered *x* LMS algorithm (Elliott *et al.*, 1988).

The feedback system, illustrated in Fig. 11.4(b), by contrast is generally implemented with a fixed controller and so can be efficiently built using analogue electronics. The feedback system has several other advantages, such as not requiring a reference signal, but also has a number of significant disadvantages. One disadvantage is that the control is not selective, i.e. any signal will be attenuated, not just those correlated with the reference signal. Another disadvantage is that the error sensor, which is the microphone in Fig. 11.4(b), must be placed close to the secondary loudspeaker.

The fundamental trade-off in the design of any feedback controller is that between performance and stability (Franklin *et al.*, 1994; Elliott, 2001). The feedback system can become unstable when the loop gain, which includes the response between the actuator and sensor and that of the controller, has a phase shift of 180°. The feedback then changes from being negative, which leads to an attenuation of the error signal, to being positive, which leads to an enhancement of the error signal. All practical systems will have a loop gain with such a phase shift at high frequencies, due to the acoustic propagation delay from the loudspeaker to the microphone, and thus inevitably have enhancement at some frequencies. If, however, the loop gain is greater than unity at the frequency where this phase shift is 180°, then the feedback system will become unstable. Some mitigation of this condition can be achieved using analogue 'compensator' circuits, but sooner or later this unstable condition will arise as the feedback gain is increased, which will then limit the performance at lower frequencies. A phase shift of 180° is reached at a frequency for which the distance between the loudspeaker and the microphone, *d*, is half an acoustic wavelength. If c_0 is the speed of sound, the upper frequency of operation of a feedback control system, $f_{(max)}$, will be significantly below this frequency, which is given by $c_0/2d$, so that

$$f_{(max)} << \frac{c_0}{2d} \qquad (11.7)$$

and, in practice, the upper frequency is about one-tenth of $c_0/2d$. One can thus see that for an active headphone, for which feedback controllers are widely used and in which *d* is about 1 cm, the maximum frequency will be about 1.7 kHz, since c_0 is 340 metres per second. For an active control

system in a car, however, where the microphone is close to the driver's head but the loudspeaker is fitted in the door or the dashboard, d will be about 50 cm and so the upper frequency will be about 34 Hz. The feedback system is thus of limited use unless either very low frequency noise is to be controlled or the loudspeaker can be brought significantly closer to the microphone, by mounting it in the headrest, for example. Laboratory versions of such headrest controllers have been demonstrated (Elliott, 2001), with performance up to about 300 Hz. At this frequency, however, the size of the zone of quiet, predicted to be one-tenth of an acoustic wavelength following the discussion in Section 11.2, is about 10 cm, so that significant active control would be experienced only if the listener's head was fairly stationary.

11.4   Commercial systems

Early automotive active noise systems were feedforward arrangements for tonal engine noise control (Elliott *et al.*, 1988), developed as part of a research programme that also focused on the active control of interior noise in propeller aircraft (Nelson and Elliott, 1992). The physical arrangement of a typical feedforward active noise control system, developed in collaboration with Lotus Engineering, is shown in Fig. 11.5, in which four of the six loudspeakers, in the dashboard and front doors, were adjusted at the engine firing frequency and its harmonics, to control the sum of the mean
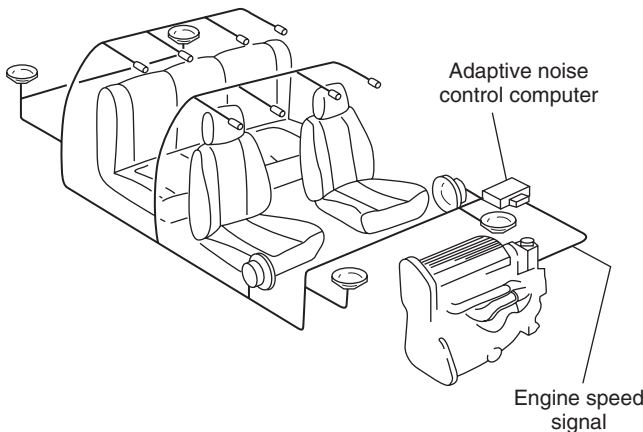
11.5 The components of an active noise control system for engine noise, showing the feedforward controller deriving a reference signal from the engine and driving four loudspeakers at a number of engine orders, adjusted in amplitude and phase to minimise the sum of the mean-square responses at eight microphones, positioned in the roof lining.
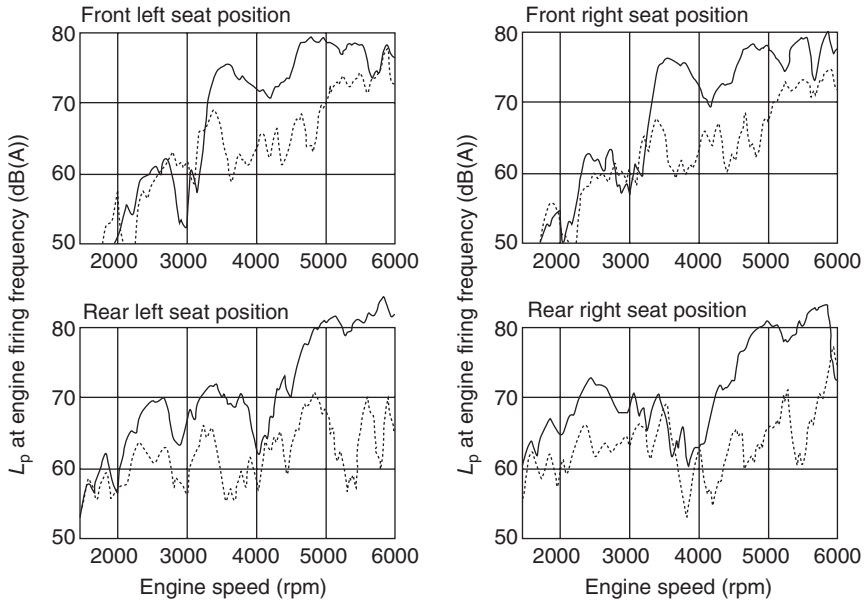
11.6 A-weighted engine second-order levels at the four seat positions as a function of engine speed as a small, four-cylinder car is accelerated along a track, without (dashed) and with (solid) the active control system shown in Fig. 11.5 operations.

square pressures at eight microphones, mounted in the head lining. The A-weighted sound pressure levels at the engine firing frequency (second order for this 1.1-litre four-cylinder car) are shown in Fig. 11.6, measured at the front seat positions using monitoring microphones separate from the error microphones used by the control system. Reductions of about 10 dB are measured in the front seats above about 3000 rpm (a firing frequency of 100 Hz), which gave an improvement in the overall dB(A) level of 4 to 5 dB(A). Reductions at lower speeds were measured in the rear due to the suppression of the first longitudinal acoustic mode, which has a nodal line near the front passengers' heads. Nissan first put such a system into production on a Bluebird vehicle in 1992 (Hasegawa *et al.*, 1992), in a system which used loudspeakers, amplifiers and processors separate from the audio system, and so was relatively expensive.

Demonstration systems were also developed for the active control of random road noise using feedforward techniques, with reference signals derived from accelerometers on the vehicle suspension and body (Sutton *et al.*, 1994; Bernhard, 1995; Dehandschutter and Sas, 1998; Mackay and Kenchington, 2004). In order to obtain reasonable levels of active control, however, it was found that about six such reference signals were required. This is because the tyre vibration is relatively uncorrelated in its various

Z direction

X, Y, and *Z* tri-axial
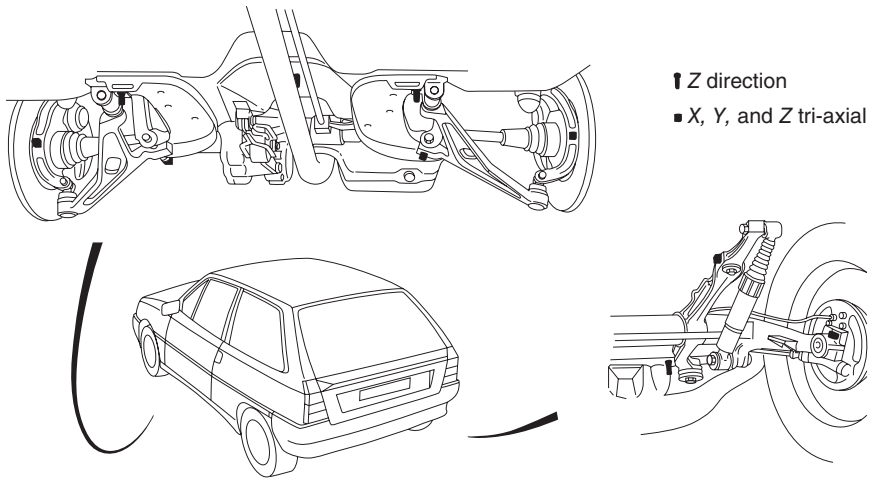
11.7 Typical locations of the accelerometers used to obtain the six reference signals in a feedforward active control system for road noise.

degrees of freedom, and reference signals have to be used for all the significantly contributing sources (Sutton *et al.*, 1994). Typical locations for the accelerometers used to generate the reference signals are shown in Fig. 11.7. The A-weighted spectrum of the pressure at the driver's ear using a real-time feedforward system is shown in Fig. 11.8 (Sutton *et al.*, 1994), which shows that from 100 Hz to 200 Hz reductions of up to 10 dB are measured. The additional expense of these accelerometers has prevented the mass production of such feedforward active control systems for road noise. In 2000, however, Honda demonstrated a mainly feedback system to control a 40 Hz boom in the front of their Accord wagon car (Sano *et al.*, 2001). A fixed feedforward system was then used to prevent the noise in the rear of the car being amplified. This excitation was relatively narrowband and the microphone was placed fairly close to the loudspeakers, compared with the wavelength at 40 Hz, so that good performance was obtained in suppressing this resonant boom. Figure 11.9 shows the configuration of the active control system, from Sano *et al.* (2001), and Fig. 11.10 shows the measured spectrum at a front seat, illustrating the suppression of the narrowband boom at 40 Hz by about 10 dB. An important aspect of reducing the cost of this system, so that it could be used in mass production, was the integration of the loudspeakers with the audio system, although at that time a separate active control unit was used from the audio system, since a number of different audio head units were offered on this vehicle. It is the full integration of the active control system with the audio system that would make this technology affordable on many vehicles.
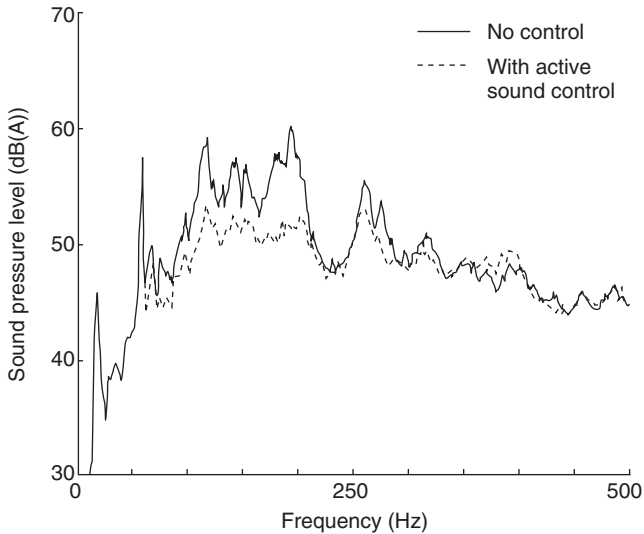
11.8 Spectrum of the A-weighted sound pressure level in a small car using a real-time active control system for road noise, measured at the driver's ear. Vehicle speed was 60 km/h over asphalt and coarse chippings.
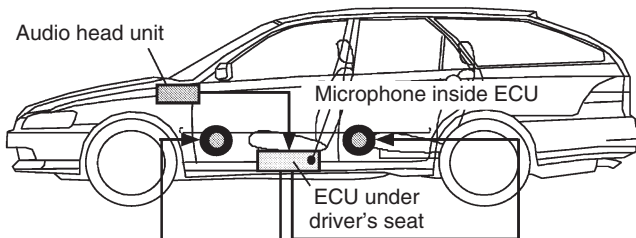
11.9 Configuration of the active control system in the Honda Accord (Sano *et al.*, 2001).

Since 2000, active engine noise systems have been introduced on vehicles in Honda for variable cylinder management systems (Inoue *et al.*, 2004) and hybrid vehicles (Honda, 2005), and in Toyota for hybrid vehicles (Toyota, 2008), to improve the sound quality inside the vehicle. The synthesis of external noise on hybrid vehicles has also been suggested in order for them to be safer for pedestrians (Lotus, 2008).

Systems for the active control of vibration in vehicles have tended to concentrate on active engine mounts, which may also reduce internal noise. Nissan, for example, used two electromagnetic engine mounts to reduce the vibration in a four-cylinder direct injection diesel in 1998 (as discussed by Sano *et al.*, 2002), which used feedforward control operating from 20 Hz to 130 Hz and a load cell on the body to provide an error signal. Figure 11.11
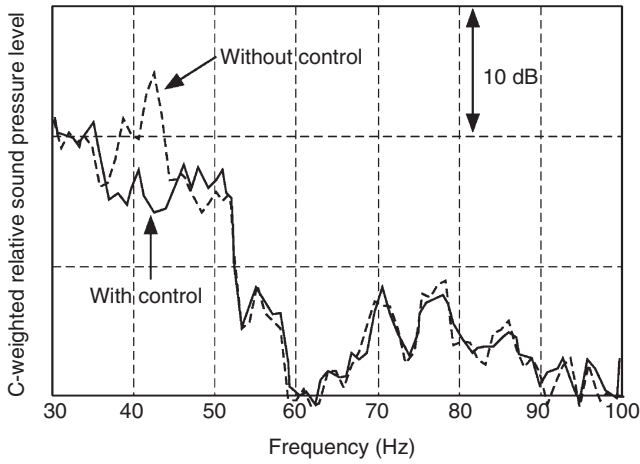
11.10 Spectrum of the C-weighted pressure in the front seat of a Honda Accord (Sano *et al.*, 2001).
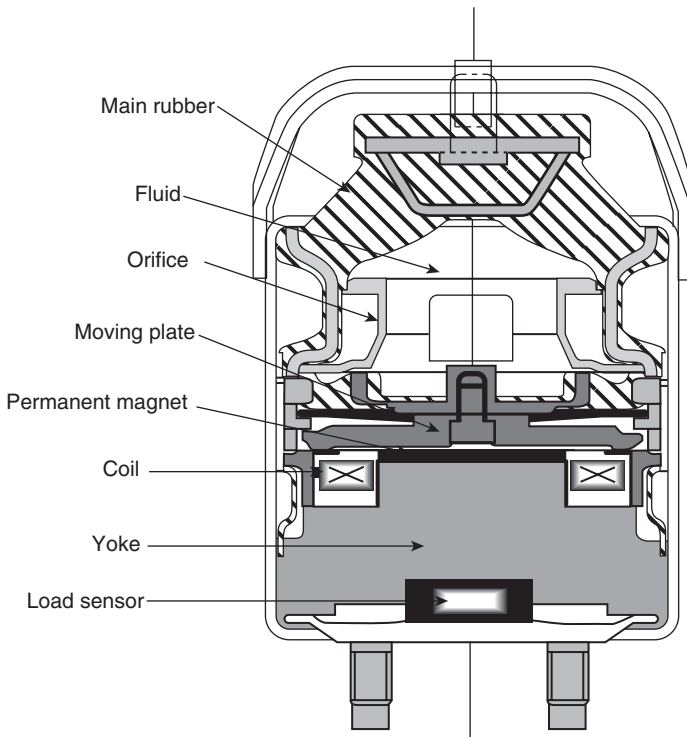
11.11 Components of an active engine mount (Sano *et al.*, 2002).
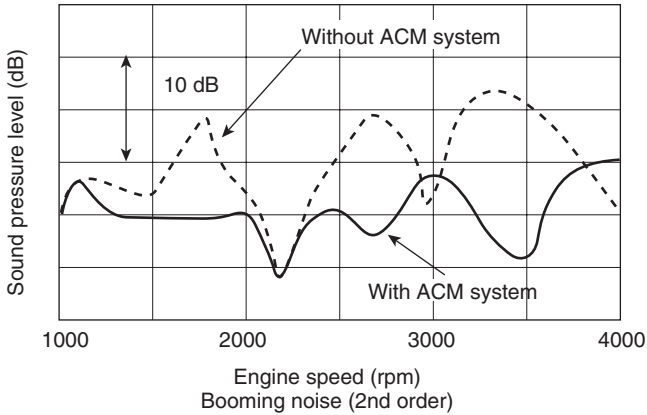
11.12 Measured spectrum of the sound in a diesel vehicle fitted with active engine mounts (Sano *et al.*, 2002).

shows the main components of such an active engine mount, which integrates an electromagnetic actuator capable of generating about 50 N into a conventional hydromount. The reduction in internal noise when such mounts are used in a diesel vehicle is illustrated in Fig. 11.12. Honda also has introduced active engine mounts on vehicles with variable cylinder management in addition to engine noise systems to keep six-cylinder noise and vibration quality during three-cylinder operation (Matsuoka *et al.*, 2004). More recently, Jaguar has used Avon electromagnetic engine mounts to control the vibration on the diesel version of their XJ vehicle (Avon Rubber, 2005), again largely for sound quality reasons rather than to reduce the noise level.

11.5   Future trends

An important overall trend in the automotive industry is clearly the design of more fuel-efficient vehicles. One of the main ways in which improvements in fuel efficiency can be achieved is by reducing weight. Reducing the weight of the body panels inevitably degrades their ability to attenuate low frequency noise, and so increases noise levels within the vehicle in this frequency range. Passive methods of noise control using absorption are very effective from mid-frequencies upwards, but generally rely on tuned systems to provide significant low frequency control. These tuned systems are only suitable for certain frequencies and themselves add weight to the vehicle. The drive towards more fuel-efficient vehicles thus provides a real opportunity for active systems to be used to control low frequency noise and vibration without significantly increasing weight.

Another trend is the active control of the overall sound quality in a vehicle, rather than just the sound level (Gonzalez *et al.*, 2003). This may become important with the use of hybrid vehicles and in vehicles with variable cylinder management, since the changes in the quality of the sound inside these vehicles as the power source changes character can be disconcerting to the driver. The active control of sound quality generally involves a control system that drives the microphone signals inside the car towards a target, or command, signal, rather than just minimising it. This has been termed 'noise equalisation' (Ji and Kuo, 1993), 'sound synthesis' (McDonald *et al.*, 1994), 'active design' (Scheuren *et al.*, 2002) and 'sound profiling' (Rees and Elliott, 2006), and can include the use of psychoacoustic models (Rees and Elliott, 2004). Recent trends also include the use of active control systems to provide a smoothly changing sound profile with engine speed, but with an emphasis on sporty sound during acceleration, to make the vehicle 'fun to drive' (Kobayashi *et al.*, 2008). Further development along these lines is also possible, by providing an acoustic environment inside the vehicle that encourages the owner to drive in a more fuel-efficient way, for example. There has been some resistance to this trend towards active control of sound quality in some parts of the automotive industry, who see such electronic sound control as 'cheating' compared to mechanical redesign. As more virtual systems are introduced in vehicles, however, with active braking, stability and steering, and with a younger generation of customers who are more used to audio manipulation, these objections are likely to die away.

Another important development is in the integration of electronic vehicle systems. Early active control systems were completely stand-alone, which meant that amplifiers, loudspeakers and processors were all duplicated in the audio and active control systems. This duplication has continued, to some extent because of the different responsibilities of the vehicle manufacturer and audio supplier, and the requirement that a given vehicle may be fitted with a number of different audio systems. It is a paradox that a customer can be sold a very expensive audio system in a vehicle for which the low frequency vehicle noise impairs their enjoyment of the audio system, and yet the additional cost of an active control system would be small compared with that of the audio system if it was fully integrated.

It is clear that active control can have the most impact on lightweight vehicles and that in these vehicles the active noise control system could be effectively integrated with the audio system, reducing the cost considerably. The loudspeakers may need to be upgraded for low frequency active control use, but this is still considerably less expensive than having two systems with duplicate drivers, wiring and amplifiers. Many audio systems now also contain considerable digital processing power, for CD and MP3 players, radio tuning and audio effects. This processing power is no longer

expensive and can also be used to implement active control algorithms. The microphones and associated wiring remain an additional cost for active control systems on some vehicles, although others already have microphones fitted as standard, for hands-free telephone operation, for example. A fully integrated system could then be achieved if these microphones could be positioned so that they effectively measured the noise field in the car as well as the driver's voice, and their signal could be integrated into the audio system.

11.6   Sources of further information and advice

The physical basis of active noise control is explained in the textbook *Active Control of Sound* by P.A. Nelson and S.J. Elliott (1992). The principles of feedforward and feedback control, together with a more detailed discussion of the control algorithms used and an introduction to hardware and optimum placement of actuators and sensors, are described in *Signal Processing for Active Control* by S.J. Elliott (2001).

A good review of the development of automotive active noise and vibration control is provided by Sano *et al.* (2002) and an interesting discussion of the integration of active and passive control to reduce cost is provided by Su (2002).

Further information on individual systems can be found on the following websites:

http://www.isvr.soton.ac.uk/ACTIVE/Introduction.htm
http://www.mecheng.adelaide.edu.au/avc/projects/
http://www.mech.kuleuven.be/mod/other/topic_03_08
http://www.grouplotus.com/mediacentre_pressreleases/view/406

For movies see the following websites:

http://www.thefutureschannel.com/dockets/critical_thinking/bose/index.
   php
http://cnettv.cnet.com/?type=externalVideoId&value=6214373
http://uk.youtube.com/watch?v=zOtTX_NPPBs

11.7   References

Avon Rubber (2005) Vibramount brochure. Avon Rubber plc, Melksham, Wilts, UK.
Bernhard, R.J. (1995) Active control of road noise inside automobiles. *Proc. ACTIVE 95*, 21–32.
Dehandschutter, W. and Sas, P. (1998) Active control of structure-borne road noise using vibration actuators. *Journal of Vibration and Acoustics*, **120**, 517–523.
Elliott, S.J. (2001) *Signal Processing for Active Control.* Academic Press, London.

Elliott, S.J., Stothers, I.M., Nelson, P.A., McDonald, A.M., Quinn, D.C. and Saunders, T. (1988) The active control of engine noise inside cars. *Proc. Inter-Noise 88*, 987–990.

Franklin, G.F., Powell J.D. and Emani-Naeini, A. (1994) *Feedback Control of Dynamic Systems*. Addison Wesley, 3rd Edition.

Gonzalez, A., Ferrer, M., de Diego, M., Pinero, G. and Garcia–Bonito, J.J. (2003) 'Sound quality of low-frequency and car engine noises after active control', *Journal of Sound and Vibration*, **265**, 663–679.

Hasegawa, S., Tabata, T. and Kinoshita, T. (1992) The development of an active noise control system for automobiles. *Society Automotive Eng., Tech. Paper*, 922 086.

Honda (2005) *Honda Accord hybrid sedan interior*. Press release.

Inoue, T., Takahashi, A., Sano, H., Onishi, M. and Nakamura, Y. (2004) NV countermeasure technology for a cylinder-on-demand engine – Development of active booming noise control system applying adaptive notch filter. *Proc. SAE*, 976.

Ji, M.T. and Kuo, S.M. (1993) Adaptive active noise equaliser. *Proc. ICASSP-93*, **1**, 189–192.

Kobayashi, Y., Inoue, T., Sano, H., Takahashi, A. and Sakamoto, K. (2008) Active sound control in automobiles. *Proc. Inter-Noise 2008*.

Lotus (2008) www.greencarcongress.com/2008/08/Lotus-engineer.html

Mackay, A.C. and Kenchington, S. (2004) Active control of noise and vibration – A review of automotive applications. *Proc. ACTIVE 2004*, Williamsburg, VA.

Matsuoka, H., Mikasa, T. and Nemoto, H. (2004), *SAE paper* 04Annual-714.

McDonald, A.M. *et al.* (1994) Sound synthesiser in a vehicle. *US Patent* 5381902.

Nelson, P.A. and Elliott, S.J. (1992) *Active Control of Sound*. Academic Press, London.

Olsen, H.F. and May, E.G. (1953) Electronic sound absorber. *J. Acoustical Society of America*, **25**, 1130–1136.

Rees, L.E. and Elliott, S.J. (2004) Psychoacoustic modelling for active sound profiling in automobiles. *Proc. UK Inst. of Acoustics*, **26**(2), 337–347.

Rees, L.E. and Elliott, S.J. (2006) Adaptive algorithms for active sound profiling. *IEEE Trans. Speech and Audio Processing*, **14**(2), 711–719.

Sano, H., Inoue, T., Takahashi, A., Terai, K. and Nakamura, Y. (2001) Active control system for low-frequency road noise combined with an audio system. *IEEE Trans. Speech and Audio Processing*, **9**, 755–763.

Sano, H., Yamashita, T. and Nakamura, M. (2002) Recent applications of active noise and vibration control in automobiles. *Proc. ACTIVE 2002*, ISVR, Southampton, 29–42.

Scheuren, J., Shirmacher, R. and Hobelsberger, J. (2002) Active design of automotive engine sound. *Proc. Internoise 2002*, paper N629.

Su, J. Hannsen (2002) A proposal for affordable applications of active control technology. *Proc. Internoise 2002*, paper N109.

Sutton, T.J., Elliott, S.J. and McDonald, A.M. (1994) Active control of road noise inside vehicles. *Noise Control Engineering Journal*, **42**, 137–147.

Toyota (2008) *Toyota cuts 'muffled noise' in Crown Hybrid*. Tech-on, 23 June.

Widrow B. and Stearns, S.D. (1985) Adaptive signal processing, Prentice Hall.

12

Noise and vibration refinement of powertrain systems in vehicles

D. C. BAILLIE, General Motors Holden Ltd, Australia

Abstract: The noise level and sound quality of the powertrain system is arguably one of the most significant influences on the customer's perception of a new car. This chapter describes the process for integrating the powertrain into passenger vehicles. The first step in the process is to set targets for the vibration source levels and isolation of paths to meet the noise level requirements. The second step is to incorporate enablers to tailor the induction and exhaust sound quality in order to meet the customer's expectation of the vehicle. The chapter concludes with a review of future powertrain trends and the challenges they pose for noise and vibration refinement.

Key words: noise, vibration, powertrain, engine, transmission, driveline, exhaust, induction.

12.1 Introduction

The primary motivation to improve noise and vibration in motor vehicles has traditionally been to eliminate any unusual or unexpected noises. The customer perceives a quiet car as a well-built quality vehicle, and any unexpected noises can be a concerning sign of impending failure. The noise level and sound quality of the powertrain system is arguably one of the most significant influences on the customer's perception of his or her new car. The owner of an expensive luxury saloon expects to be propelled along by a whisper-quiet and silky-smooth engine. At the other extreme, the owner of a shiny new sports car expects a loud and exciting note from the exhaust on every stab of the throttle. Thus powertrain noise and vibration refinement does not merely involve the elimination of unusual noises, but increasingly involves sound quality engineering to mould the aural excitement of a new car.

This chapter begins with a review of the key powertrain noise targets and how the targets are rolled down from vehicle-level to powertrain system-level to achieve the noise level requirements. A refresher on order tracking analysis is also covered, since this is the language of describing powertrain noise and vibration performance.

The powertrain hardware is introduced in a series of tables documenting the sources and paths of powertrain noise. These sources and paths sum

together to create the net engine sound level and character received by the driver and the occupants in the vehicle. A review of the many hardware enablers to ensure refinement of the engine, transmission, driveline, induction and exhaust systems is presented along with numerous and interesting examples.

Powertrain systems are continually evolving, and this chapter considers the future trends in hardware enablers for enhanced engine sound quality. But the biggest influence on noise and vibration refinement in the future will no doubt be the ever-increasing push for better fuel economy. The challenges this presents to the noise and vibration engineer are outlined at the end of the chapter.

12.2   Principles and methods

12.2.1 Requirements

The requirements or targets for powertrain noise and vibration performance in a new vehicle program can be considered as the minimisation of any unusual or unexpected noises under all driving conditions. At the highest level, the requirements can be summarised as:

- Smooth idle
- Quiet cruising (under light engine loads)
- Smooth and linear acceleration (under high engine loads)
- A sound character appropriate for the class of vehicle.

Unexpected noises are often due to a system resonance being excited by the powertrain under a specific operating condition. For example, an exhaust boom might be noticeable to the driver on each occasion when he or she drives away from a standstill. On further investigation, it could be apparent that the boom noise is always evident when the engine speed is 1200 rpm, and seems to be more severe under higher engine loads. A V6 engine has an engine firing frequency of 60 Hz at 1200 rpm, and in this case the forces from the engine were found to excite a 60 Hz bending mode of the exhaust system. This example illustrates that a powertrain refinement problem will typically involve a natural resonance of a system (whether it is structural or acoustic) that is excited by forces from the powertrain when the frequencies of both coincide. Targets and requirements of powertrain refinement are set during the development of a new vehicle program to define acceptable levels as well as to provide strategies to avoid these issues.

12.2.2 Development process

As mentioned in Chapters 1 and 2, development of a refined powertrain for a new vehicle has the same key processes as the general vehicle

development process. The key steps in the integration and development of a refined powertrain are:

1. Target setting
   - Set vehicle-level targets:
     - Define noise and vibration levels at driver interfaces over the operating range of the powertrain.
   - Set powertrain system and component-level targets:
     - Set targets for powertrain components based on the vehicle requirements.
     - Vehicle body transfer functions are utilised to calculate system source and isolation requirements.
     - Component targets allow for systems to be developed without the need for a vehicle, which is very important for external suppliers and keeping development costs low.
2. Development and design of components
   - Mathematical and CAE tools are used to develop components.
   - Experimental tests are run on a rig or a prototype vehicle.
3. Verification
   - Confirmation tests are run to show that the system meets the targets. They are usually experimentally verified on the vehicle.

Component noise and vibration targets need to be defined as objective measurements so that mathematical analysis and experimental analysis can be carried out interchangeably. Objective targets also allow for clear verification results so that pass/fail criteria can be based on an objective measurement.

12.2.3 Measurement methods

To assess the noise and vibration refinement of the vehicle's powertrain, measurements need to be made across the range of operating conditions. Run-up sweeps are performed by ramping up the engine speed over a short period of time, thus covering a range of operating conditions in one measurement set. The run-up sweeps can be performed at low load and repeated at full load to further extend the range of operating conditions. If the engine speed is recorded at the same time as the noise and vibration signals, then a spectral order map can be generated for the run-up sweep as shown in Fig. 12.1. An *order* is defined as a harmonic corresponding to the rotational speed of the engine. For run-up sweeps, orders are a useful alternative to frequency measured in hertz, since engine forces are synchronised to the rotating speed of the engine. To calculate the frequency of the Nth order at a particular engine speed, Equation 12.1 is used:

$$\text{Frequency of the } N\text{th order (Hz)} = N \times \text{rotational speed (rpm)}/60 \text{ (seconds)} \tag{12.1}$$
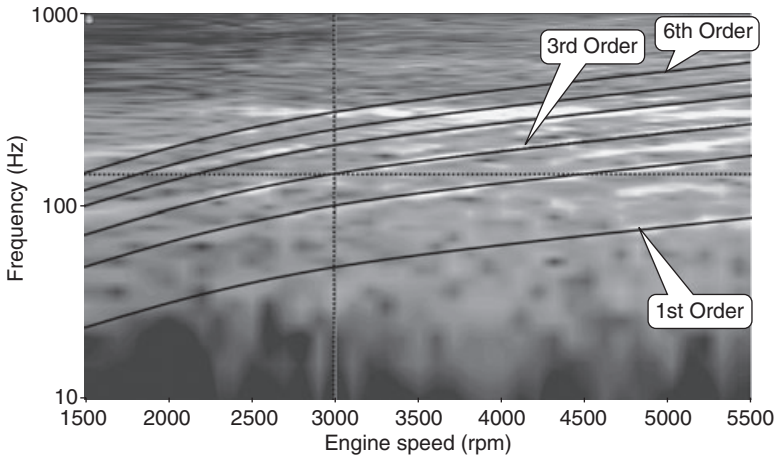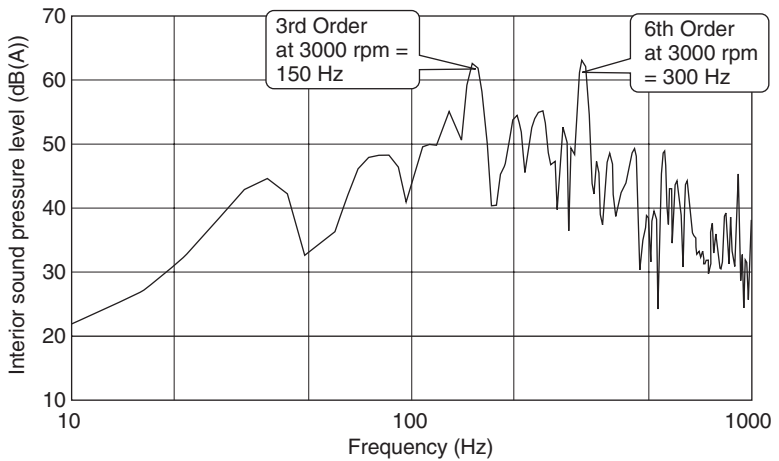
12.1 (a) A spectral order map, and (b) a 3000 rpm spectral cut for interior sound pressure level during a full-load run-up sweep.

For example, a V6 engine running at 3000 rpm has a first-order frequency of 50 Hz and a third-order frequency (engine firing rate) of 150 Hz (see Fig. 12.1).

The *spectral order map* consists of the computed spectrum at each engine speed increment during the run-up sweep. Overlaid on the diagram are order lines that indicate harmonics of the engine rotational speed at each engine speed increment. A high level of noise at a constant frequency in the spectral order map is indicative of a resonance in the system (evident as visible horizontal bands in Fig. 12.1). When the engine speed sweeps through a resonance and the engine forces excite it, we get a resulting

increase response in noise level. This response can create that unexpected noise that can alert the driver that his or her new car is not a quality engineered car after all.

Whether noise and vibration development is to be carried out experimentally or by computer-aided mathematical analysis, the use of run-up sweeps and order tracking for powertrain measurements is a fundamental tool. However, if a particular problem has been identified at a steady operating speed and load, steady-state measurements can also be taken and the narrowband FFT calculated for analysis.

12.2.4 Acquiring engine speed

For experimental measurements, an engine speed signal is necessary to perform order tracking of the noise and vibration data. Engine speed is acquired using an engine tachometer. Alternative tachometers available for order tracking include:

- Optical tachometers. These typically require a reflective mark placed on the crankshaft. They can be the most precise, and can also be used to provide a phase signal. However, they can take the technician some time to install and set up on a vehicle.
- The engine management tachometer signal used by the engine computer can sometimes be tapped into (if you know how) but it might not be very accurate.
- Vehicle data bus tachometers. These generate an engine speed pulse from the vehicle's data bus (e.g. CAN) and are convenient to use since they are simple to plug into the connector under the steering wheel. The downside is that they generate an artificial signal to replicate the engine speed and thus cannot be used for phase measurements.

Order tracking measurements are commonly referenced to the engine speed, since engine forces generate many vehicle noise and vibration problems. However, when working on transmission or driveshaft problems, it makes sense to refer orders back to the transmission or driveshaft speed. In this case, you will need a tachometer that measures driveshaft speed rather than engine speed. As an alternative, some analysis software allows the application of a multiplier to the engine tachometer to derive another tachometer signal.

12.3   Powertrain noise sources and paths

12.3.1 Source, path and receiver model

The focus of this section is primarily on how to integrate the powertrain system into the vehicle. This is presented by identifying the sources of

vibration from each powertrain subsystem and the airborne and structure-borne paths of each into the vehicle.

The source/path/receiver model of noise and vibration is a powerful concept in engineering powertrain refinement. This fundamental concept is used in the target setting process, and extends into the development of vehicles and as a tool in the analysis of noise and vibration problems. Figure 12.2
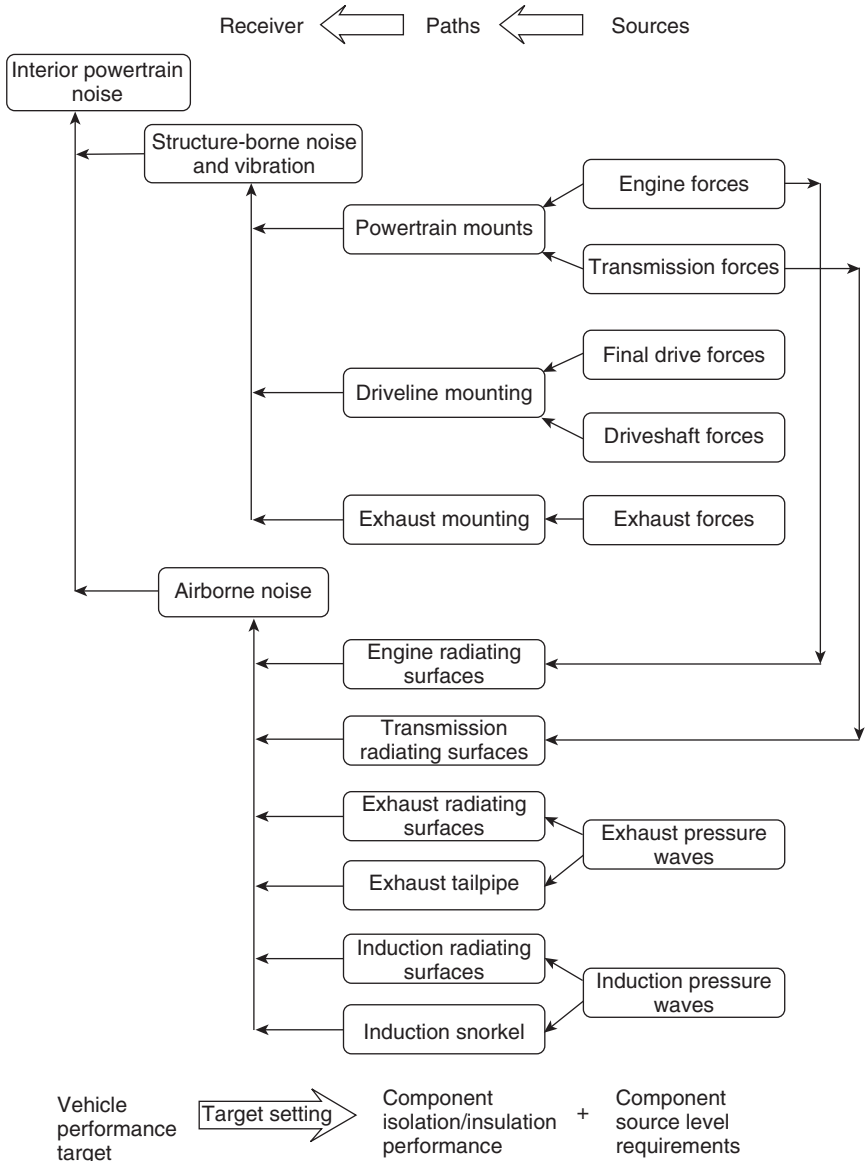
12.2 Simplified powertrain noise source/path/receiver model.

Table 12.1 Definition of frequency ranges

Term	Frequency range	Typical sensation
Low-frequency	Sub-firing frequency range, typically <20 Hz	Vibration – shake Noise – inaudible
Mid-frequency	Firing frequency range (idle to red line), typically 20–400 Hz	Vibration – roughness, harshness Noise – boom, moan
High-frequency	Super-firing frequency range, typically >400 Hz	Vibration – tingling Noise – whine, whistle

presents a simplified diagram of some powertrain noise and vibration sources, and their paths to the receiver inside the vehicle.

12.3.2 Noise sources

Table 12.1 provides the definitions of low, mid and high frequency ranges relating to powertrain noise and vibration used in this chapter. Table 12.2 is a summary of the sources of forces produced by the powertrain systems (refer to Eshleman (2002) and Wowk (1991) for further examples relating to general rotating machinery). Included in the table is a guide to the frequency range of forces, and this information will be used later in this section to assist in developing a vehicle mode map to ensure that vehicle and system response modes are well separated from excitation forces.

The mechanical structure of the powertrain systems will have vibration modes (natural resonances) that are likely to be excited by the powertrain forces described in Table 12.2, or in some cases from other inputs such as a rough road or wheel imbalance. Table 12.3 lists some significant powertrain system modes that must be managed to ensure adequate refinement of a passenger vehicle.

In setting the design parameters in order to minimise the source and amplification of powertrain forces for a future model vehicle, the source excitation frequencies should be kept separated from the powertrain modes where possible. By combining the information of the source forces in Table 12.2 and the system mode responses in Table 12.3, a mode placement map can be produced. Figure 12.3 shows an example of a powertrain mode placement map for a typical passenger car vehicle.

12.3.3 Noise paths

Table 12.4 lists the typical path of the powertrain forces into the vehicle. An airborne path refers to noise radiated from the powertrain components

Table 12.2 Sources of powertrain noise and vibration

Component	Direction of force	Excitation frequency	Low-frequency range	Mid-frequency range	High-frequency range
IC engine					
Engine rotating unbalance	Translational	First-order shake/vibration	×		
Engine reciprocating unbalance/unbalanced inertial forces	Translational	First-order and harmonics (dependent on cylinder configuration)	×	×	
Engine reciprocating unbalance/unbalanced moments	Moment	Nth order and harmonics (dependent on cylinder configuration)	×	×	
Engine reciprocating unbalance/inertial torques	Torsional	Nth order and harmonics (dependent on cylinder configuration)	×	×	
Combustion gas pressure	Torsional	Firing order (and harmonics)		×	×
Combustion gas pressure – random misfire component	Torsional	Broadband	×		
Combustion gas pressure – driver commanded step-input	Torsional	Broadband	×		
Engine combustion noise	Translational	Broadband			×
Fuel injector and valve train	Translational	Broadband			×
Forced induction pumps (turbo or superchargers)	Translational	Blade pass frequency			×
Engine accessories	Multiple	Pulley ratio and vane/blade/pole passing		×	×

Table 12.2 Continued

Component	Direction of force	Excitation frequency	Low-frequency range	Mid-frequency range	High-frequency range
Transmission					
Transmission gear whine	Multiple	Gear tooth meshing frequency (= shaft speed × number of teeth)			×
Driveline					
Coupling misalignment	Multiple	Shaft speed (and harmonics)	×	×	
Driveline imbalance	Translational	Shaft speed	×	×	
Final drive module gear whine	Multiple	Gear tooth meshing frequency (= shaft speed × number of teeth)		×	×
Exhaust and induction					
Exhaust noise	Wave	Firing order (and harmonics)		×	
Flow induced noise	Wave	Broadband			×
Induction noise	Wave	Firing order (and harmonics)		×	

Table 12.3 System-level structural vibration modes

Powertrain mode	Mode type	Low-frequency range	Mid-frequency range	High-frequency range
Powertrain mounting	Rigid body	×		
Driveline/ propshaft	Rigid body	×		
Driveline surge	First elastic torsional	×		
Exhaust flexural	Elastic bending		×	
Final drive module (FDM) mounting	Rigid body		×	
Driveline bending	First elastic bending		×	
Gear rattle	Second elastic torsional		×	
Gear whine	Third elastic torsional			×

into the surrounding air that can find its way into the cabin unless it is sufficiently insulated. Structure-borne paths refer to forces transmitted directly into the vehicle body where they can directly generate noise and vibration of the vehicle. The structure-borne paths are usually isolated by elastomeric mountings to minimise force input into the vehicle structure. Development of a future model vehicle involves setting suitable specifications for insulating and isolating each of these paths.

12.3.4 Noise receiver

The noise receiver of interest is usually the occupants inside the vehicle cabin. The reader is directed to Chapter 13 for a description of the sound propagation characteristics inside the cabin.

12.4   Enablers and applications

12.4.1 Internal combustion engine

This section discusses the key powertrain subsystems and the design factors that influence noise and vibration refinement. The powertrain subsystems covered include the engine, transmission, driveline, induction and exhaust
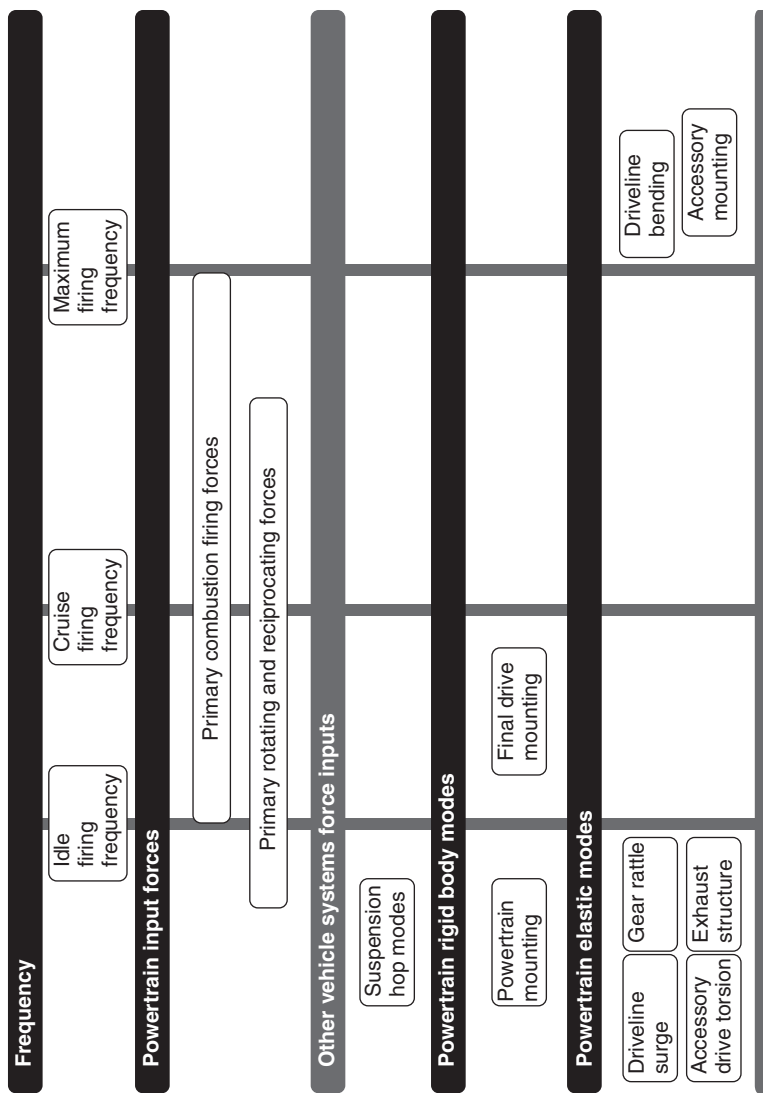
12.3 Target setting mode placement map.

Table 12.4 Paths for each powertrain source

Noise source	Airborne path	Structure-borne path
IC engine		
Engine rotating unbalance		Engine and transmission mounting
Engine reciprocating unbalance/ unbalanced inertial forces		Engine and transmission mounting
Engine reciprocating unbalance/ unbalanced moments		Engine and transmission mounting
Engine reciprocating unbalance/ inertial torques		Engine and transmission mounting
Combustion gas pressure		Engine and transmission mounting
		Exhaust mounting
		Driveline and axle mounting
Combustion gas pressure – random misfire component		Engine and transmission mounting
Combustion gas pressure – driver commanded step-input	Engine and transmission	Engine and transmission mounting
	Driveline and axle	Driveline and axle mounting
Engine combustion noise	Engine block and covers	Engine and transmission mounting
		Exhaust mounting
		Driveline and axle mounting
Fuel injector and valve train	Engine block and covers	
Forced induction pumps (turbo or superchargers)	Induction inlet Induction ducts	
Engine accessories	Accessories housing	Engine and transmission mounting
	Brackets	
Transmission		
Transmission gear whine	Transmission housing	Engine and transmission mounting
		Driveline and axle mounting
Driveline		
Coupling misalignment		Driveline and axle mounting
Driveline imbalance		Driveline and axle mounting
Final drive module gear whine		Driveline and axle mounting
Exhaust and induction		
Exhaust noise	Exhaust tailpipe	Exhaust mounting
	Muffler shells	Engine and transmission mounting
Flow-induced noise	Exhaust tailpipe	
Induction noise	Induction inlet	Induction mounting

© Woodhead Publishing Limited, 2010

systems. Countermeasures or enablers to aid in refinement are introduced for each subsystem, and their use is explained with examples.

The reciprocating four-stroke internal combustion engine is the class of engine installed in the majority of today's gasoline and diesel passenger cars. Not surprisingly, the reciprocating engine is a significant generator of forces that need to be managed systematically to avoid any unexpected noises that might upset the owner of a new car.

Forces generated by the rotating crankshaft and forces generated by the reciprocating motion of the pistons generate vibration loads that are proportional in amplitude and frequency to the engine speed. These forces are generated in all directions (translation, moments and torsion) and vary depending upon the number of cylinders, the configuration of the engine, and the mass and inertia of the reciprocating components. To counteract some of these forces, additional balance weights can be applied to the crankshaft. One noticeable exception is that the reciprocating force generated by a four-cylinder in-line engine require balance shafts (however, to save costs, balance shafts are often not included in the design of engines smaller than 2 litres displacement). Table 12.5 provides a summary of the forces and methods used to counterbalance the forces. Refer to Rao (1986) for derivation of the unbalance forces and Bosch (1986) for a summary of the magnitudes.

The valve train also generates inertial imbalance forces as the engine rotates. For example, the rotating cam lobes on the camshaft can induce an unbalance moment, but these are generally not a significant concern.

The combustion gas pressure forces that act on the piston during firing generate a significant torsional vibration in the crankshaft. This is due to increase in rotational speed of the crankshaft during each downward expansion stroke of the pistons. While the frequency of the gas forces is dependent on the engine speed, the amplitude of the torsional moment is proportional to the torque or load output of the engine. Table 12.6 shows the periodic torsional moments due to engine combustion for various cylinder configurations.

In addition to the periodic combustion gas forces, Table 12.6 also shows that additional forces can be generated due to irregularities in the combustion process. These irregularities can be periodic or random in nature depending upon what is causing them.

The low and midfrequency forces generated by the rotating and reciprocating motion of the engine are capable of exciting the vibration modes of engine components, so they must be designed to avoid resonances in the engine operating range. Significant considerations include:

• Frequency of the first bending mode of the engine block and transmission. Besides driving targets for engine block and transmission casing

Table 12.5 Engine configuration and reciprocating imbalance forces

Engine configuration	First-order force	First-order moment	Second-order force	Second-order moment	Counterbalancing
Inline four-cylinder	0	0	Yes	0	Second-order requires counter-rotating balance shafts
Inline six-cylinder	0	0	0	0	Not required
V6 cylinder with 60° bank angle	0	Yes	0	Yes	First-order requires additional crank balancing Second-order requires balance shaft
V6 cylinder with 90° bank angle	0	Yes	0	Yes	First-order requires crankshaft balancing and balance shaft Second-order requires balance shaft
V8 cylinder with 90° bank angle	0	Yes	0	0	First-order requires additional crank balancing

Table 12.6 Engine configuration and combustion gas torque forces

Engine configuration	0.5 order	1.5 order	2 order	3 order	4 order
Inline four-cylinder	Single cylinder variation		Primary		Harmonic
Inline six-cylinder	Single cylinder variation			Primary	
V6 cylinder with 60° bank angle	Single cylinder variation	Bank-to-bank variation		Primary	
V6 cylinder with 90° bank angle	Single cylinder variation	Bank-to-bank variation		Primary	
V8 cylinder with 90° bank angle	Single cylinder variation		Bank-to-bank variation		Primary

stiffness, the bolted joint between the two must also be sufficiently stiff to ensure the whole system meets it target.

- Frequency of the first torsion mode and bending mode of the crankshaft. The crankshaft modes are susceptible to being excited to the gas pressure loads. Tuned crank pulley dampers are often used as a countermeasure.
- Frequency of the bending modes of the engine mounting brackets. Since the engine forces are reacted through the engine mounting system, any amplification of engine vibrations by brackets in resonance must be avoided (refer to the later discussion on engine mounting).

Besides the significant low and mid-frequency vibrations generated by the rotation and combustion forces of the engine, there are high frequency sources of noise that affect the sound quality of the engine. The combustion wavefront within the cylinder generates high frequency pressure pulses that are audible as high frequency noise. The level of combustion noise produced is proportional to the rate of pressure rise during combustion. Figure 12.4 shows a comparison of cylinder pressures during combustion in typical gasoline and diesel engines. Diesel compression ignition engines have a more abrupt explosive combustion process than spark ignition gasoline engines, and so have a noisier and higher frequency content. The higher cylinder pressures in diesel engines also result in high potential for piston knocking in the cylinder clearances.
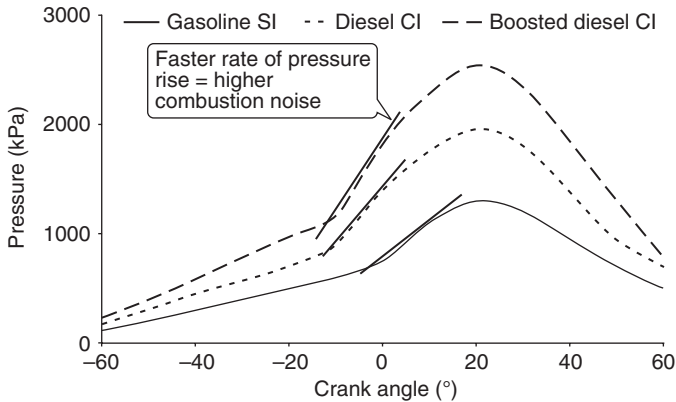
12.4 Cylinder pressure comparison.

Impacts during operation of the valve train also contribute to high frequency tapping noises, and timing chain or gears are also sources of high frequency noise within the engine.

Sources of high frequency noise are often transmitted as airborne noise radiated from the engine surfaces. Most airborne noise is radiated from the large thin panels on the engine. These can include cam covers, front cover, inlet manifolds, oil pan, exhaust pipes and heat shields. The best noise reduction countermeasure is to provide isolation of these surfaces. Where a soft isolating joint is not acceptable, other treatments include ribbing, dished concave/convex surfaces, laminated layers, and exterior acoustic covers.

Examples of countermeasures applied for airborne noise include:

- Isolation of the crank pulley to the crankshaft. The crank pulley can radiate combustion noise because it is directly mounted on the crankshaft. Radiated noise can be minimised by isolation and designing spokes instead of a flat disc hub.
- Laminated heat shields on the exhaust manifold. Plain steel heat shields mounted directly on the exhaust system are efficient radiators of noise. Due to the high temperatures, it is not practical to design an isolated connection. Choosing a multi-layer material that sounds dead due to internal damping is a common method of noise reduction.
- Acoustic cover over the inlet manifold. Inlet manifolds often have comparatively thin walls with large surface areas and also act as efficient radiators of noise. A separate, acoustically treated cover placed over the engine is often used to absorb the radiated noise.

Engine mounts are the key defence in isolating engine forces from the vehicle structure, whilst also performing the key function of restraining the

engine in the engine bay. Although they may often appear very simple devices, the design and placement of the mounts need to be very carefully optimised in order to achieve satisfactory refinement. In order to achieve the best isolation from engine vibrations, the rigid body mounting modal frequencies of the mount system need to be set very low. But soft mounts must be sufficiently durable for the life of the vehicle, as well as acting to control the motion of the engine to prevent it from colliding into anything housed in the engine bay.

The design considerations for engine mounting, whether front wheel drive (FWD) or rear wheel drive (RWD), are covered in the following steps:

- The first consideration is to target the roll frequency of the engine. The rate of the mounts must be soft enough to isolate the low frequency torsional vibrations from the engine. In normal operation of the vehicle, the lowest frequency vibration of concern is at idle engine speed. Thus the rate of the mounts is chosen to provide a rigid body modal frequency in the roll direction (torque reaction of the engine) much lower than the engine firing frequency at idle.
- The second consideration is to ensure the bounce frequency of the engine is separated from the vehicle suspension vertical (hop) modes. It normally follows that if the roll frequency is quite low (approximately 10 Hz), then the bounce frequency will also be quite low. Humans are sensitive to low frequencies, and should the road input excite the engine into bounce, the ride quality of the vehicle can be seriously compromised. So the desire is to separate the bounce mode of the engine from the hop modes of the suspension. On modern cars this often is not enough, and hydraulically damped engine mounts are used to control engine bounce. The maximum hydraulic damping is normally specified to match the bounce frequency of either the engine or vehicle suspension.
- Designing separation (decoupling) of all rigid body engine modes. This ensures that engine or road inputs do not generate excessive motion of the engine in any direction (e.g. suspension vertical input must not excite the engine in its pitching or bounce modes).
- Placement of mounts at nodes of the powertrain elastic bending mode. Transmission of mid-frequency vibrations can be minimised by placing mounts at the node position.
- Snubbers/progressive mount rates. The ideal requirement is to restrain engine roll under full load, but at the same time to maximise isolation. If the mount stiffness is too soft, mounts could bottom-out when the engine is under full load, causing harsh engine sound.
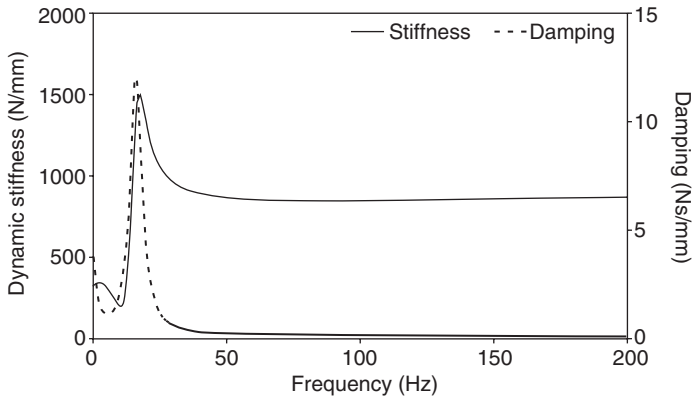
12.5 Hydraulic engine mount dynamic stiffness and damping.

- High frequency isolation is usually designed by targeting high stiffness of the mount brackets and supports. As a rule of thumb, the mounting system is targeted to provide 20 dB of isolation in high frequency vibration, and this is done by ensuring the dynamic bracket stiffness is at least 10 times the dynamic stiffness of the mounts.

Figure 12.5 shows an example of the dynamic stiffness and damping characteristics of a hydraulically damped engine mount. The hydraulic damping in this mount has been designed to reach a maximum at approximately 15 Hz to minimise bounce of the engine by having it tuned at the frequency of the vertical mode. The dynamic stiffness curve shows the typical behaviour of a hydraulic engine mount. Dynamic stiffness is often at a minimum prior to the peak damping frequency, and reaches a maximum just above the peak damping frequency. A drawback of the hydraulic engine mount is that it also behaves dynamically stiffer at mid- to high frequencies compared to a simple rubber elastomer mount, and so there is a loss in isolation performance of the engine mounting system. An emerging trend is to use actively controlled engine mounts to switch the hydraulic damping off at idle to enable a smooth and refined idle sound quality (there is no need for damping to restrain engine bounce when the vehicle is stationary).

12.4.2 Accessories

The engine in a passenger vehicle will typically be used to drive a series of accessories via a belt drive. The accessories include an alternator, an air-conditioning compressor and a hydraulic power steering pump. Quite

surprisingly these accessories can generate equivalent noise levels to the engine, especially under idle conditions. Thus it is important to have targets and strategies to minimise the noise component of the accessory systems.

Each individual accessory can generate its own particular noise source, but they are common in that the rotating components can generate an unbalance force in addition to a periodic operating force. For a vane power steering pump and reciprocating air-conditioning compressor, the periodic force is due to the pumping action of the fluid. For alternators, the periodic force is generated by the magnetic flux variation as the rotor passes the poles.

The accessory drive system is connected together by the drive belt. The belt drive system is tuned to avoid belt slippage that can generate an alarming squealing noise. Slippage can occur due to loss of tension in the belt, under high loads, or under high crankshaft torsional vibration. For example, starting or stopping the engine can cause slippage on the crank pulley and possibly excite the tensioner into resonance. Belt slippage will often occur at the alternator pulley because the alternator has the highest angular momentum of the accessories due to its high rotational speed. One solution is to make use of a one-way decoupling clutch on the pulley (King and Monahan 1999). This is effective but can be a costly solution.

The accessory drive system has torsional vibration modes, with the belt acting as the spring elements and the accessories as lumped inertias. The objective is to ensure that the first torsional mode is low enough in frequency that the engine will not excite it at idle. A crankshaft damper is often used to lower the torsional modal frequency of the accessory system.

Each of the accessories is bolted to the engine either directly or to a support bracket. In both cases, the objective is to ensure that the first bending frequency of the accessory mounting is sufficiently high to avoid being excited from either the engine or the accessory unbalanced forces. Normally a target based upon the maximum engine firing frequency is specified for these purposes. The bracket design must also ensure that belt alignment is accurate, and the surfaces are not efficient radiators of noise.

As a case study, we can consider the development of a mounting bracket stiffness target for an alternator mounted to a V6 engine. The desire is to ensure that the first modal frequency of the mounted alternator lies above the engine firing frequencies as well as above the rotating unbalanced frequencies of the alternator. Figure 12.6 shows that a Campbell diagram can be drawn to help establish the bracket modal frequency target. In this example, the V6 engine has an operating range to 6200 rpm, and the third-order combustion forces will have a limit of 310 Hz. Initially an alternator pulley ratio of 3.05:1 is chosen, and that results in the alternator imbalance forces reaching a maximum range of 315 Hz. However, a higher pulley ratio should be selected to avoid the potential of beating noise between the
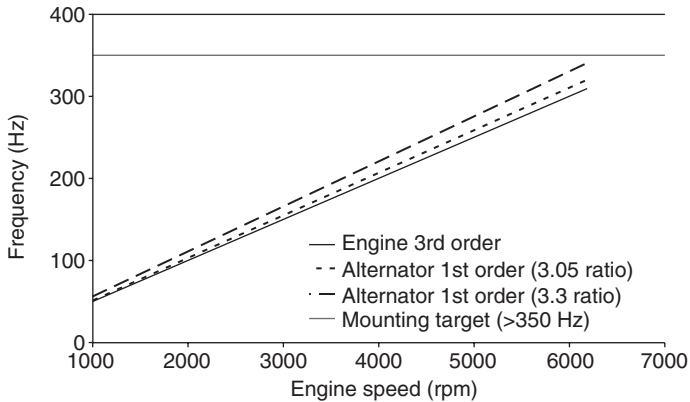
12.6 Campbell diagram for alternator mounting target.

engine firing frequency and alternator imbalance. For a pulley ratio of 3.3:1, the maximum frequency from alternator imbalance increased to 341 Hz. Thus the design target for the alternator mounting modal frequency was set at greater than 350 Hz (incorporating a margin of approximately 10 Hz in this example).

12.4.3 Manual transmissions

While the gear sets in a transmission are carefully optimised to minimise sources of noise by the manufacturer, the vehicle platform engineer must carefully consider the successful integration of the transmission into the vehicle system. Often there are many arguments about who is to blame for gear whine in a new model vehicle: when the transmission manufacturer is summoned to fix the transmission, he may instead point towards weaknesses of the installation in the vehicle as the contributor.

The gear sets in a transmission are helical-cut to minimise generation of gear noise, which normally manifests itself as a whine during run-up or run-down. The manufacturer will do his best to ensure smooth engagement of gear teeth to minimise forces and will design a stiff casing to minimise radiated noise. Structure-borne whine can be minimised by following good mounting practices to the body, using stiff brackets and soft isolators (refer to Section 12.4.1 on engine mounting). Gear whine structure-borne paths can also include the driveshafts and the shifter linkage.

Gear rattle is a phenomenon that plagues manual transmissions. Under situations of high torsional vibration from the engine, the variation in rotational speed of the input shaft can cause clashing of teeth between mating pairs, causing a disturbing rattling noise. The transmission manufacturer will remind you that a balance needs to be struck between the amount of

gear lash required for economical production, and the tighter requirements on lash to minimise rattle. So in the end, it comes down to minimising source levels of torsional vibration from the engine and providing good isolation of the noise transfer paths.

The flywheel and clutch are your allies in controlling engine torsional vibration inputs into the transmission. The inertia of the flywheel assists in smoothing engine torque, but a good balance needs to be made with engine responsiveness. The damping springs in the clutch plate are tuned to assist in torsional isolation. In some instances, frictional damping in the damping springs can be applied to overcome low frequency induced gear rattle, but needs to be treated with caution to ensure there is no noticeable degradation in high-frequency isolation. The dual mass flywheel is a recent invention that has been used to lower the torsional modal frequency associated with gear rattle to a frequency well below the idle speed of the engine (Wolfgang 1990).

12.4.4 Automatic transmissions

In many parts of the world, automatic transmissions have almost completely penetrated the automotive market. In some respects this is a blessing to noise and vibration engineers because the torque converter in its slipping state provides isolation of the torsional vibrations from the engine crankshaft. Torsional vibration problems on manual transmissions such as gear rattle and driveline resonances are unheard of in automatics running in the unlocked state. But unfortunately the torque converter does not always operate in the unlocked state. When the clutches lock up the torque converter there is a loss of isolation to the engine. The locked state is normally restricted to light cruise loads where engine combustion torque is near its minimum.

To further achieve the fuel economy benefits of a locked converter, electronic controlled slip has been adopted to enable some degree of torsional isolation from the engine. With a controlled amount of slip (typically 20 to 80 rpm) full isolation can be maintained. The noise and vibration engineer will need to work with the transmission calibration engineer to determine minimum acceptable levels of slip for good noise and vibration refinement. The transmission calibration engineer must ensure that this minimum level of slip is carefully controlled so as not to lose slip speed, especially under change in engine torque commanded by the driver. More discussion on the challenges of the increasing use of a locked torque converter is covered in Section 12.5.

Figure 12.7 shows an example of the torsional vibration isolation of an unlocked torque converter compared to a fully locked torque converter. For comparison there is also a plot of torsional vibration transmitted by a
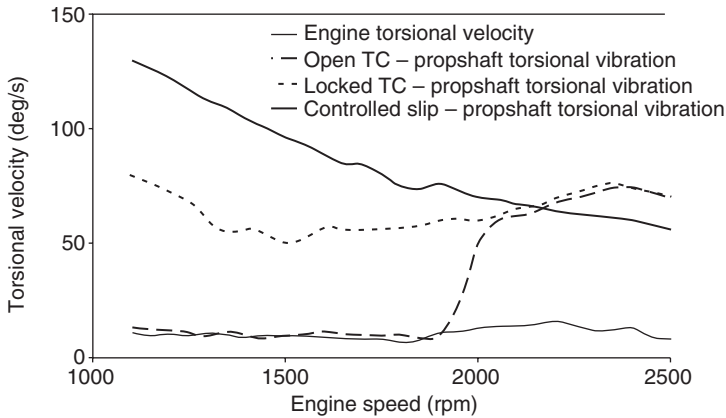
12.7 Driveline torsional vibration comparison between a locked, an unlocked and a controlled slip torque converter.

torque converter running electronically controlled slip up to 1900 rpm, whereafter the torque converter goes into the fully locked state. The chart shows how effective controlled slip can be in reducing torsional vibration from the engine.

12.4.5 Driveline

Many newcomers to automotive engineering find it surprising that the vehicle driveline can generate many noise and vibration challenges. Like every other powertrain subsystem, the driveline can generate sources of vibration, have influence on powertrain system modes, as well as act as structure-borne paths.

In this chapter, the *driveshaft* is defined as the shaft that connects the final drive module to the wheels, and the *propshaft* as the shaft that connects the transmission to the final drive module in RWD vehicles. The levels of imbalance are more critical on propshafts, since propshafts rotate faster than driveshafts. For example, if we assume a final drive ratio of 3:1, then the imbalance force generated for the same out-of-balance mass will be nine times greater on the propshaft compared to the driveshafts. This drives the need for tighter requirements for residual imbalance and radial run-out for propshafts. Radial runout can often account for the majority of imbalance forces generated and the solution is to ensure the propshaft stays straight and centred. Bolted joints require a spigot for guidance, and if splined joints are used they need to be tight to ensure the torque load does not drive the propshaft up the splines.

The couplings at each end of a driveshaft are also a significant source of vibration if not properly designed. The couplings are designed to enable

transmission of torque through an angular misalignment to account for relative movement between the driveline and suspension. Constant-velocity couplings are exclusively used on driveshafts because of the large excursion of angles encountered during operation but come at a cost because of their complexity. In situations where the angular misalignment is less than 1° on a propshaft, a universal joint might be used to keep costs down. However, universal joints are not constant-velocity and this means that the shaft output speed will vary in proportional to the angle across it and generate a second-order torque, so it is important to note that universal joints are only suitable for driving across small angles if good noise and vibration refinement is required.

A long propshaft will need to be designed as two or more sections of tube to avoid whirling or bending at high vehicle speeds. A multi-tube propshaft will require support bearings placed next to the centre joints. A propshaft support bearing will be rubber mounted to isolate it from the vehicle body. In order to minimise the path of high frequency vibrations transmitted from the engine, support bearings with low natural frequencies and low damping are desirable. However, the low-frequency bounce mode of the propshaft can be excited if the sources of vibration mentioned above are not controlled adequately.

The final drive module houses the final gear set and differential. In FWD vehicles it is incorporated into the transmission, and on RWD vehicles it is mounted at the rear of the vehicle. The gear set in a final drive module is a source of gear whine, particularly noticeable under light loads. This is because a hypoid gear tooth profile is used on the crown and pinion gears, and under low loads, and hypoid gears tend to have higher transmission errors.

The housing of the final drive module has traditionally been cast from iron. One of the benefits of iron is that the thermal expansion of the housing matches the gear sets, thus minimising gear tooth transmission meshing error as the temperature of the module varies. But a cast iron final drive module is very heavy and has become a target for vehicle mass reduction. Aluminium housings are now used extensively but suffer from potentially higher levels of gear whine due to thermal expansion in operation.

Sometimes RWD final drive modules are directly mounted on the vehicle's rear suspension sub-frame, but this provides poor isolation of mid- to high frequency vibration such as gear whine. Conversely, the module can be mounted on rubber isolators but needs careful management of rigid body modes to ensure that modes are not excited by the driveline imbalance forces.

Figure 12.3 presented some elastic modes that are associated with the engine–transmission–driveline system. Figure 12.8 provides an indication of the elastic torsional mode deflection shapes of the driveline system.
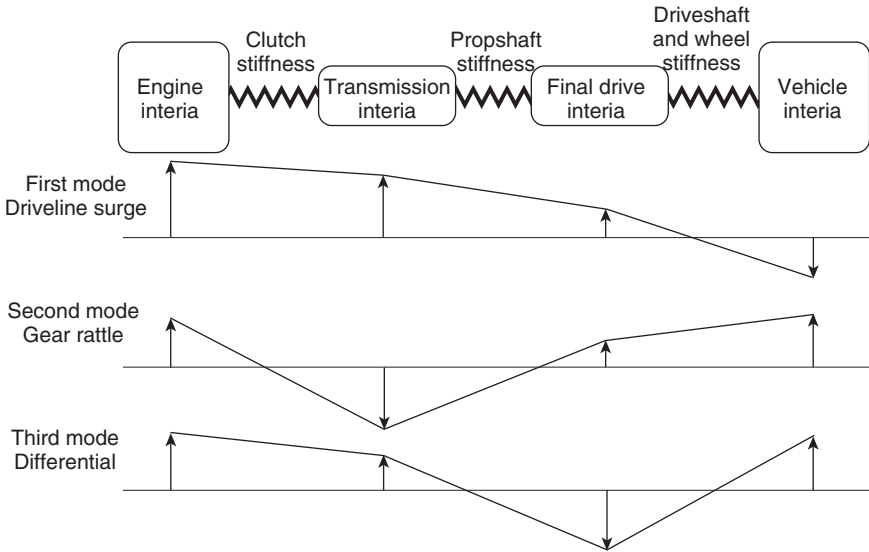
12.8 Driveline torsional mode shapes.

The first torsional elastic mode of the driveline system is referred to as the *driveline surge mode*. The surge mode is felt as a longitudinal surge or jerk by the driver as he rapidly steps on or off the throttle pedal and the engine produces a rapid change in torque. This broadband excitation provides the source input to excite the low frequency mode. Figure 12.8 shows that the torsional stiffness of the driveline and the inertia of the vehicle are the controlling parameters of the mode. In a manual transmission, it is very difficult to dampen this mode, and the mode is usually avoided by tuning the engine calibration to reduce the rate of torque change when commanded by a throttle input from the driver. The driveline surge mode can cause audible clunks in the driveline system at locations where there is mechanical lash. An example is from the clashing of gear teeth in the transmission or differential. In the case of an automatic transmission, this mode is reduced by the isolation provided by an unlocked torque converter.

The second torsional mode of the driveline is often associated with gear rattle in manual transmissions. This is because the gear sets are at the location of an anti-node or maximum torsional velocity. The torsional velocity fluctuations in the gears cause clashing of the gear teeth that creates a rattling noise. Refer back to the discussion in Section 12.4.3 on methods used to control gear rattle.

Higher torsional modes of the driveline can amplify whine from the final drive gear set. In this case, high frequency vibrations from the tooth meshing can excite this mode and amplify gear whine. The mass of the differential

crown and pinion gears and the axle shaft stiffness are controlling properties of the mode.

Apart from torsional modes of the driveline, there are also bending modes. The first bending mode of the driveline is in the mid-frequency range and can be excited by reciprocating or rotating imbalance forces from the engine. It is often the cause of a booming noise inside the vehicle at a given engine speed. Refer to the discussion on engine mounting in Section 12.4.1 on placement of the engine mounts at the node points in order to minimise the transfer path of the noise into the body.

12.4.6 Induction

The induction and exhaust system generate a significant proportion of noise from the powertrain when the engine is operating under high load. In addition to managing the resonances or transfer paths that can generate unwanted noises, the induction noise sound quality can be tuned to give the car the desired character.

The source of induction noise is the airborne pressure pulses generated when the engine inlet valves shut. Since this occurs at the same rate as engine combustion, the induction noise has a primary frequency the same as the engine firing order. Harmonic content depends upon the speed of the inlet valve closure, and is affected by acoustic tuning or resonances of the inlet manifold and runners. To achieve a smooth and refined character of induction noise, it is desirable to have a primary order that increases linearly with engine speed and less contribution from the harmonic orders. On the other hand, a sporty note requires tuning of the system to achieve a modulated combination of the harmonic orders.

The induction noise is very dependent upon the position of the throttle blade valve in a gasoline engine. Induction noise is most prominent when the throttle valve is open and the engine under high load. When the throttle valve is nearly closed, it reflects the pressure pulses back to the engine, and induction noise is reduced (except for any whistles generated by the high velocity air flowing past any sharp edges near the throttle blade). This makes induction noise very apparent to the driver as he accelerates, and hence this is key to providing the character that the vehicle portrays.

The induction pressure pulses are radiated as airborne noise at the mouth of the induction system. The amplitude and frequency content of the noise emanating from the mouth is a function of the acoustic properties of the ducts and expansion chambers incorporated into the induction system. Standing waves, and hence potential boom noises, are dependent upon the length of the ducting and runners in the system. It has become usual practice to reduce the standing waves that cause problems by incorporating reactive resonators. An expansion chamber is incorporated into most

designs in the guise of the air filter box. Although the primary function is to house the filter element, the filter box is a large expansion chamber that assists in broad attenuation of the induction noise. A rule of thumb in designing the filter box is to package a volume of three times the engine capacity.

Tuned reactive resonators such as quarter-wave or Helmholtz resonators are also commonly employed to attenuate noise at specific frequencies that may cause excessive interior or exterior noise. They are incorporated as branches connected to the induction ducts.

Airborne noise can also be radiated from walls of the induction system components. The filter box is generally the most susceptible due to its large and flat thin walls. By incorporating ribbing, the filter box walls should be designed so that the panel modes are above the primary excitation frequency of the induction system. Likewise, induction and engine noise can be readily radiated from the inlet manifold system, since this also usually incorporates large flat surfaces.

The filter box and ducting should be isolated from the vehicle body to ensure that there are no structure-borne paths of the system into the vehicle body.

Figure 12.9 provides an example of the contribution of the induction system noise inside the vehicle during a wide-open-throttle run-up. A common experimental technique is to fit an additional large muffler to the induction system in order to silence it, and repeat the run-up measurements. The result in Fig. 12.9 clearly demonstrates that the peaks in noise
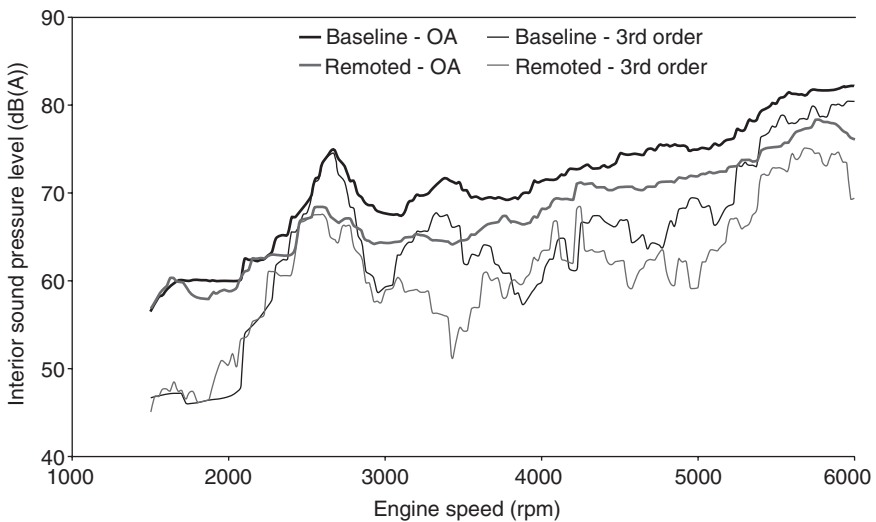
12.9 V6 induction noise measured during a full-load run-up and compared with the induction system silenced.

levels at 2500 rpm and 3200 rpm are associated with noise from the vehicle's induction system.

12.4.7 Exhaust

The level and character of the noise from the exhaust system has a significant effect on the perceived powertrain refinement of the vehicle. As such, a set of well-defined targets is usually established very early in the development of a new vehicle.

The contributors to exhaust sound quality are:

- Low frequency vibration modes of the exhaust system creating structure-borne booms
- Mid-frequency airborne noise from the tailpipe
- Mid-frequency airborne noise radiated from the muffler shells and pipes
- High frequency rush/hiss of the exhaust gas exiting the tailpipe.

In addition to meeting the above sound quality objectives, the exhaust system design must meet government exterior noise regulations and opposing powertrain performance requirements.

Tailpipe noise is generated from the exhaust gas pulses leaving the engine. The primary frequency is at the firing frequency of the engine and it also contains harmonics. Where pipe lengths may be uneven between cylinder banks, or uneven firing occurs, half-orders can also be generated. The crudest method to reduce tailpipe noise is to put a restriction in the exhaust system, but this significantly affects back-pressure and leads to an unacceptable loss of engine power. As a rule of thumb, a 5 kPa increase in back-pressure can result in a 1% loss in engine peak power. Thus a series of reactive and absorptive muffler elements are used to control exhaust tailpipe noise.

Reactive mufflers are designed with the principle of using reflection to change the phase of waves and resultant attenuation due to phase cancellation. Reactive mufflers consist of combinations of reactive tuning elements, including expansion chambers, quarter-wave resonators and Helmholtz resonators. It is important that a reactive muffler be positioned at an anti-node point in order for it to function optimally. Table 12.7 provides a guide for the total muffler volume required to reduce exhaust noise to an acceptable level.

Resistive mufflers make use of absorption to reduce noise. Thus resistive mufflers are useful for reducing broadband noise, and are more effective at reducing high frequency noise compared to reactive mufflers. They can generally be located in any position in the exhaust system because the absorption process is relatively independent of phase. Typical porous materials used in mufflers include fibreglass roving or stainless steel mesh. A

Table 12.7 Estimate for total muffler volume

Vehicle class	Four-cylinder engine	Six-cylinder engine	Eight-cylinder engine
Sporty car	Four times engine displacement	Three times engine displacement	Three times engine displacement
Quiet car	Ten times engine displacement	Seven times engine displacement	Six times engine displacement
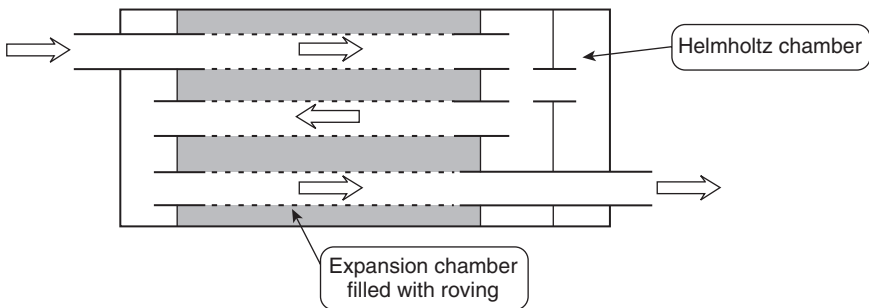
12.10 Tri-flow muffler layout.

higher density of absorber means better acoustic performance; however, this comes at a cost of increased weight and cost.

A tri-flow muffler is typical of a muffler used on passenger vehicles (see Fig. 12.10). It is a combination of perforated tubes and chambers separated by baffles to dissipate and reflect the sound waves. It can contain all of the above methods to reduce noise in a single package.

Flow noise in exhaust systems is generated by turbulence in the high velocity gas flow. The noise is broadband in character, and is typically centred from 1 to 3 kHz. To avoid this problem, use a large diameter pipe to reduce gas velocity, and avoid sharp edges and bends to minimise flow disturbances.

Exhaust noise can be radiated from the walls of pipes and mufflers due to the high sound pressure levels in the exhaust gas. Pressed muffler shells that have ribbing to provide stiff surfaces are commonly used. Mufflers and exhaust pipes incorporating laminated layers are also commonly used in minimising radiated noise.

Since the exhaust system is constructed from long lengths of steel pipe with lumped masses attached (mufflers), bending modes of the exhaust system may cause severe problems because the long steel pipes act as springs with very little damping. These modes are in the low to mid-frequency range, and as chance has it, a mode will often be precariously

placed near the idle speed of the engine, causing an excessive level of boom and vibration. The most important action to minimise the transfer path of exhaust vibration is to ensure adequate isolation of the exhaust system from the body. The exhaust hanger brackets must be stiff and mounted to the body on an isolated frame or stiff section, and the rubber hangers should be as soft as possible to ensure good isolation.

Other countermeasures to minimise exhaust vibration include optimising the exhaust pipe stiffness (i.e., wall thickness or diameter, or bracing) to avoid bending modes near engine idle and cruising speeds. Flexible couplings are useful in isolating the exhaust system from the engine, as well as providing relative movement between exhaust and engine.

12.5   Future trends

12.5.1 Sound quality

To better differentiate a brand of motor car from its competitors, in the future vehicle manufacturers are more likely to make more use of sound quality engineering to produce a unique brand character. This section reviews new hardware designed to give manufacturers the tools they need to deliver a unique brand sound.

Future trends will affect the sophistication of exhaust systems and the sound quality requirements placed on them, and active exhaust tuning systems are becoming an important enabler for meeting sound quality objectives. An active exhaust system refers to a switch in exhaust tuning under driving conditions. A switchable exhaust can have one tuning for low engine speed or low load, and another tuning for high speed or high load, allowing for a reduction in back-pressure to reach engine performance targets (Hill 2002).

Typically referred to as a *semi-active system*, a spring-loaded flapper valve is a means of implementing switchable exhaust tuning. The valves are normally placed in the exhaust path inside a muffler. Under low load conditions, the valve remains shut and exhaust gas is routed through a path that provides maximum noise attenuation. As engine load and speed increase, the gas flow opens the valve, providing an alternative path for the exhaust gas and resulting in less noise attenuation and back-pressure. These semi-active valves are ideally suited to solving exhaust noise problems at low loads, such as idle boom or cruising exhaust boom.

Figure 12.11 shows an example of a semi-active valve in the left rear muffler of a passenger vehicle. In this case, the vehicle had a dual exhaust system with twin rear mufflers but suffered from an exhaust boom at idle. The incorporation of the valve in one of the mufflers increased back-pressure and considerably reduced the boom at idle. At higher engine
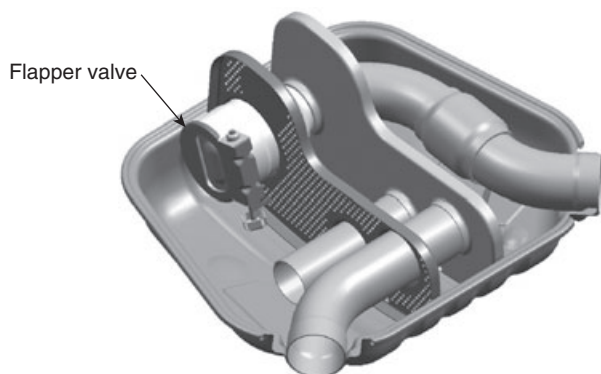
12.11 Muffler cutaway revealing a semi-active exhaust valve.

speeds, the light spring loading enabled the valve to open, and the exhaust functioned normally as a low back-pressure system and generated a purposeful exhaust note.

An *active system* is used to refer to an exhaust valve that can be commanded open or shut by the engine controller. This flexible control allows the point of exhaust tuning switchover to be precisely controlled, providing optimal noise performance as well as optimal engine performance. However, the drawback is the expense of these systems. Vacuum-operated valves are more reliable than electric valves due to the heat in the exhaust system, and this drives the added complexity of vacuum valves, lines and reservoirs to service the actuator.

Induction noise is an equally important key to providing a specific sound character. There is increasing use of turbochargers in sports cars, but a turbocharged system naturally has a quieter induction note than a normally aspirated engine. One approach to bring the excitement of induction noise back to a turbocharged engine is to utilise devices to enhance the induction noise. A device currently appearing on the market consists of a side branch in the induction system that terminates with a soft membrane. By tuning the length of the side branch and the stiffness properties of the membrane, a pleasing induction noise can be generated. In order to minimise exterior pass-by noise, the outlet from the membrane can be ducted directly into the cabin so that the induction noise is apparent to the occupants. A similar device has also been proposed to enhance exhaust noise (Wolf *et al.* 2003).

Lower costs of electronics and microprocessors will also have a role to play in tailoring vehicle noise and vibration character, despite limited applications at the moment. Active noise control (ANC) and active vibration control (AVC) can be considered as the epitome in tuned vibration absorber evolution.

The principle of an active control device is to produce a force or pressure out of phase with that from the powertrain to provide phase cancellation. Where the excitation is a structure-borne vibration, such as engine noise through the mounts, it makes sense to use a method of AVC. However, AVC may never become viable in the automotive market because the cost and mass of actuators to generate an opposing force can be high. One variation is to use a resonant spring–mass system to provide a high force output. For example, this method has been used inside engine mounts to generate a high opposing force, but has the limitation of providing a sufficient output only over a narrow frequency range (Lee and Rahbar 2005). The existing technology of switchable damping in hydraulic mounts will probably take the position as the preferred method of isolating the engine from the body.

ANC has its problems as well. Due to the spatial dependence of noise in the cabin, often an array of microphones and speakers are required to effectively provide noise cancellation at all seating locations. Thus the higher the frequency of noise to be cancelled, the higher the cost of electronic hardware and the complexity of the software. One proposal to overcome this problem is to cancel the noise at its source, for example by placing the feedback speaker inside the exhaust system (Garabedian and Zintel 2001) or induction system (Vaishya 2005).

12.5.2 Fuel economy challenges

Ultimately the greatest challenge in the future will be maintaining good noise and vibration refinement while meeting ever-tightening fuel economy requirements of the vehicle. The challenges driven by fuel economy can be categorised as a 'triple-whammy' for noise and vibration engineers:

- Greater source excitation from internal combustion engines
- Vehicle mass reductions
- Engineering budget biased towards fuel economy improvements.

New and higher vibration sources can be expected in the evolution of the internal combustion engine and driveline. Already we are seeing early lockup of the torque converter on automatic transmissions (Hage and Szatkowski 2007). Even if electronic slip control is used to maintain torsional isolation from the engine, the result is engine speeds at highway cruise extending down to lower speeds than before. Designing for cruising refinement means that all vibration modes in the extended cruise window of operation must be controlled.

New engines will also bring higher loads and forces to contend with. Diesel engines, although not exactly new, provide a good example. Higher torque levels from diesel engines generate larger torque pulses that result in many driveline vibration challenges. Diesel engines also present a problem of high-frequency airborne noise levels from their high-pressure

Table 12.8 New engine technologies

Engine technology	Noise and vibration challenges	Noise and vibration enablers
Early torque converter lockup	Loss of driveline torsional vibration isolation at low speed	Driveline tuned vibration damper Separation of system modes
Low idle speed	Poor isolation of engine mounting system	Soft or switchable/active engine mounts
	Exhaust resonances	Separation of system modes from idle speed
	Shake due to poor combustion stability of engine	Hydraulically damped engine mounts
Engine shut-off at idle	Shake on start-up	Hydraulically damped engine mounts
	Noisy electrically driven accessories	Variable-speed accessories
Diesel engine	High combustion noise and rattle	Additional vehicle insulation package and controlled fuel injection
	Idle vibration/boom	Soft or switchable/active engine mounts
	Driveline vibration/boom	Driveline tuned vibration damper
Direct injection gasoline engine	Fuel system ticking noises	Additional vehicle insulation package
Turbo-charging	Turbo whine	Induction system resonators
	Higher combustion noise	Additional vehicle insulation package
Cylinder deactivation	High driveline torsional vibration	Driveline tuned vibration damper
	Loss of engine mounting isolation	Soft or switchable engine mounts
	Exhaust booms	Exhaust acoustic and structural tuning

fuel injection noises and high rate of compression combustion noise (Wang *et al.* 2007). Gasoline engines also are evolving towards characteristics of diesel engines. Already on the market are direct injection gasoline engines, which have the characteristic high-pressure fuel delivery ticking noises of a diesel. In the future, gasoline engines are expected to further evolve to take on diesel-like compression ignition modes of operation under cruising conditions.

Table 12.8 lists a number of engine technologies that are being phased into production by the world's vehicle manufacturers in response to improving fuel economy. Each of these presents new forces and vibration sources that must be designed for.

If you are dealing with a noise and vibration problem caused by one of the above engine technologies, you probably have plans to add counter-measures. But these add mass, and extra mass has now become an unmentionable word in the automotive world. Even if you do get to add mass, you will probably need to do a deal with your engineering manager to balance it by taking mass out elsewhere. And every little piece of the car will repeatedly go under the microscope for any opportunities for mass reduction. What this potentially means is less stiff components and fewer add-on vibration absorbers. Make sure you have done your homework, and can argue your case to maintain subsystem targets.

Last but not least come considerations of cost. The priority of spending will be meeting the fuel economy targets of the vehicle program. Whether that includes fixing the noise and vibration problems it causes will vary from program to program. You will need to prove that you have optimised your solutions with regard to cost and mass, and this is where mathematical analysis models help to gain a better understanding and optimised solutions to noise and vibration refinement.

12.6   Conclusions

Integration and sound quality engineering of the powertrain is a critical factor in meeting customer expectations due to the inevitable link between vehicle noise and the perception of quality. This chapter has described the process for integrating the powertrain into passenger vehicles. The first step in the process is to set targets for the vibration source levels and isolation of paths. The second step is to make use of enablers to tailor the induction and exhaust character to meet the customer's expectation of the vehicle.

In summary, a good powertrain noise and vibration engineer will apply the following practices:

*   Set targets prior to development.
*   Thoroughly validate the vehicle under all operating conditions and measure against the targets.
*   Use a methodical approach to solve the problem. For example, consider the role of the source, path and receiver.
*   Consider and balance aspects of the solution. For example, determine trade-offs between noise performance, cost, mass and manufacturing impact.

12.7   References

Bosch (1986), *Automotive Handbook*, 2nd edition, Stuttgart, Robert Bosch GmbH

Eshleman R L (2002), Torsional vibration in reciprocating and rotating machinery, in *Harris' Shock and Vibration Handbook*, Harris C M and Piersol A G, New York, McGraw-Hill

Garabedian C and Zintel G (2001), Active noise control: Dream or reality for passenger cars?, SAE paper 2001-01-0003

Hage A and Szatkowski A (2007), Improving low frequency torsional vibrations NVH performance through analysis and test, SAE paper 2007-01-2242

Hill W E (2002), The pros and cons of valves in automotive exhaust systems, in *Proc. Inter-Noise 2002*, the 2002 International Congress and Exposition on Noise Control Engineering, Dearborn, MI

King R and Monahan R (1999), Alternator pulley with integral overrunning clutch for reduction of belt noise, SAE paper 1999-01-0643

Lee P and Rahbar A (2005), Active tuned absorber for displacement-on-demand vehicles, SAE paper 2005-01-2545

Rao S R (1986), *Mechanical Vibrations*, Reading, MA, Addison-Wesley

Vaishya M (2005), Unified strategy for active control of induction air sound, SAE paper 2005-01-2535

Wang P, Song X, Xue D, Zhou H and Ma X (2007), Effect of combustion process on DI diesel engine combustion noise, SAE paper 2007-01-2076

Wolf A, Gaertner U and Droege T (2003), Noise reduction and sound design for diesel engines – An achievable development target for US passenger cars?, SAE paper 2003-01-1719

Wolfgang R (1990), Torsional vibrations in the drive train of motor vehicles – principal considerations, in *4th LuK Symposium*, Germany, LuK GmbH

Wowk V (1991), *Machinery Vibration: Measurement and Analysis*, New York, McGraw-Hill

Vehicle interior noise refinement – cabin sound package design and development

D. VIGÉ, Centro Ricerche Fiat, Italy

Abstract: The topic of this chapter is the analysis of the main vibroacoustic problems related to the sound package design and development of a vehicle. This chapter presents an overview of the noise paths for vehicle interior noise, followed by a description of the basic acoustic principles for analysis of the performance of commonly used acoustic materials and for solutions currently applied to modern vehicles, including a short description of the available simulation tools and the design process for cabin sound package development.

Key words: sound package design, vehicle interior noise, acoustics materials, sound absorption, sound isolation.

13.1 Introduction

In today's market the perceived quality of a vehicle is one of the main aspects that customers take into account in choosing the vehicle to buy. A very important component of perceived quality is the noise inside the cabin. This is confirmed by 'buyer selection criteria' surveys, which show that the ranking of noise is quite high among all the other parameters playing a role in the customer's vehicle choice. For these reasons the design of the sound package is a key feature in vehicle development. To improve this comfort factor related to vehicle acoustics, products such as absorption and damping materials are currently available on the market but, unfortunately, they are very heavy and expensive. Moreover, the acquired noise and vibration benefits have penalties in terms of additional cost and weight, whereas the fuel consumption requirements push towards low-weight solutions and the need for reducing costs requires low-priced solutions. All these aspects make the sound package design of a vehicle an important challenge driven by a big effort of optimisation to find a good balance between acoustic performance, weight and cost.

13.2 Internal noise sources in a vehicle

The sound package design of a vehicle for the reduction of internal noise requires knowledge of the different sources of noise, in order to find and

286

analyse the different transmission paths: the sound isolation of the vehicle's panels should be balanced according to the strength and positioning of the different sources.

There are many sources of noise in a vehicle: in the past the engine was the most important, and the first NVH studies were applied to reduce noise and vibrations generated by the engine and powertrain. As a result current engines and powertrain systems show a strongly reduced level of noise, and consequently other sources of noise such as road noise become very significant. Moreover, the increase of the speed of vehicles has strongly increased the importance of aerodynamic noise (George, 1990). Below is a short description of the main noise sources in vehicles.

13.2.1 Engine and powertrain

The engine plays a very important role for internal noise of vehicles. Internal combustion engines are generally strong sources of noise and vibration, whereas electric engines are often much quieter. The vibrations from the engine are mainly generated by the reciprocating and rotational masses such as pistons, connecting rods and shafts; for this reason balancing of these masses is very important and an increased number of pistons allows one to reduce the effect of the lower orders of the engine: for a four-cylinder engine the second order is the most important, whereas for a five-cylinder it is order 2.5 and for a six-cylinder it is the third order. Other sources of vibration come from the gearbox, the differential and the structural modes of the exhaust system. For airborne noise there are many acoustic sources in the powertrain system, like the vibrating panels of the engine body itself, pumps, electric generators, valves, belts and chains, but the most important are the intake and exhaust tailpipes, which act as very efficient acoustic sources as they are almost monopole sources (Roger, 1996). The intake, the exhaust and the number of cylinders play important roles in the typical sound of a car and allow for brand-noise customisation by car makers.

13.2.2 Suspensions

The vehicle suspension system is located in the structure-borne transmission path between the road–tyre interaction and the vehicle body, so the design of this system must be done carefully taking into account its behaviour in vibration transmission. The suspension geometry, the stiffness of the bushings connecting different components of the system, the flexibility and the mass distribution of brackets and other suspension components are very important factors for the dynamic behaviour of this system and its capability to filter or amplify the vibrations coming from the wheels to the vehicle

body. The suspension system can also self-generate noise: the flow noise of the oil inside the shock absorbers and the maximum displacement bump of the bushing in high-load conditions are frequent examples.

13.2.3 Tyres

The tyres are the vehicle parts in contact with the rough road surfaces. They have a dual role in road-noise generation and transmission. The geometry of the tread and the vibrations of the tyre surfaces in contact with the road are important airborne paths for noise emission; air pumping into the tread is also an aerodynamic source of noise. For the structure-borne path the tyres and their dynamic behaviour are very important, as they are responsible for the transmission of the forces between the road and the wheels; the air cavity inside the tyre and its acoustic modes must be taken into account as these resonances increase the transmission of forces.

13.2.4 Aerodynamic sources

The importance of aerodynamic noise in cars has considerably increased. In the 1970s this source of noise was only perceived at over 160 km/h, but in today's cars it reaches the same level as other sources already at 100 km/h. At higher speeds it quickly becomes one of the most important noise sources, as the intensity of the aerodynamic noise in a car follows the behaviour of a dipole source, which is proportional to the sixth power of the speed:

$$I \propto V^6 \tag{13.1}$$

There are different aerodynamic sources in a vehicle:

- Global flow separation, with big vortexes in the low-frequency range
- Local flow separation, with local vortexes in the mid- to high-frequency range (the most important regions for a car are the A-pillar, the windshield, the underneath flow, the accessories like rear mirrors and windshield wipers, the radio antenna, etc.)
- Turbulence and boundary layer noise (typically a broadband noise)
- Leakage noise from seals, with or without net flow (see Fig. 13.1, Vigé, 1999).

13.2.5 Squeaks and rattles from interior dashboard and trimmings

These represent an indirect source of noise in a vehicle, as they are generated by the dynamic displacement of the surfaces of the dashboard and
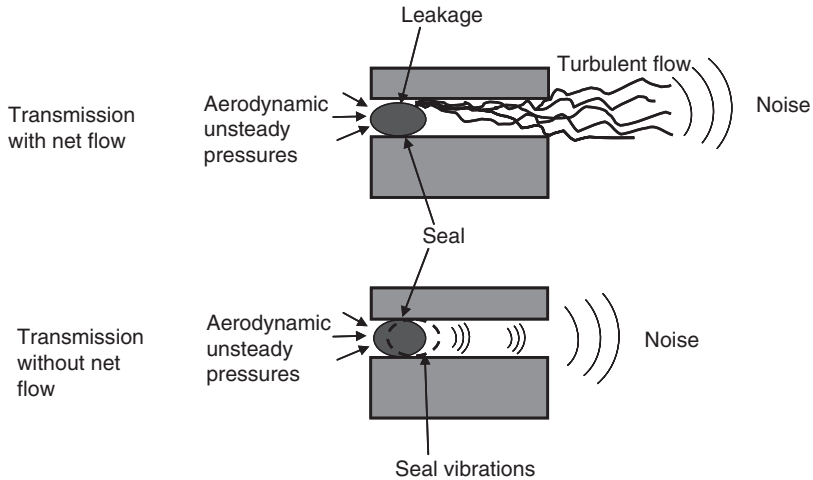
13.1 Noise from seals with and without net flow (Vigé, 1999).

internal trimmings, which is caused by the sources of vibrations in a car (mainly the road and powertrain excitations). Squeaks are given by stick and slip phenomena, where surfaces in contact are switching between contact and slipping conditions. Rattles are generated by impacts of adjacent surfaces. The noise generated by these sources is generally in the high-frequency range (500–5000 Hz for squeaks and 200–2000 Hz for rattles), even though the road and engine excitations responsible for these phenomena are in the very low frequency range. Both squeaks and rattles can be reduced by control of tolerances and an appropriate choice of materials.

13.2.6 Other sources

Besides the above main sources of noise in a vehicle there are many other secondary sources, such as brakes (responsible for the annoying brake squeal noise), electrical and mechanical accessories, etc.

13.3   Vehicle noise paths

Internal vehicle noise does not depend only on the acoustic and vibration sources; very important roles are also played by the different transmission paths between the sources and the receivers (i.e. the driver's and passengers' ears). In a vehicle there are two different categories of transmission paths: structure-borne and airborne paths. They are related to completely different mechanisms of energy transmission. In a common vehicle (like a car) experience shows that very often the structure-borne noise
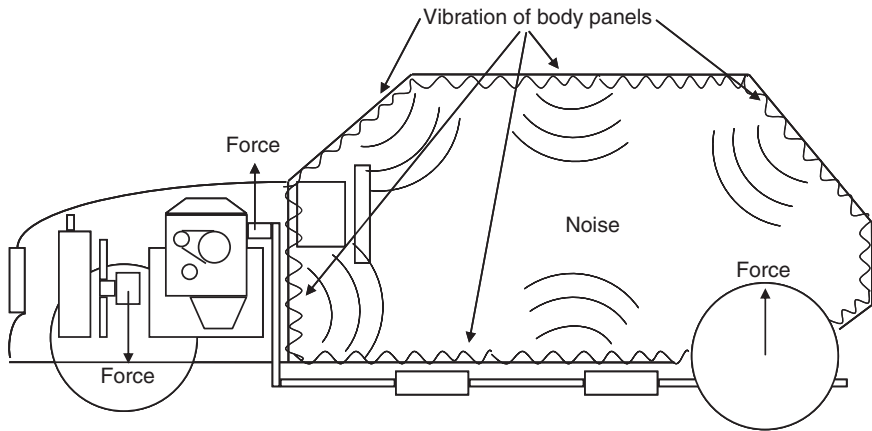
13.2 Structure-borne paths.

transmission path dominates at low frequency (<200 Hz) while the airborne noise transmission path dominates above 500 Hz. In the mid-frequency range, both transmission paths have commonly the same level of importance.

13.3.1 Structure-borne noise transmission paths

The structure-borne path is a vibration transmission path, in which noise is emitted by the panels surrounding the internal cabin. A simple example is the case of the engine of a vehicle: if we consider the engine when running as a source of vibrations (Fig. 13.2), the energy associated with this vibration will be transferred to the vehicle structure through the engine mounts, then the vibration will propagate over the whole vehicle structure onto the panels facing the passenger compartment. The vibration of these panels will transfer the energy to the air cavity inside the cabin, generating the noise perceived by the occupants. The reduction of structure-borne noise is therefore focused mainly on the structure and the isolation of the vibrations: in this example the engine mounts play an important role in the attenuation of the level of vibration, the vehicle structure should have a low sensitivity to the forces coming from the mounts, and the panels should have a low radiation efficiency and possibly be damped to reduce their levels of vibration.

13.3.2 Airborne noise transmission paths

The airborne path is a completely different transmission mechanism, as it is an acoustic transmission path. A simple example is still the engine in
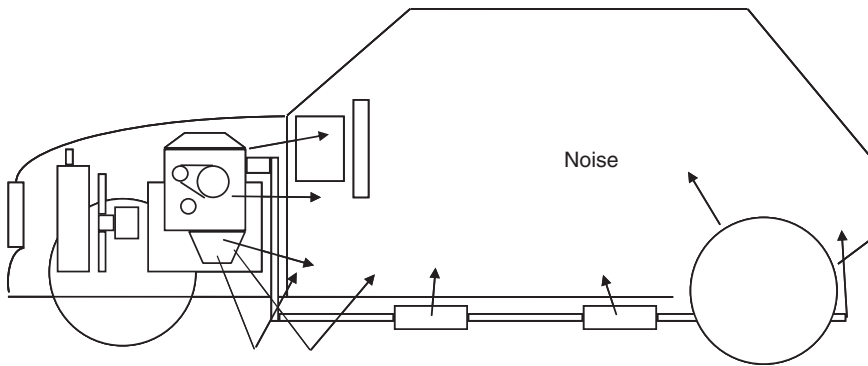
13.3 Airborne paths.

running conditions (Fig. 13.3): if we consider the engine as an acoustic source (i.e. the noise generated by the vibrating panels of the engine body), in this case the noise propagates through the air, through holes and across the surfaces of the structure. In the latter case the acoustic propagation will involve also the vibration of the panels of the structure but we are still dealing with an airborne path (the noise outside the panel makes it vibrate, and the panel will generate noise inside the passenger compartment). For these reasons the reduction of airborne noise is more focused on the acoustic path (particular attention should be paid to avoid holes and leakages), on the structure (which should work in acoustic isolation) and on acoustic absorption inside the cabin (this could be done also for structure-borne noise, but the common acoustic materials show better performance in the high-frequency range, where the noise is dominated by the airborne path).

The cabin sound package design, which is the central topic of this chapter, is then mainly related to the airborne path of noise transmission.

13.4   Basic principles

Control of airborne noise transmission is obtained by two different actions: sound isolation and sound absorption of the vehicle cabin. The first action is focused on keeping acoustic energy out of the cabin, whereas the second acts to absorb the acoustic energy in order to reduce the residual noise inside the passenger compartment. In this section the basic principles of sound isolation and absorption are underlined, including the description of the measuring facilities and the material properties related to these actions.

13.4.1 Sound transmission loss

The sound isolation capability of a given partition (window, panel, wall, etc.) is very important for airborne noise transmission in a vehicle as most

of the acoustic sources are external to the cabin: a good level of isolation is then a good starting point to reduce the interior noise. This acoustic isolation capability of the structures is measured by the definition of the sound transmission loss (TL):

$$TL(\beta, f) = 10 \log \frac{W_{in}(\beta, f)}{W_{out}(\beta, f)} \tag{13.2}$$

where:

β is the angle of incidence of the sound wave over the surface of the given partition

f is the frequency of the considered sound wave

W_{in} is the sound power incident at the source side

W_{out} is the sound power radiated at the opposite side of the partition.

One important fact is that the TL depends on the angle of incidence of the sound. The simplest situation is the case of acoustic plane waves normal to the surface: in this case we can define the transmission loss for normal incidence:

$$TL_N(f) = 10 \log \frac{W_{in}(f)}{W_{out}(f)} \tag{13.3}$$

The typical shape of the TL curve is shown in Fig. 13.4; there are different ranges of frequency with different behaviour of the TL. For very low frequency, below the first resonance mode of the structure, there is the 'stiffness controlled region', where the stiffness of the plate influences the level of the TL. The second region is the 'resonant region', dominated by the resonances of the structure and their level of damping. Increasing the frequency, the modal density increases and the effect of individual modes is no longer noticeable. In the 'mass-controlled region', the TL is dominated by the mass per unit surface area of the structure. The final region shown in Fig. 13.4 is controlled by the 'critical frequency' (f_c), due to the coincidence of the wavelength in the structure and in air (see below); the level of the response in this region is controlled by the damping of the structure.

Usually at low frequency the internal noise is dominated by the structure-borne path of transmission; for this reason the most important regions of the TL curve in common vehicle applications are the high-frequency regions (where the airborne noise path is dominant): the mass-controlled region and the coincidence frequency region.

Mass law

In the mass-controlled region the TL follows the so-called 'mass law'. In the simple case of normal incidence waves on an infinite uniform plate, it
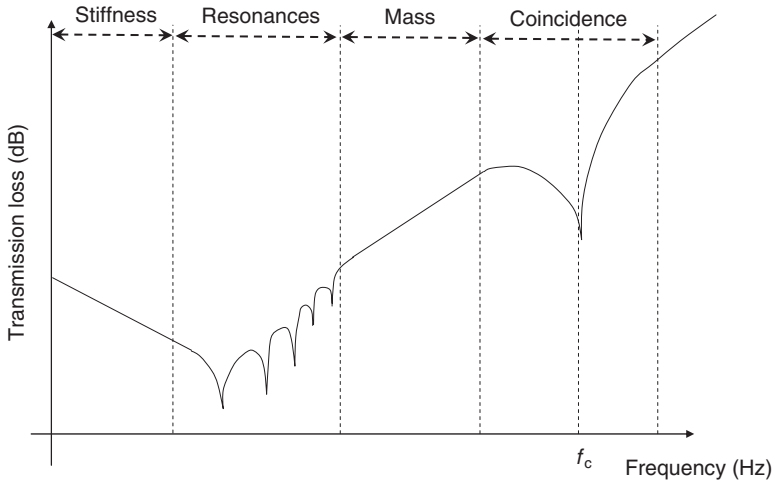
13.4 Typical behaviour of the TL for a real partition.

is possible to find an analytical solution to calculate the TL. In this case the normal incidence mass law (valid for compression wave lengths $\gg$ plate thickness) is given by:

$$\text{TL}_{\text{N}}(f) = 10 \log\left(1 + \frac{2\pi f \rho_{\text{S}}}{2\rho_0 c_0}\right) \tag{13.4}$$

where:

ρ_{S} is the mass per unit surface area of the plate
$\rho_0 c_0$ is the characteristic impedance of the gas (air) of mass density ρ_0 and speed of sound c_0.

It is easy to see that in the mass law region the TL increases by 6 dB when doubling the frequency or doubling the mass per unit surface area. Also, Equation 13.4 shows that for a given gas (usually air) the TL in the mass law region depends only on the mass per unit surface area; any modification of the plate's stiffness or damping cannot change the level of the TL in this region. For better sound isolation without increasing the weight too much, it is possible to adopt specific solutions, such as double wall barriers (see Section 13.5.1).

In practical applications it is more common to deal with incident sound fields where the angle of the acoustic waves varies randomly from 0° to 90° with about the same level of probability. For this reason, it is usual to define a 'random incidence transmission loss' (TL_random). Comparison of the predicted values of TL with the measured value (see Section 13.4.3) shows that better agreement is achieved by considering a random field with incident angles in the range 0° to 78° (defined as 'field transmission loss', TL_field)

rather than between 0° and 90°: the reason is that in practice it is very difficult to obtain a real diffuse field in all directions. The relationships between these values in the low-frequency range ($f \ll f_c$) are as follows:

$$TL_{random} = TL_N - 10 \log(0.23 TL_N) \tag{13.5}$$

$$TL_{field} = TL_N - 5 \tag{13.6}$$

Coincidence frequency

Wave coincidence is a phenomenon that occurs when the length of an acoustic wave in air is coincident with the wavelength of the structural bending wave in the panel: in this situation the panel is driven by a strong excitation in a resonance condition, and vibrates with an amplitude very close to the amplitude of the displacement of the air particles associated with the acoustic wave. The TL of the panel falls to a very low value, which would be zero theoretically in the case of no structural damping. The minimum TL in this region is then controlled by the damping value of the structure, as in the dynamic resonance phenomenon.

There is a wave coincidence when the wavelength of the bending structural wave is equal to the wavelength of the sound wave in air projected to the panel (see Fig. 13.5):

$$\sin \beta = \frac{\lambda}{\lambda_s} \tag{13.7}$$
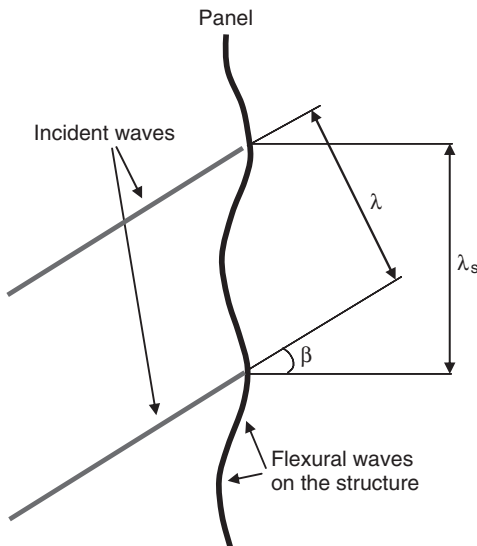
13.5 Wave coincidence.
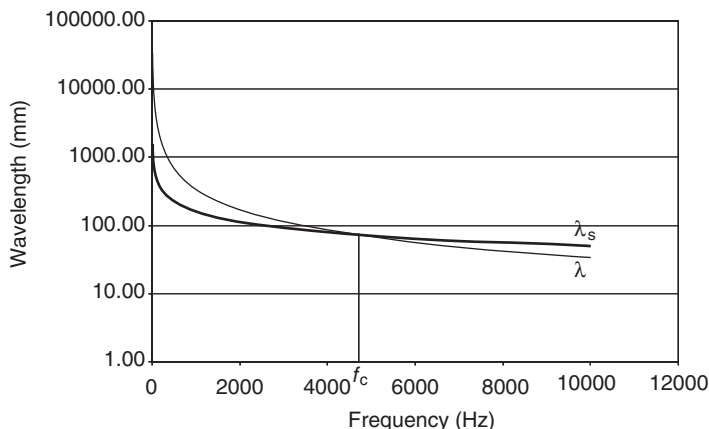
13.6 Coincidence frequency.

where:

β is the angle of incidence of the sound wave over the surface of the given panel

λ is the wavelength of the acoustic wave in air

λ_s is the wavelength of the bending wave in the structure.

The frequency at which this occurs is called the 'coincidence frequency'.

It is easy to see from Equation 13.7 that if the wavelength of the sound in air is greater than the wavelength of the bending waves in the structure there are no wave coincidence phenomena. Usually at low frequencies λ is much greater than λ_s. Furthermore, as frequency increases, λ decreases more quickly than λ_s (see Fig. 13.6), so there is always a frequency where the two wavelengths are the same: the 'critical frequency' f_c is defined as the minimum frequency at which a wave coincidence may occur, so it is the minimum possible value for the coincidence frequency. From Equation 13.7 it can be seen also that over the critical frequency there is always a given angle of incidence β at which the wave coincidence phenomenon may occur.

It can be shown (Beranek, 1960) that:

$$f_c = \frac{c_0^2}{1.8 c_l h \sin^2 \beta} \tag{13.8}$$

where:

c_l is the speed of longitudinal waves in the plate

h is the thickness of the plate structure.

In the panels of a common car this frequency is usually very high (often above the frequency range of interest), but for very thick panels and for all

the glass of the car it falls within an important frequency range (i.e. 3000–5000 Hz).

13.4.2 Sound absorption

Sound absorption is a very well-known and commonly used solution to reduce noise. It exploits the characteristics of some materials that are able to dissipate the acoustic energy. In current vehicles sound absorbing materials are applied in the passenger cabin and often in the engine bay, to reduce the interior and sometimes the exterior noise.

There are three main physical phenomena related to sound absorption. The first mechanism is the frictional losses of the air molecules; a sound wave causes an oscillation in the position of the air particles: the molecules of the air interact with the pores or the fibres of the absorbing materials and are subjected to friction phenomena, causing a loss of energy (the friction slightly increases the temperature of the air and the material). A second mechanism is related to heat exchange; the sound wave generates pressure fluctuations in the air; in the free field this is an adiabatic transformation, whereas on the boundaries the presence of absorbing materials (with a large surface to volume ratio) causes a heat exchange between the air and the surrounding materials. The transformation is no longer adiabatic and shifts towards an isothermal transformation, causing a loss of energy in the sound wave. This could happen mainly at low frequencies, where there is more time during a cycle for heat exchange (at high frequency the heat exchange becomes so small that it can be neglected). The third mechanism is related to the internal losses of the acoustic materials subjected to the forced mechanical oscillations caused by the acoustic pressure: this is true mainly for closed-cell porous materials, whereas in fibrous and open-cell porous materials this effect is so low that it can generally be neglected.

The most important characteristics of the sound absorbing materials are listed below.

Normal specific acoustic impedance

At the boundary between the air and a denser medium like an absorbing material the air particles are moving in the presence of an acoustic wave: their velocity u is an alternate velocity in a given direction through the material's surface. The direction depends on the angle of incidence of the acoustic wave and on the properties of the absorbing material. A first important definition for the properties of an acoustic material is the 'normal specific acoustic impedance' (Z_n):

$$Z_n = \frac{p}{u_n} \qquad (13.9)$$

where:

p is the sound pressure on the boundary between the air and the material's surface

u_n is the normal component of the particle's velocity at the material's surface.

Z_n is a complex value and is an important property that describes the behaviour of an absorbing material in the presence of normal incident sound waves.

Energy absorption coefficient

The most important definition for the characterisation of an acoustic material is the 'energy absorption coefficient' (α), which is defined as the ratio between the absorbed acoustic energy and the total incident acoustic energy. In all the reflections of acoustic waves on a surface the energy is partially reflected and partially absorbed by the material, and this coefficient represents the capability of the material to absorb the acoustic energy. The value $\alpha = 1$ means that all the energy is absorbed, so there are no reflected waves by the surface; a value $\alpha = 0$ means that there is perfect reflection, without any loss of energy.

The coefficient α depends on the material properties and the thicknesses of all the layers applied on the surface (absorbing materials, air gaps, etc.). Also, α is usually a function of the frequency and the angle of incidence of the sound wave, as in the case of the TL. For this latter reason it is common to define an absorption coefficient for a diffuse field (α_d), where the angle of incidence covers all the angles between 0° and 90°.

Closed rooms, reverberation time, Eyring and Sabine theory

For a given closed room (like a vehicle cabin) it is possible to define an 'average diffuse field sound absorption' ($\bar{\alpha}_d$) (Beranek, 1960):

$$\bar{\alpha}_d = \frac{\sum_i S_i \alpha_{di}}{\sum_i S_i} \qquad (13.10)$$

where:

i is the number of surfaces closing the room
α_{di} is the diffuse field absorption coefficient for the ith surface
S_i is the area of the ith surface.

The sound absorption of a closed room can be measured by its 'reverberation time' (T_{60}), defined as the time required (in seconds) to reduce the noise by 60 dB after turning off the acoustic sources inside the room. There are many diffuse field models, the most interesting for vehicle applications being the Sabine theory. In order to better understand the Sabine formulas it is possible to start with the most generally applicable diffuse field model, the Eyring theory, applicable for a point source:

$$L_p(r) = L_w + 10 \log\left(\frac{Q}{4\pi r^2} + \frac{4}{R}\right) \tag{13.11}$$

valid for steady-state conditions, where:

L_p is the sound pressure level
L_w is the sound power level of the source
Q is the directivity factor for the point source (the ratio of the sound power radiated in the receiver direction to the mean sound power radiated in all directions; equal to 1 for a homogeneous sound source)
r is the distance between the point source and the receiver
R is the so-called room constant, given by:

$$R = \frac{4mV - S \cdot \ln(1 - \bar{\alpha}_d)}{1 - \bar{\alpha}_d} \tag{13.12}$$

where:

$2m$ is the energy air absorption exponent (Beranek, 1960)
V is the room volume
S is the whole surface of the room.

Equation 13.11 describes the sound field in a room as the summation of a direct and a reverberant component (the two terms in the parentheses). Also, the Eyring theory states that the reverberation time is given by (in SI units):

$$T_{60} = \frac{55.3V}{c[4mV - S \cdot \ln(1 - \bar{\alpha}_d)]} \tag{13.13}$$

where c is the speed of sound in air.

In practical vehicle applications the average diffuse field sound absorption coefficient is usually quite small (<0.25); in this case it is better to use the Sabine theory. Also, the air absorption can be neglected, that is $2m = 0$ (it is only important for propagation distances greater than about 10 m). In this case Equations 13.12 and 13.13 become:

$$R = \frac{\bar{\alpha}_d S}{1 - \bar{\alpha}_d} \tag{13.14}$$

$$T_{60} = \frac{55.3V}{c\bar{\alpha}_{d}S} \tag{13.15}$$

Equations 13.11 and 13.14 show that the direct field (dominating near the source) decreases by 6 dB when doubling the distance from the source, whereas the reverberant field (dominating far from the source) depends only on the absorption of the room, and is about inversely proportional to $\bar{\alpha}_{d}$ and S (for small values of $\bar{\alpha}_{d}$). Equation 13.15 shows that the reverberation time is directly proportional to $V/\bar{\alpha}_{d}S$. These equations allow for measuring an absorption coefficient by measuring the reverberation time. The term $\bar{\alpha}_{d}S$ is also called the 'total room absorption' or 'equivalent area of absorption of the room' and represents the equivalent area with absorption coefficient equal to 1.

It is important to know that for normal incidence acoustic waves it is sufficient to measure the normal impedance of the material without measuring the diffuse field absorption coefficient.

13.4.3 Measuring facilities

There are different testing facilities and procedures for measurement of the acoustic properties of the acoustic package. The most interesting for vehicle applications are described below.

Anechoic and semi-anechoic rooms

Anechoic rooms are closed rooms with all the walls (including floor and ceiling) covered by strong absorbing materials, usually cones made of mineral or glass fibres. An ideal anechoic room should have a unit absorption coefficient in all the walls, in order to have a free-field radiation condition inside the room. Obviously this is not completely feasible, mainly at low frequencies where it is really hard to achieve a high level of absorption. For this reason an anechoic room has a minimum working frequency (usually 100–200 Hz) and measurements inside the room can be made only at higher frequencies.

In order to allow work inside an anechoic room (where also the floor is covered by acoustic treatments) it is usual to build a suspended floor made of metal wires with a small reflecting surface. Semi-anechoic rooms are the same as anechoic rooms except that the floor is a reflecting surface: in this way it is possible to reproduce a free-field radiation in the presence of a reflective ground, like the road for vehicles.

Reverberant rooms

Reverberant rooms are the opposite of anechoic rooms, as the goal is to reproduce a reverberant and diffuse field inside them. For this reason all

the walls, including floor and ceiling, have to perfectly reflect the sound waves. Furthermore, to avoid cavity resonance phenomena it is usual to build non-parallel walls (including the ceiling), and sometimes to add reflecting and non-planar shields in random positions to reflect and diffuse the waves in all possible directions, to generate a field with waves travelling with all the angles of incidence (diffuse field). In the low-frequency range the cavity resonance phenomena are still important, so there is a transition frequency above which the field can be described in statistical terms. The sound field obtained is still not perfectly uniform and diffuse, so it is necessary to take some spatial averages of the sound pressure in order to have reliable measurements.

Reverberant rooms are used to measure the absorption of a given material or component by exploiting the Sabine formula (Equation 13.15); by measuring the reverberation time with and without the component it is possible to find its absorption coefficient. This measurement is defined by the international standard procedure ISO 354-1985 and requires a reverberation room of at least 294 m^3.

Alpha cabin

In the automotive field it has become a common standard to use reverberation rooms (known as alpha cabins) that are smaller than the standard ISO requirements for measurement of the acoustic absorption of the materials. The basic principle of measurement is the same.

Kundt's tube

Measurement of the normal impedance and the absorption coefficient for normal incidence waves can be done in the laboratory with a smaller facility than a reverberant room. This is the impedance tube or Kundt's tube (see Fig. 13.7), and the international standard procedures for the measurement are ASTM-E 1050 and DIN 52215. A disc of the test material is placed in the side opposite to the acoustic source (loudspeaker) and the acoustic normal impedance is calculated by the sound pressure levels measured by the microphones inside the tube.

Transmission loss measurement

The measurement of the TL of a given partition is defined by international standard procedures, in particular ISO 140/3–1995 and ASTM E90-74. They require the use of two reverberant rooms (with a volume of at least 64 m^3) both facing the same window where the test partition can be placed (see Fig. 13.8). The window (and consequently the partition) has dimen-
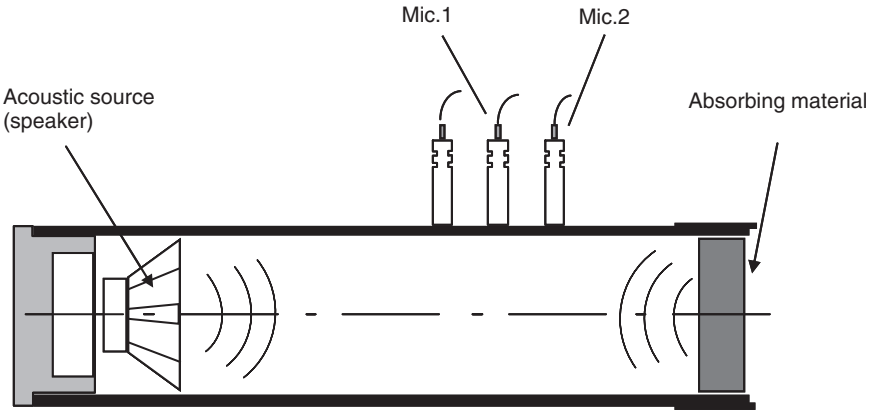
13.7 Kundt's tube.
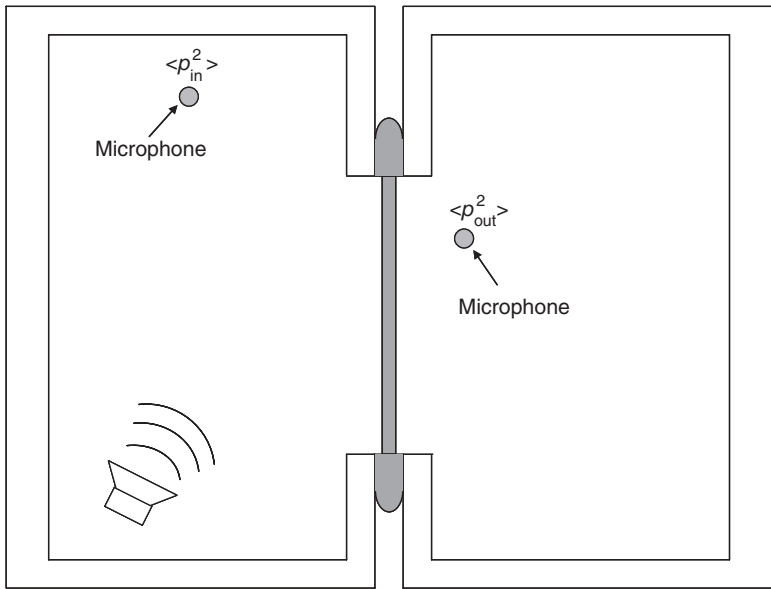
13.8 Transmission loss measurement.

sions of 2.8 by 3.6 m. The first room is used for the source, using one or more loudspeakers covering the whole frequency range of interest and generating a diffuse field. In the second room the noise attenuated by the test partition is measured: it is very important to have only the acoustic path that comes through the test partition, avoiding any leakages and with very good isolation of the common wall between the two reverberant rooms.

The measurement procedure follows three steps:

1. Measurement of the incident acoustic field
2. Measurement of the transmitted acoustic power through the partition
3. Measurement of the total absorption area of the receiver room.

Equation 13.2 requires the measurement of the incident and transmitted sound power. If we consider an incident diffuse field, the incident sound power will be:

$$W_{in} = I_{in}S_p = \frac{\langle p_{in}^2 \rangle S_p}{4\rho_0 c_0}$$

(13.16)

where:

I_m is the sound intensity in the source room

S_p is the area of the test partition

$\langle p_{in}^2 \rangle$ is the time and space averaged mean-square sound pressure in the source room (it should be constant in a real diffuse field, but considering that a reverberant room cannot give an exact diffuse field this pressure has to be averaged with spatial sampling).

The measurement of the transmitted power through the partition can be obtained by a power balance in the receiver room:

$$W_{out} = \frac{\langle p_{out}^2 \rangle A_{rec}}{4\rho_0 c_0}$$

(13.17)

where:

$\langle p_{out}^2 \rangle$ is the time and space averaged mean-square sound pressure in the receiver room

A_{rec} is the equivalent absorption area of the receiver room.

Equation 13.2 then gives (for a diffuse incident field):

$$\begin{aligned} TL &= 10\log\frac{W_{in}}{W_{out}} = 10\log\frac{\langle p_{in}^2 \rangle S_p}{\langle p_{out}^2 \rangle A_{rec}} \\ &= \langle L_p \rangle_{in} - \langle L_p \rangle_{out} + 10\log\frac{S_p}{A_{rec}} \end{aligned}$$

(13.18)

where:

$\langle L_p \rangle_{in}$ is the time and space averaged sound pressure level in the source room

$\langle L_p \rangle_{out}$ is the time and space averaged sound pressure level in the receiver room.

The measurement of the TL of vehicle components commonly uses slightly smaller rooms (with some restrictions in the frequency range).

Often, the receiver room used is an anechoic room: Equation 13.18 shows that it is still possible to measure the TL, just by measuring the total equivalent absorption area of the receiver room. The advantage is that with such a facility it is also possible to make sound intensity measurements in the receiver room in the near field of the test partition, obtaining acoustic maps that qualitatively show the areas of the partition with the high level of transmission.

13.4.4 Acoustic material characteristics

There are some physical properties that make certain materials suitable for use as acoustic treatments (Beranek and Ver, 1992). The first important property is the resistance that the material offers to an airflow through it (as described in Section 13.4.2, one of the mechanisms of acoustic energy absorption is the friction of the air and the fibres or the pores of the material). One of the most important quantities is then the 'specific flow resistance' (σ):

$$\sigma = \frac{\Delta p}{ud} \tag{13.19}$$

where:

Δp is the pressure difference between the two sides of the material specimen
u is the mean air particle velocity through the specimen
d is the thickness of the specimen crossed by the airflow.

A second important property is the density of the material and its 'porosity' (Φ):

$$\Phi = \frac{V_a}{V_m} \tag{13.20}$$

where:

V_a is the volume of the air included in the material
V_m is the total volume of the material, including the air inside it.

The flow resistance is related to the porosity, the fibre diameter and the so-called 'structure factor' or 'tortuosity', which depends on tortuous paths that the air has to follow crossing the material: it takes into account the effect of openings that are perpendicular to the propagation direction of the sound wave.

Another parameter, important only for materials with a consistent structure, is the 'volume coefficient of elasticity of the skeleton' (Q), which measures the compression stiffness of the material: it is measured using a

flat layer of material (with a thickness d) compressed with a force (F) that acts uniformly on the entire surface of the material (of area S). The measurement of the thickness reduction (Δd) gives the coefficient Q:

$$Q = \frac{F}{S} \frac{d}{\Delta d} \qquad (13.21)$$

Another property of materials for noise control applications is the 'loss factor' (η), which is important for the reduction of the structure vibrations. It comes from the measurement of the complex Young modulus (E) of the material subjected to a dynamic load:

$$E = E' + iE'' \qquad (13.22)$$

$$\eta = \tan \delta = \frac{E''}{E'} \qquad (13.23)$$

where:

E' is the 'storage modulus' (real part of the complex Young modulus)
E'' is the 'loss modulus' (imaginary part of the complex Young modulus)
δ is the phase angle.

The most common materials used on vehicle applications are described below.

Porous materials

All materials with a given porosity on their surface have some sound-absorbing properties. Usually the materials used are open-cell foams (i.e. polyurethane); closed-cell foams are not very useful for acoustics applications, as they work only on their surface and do not allow air to flow through them (the flow resistivity is very high). The common open cells used in acoustics have pores smaller than 1 mm, so they are much smaller than the wavelength. In many porous materials the continuous solid structure behaves also as an elastic structure, adding stiffness and damping to the panels of the structures: in this case they are called *poroelastic materials*.

Fibrous materials

Fibrous materials are very common in sound absorbing isolation as they may be optimised to have the required specific flow resistance, porosity and tortuosity, by changing the diameter of the fibres and their geometrical orientation. Fibrous materials are in general based on mineral, glass or natural fibres.

Damping materials

In this category falls all the materials applied to add damping on the structure. The most common are viscoelastic materials, which show both damping (high loss factor) and structural capability.

13.4.5 Interior sound quality

The level of interior noise reduction is very important for the acoustic comfort of the occupants but it is not sufficient by itself. Another important factor that has to be taken into account is the quality of the noise. In recent years there have been many sound quality studies and analyses in order to define the criteria for a noise that is not just quiet but also pleasant. The topic of sound quality is quite complex and many studies are still running, so a general description of this discipline is beyond the scope of this book; a basic description of a few of the most commonly used parameters in the industry is outlined below, but many other parameters can be taken into account (i.e. tonality, roughness, speech transmission index, speech interference level, etc.).

The articulation index (AI)

This is a measure of the intelligibility of voice signals, expressed as a percentage of speech units that are understood by the listener when heard out of context. There are different algorithms for the calculation of the AI. The method used in the automotive field is based on the 1/3-octave band levels in dB(A) between 200 Hz and 6300 Hz, taking strongly into account the frequency bands where the typical speech frequencies are more important.

Loudness

The loudness level refers to the perceived intensity of sound. It is based on the statistical response of the ear as a function of frequency for a statistically significant number of people. Its measurement is defined by the international standards ISO 226, ISO 532 and DIN 4563. Its unit can be sone or phon.

Sharpness

The sharpness is an important measure that takes into account the frequency content of the noise. It is defined as the ratio between the high-frequency noise level and the overall level; it is not related to sound

intensity, but it is high for metallic noise components that are generally considered annoying and correlated with bad quality of the vehicle.

13.5   Sound package solutions to reduce the interior noise

The sound package design of a vehicle requires knowledge of vehicle's acoustic targets, the main noise sources in the vehicle, the transmission paths of the noise and the characteristics of the materials available in the market that can be used to improve the NVH performance: a good design requires the use of appropriate solutions in terms of materials, costs and performance. Not all the acoustics materials available in the market satisfy the requirements for a vehicle application (recyclability, flame resistance, cost, weight, etc.). Also, design optimisation of current vehicles is often performed in strong collaboration between materials suppliers and car makers, and this allows for developing specific solutions for vehicle applications.

13.5.1 Acoustic isolation

The acoustic isolation capability of the vehicle's panels and windows is very important for their NVH performance, as most of the noise sources are external to the vehicle's cabin. This performance is measured by the transmission loss (see Section 13.4.1) of the given panel or component. The performance of the whole vehicle is usually (by most car makers) expressed in terms of *acoustic transparency* of the cabin, measuring the internal sound pressure level for some predefined positions of external noise sources. This performance obviously depends on the transmission loss of all the components of the cabin, including panels, acoustic treatments, glass windows, seals and any other possible paths of transmission. One really important matter is that the global performance is strongly reduced if just a few transmission paths are not well isolated. In other words, a vehicle cabin with a very good level of isolation in the panels and windows could show poor performance if there is a lack of isolation in just one leakage. For this reason it is really very important to find which are the most effective paths of transmission (weak paths) and to work on them.

Panels

As discussed in Section 13.4.1 the airborne transmission of the vehicle's panels follows the mass law in the most important frequency range. The panels usually show their coincidence frequency only at very high frequen-

cies, and only for thick steel panels. For this reason it seems that the only solution is to add mass to the panels in order to reduce their transmission loss, but there are other possible solutions that could help to boost this performance. The most important property that can be exploited is the behaviour of double walls: using two separate partitions separated by an air gap it is possible to obtain an equivalent transmission loss that is much higher than the summation of the transmission losses of the two separated walls. Also, filling the air gap with sound-absorbing material may further increase their performance. Very common solutions in vehicle applications are made by a double wall composed of the metal panel and a so called 'heavy layer' (usually bitumen or heavy rubber), separated by a fibrous absorbing material: in this way the system works as an *acoustic barrier*, with a high level of transmission loss. The design of these solutions allows for the largest noise reduction in the optimised frequency range by working on material properties and thicknesses of each layer. Particular care has to be taken to avoid resonance phenomena in which a double wall system adds to the critical frequencies of the two partitions a third resonance, called the double wall resonance, at which the transmission loss shows a strong reduction. Acoustic barriers in cars are commonly applied on the firewall and floor.

Glass windows

Glass windows on vehicles are often weak paths as they cannot be treated with added mass or double walls (double glazing is not suitable for vehicle applications), and their coincidence frequency is in a frequency range (near 3000 Hz) where the contributions of noise sources are substantial. This latter fact allows for increasing the transmission loss of the windows by adding damping (see Section 13.5.3).

Leakages

Particular care has to be taken with all the openings that connect the cabin and the external sources of noise, particularly in the firewall region. There are many reasons to have some openings in the metal panels, in order to allow the passage of electric cables, air pipes for the ventilation of the cabin, the mounting of the brake assist system, the steering column, etc. All these openings must be firmly closed and isolated using caps or sealants, avoiding any residual leakage.

Seals

Seals of doors and windows are very important for the reduction of aerodynamic noise. Particular care has to be taken on geometric tolerances and

on the dynamic behaviour of compressed seals in the presence of aerody-
namic unsteady pressures acting on them, to reduce possible noise transmis-
sion through them, both with and without net flow (see Fig. 13.1). In the
first case the aerodynamic pressures are capable of deforming the sealant
to such an extent that it becomes detached from the door or body surface,
allowing an airflow passage: this noise source is really strong as it behaves
as a very efficient monopole source. In the second case the aerodynamic
pressures acting on the seal surface make it move and the vibrating seal
surface on the interior side acts as an acoustic source.

13.5.2 Acoustic absorption

The second class of solutions for noise reduction in a vehicle's cabin is the
absorption of the energy associated with the acoustic waves. As stated in
Section 13.4.2 this is possible thanks to the sound absorption properties
shown by some materials. The use of these materials inside the passenger
cabin is very common in current vehicles. Moreover, some sound sources
can be attenuated by surrounding them with absorbing materials. A fre-
quent application is in the engine compartment, where the main vehicle's
noise source (the engine) is attenuated by covering the internal walls of the
engine compartment with absorbing materials. The current and probably
future trend is to try to encapsulate as much as possible the engine with
absorbing covers and shields surrounding it, adding their absorbing proper-
ties with a sound isolation capability. Obviously this kind of solution must
take into account the problems related to the cooling requirements of the
engine itself.

The design of the acoustic absorbing treatments requires good knowl-
edge of the physical properties of the materials: by optimising their flow
resistance, porosity, density, tortuosity, etc. (acting in the pores or the fibres
and their dimensions and geometrical orientation) it is possible to optimise
the acoustic absorption of a given treatment in the defined frequency range
according to the defined targets, keeping the weight to the minimum
required.

There are some general rules that can be taken into account:

- The porosity has to be very high (typically between 0.95 and 0.99).
- The flow resistance must be optimised, as too high values cause waves
  to be reflected, whereas too low values mean inefficient absorption.
- The thickness of the absorbing materials should be more than a quarter
  of the wavelength at the considered frequency.

In automotive applications, trim materials are commonly based on felt,
mineral or glass fibres, polyester or polypropylene (such as Thinsulate or
Politex) or other textile fibres.

Multilayer absorbers are commonly used in vehicle applications. They can be composed of more layers of different absorbing materials (optimised in thickness and properties to give the desired level of absorption in the defined frequency range), or an absorbing layer with an air gap behind, allowing the total absorption coefficient to be increased in the specified frequency ranges.

An important fact is that the treatments for a given part of the vehicle are usually obtained by a stamping process (in order to give the treatment the same shape as the part of the vehicle to be covered, including beads); the acoustic properties of the treatments obtained by such a process must be carefully analysed in the design phase, as the resulting variation of thickness results in different fibre or pore densities (and consequently modified flow resistance, porosity, etc.).

Absorbing treatments in cars are often applied to all the available surfaces of the cabin, in order to maximise the total absorption of the cabin. Particular care has to be taken in seats, as they are responsible for 50% of the total absorption of the passenger compartment. The choice of the materials for the seats (foams and fabrics) is then very important for the whole acoustic behaviour of the cabin. Another important component is the headliner. Because of its large surface area it can reach 25% of the total absorption of the passenger compartment, so it must be carefully designed from the point of view of acoustic absorption.

13.5.3 Damping materials solutions

Damping materials are commonly used to reduce the vibration of the structure for structure-borne noise reduction. The most common solutions in the vehicle's steel panels are the 'free layer damping treatments' (FLDT, see Fig. 13.9(a)) and 'constrained layer damping treatments' (CLDT, Fig. 13.9(b) and (c)) (Danti *et al.*, 2005). Free layer damping treatments have a damping material (usually a viscoelastic material) with a free surface; the material adds damping in its tension–compression deformation. They are used in most vehicles, usually by gluing damping patches to the panels. In recent years, there has been increasing use of an alternative solution, where the damping material is sprayable and can be applied by robots in the vehicle's production facilities. The damping effect of the materials can be increased by using constrained layer damping treatments. There are two different solutions: the first is described in Fig. 13.9(b) and is similar to the FLDT with an additional thin metal cover (usually aluminium or steel). In this way the damping material is constrained by the two metal sheets and works with shear deformations. It can be very effective in terms of added damping but this solution is not often used because of its weight and cost. The most common CLDT solution is depicted in Fig. 13.9(c). In this case

Damping patch
Steel panel

(a)

Metal cover
Damping patch

Steel panel

(b)

Steel layer
Damping layer
Steel layer

(c)
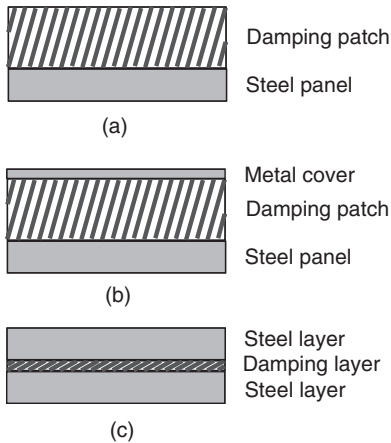
13.9 Damping materials solutions: (a) free layer; (b) and (c) constrained layer.

the damping layer is really thin (i.e. 20–50 microns) and the sandwich structure comes as a single panel (the viscoelastic layer is directly inserted during the stamping process), with a total thickness similar to that of the single sheet steel panel. In this solution the viscoelastic layer is subjected to strong shear deformations and is able to add strong damping despite its very low thickness. This solution allows for keeping the weight low in the damped structure.

Another application similar to the latter is the use of acoustic PVB (polyvinyl butyral) in window glasses (Mezzomo, 2003). Common laminated glasses, such as those used in the windscreens of cars and trucks, are composed of two glass layers separated by a thin PVB layer. Common PVB layers are able to increase the damping of the windscreen, with some improvements in sound transmission in the coincidence frequency region of their transmission loss. A much bigger effect can be obtained by means of special acoustic PVB that has been optimised in terms of damping added to the glasses, allowing a strong improvement of their transmission loss in the coincidence frequency region.

13.5.4 The importance of the balance between isolation and absorption

As described above, noise inside a vehicle's cabin can be reduced by two different means: sound isolation and sound absorption. The balance between them is very important. A solution based on strong isolation with low absorption is probably not optimised in terms of weight and cost (this is easy to understand considering the mass law mechanisms in sound trans-

mission). An optimal solution requires a balance between the two solutions. Moreover, a too high level of sound absorption could give a poor result in terms of speech intelligibility inside the cabin. The lack of reflections of the speech sound waves would make it difficult to understand the words. This phenomenon can be easily observed in an anechoic chamber. Therefore, a good balance should take into account all considerations related to cost, weight and sound quality.

13.6   Simulation methodologies for interior noise

Many simulation methodologies are currently available for the simulation of interior noise. A complete analysis of these methodologies is beyond the scope of this book, but a short description of the main methodologies in current use in vehicle applications may be useful as a starting point for further and deeper studies.

13.6.1 Finite element method (FEM)

Finite element methods are well known and common in vehicle design and in the analysis of many aspects of structural performance and do not need to be described in detail here. For vehicle acoustic applications, they are suitable for low-frequency range simulation of structure-borne transmission paths. Usually linear FEM solutions are sufficient for acoustic analysis, except in particular cases that involve non-linear phenomena such as strong deformations in some components (i.e. bushings and tyres under conditions of large loads). In order to estimate the vibroacoustic behaviour of a vehicle, it is necessary to model both the solid structure (including all the non-structural components and masses such as carpets, seats, the battery, etc.) and the fluid cavities: cabin (including the volume and absorption effect of components such as seats, dashboard and parcel shelf), baggage compartment, and for rolling noise analyses also the tyre cavity. Figure 13.10 shows an example of a structure and cavity model for the interior structure-borne noise of a car (Danti *et al.*, 2001). The cavity is simulated by FEM commercial software using appropriate characteristics for the fluid elements. The suitable commercial software allows for performing a fully coupled solution between the structural accelerations and the pressure inside the cavity (taking into account both the effect of the structural vibrations on the cavity's pressure and vice versa the effect of the internal pressure on the structure's accelerations). This allows for calculating internal noise for a given dynamic force applied on the structure (i.e. the engine or suspension attachments). The modal solution is often more suitable than a direct frequency response in terms of simulation time required.
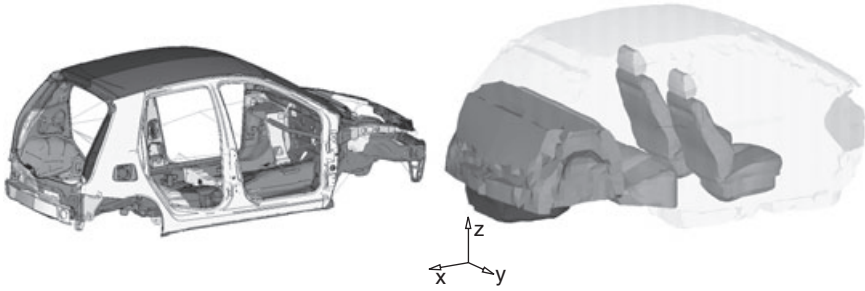
13.10 Finite element model of a car's structure and acoustic cavity (Danti *et al.*, 2001).

13.6.2 Boundary element method (BEM)

The boundary element method has been developed since the late 1970s. It is less generally known than the FEM but is very common in the acoustic field. The main difference between the FEM and the BEM is the way the domain is discretised. In both of them the problem domain is divided into finite elements. The FEM requires a discretisation of the entire domain, preserving the dimensional order of the problem, i.e. a 3D problem will require 3D equations. On the contrary, the BEM operates on the discretisation of the boundaries, which reduces the terms of the problem by one dimension. As only the bounding surface of the domain is divided (see Fig. 13.11; Maquet, 2005; Vigé *et al.*, 2008), the elements are therefore called boundary elements.

There are two kinds of BEM. The direct one (DBEM) requires a closed boundary so that physical variables (pressure and normal velocity in acoustics) can only be considered on only one side of the surface (interior or exterior), while the indirect one (IBEM) can consider both sides of the surface and does not need a closed surface. Both are based on the direct solution of the Helmholtz equation, which is quite time-consuming for the BEM (as it generates a full coefficient matrix), making the BEM suitable only for models that are not too big. For the same reason, they are not suitable for simulation in very high frequencies, as they require very fine models with a large number of elements. The main advantage of the BEM for acoustic analysis is that the Helmholtz equation (together with the boundary conditions) allows one to easily simulate both closed and open acoustic fields, including the presence of acoustic treatments by use of their surface impedances. The FEM is less suitable for the simulation of acoustic treatments and for dealing with open acoustic fields.

In recent years a new approach known as the fast multipole BEM has been implemented. It is an approximation of the standard BEM which
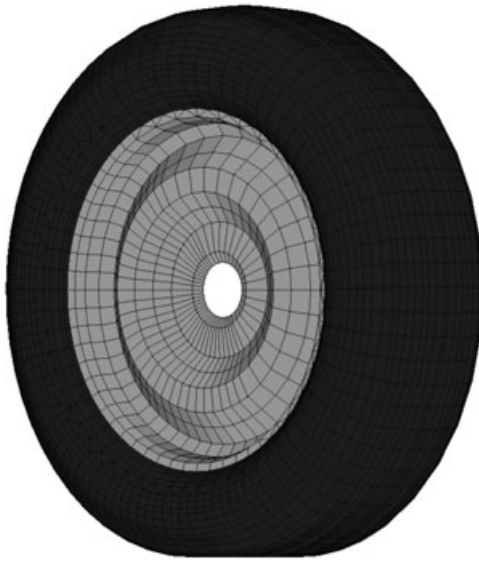
13.11 Boundary element model of a car's wheel (Maquet, 2005; Vigé *et al.*, 2008).

allows one to deal with larger models with a reduced time requirement for the simulation.

13.6.3 Infinite element method (IEM)

The infinite element method has been developed as an alternative to the BEM. In fact, the main drawback of the BEM is its cost in terms of computation time. An alternative to boundary representations is the domain representation. Domain-based methods do not seek exact solutions of the field equations but approximate their solutions within a finite region close to the radiating body. This is generally achieved by means of a conventional volume discretisation, most commonly through the FEM, in which case the unknowns become nodal values of the acoustic pressure. The anechoic termination of the FEM domain then forms a finite boundary on which a '$\rho_o c_o$ impedance boundary' is applied. Such an approximation is valid only if the boundary is sufficiently distant from the radiating source. A more radical approach to domain-based computation is embodied in the infinite element concept. Instead of applying boundary conditions on the termination of the FEM domain, elements of infinite extent are created to model the unbounded domain in its entirety (Fig. 13.12; Fuccelli, 2006). These incorporate oscillatory shape functions whose amplitude decays with radial distance to model the behaviour of a spherical or cylindrical wave. The field of application of the IEM method is similar to that of the BEM, which
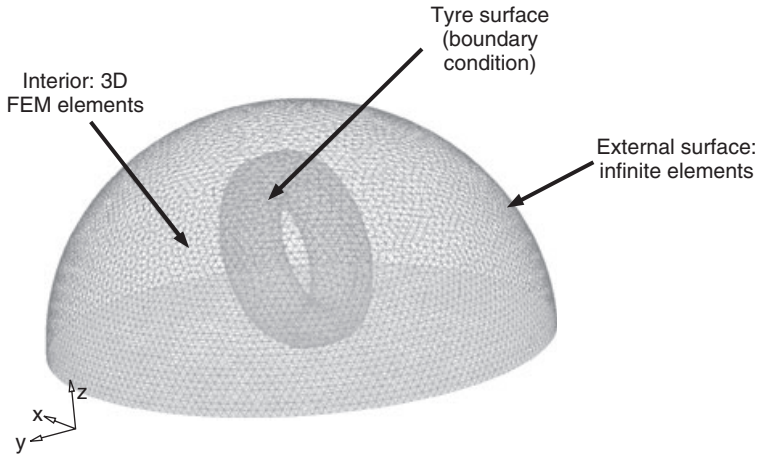
13.12 Infinite element model of a car's wheel (Fuccelli, 2006).

works very well for low and medium frequencies in an open acoustic field and allows one to easily apply specific boundary conditions for the acoustic treatments.

13.6.4 Statistical energy analysis (SEA)

All the previous methodologies are constrained by having an upper limit in the frequency range. For high-frequency airborne noise simulation, the most used and most reliable method in vehicle design is 'statistical energy analysis' (Lyon, 1995). The idea is completely different from the FEM, BEM or IEM methods. In SEA, the vibroacoustic problem can be linked to an equivalent thermal (or electrical) analogy in which vibration or acoustic energy is related to the temperature (or voltage). The whole structure and acoustic cavity system is considered as a network of subsystems coupled through joints. A subsystem is defined as a finite region with a resonant behaviour, involving a number of modes of the same type. Each subsystem's response is represented by a space and frequency band-averaged energy level. Based on the principle of conservation of energy, a band-limited power balance matrix equation for the connected subsystems can be derived, and easily resolved. Because of the reduced number of degrees of freedom of the models, SEA calculations are usually very fast (from a few minutes to a few hours), allowing fast analysis in the design phase. Moreover, the properties of the acoustic treatments can be described in detail, allowing reliable simulations. The validity of the SEA technique depends on a number of fundamental assumptions, and the extent to which they are justified in various practical situations is often difficult to deter-

mine and requires a certain experience. Furthermore, some of the parameters required in the application of SEA are difficult to obtain in certain situations and require some specific testing measurements.

13.7   Target setting and deployment on vehicle subsystems

The design of a vehicle's acoustic sound package can be divided into three main tasks. The first step is to define the global vehicle noise targets, the second is deployment of the subsystem's targets, and the final task is the design of the sound package for the given targets by an optimisation process. It is important to underline that the third step cannot be completed properly without the previous two steps of target setting activities, as a good sound package solution requires a good balance of the component's targets.

13.7.1 Vehicle noise targets

The first requirement for designing an acoustic package is knowledge of the global acoustic targets of the vehicle (Baret *et al.*, 2003). It is important that the targets should be well focused on the customer's requests, which are not easy for acoustic performance, as noise perception is strongly subjective. For this reason, vehicle makers usually conduct surveys among different customers and collect their judgements from testing different vehicles in different running conditions. The difficult part is establishing objective and measurable targets that are well correlated with the subjective judgements. This is obtained by measuring different acoustic data (such as sound pressure level, loudness, articulation index, sharpness, etc.) on the same vehicles and in the same test conditions as the subjective tests, and trying to find which measurement results correlate with the subjective judgements. This allows for definition of the vehicle noise targets under different running conditions.

13.7.2 Deployment at subsystem level

After setting up the previous global vehicle targets the second step is to cascade these global targets into sub-targets at levels of subsystems (components). This is important as the design process is much simpler if a given acoustic target is defined for each of the different subcomponents, which is often a requirement as some subcomponents can be designed or co-designed by different suppliers. As an example, the overall vehicle's acoustic target in a given condition is first divided into global structure-borne and airborne noise performance targets. If we consider the airborne noise target we can then assign a target for the sound isolation and sound absorption of each

component of the cabin (front floor, rear floor, baggage compartment floor, roof, firewall, etc.). This target definition is often obtained using the available simulation methodologies which allow one to find a good balance between the sub-targets, avoiding the risks of setting up too high or too low requirements to specific components that would result in final design solutions being not well optimised in terms of cost and weight. For the same reason, intensive benchmarking measurements and tests on existing vehicles are very common in this phase.

13.7.3 Target achievement and optimisation process of the sound package design

Once the acoustic targets have been defined, design of the sound package can start. The appropriate solutions and materials for both sound isolation and sound absorption have to be selected according to the given targets: specific experimental tests and numerical calculations allow one to verify the achievement of the acoustic requirements. A good design process must be focused on the optimisation of design solutions in order to find the best compromise in terms of acoustic performance, weight and cost. The cost must include not only the rough material cost but also the cost, time, problems and risks related to their application in the vehicle's production facilities.

13.8   Conclusions

In this chapter the relevant topics related to the vehicle's sound package design have been underlined. After a short introduction describing the sources and main paths of noise in a vehicle, attention has been paid to the two main solutions adopted for noise reduction, which are sound isolation and sound absorption. The chapter then described the material characteristics and measuring facilities in this field of application, and finally some of the solutions adopted in vehicle sound package design, including the target setting criteria and a short description of the available simulation methodologies for interior noise.

13.9   References

Baret C., Nierop G. and Vicari C. (2003), New ways to improve vibro-acoustic interactions between powertrain and car body, Graz, Austria, 2nd Styrian Noise Vibration and Harshness Congress
Beranek L. (1960), *Noise Reduction*, New York, McGraw-Hill
Beranek L. and Ver I. (1992), *Noise and Vibration Control Engineering, Principles and Applications*, New York, Wiley-Interscience

Danti M., Nierop G. and Vigé D. (2001), FE simulation of structure-borne road noise in a passenger car, Lake Como, Italy, NAFEMS World Congress

Danti M., Nierop G. and Vigé D. (2005), A tool for the simulation and optimization of the damping material treatment of a car body, Traverse City, MI, SAE NVH Conference

Fuccelli A. (2006), Metodologia numerico – sperimentale per l'analisi del rumore di rotolamento di un pneumatico trasmesso per via aerea, MSc Thesis, Torino, Politecnico di Torino, Italy

George A. (1990), Automobile aerodynamic noise, SAE paper 900315

Lyon R.H. (1995), *Statistical Energy Analysis of Dynamical Systems: Theory and Application*, Cambridge, MA, MIT Press

Maquet T. (2005), Étude de l'influence du matériau et de la géométrie du passage de roue sur la propagation acoustique du bruit de roulement, MSc Thesis, Compiègne, Université de Technologie de Compiègne, France

Mezzomo F.F. (2003), Determination of the acoustic transparency in laminated glasses, MSc Thesis, Torino, Politecnico di Torino, Italy

Roger M. (1996), *Fundamentals of Acoustics*, von Karman Institute for Fluid Dynamics, Lecture Series 1996–04

Vigé D. (1999), Modelli predittivi di campi aeroacustici per applicazioni automo-bilistiche, MSc Thesis, Torino, Politecnico di Torino, Italy

Vigé D., Bonardo E., Chiesa L., Vanolo M. and Vicari C. (2008), An hybrid experi-mental–numerical methodology for the prediction of the external rolling noise in running conditions, Graz, Austria, Styrian Noise, Vibration and Harshness Congress

14

Noise and vibration refinement of chassis and suspension

B. R E F F, Ford-Werke GmbH, Germany

Abstract: Today, people spend more time in their cars, as average traffic speeds are reduced while distances travelled increase. So noise and vibration performance gain in importance, while the car should still offer an active driving experience in case the road allows. This chapter deals with the influence of the suspension type and the adjustable suspension parameters upon the achievable refinement. Special insight into the acoustic properties of tyres, suspension components and isolators is given, including from the viewpoint of tuning, weight restrictions and other expectations.

Key words: road NVH, road-induced noise, comfort, impact, tyres, isolation.

14.1   Introduction

Nowadays, many people drive longer distances in their cars, partly for private purposes, partly for commuting to and from work. With average speeds tending to decrease, people are spending more time in their cars, so comfort in the vehicle is becoming more important. People want to be transported as comfortably as possible with little tiredness, while the vehicle should still offer an active and agile driving experience in situations when traffic allows it.

The focus of this chapter is on noise and vibration optimization of the chassis. This area contains all the audible responses that are due to the vehicle rolling on the road, and also the respective vibrations, as perceived by the driver and passengers. The lower frequencies of these local vibrations overlap with the low-frequency motions of the full vehicle on undulating roads, which are known as ride comfort. This overlap is in the range of the so-called secondary ride, which spans frequencies from 3 to 20 Hz. The resulting responses can be airborne or structure-borne, as well as the excitations. The area of chassis refinement is also called 'Road-induced NVH' where NVH stands for noise, vibration and harshness (with reference to the exciting source, in contrast to, e.g., 'powertrain NVH'). In this chapter, 'road-induced NVH' and 'chassis refinement' are used synonymously.

318

All items that are relevant for the attenuation of other structural or air-borne excitations (e.g. powertrain noise) are also relevant for road-induced NVH. Also, all foundations of the body treatment for increased isolation as well as for radiation control and sound attenuation or absorption are also valid for road-induced NVH. Hence, the reader is asked to refer to the respective chapters in this book. Many relevant topics can be mentioned, but most topics must be kept very short, so that the references given at the end of the chapter should be used to go into more detail.

14.2   Road-induced noise, vibration and harshness (NVH) basic requirements and targets

14.2.1 Load cases: cruising versus impact

Typically a cruising condition is the vehicle excitation due to the road surface texture and the tyre–road interaction, and is regarded as time-invariant. An impact condition is due to single or repeated events. Cruising data is mostly analysed in the frequency domain by means of a stationary frequency analysis. A constant-bandwidth analysis by means of a fast Fourier transform (FFT), usually as an autopower spectral density (PSD), gives detailed information about the frequency content, e.g. resonances, and allows analysis of the root cause by comparing auditory or tactile response with chassis accelerations, forces, etc., or by means of more sophisticated approaches like transfer path analysis (TPA); see also Section 14.2.3. TPA is based on the assumption of linearity around a working point of all relevant systems and components, which can be expected as long as the road excitation levels are not too high. Impact data can be analysed in the time domain as well as in the frequency domain. The time domain analysis can take into account non-linearities in the suspension due to larger chassis deflections, because all non-linear relationships can be displayed correctly (e.g. force over deflection in a chassis bush).

In order to additionally obtain frequency domain information, which is very helpful in tracing back for resonances, it is not sufficient to simply apply a kind of FFT on a time record of a microphone or acceleration responses. In order to enhance the poor frequency resolution of a short time history of an impact response, sophisticated techniques are required to separate front and rear suspension responses as well as to average away undesired uncorrelated noises by triggered averaging of several measure-ment runs over one type of impact. Due to the time-variant and finite character of the signal, the analysed spectra are energy spectral densities (ESDs).

Figure 14.1 shows examples of the time history and the spectra for cruis-ing and impact load cases of a C-car vehicle. Note that in order to show the
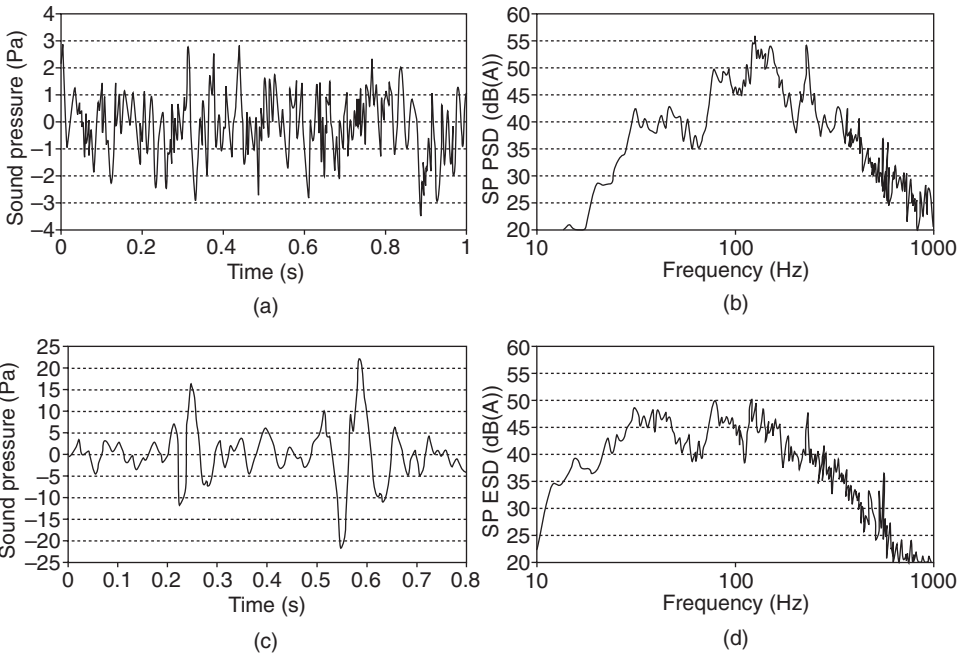
14.1 Time history and frequency responses for cruising and impact cases: (a) time history, cruising; (b) frequency response, cruising; (c) time history, impact; (d) frequency response, impact. PSD = autopower spectral density; ESD = energy spectral density.

stochastic characteristics of the cruising excitation, the time history of the signal spans only one second, which is, of course, much too short for a statistically relevant analysis. Similarly for impact, the response for only one impact event is shown – one local peak for the front suspension hitting the impact, and one for the rear suspension. The frequency content shown is an average of several of these events. With regard to the spectral content, both excitation types resemble one another in the frequency analysis but have different spectral balance. In addition, due to the non-linearities of the vehicle that are especially relevant for the impact case, the relative amplitudes of different peaks will be different between both excitations, and slight frequency shifts can also occur.

14.2.2 Road types and spectra

Public roads show a large span of excitation levels and spectra (Fig. 14.2). Textural levels vary from smooth asphalt surfaces with subjective dominance of tyre airborne noise through coarse aggregate chipping surfaces, which are subjectively dominated by low-frequency structure-borne noise,

(a)   (b)   (c)
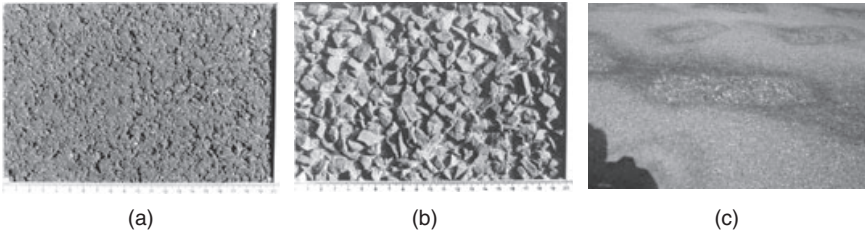
14.2 Examples of (a) smooth, (b) coarse and (c) rough surfaces. Smooth and coarse: macrotextural view (20 × 13 cm); rough: inclined view on area approximately 1 × 1.5 m.
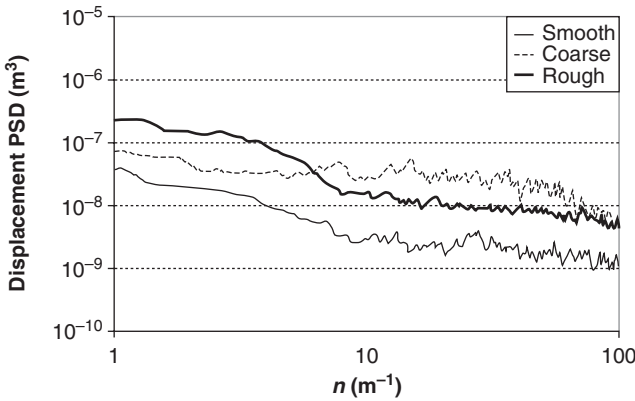
14.3 Spectra of smooth, coarse and rough surfaces.

up to rough surfaces with bumps, holes and undulations, which are often a combination of a constant cruising load case with arbitrarily repeated single events.

The amplitude of road excitation spectra (Fig. 14.3) usually decreases with frequency, but the slope can differ between the surfaces, and also some wavenumber ranges may be emphasized by, e.g., road manufacturing issues, or pavement structures such as Belgian Blocks.

For setting spectral targets for interior road noise and cascaded quantities, it is important to know the properties of the reference surface, which should have a smooth spectrum. Only if this is given can one identify peaks in the response with vehicle root causes, rather than seeing a quite undefined mixture of road excitation peaks and vehicle responses. Figure 14.4 shows a surface which is not optimal for development purposes, because it creates a high vehicle response around 90 Hz due to its uneven spectrum.
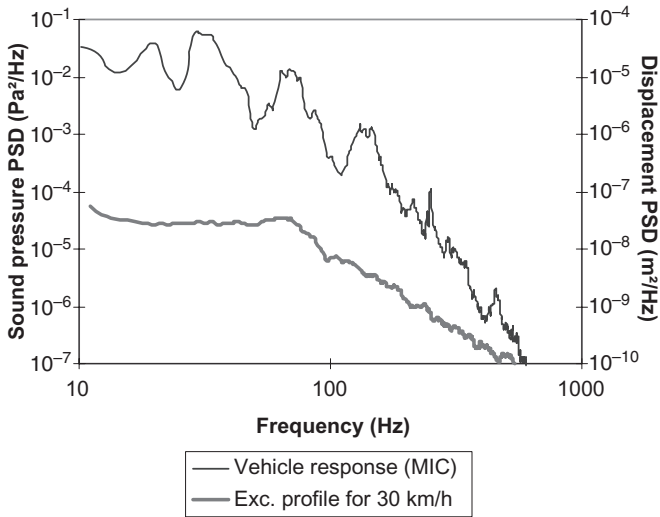
14.4 Comparison of road excitation spectrum and resulting interior noise. Note that the area around 80 Hz is emphasized not due to the vehicle, but due to the road.

14.2.3 Target quantities for full vehicle and target cascading

On the full vehicle level, aural as well as tactile responses can be targeted. The aural responses are sensed by microphones or acoustic heads, the tactile responses by accelerometers, e.g. at seat track, steering wheel, gear lever, pedal box, etc. The quantities can be frequency spectra, band levels, overall levels or characteristic values of the time history of the responses. Spectra can have an equally spaced, narrowband *x*-axis, which enables tracing back resonances and combination with narrowband transfer functions, or can have fractions of an octave (typically three or 12, rarely 96) as the *x*-axis. A 1/3-octave analysis results in better correlation to the subjective spectral balance, while a 1/12-octave achieves almost the frequency resolution of a narrowband FFT for lower frequencies but still shows lower 'noise' in higher frequency ranges. Lower frequencies are dominated by structure-borne noise, higher frequencies by tyre airborne noise; the borderline is between 400 and 800 Hz, depending on speed and road. All of these considerations are summarized in Fig. 14.5 and Table 14.1.

Many applications exist which calculate complex quantities from the measured physical values for sound pressure or acceleration. These complex quantities are able to better correlate to subjective perception, but usually are hardly cascadable, especially when reduced to two or even one dimension. Examples are psychoacoustic loudness, articulation index (AI), and values describing human tactile perception.
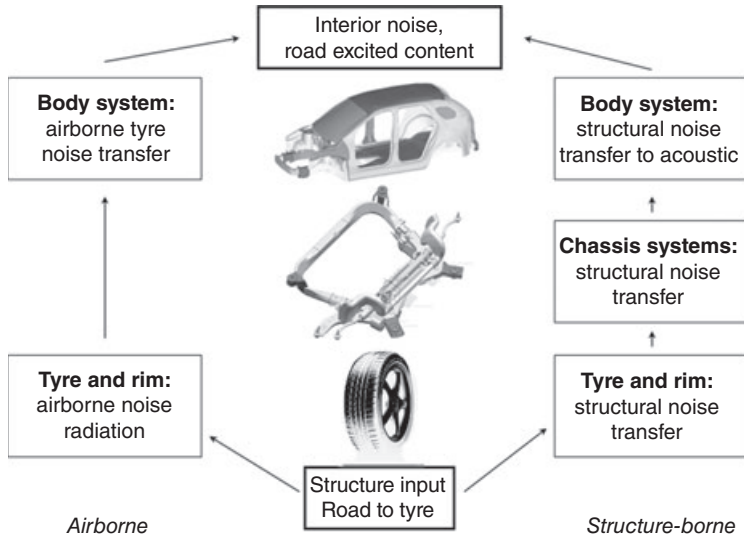
14.5 Vehicle systems cascade.

Table 14.1 Vehicle targets and cascaded targets (generic)

System	Structure-borne noise	Airborne (tyre) noise	Vibrations
Full vehicle	Interior noise spectrum for coarse road	Interior noise spectrum for coarse road	Vibration levels/spectra at comfort points
Body system	NTF (Pa/N)	NTF (Pa/Pa)	VTF (m/s^2/N)
Chassis system	VTF (N/N)*	n.a.	VTF (N/N)*
Tyre–rim system	Spindle force for coarse road	Nearfield noise (Pa)	Spindle force for coarse road

*Different units possible, depending on approach.

14.3 Foundations of road-induced noise, vibration and harshness

Three fundamentals are defined for the vehicle potential of road-induced NVH performance. The first is the suspension concept, to be chosen in the framework of vehicle class, performance targets, manufacturing restrictions, existing vehicle platform requirements, and specific desired performance profiles (e.g. handling versus comfort dominated). This defines the range of the final refinement performance. Of course, the refinement ranges of different suspension types overlap. Secondly, within a specific suspension

concept, the achieved kinematics can vary quite a lot. As an example, the damper position can be very different. The lower attachment position of the damper and its inclination influence the damper ratio, the ratio influences the required upper attachment mount stiffness, and this together with the mount design and the attachment stiffness of the vehicle body defines the degree of noise isolation at the damper path. Thirdly, only the tuning of the components enables the greatest compromise to be achieved between a concept and its kinematics. Such a compromise may partly compensate for weaknesses of one of the other foundations.

We start with some details of the concepts and the kinematics. The component potential is handled in Sections 14.4–14.6.

14.3.1 Suspension concepts

In the first instance, the list of functional requirements to a suspension is quite complex: see Table 14.2 for a rear suspension (it is similar for a front suspension, plus some additional steering-related items).

Table 14.2 Key requirements for rear suspensions

Factor	Requirements
Camber, castor, toe	Toe and camber low for tyre wear. Toe adjustable with minimal effect to camber (enabled by low castor angle).
Bump camber	(Negative) camber angle should increase with bump travel.
Roll centre	Roll centre not too high for straight-ahead stability.
Longitudinal wheel recession	Wheel should move rearward at bump travel for good impact harshness.
Longitudinal compliance	In addition the suspension should be compliant in the longitudinal direction.
Aligning torque compliance	Suspension should be stiff around the wheel z-axis to provide understeer for higher pneumatic trails (robust for varying tyre widths).
Lateral compliance steer	Toe-in under lateral forces is required for cornering stability, especially for RWD vehicles.
Longitudinal compliance steer	Toe-in under braking forces is required for brake in turn stability.
Camber compliance	High camber stiffness or lateral stiffness is required for straight-ahead stability, steering feel and high agility.
Castor compliance	Castor change under braking or lateral forces to be minimized to increase stability and minimize shake and brake judder.
Anti-lift, anti-squat	High anti-lift and anti-squat are required to minimize vehicle pitch at braking and acceleration.

Source: Zandbergen (2008).

Table 14.3 Suspension load cases

Case	Regarded frequency range	Directions of excitation at tyre	Transfer directions through suspension[1]
Road NVH	20–500 Hz[2]	z, x	z, x, y[4]
Cornering[3]	Steady state	y	y, (x, z)[5]
Ride	0–30 Hz	z, x	z, x (y)[5]
Braking	Steady state	x	x, z[6], y[5]

[1] Directions of secondary importance in brackets.
[2] The upper limit of the relevant range is dependent on road and speed.
[3] The term 'cornering' was chosen, because 'handling' comprises more than the steady-state cornering situation, which should be discussed here.
[4] The transfer of the road NVH tyre input into the lateral suspension direction can be reduced by higher compliance in the *x*-direction and optimization of lever arms within the suspension, especially at the knuckle.
[5] Including vehicle reaction.
[6] Transfer into *z* due to braking moment and resulting dive/lift.

In order to provide sufficient potential for noise and vibration refinement and ride as well as for handling and steering, an essential approach comprises the kinematic decoupling of the suspension's reaction to different inputs. The input types in this case are the vertical (road profile), longitudinal (braking/accelerating, impact) and lateral (cornering, aligning) forces that are acting upon the tyre patch. The different concepts with countless variations in execution support this approach to different degrees. In order to get this sorted, we introduce different load cases as shown in Table 14.3.

We see that although a specific direction is hardly excited at the tyre patch, it might be generated in the suspension (for example, the very important *y*-direction for road-induced NVH). This is an effect resulting from the static geometry, independent of the modal properties of the components, which also 'creates' vibrations in directions that have not been directly excited (see Section 14.5). There is some overlap between the load cases, e.g. between ride and road-induced NVH. Most relevant for the decoupling of suspension reactions, hence for the refinement potential, are the 'road NVH' and the 'cornering' load cases. As an example, we look at the potential of three different trailing arm rear suspension concepts, and additionally two advanced concepts. The so-called 'trailing arm concepts' have a longitudinal arm which is mounted with a bush directly to the vehicle body, while the 'advanced' concepts carry also the longitudinal input within the isolated subframe. The variants span over different vehicle classes, so in real life one may have to do such a comparison with a different set of concepts, and with more parameters. Note that for the 'road NVH' load case the cruising and the impact excitation is summarized.

Table 14.4 Reaction forces of rear trailing arm suspension concepts
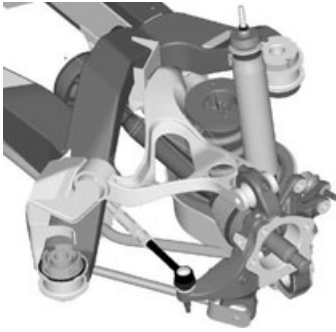
Component	Twistbeam	Quadralink – McPherson	Trailing-arm SLA
Longitudinal arm bush	Road NVH; cornering: *x, z; y*	Road NVH: *x*	Road NVH: *x, z*
Bushes lower lateral arms/ semi-trailing arm	n.a.	Cornering: *y*	Cornering: *y*
Bushes upper lateral arms	n.a.	n.a.	Cornering: *y*
Top mount	Road NVH: *z,* [*y, x*]	Road NVH; cornering: *x* and *z*, [*y*]; *y*	Road NVH: *z,* [*y, x*]

Note: The *x*, *y*, and *z* directions are in global coordinates, with secondary directions or directions created in the suspension in square brackets.

The three chosen concepts of Table 14.4 all show a relatively simple geometry, compared to advanced suspensions which may have arms located at various angles to all axes and so are less easy to understand. Also for these complex geometries, it is a valid approach to separate load cases into different components and directions of the reaction force, but we may have to reorganize the table syntax: see Table 14.5. Details of the influence of all single kinematic parameters are found in Zandbergen (2008).

Note that for these advanced suspensions, the concrete geometry largely influences the contributions of bushes and directions. If, for example, the upper arm of the 4-link shown is changed to a pure L-arm, the *x*- and *y*-contributions change significantly. So in order to make a really detailed comparison of options, you need to think about the geometry carefully, and need to fully explore the constraints of the installation. Once these are known, one can dive deeper into, e.g., the capabilities of a trailing-arm SLA versus a 4-link suspension, by comparing, for example, kinematic recession, longitudinal wheel recession, parasitic wheel rates from rotational and cardanic bush loads, etc. Also kinematic and elastokinematic properties which are primarily important for vehicle dynamics, such as bump steer (toe versus vertical wheel travel) and camber steer (toe versus sideforces), but which indirectly influence refinement, need to be taken into account (see also Table 14.2).

Table 14.5 Reaction forces of advanced rear suspension concepts

Load case	Integral link	4-Link
Cornering	UCA: *y* LCA front: mainly load-free LCA rear: *y* [TL: *y*]	UCA front & <u>rear</u>: *y* (<u>rad</u>, ax) [FLA: *x-y* (rad)] LCA: *y* [TL: *y*]
Road NVH	LCA front: *y* (esp. for impact), [*z*] LCA rear: rot(*z*), [*y*], [*z*] IL: *z* TM: *z*	UCA front: *y* (<u>rad</u>) UCA rear: rot(*z*) FLA: *x-y* (rad) [LCA: *y*, *z*] TM: *z*
Remarks	• Geometry shown has a soft LCA front bush, and a stiff LCA rear bush or balljoint, separating longitudinal and lateral response characteristics. • Stiff integral link bushes support braking and also driving torque (for all-wheel-drive), as well as *z*-reaction upon impact, enabling soft LCA bushings without suspension winding up.	• Both road NVH and cornering forces are supported by the arrangement of FLA, LCA and UCA bushings, but with different contributions from radial and axial directions.
Abbreviations	TL: toe link (front lower arm) LCA: lower control arm, with front and rear bushes UCA: upper control arm IL: integral link TM: top mount	TL: toe link FLA: front lower arm (diagonal) LCA: lower control arm (spring link) UCA: upper triangular arm, with front and rear bushes TM: top mount

Note: The *x*, *y* and *z* directions are in global coordinates, dominant directions are underlined, and secondary directions or directions created in the suspension are in square brackets; 'ax(ial)', 'rad(ial)' and 'rot(ational)' refer to the affected bushings. Resulting moments are resolved into the reaction forces.

14.3.2 Achieved kinematics and vehicle topology

Having chosen a suspension concept, it is necessary to work on the concrete design in order to get as much as possible out of the concept. One parameter is kinematics, where especially the kinematic wheel recession plays an important role in realizing the concept's potential. For large road excitations such as in impact, but also for smaller load cases, it is important that the kinematics allow the wheel to move backwards when the road undulations hit the tyre. This can be achieved for a suspension with longitudinal links by positioning the front pivot point sufficiently above the wheel centre, otherwise the x-axis, around which the knuckle is rotating for jounce, must be inclined. That is called a negative wheel recession (due to the coordinate system with the positive x-direction in the forward driving direction), and it softens the load peaks in the suspension, and hence the noise and vibration response. In the case of a positive wheel recession, the wheel is forced to move forward, i.e. into the bump, when the suspension goes into the jounce direction, and this largely increases the impressed knuckle acceleration (see Fig. 14.6). Even if large bush compliances can reduce the severity
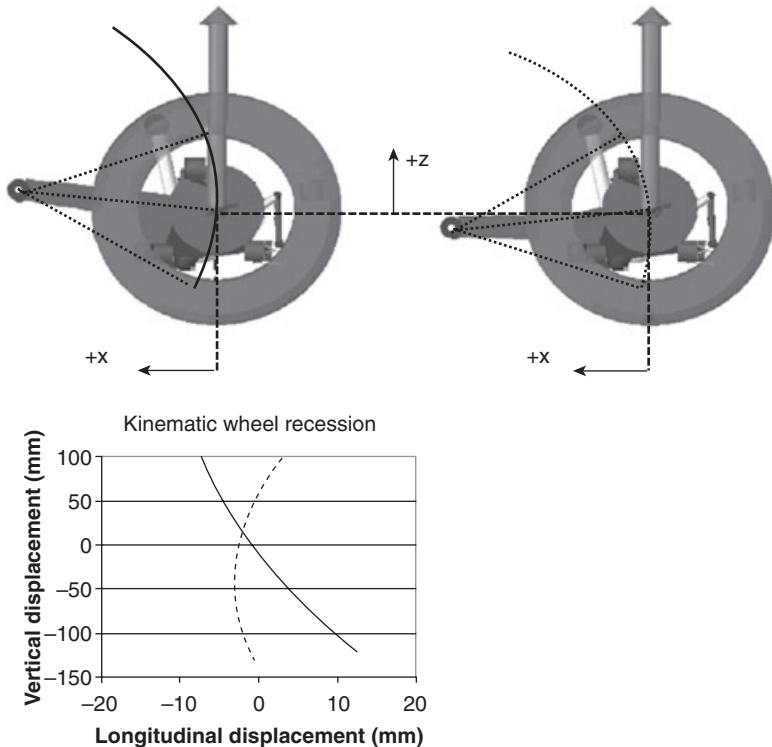
14.6 Wheel recession curve. Two different heights of the trailing arm front bush, leading to different kinematic wheel recession.

of such a geometry, the basic disadvantage will remain. For a detailed introduction into the suspension kinematics, see Arkenbosch *et al.* (1992).

Another parameter is the working environment of the damper. A damper has to damp away undesired oscillations and overswings of the unsprung masses. To build up damping forces, the compliances of the damper connection to the driving suspension and to the body need to be low enough to force the damper to break free at forces as low as possible, otherwise the suspension vertical motion would easily be stored in the bottom or in the top mount of the damper and given back to the suspension as kinematic energy, rather than creating damping forces in the damper. This can create a floating ride, undesired vertical abruptness of the car, or non-linear steering behaviour.

Parameters which support this requirement are a stiff connection of the lower damper end to the suspension, and sufficient stiffness of the damper top mount, which subsequently requires a stiff body structure to allow isolation of noise transfer, and a good damper ratio. The damper ratio describes the relationship between the vertical travel of the wheel centre and the deflection of the damper. The target for the suspension is usually to be as close as possible to a factor of 1. Values lower than 1 reduce damper travel and hence velocity, and so require damper forces (as a function of damper velocity) to increase accordingly by the square of this ratio. In most cases this requires one to stiffen the top mount accordingly, to ensure sufficient initial damper forces at the wheel. Having the top mount stiffened for these reasons, we are back into the isolation dilemma: the stiffer the top mount of a damper, the stiffer the body attachment needs to be in order to provide sufficient isolation capability. Formerly, a rule of thumb was to achieve a stiffness ratio of 10 between the structural environment and an isolator (i.e. bush or mount) to be on the safe side. Often, this is not achievable today, which makes many designs sensitive to small changes in the impedance of the mounts and the connected chassis and body components. Note that these basic relationships, due to the three-dimensional vibrational capability of each structure, are valid not only in the vertical but also in all three spatial directions.

In other words, we always have to see the full picture: a better concept may lose its advantages when kinematically not optimized. Because many design constraints for the suspension are imposed by the basic vehicle topology with regard to package, underbody geometry, manufacturing capabilities, etc., in some cases a more basic suspension with a refined geometry can perform better than a highly sophisticated concept with constrained kinematics.

While wheel recession directly influences chassis refinement, there are many other kinematic parameters that indirectly can degrade or improve comfort, because every suspension has to guarantee safe driving under all

circumstances. These days, this is mostly identified with a defined under-steer in all conditions. Therefore, it is required to choose the geometry of arms, links, stabilizer bars and bushes in such a way that an internal or external input that deflects the suspension (symmetrical and asymmetrical jounce and rebound wheel deflection, braking and accelerating, cornering, and combinations of all these) will always lead to a toe-in of the affected axle. This can lead to some bushes being stiffer than appropriate for comfort. An example is the pivot bush of the twistbeam suspension, which is much stiffer than the corresponding longitudinal arm bushes of other suspensions such as SLA and Quadralink, in order to reduce the undesired rotation of the complete suspension around a vertical axis in case of cornering.

14.4   The tyre: the most complex component?

The tyre is clearly a very special component. It is the component with the shortest lifetime, because it needs to be replaced several times during a vehicle's lifetime. It has many contradictory requirements with regard to safety, durability, dynamics, comfort, environment, etc. And everything the driver wants from a car, whether at 20 or 200 km/h, needs to be transferred to the road by four areas each only the size of a palm. Although the customer often does not value these high-tech components adequately, he or she surely recognizes the individual noise and vibration performance of different tyres after they have been changed.

For the vehicle manufacturer, the tyre is a very powerful component due to its ability to fine-tune aspects of comfort and driving dynamics, but at the same time it is a very difficult component to manage because it interacts with so many of the full vehicle's properties, such as fuel consumption, cost of ownership, brake performance (safety!), etc. Figure 14.7 shows the
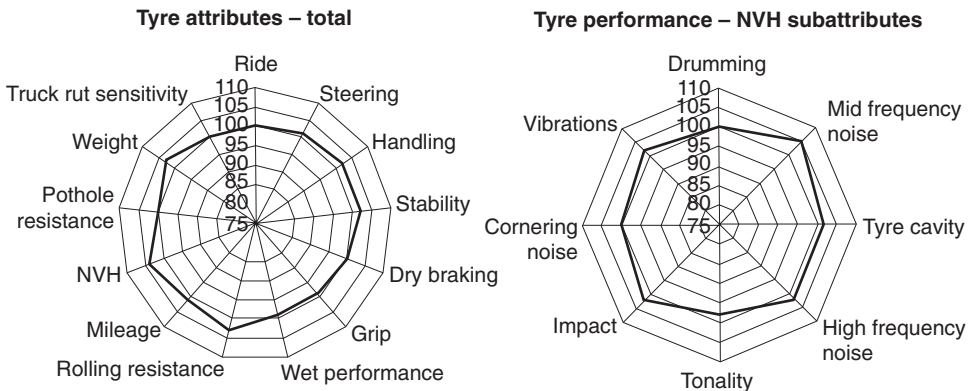
14.7 Tyre performance attributes.

attributes in total, of which NVH is only one of many, and a list of the NVH subattributes.

This section concentrates on the audible noise aspects of the tyre, rather than on the large field of fundamental vibrations at tyre orders (harmonics of the tyre rotational frequency), which is connected, amongst other parameters, to tyre and wheel imbalance and non-uniformity. For balancing and matching, refer to Chapter 16 and Arkenbosch *et al.* (1992, p. 295).

14.4.1 Basic NVH properties

For road-induced NVH, we can differentiate three frequency regions relevant to structure-borne tyre noise: below the first vertical tyre mode, between this and the tyre cavity resonance, and above the latter. In a simple word, for excitations below the first vertical mode, the tyre reacts as a stiffness because the excitation is undercritical. Beginning with the frequency of the first vertical mode, the tyre begins to isolate road excitation similarly to an overcritically excited spring–mass system. From this frequency on, the modal properties are dominated by radial belt modes. This extends up to the first resonance of the air within the tyre torus, when one wavelength of a sine fits in the inner circumference. Above this, more local modes appear which have less impact on the noise transfer.

The following sections deal with the excitation mechanisms and specific dimensional or attribute-related effects that influence these modal properties to differing degrees, or influence the direct radiation of tyre airborne noise.

14.4.2 Excitation types

The tyre–road interaction can be very complex. Depending on the type of surface, different excitation types dominate. Not only is the texture of the road exciting the tyre, but even on a road as smooth as glass there are effects introducing vibration into the tyre and radiating airborne noise. While many tyre properties are interacting intensively, it is hardly possible to isolate one excitation type and optimize the tyre and the subsequent noise for this type alone. Nevertheless, we will briefly illustrate the different types of underlying physics and how to utilize these. There are not only excitations of the tyre from outside the borders of the tyre component, but also effects that amplify the mechanical noise transfer through the tyre to the rim or that directly create radiated airborne noise. Note that only the first three items listed are excitations in a strict understanding; the other effects either refer directly to the airborne noise radiation of the tyre, or amplify the mechanical noise transfer through the tyre to the rim. For details see Sandberg and Ejsmont (2002, Chapter 7.1).

Road texture

The road texture deflects the flat geometry of the footprint. Even without any resonances of the tyre system, these deflections would lead to mechanical noise transfer throughout the tyre as a forced response towards the rim, exciting structure-borne noise in the vehicle. The main influence in this effect is the enveloping properties of the footprint, i.e. how well the footprint isolates the full tyre against the macrotexture of the road. This, of course, is not a simple parameter in the tread compound or in the mechanical structure of the tyre, but is already a very complex property. Often this term is referred to for the excitation type of a deterministic cleat or an impact in general, but it is also valid for the statistical input of the road texture.

Block impact (leading end, snap-in)

At run-in, the tread blocks hit the road. This impact creates vibrations in the tread and belt and also in the sidewall. A too regular impact sequence of the pattern can create tyre whine. This can be influenced by the distribution of the blocks, which not only should be of varying length over the circumference, but also should not have parallel edges in the different parallel pattern rows. In addition, the imprint of the tyre patch on the road shows differences: elliptic footprints are much quieter than rectangular ones.

Adhesion (trailing end, snap-out)

At run-out, the tread blocks tend to adhere to the surface. Once these adhesive forces are overcome, the blocks contract from their elongated condition back to the nominal geometry in an oscillating, damped motion, creating radial and tangential belt excitation.

Friction and stick–slip effects

The deformation of the tyre patch and the force distribution in the patch forces parts of the patch to slightly slip over the road. This is in most cases a steady stick–slip process, creating tangential and radial tyre vibrations.

Groove resonances

Air is pumped out from the deformed lateral and circumferential grooves in the tyre patch. This pumping is repeated according to the groove

repetition sequence. Additionally, the frequencies for which the groove length forms a $\lambda/2$ pipe are amplified.

Helmholtz resonances

In circumstances like those above, when there is no groove leading to the outside with constant nominal dimensions, but a non-open lateral 'groove' between two tread blocks is being closed by the road while being run into the tyre patch, the decreasing coupling volume between the groove and the outside works as a resonance tube of a Helmholtz resonator. This refers only to airborne noise and cannot be avoided, but it may be distributed in frequency range and occurrence coincidence with all the other Helmholtz resonances, which run in parallel, by optimizing the tread pattern and footprint.

Horn effect

The tyre's outer shape in run-in and run-out, together with the road, forms a kind of horn, which amplifies the radiation in these directions. Depending on the tyre size, this may affect a frequency band in the range of 800–1200 Hz (for car tyres). This effect is especially present on smooth roads and cannot be avoided, so it may require countermeasures in the tyre patch noise transfer function in case frequencies in this range become annoying in the vehicle interior.

Mechanical tyre resonances

These are not excitation mechanisms as the first three in this list are, but amplifiers to all structure-borne input from these effects. The belt is quite stiff in the tangential direction but flexible in the radial direction. As is common for a mechanical system, various vibration modes exist. Important for noise transfer are mainly those that create a force upon the rim. The resonances (of higher order) which – in theory – create a force equilibrium upon the rim can create airborne noise radiation of the sidewall or the belt, but no force input to the spindle, and so are of secondary importance. In real life, due to the limited symmetry of real systems and additional lever arms which can transfer a vertical excitation by the road into all other directions, higher modes of the belt still affect knuckle vibrations and interior noise.

In particular, the vertical mode of modal number 'zero' has a high importance, where the belt moves as a rigid ring against the sidewall stiffness. For passenger cars, it lies typically in the range of 80–100 Hz and transfers much energy into the chassis. Additionally, it defines the frequency above which the tyre works as a resonator of first order in the overcritical range,

Air pressure   Base frequency

$$f = \frac{c}{\lambda} = \frac{c}{2\pi r_e} \cong 230 \text{ Hz}$$
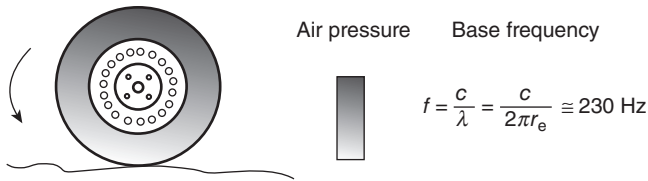
14.8 Tyre cavity resonance. A snapshot of the pressure distribution for the standing wave at the first tyre cavity frequency.

so improving the isolation against the road textural input with increasing frequency. Moving this frequency downwards is usually contradictory to steering and handling properties but gives large potential for a comfortable tyre. Belt resonances of higher order, in the frequency range above 100 Hz up to that of the tyre cavity mode, are also often visible in the interior noise spectrum, but the modal alignment to the rest of the suspension can be difficult due to the already increasing modal density in this area.

Acoustical tyre resonances

The tyre torus is a closed cavity, which is statically and dynamically deformed at the patch. The dynamic excitation of the patch leads to high broadband sound pressure in the tyre (up to 130–140 dB). This noise is amplified for wavelengths that form standing waves in the torus, returning to the patch after one circumference in the same phase. These frequencies show a super-elevation of 10–15 dB. The most important of these frequencies, as with structural resonances on page 333, is the one that forces the rim to move in the x–z plane: the first tyre cavity resonance (TCR), Fig. 14.8. For passenger cars, this resonance lies in the range of 190–240 Hz (for typical 14-inch to 19-inch tyre–rim combinations). To be correct, as soon as the tyre is loaded and subsequently deformed, the resonance splits up into two 'base frequencies' (as is normal for any not fully symmetrical mechanical structure), with dominance in x and z respectively (Fig. 14.9). Additionally, for rolling tyres the Doppler effect leads to a modification of the two peaks according to the rotation speed. One would expect both base frequencies to be modified according to the waves travelling in the forward and reverse directions. Interestingly, in most applications the lower base frequency shows only the lower sideband (the frequency decreasing with increasing vehicle speed), and the upper base frequency shows only the upper side-band (the frequency increasing with increasing speed). See Fig. 14.10 with measured data for a standard 205/50 R 16 tyre.

Two properties of the TCR make the noise created very annoying: tonality and time-variance. In contrast to most other noise forms, the TCR is very tonal and, in the interior noise spectrum, clearly rises as a sharp peak
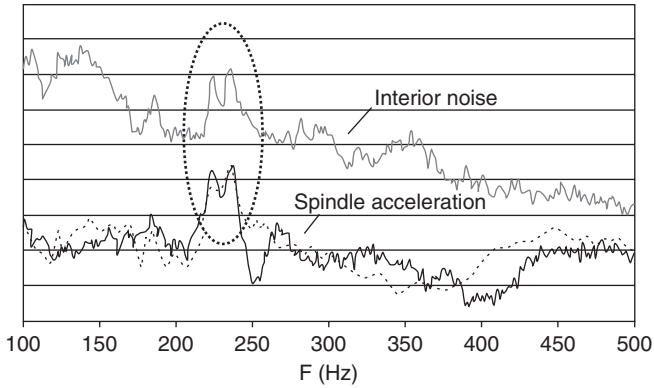
14.9 Typical interior noise and spindle acceleration spectra (*x* and *z*), showing the tyre cavity resonance.
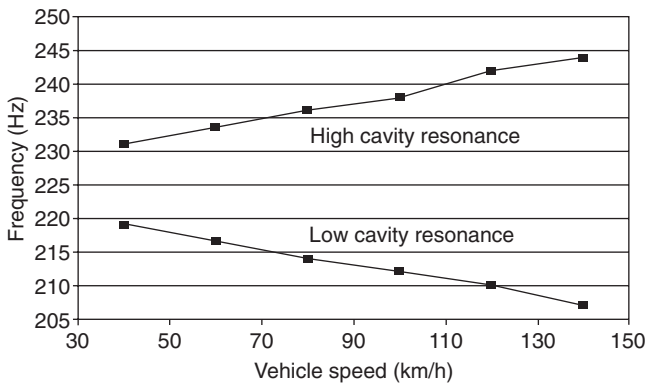
14.10 Tyre cavity resonance over speed.

above the frequency neighbourhood, so is not masked by other noises. Once perceived, the human ear becomes sensitive to it and easily finds it in every new driving situation. Additionally, often the tonal noise is not constant over time but swells up and down in loudness, being respectively re-excited with each new small impact and then ringing out (e.g. on worn concrete surfaces with lateral grooves or brushings). This modulation in the time domain additionally increases the audibility and annoyance of the effect.

The TCR reacts to changes of tyre/tread mass and to tread compound damping. It is more critical for tyres with a low aspect ratio, where the peak is sharper and higher. A perfect but quite unfeasible countermeasure for the tyre itself is a modification of the cavity properties. Introducing absorption into the torus has been tested by means of polyurethane foam (from various tyre and vehicle manufacturers), aluminium foam (Torra i Fernández,

2004) or a kind of fur whose fibres only stand upright and form an absorption volume under centrifugal forces, facilitating mounting (by Rieter and Ford Motor Company). None of these has yet made its way into mass production. Bridgestone published a modified rim with integrated Helmholtz resonators to absorb the resonance. The principle works well, but the rim is very complex and not yet in production. Modifying the cavity's medium is also an option. A helium filling basically only shifts the resonance instead of reducing its energy, but on the one hand, the modal density is higher at higher frequencies, reducing the annoyance of a specific resonance, and interestingly, also the amplitude of the resonance is lowered in most applications. Maybe the different ratio of chassis structure-borne sources to other noise sources may also help here.

Under real conditions, and also regarding the aftermarket, it is not very practical to use a medium other than air for the tyre, although helium has been used by some tyre dealers as a 'comfort filling'. This means that for refinement, we have to avoid any energy-rich suspension mode in the individual TCR range (which depends on the tyre sizes used, and in most cases refers to a speed range up to, e.g., 120 km/h, because for higher speeds the noise is usually masked by other sources). Also the isolation of all coupling elements between chassis and body needs to be evaluated carefully.

14.4.3   Performance dependency on dimensional tyre parameters

Width

Clearly, the airborne noise radiation increases with tyre width. The structure-borne noise excitation also tends to go up, but with many more possibilities for countermeasures from the choice of the compound and the inner structure of the tyre. This is valid for the cruising as well as for the impact condition. In most cases, an increased width comes together with a lower aspect ratio, in order to maintain the outer diameter of the tyre, so often the influence of these two parameters cannot be clearly separated.

Aspect ratio

The aspect ratio has more influence on structure-borne noise transfer. Even when it is not by definition a 'handling tyre', in order to maintain a safety margin for the impact case, the tyre sidewall can become stiffer, which can increase the structure-borne noise. Closely connected to this is the load capacity: with decreasing aspect ratio, the load capacity of the tyre decreases – see next section.

Maximum load capacity

The maximum load capacity for a tyre dimension is given by the standards of the ETRTO (European Tyre and Rim Technical Organisation), quoted, e.g., by Sandberg and Ejsmont (2002, p. 71). For example, the maximum load for an index of 92 is 630 kg, and for 106 is 950 kg (as examples for passenger car tyres for light and heavy vehicles). These values always refer to an inflation pressure of 2.5 bar. A lower pressure reduces the load capacity, as does the switch towards lower aspect ratios (by reducing the load index with constant tyre width and diameter). The latter tendency leads to the frequent need to upscale the load capacity for a given tyre dimension by stiffening the tyre structure (so-called 'reinforced tyres' or 'extra load (XL) tyres') and/or increasing the tyre pressure. While increasing the tyre pressure always leads to a loss in noise performance and often in ride performance, reinforcement can have a positive effect on road-induced NVH due to more tread mass.

Maximum speed

As tyres for higher speeds need, roughly speaking, to be stiffer in order to limit the total losses and so the tyre heating, refinement properties will worsen. Note that, as with load capacity, not all speed variants of one tyre type as offered in the market are really different, but they may be labelled differently only to support all market-relevant categories with a few different tyre designs. The actual influence of speed on the tyre's dynamic spring rate was reported to be greater than the influence of tyre construction with different load capacities (Gent and Walter, 2005).

14.4.4 Other relevant tyre parameters

Radial spring rate

This rate is usually the static spring rate of the inflated, loaded tyre in the vertical direction, with deflected patch and measured spindle response. This can usually be detected on a static isolated wheel as well as on a kinematic-and-compliance rig, using a full vehicle. Dynamic data from standing or rolling tyres can differ noticeably from the static values (Gent and Walter, 2005). This has to be taken into account when comparing data from different sources.

The static spring rate for passenger car tyres can vary between 150 and 300 N/mm, but is typically around 200 N/mm. The higher values are often reached for reinforced/extra load tyres, low aspect ratios or high speed variants. Higher values are connected with a worse enveloping capability, but in case this is due to a larger mass in the tread (e.g. for reinforced tyres)

these tyres do not need to be inferior compared to softer tyres, at least for the cruising situation.

Inflation pressure

The influence of inflation pressure on cruise and impact excitation is clearly important. Values for the correlations vary depending on the speed and the road surface, spanning from 0 to 0.2 dB(A) per 0.1 bar for the overall level and up to 0.35 dB(A) per 0.1 bar for specific, structure-borne relevant frequency bands. This dependency affects measurement repeatability and accuracy during development with regard to the nominal value of the pressure as well as the real road value after warm-up. Note that the inflation pressure also influences handling, safety, fuel economy and ride, in most cases contradicting the noise and vibration refinement properties.

Rolling resistance

As any material damping transfers deformation energy into heat, it increases rolling resistance. However, rolling resistance increasingly stands at the focus of efforts to reduce fuel consumption. In the US market, the customer already has an eye upon the tyres' rolling resistance, as this is a parameter that is also monitored by the very popular customer surveys. In the European Union, from around 2012 tyres will be labelled for their rolling resistance in the same way that refrigerators are for their energy consumption. By then at the latest we can expect similar customer attention in the European market. Currently, each 10% of rolling resistance reduction marks a 'new generation', and at least the first tyres that achieve the respective 'next generation' can be expected to be inferior in noise and vibration refinement to their predecessors. As an example, for a CD car, a delta of 4% in rolling resistance can affect fuel consumption by 0.4 litres per 100 km. This illustrates the importance of the parameter, and we may find that improvements in noise and vibration refinement via the tyres get more and more difficult in the coming years.

Non-uniformity and force variation levels

Due to their internal structure and manufacturing technology, tyres have limited uniformity. Non-uniformity is mostly monitored by radial and lateral force variation measurements and rarely also by tangential force variation. Data for the overall value as well as for the values of the first, second, etc., harmonic can be established. As with tyre imbalance, this can create low-frequency vibration and/or issues related to the first or second order of the variation, or interference with the spectral lines of existing

modes respectively via modulation or beat (especially for driveline frequencies). For details of root causes and measurements, see Gent and Walter (2005).

Imbalance

Similar to non-uniformity, tyre imbalance can lead to audible or tactile low-frequency issues and can create steering wheel nibble, which is the undesired oscillating rotation of the steering wheel, also influenced by elasticities in the steering system and the damping of the front suspension (i.e. the vehicle sensitivity). It can also be created from imbalance in the rear suspension, such as rear brake discs. For details see Gent and Walter (2005).

Interaction with the rim (matching)

For the last two effects – tyre non-uniformity and tyre imbalance – there is an interaction with the limited symmetry of the wheel. This can increase the problem but sometimes also gives the opportunity to match the tyres to the wheel, reducing the initial issue. This is achieved by rotating the tyre with respect to the rim to minimize force variation with respect to imbalance. For details see Chapter 16. Another method consists of grinding away material at the position of the force peak in the first radial harmonic. This is no longer used much and has been mostly replaced by matching. For a more detailed view on the dependency of noise performance and other tyre attributes upon the *internal* tyre construction parameters, see Arkenbosch *et al.* (1992, p. 222).

14.4.5 Run-flat tyres

Run-flat tyres may be driven deflated for a considerable distance without damage, until the vehicle is in a safer environment for changing the tyre. Although safety clearly increases, because dangerous tyre changes near fast-moving traffic or in unsafe neighbourhoods are no longer required, noise comfort with current run-flat tyres mostly decreases noticeably. This is true especially for the common variants that support the deflated tyre by stiff sidewalls and reinforced bead areas. Derivatives that support the tyre with a metal ring on the rim, working together with standard tyres or only slightly modified ones, are superior here but are only available for luxury vehicles due to their cost. In general, the increased stiffness can increase noise transfer in the 80–200 Hz region but has potential to noticeably decrease the excitation of the first tyre cavity mode. So, even when the overall performance of the run-flat tyre may be similar to that of a standard

tyre, the spectral balance can give a very different sound quality. For the 'next generation run-flat' the tyre industry currently promises a break-through in comfort. It will be up to the valued customer to follow this up.

14.5   Suspension

The suspension in our context is all the components 'behind' the tyre and 'before' the vehicle body, so it comprises the rim, the hub and spindle/knuckle, all linking arms with bushings and/or balljoints, units introducing wheel motion damping and, if present, any kind of subframe (isolated from the body or rigidly mounted) and anti-rollbars. It can contain additional refinement components like mass dampers or absorbers. Of course, the suspension also contains all the steering and braking components and systems. All components have specific relevance for chassis refinement, because they all have elastic vibrational modes in which they deform dynamically and are able to amplify structural noise throughput. Additionally, once a component is mounted and isolated from the next or from the body, rigid vibrational modes occur, when the rigid component mass oscillates against the stiffness of the attachment. This attachment could be an isolating mount, or a bolted stiffness attachment in case the bolting connection is noticeably softer than the component and/or the component has a large mass (e.g. disc brake caliper, mounted to the knuckle).

14.5.1 Rigid modes

The unsprung masses, by definition, have rigid modes against the sprung mass of the vehicle (or the adjacent system). For the soft-coupled, large masses of the knuckle (with rim and tyre and partly linked arms) in the longitudinal and vertical directions, the low-frequency modes 'fore–aft' and 'wheelhop' (vertical) exist, which both have relevance for ride comfort. They can be excited by road undulations or by internal suspension forces such as tyre imbalance or tyre non-uniformity or during braking due to disc brake thickness variations. Damping of these modes is essential: wheelhop is (partly) attacked by the damper, and both wheelhop and fore–aft modes either by the compound damping of the suspension mounts involved or by a hydraulic mount, transforming wheel motion into heat via a resonating hydraulic system, which is tuned to the disturbing frequency. Wheelhop as well as (especially) the fore–aft mode are dependent on the vertical (vehicle loading) and longitudinal (braking) preloads, and also on the natural vari-ance of springs and dampers over all vehicle derivatives. Resonance-based damping therefore always has to be a compromise between maximum damping performance and its effective frequency range or bandwidth.

Typical values for passenger cars for wheelhop are 10–16 Hz, with fore–aft mostly just above this. We will concentrate in this section on the modal properties of the suspension in higher frequency regions. Of course, there are also unsprung masses with rigid modes at higher frequencies, especially for suspensions with (light) linkage arms in stiff bushings. These can be translatoric modes as well as rotational modes. Also for the bushes, there are often not only translational deflections, but torsional and/or cardanic loads involved. This enables a modal shifting by modifying these two quantities but keeping the axial/radial stiffness.

14.5.2 Flexible modes

Besides the rigid modes, most components have flexible modes, where the geometry is deformed and oscillates. This can be bending, torsion or arbitrary combinations of these deformations. Here the rule applies that usually the modes of low order carry higher energy and so are more relevant.

14.5.3 Sprung masses

Basically, the above remarks on rigid and flexible modes also apply to sprung masses, because a sprung mass can also be isolated from the vehicle body (e.g. isolated crossmembers). Chassis systems and components which are coupled stiff to the vehicle body can usually show only flexible modes (if the coupling is stiff enough compared with the driven mass of the system).

14.5.4 Dampers

The requirements of the damper towards its environment have been explained already in Section 14.3. But the damper itself also has some properties that are relevant to refinement. Apart from the working principle, different valve sets are always responsible for compression and rebound damper force buildup, between which a phase of stiction exists. So at any of these discontinuities, there will be a pulsation in the hydraulic system once the damper brakes free from stiction or when a main valve or a checkvalve opens or closes. For NVH, these processes have to be soft enough not to create knocking noises or damper chuckle, and also the high-frequency noise of the oil pressed through the valves for a specific damper velocity, called swish, needs to be below a specific limit, which is related to the airborne noise transfer into the vehicle. These effects are often classified separately from the classical noise at cruising or impact and can be called 'suspension noise', together with suspension-based squeaks and rattles.

Besides these types of noises, the damper has 'classic' modes based on its mechanical setup: a tube in which a piston is slipping, sealed to the tube with a moving seal at the piston and a stationary seal at the upper tube end. Here, as a first approach, the lateral modes of piston and piston rod against the seals are relevant, also known as 'damper bending'. These are primarily dependent on the masses, less on seal friction. The resonance can be between 150 and 200 Hz and so in a very well audible range. In order to maintain the function of the damper, this mode cannot be deleted by design, but in some applications strut absorbers are used. A basic introduction into damper types is given in Causemann (1999), with more details in Arkenbosch *et al.* (1992, p. 488) and a detailed example of the complex breakdown of a damper noise issue from the full vehicle to the component in Kruse (2002).

14.5.5 Modal strategy

Not all modes are equally relevant. This has to be taken into account when calculating modal alignment based on computer-aided engineering (CAE). Only CAE can cover vehicle or suspension variants in an early design phase, and can reasonably cover tolerance studies of geometries, masses and (bush) stiffnesses. The modal alignment, to be complete, needs to cover not only suspension modes but also fundamental tyre modes (first vertical and tyre cavity mode range) and main body/greenhouse modes. In order to still have a mode list which can be handled, it is necessary to extract the important modes (high modal energy, critical mode shape with respect to the force input/output locations) by hand, which is very time-consuming. Comparison of modal analysis and simple measurement or calculation of a forced response shows that many modes exist which, in real life, are not excited. So, in the case of complex vehicle programs (e.g. transporters with numerous combinations of chassis settings and body styles), as an alternative to real modal alignment based on modal analysis, just the forces at the chassis-to-body attachments can be reviewed for the variants. Only in the case of violations of the targeted values (i.e. force frequency spectra), which can be detected very easily, is a root cause analysis, e.g. by means of a modal analysis, performed.

14.5.6 Hardware tricks and late changes

In case a design cannot be optimized right from the beginning, or should a new derivative be covered by a concept which is originally not able to deliver the performance, there are still some tricks available. In order to improve isolation, an additional mass on the receiver side of a path isolation can increase the inertia and so provide a larger impedance change. Another

trick is the application of a tuned absorber in resonating systems. As absorbers increase weight and cost, it is desired to use existing components for the realization of the absorber. Examples are radiators of engine cooling systems absorbing body front-end modes, or the elastic suspension of a steering wheel airbag compensating for the fundamental steering column bending mode.

Additionally, it is possible to change either the geometry or the mass distribution in a way that moves the node of a critical mode into the coupling to the receiver system. As an example, a damper piston rod, which transfers usually a portion of the modal energy of the damper bending via the top mount into the vehicle structure, can be modified with a mass to shift the node of the bending shape down into the top mount.

14.6   Mounts and bushes – the art of isolation

Mounts and bushes should couple some degrees of freedom elastically, isolate others as much as possible, support distinctive elastokinematics, be dynamically as soft as possible, control some components or systems via damping, achieve low tolerances, last usually for a vehicle's lifetime under all conditions with low functional deterioration, be failsafe under all circumstances, and (based on high volumes) have a very low unit cost. This sounds like a job almost as difficult as that for a tyre.

14.6.1 Basic isolator types

There is a large variety of bush and mount types, which can be categorized in different ways: for details refer to Walter (2009). Most of the standard rubber–metal bushings are manufactured by casting an elastomere into a closed form while introducing a vulcanizing agent. During a heating process, which can last several hours, the rubber vulcanizes. The mounts need to cool down and constitute for 24 hours before they can be measured or used in a vehicle. It is important to differentiate between two types of mounts: single-bonded and double-bonded. Double-bonded bushes have a bonded connection to the inner core as well as to an outer tube. Due to the vulcanization process, the rubber shrinks, and the mount needs a compression of the outer tube to reduce the inner stress within the rubber and support the durability requirements. This reduction is called calibration and is made in hydraulic presses which reduce the outer diameter. A rolling of the ends of the outer tube is also possible, largely securing the bush against axial loads. The stiffness of the bush is increased respectively, which has been taken into account in the design.

Single-bonded bushes have an inner core around which the rubber corpus is vulcanized. There is no outer tube of the bush, the outer surface of the

rubber corpus forming the shape of the bush. They are pressed into their working positions in the chassis components. Due to the missing outer tube, there is no shrinkage effect to be compensated for, but the calibration of the double-bonded bush is much more capable of securing the bush against internal overload. This often leads to a higher shore value of single-bonded bushes compared with double-bonded in the same position, which usually builds up a risk of a worse dynamic restiffening. Additionally, the single-bonded bush always has a risk of rotating in the working position, usually occurring in a type of slip–stick motion which can create squeaking noises, rather than transferring rotational loads.

14.6.2 Stiffness and damping foundations

Mounts and bushes are usually passive components that provide a coupling function between chassis parts or between the chassis and body system. The term 'mount' is mainly used for softer applications like engine mounts or subframe-to-body mounts, while 'bush' mostly refers to stiff cases such as link arm bushes in suspensions. They are the main contributors to the elastokinematic properties of the suspension. Depending on design, static loads or moments are elastically coupled, while high-frequency excitations due to the road or system resonances can be isolated. The lower limit of 'high-frequency' depends here on the relation of the mount stiffness to the affected masses, i.e. usually isolation can be obtained when the excitation is overcritical with regard to the basic spring–mass resonances of the different translational and rotational directions.

The high-frequency isolation is not a property of the mount alone, but of the interaction of the source side stiffness, the isolator, and the receiver side stiffness. Only if these stiffnesses differ substantially can a good isolation be obtained due to the misalignment of these three mechanical impedances.

In the first instance, one describes the three stiffnesses in terms of the modulus of the stiffnesses. However, the term 'impedance', as used above, already implies that these stiffnesses do not need to have only a real part. In fact, at least the isolator stiffness is complex, either based on the damping of the rubber compound or because of a built-in hydraulic feature (as used often for control arm bushes or subframe-to-body mounts).

The damping is given in degrees of phase angle between the force and the deflection for the application of a sinusoidal dynamic load. The loss angle is denoted by δ (Greek delta), sometimes also as the loss factor 'tan δ'.

The hydraulic effect, which is usually tuned to the disturbing resonance frequency of the affected system, does not simply reflect portions of the mechanical energy back into the source, as fully real isolators would do,

but absorbs mechanical energy by transfer into heat. Typical values reached are up to 25°, in some applications even much more. Note that, as for each resonating system, the bandwidth and the maximum damping at tuning frequency are anti-proportional.

Pure rubber bushes (non-hydraulic) provide relatively low damping values, as a function of the rubber compound and the design (rubber is able to provide damping under shear load), of typically up to 8–10°. For a detailed explanation of the physics of rubber for static and dynamic loads, see Vibracoustic (2002) and Walter (2009), and for the influence of the clamping of bushes upon the stiffness in real mounting cases see Walter (2009).

Isolators can also be described by means of a quadrupole. This is a mechanical translation from the electronic domain, in which voltage and current may be identified with force and velocity. This is not a very common approach, but it enables one to correctly describe all cross-couplings, including the crossover from the receiver back to the source. Impedance misalignment can be optimized more easily, reflected and absorbed energies get more demonstrative, and also active mounts can be described. For details see Sell (2005).

14.6.3 Stiffness and damping measurements

Static and dynamic component stiffness are measured in different ways. Static stiffness c (Fig. 14.11(a)) is measured with slow sawtooth-like signals between force limits representing normal usage of the full vehicle (or also maximum durability loads). The time history of applied force and resulting mount deflection is recorded and displayed in a four-quadrant graph. The hysteresis of the curves is a measure of the component damping. A single value for the stiffness can be obtained from the slope of the hysteresis curve at a working point (with or without preload).

Dynamic stiffness k (Fig. 14.11(b)) is measured with sinusoidal stepped sweeps of constant amplitude. The stiffness at a specific frequency is the quotient of the maximum force and maximum deflection, the phase angle between both quantities being the loss angle δ. Stiffness and damping values are plotted against frequency in the figure.

For data compatibility, it is important to define the speed of measurement as well as the amplitude of both the static and the dynamic measurement. Common values for the measurement speed are 10–30 mm/min for the static data with application-specific maximum force values. The amplitude of the sinusoidal dynamic measurement can vary, but for 'pure' Road NVH load cases it may go down to e.g. ±0.025 mm, while spanning frequencies up to 500 Hz, establishing high requirements to the measurement rig hardware. Note that a mount will be measured softer with increasing
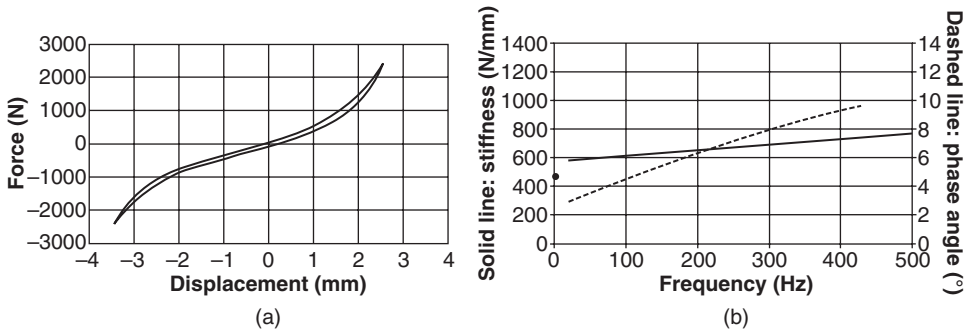
14.11 (a) Static and (b) dynamic axial stiffness data. Measured data for a damper top mount. The resulting static stiffness around the origin – 430 N/mm – is marked in the dynamic curve at 0 Hz.

amplitudes, which is valid for static as well as for dynamic load cases. For the amplitude-related reversible and non-reversible effects on the stiffness (Payne effect, Mullins effect), see Walter (2009).

14.6.4 Dynamic isolation capability

All bushings and mounts are stiffer for dynamic loads than for static loads (the higher the frequency, the stiffer). Here we have to differentiate between properties of the compound only and properties of the complete component. While usually a bush supplier will not discuss pure compound data with a vehicle manufacturer (which would be data from pure rubber test probes with common, standardized geometry), all data available for the vehicle manufacturer is established on the actual design of the rubber–metal bushes. To still enable a differentiation between compound influence and design influences, different values can be established from the static and dynamic stiffness measurements. In most cases, an estimation of the dynamic isolation capability of the compound can be obtained from the ratio of the dynamic stiffness at 100 Hz to the dynamic stiffness at 1 Hz. This 'dynamic restiffening ratio' R_k is given by

$$R_k = \frac{k_{(100\,\mathrm{Hz})}}{k_{(1\,\mathrm{Hz})}} \tag{14.1}$$

and is influenced mainly by the compound, while the bush design, i.e. the ratio of shear loads to compression, largely influences the difference between static and dynamic response. The latter is important in evaluating the compromise between vehicle dynamics load cases and NVH properties. So, to quantify the mount behaviour between (quasi-)static load cases with larger amplitudes and dynamic loads of small amplitudes, we establish a dynamic-to-static stiffness ratio R_{ck} with

$$R_{ck} = \frac{k_{(100\,Hz)}}{c} \tag{14.2}$$

Note that this latter metric leads to higher values for the stiffening factor, but might be the preferred one for a vehicle manufacturer, compared to a bush manufacturer. Typical values are between 1 and 2. To optimize a bush for low R_{ck} makes sense only for the case of a low damping compound. At locations which require a high damping compound, R_{ck} may be much higher, but the advantage then lies in the damping of oscillations rather than in a soft decoupling.

Note that the use of 'c' for the static and 'k' for the dynamic stiffness is in accordance with VDA 675 460 and 675 480. See there for more details. Different standards may use different symbols, e.g. 'k_0' for the static stiffness.

14.6.5 Shore hardness

The frequently used shore value for the specification of the hardness of the rubber compound has only restricted meaning with regards to NVH. The shore hardness cannot replace the correct establishment of the static and dynamic stiffness of the component. The higher the shore value is, the higher the dynamic restiffening tends to be. This shows the limitation in simply modifying bushes for a higher load case by increasing the shore hardness of the rubber compound. Depending on the application, usually a shore value of 50–55 should not be exceeded in order to maintain proper dynamic isolation capability.

14.6.6 Tuning options in geometry and material

For tuning the properties into the desired direction, different options are available. Either the integration of specific features into the mount will improve the performance, or a review of the basic design (when iterating from an existing mount to a similar application) can help. For the latter case, it is important to see the basic requirements for the geometry, to have a sufficient bonded area to ensure durability, and to have as few restrictions as possible to maximize shear loads against compression. So for an existing design, a marginal change of the areas that are bonded to the inner or outer core may deliver some refinement. This may be an option, for example, if original durability loads and/or peak loads can be detected as overstrict, then the bonding change potentially reduces either translatoric stiffness or rotational (cardanic and torsional) stiffness, while keeping the radial properties. Other options require one to integrate specific features or components into the mount. For example, the reduced cardanic and torsional

stiffness mentioned above can also be obtained by introducing additional curved inner tubes in a radial mount, transforming compression into shear load.

Very different load cases in the different directions require different rates in all directions. This can be obtained either by orienting the mount accordingly (the radial directions are usually much stiffer than the axial one) or by splitting the radial stiffnesses either by voids in the rubber corpus or by introducing outside clips or inside inserts to the mount. Snubbers or bump stops can be internal or external, providing an enhanced tuning range between soft initial stiffness and increasing progression over deflection. Quite new are mounts which are manufactured using different compounds for specific parts of the mount.

14.7   Future trends

14.7.1 Future targets

The future evolution of road-induced NVH targets may be dependent on the vehicle class. While luxury products still tend to shift the comfort borderline further and further (or lift the compromise between the attributes to higher and higher levels), in the medium and small vehicle segments often stagnation can be experienced when comparing new vehicles with their predecessors. Cost pressures and flexibility requirements with regard to modularity may restrict the potential for improvement. Especially for tyres, it is expected that safety and fuel economy aspects will dominate development in the near future above the other attributes, both aspects complicating refinement improvements.

14.7.2 Robustness and efficiency

Today, a vehicle platform for a mass product also has to support the derivation of niche products with relatively low sales volumes but high scheduled market penetration. So, apart from mass products, which are balanced to show the performance of all attributes on a relatively high level, the concept also has to support the tuning of a vehicle towards a sport sedan (tuned towards vehicle dynamics), a light off-road vehicle (wheel travel, off-road loads, etc.), a SUV or medium van (high loads), etc. So it makes no sense to use a suspension concept that can be developed only for one specific application; instead we need a robust tuning bandwidth for all required vehicle derivatives while keeping the refinement level high in terms of kinematic and elastokinematic parameters. Also, the capability of suspensions to work, for example, with an isolated subframe as well as a fixed bolted one can be relevant, and compatibility with different springs (e.g.

steel coil spring versus air spring) and dampers (standard dampers versus self-levelling), with all-wheel-drive, or with add-on features such as active steering, active roll control, etc., is important in enhancing the spectrum of applications. This flexibility in most cases will be limited automatically by the amount of 'overdesign' that will be accepted for the standard, i.e. volume application.

14.7.3 Consequences of light weight

For airborne noise attenuation as well as for structural noise transfer, the mass of the affected components or systems is an important parameter. So, as a result of overall vehicle weight reduction, the mass law forces an increase of the transferred airborne noise from tyre patch to the vehicle interior, unless countermeasures are taken. Since, as always, the primary line of attack has to be to the main path, which is a very individual one, no general rules can be given here. In order not to lose the weight advantages with these counter-measures, it has to be carefully evaluated whether the original isolation should be reconstituted or whether a secondary means (e.g. interior absorp-tion) is more efficient. For structure-borne noise transfer similar relations are valid. In most chassis locations, pure inertia supports better isolation, espe-cially in the environment of bushings. So it is again a matter of individual tuning to achieve comparable structure-borne noise isolation with weight-reduced components. Modal alignment here plays a major role in adjusting modified system components to match the vehicle environment.

14.7.4 Future features

Controlled dampers and active dampers

Dampers with continuously controlled damping by means of switchable or analogue-controllable valves have slowly spread from the luxury class to mass products, having a moderate potential to combine a smooth ride and a few noise improvements with good suspension control in the – mostly only few – required moments. The next generation of dampers, which are really active, i.e. able to control wheel motion by expanding and compress-ing the damper actively, are currently still in a prototype phase. They show much potential to improve ride comfort but face issues of power consump-tion, controlling algorithms and cost, so it is expected that they will slowly enter the luxury vehicle class only.

Active mounts and active absorbers

In contrast to the above ride-oriented technologies for dampers, the appli-cation of active mounts or active absorbers is aimed directly at noise and/

or vibration improvements with regard to nominal performance as well as robustness. Active mounts, positioned in the load path of the mount, have been found to be difficult to implement due to the high loads that have to be transferred through them. In contrast, active absorbers in the vicinity of the input location can be tuned to minimize the transferred vibrational energy and can be expected to be used more as they improve construction efficiency and integration into the vehicle infrastructure. Depending on the sensors and algorithm, the target function could be the minimization of road-induced vibration, tyre first-order imbalance, or the fundamental engine orders at an engine mount. See Vibracoustic (2002) and Hofmann (2002).

14.8   References

Arkenbosch, M., Mom, G. and Nieuwland, J. (1992), *Das Auto und sein Fahrwerk* ('Steinbuch'). Stuttgart, Motorbuch-Verlag.

Causemann, P. (1999), *Kraftfahrzeugstossdämpfer: Funktionen, Bauarten, Anwendungen*. Landsberg/Lech, Verlag Moderne Industrie.

Gent, A.N. and Walter, J.D. (2005), University of Akron, *The Pneumatic Tire*. Washington DC, NHTSA.

Hofmann, M. (2002), Trelleborg GmbH, *Antivibration Systems: Fundamentals, Designs, Applications*. Landsberg/Lech, Verlag Moderne Industrie.

Kruse, A. (2002), 'Characterizing and reducing structural noises of vehicle shock absorber systems'. ZF Sachs AG, SAE paper 2002-01-1234.

Sandberg, U. and Ejsmont, J. A. (2002), *Tyre/Road Noise Reference Book*. Kisa, Sweden, Informex.

Sell, H. (2005), 'Charakterisierung des dynamischen Verhaltens von elastischen Bauteilen im Einbauzustand'. Weinheim, Germany, Vibracoustic GmbH.

Torra i Fernández, E. (2004), 'Tyre air cavity acoustic modes and their influence on the automobile interior noise'. Licentiate Thesis KTH, Stockholm.

Vibracoustic GmbH & Co KG (2002), *Schwingungstechnik für Automobile*. Weinheim, Germany.

Walter, H. (2009), 'Untersuchung der Steifigkeit von Fahrwerklagern bei idealen und realen Einspannbedingungen'. Diploma thesis, Rheinische Fachhochschule, Köln, Germany.

Zandbergen, P. (2008), 'Design principles for multi-link rear suspensions'. Ford Motor Company, 6. Tag des Fahrwerks 2008.

15

Body structure noise and vibration refinement

G. M. GOETCHIUS, Material Sciences Corporation, USA

Abstract: The body structure of an automobile is a critical part in determining the overall levels of noise and vibration which reach the vehicle occupants. It is the body structure which separates, and therefore insulates, the occupants from the many and varied sources of noise generated while a vehicle is in operation. As a result, the body structure must be carefully engineered to block incoming noise and vibrational energy, and to minimize the effects of whatever energy does ultimately get into the body structure. This chapter focuses on the basic mechanisms which affect both structure-borne and airborne noise transmission in the body, and offers specific design practices and generic targets for many of the attributes which are critical to achieving overall noise and vibration goals of the vehicle.

Key words: noise, vibration, body, structure, stiffness, panel.

15.1   Introduction

All noise and vibration which reaches the occupants of an automobile must, by definition, travel through the body structure. As a result, the body structure plays a critical role in determining the overall levels and the quality of the noise inside the car. How well the body structure blocks incoming energy and how the various resonances of the body structure (there are many) affect that energy as it travels through the body structure are critical issues and will be the focus of this chapter.

This chapter separates the body into three main areas:

1. Global body structure
2. Body attachments
3. Body panels.

For each of these three main areas, best practice design guidelines and generic targets are offered, along with the description of the physical mechanisms which govern their behavior. The intent of the chapter is to provide the reader with a basic understanding not only of the 'what' and 'why' of automotive body NVH, but also of the 'how'.

Since NVH is a highly complex field, and since specific design practices will always depend on the unique situation of every car design, the design practices proposed here should be thought of as generalizations. Nonetheless,

351

they form a solid starting point from which a strong foundation can be constructed and upon which future refinement can be accomplished.

15.2   Basic principles

The basic principles which govern the behavior of body structure NVH must be understood before establishing design guidelines and generic targets. Therefore, this chapter will discuss the fundamental principles of the source–path–receiver model, the importance of separating structure-borne noise and airborne noise, the two main ways in which NVH energy is attenuated (energy impedance and energy dissipation), and finally, the importance of a systemic or 'holistic' approach to applying all design strategies.

15.2.1 Source–path–receiver model

No discussion of noise and vibration would be complete without an introduction to the 'source–path–receiver' concept. All noise and vibration phenomena can be broken down into their constituent parts: source(s), path(s) and receiver(s). In an automobile, there are many sources which are often acting simultaneously on the body structure. Furthermore, each individual source can have many paths through which energy can reach the vehicle's occupants. Finally, the 'receivers' (the human occupants) receive and perceive multiple noise and vibration signals through different parts of their anatomy. Figure 15.1 shows a typical set of sources and paths for powertrain-induced noise and vibration.

Note that the first 'path division' is between structure-borne and airborne noise. This distinction is important since the mechanisms by which noise and vibration enter the body structure are significantly different between structure-borne and airborne noise. Also notice that there are multiple sources and multiple paths, so the resulting energy flow is extremely complex.

The 'golden rule' of NVH attenuation with respect to the source–path–receiver model is to reduce the energy at the source first. This seems logical, but its importance cannot be overstated. Since most sources (engine, tires, wind, etc.) have many paths through which energy can penetrate the body, if the energy is not controlled or stopped at the source, one must 'chase' the energy through the many paths into the body. The effort to treat the paths becomes more difficult, less efficient and ultimately more costly than treating the source.

Having said that, it is often the case that the source is a fixed quantity and cannot be changed, and in this case, one has no choice but to work on the paths. Since the body structure is, in fact, a set of many paths for energy
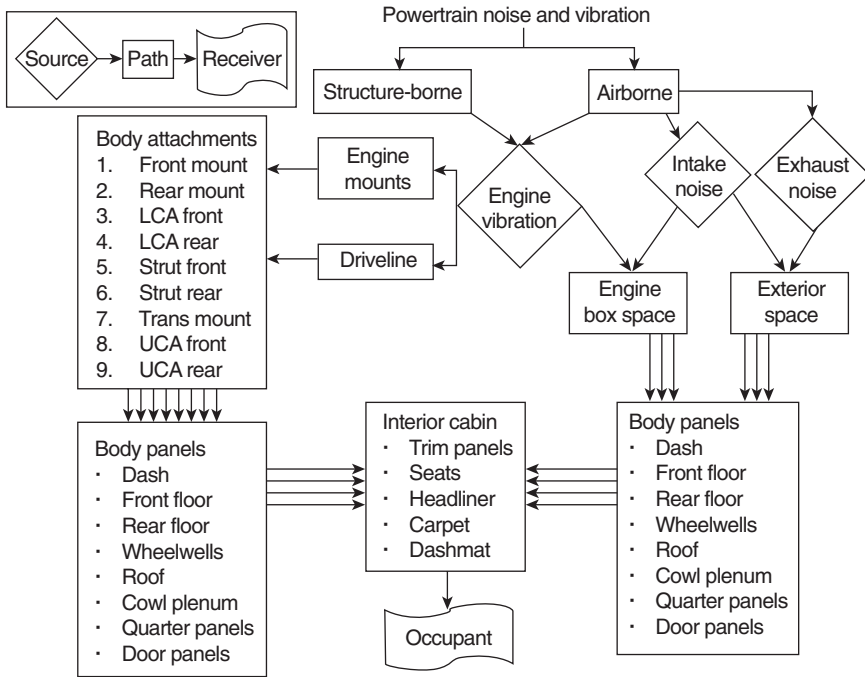
15.1 Source/path/receiver example.

to pass through, much of the focus in this chapter will be on addressing path issues with respect to the body structure.

15.2.2 Structure-borne and airborne noise

It is important to define what is meant by the terms 'structure-borne' and 'airborne' noise, since the governing physics and the actual body components involved in these two areas are markedly different. Structure-borne noise is defined as noise which reaches the car interior by virtue of mechanical vibration transmitted through attachment points of the powertrain, chassis and other vibration sources. Airborne noise is defined as noise which reaches the car interior by virtue of sound pressure waves impinging on the various surfaces and panels of the body. It can be seen, then, that the definition of structure-borne and airborne revolves around how the energy gets into the body structure.

Structure-borne noise is generally limited to the frequency range of 20–600 Hz but can vary depending on the specifics of each vehicle. Airborne noise is generally limited to the frequency range of 400–10,000 Hz but can also vary depending on the vehicle. Figures 15.2 and 15.3 illustrate the basic mechanisms for structure-borne and airborne noise. Figure 15.4 shows the
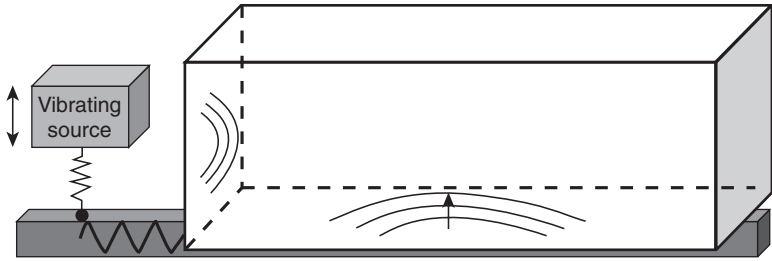
15.2 Structure-borne noise: basic mechanism.
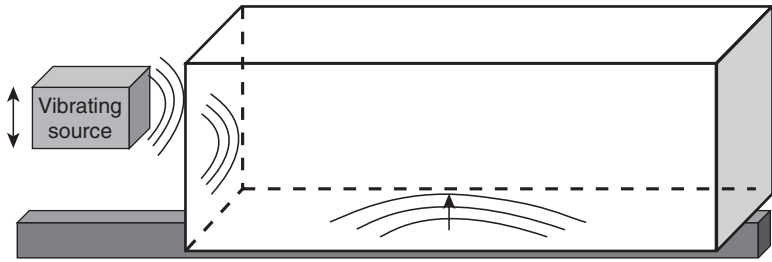
15.3 Airborne noise: basic mechanism.
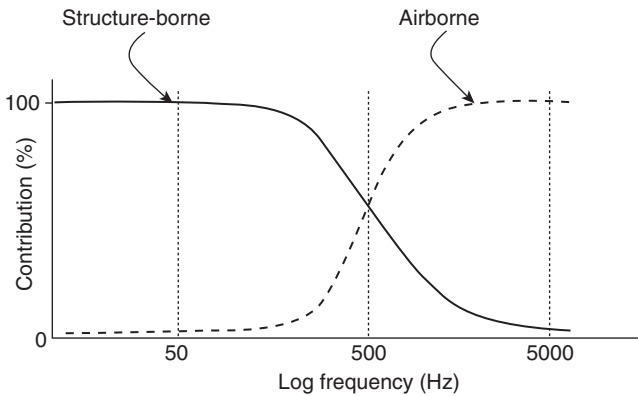
15.4 Structure-borne noise and airborne noise contributions to total noise.

relative contribution of structure-borne and airborne noise contribution for most automotive applications over the entire automotive frequency range.

15.2.3 Basic vibration attenuation strategies

Body structure NVH control can be broken down into two fundamental strategies:

1. Incoming energy impedance
2. Resonance management.

All subsequent principles discussed in the chapter are based on these two fundamental strategies.

Incoming energy impedance

The concept here is simple: the body structure must be designed to block as much of the incoming energy as possible. Thinking, for the moment, of the body structure as a complete system (it is part of a larger system, the car), this is the principle of 'treating the noise at its source'. Sound and vibration energies are attempting to enter the body at all of the mounting points for the engine and chassis (structure-borne) and through all of the body panels, doors and glass (airborne). It is critical to design these systems to block as much of the energy as possible at these critical interfaces.

This is the first line of defense against noise and is arguably the most important. Despite our best efforts, however, not all energy can be blocked at these interfaces, and the resulting energy which is transmitted into the body must be dealt with carefully. That is the next principle.

Resonance management

Once energy is allowed into the body structure, the way that this energy is converted to interior noise is a function of how the resonances of the body structure affect the vibration along the way. There are resonances in every part of the body: in the frame rails, in the body panels, in the fixed and movable glass, in the door systems, and so on. All of these resonances are potentially important and need to be carefully understood and 'managed'. This is true for structure-borne as well as airborne noise. How these resonances are managed varies widely, and will be described in detail in upcoming sections.

15.2.4 Systems approach to NVH

An automotive body structure is a complex system with many reinforcing and competing attributes. As a result, successful noise and vibration control is always the result of many incremental improvements which are based on 'best practice' design guidelines, and are executed at *every available opportunity* throughout the body structure. Each incremental improvement may seem insignificant when viewed alone, and in fact may be difficult to justify by itself, but combined together with all of the other individual improvements will result in successful noise control. Therefore, the design principles

discussed in this chapter must not be considered in isolation but must be integrated 'holistically' into the design of the body structure.

One way to illustrate this is to consider the spot welds of an automotive body structure. A typical body has 3000–4000 welds (some more, some less). It is unlikely, if not impossible, for the best scientific method to quantitatively show the effect of a single spot weld on overall body stiffness, durability and NVH. Therefore, one might be tempted to delete that particular spot weld from the design. If this 'justify-or-delete' strategy were applied to each successive spot weld, the cumulative effect would be devastating, but there would be no point at which the effect of one single spot weld would become significant enough (compared to the previous deletion) to stop the deletion process. It is the cumulative effect of all of the spot welds working together which helps the body to achieve its overall structural goals.

The same is true for body design principles aimed at noise and vibration control. All design principles, inconsequential as they may seem by themselves, must be executed well and at every available opportunity in and around the body structure in order to achieve the levels of refinement which are required by the automotive buying public.

15.3   Global body stiffness

The body structure can be thought of as the 'backbone' of the car and so its overall stiffness and structural continuity are of critical importance in meeting the basic strategies outlined above. Global body stiffness is achieved by carefully designing the body with the following in mind:

- Body modes: mode management
- Structural continuity
- Body cage strategy: unstressed and stressed members
- Beam integration
- Welding.

15.3.1 Mode management

Minimizing vibrations in body structures is often a matter of precisely locating the various modes (or resonances) of the body such that they are not excited by body input forces nor do they interfere with other modes of the vehicle. This is referred to as 'mode management'. Mode management requires that the resonant frequencies of all of the major subsystems of a vehicle (body, engine, suspension, exhaust, etc.) be characterized. Additionally, all of the major excitation sources must then be characterized in terms of their frequency content and probable amplitudes.
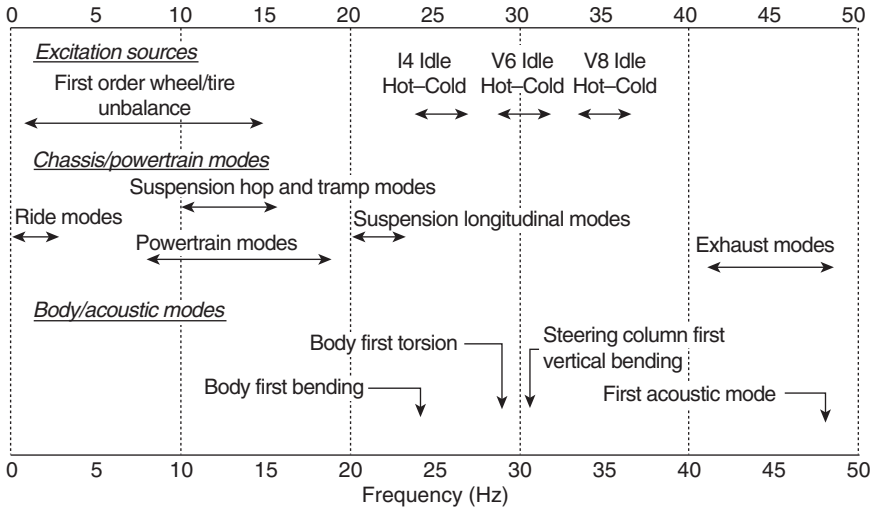
15.5 Vehicle mode management strategy example (Duncan *et al.*, 1996).

Any potential alignments of excitation frequencies and body structural resonances must be minimized by changing the excitation frequencies, the resonant frequencies, or both. This is in contrast to the popular belief that 'stiffer is better', where the objective is to achieve the highest possible modal frequencies. The exercise of mode management may, in fact, lead the structural designer to reduce the frequency of selected subsystems, including the body, to achieve better NVH.

When developing the overall mode management strategy, it is important to follow these two basic rules (in order of importance):

1. Separate modes from excitations.
2. Separate modes from each other.

A general rule-of-thumb for what constitutes minimum frequency separation is 10% (Duncan *et al.*, 1996). Figure 15.5 shows a typical example of a vehicle mode management strategy.

15.3.2 Structural continuity

Structural continuity of the body is a key component in reducing noise and vibration levels in the body. Body structures which achieve 'beam-like' continuity distribute strain energy more evenly over the structure. Energy dissipation occurs when the material of the body is strained. If local discontinuities exist, then strain energies are focused at these points and the rest of the structure is not used to dissipate the energy. The structural continuity
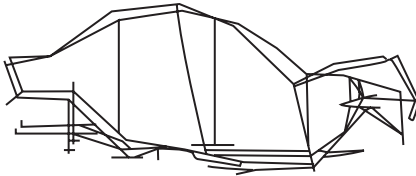
15.6 Discontinuous body bending mode shape (Achram *et al.*, 1996).
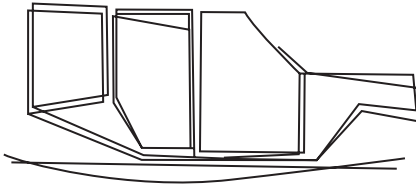
15.7 Continuous body bending mode shape (Achram *et al.*, 1996).

of a body can be assessed by examining the static deflection shapes of the body under various loadings, and also by examining the resonant mode shapes of the body at various frequencies. A continuous structure will exhibit 'classical' beam shapes, i.e. first bending, first torsion, second bending, etc. Figures 15.6 and 15.7 are examples of discontinuous and continuous resonant mode shapes. In Fig 15.6, the bending mode shape shows that most of the motion is in the front end of the body with a discontinuity at the base of the A-pillar. In Fig 15.7, the bending mode shape is more continuous and therefore represents a body structure with better overall structural continuity.

Structural discontinuities are often the result of poor beam integration and general structural weakness in the major joints of the body structure. These areas will be addressed in the next sections.

15.3.3 Body cage concept

Most automotive body structures are constructed from beams which form a 'cage', and panels which close off the interior cavity. It is desirable for the body cage to carry all of the structural and vibrational loads of the body, and not to rely on the panels for these tasks. The panels of a body are the main radiation surfaces for noise inside the vehicle. Therefore, if the panels become structural participants, then energy must pass through them, and this energy can, in turn, be radiated as noise. All of the beams in the body must then be constructed so as to minimize the energy transmitted to the panels. A practical application of this concept can be seen in body struc-
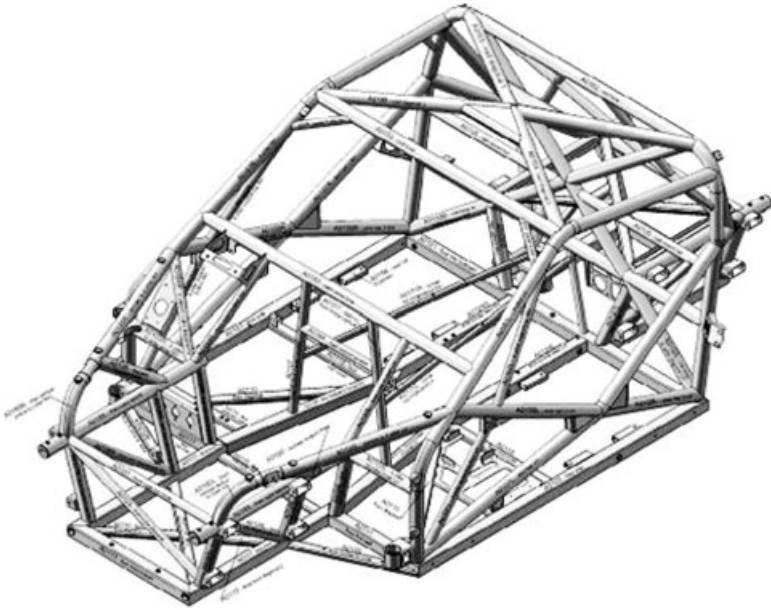
15.8 Body cage example: racing car tubular chassis.

tures where beams exist to perform limited tasks such as supporting the seat or steering column. Often, these beams are not designed to be a part of the 'body cage' and therefore do not provide much structure, consequently forcing the panels to carry more load. Since the cost and weight of these beams is already in the vehicle, it makes sense to integrate them into the body cage.

Another illustration of this concept is a typical racing car chassis, which is generally made up of welded tubing forming a 'cage' (Fig. 15.8). This has proven to be the lightest and most efficient means to achieve good structural performance. Years of evolution and engineering refinement in the racing industry have resulted in an architecture in which all structural loads are carried by beams. The sheet metal on a racing car is strictly for aerodynamics, aesthetics and generating sponsorship opportunities.

15.3.4 Beam integration design strategies

As a member of a larger structure, a beam is only as good as its end conditions. Poor beam end condition often results from practices such as access holes and cut-outs near the beam ends, beams that flatten or lose section

just before a joint with another beam, and slip planes in the joint which allow for build tolerances, among others. The objective in designing beam end conditions is to maximize the moment-carrying capability of a given joint by using all of the available section of the beams which make up the joint. Without good beam integration, the integrity of the body cage is compromised. In fact, for beams which are not well tied together, the sections of the beams must grow large to achieve the same overall stiffness. The result is added cost and weight to the body.

15.3.5 Welded joint design strategies

A key factor in assuring good structural continuity in an automotive body is how well it is welded together. Welding, in general, is one of the most effective ways to obtain 'synergy' between structural elements without adding unnecessary weight. With respect to spot welds, more is generally better. Continuous welding (Mig, laser, etc.) provides better structural continuity than spot welds and should be used wherever the manufacturing process and cost restraints allow.

Most body structures are, in fact, welded together with spot welds. In general, the desirable weld spacing (also known as 'weld pitch') for good overall structural performance is 30 mm (Huang and Sin, 2001; Gogate and Duncan, 2001). This may be lower for critical areas (e.g. complex joints where multiple beams are interfacing), and sometimes higher for non-critical areas. Weld pitch should not exceed 50 mm both for structural reasons (i.e. 'holistic' design principles) and for water- and noise-sealing reasons through the weld flange.

Following the guidelines and principles in this section will help establish the basic structural integrity of the body in terms of static stiffness and low-frequency modal performance of the body. However, significant attention must be given to the body attachments and the body panels. These will be covered in the following sections.

15.4   Body attachment behavior

The execution of good structure in the areas where vibration sources are attached to the body is arguably the single most important aspect of a good body design for structure-borne NVH. To support this discussion, the following topics will be covered:

* Transfer path analysis: importance of stiff attachments
* Generic targets for body attachments
* Bolted joints
* Bulkheads/local reinforcements
* Cantilevered attachments.
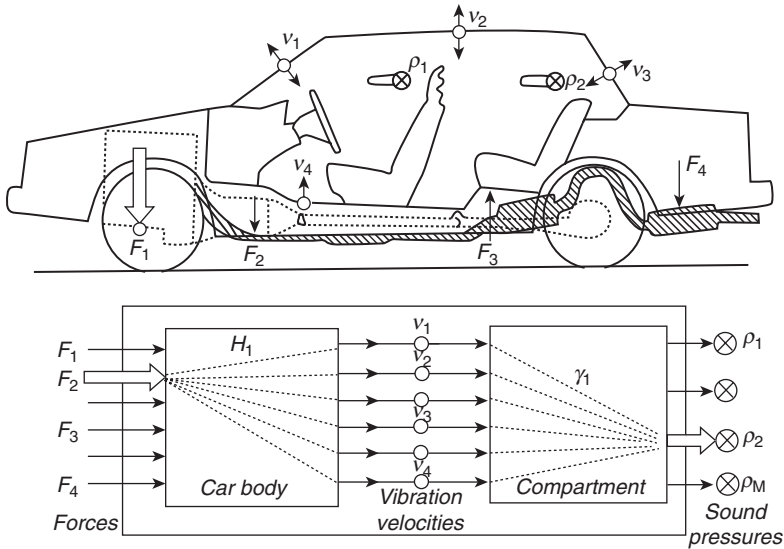
15.9 Transfer paths into a body structure (Plunt, 2005).

15.4.1 Transfer path analysis

Achieving high impedance (stiffness) at body attachment points allows the body to block the incoming vibration energy. However, the question might be asked: 'how stiff should these attachments be?' The answer is that it depends on a very specific set of relationships between the body structure and the systems which are attached to it, namely the isolator stiffness (if present) and the stiffness of the structure attaching to the body (e.g. engine mount). The process by which we define the appropriate attachment stiffness will rely on transfer path analysis, where the individual noise levels through each attachment are quantified and broken down into their respective contributions. With this method, individual path-based targets can then be set, including body attachment stiffness (Dong *et al.*, 1999).

Figure 15.9 shows a set of loads applied to the body and the subsequent transfer paths of energy to the occupants' ear locations. The loads could be the result of engine vibrational loads, tire/road inputs, or any other operational force acting on the body. There are generally several dozen of these loads acting on the body at any given moment when in operation. The goal of the noise path study is to determine the noise level flowing through each structural path into the body. With this information, dominant paths can be identified and reduced via various countermeasures, including changes to the local body structure design.

The level of noise 'flowing' through each path into the body is referred to as the 'partial pressure' for that path. The expression for partial pressure P_i for an individual path i is given by:

$$P_i = \left(\frac{P}{F}\right)_i * F_i \tag{15.1}$$

where $(P/F)_i$ is the body acoustic transfer function at the force input location on the body. It is defined as the sound pressure at a particular location inside the vehicle with respect to a unit force at a particular attachment location. F_i is the force measured at the same input path during an actual operating condition. Considering all of the structural load paths into the body, the total sound pressure P_t is the sum of the all the individual partial pressures:

$$P_t = \sum P_i = \sum \left[\left(\frac{P}{F}\right)_i * F_i\right] \tag{15.2}$$

15.4.2   Body transfer function targets

The key to establishing path-based targets is to first establish the system-level response target, in this case the target noise level, P_t (for eq. 15.2). This could be, for example, 3 dB less than the current noise level. Since the sum of the partial pressures equals the system noise level, a new set of partial pressures ($\overline{P}_i$) can be derived whose sum equals the new target noise level. These new partial pressures will be reduced compared to the original values by a factor R_i. Each partial pressure should be reduced by a different amount depending on the overall contribution of that particular path. However, the result of the summation of the new partial pressures will be a total sound pressure level which meets the target level inside the vehicle:

$$\overline{P}_i = P_i * R_i \tag{15.3}$$

$$\overline{P}_t = \sum \overline{P}_i \tag{15.4}$$

If we assume that the forcing function (F) is constant, then the reduction in the partial pressures can be used to calculate new (P/F) transfer functions for the body. The same unique path reduction factors which are applied to the partial pressures can be applied to the body acoustic transfer function, (P/F):

$$\overline{\left(\frac{P}{F}\right)_i} = \left(\frac{P}{F}\right)_i * R_i \tag{15.5}$$

We now have targets for the individual body acoustic transfer functions which are based on the relative importance of each path.

However, the (P/F) transfer function includes the effects of the entire path from the point of load application, all the way to the ear response point inside the passenger compartment. In designing good body structures

for NVH, a more specific measure is needed which focuses specifically on the body attachment structure. The driving point mobility transfer function (V/F) is one such measure.

The driving point mobility (V/F) transfer function is defined as the velocity response at a given input location to the body, with respect to a unit force input at that same location. Intuitively, it characterizes the dynamic attachment stiffness of the body at a particular attachment. In fact, integrating the (V/F) function and taking the reciprocal directly yields the dynamic attachment stiffness of the body. The reason for using point mobility is that for most body structure attachments, it is relatively flat with frequency, which allows a single value target to be set across the entire structure-borne noise frequency range.

Targets for (P/F) can be related to targets for (V/F) by relying on the following equation:

$$\left(\frac{P}{F}\right)_i = \left(\frac{V}{F}\right)_i * \left(\frac{P}{V}\right)_i \tag{15.6}$$

A new function, (P/V), has been introduced here that essentially characterizes the 'downstream' performance of the body (trim, panels, acoustic cavity, etc.) where the (V/F) characterizes the local attachment stiffness of the body only. The (P/V) function is more or less a mathematical construct and using it in this equation as such requires one to assume that (V/F) and (P/V) are linearly independent variables. This is not generally true, but for the purposes of this attachment stiffness target-setting discussion, we will make that assumption here. Assuming (P/V) to be constant (and independent from (V/F)), the reduction factors calculated for (P/F) functions can now be applied to (V/F) functions.

$$\overline{\left(\frac{V}{F}\right)_i} = \left(\frac{V}{F}\right)_i * R_i \tag{15.7}$$

In this way, point mobility targets for each body attachment can be derived from a transfer path analysis, which can be performed experimentally on an operating vehicle, or by using a computer aided engineering (CAE) method such as finite element analysis (FEA). The advantage of setting path-based targets is that the resulting body structure design will only need to achieve the performance which is required to match the incoming energy to the body at the various attachments. The result is a more optimized design in terms of cost and weight.

In many cases, however, the opportunity to perform this detailed (and often complex) transfer path analysis is not available. In these cases, generic targets for the body acoustic transfer function (P/F) and point mobility (V/F) can be used to establish basic performance of the body attachments.

Generic targets are useful in establishing a solid foundation for body attach-
ment design, but often, body designers will find that these designs will need
to be optimized later in the design process once the performance can begin
to be assessed. As such, generic targets should be thought of as a starting
point for the design.

Studies have shown that a (P/F) performance level of less than or equal
to 60 dB/N is generally found to be acceptable (Williams and Balaam,
1989). For (V/F) the generally accepted generic target is −10 dB (reference:
1 mm/sec/N) (Dunn, 1978). Note that these targets are constant with respect
to frequency and can be applied uniformly across the structure-borne noise
frequency range (20–600 Hz).

15.4.3 Attachment stiffness and force transmissibility

While an excellent starting point, generic point mobility targets do not take
into account the incoming energy to that attachment. In particular, many
engine and chassis attachments to the body include a rubber isolator or
bushing. Basic physics dictates that a stiffer bushing will increase the force
(energy) transmitted to the body. It is desirable to develop a generic target
which is somehow linked to the isolator stiffness. In order to do this, we
will introduce the concept of transmissibility using simple multiple degree
of freedom (MDOF) systems (Duncan *et al.*, 2009).

Figure 15.10 shows a simple system containing a source and a receiver
with no isolator between them and through which force is being transmit-
ted. In this system, we are assuming that both the source (e.g. engine mount
bracket) and the receiver (e.g. body attachment) are flexible, and therefore
have a specific mobility value. For this system, the reaction force at the
source (F_s) is given by:
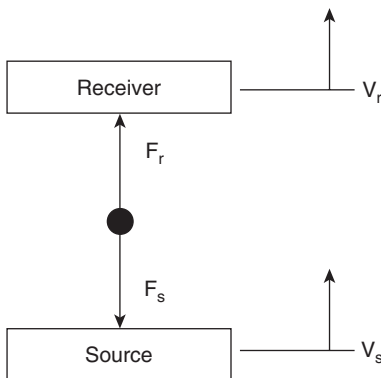
15.10 Source–receiver system with no isolator (Duncan *et al.*, 2009).
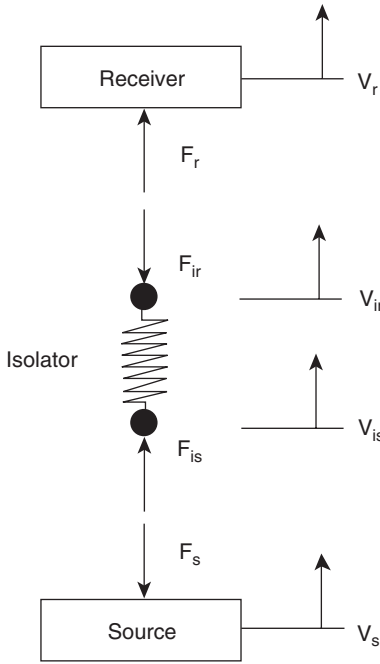
15.11 Source–receiver system with isolator inserted between source and receiver (Duncan *et al.*, 2009).

$$F_s = \frac{V}{Y_r + Y_s} \tag{15.8}$$

where

$V_r = V_s = V$ = velocity
Y_r = mobility of receiver
Y_s = mobility of source.

Considering the same system, but inserting an isolator between the source and receiver as shown in Fig. 15.11, the force at the source is now given by:

$$F_s = \frac{V}{Y_i + Y_r + Y_s} \tag{15.9}$$

where Y_i is the mobility of the isolator.

The transmissibility ratio (TR) can be defined as the ratio of the force from the source *with an isolator*, divided by the force from the source *without an isolator*, as follows:

$$\text{TR} = \frac{Y_r + Y_s}{Y_i + Y_r + Y_s} \tag{15.10}$$
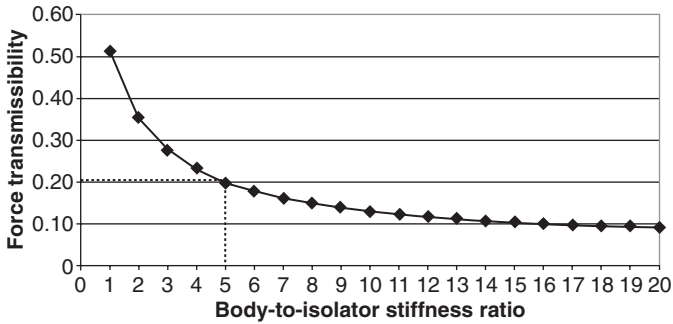
15.12 Body-to-isolator stiffness ratio effect on force transmissibility (Duncan *et al.*, 2009).

Minimizing the force at the body would mean minimizing the transmissibility ratio. From eq. 15.10, it can be seen that in order for the TR to be less than or equal to 1 (and therefore provide isolation from the source), the mobility of the isolator must be equal to or greater than the sum of the source and receiver mobilities. In other words, the isolator must be 'soft' relative to the 'stiffness' of the source side structure and the body side structure. This is intuitive, since rubber isolators are generally softer than metal structures. If we express the mobility (V/F) in terms of stiffness (F/X), where stiffness is inversely proportional to mobility, we can then establish stiffness ratio targets for body attachments:

$$K = \left(\frac{F}{X}\right) \propto \frac{1}{(V/F)} \tag{15.11}$$

where X is displacement and K is stiffness.

Figure 15.12 shows the calculated TR as a function of body-to-isolator stiffness ratio (K_{body}/K_{isol}), where the ratio of the source-to-isolator stiffness is assumed to be very high (e.g. engine mount brackets are generally much stiffer than the rubber engine mounts). The chart clearly shows the inverse exponential effect which the body-to-isolator stiffness ratio has on the force transmitted to the body. In fact, it can be seen that by achieving a stiffness ratio of 5:1, the transmissibility ratio is 0.2. This means that only 20% of the force from the source has reached the body. In general, it is desirable to achieve a minimum body-to-isolator stiffness ratio of 5:1. Higher ratios would provide better isolation, but in many cases where isolators can be very stiff (e.g. suspension control arm bushings), achieving higher ratios than 5:1 is not practical and would drive very high cost and complexity into the attachment structure design.

15.5   Body attachment design strategies

Body attachments should be designed carefully and with detailed knowledge of the energy flowing through each body attachment path. If available, a detailed noise path analysis can help set very specific and 'tailored' targets for that particular vehicle. In absence of this, generic targets can be used for point mobility and/or body-to-bushing stiffness ratio, if the bushing rates are known.

Now that targets have been established for body attachments, design principles needed to achieve these levels can be discussed.

15.5.1 Bolted joints

Beam integration focuses on beams within the body structure, but the same concept applies to components which are attached to the body via fasteners (i.e. suspension crossmembers, engine mounts, etc.). These attachments must not only allow the component to add to the body cage but also provide a high level of attachment stiffness. As discussed in the last section, high attachment stiffness can also be expressed as high mechanical impedance (or low point mobility). As with beam end conditions, the use of the entire available section of the beams involved in the attachment is critical in achieving high mechanical impedance. One example of how this can be accomplished is by incorporating 'double-shear' attachments. A double-shear attachment provides moment reactions at two points inside the beam through the use of tubes or internal bulkheads. Figures 15.13 and 15.14 illustrate the difference between the single-shear and double-shear concepts. In general, design practices such as single-shear bolted attachments, oversize bolt holes, loose attachment nuts (i.e. J-nuts, floating tapping plates, etc.), cut-outs and holes for access, etc. should be avoided.

Figure 15.15 shows an example of a crossmember with a good attachment to the body, and Fig. 15.16 shows an example of a crossmember with a poor
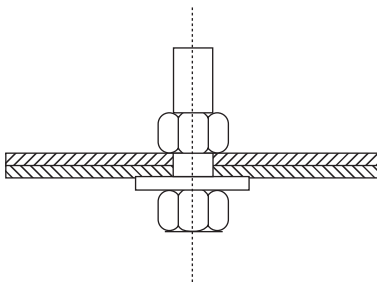
15.13 Bolted joint example: single shear (Achram *et al.*, 1996).
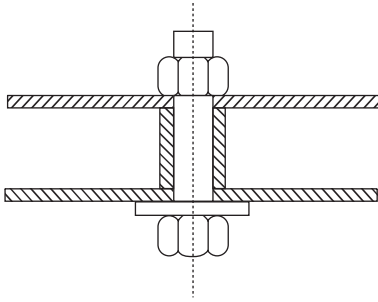
15.14 Bolted joint example: double shear (Achram *et al.*, 1996).

15.15 Example of good bolted beam end condition (Achram *et al.*, 1996).
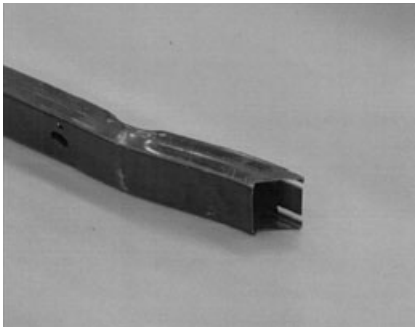
15.16 Example of weak bolted beam end condition (Achram *et al.*, 1996).

attachment to the body. The crossmember with the poor attachment not only loses section at its end, but the crossmember is attached through slotted holes using a single-shear design. The crossmember with the better attachment uses double-shear attachments both in the crossmember and inside the body, or effectively a 'quad-shear' design. The moment-carrying

capability of this attachment is substantially higher than that of the poorly attached crossmember. Consequently, the gauge of the steel in the poorly designed crossmember must be very high in order to achieve sufficient attachment moment-carrying capability, resulting in unnecessary mass and cost of the part.

15.5.2 Bulkheads and internal frame rail reinforcements

The 'double-shear' strategy makes use of internal structures within the frame rail to allow a high moment-carrying capability of the joint. In more general terms, internal rail bulkheads and reinforcements are usually needed to provide a low compliance structure to which the engine or chassis component is attached. In some cases, these reinforcements are needed to provide static stiffness for the bolted joint, and in other cases (especially when point mobility targets exceed targets at specific frequencies), the reinforcements are needed to address localized resonances of the rail and bolted structure.

Here, FEA is an extremely powerful tool, since it allows the calculation not only of the point mobility function, but also of the deformed mode shape of the local structure. The visualization of these deformed shapes allows the engineer to clearly see areas of weakness and develop reinforcement strategies to address the problem. Figure 15.17 shows an FEA representation of a reinforced frame rail internal bulkhead design compared to the baseline, unreinforced design. This internal bulkhead design resulted in the body attachment achieving its point mobility and body-to-isolator stiffness targets.

15.5.3 Cantilevered attachments

In many cases, packaging the various components which attach to the body requires the body structure to 'reach out' over a distance to attach to the component. This results in a cantilevered attachment and a corresponding loss of moment-carrying capability. In many cases, cantilevered designs can be avoided altogether by choosing alternative packaging solutions. In other cases, where a cantilevered structure is unavoidable, sufficient moment-carrying structure must be added to the design.

Figure 15.18 shows a set of engine mounts cantilevered from a fore/aft engine crossmember. The effect of this poorly designed cantilevered structure is to significantly degrade the attachment stiffness of the engine mount attachments. In this case, note the large, added-on reinforcement bracket at the rear mount (left side of image). This is an excellent example of how an inefficient design can result in inelegant, heavy and costly design fixes in order to meet basic structural requirements.

Baseline design (A)

Body rail

Two bolts through
metal thickness
(rail to x-mbr)

Transmission
cross-member

Proposed design (C)

Two through-bolts in
double shear

Body rail

Cover plate

Bracket

Two bolts
(through
section)

Floating
tapping
plate

Rail sleeve

Cross-member
sleeve

Transmission
cross-member
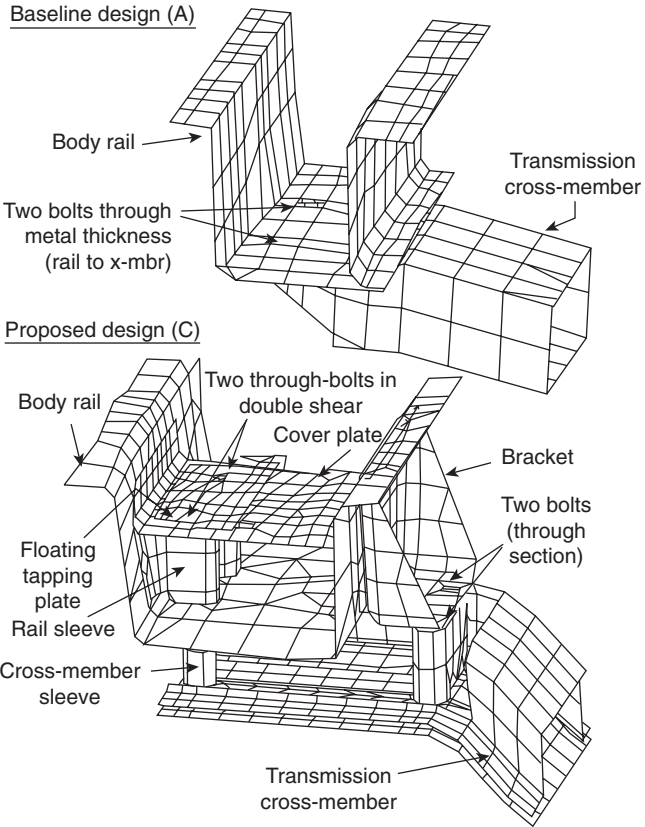
15.17 Example of frame rail internal bulkhead reinforcements (Achram
et al., 1996).

15.18 Example of cantilevered engine mount attachment design
(Achram et al., 1996).

Good structural–acoustic performance of each body attachment path is critical in achieving overall structure-borne noise level targets. From the previous section, we know that a significant enabler for this performance is the attachment point mobility and/or the attachment-to-isolator stiffness ratio. But it is entirely possible that even with sufficient attachment performance, the overall structural–acoustic performance of the body will be insufficient, in particular the individual path (*P*/*F*) transfer functions. In the next section the major contributors to this will be considered, i.e. all of the 'downstream' structures which ultimately convert the vibrational energy into interior sound levels: the body panels.

15.6   Body panel behavior

Once energy (structure-borne or airborne) reaches a panel, measures must be taken to prevent the energy from being converted into noise. Before body panel design principles can be proposed, it is important to establish the basic physical mechanisms by which noise is radiated from body panels.

Body panel radiated noise will be broken down into three sections:

1. Body panel structure-borne noise mechanisms
2. Body panel airborne noise mechanisms
3. Basic design principles.

15.6.1 Structure-borne noise mechanisms

Body panels radiate noise in the structure-borne noise range due to a combination of forced vibration and resonant vibration. Forced vibration is simply the 'rigid' response of the panel to forces acting on it from its attachment boundaries. This is analogous to the noise radiated by a moving rigid piston. Resonant vibration is the result of the same forces acting on the attachment boundaries, but which also excite the various resonances of a panel. These resonances have unique mode shapes, which in turn determine how strongly coupled the panel vibrations are to the acoustic medium (passenger space air cavity).

Reducing the rigid or forced vibration of the panel is achieved by addressing the upstream areas of the body structure, namely the body attachments and the global body stiffness (covered in Sections 15.3 and 15.4). Managing panel resonant energy to reduce unwanted radiated noise can be accomplished with various combinations of mass, stiffness and damping in the panel. Mass and stiffness affect the resonant frequency directly, but also affect the amplitude of the resonance (to a lesser degree). Damping affects the amplitude of the resonance, but also the frequency (to a lesser degree). In other words, body panel resonances in the structure-borne noise
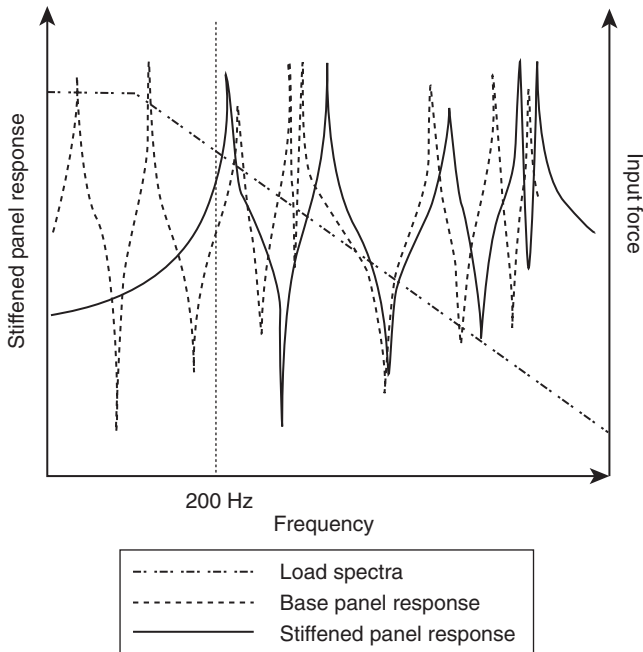
15.19 Stiffened panel resonances and input load spectrum.

range can be either managed by shifting their frequencies using mass and stiffness or damped using various types of damping treatments. In some cases a combination of frequency shifting and damping will be required to achieve the best result.

As a general rule, designing a panel such that its first mode (commonly referred to as the 'pumping' or 'breathing' mode) is above 200 Hz will help prevent low-frequency boom issues, because the input forces to the body from the engine and tire/road decline rapidly above 200 Hz due to the isolation effect of the rubber bushings. This is illustrated in Fig. 15.19 which shows the input loading spectrum and an example of a stiffened panel response (resonances shifted higher). Figure 15.20 shows the same load spectrum with a damped panel response (resonant amplitudes reduced). In each case, it can be seen that the goal is to reduce the panel resonant behavior in the low-frequency range (below 200 Hz) where the input load is the highest.

Panel acoustic contribution

In the structure-borne noise region, it has already been established that individual panel resonances are a significant noise-generating mechanism for body panels. One important and often missed aspect of this is that each
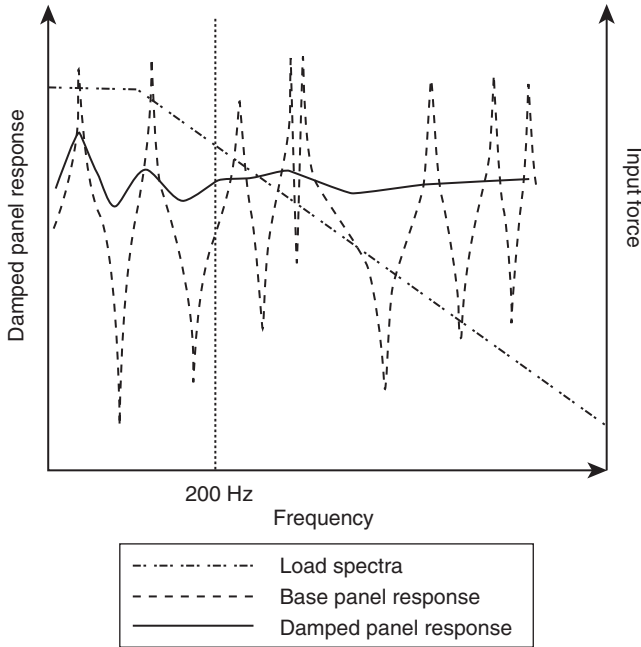
15.20 Damped panel resonances and input load spectrum.

panel resonance has both mode shape and phase with respect to all of the other panels that make up the body. Furthermore, these panel resonances are dynamically coupled to the resonances and other dynamic behavior of the interior air cavity. As a result, noise radiating from panels into the interior of the body can have both negative and positive interaction.

A simple example of this is two panels opposite each other in a closed box with equal resonant amplitude and the same phase (Fig. 15.21). In this case the net dynamic volume change (and therefore the net dynamic pressure change) inside the box is exactly zero. Eliminating the motion of one of the two panels would have the adverse effect of increasing the sound pressure level inside the box!

The opposite case is when the two panels have the same resonant amplitude but with opposite phase (Fig. 15.22). In this case, the net pressure fluctuation would be the highest (loudest). The coupling of the acoustic air space with the structural modes of the body is an important factor since the air cavity has its own resonances. Eliminating the motion of one of the two panels would now decrease the sound pressure level in the box.

Therefore, great care must be taken when targeting the vibration reduction of specific body panels. In these cases, detailed knowledge of the panel mode shapes, amplitudes and phase relationships is necessary to prevent unwanted noise increases due to panel-to-panel and panel-to-acoustic space
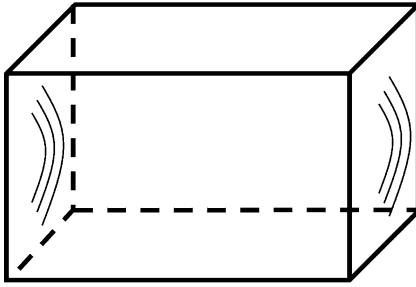
15.21 Closed-volume box with opposite panel modes in-phase.
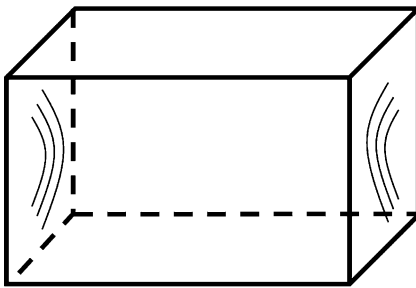
15.22 Closed-volume box with opposite panel modes out-of-phase.

interactions. Advanced tools such as panel contribution analysis can assist the development engineer in this exercise and help navigate the potential minefield of panel interactions.

15.6.2 Airborne noise mechanisms

The basic mechanism which governs the ability of a body panel to block airborne noise is known as sound transmission loss (STL). STL is defined as the ratio of the sound energy emitted by an acoustical material or structure to the energy incident upon the opposite side. Figure 15.23 shows the theoretical response for the STL of a flat panel. From this figure it can be seen that STL through a panel is governed by different factors in different frequency ranges. Stiffness and damping dominate in the very low and very high frequency ranges, and mass dominates in the middle frequency range. Automotive body panels are more complex than simple flat panels, and their STL behavior can deviate significantly from flat panel behavior. This will be discussed in the following sections.

Sound transmission through a panel can be broken down into two distinct energy paths:
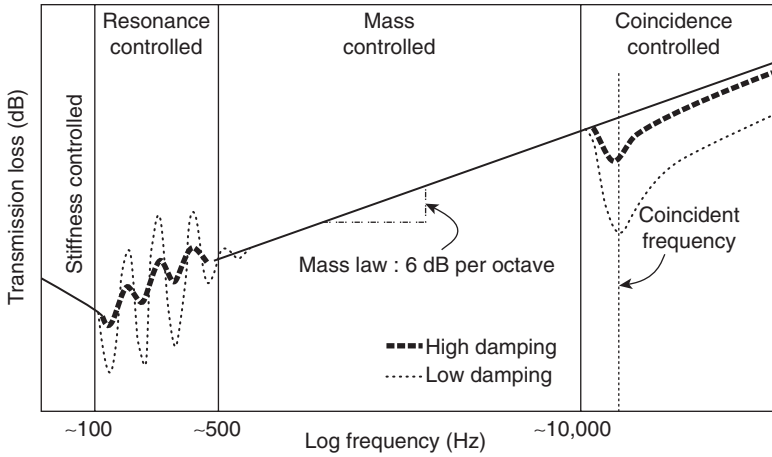
15.23 Sound transmission loss behavior for a flat plate (Norton, 1989).
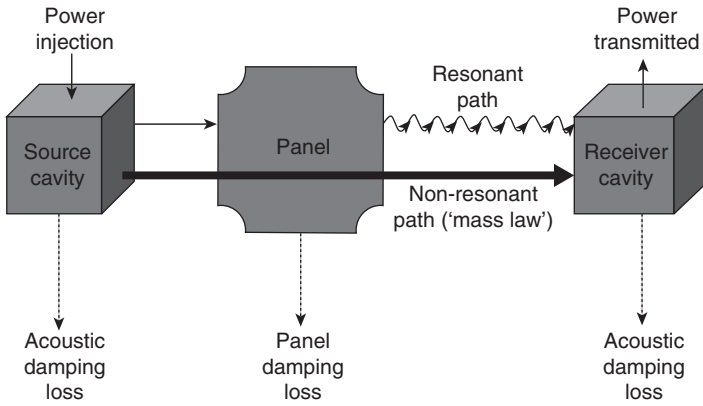
15.24 Sound transmission mechanisms through panels.

1. Non-resonant path ('mass law')
2. Resonant path.

This is shown conceptually in Fig. 15.24 along with the associated dissipation mechanisms.

When testing a panel for STL, the acoustic damping losses can generally be ignored, since the source and receiver cavities and the test methods minimize the impact of these losses on the transmitted noise.

The non-resonant path of the panel is governed only by mass: the more mass, the lower the vibration and the lower the noise. This comes directly from Newton's second law, and is often referred to as the 'mass law'. The mass law portion of STL is defined as (Raichel, 2006):

$$TL = 20\log(mf) - 47 \tag{15.12}$$

where m is mass per unit area (kg/m^2) and f is frequency.

From eq. 15.12, it can be seen that by doubling the mass of the panel, the mass-law portion of STL is increased by 6 dB. Therefore, one way to increase the ability of a body panel to block airborne noise is to increase its mass. This can be done by adding heavy asphaltic or bitumen patches to the panel, or by increasing the panel thickness. However, great care should be taken when increasing panel thickness, since this not only increases the mass but also increases the stiffness (and therefore the resonant portion) of the panel radiated noise. This will be covered in detail in the following section.

The resonant portion of panel noise radiation is governed by the bending (flexural) resonances of the panel. Vibration waves traverse across the panel in bending waves and longitudinal waves. Since bending waves create motion normal to the panel surface, it is the bending waves which are dominant in radiating noise.

Resonant bending waves of a panel travel along the panel as dipoles. Dipoles, by definition, have no net noise radiation and so the resonant radiation of a panel is nearly equal to zero so long as there are no stiffness discontinuities along the path of the bending wave to disrupt the dipole. When bending waves encounter a stiffness discontinuity, such as the panel edge or a stiffening bead, the dipole can be disrupted and converted to a monopole. A monopole radiates noise in proportion to its surface velocity. Figure 15.25 illustrates this concept. This means that stiffening beads and other structural features of the panel can actually increase the high-frequency noise radiation of a body panel.

Finally, the concept of 'coincident frequency' must be discussed, which is directly related to the resonant part of the noise radiation. The coincident frequency is the frequency at which the wavelengths of the bending resonances in the body panel exactly match the wavelengths of the propagating air pressure wave. At this frequency, the panel becomes a very efficient radiator and bending waves are easily converted into radiated noise. For most steel body panels, this phenomenon occurs above 10,000 Hz, but in a somewhat counterintuitive way, the coincident frequency actually decreases as the stiffness of the panel increases. This is due to the fact that as the panel becomes stiffer, the wavespeed of the flexural modes increases, and therefore the wavelengths at a given frequency become longer. These longer wavelengths will then match up with the wavelengths of sound pressure waves in the air at a lower frequency.

Since automotive body panels are far from flat, and are instead highly formed, their STL behavior can deviate significantly from flat panel behavior due to the strong influence of the resonant path. This means that any
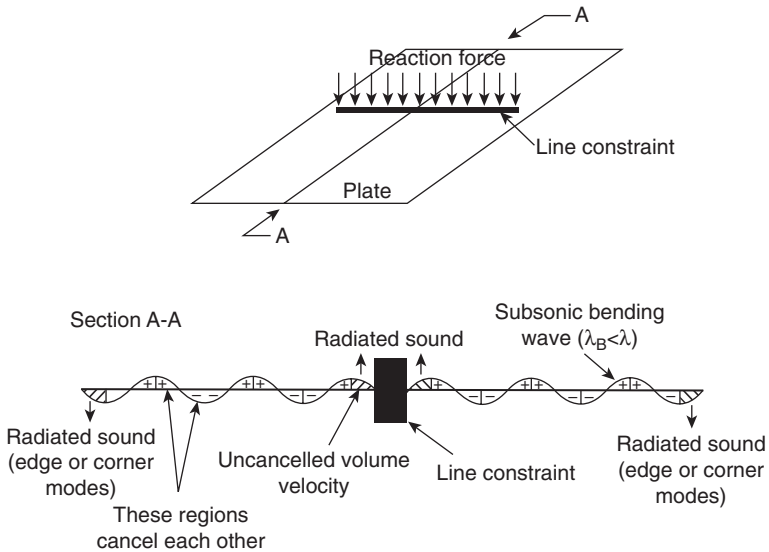
15.25 Flexural waves in a panel interrupted by stiffness discontinuity (Norton, 1989).

design strategies which increase the stiffness of a panel for low frequency will have an adverse effect at high frequencies. This dilemma can be avoided altogether by introducing sufficient damping into the panel, which essentially eliminates the bending resonances of the panel (Patil and Goetchius, 2009).

15.7   Body panel design strategies

With the basic principles of body panel dynamics established, a series of design guidelines can now be discussed, each relating back to one or more of the panel noise radiation principles covered above. The basic strategy for body panel design is as follows:

1. Design the surrounding beam structure to minimize the energy transmitted into the panel.
2. Manage individual modes of the panel to avoid excitation sources and other nearby resonances.
3. Carefully optimize the gauge. Manage the conflicting requirements of global body static stiffness, modal resonant response and high-frequency noise radiation.
4. Introduce damping into the panel to minimize resonant noise radiation.

15.7.1 Panel boundary structure

In previous sections, it has been established that providing a strong and continuous 'cage' structure is critical to overall NVH performance of the body. A strong cage structure will minimize the amount of energy transmitted to the panels and therefore minimize the noise radiating from the panels. The strategies for accomplishing this have been covered in previous sections in this chapter.

15.7.2 Panel mode management

In many cases, the resonances of a body panel will coincide with other resonances of the vehicle (acoustic cavity, suspension, etc.) and, more critically, they can coincide with energy peaks in the forcing function entering the body. The same rules for global body mode management also apply to body panels (in order of importance):

1. Manage panel resonant frequencies away from excitation source frequencies.
2. Manage panel resonant frequencies away from other coupled resonant systems (i.e. acoustic cavity modes, other nearby panels, etc.).

The most common methods to accomplish this panel mode management strategy are to change the panel gauge and to introduce bead patterns, dome patterns and other panel formations to stiffen, and therefore shift the panel resonant frequencies. Due to the negative impact that panel stiffening can have on high-frequency radiated noise, it is critical to combine stiffness increases with sufficient damping so that the high-frequency resonant behavior is controlled (Patil and Goetchius, 2009).

Panel beads can be thought of as miniature beams, and as such follow basic beam theory. Bead design guidelines are as follows (Onsay *et al.*, 1999):

• Beads should be straight.
• Beads should span the shortest distance between structural boundaries.
• Beads should not be 'broken' or discontinuous across the length of the bead.
• Beads should terminate close to or at the structural boundaries of the bead.
• Beads should not cross.

Figure 15.26 shows examples of good panel bead designs and Fig. 15.27 shows examples of less efficient and generally undesirable panel bead designs.
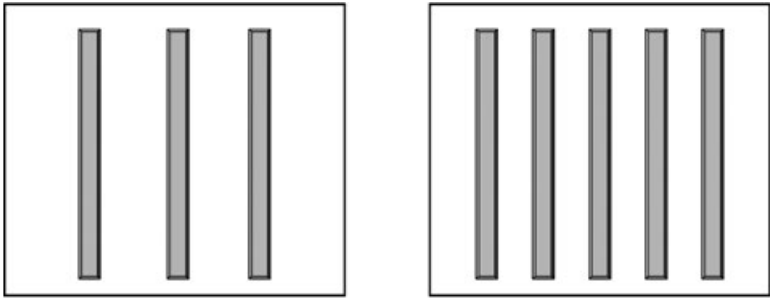
15.26 Preferred panel bead stiffening examples.
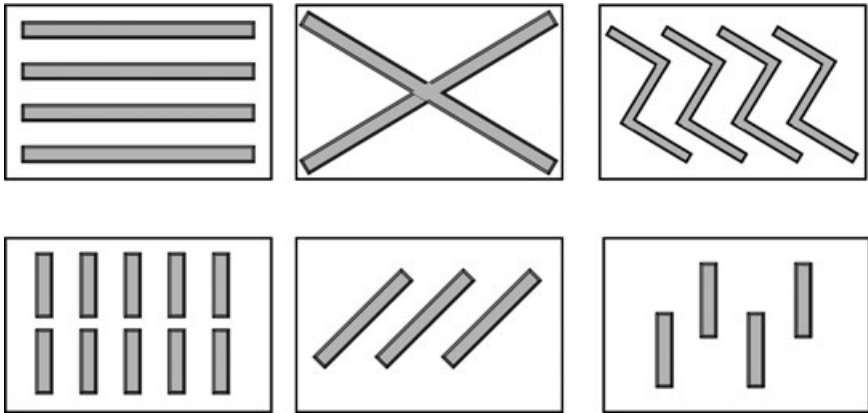
15.27 Inefficient panel bead stiffening examples.

15.7.3 Panel gauge optimization

The effect of panel gauge (thickness) on NVH is important. The flexural stiffness of a panel can be expressed as bending rigidity, which is given by (Norton, 1989):

$$B = E\left(\frac{t^3}{12(1-v^2)}\right) \tag{15.13}$$

where:

B = bending rigidity
E = Young's modulus
t = panel thickness
v = Poisson's ratio.

Also note that the mass of a panel can be given by:

$$M = A*t \tag{15.14}$$

where:

M = mass
t = panel thickness
A = panel area.

Noting that mass changes proportionally to panel thickness and stiffness changes as the cube of thickness, it can be seen that the net effect of panel thickness change is a change in the natural frequencies of the panel resonances. This means that optimizing the panel gauge is another tool for panel modal management.

As always, it is important to understand the implications of changing the panel gauge (and therefore stiffness and mass) on both structure-borne and airborne noise. Increasing the panel gauge will shift the resonant energy to a higher frequency range, which can be useful in managing panel modal energy which is in the vicinity of excitation forces or other resonances. It also increases the mass of the panel, which can add extra STL performance in the mass-law range of the panel. However, if left undamped (or under-damped), a thicker panel is subject to higher noise radiation in the high-frequency airborne noise range due to the increased resonant path in the panel's STL performance. Therefore, caution must be exercised when changing panel gauges, and the proper balance between structure-borne and airborne noise must be maintained.

15.7.4 Panel damping

Introducing damping into a body panel can significantly improve both the structure-borne and airborne noise performance of the panel. Damping is often characterized by the term 'loss factor'. Conceptually, the loss factor is the ability of a material to dissipate resonant energy, and can range from 0 to 1. A loss factor of 1 means that all resonant energy is completely damped out (time domain impulse response would have no oscillation), and a loss factor of 0 means that no resonant energy is damped out (time domain impulse response would oscillate forever). Table 15.1 shows the loss factor of several familiar materials.

Achieving high loss factors (high damping) in body panels requires the introduction of various materials to the panel, since body panel materials (steel, aluminum, etc.) have very low inherent damping (loss factor less than 0.01). General practice has shown that loss factors above 0.1 provide sufficient damping for most body panel applications.

Table 15.1 Loss factor values for common materials

Material	Loss factor
Asphalt	0.055–0.38
Light concrete	0.01
Oak	0.01
Plywood	0.01–0.05
Gypsum board	0.004–0.03
Glass	0.0008–0.002
Dry sand	0.06–0.12
Steel	0.001
Steel with unconstrained damping sheet	0.1
Steel with constrained damping sheet (including laminated steel)	0.25
Aluminum	0.0001
Lead	0.02–0.03

Source: Cremer and Heckl (1988).

Unconstrained (extensional) damper

Viscoelastic layer

Base panel

Constrained (shear) damper

Constraining panel
Viscoelastic layer
Base panel
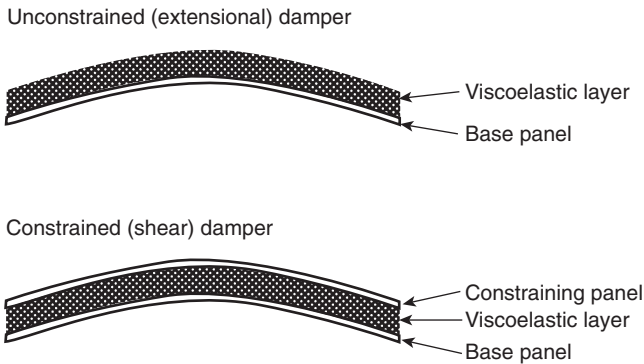
15.28 Unconstrained and constrained layer panel damping treatments.

There are two kinds of damping mechanisms for sheet metal panels:

1. Unconstrained layer (extensional) damping
2. Constrained layer (shear) damping.

Figure 15.28 illustrates these two types of damping treatments.

Unconstrained damping makes use of a single layer of bitumen or asphaltic material which is essentially 'stretched' or 'compressed' as the bending waves deform the panel. For this reason, unconstrained damping treatments are often referred to as 'extensional' dampers, since the basic strain mechanism is extensional strain. Extensional strain is much less efficient in dissipating energy than shear strain, since the polymer molecule chains do

not slide across each other as much as in the shear strain case. Therefore, extensional dampers are less effective than constrained layer dampers. However, extensional dampers are often cheaper and can be easier to apply than constrained layer damping materials.

Constrained layer damping makes use of a stiff constraining layer and a soft viscoelastic layer on top of the base sheet metal. The result is a high level of shear strain imparted on the viscoelastic core when bending waves deform the panel. Shear strain is highly effective in dissipating vibrational energy due to the way the polymer molecule chains in the viscoelastic material are forced to slide against and across each other. For this reason, constrained layer damping treatments are often referred to as 'shear' dampers, since the basic strain mechanism is shear strain. Figure 15.29 shows how the constraining layer shears the core material under bending. Constrained layer damping materials can be either added on to the base panel or included in the base panel itself using a laminated metal approach.
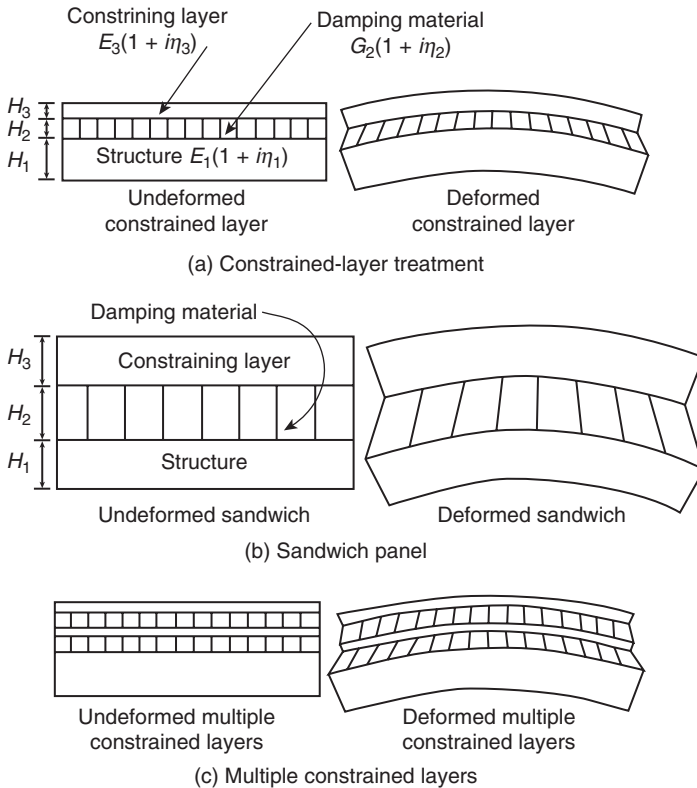
15.29 Shear mechanism of constrained layer damper in bending (Nashif et al., 1985).

    In the case of add-on damping treatments (both constrained and uncon-
strained), a minimum coverage area is needed to affect both structure-
borne and airborne noise. For structure-borne noise, add-on damping
treatments can be applied only to the areas of the panel which are exhibit-
ing high modal strain energy (high motion). However, in order to combat
the resonant path in the high-frequency airborne noise range, it is necessary
to cover at least 70% of the panel area which is exposed to the airborne
noise source. In many cases, it can be found that the damping coverage area
needed for structure-borne noise would not sufficiently cover the panel to
address the resonant path at high frequencies. In these cases, the laminated
metal approach can be an alternative since it has, by definition, 100%
damping area coverage.

15.8   Future trends

As with most automotive systems, the drive towards higher fuel economy,
lower emissions and more eco-friendly materials will have a significant
impact on body structure NVH in the future. This will manifest itself in
several ways:

1. Alternative (high efficiency) propulsion systems will have dramatically
    different operational loads on the body structure in terms of both overall
    levels but also frequency content. This could fundamentally shift the
    basic understanding of the split between structure-borne and airborne
    noise contributions.
2. Reducing weight in vehicles has always been a top priority. However,
    the recent global emphasis on reducing fuel consumption and emissions
    has escalated weight-savings initiatives to the top of most automotive
    engineers' lists. As a result, lighter-weight materials will find their way
    into the automotive body structure. Aluminum body structures have
    been introduced on several production vehicles, but this practice has
    not become mainstream due to cost and manufacturability concerns.
    This may change under the current weight reduction pressures. More
    'exotic' materials (e.g. graphite epoxy composites) commonly found on
    racing cars and high-end performance cars may also begin to become
    more mainstream. In both of these cases, the challenge for body NVH
    control will be daunting since we know that very stiff and very light
    structures are also very loud (just ask any loudspeaker designer!). This
    also means that some of the more practical and economical solutions
    for noise control in the body structure may need to be replaced with
    more expensive systems to deal with the lighter-weight materials.
3. Regardless of the materials which will be used in future body structures,
    they will all most certainly face tougher requirements with respect to

environmental impact and recyclability. Certainly, steel and aluminum are highly recyclable and mature programs have existed for decades for recycling automotive body structures. However, many of the noise and vibration treatments applied to the body are not recyclable and neither are many of the new and exotic composite materials which may find their way into future body structures.

4. As vehicles get lighter, even more emphasis will be placed on crashworthiness. Much of the crashworthiness of a vehicle comes from the body structure, and new lightweight materials, along with the different behavior of the aforementioned alternative propulsion systems, will create new and unimagined challenges for the body structure designer, and therefore potentially create an even tighter set of criteria within which body structure NVH must be developed.

5. The use of computer aided engineering (CAE) tools to assist engineers in designing and refining the NVH performance of the body structure much earlier in the product life cycle will continue to grow. Today, CAE methods for body NVH are widespread and fairly mature. They are used extensively at many automotive original equipment manufacturers (OEMs) early in the design process. However, there are still many weaknesses in the CAE process which will need to be addressed and improved in the future, especially as the cost of building prototypes continues to limit the availability of hardware on which to do development testing. These weaknesses include frequency constraints on structure-borne and airborne noise analysis types, lack of statistical sampling and probabilistic methods, and lack of a mature understanding of the forces generated by new and as yet undeveloped propulsion technologies which act on the body structure, among many others.

15.9   Conclusions

Every aspect of body structure design has an effect on the noise and vibration level which ultimately reaches the vehicle occupants. As a result, great care and diligence are required in understanding all of the sources and paths of noise and vibration energy. Sources and paths for both structure-borne noise and airborne noise must be well understood, since design concepts and countermeasures for one often result in poor performance in the other. The 'best practice' design concepts and 'generic targets' proposed in this chapter should be used as the starting point for the evaluation and design of any automotive body structure. However, realizing that each vehicle is a unique and complex system, it is critical that the specific performance of each body structure be carefully crafted to meet the specific needs of the vehicle of which it is a part. This can be done using a combination of experience, predictive methods (CAE) and development testing.

Table 15.2 Generic target and best practice summary

Generic target/best practice	Value	Comments
Point mobility (*V/F*)	−10 dB	mm/sec/N (reference: 1 mm/sec/N)
Body-to-isolator attachment stiffness ratio (K_{ratio})	5:1	Unitless ratio
Body acoustic transfer function (*P/F*)	60 dB(Pa)/N	(reference: 2e − 5 Pa)
Body panel loss factor	0.1	Unitless ratio
Body panel first mode	200 Hz	
Body panel damping area coverage	70%	
Modal separation (mode management)	10%	Global body modes and panel modes
Spot weld pitch	30 mm	

In previous sections, generic targets for various body NVH metrics have been proposed. These targets are summarized in Table 15.2.

15.10 References

Achram L, Chidamparam P, Goetchius G, Thompson J (1996), 'Applying NVH basics to body design', *Proceedings of the 1996 International Body Engineering Conference*.

Cremer L, Heckl M (1988), *Structure Borne Sound*, Springer-Verlag, New York.

Dong B, Goetchius G, Duncan A, Balasubramanian M, Gogate S (1999), 'Process to achieve NVH goals: Subsystem targets via "digital prototype" simulations', *Proceedings of the 1999 SAE Noise and Vibration Conference*.

Duncan A, Su F, Wolf W (1996), 'Understanding NVH basics', *Proceedings of the 1996 International Body Engineering Conference*.

Duncan A, Goetchius G, Guan J (2009), Structure Borne Noise Workshop, 2009 SAE Noise and Vibration Conference.

Dunn J (1978), 'Standardization techniques for the dynamic performance of monocoque vehicle structures', *Proceedings of the Inst. Measurement and Control Symposium, Vehicle Ride and Maneuvering Characteristics Volume*.

Gogate S, Duncan A (2001), '"Digital prototype" simulations to achieve vehicle level NVH targets in the presence of uncertainties', *Proceedings of the 2001 SAE Noise and Vibration Conference*.

Huang J, Sin H (2001), 'Aluminum rail rivet and steel rail weld DOE and CAE studies for NVH', *Proceedings of the 2001 SAE Noise and Vibration Conference*.

Nashif A, Jones D, Henderson J (1985), *Vibration Damping*, John Wiley & Sons, New York.

Norton M (1989), *Fundamentals of Noise and Vibration Analysis for Engineers*, Cambridge University Press, Cambridge.

Onsay T, Akanda A, Goetchius G (1999), 'Vibro-acoustic behavior of bead-stiffened flat panels: FEA, SEA, and experimental analysis', *Proceedings of the 1999 SAE Noise and Vibration Conference*.

Patil A, Goetchius G (2009), 'Effect of damping on sound transmission loss through automotive body panels', *Proceedings of the 2009 SAE Noise and Vibration Conference*.

Plunt J (2005), 'Examples of using Transfer Path Analysis (TPA) together with CAE-models to diagnose and find solutions for NVH problems late in the vehicle development process', *Proceedings of the 2005 SAE Noise and Vibration Conference*.

Raichel D (2006), *The Science and Applications of Acoustics*, Springer, New York.

Williams R, Balaam M (1989), 'Understanding and solving noise quality problems', *Proceedings of the 1989 Auto Tech Conference*.

16

Vehicle noise and vibration strategy-based diagnostics

X. WANG, RMIT University, Australia

Abstract: This chapter introduces noise and vibration induced by run-outs, material property variations, imbalance of tyre/wheel and propshaft, and incorrect driveline angles. Root-cause diagnosis methods and problem-solving methodology are illustrated in detail in order to help eliminate conventional customer complaints in terms of vehicle noise and vibration problems.

Key words: run-out, static imbalance, dynamic imbalance, first-order vibration, second-order vibration, tyre/wheel balance, propshaft balancing, driveline angle, propshaft phasing, tyre/wheel force variation.

16.1 Introduction

When a person does not feel well, with symptoms such as high temperature, vomiting, diarrhoea, dizziness, headache, etc., he goes to see a medical doctor. The doctor would listen to his description of the symptoms, collect the information, and carry out a series of medical tests in order to identify the root causes for his sickness and make decisions for the solutions such as prescriptions, surgery, etc. A machine or a vehicle will have noise and vibration symptoms if it is poorly designed or is liable to mechanical or structure failure. The mechanic follows the same diagnosis and solution process, which is to collect information by talking with customers and to reproduce the symptoms by doing test drives in relevant driving conditions. A series of noise and vibration tests are carried out to identify the root causes for the noise and vibration problems, and solutions such as modification of the source, structure or transmission path are determined.

Customer complaints or callbacks are common issues in vehicle warranty periods. A lot of complaint issues concern noise and vibration symptoms. In order to resolve them in a reasonably short period of time (such as one or two weeks) and satisfy the customers, noise and vibration-based diagnosis strategy or methodology is necessary for both engineers and their employers.

The objective of this chapter is to formulate systematic noise and vibration diagnosis strategy or methodology and solutions by investigating the

387

① **Diagnostic flow**
Verify complaint

② Preliminary checks (visual, operational, DTC)

③ Check bulletins and trouble-shooting highlights

④ Perform service manual system check(s)

⑤ a **Hard code**
Perform service manual diagnostic procedures

⑤ b **No code**
Select symptom from service manual symptom chart and perform procedure

⑤ c **No matching symptom in service manual**
Analyse and develop diagnostics from wiring chart and theory

⑤ d **Intermittent**
Refer to intermittent diagnostic details

⑤ e Operating as designed
Call or explain to customer

Find/isolate the problem — No → Re-examine the complaint ⑥

⑦ Repair/resolve and verify fix — Yes

16.1 Noise and vibration strategy-based diagnostics.

root causes such as run-outs, force variations, imbalances of tyres/wheels and propshaft, and driveline angles, which can be used to resolve most noise and vibration issues.

A conventional vehicle noise and vibration strategy-based diagnostics process flow is shown in Fig. 16.1 in which seven steps are followed. Before getting started, a few basic concepts must be understood. As in any diagnostics process, one must gather information, decipher it, and perform a

correction based on the results. Basically, we follow a process of elimination. For example, the following is such an elimination process:

1. A customer brings his/her vehicle to the dealer complaining of a pulsation when the brakes are applied.
2. The service advisor questions the customer and writes the pertinent details on the repair order.
3. Next, the technician reads the information, and road tests the vehicle using the normal and the parking brake to stop the vehicle. He is gathering information.

If the pulsation was present only while using the parking brake, the logical approach would be to inspect the rear brakes first for an out-of-round or similar condition. This would, in turn, dictate the type of repair necessary to eliminate the complaint. If the technician measured the rear brake drums and found excessive run-out present, he would then most likely resurface the drums and evaluate the vehicle to make sure that the method of repair he chose was the correct one, based on the information that was gathered.

This process of elimination can be very useful when applied to correcting vibrations in two steps:

1. The service advisor gathers information about the complaint from the customer.
2. The technician then road tests the vehicle in a manner intended to systematically eliminate different parts of the vehicle. This information supplements the customer information.

By concentrating repair efforts on the areas that have not been eliminated, repairs can be made more quickly and effectively.

To take another example, a customer brings his or her car to the dealership, complaining of a vibration at 60 km/h. During the road test, the technician discovers the same vibration can be felt while the car is stopped at the same time revving the engine to about 1200 rpm. The logical approach, based on this information, would be to concentrate on components related to the engine, since tyres, wheels and the driveline have already been eliminated as a possible cause. This is because they are not rotating when the vehicle is standing still. Take the time to gather additional information relating to the complaint. It saves a tremendous amount of time in the long run.

16.2   Wheel and tyre vibrations

Vibrations related to wheel and tyre are low-frequency vibrations and sensitive to vehicle speed. In this section, the following specific vehicle components will be addressed according to vibration frequency and systems:

- Tyres
- Wheels
- Wheel hubs
- Brake rotors.

We will go through the steps necessary to systematically approach and repair problems found in these areas.

16.2.1 First-order vibrations

The following are symptoms of first-order vibrations caused by tyre/wheel assemblies:

- They are always vehicle-speed related. If the vibration is affected by the speed of the engine, or is eliminated by placing the transmission in neutral and coast down test vehicle, then it is not related to the components in this group.
- The vibration will 'feel' like a shake, usually in the steering wheel or seat.
- At low speed (10 to 60 km/h) the customer may complain of a 'waddle' (see Section 16.3.6 Lateral force variation).

The frequency of the vibration will correspond to the first-order of tyre rotation. This will usually be in the 10–20 Hz range, depending on the speed of the vehicle and the size of the tyre. The smaller the tyre, the faster it will rotate at any given speed.

The available range of human hearing begins at 20 Hz. For this reason, first-order tyre vibrations rarely produce a noise. The exception to this would be if the tyres display an irregular tread pattern or flat spots, causing a 'growling' or 'slapping' noise. Tyre/wheel vibrations felt in the steering wheel are most likely related to the front tyre/wheel assemblies. Tyre/wheel vibrations felt in the seat or floor are most likely related to the rear tyre/wheel assemblies. This may not always hold true but is a general rule that may serve to initially isolate a problem to the front or rear.

First-order tyre/wheel vibrations are usually the result of one of five conditions:

- Excessive radial run-out
- Excessive lateral run-out
- Excessive imbalance
- Excessive radial force variation
- Excessive lateral force variation.

All five of these conditions must be eliminated step by step, in order to attain a set of tyres free from vibration-causing elements. Substituting a set

of tyres from another vehicle should only be performed as a last resort, and then only if the tyres used have been evaluated on a similar vehicle under the same conditions.

Due to vehicle-to-vehicle sensitivities and differences between the mounting hubs of any two vehicles, correcting the existing tyre/wheel assemblies is the most accurate and least time-consuming approach in the long term.

16.2.2 Run-out

Because the run-out of a tyre/wheel assembly will directly affect the amount of imbalance and radial force variation, radial and lateral run-out can be corrected at the same time. There are two methods to measure run-out of tyre/wheel assemblies:

- On the vehicle (mounted to the hub – the wheel bearing must be in good condition)
- Off the vehicle (mounted on a spin-type wheel balancer)
- Initial on-car inspection should be made prior to off-car runout check.

Measuring the tyre/wheel run-out off the vehicle is easiest. It is usually easier to mount a dial indicator in the correction location as shown in Fig. 16.2, and the chances of water, dirt or slush getting on the indicator are decreased. Once the run-out has been measured and corrected off the vehicle, a quick visual recheck of run-out on the vehicle will indicate if any further problems exist. If there is a large difference in the run-out measure-ments from on-vehicle to off-vehicle, then the run-out problem is due to either stud pattern run-out, hub flange run-out, or a mounting problem between the wheel and the vehicle.

(a)   (b)
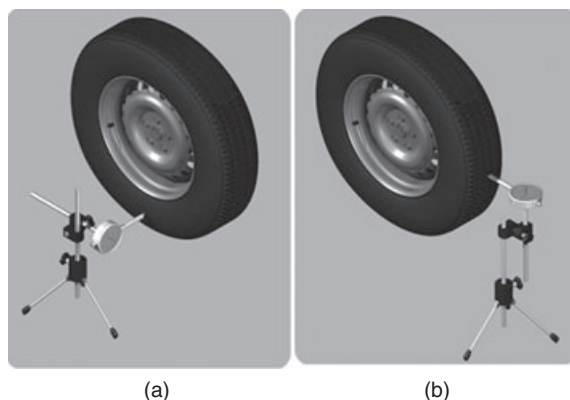
16.2 (a) Radial and (b) lateral run-out.

Before measuring or attempting to correct excessive run-out, carefully check the tyre for uneven bead seat. The distance from the edge of the ring to the concentric rim locating ring should be equal around the entire circumference. If the beads are not seated properly, the tyre should be remounted, otherwise excessive run-out and imbalance may result.

16.2.3 Measuring tyre/wheel assembly run-out

If the vehicle has been sitting in one place for a long time, flat spots may exist at the point where the tyres were resting on the ground. These flat spots will affect the run-out readings and should be eliminated by driving the vehicle long enough to warm up the tyres. Do this before any run-out measurements are taken, and do the following:

1. Lift the vehicle on a hoist or support with jack-stands.
2. In order to get an initial indication of how much run-out exists, spin each tyre and wheel on the vehicle by hand (or at a slow speed using the engine to run the drive wheels), visually checking the amount of run-out from the front or rear.
3. Mark the location of each tyre/wheel assembly in relation to the wheel studs and to their position on the vehicle (right front, left rear, etc.) for future reference.
4. Remove the tyre/wheel assemblies one at a time and mount on a spin-tyre wheel balancer.
5. Measure the tyre/wheel assembly run-out as shown in Fig. 16.3.

On tyres with an aggressive tread pattern, it will be necessary to wrap the outer circumference with tape when measuring radial run-out. This allows for a smooth reading to be obtained from the dial indicator. Lateral run-out should be measured on a smooth area of the sidewall, as close to the tread as possible. Any jumps or dips due to the sidewall splices should be ignored and an average amount of run-out obtained by the following procedure:
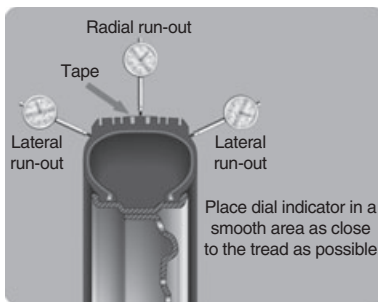
16.3 Measuring tyre/wheel assembly radial and lateral run-out.

1. Slowly rotate the assembly one complete revolution and 'zero' the dial indicator on the spot.
2. Rotate the assembly one more complete revolution and note the total amount of run-out indicated.

The maximum allowable assembly radial and lateral run-out is 1.5 mm when measured off the vehicle and 1.8 mm on the vehicle.

16.2.4 Match-mounting

If the run-out is excessive, mark the location of the high and low spot on the tyre and the wheel. The next step is to determine if the run-out problem exists in the tyre, wheel or a combination of both, then to correct it. The procedure used to accomplish this is called match-mounting or system matching:

1. Place a mark on the tyre sidewall at the location of the valve stem. This will be referred to as the 12:00 position. The location of the high spot will always be referred to in relation to its 'clock position' on the wheel.
2. Mount the tyre/wheel assembly on a tyre machine and break down the bead. Do not dismount the tyre from the wheel at this time.
3. Rotate the tyre 180° on the rim so the valve stem reference mark is now at 6:00 in relation to the valve stem itself. Reinflate the tyre and make sure the bead is seated properly. The bead may have to be lubricated in order to easily rotate the tyre on the wheel.
4. Mount the assembly on the tyre balancer and remeasure the run-out. Mark the new location of the run-out high point on the tyre. If the run-out is now within tolerance, no further steps are necessary. The tyre may be balanced and mounted on the vehicle.
5. If the clock location of the high spot remained at or near the clock location of the original high spot, the wheel is the major contributor to the run-out problem as shown in Fig. 16.4. It should be measured for excessive run-out and replaced if that is the case.
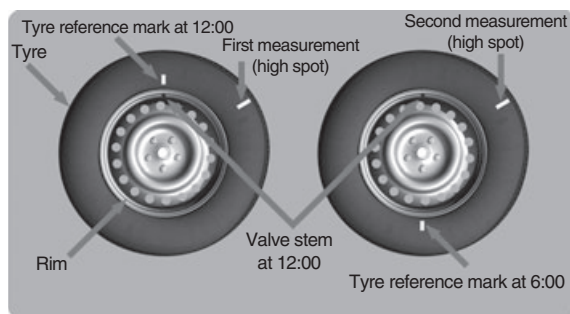
16.4 Match-mounting (1): the wheel is the major run-out contributor.
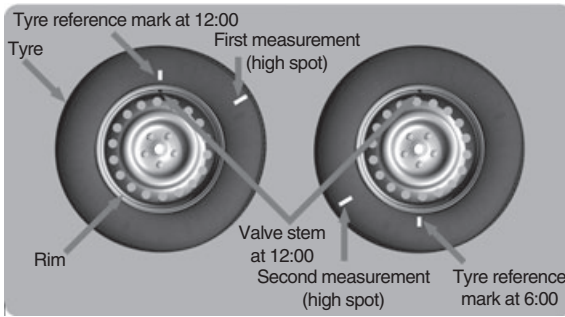
16.5 Match-mounting (2): the tyre is the major run-out contributor.

Always measure the run-out of new wheels when replacing old ones. Do not assume that a new wheel is automatically a 'known good' component. If the high spot is now at or near a position 180° (6 hours) from the original high spot, the tyre is the major contributor and should be replaced as shown in Fig.16.5. Always measure the tyre/wheel assembly run-out after replacing the tyre and make sure the run-out is within tolerance before continuing. In the majority of cases, the first 180° turn of the tyre will either correct the run-out problem or indicate which component to replace. If the high spot is between these two extremes, then both the tyre and the wheel are contributing to the run-out. Try rotating the tyre an additional 90° (3 hours) in both clockwise and counterclockwise directions, measuring the run-out after each rotation. Once run-out has been brought within the tolerance, the assembly should be balanced.

16.2.5 Wheel run-out

If run-out cannot be brought within tolerance by match-mounting, dismount the tyre from the wheel and measure wheel run-out. Wheel run-out should be measured on the inside bead area of the wheel. Measure the run-out in the same fashion as tyre run-out. Ignoring any jumps or dips due to paint drips, chips or welds, measure both inboard and outboard as shown in Fig. 16.6.

If the run-out of the wheel is within tolerance, and the tyre/wheel assembly run-out cannot be reduced to an acceptable level by using the match-mounting technique, the tyre must be replaced. Always remeasure assembly run-out after replacing the tyre. If there is a large difference in the run-out measurement from on-vehicle to off-vehicle, the run-out problem is due to either stud pattern run-out, hub flange run-out, or a mounting problem between the wheel and the vehicle. If run-out measurements are within tolerance but are marginal, some sensitive vehicles may still be affected. It
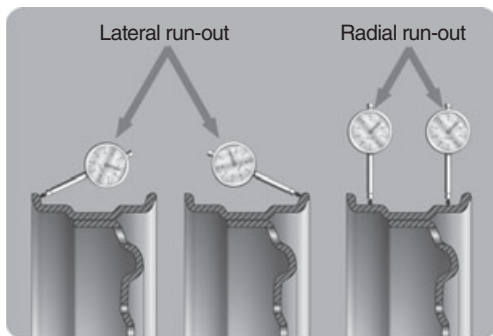
16.6 Lateral and radial run-out.
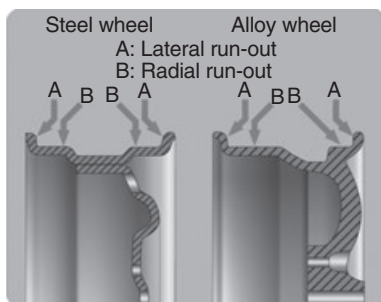
16.7 Steel and alloy wheel run-out.

is always advisable to reduce run-out as far as possible in order to obtain optimum results under all conditions.

Figure 16.7 shows lateral and radial run-out measurement locations for steel and alloy wheels.

16.2.6 Fitting new tyres

When fitting a new tyre to a wheel, it is important to ensure that the tyre is correctly indexed to the wheel, i.e. the first harmonic high point of the tyre should be fitted so that it is matching the first harmonic low point of the wheel. The matching minimizes the effects of force variation inherent in tyre manufacture.

All wheels have a mark on the outer flange indicating the first harmonic low point (a drill point), a paint mark or an 'O'. Australian manufactured tyres have a red dot on the sidewall indicating the first harmonic high point. European manufactured tyres have a white dot on the sidewall indicating the first harmonic low point. Some Japanese manufactured tyres have a red dot on the sidewall indicating the first harmonic high point and a yellow dot indicating a static balance point.

16.3   Balancing

The purpose of wheel balancing is to undo the wheel vibrations, or at least to reduce them to an acceptable limit, thus avoiding all consequent troubles and damage such as:

- Tyre wear
- Early bearing wear
- Damage to shock absorbers and other steering parts
- Loosening of the vehicle body and screw bolts
- Detachment or peeling of electric wires
- Difficult drive and lower road control due to wheel tripping and shimmy effects
- Reduced comfort for passengers.

Wheel balancing is achieved by applying some masses with suitable weights on the wheel in such a way as to avoid vibration.

The centrifugal force is due to the unbalance mass. If p is the unbalance weight and its mass is given by $m = p/g$ (g = acceleration due to gravity), the centrifugal force is then:

$$F = rm\omega^2 = r\frac{p}{g}\omega^2 \tag{16.1}$$

where ω is angular speed. If $p = 50$ g, in a wheel having an outer diameter $D = 600$ mm and running at $V = 120$ km/h, the weight generates a centrifugal force:

$$F = \frac{pV^2}{63.6D} = \frac{50 \times 120^2}{63.6 \times 600} = 18.9\,\text{kg} \tag{16.2}$$

Also, a little centre error e (mm) on a wheel having a weight P (kg) generates an unbalance

$$p = \frac{2000Pe}{D} \tag{16.3}$$

If a wheel has a weight P of 20 kg, a centre error e of 0.3 mm would cause an unbalance of

$$p = \frac{2000 \times 20 \times 0.3}{600} = 20\,\text{grams}$$

and a centrifugal force of

$$F = \frac{20 \times 120^2}{63.6 \times 600} = 7.6\,\text{kg}$$

16.3.1 Wheel balancing methods

Two balancing methods are available:

- Wheel balancing separately, off the vehicle, by means of suitable balancing machines
- Wheel balancing on the vehicle by means of suitable units.

These two methods differ either because of their different peculiarities of use or because they involve different results from a technical viewpoint, owing to their different limits and possibilities.

Wheel balancing is necessary in the following circumstances:

- When each tyre is changed
- After about 20,000 km running either in the case of a new vehicle or in the case of a new tyre
- For a sports car, after 5000 km and every 10,000 km
- When a tyre is refitted after repair or every time vibration or shimmy effects are noted
- On the spare wheel.

16.3.2 Static and dynamic balance

There are two types of tyre/wheel balance – static and dynamic:

- Static balance affects the distribution of weight around the wheel circumference.
- Dynamic balance affects the distribution of weight on each side of the lateral tyre/wheel datum plane.

As a rule, vehicles are more sensitive to static imbalance than to dynamic imbalance, with as little as 5 grams capable of inducing a vibration in some models. Vibration induced by static imbalance will cause a vertical or 'bouncing' motion of the tyre. Static imbalance is shown in Fig. 16.8, and the vibration patterns in a wheel due to a static imbalance are shown in Fig. 16.9 where the effects of the static imbalance are vertical rebound, surging, shimmy and wear.
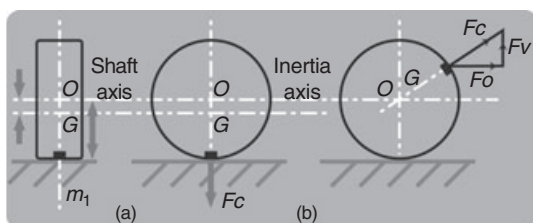
16.8 Static imbalance.

16.11 Shimmy, caused by dynamic imbalance.

16.9 Vibration patterns due to static imbalance.

16.10 Dynamic imbalance.

© Woodhead Publishing Limited, 2010
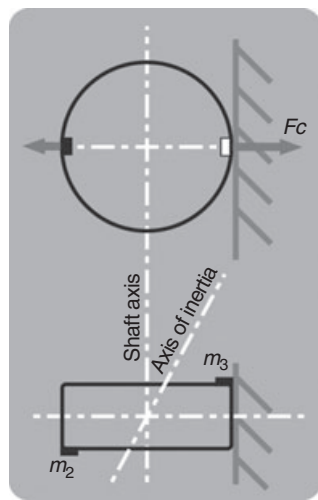
Dynamic imbalance is shown in Fig. 16.10. It results in a side-to-side motion of the tyre sometimes referred to as shimmy, as shown in Fig. 16.11. The difference between static and dynamic wheel balance is shown in Fig. 16.12.

All four tyre/wheel assemblies should be balanced as close to zero as possible, carefully following the wheel balancer manufacturer's instruction
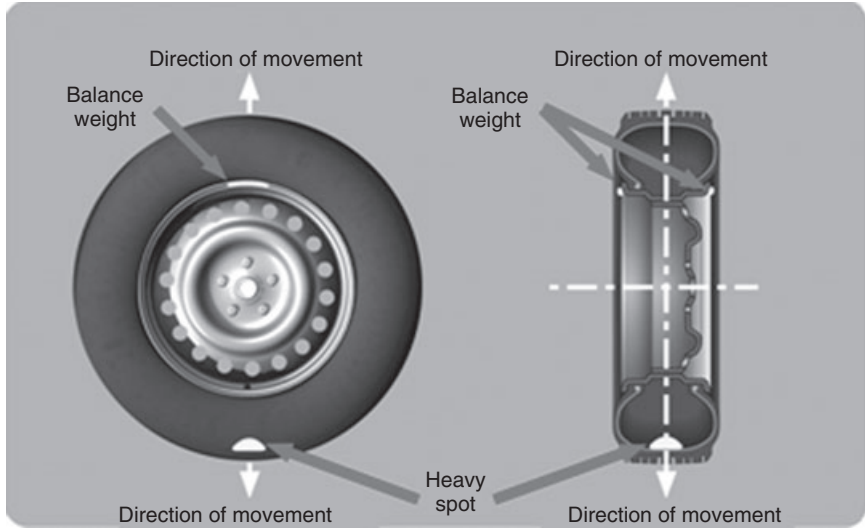
(a)
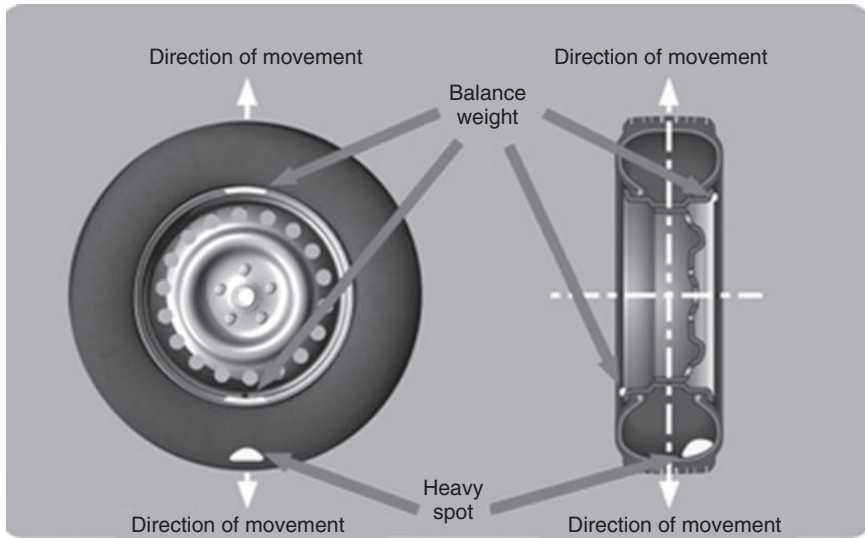
(b)

16.12 The difference between (a) static balance and (b) dynamic balance.

Table 16.1 Standard wheel balancing tolerance rates

Balancing grade (G)	Vehicle types	Tolerance (grams)
12	Fast cars and motorcycles	5
14	Standard cars and motorcycles	10
16	Light motor lorries	30
18	Standard motor lorries	60
20	Heavy trucks	150

for proper mounting techniques to be used on different types of wheels. The standard balancing tolerance rates, valid for each wheel side, are indicated in Table 16.1.

For special cases, the balancing tolerance can be determined by the following formula:

$$p = 3.67 \frac{D}{d} \frac{P}{v} G \qquad (16.4)$$

where:

p = balancing tolerance (g)
P = wheel weight (kg)
D = wheel outer diameter (road contact) (mm)
d = diameter where counterweights can be put (rim diameter) (mm)
v = maximum vehicle speed (km/h)
G = balancing grade (see Table 16.1).

For standard cars, the ratio D/d is about 1.3 and the balancing tolerance can be determined from Fig. 16.13 as a function of the car's top speed on the road and the wheel weight.

Once all four tyre/wheel assemblies have been corrected for run-out and imbalance, reinstall them on the vehicle and double check the on-vehicle run-out. It must remain within tolerance. Evaluate the vehicle at the speed to which the complaint related and note if the vibration has been corrected. In most cases, the above procedures will reduce the vibration to an acceptable level, especially if the run-out has been reduced to an absolute minimum.

If the vibration is still present, or is reduced but still unacceptable, one of two possibilities exists:

- For on-vehicle imbalance, the imbalance may result from the components other than the tyre/wheel assemblies such as hubs, rotors, etc., having imbalance.
- Radial or lateral force variation.
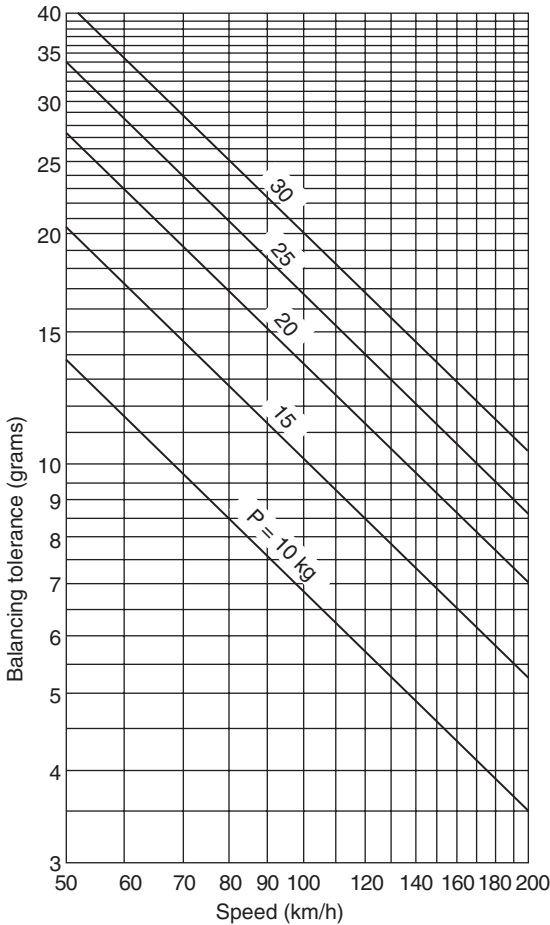
16.13 Balancing tolerance.

16.3.3 Vehicle wheel balancing

Wheel unbalances can always be traced back to a static unbalance m_1 and couple unbalances m_2 and m_3 as shown in Fig. 16.14.

Wheel balancing is an operation by which some masses are applied on the two wheel sides. Due to the fact that the planes in which to apply balancing masses are the same as those in which m_2 and m_3 are lying, it is necessary to split m_1 into masses m_4 and m_5 lying on such planes as shown in Fig. 16.15. By adding m_2 and m_4 on the left plane S and m_5 and m_3 on the right plane D, two masses m_s and m_d are obtained. The balancing of the wheel is then achieved by applying two masses having the same values as m_s and m_d but diametrically opposed to m_s and m_d on the two wheel sides.
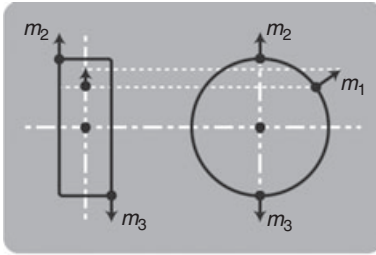
16.14 Couple unbalance.
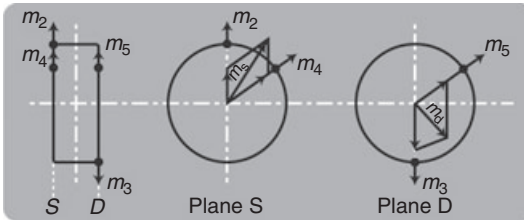
16.15 Plane *S* and plane *D*.
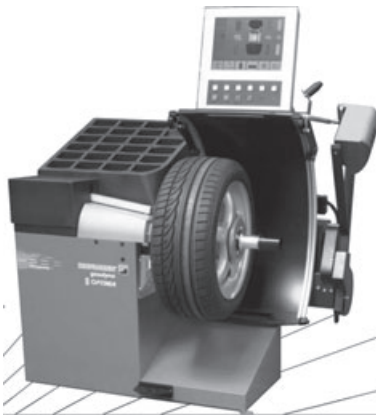
16.16 Off-vehicle wheel balancer.

Unbalanced corrections are made by applying counterweights in hard lead alloy which are fixed to the rims by means of a steel spring or are self-adhesive.

Tyre/wheel assemblies can be balanced off the vehicle or on the vehicle. On-vehicle balancing is the best choice as the balance is not affected when the tyres are rotated. Also, on-vehicle balances are generally more accurate than off-vehicle balances (as shown in Fig. 16.16) and can perform dynamic as well as static balance.

16.17 Various types of counterweights for vehicles.

Adhesive
wheel weight
placements

Wheel
weight
placements
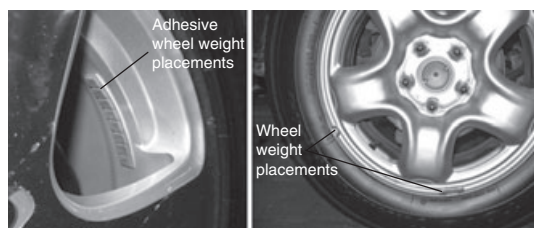
16.18 Balancing counterweight applied on a wheel fitted in a
balancing machine.

Deposits of foreign material must be cleaned from the inside of the
wheel. Stones should be removed from the tread in order to avoid operator
injury and to obtain a good balance. The tyre should be inspected for any
damage, then balanced according to the equipment manufacturer's instruc-
tions. Always use coated weights on aluminium wheels to prevent cosmetic
damage to the wheel finish. Figure 16.17 shows various types of weights,
and Fig. 16.18 shows a weight applied to a wheel in a balancing machine.

Wheel balancers can drift out of calibration, or can be inaccurate as a
result of abuse. This can happen without any visual clue that a problem
exists. Even though the equipment indicates that an assembly is balanced,
an imbalance may still be present. A quick calibration check can be made
using the following procedure:

1. Spin the balancer without a wheel, or any of the adaptors on the shaft.
   The readings should be 0 ± 5 grams.
2. Next balance a tyre/wheel assembly that is within radial and lateral
   run-out tolerances to 'zero', using the balancer.
3. Add a 50 gram test weight to the wheel at any location and re-spin the
   assembly. The balancer should call for 50 grams of weight, 180° opposite
   the test weight, in the static and dynamic modes. In the dynamic mode,
   the weight should be called for on the flange of the wheel opposite the
   test weight.

16.19 Balancing on-vehicle wheel by means of on-vehicle balancer.

4. With assembly imbalance to 50 grams, cycle the balancer fives times. The balance readings should not vary by more than 5 grams.
5. Index the wheel assembly at four separate locations on the balancer shaft, 90° apart. Cycle the balancer with the assembly at each location and record the results. The readings should not vary by more than 5 grams.

If the balancer fails any of the above tests, it should be checked by the manufacturer for defects. Balancer calibration should be checked at least every two weeks or whenever the balance readings are questionable.

16.3.4 On-vehicle balancing

If checking and/or correcting these components off the vehicle are not possible or do not correct the vibration, it may be necessary to balance the tyre/wheel assemblies while they are mounted on the vehicle using an on-vehicle, high-speed balancer (Fig. 16.19). This will balance the hubs, rotors and wheel simultaneously. Also it can compensate for any amount of residual run-out encountered as a result of mounting the tyre/wheel assembly on the vehicle, as opposed to the balance that was achieved on the off-vehicle balancer.

Follow the on-vehicle balancer manufacturer's operator's manual for specific instructions while keeping the following tips in mind:

- Do not remove the off-vehicle balance weights. The purpose of on-vehicle balance is to 'fine tune' the assembly balance already achieved, not to start all over again.
- Leave all wheel trim installed whenever possible. Some wire wheel covers have been known to induce static imbalance. If you suspect wheel trim to be causing the vibration, it can be eliminated by road testing the vehicle with the wheel trim removed. Remember the process of elimination: it works.
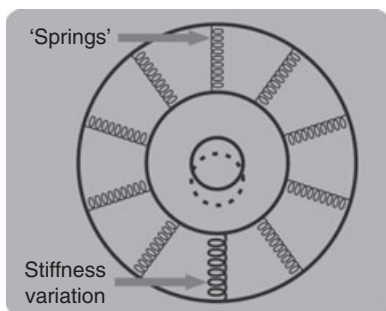
16.20 Radial force variation.

- If the on-vehicle balance calls for more than 10 grams of additional weight, split the weight between the inboard and outboard flanges of the wheel, so as not to upset the dynamic balance of the assembly achieved in the off-vehicle balance.
- Evaluate the condition after the on-vehicle balance to determine if the vibration has been eliminated.

16.3.5 Radial force variation

Radial force variation (Fig. 16.20) refers to a difference in the stiffness of a tyre sidewall as it rotates and contacts the road. Tyre/wheel assemblies have some of this due to splices in the different piles of the tyre, but they do not cause a problem unless the force variation is excessive. These 'stiff spots' in the sidewall can deflect the tyre/wheel assembly upward as they contact the road. If there are two 'stiff spots', they can cause a second-order vibration. First- and second-order tyre/wheel vibrations are the most common to occur as a result of radial force variation. Higher orders (third, fourth, etc.) are possible but quite rare, caused, for example, by a squared wheel (fourth order) or polygon (higher order).

The most effective way to minimize the possibility of force variation is to ensure tyre/wheel assembly run-out is at an absolute minimum. Some tyre/wheel assemblies may exhibit vibration caused by amounts of force variation even though they are within run-out and balance tolerances. Due to tighter tolerances and higher standards in manufacturing, these instances are becoming rare. If force variation is suspected as a factor, substitute one or more 'known good' tyre/wheel assemblies for the suspected assemblies. If this rectifies the problem replace the offending tyre.

16.3.6 Lateral force variation

This is based on the same concept as radial force variation, except that lateral force variation tends to deflect the vehicle sideways or laterally, as

the name implies. It can be caused by a 'snaky' belt inside the tyre. Tyre replacement using the substitution method may be necessary. This condition is very rare and again the best way to eliminate it as a factor is to ensure that the lateral run-out of tyre/wheel assemblies is at an absolute minimum. In most cases where excessive lateral force variation exists, the vehicle will display a 'wobble' or 'waddle' at low speeds (8 to 40 kph) on a smooth road surface. The condition will usually be related to the first order of tyre/wheel rotation.

16.4   Driveline vibration

Driveline vibrations can be related to one or more of the following components:

• Transmission output shaft
• Propshaft
• Pinion flange
• Pinion gear.

These four components are all either bolted or spined together. They all rotate at exactly the same speed. This means that any vibrations they may cause will produce the same frequencies and the same symptoms. These variations may be related to either the first or second order of driveline rotation. Each will be treated separately. Driveline variations, as a whole, are vehicle-speed related. In many instances, the disturbance is torque sensitive, meaning the vibration is present or worse when accelerating, decelerating or crowding the throttle. However, the disturbance will always a appear at the same vehicle speed. This characteristic of being torque sensitive and vehicle speed sensitive is always a clue in pointing to the driveline as a cause (tyre/wheel vibrations are also vehicle-speed related but are not torque sensitive, as a rule).

16.4.1 First-order driveline vibration

This vibration may be torque sensitive. Its symptoms are that:

• The vibration is related to vehicle speed (km/h dependent).
• Noise may be present (usually a 'boom' or 'moan').
• The vibration may occur at as low as 50 km/h, but most commonly in the range of 70 km/h and above.
• The vibration may be felt in the seat, floor or steering wheel as 'roughness' or 'buzz'.
• The frequency of the vibration will equal the first order of driveline rotation – 25 to 60 Hz depending on the rotational speed of the propshaft.

16.21 Propshaft balancer.

16.4.2 Correcting first-order driveline complaints

The cause of first-order driveline vibrations is usually excessive run-out or unbalance of a component. In order to quickly determine which component is at fault, the following procedure offers a systematic process of elimination:

1. Check and correct propshaft and pinion flange run-out in the same way as tyre/wheel assembly.
2. Balance the propshaft using a propshaft balancer as shown in Fig. 16.21.

16.4.3 Second-order driveline vibration

As explained previously, first-order driveline vibrations are mostly the result of excessive run-out or imbalance of a driveline component. Second-order driveline disturbances are independent of these factors. Due to operational characteristics of universal joints a vibration that occurs twice per revolution of the propshaft may occur. In order to clearly understand where the second-order driveline vibrations come from – and why they do – we should review the basic theory of operation.

As the propshaft rotates, the universal joints actually speed up and slow down, twice for every revolution of the propshaft. As previously mentioned, a vibration that occurs twice per revolution of a component is termed second-order. The acceleration and deceleration of the universal joints cannot always be seen, but in the case of vibration complaints it may be felt or heard.

Compare the universal joint in a vehicle to a universal-type socket in your toolbox. Picture a universal socket to tighten a belt. As the angle through which you operate the socket increases towards 90°, the universal joint will bind and release as you turn the socket. This bind and release occurs twice for each revolution of the socket.

The same condition occurs in the universal joints of vehicles as they operate through an angle: the greater the angle, the more pronounced the effect. Because the transmission output is constant, this binding and releasing of the universal joints is better described as an acceleration and deceleration that occurs twice per revolution of the propshaft. If you run the propshaft slowly you can actually perceive the acceleration and deceleration effect. It can create a vibration due to the fluctuations in force that are generated at high speed.

Drivelines are designed in a manner that allows for these accelerations and decelerations to be cancelled out, in order to produce a smooth and constant power flow. The transmission is driving the front yoke of the propshaft at a smooth and constant speed. As the power travels through the first universal joint, it fluctuates twice per revolution of the propshaft. The second universal joint is oriented in a manner that allows the power flow to fluctuate opposite that of the first joint. As the first joint is slowing down or binding, the second joint is speeding up or releasing. This creates the effect of one universal joint cancelling out the other, and results in a smooth, constant power flow from the output yoke of the propshaft. Second-order driveline vibrations occur when the cancellation becomes unequal between the front and rear joints.

The symptoms of second-order driveline vibrations are that:

• They are always vehicle-speed related.
• They are usually torque sensitive, and generally worse under torque.

One of the most common complaints is initial acceleration shudder (take-off shudder). This occurs on acceleration from a standing start at speeds of 0 to 40 km/h. The vibration appears as a low-frequency shake, wobble or shudder. It is felt in the seat or steering wheel at low speed (0 to 25 km/h) and will increase in frequency as vehicle speed increases. Eventually it feels more like driveline roughness at higher speeds (15 to 40 km/h), or acceleration-delayed shudder. At high speeds the vibration generally disappears. The vibration frequency is equal to that of second-order driveline rotation. However, due to the nature of take-off, it is usually difficult or impossible to acquire frequency information.

16.4.4 Correcting second-order driveline vibration

Correcting the conditions that interfere with the proper cancellation effect of the universal joints is the main objective. The most common condition by far, especially where take-off shudder is concerned, is incorrect driveline working angles. However, other factors which may aggravate the condition must be addressed before attempting to measure or correct driveline working angles. These include:
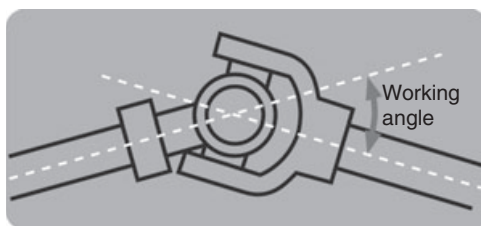
16.22 Working angle.
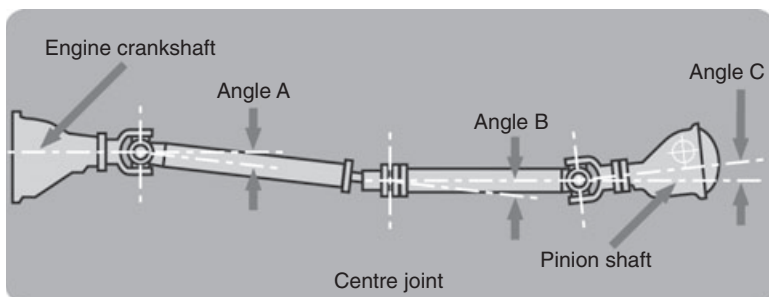
16.23 Driveline angles to be measured.

- Tight, worn, failed, damaged or improperly installed universal joints
- Worn, collapsed or incorrect powertrain mounts
- Worn, collapsed or incorrect centre bearing or mount
- Worn, collapsed or incorrect suspension control arm bushes
- Incorrect vehicle trim heights. This includes trim heights that are too low or too light on a rear-wheel-drive vehicle, when the pinion nose will tilt upward as the rear trim height is lowered. This condition tends to aggravate take-off shudder.

16.4.5 Driveline working angles

Driveline working angle does not refer to the angle of any one shaft, but to the angle formed by the intersection of two shafts (see Fig. 16.22). An inclinometer or an equivalent tool will be necessary to perform these measurements. The bubble inclinometer has a magnetic base for mounting on the joint bearing caps, along with a bubble level and angle scale for taking accurate measurements.

Referring to Fig. 16.23, symptoms and causes of driveline angle-related problems are:

- Initial acceleration (take-off) shudder. A pronounced shudder that occurs during forward acceleration could be caused by an excessive angle 'A'.
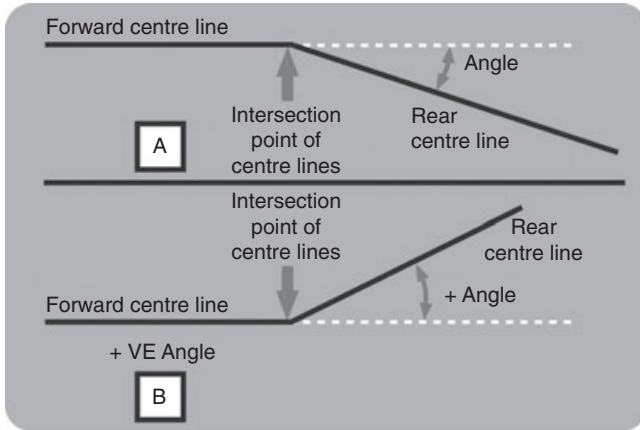
16.24 Driveline angle evaluation.
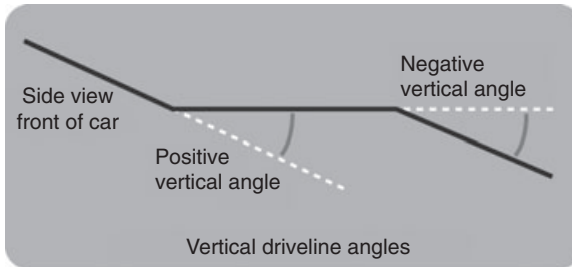
16.25 Driveline angle sign evaluation.

- Acceleration-delayed shudder. A vehicle may accelerate smoothly from standstill yet begin to shudder from 15–40 km/h. This condition is usually worse when the vehicle is heavily laden and can be caused by an insufficient angle 'C' (only applies to five-link rear suspension) as shown in Fig. 16.23.
- Boom or rumble. Vehicles with an excessive angle 'C' may suffer from cabin boom or rumble from 40 km/h on overrun/coast. The condition is usually worse when the vehicle has a minimal load in the rear. Acceleration in reverse with an excessive angle 'C' will cause severe driveline vibration (only applies to five-link rear suspension).

Figure 16.24 shows the precise way in which driveline angles are evaluated. The maximum allowable tolerance is ±0.5° for the nominal angle. To determine if a driveline angle is positive or negative, refer to Fig. 16.25.

If driveline angles are to specification, start by raising or lowering the centre bearing relative to the underbody by adding, repositioning or sub-

tracting spacers between the centre bearing carrier and underbody or between the centre bearing carrier and centre bearing. Raising the centre bearing by 7 mm will increase angle 'A' (or make it more positive) by +0.7° and increase angle 'C' (or make it more positive) by +0.6°. Note the following:

- Achievement of correct angle 'B' (at constant velocity joint) is not as critical as angles 'A' and 'C' for minimizing noise and vibration.
- This is the only adjustment available for changing driveline angles in propshafts fitted to independent rear suspension (IRS) equipped vehicles.

For vehicles with five-link rear suspension, minor angle 'C' corrections can also be made by loosening all the rear suspension control arm attaching bolts and nuts and repositioning the pinion nose up or down. This takes advantage of all the bolt-hole tolerances in the control arm mountings. If angle 'C' corrections of more than 1° are required, rear suspension lower control arms with different lengths should be tested.

Retighten control arm attaching bolts and nuts to the correct torque specification. When driveline angles are to specification, remove the inclinometer, reinstall underbody centre-bearing cross-member brace attaching bolts and tighten to the correct torque specification.

16.4.6 Checking driveline angles

The following checks must be conducted before carrying out the driveline angle measurement:

- Inspect all universal joints and centre bearing for wear and/or damage, i.e. dust seals broken, retaining snap rings broken or any movement in the universal joints or centre bearing.
- Check engine and transmission mountings and tightness of all bolts.
- Ensure that the rear suspension height is maintained at the specified dimensions when taking angle readings. The height measurement is to be taken from the underside of the rear fender opening and the lower, outside face of the wheel rim. The vehicle is also to be checked while at kerb weight, i.e. fuel tank full without driver, passengers or luggage.
- To enable clear access to both the front and rear universal joints, either partial or total removal of the exhaust system components may be required.
- Check that the centre bearing support bracket is correctly oriented, relative to the rear suspension fitted to the vehicle. The bracket fitted to a vehicle with five-link rear suspension is shown in Fig. 16.26 where the arrow with that label is facing to the front.
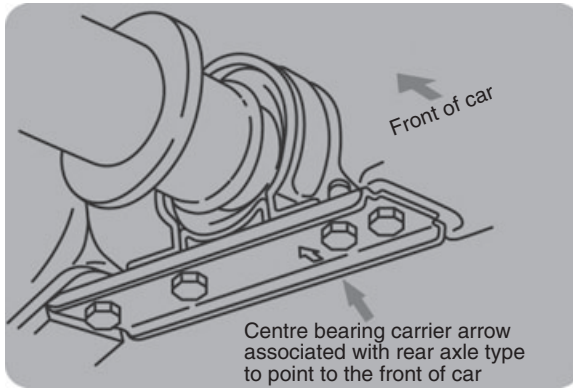
16.26 Orientation of centre bearing support bracket.

• Balance all road wheels, paying particular attention to the rear wheel/ tyre balance.

Figure 16.23 illustrated the driveline angles which are to be measured, and provided an indication of positive angles. Table 16.2 lists the various *typical* driveline angle specifications.

Before proceeding any further with the driveline angle measurement, note the following points:

• At no stage is the vehicle to be moved by twisting the propshaft.
• Ensure that all inclinometer readings are taken from the right-hand side of the vehicle, i.e. the scale is facing towards the right-hand side of the vehicle.
• Mark all universal joint caps from which measurements are taken, so that later measurements can be taken from the same caps.
• Ensure that universal joint caps are clear and free from paint and dirt.
• Ensure that the magnet on the inclinometer sits squarely on the universal joint caps.
• Ensure that the inclinometer is positioned and read at each location with the 50° end towards the front of the vehicle.

16.5   Propshaft phasing

Before attempting to diagnose propshaft phasing-induced vibrations, the following stages must be complied with first, in all aspects:

1. Driveline angles must be set to specification.
2. Check that rear axle pinion flange and propshaft rear universal joint flange aligning paint marks are matched as closely as possible.

Table 16.2 Typical driveline angle specification for vehicles with five-link rear suspension and with independent rear suspension

(a) Vehicles with five-link rear suspension

Body style (V6 or V8 engine)	Suspension type	Angle 'A' (degrees)	Angle 'B' (degrees)	Angle 'C' (degrees)	Rear suspension height (ref.) (mm)
Sedan	Standard	+1.0	−1.0	+4.0	601
	FE2 'Sports'	+1.0	+0.5	+3.5	576
	V5W 'Country'	+1.0	−1.0	+3.0	615
Station wagon	Standard	−1.0	+1.0	+3.5	589
	V5W 'Country'	−1.0	+0.5	+2.5	601
Utility	All	−1.0	+0.5	+3.0	610

Notes:
1. Tolerance on all drivelines (±0.5°).
2. All rear suspension heights are to be taken while the vehicle is at kerb height with full fuel tank.
3. Five-link rear suspension heights are for reference only to maintain a standard specification during measurements.

(b) Vehicles with independent rear suspension

Driveline angle	V6 automatic	V8 automatic	Short wheelbase	Long wheelbase
Angle 'A'	+1.0° ± 0.5°	0.0° ± 0.5°		
Angle 'C'			−1.5° ± 0.5°	−1.0° ± 0.5°

3. Check that all propshaft assembly attaching bolts and nuts are tightened to the correct torque.
4. Balance wheels and tyres.
5. Road test vehicle and check for:
   • rumble noise and vibration throughout the vehicle speed range (usually worse during 'float' or 'overrun' conditions)
   • a 'beat' that may develop at higher speeds.

A rumble is a constant sound, e.g. 'the rumble of distant thunder', while a beat is a low-frequency cycling of the rumble noise. If the vehicle exhibits any of the symptoms in step 5, proceed with the propshaft phase angle procedure. Figure 16.27 shows the conversion scale fitted to the inclinometer to check the propshaft phase angles.

There are phase specifications for different vehicles. Figure 16.28 shows negative and positive phase angle where a positive phase angle indicates that the rear universal joint leads the front, whereas a negative angle is the reverse situation. If the phase angle is to specification, remove the
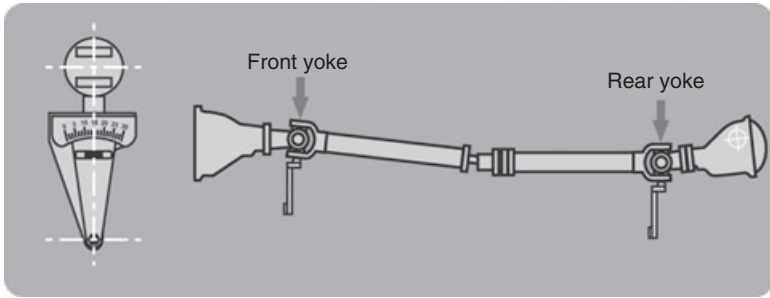
16.27 Checking propshaft phase angles.
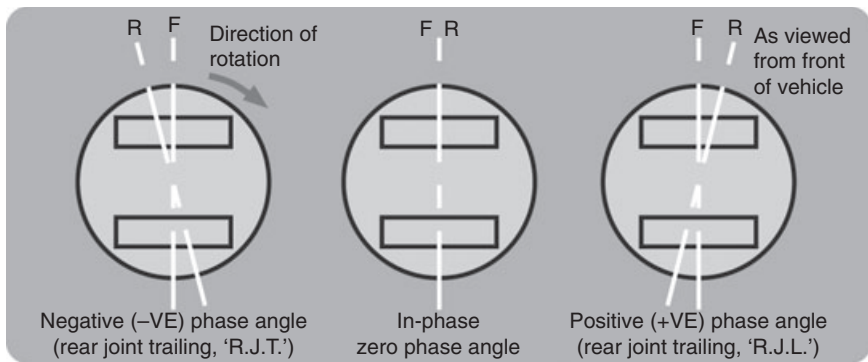
16.28 Negative and positive phase angles.

inclinometer, reinstall the centre-bearing cross-member brace bolts and tighten to the correct torque specification. To correct an out-of-specification phase angle, install the constant velocity joint around one spline from the original position. Once the propshaft phase angle has been corrected, the assembly must be rebalanced.

16.6   Bibliography

Andreescu, C.N. and Beloiu, D.M. (2005). Modelling and simulation of cylinder head vibration using multibody dynamics approach and wavelet analysis, SAE paper 2005-01-2530.

Badawi, B., Kholosy, A.M., Omer, A.A. and Shahin, M.A. (2007). Identification of diesel engine events from acoustic signals using independent component analysis and time-frequency analysis, SAE paper 2007-01-2278.

Beniwal, R. and Wu, S. (2007). System level noise source identification and diagnostics on a vehicle door module, SAE paper 2007-01-2280.

Chiavola, O., Arnone, L., Recco, E., Conforto, S., Boni, M. and Manelli, S. (2009). Block vibration measurements for combustion diagnosis in multi-cylinder common rail diesel engine, SAE paper 2009-01-0646.

Chiavola, O., Conforto, S., Boni, M., Manelli, S., Recco, E. and Arnone, L. (2009). Diesel engine combustion monitoring through block vibration signal analysis, SAE paper 2009-01-0765.

Demers, M.A. (2001). Steering wheel vibration diagnosis, SAE paper 2001-01-1607.

Fleszar, A., Van der Linden, P., Johnson, J.R. and Grimmer, M.J. (2001). Combining vehicle and test-bed diagnosis information to guide vehicle development for pass-by noise, SAE paper 2001-01-1565.

Huang, Q., Liu, Y. and Liu, H. (2003). A new vibration diagnosis method based on the neural network and wavelet analysis, SAE paper 2003-01-0363.

Jen, M.-U. and Lu, M.-H. (2003). Experimental root cause diagnosis for scooter NVH problem, SAE paper 2003-01-1426.

Johnson, O. and Hirami, N. (1991). Diagnosis and objective evaluation of gear rattle, SAE paper 911082.

Newland, D.E. (1993). *An Introduction to Random Vibrations, Spectral and Wavelet Analysis*, John Wiley & Sons, New York.

Poradek, F., Rao, M.D., Kang, J., Jeon, B. and Lee, H. (2007). Application of signature analysis and operating deflection shapes to identify interior noise sources in an excavator, SAE paper 2007-01-2427.

Randall, R.B. (1987). *Frequency Analysis*, Brüel & Kjær.

Shih, S., Yruma, J.G. and Kittridge, P. (2001). Drivetrain noise and vibration troubleshooting, SAE paper 2001-01-2809.

Shivashankaraiah, K. (2009). Measurement and analysis of cam chain noise for source identification and mitigation, SAE paper 2009-01-2167.

Van der Linden, P.J.G. (1999). Modular vehicle noise and vibration development, SAE paper 1999-01-1689.

Wowk, V. (1991). *Machinery Vibration – Measurement and Analysis*, McGraw-Hill, New York.